EPA-600/3-77-001a
January 1977

Ecological Research Series

INTERNATIONAL CONFERENCE ON PHOTOCHEMICAL OXIDANT POLLUTION AND ITS CONTROL

Proceedings: Volume I

Environmental Sciences Research Laboratory
Office of Research and Development
U.S. Environmental Protection Agency
Research Triangle Park, North Carolina 27711

RESEARCH REPORTING SERIES

Research reports of the Office of Research and Development, U.S. Environmental Protection Agency, have been grouped into five series. These five broad categories were established to facilitate further development and application of environmental technology. Elimination of traditional grouping was consciously planned to foster technology transfer and a maximum interface in related fields The five series are:

1. Environmental Health Effects Research
2. Environmental Protection Technology
3. Ecological Research
4. Environmental Monitoring
5. Socioeconomic Environmental Studies

This report has been assigned to the ECOLOGICAL RESEARCH series. This series describes research on the effects of pollution on humans, plant and animal species, and materials. Problems are assessed for their long- and short-term influences. Investigations include formation, transport, and pathway studies to determine the fate of pollutants and their effects. This work provides the technical basis for setting standards to minimize undesirable changes in living organisms in the aquatic, terrestrial, and atmospheric environments.

This document is available to the public through the National Technical Information Service, Springfield, Virginia 22161.

EPA-600/3-77-001a
January 1977

INTERNATIONAL CONFERENCE ON PHOTOCHEMICAL OXIDANT POLLUTION AND ITS CONTROL

Proceedings: Volume I

Hosted by the United States Environmental Protection Agency
September 12-17, 1976
Raleigh, North Carolina

Coordinated by the Triangle Universities
Consortium on Air Pollution

with the patronage of
Organization for Economic Cooperation and Development

Edited by

Basil Dimitriades
Environmental Sciences Research Laboratory
Research Triangle Park, N. C. 27711

Environmental Sciences Research Laboratory
Office of Research and Development
U. S. Environmental Protection Agency
Research Triangle Park, North Carolina 27711

DISCLAIMER

This report has been reviewed by the Environmental Sciences Research Laboratory, U.S. Environmental Protection Agency, and approved for publication. Approval does not signify that the contents necessarily reflect the views and policies of the U.S. Environmental Protection Agency, nor does mention of trade names or commercial products constitute endorsement or recommendation for use.

In general, the texts of the papers included in this report have been reproduced in the form submitted by the authors.

Any papers included in the Program and not included herein were not submitted for publication.

PREFACE

Since the late 1940's when the first studies of atmospheric pollution began, photochemical smog has been evolving into a full-fledged problem with an enormously strong and complex impact upon man's lifestyle. Smog is no longer a subject of mainly academic interest. Its presence and consequences are now fully felt by the layman and perhaps most painfully by the automobile user. The use of automobiles is being restricted in the large urban centers in the U. S., and even more restrictive measures including gasoline rationing have been considered. The merits of the economic incentives traditionally associated with industrial growth are now being seriously questioned, and pressures grow stronger for a review and a more realistic appraisal of the environmental, energy, and industrial growth priorities. Such a strong and multifaceted impact of the photochemical pollution problem makes it imperative that all judgment regarding the causes, occurrence, and solution or alleviation of the problem be made responsibly and with the highest degree of confidence. Thus, while it is extremely important that the health and welfare of the people be protected, it is equally important to ascertain that such protection is really achieved and that the health danger is not traded for other equally bad or worse problems.

Intensive studies conducted in the past 3-4 years have resulted in an abundance of suggestive evidence that in part supported and in part refuted the earlier understanding, but did not resolve all existing issues. Thus, the international scientific community is still divided on the issue of the justification of the 0.08-ppm ambient air quality standard for oxidant, one objection arising from the questionable achievability of such a standard. A newly revived issue of major importance pertains to the relative roles of the hydrocarbon and nitrogen oxide precursors in the urban and rural oxidant formation processes. The viewpoint of the U.S. Environmental Protection Agency supporting maximum control of the hydrocarbon and limited control of the NO_x emissions is challenged in several Conference papers. More specific issues raised by the new evidence, and debated in the Conference, are the achievability of the ambient oxidant standard, the role of stratospheric ozone, the role of the natural ozone precursors, the utility of current air quality simulation models, and the significance of short- and long-range photochemical pollution transport.

Aside from the debate on the above issues, the Conference will gather and bring into focus the latest developments in the areas of physical-chemical research methodology, biological effects of oxidants, and emission control methods. It was felt that inclusion of such widely diverse subject areas would be essential for examining the balance, rationality, and effectiveness of the entire oxidant control effort.

The Conference is expected to be extremely valuable to the U.S. Environmental Protection Agency in that it will provide a forum for presenting the Agency's evolving viewpoint on oxidant control strategies, and for sounding out scientific receptivity to this viewpoint. The Conference is of value also to the international community of scientists and government administrators in that it will provide an opportunity for comparing the problems, experiences, and control policies of one country with those of others. Considering the now established international range of pollution transport, and the implications of oxidant-related control upon international trade, such interaction among countries is more than justified. For these reasons the organization of the Conference was undertaken by the U.S. Environmental Protection Agency, with the patronage of the Organization for Economic Cooperation and Development.

B. Dimitriades

CONTENTS

PREFACE iii

ACKNOWLEDGMENT xv

SESSION 1 - ANALYTICAL METHODS FOR OXIDANTS AND PRECURSORS - I 1
Chairman: K.H. Becker

1-1 METHODOLOGY FOR STANDARDIZATION OF ATMOSPHERIC OZONE MEASUREMENTS 3
J.A. Hodgeson, E.E. Hughes, W.P. Schmidt, and A.M. Bass

1-2 ULTRAVIOLET PHOTOMETER FOR OZONE CALIBRATION 13
A.M. Bass, A.E. Ledford, Jr., and J.K. Whittaker

1-3 HYDROCARBON AND HALOCARBON MEASUREMENTS: SAMPLING AND ANALYSIS PROCEDURES 19
R.B. Denyszyn, L.T. Hackworth, P.M. Grohse, and D.E. Wagoner

SESSION 2 - ANALYTICAL METHODS FOR OXIDANTS AND PRECURSORS - II 29
Chairman: K.H. Becker

2-1 A NEW CHEMILUMINESCENT OLEFIN DETECTOR FOR AMBIENT AIR 31
K.H. Becker, U. Schurath, and A. Wiese

2-2 GC-CHEMILUMINESCENCE METHOD FOR THE ANALYSIS OF AMBIENT TERPENES 41
R.L. Seila

2-3 MEASUREMENTS OF SULFATE, INORGANIC GASEOUS NITRATE AND OTHER CONSTITUENTS IN THE ATMOSPHERE 51
T. Okita

2-4 A PORTABLE INSTRUMENT FOR THE CALIBRATION OF OZONE ANALYZERS BY OPTICAL ABSORPTION MEASUREMENTS 59
K.H. Becker, A. Heindrichs, and U. Schurath

2-5 STATUS OF CALIBRATION METHODS FOR OZONE MONITORS 67
R.J. Paur, R.K. Stevens, and D.L. Flamm

SESSION 3 - SOURCES OF TROPOSPHERIC OZONE - I 73
Chairman: R.A. Rasmussen

3-1 METEOROLOGICAL CONDITIONS CONDUCIVE TO HIGH LEVELS 75
OF OZONE
T.R. Karl and G.A. DeMarrais

3-2 OZONE IN RURAL AND URBAN AREAS OF NEW YORK STATE - 89
PART I
P.Coffey, W. Stasiuk, and V. Mohnen

3-3 OZONE MEASUREMENT AND METEOROLOGICAL ANALYSIS OF 97
TROPOPAUSE FOLDING
V.A. Mohnen, A. Hogan, E. Danielsen, and P. Coffey

3-4 METEOROLOGICAL FACTORS CONTROLLING PHOTOCHEMICAL 109
POLLUTANTS IN SOUTHEASTERN NEW ENGLAND
R.A. Dobbins, J.L. Nolan, J.P. Okolowicz, and
A.J. Gilbert

SESSION 4 - SOURCES OF TROPOSPHERIC OZONE - II 119
Chairman: R.A. Rasmussen

4-1 AN ASSESSMENT OF THE CONTINENTAL LOWER TROPOSPHERIC 121
OZONE BUDGET
R. Chatfield and R.A. Rasmussen

4-2 URBAN KINETIC CHEMISTRY UNDER ALTERED SOURCE CONDITIONS 137
L.A. Farrow, T.E. Graedel, and T.A. Weber

4-4 THE EFFECT OF OZONE LAYERS ALOFT ON SURFACE 145
CONCENTRATIONS
T.N. Jerskey, T.B. Smith, and W.H. White

SESSION 5 - SOURCES OF TROPOSPHERIC OZONE - III 155
Chairman: R.A. Rasmussen

5-1 OZONE CONCENTRATIONS IN POWER PLANT PLUMES: 157
COMPARISON OF MODELS AND SAMPLING DATA
T.W. Tesche, J.A. Ogren, and D.L. Blumenthal

5-2 OZONE AND NITROGEN OXIDES IN POWER PLANT PLUMES 173
D. Hegg, P.V. Hobbs, L. Radke, and H. Harrison

5-3 THE ANALYSIS OF GROUND-LEVEL OZONE DATA FROM NEW JERSEY, NEW YORK, CONNECTICUT, AND MASSACHUSETTS: DATA QUALITY ASSESSMENT AND TEMPORAL AND GEOGRAPHICAL PROPERTIES 185
W.S. Cleveland, B. Kleiner, J.E. McRae, and R.E. Pasceri

5-4 CHEMICAL AND METEOROLOGICAL ANALYSIS OF THE MESOSCALE VARIABILITY OF OZONE CONCENTRATIONS OVER A SIX-DAY PERIOD 197
W.D. Bach, Jr., J.E. Sickles, II, R. Denyszyn, and W.C. Eaton

5-5 OZONE AND HYDROCARBON MEASUREMENTS IN RECENT OXIDANT TRANSPORT STUDIES 211
W.A. Lonneman

SESSION 6 - OZONE/OXIDANT TRANSPORT - I 225
Chairman: A.P. Altshuller

6-1 TRANSPORT OF OZONE BY UPPER-LEVEL LAND BREEZE - AN EXAMPLE OF A CITY'S POLLUTED WAKE UPWIND FROM ITS CENTER 227
E.K. Kauper and B.L. Niemann

6-2 OZONE FORMATION IN THE ST. LOUIS PLUME 237
W.H. White, D.L. Blumenthal, J.A. Anderson, R.B. Husar, and W.E. Wilson, Jr.

6-3 LONG RANGE AIRBORNE MEASUREMENTS OF OZONE OFF THE COAST OF THE NORTHEASTERN UNITED STATES 249
G.W. Siple, C.K. Fitzsimmons, K.F. Zeller, and R.B. Evans

6-4 AIRBORNE MEASUREMENTS OF PRIMARY AND SECONDARY POLLUTANT CONCENTRATIONS IN THE ST. LOUIS URBAN PLUME 259
N.E. Hester, R.B. Evans, F.G. Johnson, and E.L. Martinez

6-5 OZONE IN HAZY AIR MASSES 275
R.B. Husar, D.E. Patterson, C.C. Paley and N.V. Gillani

SESSION 7 - OZONE/OXIDANT TRANSPORT - II 283
Chairman: A.P. Altshuller

7-1 THE TRANSPORT OF PHOTOCHEMICAL SMOG ACROSS THE SYDNEY BASIN 285
R. Hyde and G.S. Hawke

7-2 OXIDANT LEVELS IN ALBERTA AIRSHEDS 299
H.S. Sandhu

7-3 AN INVESTIGATION OF LONG-RANGE TRANSPORT OF OZONE ACROSS THE MIDWESTERN AND EASTERN UNITED STATES 307
G.T. Wolff, P.J. Lioy, G.D. Wright, R.E. Meyers, and R.T. Cederwall

7-4 OXIDANT AND PRECURSOR TRANSPORT SIMULATION IN THE RESEARCH TRIANGLE INSTITUTE SMOG CHAMBERS 319
J.E. Sickles, II, L.A. Ripperton, and W.C. Eaton

7-5 OZONE EPISODES ON THE SWEDISH WEST COAST 329
P. Grennfelt

SESSION 8 - IMPACT OF STRATOSPHERIC OZONE 339
Chairman: R. Guicherit

8-1 OZONE OBSERVATIONS IN AND AROUND A MIDWESTERN METROPOLITAN AREA. 341
G. Huffman, G. Haering, R. Bourke, P. Cook, and M. Sillars

8-2 A "TEXAS SIZE" OZONE EPISODE TRACKED TO ITS SOURCE 353
J.W. Hathorn, III and H.M. Walker

8-3 APPLICATION OF 1960's OZONE SOUNDING INFORMATION TO 1970's SURFACE OZONE STUDIES 381
P.R. Sticksel

8-4 THE ROLE OF STRATOSPHERIC IMPORT ON TROPOSPHERIC OZONE CONCENTRATIONS 393
E.R. Reiter

SESSION 9 - THEORIES ON RURAL OZONE/OXIDATES 411
Chairman: B. Dimitriades

9-1 RESEARCH TRIANGLE INSTITUTE STUDIES OF HIGH OZONE CONCENTRATIONS IN NONURBAN AREAS 413
L.A. Ripperton, J.J.B. Worth, F.M. Vukovich, and C.E. Decker

9-2 IMPORTANT FACTORS AFFECTING RURAL OZONE CONCENTRATION 425
F.L. Ludwig, W.B. Johnson, R.E. Ruff, and H.B. Singh

9-3 A MECHANISM ACCOUNTING FOR THE PRODUCTION OF OZONE IN RURAL POLLUTED ATMOSPHERES 439
M. Antell

9-4 NET OZONE FORMATION IN RURAL ATMOSPHERES 451
T.Y. Chang and B. Weinstock

9-5 THE KINETIC OZONE PHOTOCHEMISTRY OF NATURAL AND PERTURBED NONURBAN TROPOSPHERES 467
T.E. Graedel and D.L. Allara

SESSION 10 - PHYSIOLOGICAL EFFECTS OF OXIDANTS - I 475
Chairman: J. Knelson

10-1 ON THE RELATIONSHIP OF SUBJECTIVE SYMPTOMS TO PHOTOCHEMICAL OXIDANTS 477
I. Mizoguchi, K. Makino, S. Kudou and R. Mikami

10-2 EFFECTS OF OZONE PLUS MODERATE EXERCISE ON PULMONARY FUNCTION IN HEALTHY YOUNG MEN 495
B. Ketcham, S. Lassiter, E. Haak, and J.H. Knelson

10-3 EFFECTS OF OZONE AND NITROGEN DIOXIDE EXPOSURE OF RABBITS ON THE BINDING OF AUTOLOGOUS RED CELLS TO ALVEOLAR MACROPHAGES 505
J.G. Hadley, D.E. Gardner, D.L. Coffin, and D.B. Menzel

10-4 RELATIONSHIPS BETWEEN NITROGEN DIOXIDE CONCENTRATION, TIME, AND LEVEL OF EFFECT USING AN ANIMAL INFECTIVITY MODEL 513
D.E. Gardner, F.J. Miller, E.J. Blommer, and D.L. Coffin

10-5 DEVELOPMENT OF OZONE TOLERANCE IN MAN 527
M. Hazucha, C. Parent, and D.V. Bates

SESSION 11 - PHYSIOLOGICAL EFFECTS OF OXIDANTS - II 543
Chairman: J. Knelson

11-1 TOXIC INHALATION OF NITROGEN DIOXIDE IN CANINES 545
T.L. Guidotti and A.A. Liebow

11-2 THE EFFECT OF OZONE ON THE VISUAL EVOKED POTENTIAL OF THE RAT SUPERIOR COLLICULUS AND VISUAL CORTEX 555
B.W. Berney, R.S. Dyer, and Z. Annau

11-3 HEALTH EFFECTS OF SHORT-TERM EXPOSURES TO NO_2-O_3 MIXTURES 565
E. Ehrlich, J.C. Findlay, J.D. Fenters, and D.E. Gardner

11-4 BIOCHEMICAL INDICES OF NITROGEN DIOXIDE INTOXICATION OF GUINEA PIGS FOLLOWING LOW LEVEL-LONG TERM EXPOSURE 577
B. Menzel, M.B. Abou-Donia, C.R. Roe, R. Ehrlich, D.E. Gardner, and D.L. Coffin

11-5 BENEFIT EFFECTIVE OXIDANT CONTROL 589
R.A. Bradley, M. Dole, Jr., W. Schink, and S. Storelli

SESSION 12 - EFFECTS OF OXIDANTS ON VEGETATION - I 599
Chairman: W.W. Heck

12-1 OZONE INDUCED ALTERATIONS IN PLANT GROWTH AND METABOLISM 601
D.T. Tingey

12-2 OXIDANT LEVELS ON REMOTE MOUNTAINOUS AREAS OF SOUTHWESTERN VIRGINIA AND THEIR EFFECTS ON NATIVE WHITE PINE (PINUS STROBUS L.) 611
E.M. Hayes, J.M. Skelly, and C.F. Croghan

12-3 THE EFFECTS OF OZONE ON PLANT-PARASITIC NEMOTODES AND CERTAIN PLANT MICROORGANISM INTERACTIONS 621
D.E. Weber

SESSION 13 - EFFECTS OF OXIDANTS ON VEGETATION - II 633
Chairman: W.W. Heck

13-1 GROWTH RESPONSE OF CONIFER SEEDLINGS TO LOW OZONE CONCENTRATIONS 635
R.G. Wilhour and G.E. Neely

13-2 MACROSCOPIC RESPONSE OF THREE PLANT "SPECIES" TO OZONE, PAN, OR OZONE + PAN 647
D.D. Davis and R.J. Kohut

13-3 RELATIVE SENSITIVITY OF EIGHTEEN HYBRID COMBINATIONS OF PINUS TAEDA L. TO OZONE 655
L.W. Kress and J.M. Skelly

13-4 EFFECTS OF OZONE AND SULFUR DIOXIDE SINGLY AND IN COMBINATION ON YIELD, QUALITY, AND N-FIXATION OF ALFALFA 663
G.E. Neely, D.T. Tingey and R.G. Wilhour

SESSION 14 - REACTIVITY AND ITS USE IN OXIDANT-RELATED CONTROL 675
Chairman: J.G. Calvert

14-1 MULTIDAY IRRADIATION OF NO_x ORGANIC MIXTURES 677
W.A. Glasson and P.H. Wendschuh

14-2 HYDROCARBON REACTIVITY AND THE ROLE OF HYDROCARBONS, OXIDES OF NITROGEN AND AGED SMOG IN THE PRODUCTION OF PHOTOCHEMICAL OXIDANTS 687
J.N. Pitts, A.M. Winer, G.J. Doyle, K.R. Darnall and A.C. Lloyd

14-3 APPLICATION OF REACTIVITY CRITERIA IN OXIDANT- RELATED EMISSION CONTROL IN THE USA 705
B. Dimitriades and S.B. Joshi

14-4 PHOTOCHEMICAL REACTIVITY CLASSIFICATION OF HYDROCARBONS AND OTHER ORGANIC COMPOUNDS 713
F.F. Farley

SESSION 15 - ATMOSPHERIC CHEMISTRY AND PHYSICS 727
Chairman: J.G. Calvert

15-1 DECOMPOSITION OF CHLORINATED HYDROCARBONS UNDER SIMULATED ATMOSPHERIC CONDITIONS 729
F. Korte and H. Parlar

15-2 PHOTOOXIDATION OF THE TOLUENE-NO_2-O_2-N_2 SYSTEM IN A SMALL SMOG CHAMBER 737
H. Akimoto, M. Hoshino, G. Inoue, M. Okuda, and N. Washida

15-3 THE CHEMISTRY OF NATURALLY EMITTED HYDROCARBONS 745
B.W. Gay, Jr. and R.R. Arnts

15-4 MEASUREMENT OF PHOTONS INVOLVED IN PHOTOCHEMICAL OXIDANT FORMATION 753
D.H. Stedman, R.B. Harvey, and R.R. Dickerson

15-5 ACTIVE SOLAR FLUX AND PHOTOLYTIC RATE IN THE TROPOSPHERE 763
J.T. Peterson, K.L. Demerjian, and K.L. Schere

SESSION 16 - MATHEMATICAL MODELS OF OZONE/OXIDANT AIR QUALITY - I 775
Chairman: K. Demerjian

16-1 PHOTOCHEMICAL AIR QUALITY SIMULATION MODELLING: CURRENT STATUS AND FUTURE PROSPECTS 777
K.L. Demerjian

16-2 THE SYSTEMS APPLICATIONS, INCORPORATED URBAN AIRSHED MODEL: AN OVERVIEW OF RECENT DEVELOPMENTAL WORK 795
S.D. Reynolds

SESSION 17 - MATHEMATICAL MODELS OF OZONE/OXIDANT AIR QUALITY - II ... 803
Chairman: K. Demerjian

17-1 A SURVEY OF APPLICATIONS OF PHOTOCHEMICAL MODELS 805
J.E. Summerhays

17-2 TESTS OF THE DIFKIN PHOTOCHEMICAL DIFFUSION MODEL USING LOS ANGELES REACTIVE POLLUTANT PROGRAM DATA 817
G.H. Taylor and A.Q. Eschenroeder

17-3 DEVELOPMENT OF A MARKET CHAIN MODEL FOR PHOTOCHEMICAL OXIDANT PREDICTION 827
J.R. Martinez

17-4 A PRELIMINARY INVESTIGATION OF THE EFFECTIVENESS OF AIR POLLUTION EMERGENCY PLANS 837
W.F. Dabberdt and H.B. Singh

SESSION 18 - OXIDANT-PRECURSOR RELATIONSHIPS AND THEIR INTERPRETATION IN TERMS OF OPTIMUM STRATEGY FOR OXIDANT CONTROL - I . 849
Chairman: J.N. Pitts

18-1 A "J" RELATIONSHIP FOR TEXAS 851
H.M. Walker

18-2 AN ALTERNATIVE TO THE APPENDIX-J METHOD FOR CALCULATING OXIDANT- AND NO_2- RELATED CONTROL REQUIREMENTS 871
B. Dimitriades

18-3 COMBINED USE OF MODELING TECHNIQUES AND SMOG CHAMBER DATA TO DERIVE OZONE-PRECURSOR RELATIONSHIPS 881
M.C. Dodge

18-4 OUTDOOR SMOG CHAMBER STUDIES: EFFECT OF DIURNAL LIGHT DILUTION AND CONTINUOUS EMISSION ON OXIDANT PRECURSOR RELATIONSHIPS 891
H.E. Jeffries, R. Kamens, D.L. Fox, and B. Dimitriades

18-5 USE OF TRAJECTORY ANALYSIS FOR DETERMINING EMPIRICAL RELATIONSHIPS AMONG AMBIENT OZONE LEVELS AND METEOROLOGICAL AND EMISSION VARIABLES 903
E.L. Meyer, Jr., W.D. Freas, III, J.E. Summerhays, and P.L. Youngblood

SESSION 19 - OXIDANT-PRECURSOR RELATIONSHIPS AND THEIR INTERPRETATION IN TERMS OF OPTIMUM STRATEGY FOR OXIDANT CONTROL - II 915
Chairman: E.L. Meyer

19-1 REPORT ON OXIDANTS AND THEIR PRECURSORS IN CANADA 917
L. Shenfeld

19-2 PRECURSOR CONCENTRATION AND OXIDANT FORMATION IN SYDNEY 927
G.H. Allen, K. Post, B.S. Haynes, and R.W. Bilger

19-3 SMOG POTENTIAL OF AMBIENT AIR, SAMPLED AT DELFT, NETHERLANDS: THE EFFECT OF INCREASING NO_x CONCENTRATION 943
J. van Ham, and H. Nieboer

19-4 SUMMARY: A PRELIMINARY INVESTIGATION OF EXPECTED VISIBILITY IMPROVEMENTS IN THE LOS ANGELES BASIN FROM OXIDANT PRECURSOR GASES AND PARTICULATE EMISSION CONTROLS 955
C.S. Burton, T.N. Jerskey, and S.D. Reynolds

SESSION 20 - CONTROL OF OXIDANT PRECURSOR EMISSIONS - I 969
Chairman: R.W. Bilger

20-1 TRAFFIC MANAGEMENT AS A MEANS OF OXIDANT PRECURSOR CONTROL FROM LOW-SPEED SATURATED TRAFFIC 971
R.B. Hamilton and H.C. Watson

20-3 CONTROL OF VEHICLE REFUELING EMISSIONS 989
A.M. Hochhauser and L.S. Bernstein

SESSION 21 - CONTROL OF OXIDANT PRECURSOR EMISSIONS - II 1001
Chairman: R.W. Bilger

21-1 NO_x CONTROL TECHNOLOGY FOR STATIONARY SOURCES 1003
G.B. Martin and J.S. Bowen

21-2 EMISSION ESTIMATES OF NO_2 AND ORGANIC COMPOUNDS FROM COAL-FIRED BED COMBUSTION 1015
P.E. Fennelly

21-3 EMISSIONS ASSESSMENT OF THE CHEMICALLY ACTIVE FLUID BED (CAFB) PROCESS 1025
A.S. Werner, R.M. Bradway, D.F. Durocher, S.L. Rakes, and R.M. Statnick

21-4 NO_x CONTROL BY ABSORPTION 1035
G. Sakash

21-5 DEVELOPMENT OF A LOW EMISSIONS PROCESS FOR ETHYLENE DICHLORIDE PRODUCTION 1039
W.S. Amato, B. Bandyopadhyay, B.E. Kurtz, and R.H. Fitch

SESSION 22 - AIR QUALITY AND EMISSION TRENDS 1051
Chairman: R.E. Neligan

22-1 THE IMPACT OF EMISSIONS CONTROL TECHNOLOGY ON PASSENGER CAR HYDROCARBON EMISSION RATES AND PATTERNS 1053
F. Black

22-2 CONTROL OF OXIDANTS IN SYDNEY 1069
D. Iverach and M.G. Mowle

22-3 OXIDANT AND PRECURSOR TRENDS IN THE METROPOLITAN 1077
LOS ANGELES REGION
J. Trijonis, T. Peng, G. McRae, and L. Lees

22-4 COMPARISON OF PAST AND PROJECTED TRENDS IN OXIDANT 1095
CONCENTRATIONS AND HYDROCARBON EMISSIONS
R.M. Angus, E.W. Finke, and J.H. Wilson

22-5 TRENDS IN AMBIENT LEVELS OF OXIDANT AND THEIR POSSIBLE 1103
UNDERLYING EXPLANATIONS
E.L. Martinez, N.C. Possiel, E.L. Meyer, L.G. Wayne,
K.W. Wilson, and C.L. Boyd

SESSION 23 - ON THE OZONE/OXIDANT CONTROL STRATEGY IN U.S. 1113
Chairman: A.B. Bromley

23-1 TRENDS IN PHOTOCHEMICAL OXIDANT CONTROL STRATEGY 1115
J. Padgett

23-2 PROBLEMS WITH CONVERTING STATE-OF-THE-ART PHOTOCHEMISTRY ... 1123
TO STATE LEVEL CONTROL STRATEGIES
W. Bonta and J. Paisie

23-3 OXIDANT CONTROL UNDER SECTION 110 OF THE CLEAN AIR ACT 1135
J.L. Pearson

23-4 OXIDANT CONTROL STRATEGY: RECENT DEVELOPMENTS 1143
B. Dimitriades

23-5 CONTROL REGULATIONS FOR STATIONARY SOURCES OF HYDROCARBONS . 1155
IN THE UNITED STATES
R.T. Walsh

PREPARED COMMENTS ON JAPANESE PHOTOCHEMICAL AIR QUALITY 1167
STANDARDS AND CONTROL STRATEGIES
Professor R. Kiyoura

ACKNOWLEDGMENT

The assistance of the Conference Program Committee members in organizing the technical program of the Conference is gratefully acknowledged. Program Committee members were: Dr. A.P. Altshuller, EPA, USA (Chairman); Dr. K.H. Becker, U. Bonn, Germany; Dr. R.W. Bilger, U. Sydney, Australia; Dr. J.C. Calvert, Ohio State U., USA; Dr. B. Dimitriades, EPA, USA; Mr. M. Feldstein, San Francisco, Calif., USA; Mr. D.R. Goodwin, EPA, USA; Dr. R. Guicherit, IGTNO, Netherlands; Dr. A.B. Bromley, OECD, France; Dr. M. Hashimoto, Environment Agency, Japan; Dr. J. Knelson, EPA, USA; Mr. R.E. Neligan, EPA, USA; Mr. J. Padgett, EPA, USA; Dr. J.M. Pitts, U. California, USA; Dr. R.A. Rasmussen, Washington State U., USA; and Mr. J.O. Smith, EPA, USA.

Conference arrangements were made by the Triangle Universities Consortium on Air Pollution, under the direction of Dr. Laurence Kornreich, through Research Grant #800916-0451.

SESSION 1

ANALYTICAL METHODS FOR OXIDANTS AND PRECURSORS - I

Chairman: K.H. Becker
University of Bonn

METHODOLOGY FOR STANDARDIZATION OF ATMOSPHERIC OZONE MEASUREMENTS

J. A. Hodgeson, E. E. Hughes, W. P. Schmidt, and A. M. Bass*

ABSTRACT

Preliminary intercomparisons have been made among several techniques for the calibration of atmospheric ozone monitors. These procedures include the 1 percent neutral buffered potassium iodide method; a modification of this method employing 0.1 molar boric acid rather than the phosphate buffer; a 3-meter double-beam ultraviolet photometer; and gas phase titration. The potassium iodide reagent with boric acid gave a more stable color development and much closer agreement with the ultraviolet measurements than that obtained with the neutral buffered reagent. Ozone calibration data with the 3-meter photometer agreed within 1 and 2 percent with gas phase titration and ultraviolet photometric ozone measurements respectively made at the Environmental Protection Agency facility in Research Triangle Park, North Carolina.

INTRODUCTION

Atmospheric ozone (O_3) monitors have normally been calibrated against manual idometric techniques. The Environmental Protection Agency (EPA) reference calibration procedure employs a 1 percent neutral buffered potassium iodide (NBKI) reagent (1). The accuracy and reproducibility of iodmetric calibration procedures have been the subject of controversy for several years. In a recent example which received considerable publicity, O_3 measurements in the city of Los Angeles were discovered to be consistently biased 30 percent lower than measurements in surrounding counties. Laboratory studies conclusively demonstrated that the cause of the bias was the use of two different iodometric calibration procedures (2). In data obtained earlier this year and not given here, simultaneous measurements were made by NBKI with two sets of samplers off a common manifold. One set of results obtained indicated higher levels than the other by 30 percent. By interchanging reagents and components the difference appeared to be attributable to an impinger effect.

Current activities of the National Bureau of Standards (NBS) have focused on the establishment of definitive methodologies for the accurate measurement of O_3 in the subpart per million range for the purpose of calibrating constant O_3 generators. Analytical techniques currently under study are the EPA refer-

*National Bureau of Standards, Washington, D.C.

ence method which is a modified iodometric procedure suggested by Flamm (3). The method employs boric acid (BA) rather than phosphate buffer to control pH. It measures O_3 by ultraviolet (UV) absorption with a 3-meter double-beam photometer (4), and by gas phase titration (GPT) of O_3 with known concentrations of nitric oxide (NO) (5). In this paper preliminary results of comparisons of these various O_3 calibration techniques are presented.

EXPERIMENTAL

Some exceptions were employed to the iodometric technique as described. Midget impingers were employed rather than the illustrated Mae West-type bubblers. We employed a calibrated wet test meter downstream of the impingers to determine the integrated volume of air sampled. This approach gives more accurate and reproducible measurements of sample volume and does not require fine flow control devices. Finally, we measured the absorbance at a fixed time of 5 minutes after ending sample collection, because of a slow color development observed in the NBKI reagent.

The wet test meter was calibrated gravimetrically by metering a fixed volume of air from a compressed air cylinder and measuring the weight loss of the cylinder with a Voland Precision Balance, Model 1115-DN. As an additional check during one of the experiments, the wet test meter measurement was compared with the volume measured by means of a soap bubble meter connected to the inlet of the sample probe. These measurements agreed within 1 percent.

The spectrophotometer employed was a Beckman Model DU with a Guilford Model 222 digital absorbance readout attachment. Checks on the photometric accuracy have been made with NBS optical glass filters which have certified absorbance values at specified wavelengths. This instrument has been periodically calibrated over several years with standard iodine solutions and has remained constant with an average calibration factor of 9.812 microliters of O_3 per absorbance unit. This value corresponds to an absorption coefficient at 352 nonometers (nm) for molecular iodine of 24,930 liters/mole·cm (log base 10). It compares favorably with a value of 24,890 $\pm$ 100 reported in another study (6).

The O_3 source was a variable photolytic generator (7). The clean air source was an Aadco Model 737 pure air generator. The reagents employed for the NBKI procedure were ACS reagent grade granular KI, potassium dihydrogen phosphate (KH_2PO_4) certified ACS grade, and anhydrous disodium hydrogen phosphate (Na_2HPO_4) analytical reagent. The boric acid modified reagent also contained 1 percent KI of the same grade and 0.1 molar boric acid ACS-CP grade. The spectrophotometer calibration curve showed no evidence of a measurable iodine demand for either of the reagents.

The primary UV photometer was a 3-meter double-beam instrument specifically constructed at NBS for the purpose of O_3 calibration in the subparts per million (ppm) range (4). The other UV system was a commercially available Dasibi Monitor Model 1003-AH. In work at NBS this instrument has been used primarily as a secondary transfer standard. The iodometric measurements and

the UV photometric measurements are currently measured in different laboratories at NBS. The Dasibi instrument was used as a transfer standard to relate O_3 measurements obtained in different laboratories. The GPT apparatus has been described previously (5).

RESULTS AND DISCUSSION

EVALUATION OF THE BORIC ACID – POTASSIUM IODIDE REAGENT

There has been considerable lack of interlaboratory reproducibility in application of the NBKI technique (8, 9). Paur (10) has summarized a number of recent studies in which the relationship of measurements by the NBKI technique was compared to measurements of O_3 by UV photometry or by GPT. The ratio of measurements by NBKI to O_3 measurements by either of these techniques has varied over a range from 1.0 to 1.2. One particular problem with this iodometric technique is the slow color development observed after the O_3 is collected. Variable results are thus obtained if the time of the absorbance measurement is not controlled.

Flamm (3) has recently performed an evaluation of iodometric techniques. He used different buffering systems and observed an absence of the slow color development either in the absence of a buffering agent or with the addition of 0.1 molar boric acid. The addition of 0.1 molar boric acid stabilizes the pH of the solution at approximately 5.3. With the boric acid-KI (BAKI) reagent, Flamm observed O_3 measurements which were 20% lower than those obtained with a NBKI reagent. Measurements with boric acid reagent were in essential agreement with a Dasibi O_3 photometer, modified such that O_3 measurements with GPT measurements are obtained (10).

We made a reagent as described by Flamm and studied the variation in absorbance after sample collection for both this reagent and the neutral NBKI reagent. The results of this study are shown in Figure 1. An O_3 sample of 0.35 ppm was collected for 10 minutes. The initial time in Figure 1 corresponds to the end of the sample collection. The color obtained with the BAKI reagent is indeed stable and the initial absorbance at 4 minutes is approximately 22 percent lower than that obtained in the NBKI reagent. The slow color development observed with the NBKI is apparently a result of a secondary reaction which slowly releases iodine.

Based on the results shown in Figure 1, O_3 measurements with the NBKI reagent are approximately 22 percent higher than with the boric acid modification, assuming that the absorption coefficient of iodine is the same in both reagents. The absorption coefficients of iodine in both reagents were measured, and the values obtained agreed within 1 percent. We observed a slow color development in the unexposed BAKI reagent (0.003 to 0.27 in a few days) when the absorbance was measured against distilled water as a reference. Therefore, in all our analyses the absorbance measurement was made against unexposed reagent as a blank.

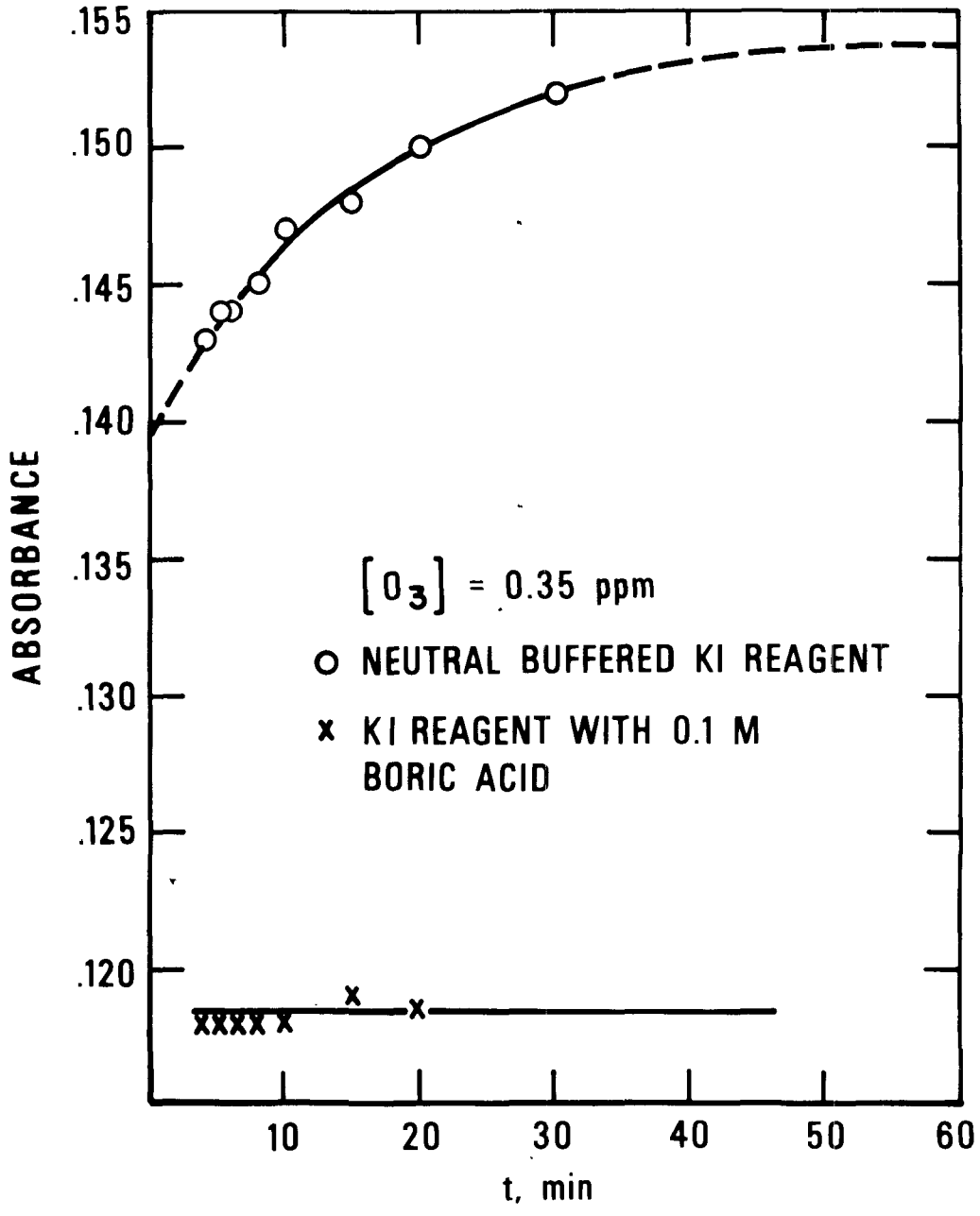

Figure 1. Absorbance versus time after sample collection.

COMPARATIVE OZONE MEASUREMENTS

We want to emphasize in the beginning that the comparative data obtained thus far are limited in number and that some of the absolute results reported here are preliminary in nature. However, in spite of the preliminary nature of these data, we present what has been obtained so far and feel that some interesting conclusions can be drawn therefrom.

The method for making the comparative measurements between different laboratories was to use the Dasibi instrument as a transfer standard. In this role the instrument has performed remarkably well in that it has maintained essentially the same calibration with respect to iodmetric measurements in the same laboratory over the past two years.

In the first comparisons given below, the Dasibi instrument was calibrated with both KI reagents. In these comparative data the Dasibi meter readings were converted to UV photometric O_3 concentrations by Equation 1. The physical path length (71 cm) of the Dasibi is assumed to be the same as the otpical path length. Also, the gas temperature inside the optical cell is assumed to be the same as the measured temperature adjacent to the cell in the instrument.

$$[O_3]_{DAS} = \frac{10^6 P_o T}{kLPT_o} \ln(I_o/I_o - \Delta I) \qquad (1)$$

where: $k = 308.6\ cm^{-1}\ atm^{-1}$ (log base e), the 253.7 nm O_3 absorption coefficient at 273 K and 1 atmosphere.

L = 71 cm, the physical path length

P_o, T_o = 1 atm and 273 K

I_o = Dasibi Span Factor

ΔI = Dasibi Meter Reading

By substituting the above values, Equation 2 reduces to

$$[O_3]_{DAS} = \frac{127T}{P} \ln(I_o/I_o - \Delta I) \ , \qquad (2)$$

where T is the temperature inside the optical cell in kelvins and P is the barometric pressure in mm mercury (Hg). For all the data in Table 1, the value used for T (313 K) was approximately the average temperature of the optical cells with the instrument in continuous operation.

The comparative data obtained are given in Table 1. The two idometric reagents were used sequentially at the same O_3 concentration and in the same sampling apparatus.

Ozone concentrations measured by the NBKI technique, $[O_3]_{NBKI}$, and O_3 concentrations measured by the boric acid version, $[O_3]_{BAKI}$, were both fitted to the O_3 Dasibi measurements by linear regression analysis.

$$[O_3]_{NBKI} = (1.35 \pm 0.01)\ [O_3]_{DAS} - (0.0015 \pm 0.003) \qquad (3)$$

$$[O_3]_{BAKI} = (1.10 \pm 0.01)\ [O_3]_{DAS} + (0.001 \pm 0.003) \qquad (4)$$

An excellent fit was obtained in both cases with no observable deviation from linearity over the range of concentrations measured. The zero intercepts are negligible. The relation between the two iodometric techniques is:

TABLE 1. CALIBRATION OF NBS-DASIBI BY IODOMETRIC METHODS

Date	$[O_3]_{DAS}$, ppm	Neutral Buffered KI, ppm	Boric Acid KI, ppm
8-19-76	.289	.383	.308
	.1725	.227	.181
	.4955	.668	.540
8-20-76	.094	.128	.108
	.233	.313	.263
	.378	.513	.422
	.130	.176	---
8-28-76	.256	.345	.285
	.3415	.458	.380
	.343	----	.379
	.462	----	.507
	.201	----	.225
	.136	----	.153
8-31-76	.476	----	.520
	.043	----	.046
	.119	----	.132
	.220	----	.241
	.323		.354
	.413		.462
	.412		.461

$$[O_3]_{NBKI} = (1.23 \pm 0.03)\ [O_3]_{BAKI} \qquad (5)$$

Flamm (3) observed a value of 1.20 for the ratio of NB to BA iodometric measurements.

On days intervening with those on which iodometric measurements were made, the Dasibi was calibrated against the NBS 3-meter double beam photometer. Multiple analyses were made at several concentrations and the averaged data are presented in Table 2.

TABLE 2. CALIBRATION OF DASIBI WITH NBS 3-METER PHOTOMETER

$[O_3]$ DAS, ppm	$[O_3]$ UV, ppm
.02531	.02157
.0989	.1001
.1695	.1733
.2999	.3006
.3578	.3688
.5192	.5265
.5193	.5245
.5238	.5372
1.0010	1.0275
1.4813	1.5045

A linear regression analysis of these data yielded,

$$[O_3]_{UV} = (1.020 \pm 0.004)\ [O_3]_{DAS} - (0.001 \pm 0.002) \qquad (6)$$

This fit also showed good linearity with a negligible intercept. By combining Equation 6 with the previous results, the following relations were obtained:

$$[O_3]_{NBKI} = (1.32 \pm 0.02)\ [O_3]_{UV} \qquad (7)$$

$$[O_3]_{BAKI} = (1.08 \pm 0.02)\ [O_3]_{UV} \qquad (8)$$

In order to obtain additional comparative data, the NBS Dasibi instrument was transported to EPA's Research Triangle Park facility. Simultaneous O_3 comparisons were made at the EPA Environmental Monitoring and Support Laboratory, where concurrent evaluations of the GPT method and a modified Dasibi photometer (10) were being performed. The comparison was made on a single date (8/24/76) using a common O_3 sampling manifold. The O_3 generator was calibrated at several fixed levels by GPT, and simultaneous measurements were made at these same levels with the NBS Dasibi and the modified EPA Dasibi photometer. The data obtained are given in Table 3.

The NBS Dasibi O_3 readings in the first column were corrected to equivalent O_3 measurements with the NBS 3-meter photometer by Equation 6. Analysis of the data yielded

$$[O_3]_{GPT}, \text{EPA} = (1.01 \pm 0.02)\ [O_3]_{UV}, \text{NBS} + (0.011 \pm 0.003) \qquad (9)$$

$$[O_3]_{UV}, \text{EPA} = (0.98 \pm 0.01)\ [O_3]_{UV}, \text{NBS} + (0.003 \pm 0.001) \qquad (10)$$

The agreement obtained on the whole was excellent among the three O_3 measurements, considering the limited time and data available during this one-day comparison.

TABLE 3. OZONE COMPARATIVE MEASUREMENTS AT EPA-RESEARCH TRIANGLE PARK

$[O_3]_{DAS}$, NBS,ppm	$[O_3]_{GPT}$, NBS,ppm	$[O_3]_{UV}$, EPA,ppm
0.053	0.061	0.056
0.125	0.142	0.127
0.203	0.223	0.205
0.285	0.309	0.290
0.371	0.390	0.374
0.456	0.481	0.459
0.619	---	0.620

SUMMARY AND CONCLUSIONS

The UV photometric measurements obtained at NBS agree within 1 and 2 percent using GPT and UV photometric measurements respectively obtained at EPA-Research Triangle Park. This is in accord with results obtained in other works (6, 10, 11). Additional comparative data will be obtained to attempt to reduce the small uncertainty remaining.

The 1 percent KI solution with 0.1 molar BA gives a stable color development. Measurements with this reagent are in closer agreement with UV photometric measurements than measurements obtained with the neutral phosphate buffered system. The BA iodometric measurements obtained here were 22 percent lower than measurements by NBKI and 8 percent higher than O_3 measurements obtained with the NBS 3-meter photometer.

We regard the absolute relations of either of the iodometric measurements to the UV photometric measurements as preliminary at this point and intend to obtain more data before reaching final conclusions. The iodometric measurements in relation to UV contradict to some degree other data which have been obtained. Flamm (3) and Paur (unpublished data) have observed closer agreement between the boric acid iodometric measurements and UV photometry. The NBKI results obtained were 35 percent higher than UV, which is outside of the 1.0-1.2 ratio range observed in other studies (10). An apparent impinger effect in analyses obtained by the NBKI procedure was noted in the introductory remarks. The impinger set used to obtain the data above was the set which apparently produced higher results. Impinger effects have been reported previously (9). Whether the impinger design or materials in fact affects the results, and whether an impinger effect applies to the BAKI reagent are questions to be answered by additional studies.

ACKNOWLEDGEMENT

The authors are particularly grateful to Mike Beard of the Quality Assurance Branch, Environmental Monitoring and Support Laboratory, EPA-Research Triangle Park for the assistance he provided in the O_3 comparisons by ultraviolet photometry and gas phase titration.

DISCLAIMER

Certain commercial equipment, instruments, or materials are identified in this paper in order to adequately specify the experimental procedure. In no case does such identification imply recommendation or endorsement by the National Bureau of Standards, nor does it imply that the material or equipment identified is necessarily the best available for the purpose.

REFERENCES

1. Environmental Protection Agency, Federal Register 36, No. 228, 22384 (November 25, 1971).

2. "Comparison of Oxidant Calibration Procedures," Final Report of Ad Hoc Oxidant Measurement Committee, California Air Resources Board, Sancramento, CA., 3 February 1975.

3. Daniel Flamm, preliminary report to the Environmental Sciences Research Laboratory, Environmental Protection Agency, Research Triangle Park, N.C., August 1976.

4. A. M. Bass, A. E. Ledford, Jr., and J. K. Whittaker, "Ultraviolet Photometer for Ozone Calibration," preprint for International Symposium on Photochemical Oxidant Pollution and Its Control, Raleigh, N.C., 12-17 September 1976.

5. K. A. Rehme, B. E. Martin, and J. A. Hodgeson, "Tentative Method for the Calibration of Nitric Oxide, Nitrogen Dioxide and Ozone Analyzers by Gas Phase Titration," EPA Report No. R2-73-246, U. S. Environmental Protection Agency, Office of Research and Development, Washington, D.C. 20460.

6. J. A. Hodgeson, C. B. Bennett, H. L. Kelly, and B. A. Mitchell, "Ozone Measurements by Iodometry, Ultraviolet Photometry and Gas-Phase Titration," publication preprint, submitted to Analytical Chemistry, 1976.

7. J. A. Hodgeson, R. K. Stevens, and B. E. Martin, ISA Trans. 11, 161 (1972).

8. J. B. Clements, "Summary Report: Workshop on Ozone Measurements by the Potassium Iodide Method," EPA-650-4-75-007, U. S. Environ-

mental Protection Agency, Office of Research and Development, Washington, D.C. 20460, February 1975.

9. H. C. McKee, R. E. Childers, and Van B. Parr, "Collaborative Study of Reference Method for Measurement of Photochemical Oxidants in the Atmosphere (Ozone-Ethylene Chemiluminescent Method), EPA-650/4-75-016, U. S. Environmental Protection Agency, Office of Research and Development, Washington, D.C. 20460, February 1975.

ULTRAVIOLET PHOTOMETER FOR OZONE CALIBRATION

A. M. Bass, A. E. Ledford, Jr., and J. K. Whittaker*

ABSTRACT

In order to provide a facility for photometric ozone measurements, we have designed and constructed a double-beam photometer for ozone concentrations in the range 0.025 - 1.0 ppm. The sample path length in this instrument is approximately 300 cm. The instrument measures changes in ozonized-air sample transmissions of mercury radiation at 253.7 nanometers where the photo-absorption cross-section of ozone has been well determined.

Radiation at wavelengths other than 253.7 nanometers from the mercury lamp is removed by passing the light through a narrow-band interference filter. The light is collimated and passed through a beam splitter which directs approximately equal intensity beams through the two cells. Clean air flows through one cell into the ozone generator and then the ozonized air flows through the second cell. The light beams are recombined on the face of a photomultiplier tube used in the photon counting mode. A rotating chopper allows the two beams to be detected sequentially so that the transmissions of the two cells may be directly observed.

Tests indicate that measurements may be made at the 0.05 ppm level with a precision of 10% or better.

INTRODUCTION

The oxidation of iodide to iodine by ozone (O_3), in a properly prepared solution of potassium iodide (KI), is the basis for the reference method specified by the Environmental Protection Agency (EPA) for the calibration of atmospheric monitors (1). Recent comparative measurements (2) of the specific iodometric methods have raised serious doubts as to the accuracy and reproducibility of iodometric calibration procedures. The report of the California Air Resources Board recommended that oxidant analyzers in California should be calibrated by an ultraviolet (UV) photometric method rather than by the iodometric method (2). In May 1975 this recommendation was accepted for that state's monitoring network. At the present time the EPA is considering two candidate methods, gas phase titration (GPT) and UV photometry as replacements for the 1% neutral-buffered potassium iodide (NBKI) procedure, the current Federal Reference Method for calibration of pollutant monitors (1).

In order to provide a facility at NBS for the measurement of O_3 concentrations, independently of GPT based on a nitric oxide (NO) standard, an ultra-

*National Bureau of Standards, Washington, DC

violet photometer with the desired sensitivity for O_3 measurements at ambient concentrations was set up (3). The desired performance for the photometer was capability for measurement of O_3 concentrations over the range 0.05 $\sim$ 1.0 parts per million (ppm) with an accuracy of approximately 0.005 ppm over the entire range.

EXPERIMENTAL

The photometric measurement method is based on the application and the validity of the Beer-Lambert Law:

$$I = I_o \exp\left(\frac{-273\ cPkL}{10^6 T}\right) \qquad (1)$$

where:

- c is given in ppm (parts per million by volume).
- k is 308.5 $cm^{-1}atm^{-1}$ (log base e), the ozone absorption coefficient (4) at 253.7 nm, 273 K, and 1 atmosphere.
- L is the path length, cm.
- P is the total pressure, atm.
- T is the temperature of the cell, ^oK.
- I/I_o is the transmittance (Tr) of the sample.

The design of the photometer is based principally on the accuracy requirement, 10% at 0.05 ppm. The quantities k, L, P, T appearing in the equation are all known or can be measured to within 1 or 2 percent. Thus the accuracy of the concentration measurement is mainly determined by the accuracy of the transmittance measurement. The error in the transmittance measurement may be expressed as

$$\frac{\Delta c}{c} = \frac{\Delta Tr}{Tr} \times \frac{1}{\ell n Tr} \cdot \qquad (2)$$

It was estimated that the transmittance measurement could be made with a precision $\left(\frac{\Delta Tr}{Tr}\right)$ of about .0005 by using photon counting. For a concentration of 0.05 ppm these conditions imply a transmittance of 0.995 which can be achieved in an absorbing path of approximately 3 m.

The design that was selected for the photometer is shown in Figure 1. It was decided that a double-beam arrangement would provide greater precision in the measurement through elimination of the effect of variability of the UV source. The cells of the photometer are made of 1-1/2" diameter pyrex pipe; teflon gaskets are used to make vacuum-tight seals for the fused silica windows. The light from a low pressure mercury discharge lamp is passed through a narrow-band interference filter in order to isolate the 253.7 nanometers (nm) emission line. The light is collimated by a fused silica lens and passed through a partially-transmitting neutral density filter which serves as a beam splitter. The two beams then pass through the two absorption cells. Adjustable aperture stops limit the diameter of the beams to ensure that there are no reflections from inner walls of the cells. The light beams emerge from the cells and are recombined on the face of a photomultiplier tube by another partially reflecting filter.

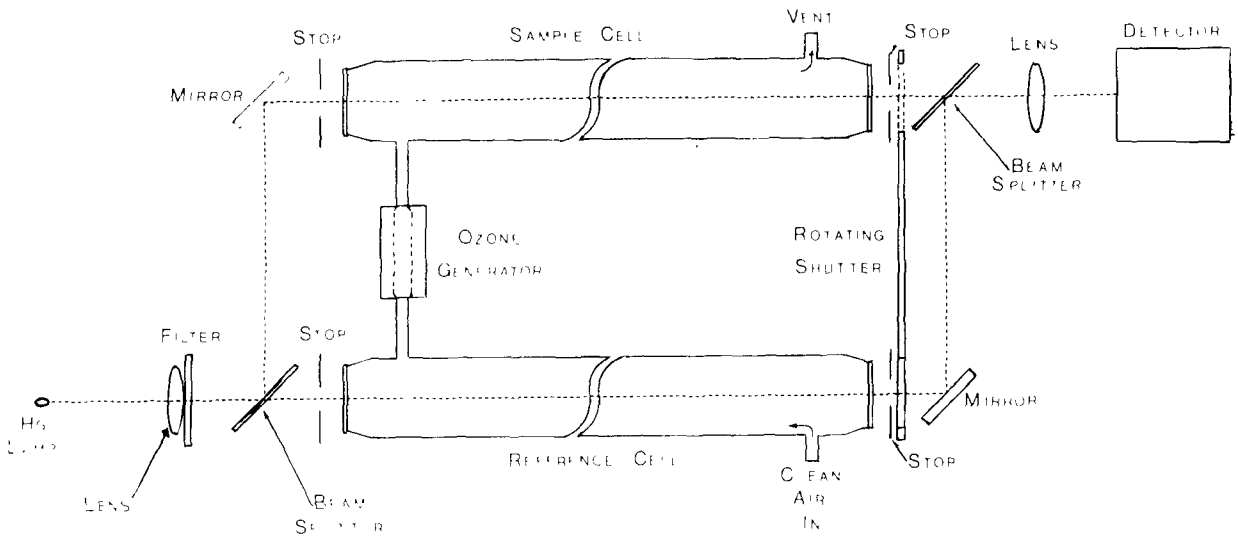

Figure 1. Double beam ultraviolet photometer for measurement of ozone concentrations.

The differential UV absorption method of photometry adopted for O_3 concentration measurements requires the precise and accurate measurement of two light intensities--one for each cell. Photon counting techniques for these intensity measurements using a UV sensitive tube with excellent single photoelectron resolution were used. If such a tube is cooled to about -20°C, the dark count rate is a few counts per second. Utilizing high-speed electronics and very precise timing methods it is possible to obtain accurate and statistically well-characterized pulse counts corresponding to incident light intensity on the photomultiplier. This method may be preferable to analog techniques which are more subject to instability, drift, and uncertain amounts of non-linearity.

The mercury vapor lamp is energized either by a 10 KHz square-wave power oscillator or by a 60 Hz commercial power supply. Light passing through each sample cell is alternately allowed to fall on the photomultiplier by means of a light chopper. A chopper blade with a single hole is driven by a hysteresis synchronous motor at a preselected rate (approximately 23 Hz) chosen to be unrelated to any harmonic or subharmonic of the line frequency. Light emitting diode-phototransistor pairs are used to sense the position of the hole in the chopper; the signal from the phototransistor triggers a discriminator to start the timing and counting cycle for each sample tube.

A logic system, triggered by the discriminators, controls the pulse counters associated with each sample tube. In order to ensure precise counting time as the photomultiplier is exposed to each tube, an electronic gate is used to ensure that the photomultiplier is fully (and not merely partly) exposed to the light beam passing through the sample.

The photomultiplier tube which must be selected for gain, low dark count rate and, most importantly, negligible afterpulsing, detects the photons as they

arrive. This type of tube, with outstandingly good single photon resolution, is essential for this measurement.

The pulse output from the photomultiplier is amplified 100 times by direct-coupled amplifiers and the pulses are detected by a high-speed pulse amplifitude discriminator. Pulse counting is performed by convential 100 MHz pulse counters and a rough guide of overall pulse rate is provided by a rate meter.

Counting time is determined by a preset counter which counts the revolutions of the chopper blade past the light-emitting diode (LED) phototransistor pairs. At the end of a counting interval, the results are printed out and the sequence repeats.

House air, dried and filtered, flows through one cell (reference cell), then into an O_3 generator (5) from which ozonized air flows through the second cell (sample cell). The measurement is made by comparing the ratio of the signals transmitted by the two cells in the presence and in the absence of O_3. This procedure provides the transmittance ($Tr = \frac{I}{I_o}$), and the O_3 concentration is determined by application of the Beer-Lambert Law, as discussed above. Since the mercury lamp is viewed, nearly simultaneously, through both cells, fluctuations in lamp intensity do not affect the measurement. Any impurities present in the air stream are observed in both cells and do not interfere with O_3 determination.

RESULTS

The performance of the photometer has been determined over the O_3 concentration range 0.020 to 1.500 ppm. At each of the measured concentrations the standard deviation was of the order of 0.005 ppm or less. A comparison of the photometric measurements with those obtained by the iodometric and GPT methods is presented at this Conference in the paper by J. A. Hodgeson, et al. (6).

REFERENCES

1. "Reference Method for the Measurement of Photochemical Oxidants Corrected for Interferences due to Nitrogen Oxides and Sulfur Dioxide," Federal Register 36, 8195-8197 (30 April 1971).

2. (a) "Comparison of Oxidant Calibration Procedures," report of the Ad Hoc Oxidant Measurement Committee of the California Air Resources Board, Sacramento, CA (20 Feb. 1974).

   (b) "Interagency Comparison of Iodometric Methods for Ozone Determination," W. B. DeMore, J. C. Romanovsky, M. Feldstein, W. J. Hamming, and P. K. Mueller, in "Calibration in Air Monitoring," ASTM Special Tech. Publ. 598, pp. 131-143 (Philadelphia, 1976).

3. J. B. Clements, "Summary Report: Workshop on Ozone Measurements by the Potassium Iodide Method," EPA-650/4-75-007, U. S. Environmental Protection Agency, Washington, D. C. 20460, February 1975, 36 pp.

4. The value of k used in this work (308.5 $cm^{-1}atm^{-1}$) is based on an evaluation by R. Hampson and D. Garvin of measurements reported in the published literature:

(a) Inn, E. C. Y. and Y. Tanaka, J. Opt. Soc. Am. 43, 870 (1953).

(b) Hearn, A. G., Proc. Phys. Soc. 78, 932 (1961).

(c) DeMore, W. B. and O. Raper, J. Phys. Chem. 68, 412 (1964).

(d) Griggs, M., J. Chem. Phys. 49, 857 (1968).

(e) Simons, J. W., R. J. Paur, H. A. Webster and E. J. Bair, J. Chem. Phys. 59, 1203 (1973).

(f) Becker, K. H., U. Schurath, and H. Seitz, Int. J. Chem. Kinet. 6, 725 (1974).

5. Hodgeson, J. A., R. K. Stevens, and B. E. Martin, ISA Trans. 11, 161 (1972).

6. Hodgeson, J. A., E. E. Hughes, and A. M. Bass, "Methodology for Standardization of Atmospheric Ozone Measurements," preprint for International Symposium on Photochemical Oxidant Pollution and its Control, Raleigh, NC, 12-17 September 1976.

HYDROCARBON AND HALOCARBON MEASUREMENTS: SAMPLING AND ANALYSIS PROCEDURES

R. B. Denyszyn, L. T. Hackworth, P. M. Grohse, and D. E. Wagoner*

ABSTRACT

During the summer and fall of 1975 approximately 3000 hydrocarbon, 500 halocarbon, and 200 heterocyclic analyses were performed in the atmospheric chemistry laboratory of the Research Triangle Institute. During this period various quality control procedures were developed to evaluate the sampling and analytical methods used to determine concentrations of various hydrocarbon and halocarbon species in ambient air as well as in smog chamber samples. Tests were performed on: (a) the stability of hydrocarbons in Teflon sampling bags; (b) permeation of hydrocarbon and halocarbons into Tedlar bags; (c) the stability of zero air and standard samples in Tedlar bags being shipped between the field and the laboratory, and (d) the accuracy of calibration.

Results of these investigations indicate the following:

- *C_2-C_5-hydrocarbons analyses at the 1-10 ppb level can be measured to a bias of 5% with 5% relative standard deviation.*
- *At concentrations of >10 ppb, C_2-C_5-hydrocarbons measurements, 2% relative standard deviation can be achieved.*
- *The relative standard deviation of Freon 11 measurements at the Research Triangle Institute are presently 3%.*
- *The stability of both reactive and unreactive hydrocarbons at the 1-10 ppb concentration range was evaluated in Tedlar bags in the dark for a 2-week period.*
- *Selected hydrocarbons and heterocyclic compounds exhibit excellent stability in Teflon bags in the dark.*
- *Contamination of Tedlar bags filled with hydrocarbon-free air is virtually negligible for hydrocarbon and some halocarbons up to 8 days.*

INTRODUCTION

During the summer and fall of 1975 approximately 3000 hydrocarbon, 500

*Research Triangle Institute, Research Triangle Park, North Carolina.

halocarbon, and 200 heterocyclic analyses were performed in the atmospheric chemistry laboratory at Research Triangle Institute (RTI). Both ambient air and smog chamber samples were included. In order to establish the credibility of these analyses quality control (QC) procedures were developed that have established the accuracy and precision of the procedures. These QC procedures have also lead to improvement in the sampling and analytical techniques.

Accuracy (bias) and precision (relative standard deviation) in hydrocarbon measurements result from attention to four parts of the measurement procedures: sampling analysis, instrument calibration, sample collection, and personnel training. If optimum procedures are applied, gas samples containing hydrocarbons or halocarbons are stable enough to allow remote analysis; measurement errors can be avoided; and a relative standard deviation of 2 percent is possible in the 10-100 ppb concentration range. If any of the critical procedures are not followed, this precision is degraded.

ANALYSIS PROCEDURES

Analysis is performed with a modified gas chromatograph (GC), the selection of which is of critical importance. A suitable GC must have detectors and signal processing electronics with proven long-term stability and must be sufficiently rugged to hold up under the rigors of continuous repetitive analysis. It is advantageous that the GC have an interface for direct coupling to a data processing computer. Additionally, the GC columns should be selected for low bleed since ambient air analysis requires the maximum detectability. The elution peaks should be well separated in order to provide maximum information from the analysis.

The specific GC employed for the hydrocarbon halocarbon analysis was the Perkin-Elmer Model 900 with dual flame ionization detectors (FID) and two electrometers. The controls were modified to allow independent operation of the detectors so as to facilitate rapid adjustment for analyses that require different flow rates and column temperatures. The valving system shown schematically in Figure 1 was built to allow the introduction of cryogenically trapped samples into the GC. Flexibility of the sample injection system is such as to accommodate samples with both ppm and ppb concentrations. This flexibility is achieved by replacing the secondary trap (liquid nitrogen trap) with a sample loop. The GC electronics interfaces with a Hewlett Packard 3352B data system.

Since hydrocarbon concentrations in ambient air are much too low for detection with direct injection gas chromatography, sample concentration is required. Concentration is usually accomplished for lower molecular weight compounds with cryogenic traps although the choice of cryogen varies among laboratories. The primary requirement of the concentration procedure is that it be quantitative--recovery must closely approximate to 100 percent.

In order to avoid the condensation of oxygen that occurs in a liquid nitrogen trap, liquid oxygen, which boils at a higher temperature than liquid nitrogen was used in our traps. The collection efficiency of the liquid oxygen traps was evaluated by testing them with ethylene and propane. When ethylene in

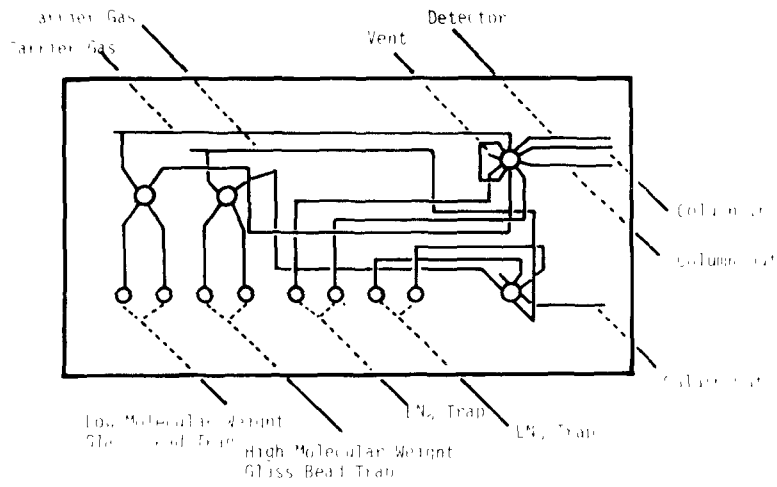

Figure 1. Valving for thermally controlled injection system.

air was passed through two traps in series, the first trap gave 4.0 ppb in subsequent analysis while the second trap gave 0.3 ppb. This indicates a collection efficiency of 93 percent for ethylene and, therefore, much better efficiences for compounds with higher boiling temperatures. In a similar experiment with propane, a collection efficiency of greater than 99 percent was obtained. Collection efficiences decreased at flow rates above 100 mℓ/min and with total sample volumes in excess of 500 mℓ as seen in Figure 2.

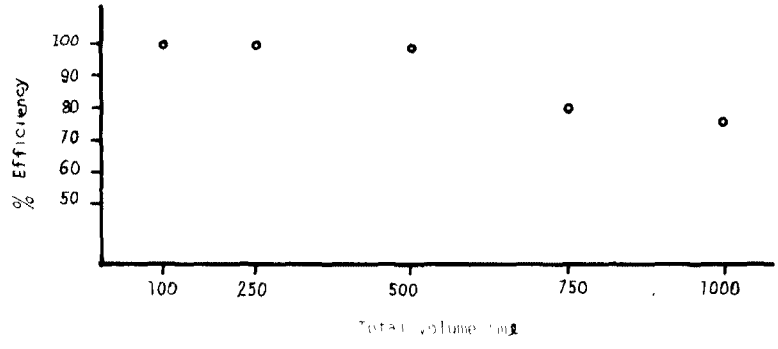

Figure 2. Dependence of collection efficiency on volume of sample.

This sample concentration and analysis system was quantitative for C_2-C_{10} hydrocarbons when the above procedures were followed.

CALIBRATION

The accuracy and precision of the analytical step was determined with the complex permeation tube system shown in Figure 3. In this system, carrier and dilution air were catalytically cleaned of hydrocarbons and other pollutants and mixed with accurate concentrations of dopant gases over broad concentration ranges. Calibration gases were propylene and n-butane. Calibration was performed using a 180 cm x 0.32 cm outside diameter (OD) column packed with 100-120 mesh n-octane Durapak maintained at 19°C with a helium flow of 20 mℓ/min. Each concentration level was measured a minimum of four times.

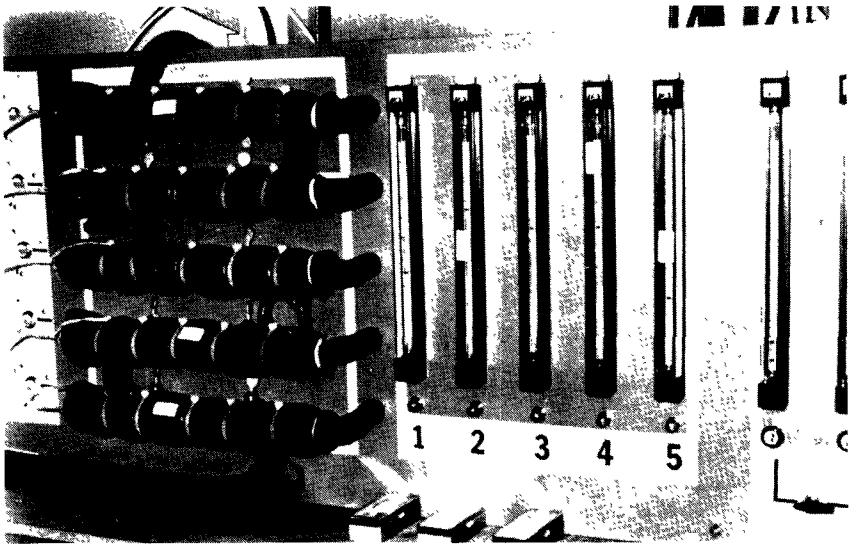

Figure 3. Permeation tube calibration system.

In these tests, a precision of 5 percent was obtained in measuring concentrations. As may be seen in Figure 4, the relative standard deviation appears to decrease with increasing concentration with a nearly linear dependence. The relative bias of the measurements plotted in Figure 5 showed no such dependence. The bias for propylene is positive and that for butane is negative; the average deviation is ±5 percent, respectively.

SAMPLE COLLECTION

Sample collection bags made of Teflon and Tedlar are commonly used in atmospheric chemistry. Their purported attributes include ease of handling, durability, chemical passivity, and low cost. Reported shortcomings include fragility, permeability, and the outgassing of various photolytic compounds by the polymeric materials of which the bags are made. Outgassing has been observed at RTI and at other laboratories.

While compounds in the C_2-C_5 molecular weight range mixed with air are stable in both Tedlar and Teflon bags, the more serious outgassing of Tedlar has led us to use Teflon bags for samples containing high molecular weight hydrocarbons, heterocyclics, and sulfur-containing compounds such as dimethyl sulfide and thiophene.

Several interesting phenomena that could result in errors have been observed in using Tedlar bags. Acetylene (in concentrations > 100 ppb) is absorbed by Tedlar and released when the bag is heated. If hydrocarbon mixtures are blended in oxygen-nitrogen mixtures obtained by liquid boil off rather than in catalytically cleaned air, the hydrocarbon concentration changes due to permeation of the bag by oxygen in establishing partial pressure equilibrium with the ambient air. Data indicating this activity are illustrated in Figure 6.

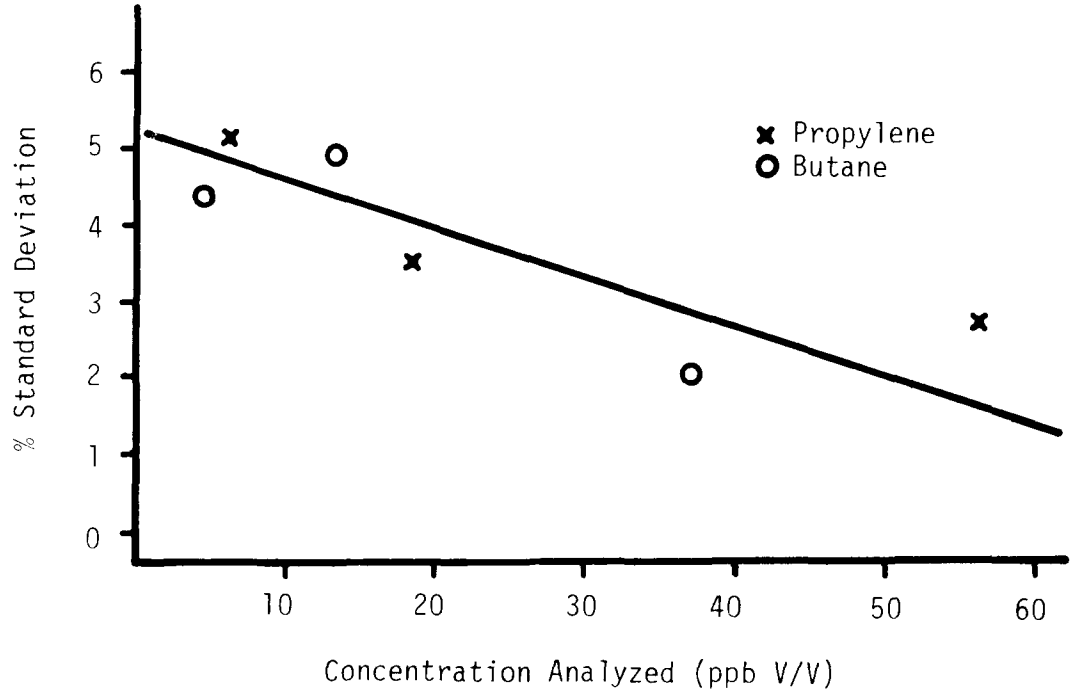

Figure 4. Precision and its relationship to concentration.

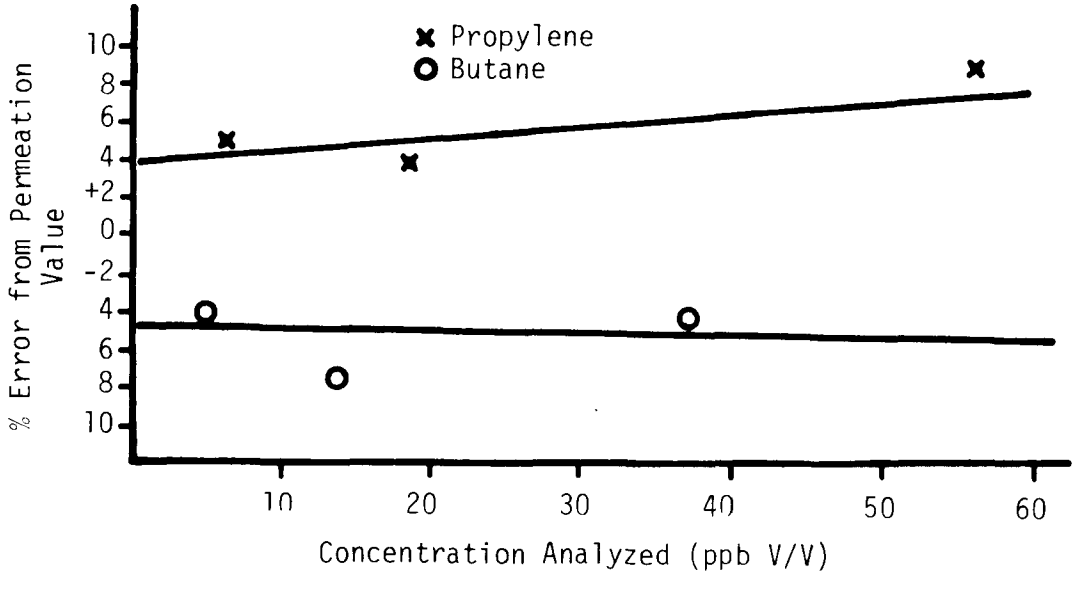

Figure 5. Bias and its relationship to concentration.

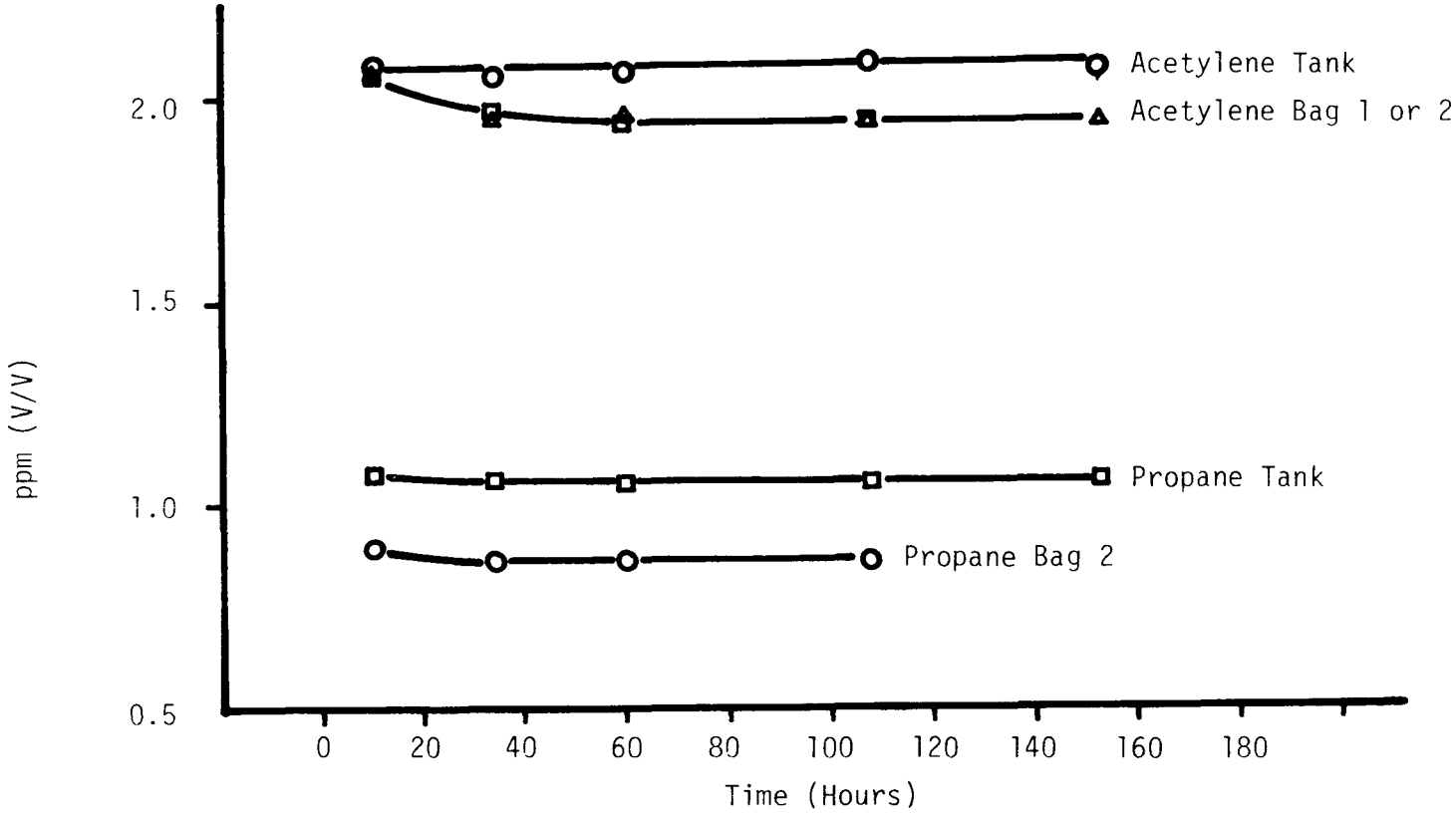

Figure 6. Instability of acetylene due to O_2/N_2 unbalance.

The stability without light of both reactive (trans-2-butene) and non-reactive (acetylene) hydrocarbon mixtures in Tedlar bags was tested for a 1-month interval. Filled Tedlar bags were stored in aluminum suitcases for periods of up to 23 days. Initial hydrocarbon concentrations were 70 ppb; after 23 days, the concentrations of trans-2-butene and acetylene were 62 ppb and 56 ppb, respectively; losses were 11 percent and 20 percent. In a test using acetylene and exposed to light, the data of Figure 7 were obtained. As shown, the average deviation is 6 percent from the mean concentration. For the 12 ppb sample used in this test, on the 5th, 6th, and 14th day the concentrations were 11.5, 11.0, and 14.0 ppb, respectively.

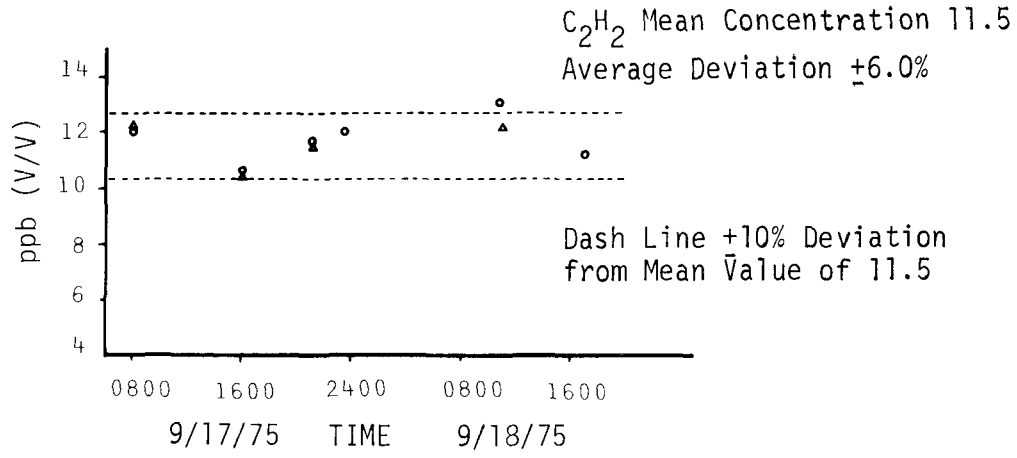

Figure 7. Stability of acetylene in Tedlar bags.

Additional stability tests were performed by exposing the sample bags to the contaminated transportation environment such as associated with a field collection program. Tedlar bags with control samples of hydrocarbon-free air were shipped by United Parcel Service and air freight to various sampling stations and then returned to the laboratory. Eight days of travel time lapsed. Test results are given in Table 1. In this test the bags were exposed to various temperatures and unusually high concentrations of hydrocarbons in the ambient air.

In contrast to hydrocarbons, halocarbon sampling is much more susceptible to contamination. In normal laboratory air the concentration of Freon 11 is several ppb so that even the fraction of a milliliter of laboratory air trapped in a Swagelock fitting may invalidate data in a sample. The permeation rates for 1,1,1-trichloroethane and tetrachloroethylene through Tedlar are much too high to use bags for sample collection. Stainless steel containers are used for halocarbon sampling by many research groups but their high cost is prohibitive for extensive sampling programs.

Aluminum sample containers (Altech Associates) appear to be excellent containers for sampling and storing both hydrocarbon and halocarbon samples. The results of a 1-month test of aluminum sample containers are given in Table 2. Both Freon 11 mixtures and undoped air were used. These aluminum cans have been found to be usable with heterocyclic compounds such as furan but serious wall interactions have been observed with sulfur compounds. The concentration of thiophene, for example, decreased 29 percent in 4 days. However their low

TABLE 1. STABILITY OF HYDROCARBON FREE AIR IN TEDLAR BAGS

Species	Bag Concentration ppb (V/V)	Cylinder Gas Concentration ppb (V/V)
ethane/ethylene	2.1	2.1
propane	0.4	0.4
propylene	0.1	0.1
acetylene	0.4	0.5
n-butane	N.D.	N.D.
butene-1	N.D.	N.D.
isobutane	N.D.	N.D.
isopentane	N.D.	N.D.
cyclopentane	N.D.	N.D.
n-pentane	0.0	N.D.
toluene	1.2	1.1
o-xylene	0.6	0.8
freon 11	13.5 ppt (V/V)	N.D.
CCl_4	N.D.	N.D.
trichloroethane	0.3	N.D.
tetrachloroethylene	<40.0	N.D.

N.D. = not detectable.

TABLE 2. FREON 11 IN ALUMINUM CANS

4-8-76	307 ppt	
4-9-76	300	4.0
4-22-76	304	
4-23-76	298	8.9
4-30-76	288	10.3
5-4-76	290	8.8
MEAN	298	8.0
S. DEV	7.5	2.8

cost, convenience in use, and stability for most compounds indicate that aluminum cans are generally excellent for sample collection.

Teflon bags are also recommended for sample collection. Wall interactions and permeation rates are low. However there is considerable variability in the quality of the bags. Some give off compounds that are detected with the FID and the electron capture detector. Because this outgassing varies with the batch, and is usually less than with Tedlar, it is necessary to condition Teflon bags with ozone and to analyze for background before being used for sampling. Table 3 gives data illustrating the excellent stability in the dark of various mixtures contained in Teflon bags.

PERSONNEL FACTORS

Training of personnel is important in operating a sampling program that is

TABLE 3. STABILITY OF VARIOUS COMPOUNDS IN TEFLON BAGS

	Net Loss After 3 Days
Dimethyl Sulfide	1%
Thiophene	5%
Dimethyl Disulfide	5%
Methyl Mercaptan	7%
Furan	14%
p-Xylene	14%
Pyrrole	23%

to obtain accurate and precise data. This training must include familiarization with GC and review of the various pitfalls that result in errors. Measurement of trace quantities of various atmospheric contaminants requires much attention to detail. Gas regulators with rubber diaphragms cannot deliver pure gases, small leaks will result in errors. Personnel must learn to discern bad from good data, and every phase of the measurement program must be given the required attention.

CONCLUSIONS

Hydrocarbon and halocarbon measurements can be made accurately and precisely if proper attention is given to the analysis procedures, calibration, sample collection, and personnel training. When this is done, C_2-C_5 hydrocarbons at < 10 ppb concentrations can be measured with a bias of 5 percent and a relative standard deviation of 5 percent. For concentrations above 10 ppb, the bias is the same but the relative standard deviation improves to 2 percent. Analysis of samples should be made within one week of collection and when possible, on-site analysis is preferable.

SESSION 2

ANALYTICAL METHODS FOR OXIDANTS AND PRECURSORS - II

Chairman: K.H. Becker
University of Bonn

A NEW CHEMILUMINESCENT OLEFIN DETECTOR FOR AMBIENT AIR

K. H. Becker, U. Schurath, and A. Wiese*

ABSTRACT

An instrument for continuous monitoring of reactive hydrocarbons in ambient air in the parts per billion concentration range is described. The new analytical method is based upon the chemiluminescent olefin – ozone reaction. The chemiluminescent olefin detector has been tested at ground level parallel to an automatic Gas Chromatograph, aboard an airplane, and as a detector adapted to a gas chromatographic column. Applications of the new instrument for air pollution control are discussed.

INTRODUCTION

In order to control photochemical oxidant precursors and their transport over long distances, there is an urgent need for a simple technique capable of measuring "reactive hydrocarbons" continuously, with high sensitivity, and good time resolution. The term "reactive hydrocarbons" is generally applied to the total amount of organic gaseous material, as measured by a Flame Ionization Detector (FID), less methane, which is considered unreactive in photochemical smog. It might, however, be more appropriate to measure the reactivity of the hydrocarbons towards ozone (O_3) to obtain an indicator of their smog forming potential. It has been shown in a number of field studies (1,2) in urban areas with unspecified emission sources that ethylene and propene are by far the most abundant unsaturated hydrocarbons which at the same time represent the most reactive organics with respect to photo-oxidant formation. Reactivity of organics is measured as rate constant times concentration. Saturated hydrocarbons, although most present at higher concentrations are less reactive. A suitable measure of the total olefin amount in ambient air may be that of the intensity of the chemiluminescent reaction with O_3, as measured in a "reversed" chemiluminescent O_3 analyzer which uses ozonized oxygen as reagent gas. The relative quantum yields of the most abundant olefins, ethylene and propene, could also be a good "weighing" factor of their relative reactivity as smog precursors.

The paper describes a rather simple chemiluminescent olefin detector which has been field tested as a continuous monitor of reactive hydrocarbons in ambient air at ground level, in parallel with an automatic Gas Chromatograph (GC) (Siemens U 180). Another version of the detector has been successfully used for olefin measurements in plumes aboard an airplane up to an

*Institut für Physikalische Chemie der Universität Bonn, Bonn, Germany.

altitude of 3000 meters. And the instrument was also adapted to a gas chromatographic column for the selective detection of unsaturated hydrocarbons. A similar technique has previously been used elsewhere (3). Part of the present work has previously been published (4,5).

EXPERIMENTAL

The construction and principle of operation of the chemiluminescent olefin detector are evident from the schematic diagram (Figure 1), which shows the version used for airborne measurements. Ozonized oxygen from a silent discharge ozonizer (2.5 liter/hour) and sample air (60 liter/hour) are drawn into a mixing chamber (volume 230 ml) by a small diaphragm pump which is protected against O_3 by an activated charcoal filter. A chamber pressure of 400-500 torr was found satisfactory. The mixing chamber is mounted in front of a photomultiplier tube (EMI-9635 QB) which, by its low quantum efficiency above 600Å, essentially eliminates interference by nitrogen oxide (NO) from its chemiluminescent reaction with O_3. The reaction chamber was drilled from solid teflon contained in a light-tight metal cylinder. Teflon has the advantage of an extremely good optical reflectivity at short wavelengths, thereby increasing the sensitivity of the detector.

The instrument was calibrated using a 425 liter evacuable glass cylinder as mixing chamber. The container was filled with ambient or pure synthetic air and spiked with the olefins by means of a precision gas syringe. Mixing was achieved by a built-in teflon fan.

To increase the long term stability of the detector background signal (photomultiplier dark current plus background chemiluminescence), the photomultiplier and reaction chamber could be thermostatized. This procedure was not necessary for shorter periods of operation, e.g., aboard an aircraft.

The sensitivity of the detector towards various olefins not only depends on the relative quantum yields of the chemiluminescent reactions, but also on the flow rate and total pressure in the chamber. Typical sensitivities, relative to ethylene taken as unity, were 2.5 for propene, 6.4 for trans-2-butene, 3.0 for cis-2-butene, and 4.4 for 1,3-butadiene.

To eliminate sensitivity changes due to relative humidity effects, an air filter filled with Sicapent (phosphorus pentoxide on a solid support) was found most satisfactory. The detector zero was checked at intervals by switching a molecular sieve filter of suitable pore size to eliminate olefins.

RESULTS

Our prototype chemiluminescent olefin detector for air analysis at ground level has been in continuous operation since May 1975. Maintenance amounts to changing the Sicapent filter every 5 days, and the ozonizer oxygen supply tank every 100 days.

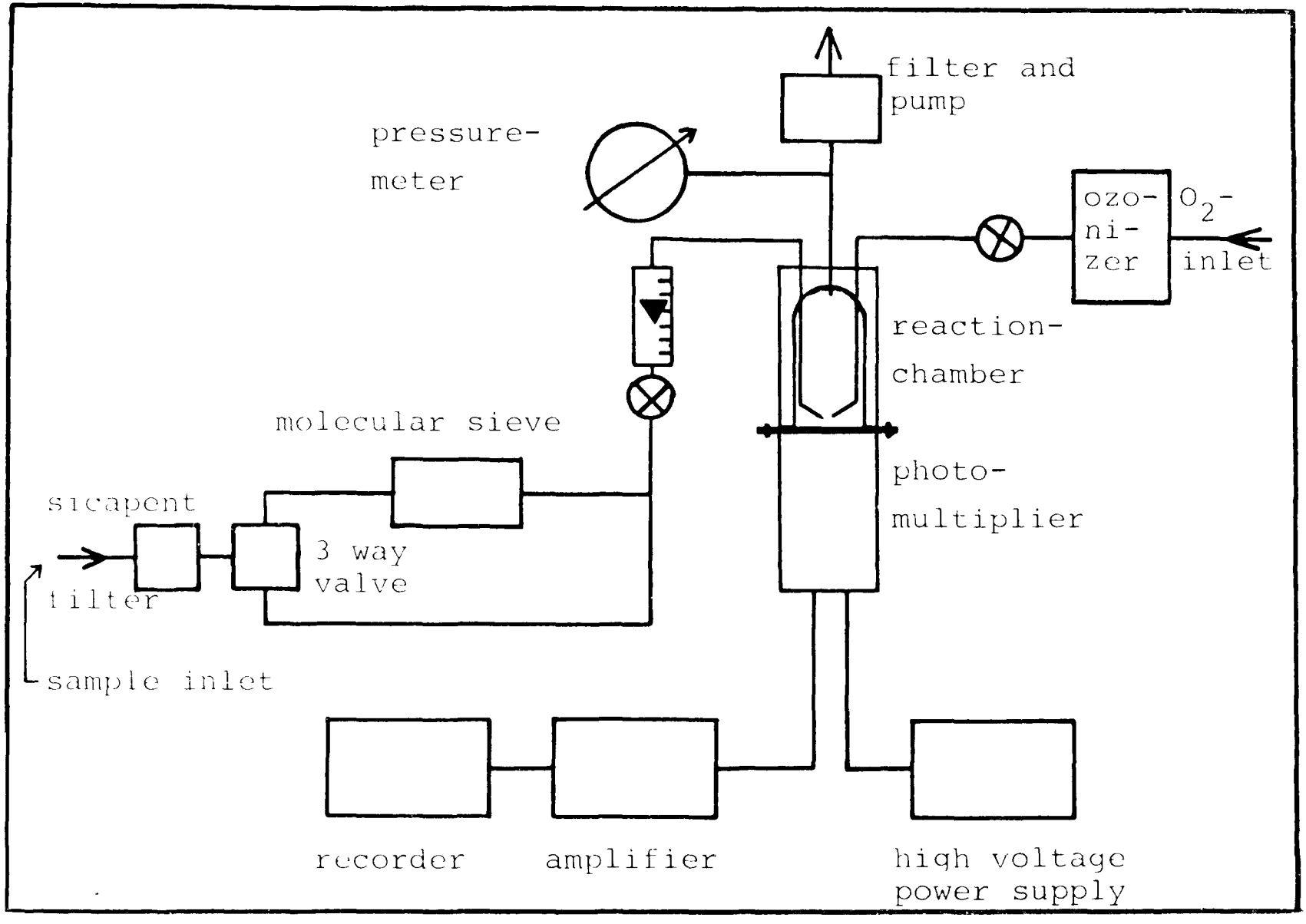

Figure 1. Schematic diagram of the chemiluminescent olefin detector.

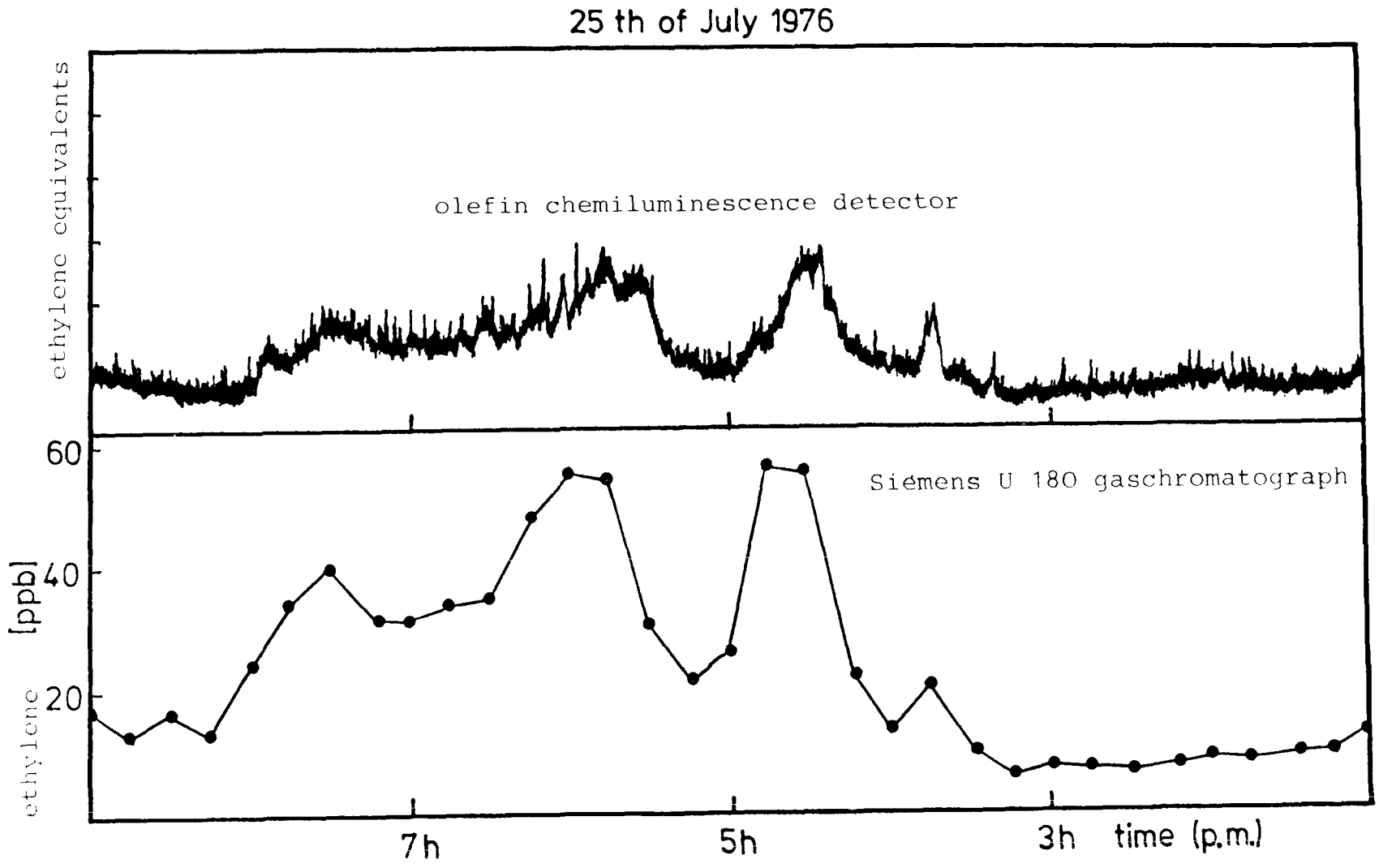

Figure 2. Ambient air analysis: Comparison of the chemiluminescent olefin detector signal with the ethylene concentration as measured by an automatic GC at 15 minute intervals.

An 8 hour recording by the detector is compared with the ethylene concentration as measured by a Siemens U 180 automatic GC (Figure 2). This GC performs a complete analysis every 15 minutes, averaging over 10 minutes by a preconcentration technique. The comparison shows a good correspondence between the detector output and the ethylene concentration which is by far the most abundant olefin in ambient air. The continuous recording shows fine structure of the concentration-time profile which is lost in the averaging process of the GC analysis. Interpretation of the chemiluminescent detector recordings is also much easier than would be an evaluation of the sometimes confusing information contained in a complete GC analysis of the light hydrocarbons every 15 minutes.

The high sensitivity and short time constant (about 3s) of the chemiluminescent olefin detector make it a valuable tool for continuous airborne measurements of reactive hydrocarbons. Figure 3 shows a recording obtained on a first test flight in the Cologne-Bonn area. The flight level was changed after passing over a lignite burning thermal power station from 4000 feet to 2600 feet (3800 to 2600 feet above ground). An extremely strong olefin signal corresponding to a maximum of 700 ppb ethylene equivalents was obtained above a petrochemical plant. It had been shown on a previous flight (6) under clear weather conditions that the O_3 concentration increased considerably above average about 20 km downwind of the petrochemical plant, at a flight level of 2500 feet. The effect was less pronounced at lower and higher altitudes.

The performance of the instrument as a GC detector is shown in Figures 4, 5, and 6. In this mode the GC column outflow is blended with 60 liter/hour of argon before analysis to reduce the residence time in the reaction chamber which was run at atmospheric pressure. Figure 4 compares analyses of identical mixtures of alkanes and olefins in synthetic air (concentrations of the order 50-100 ppm), as measured with a conventional FID, and with olefin detector. Peak-overlapping with alkanes is completely eliminated. Figure 5 shows the chemiluminescent detector response for car exhaust gas after separation on a GC column. Again, only the olefins are detected. Analysis of ambient olefins by GC with the new detector requires pre-concentration. A typical olefin analysis of ambient air is shown in Figure 6. It clearly corroborates our previous statement that ethylene and propene are a good measure of the total olefin content in ambient air under normal conditions.

CONCLUSIONS

It has been shown that unsaturated hydrocarbons can be measured continuously in ambient air and in smog chamber experiments (7) with this inexpensive rugged chemiluminescent detector. The output of the instrument is a useful measure of the total olefin content of the atmosphere, with weighing factors of 2.5 for propene, 6.4 for trans-2-butene, 3.0 for cis-2-butene, and 4.4 for 1,3-butadiene relative to ethylene as unity, taking account of the higher photochemical reactivity of the higher olefins. One version of the detector has been used successfully for airborne measurements of reactive hydrocarbons above an industrialized area with distinct sources of olefins. The instrument is also useful as a specific GC detector for unsaturated hydrocarbons which need not be separated from alkanes.

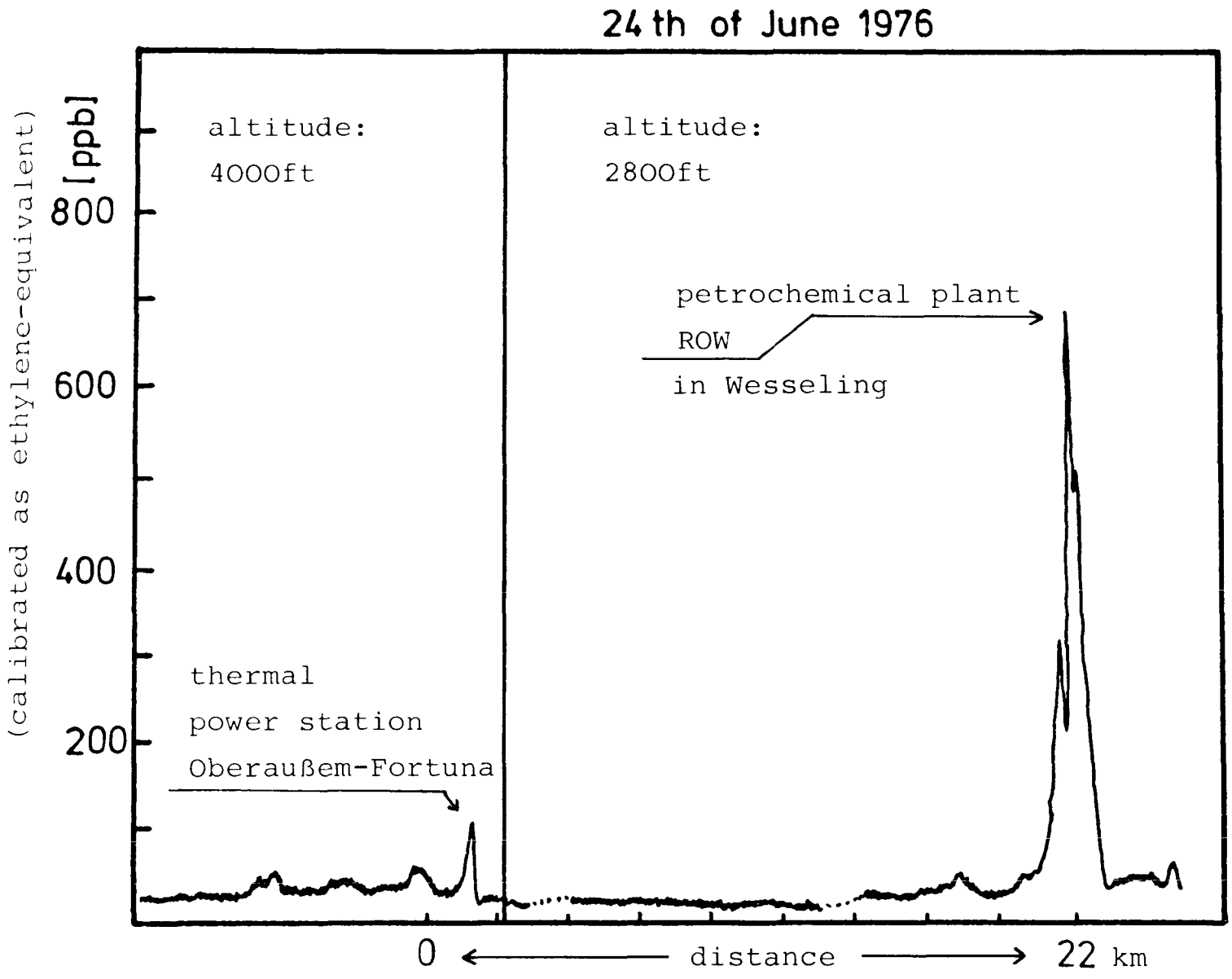

Figure 3. Airborne measurements of olefins with the chemiluminescent detector in the Cologne-Bonn area.

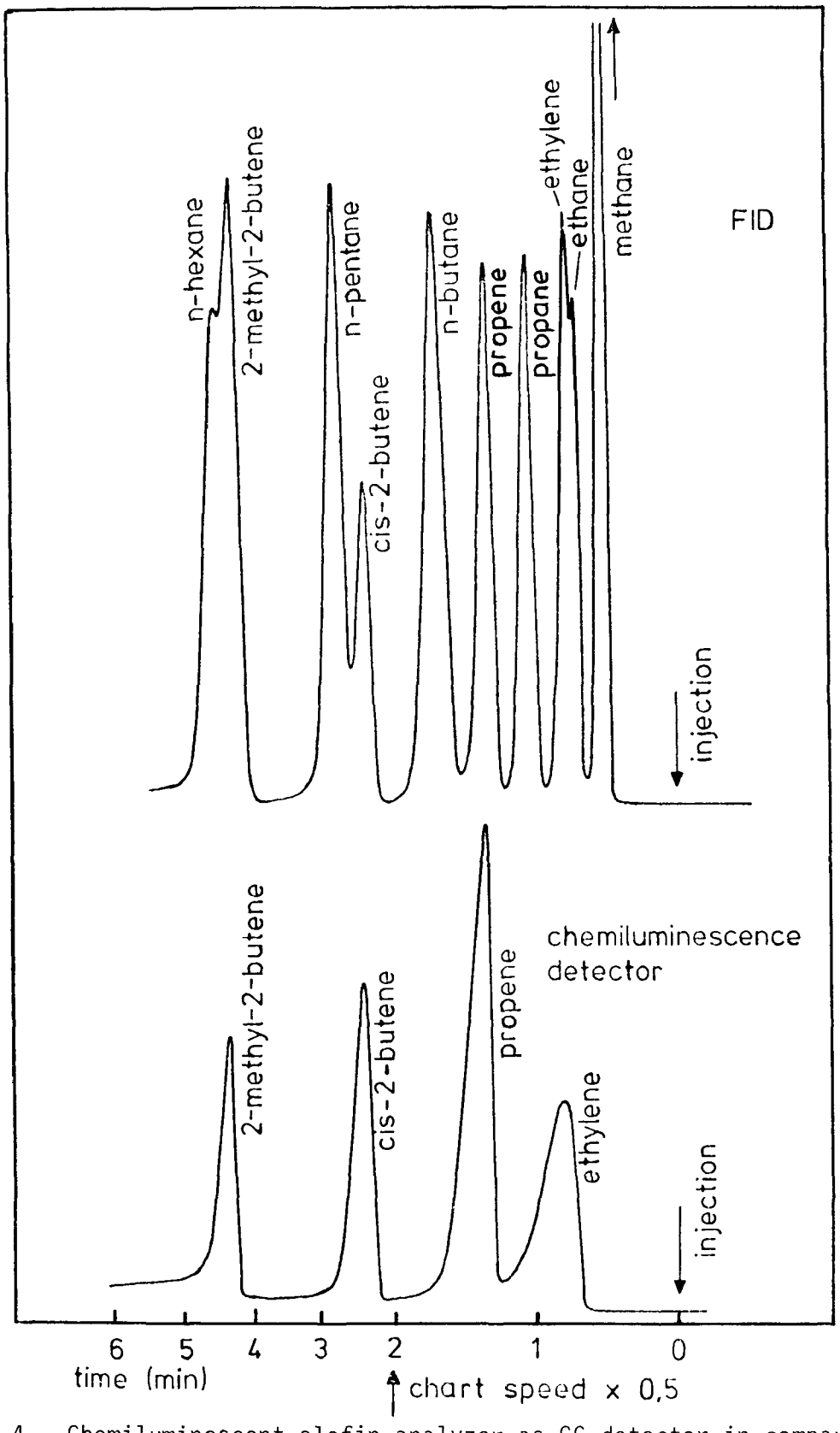

Figure 4. Chemiluminescent olefin analyzer as GC detector in comparison with an FID: Analysis of a synthetic air sample (olefin concentration in the 50 - 100 ppm range).

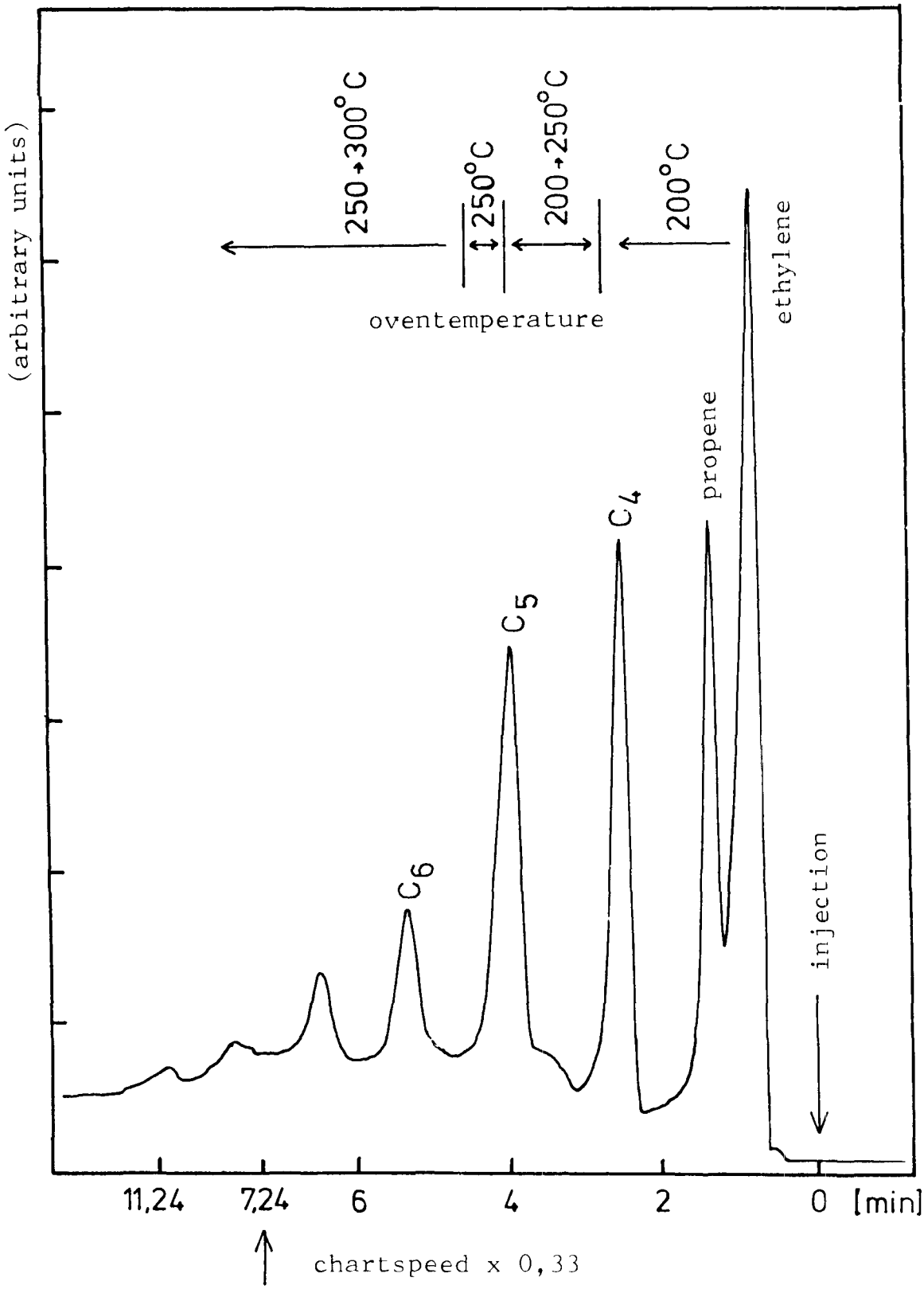

Figure 5. GC analysis of car exhaust by the chemiluminescent olefin detector.

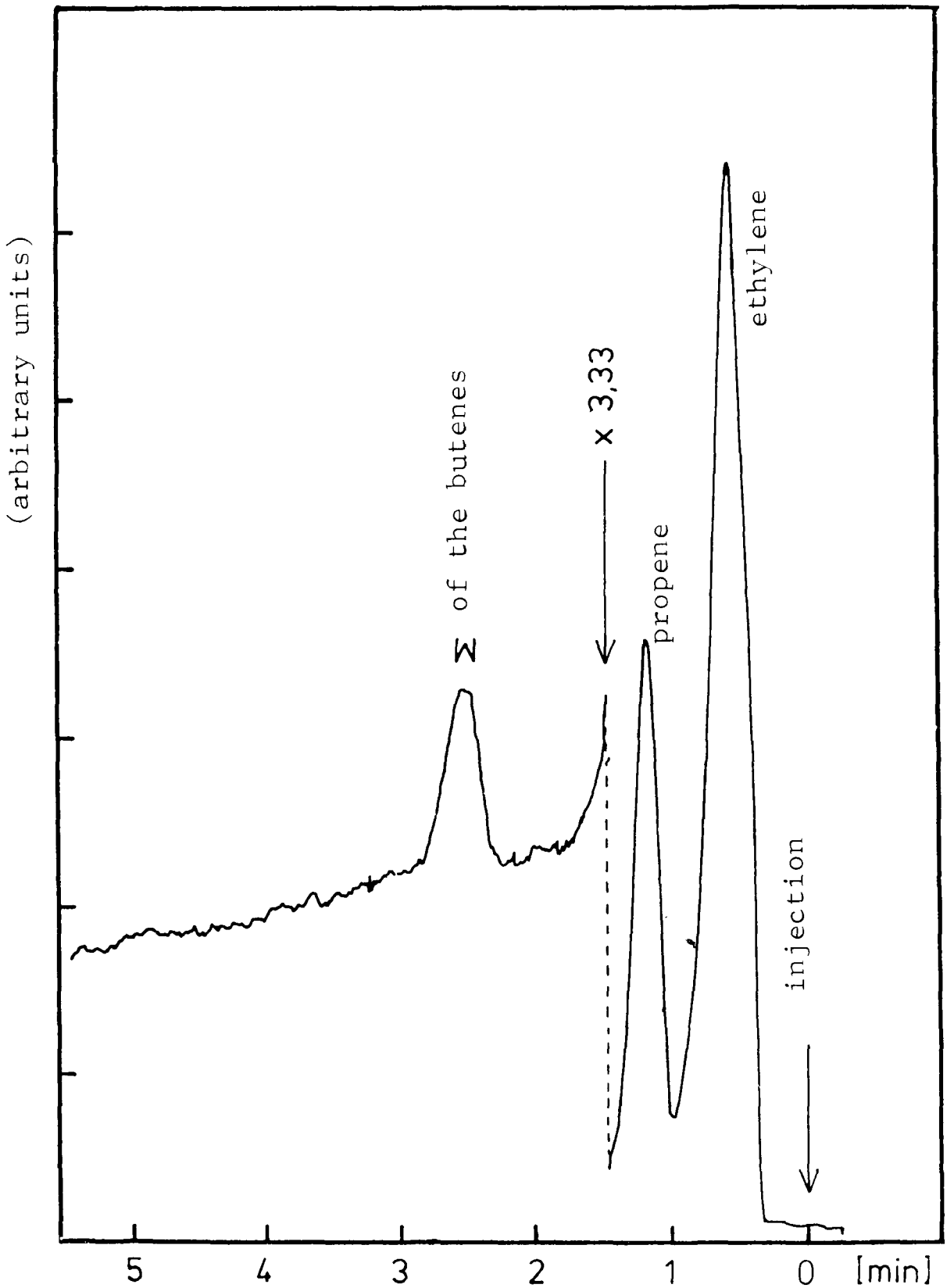

Figure 6. GC analysis of a pre-concentrated air sample by the chemiluminescent olefin detector.

ACKNOWLEDGEMENT

This work was supported by the "Bundesminister des Innern" as part of a program on photochemical air pollution control in the German Federal Republic.

REFERENCES

1. H. H. Westberg, R. A. Rasmussen, and M. Holdren. Gas Chromatographic Analysis of Ambient Air for Light Hydrocarbons Using a Chemically Bounded Stationary Phase. Anal. Chem. 46:1852, 1974.

2. W. A. Lonneman, S. L. Kopczynski, P. E. Darley, and F. D. Sutterfield. Hydrocarbon Composition of Urban Air Pollution. Env. Sci. Technol. 8:229, 1974.

3. W. Bruening and F. J. M. Concha. Selective Detector for Gas Chromatography Based on the Chemiluminescence of Ozone Reactions, J. Chromatog. 112:253, 1975.

4. U. Schurath, A. Wiese, and K. H. Becker. Ein Chemilumineszenzanalysator fur ungesättigte Kohlenwasserstoffe in der Atmosphäre. Staub - Reinhalt. Luft, 1976, in press.

5. K. H. Becker, Ulrich Schurath, and Andreas Wiese. Gas Chromatographic Detector for Olefins. Anal. Chem., 1976, in press.

6. W. Fricke and H. W. Georgii, private communication.

7. K. H. Becker, F. Bahe, W. Janek, J. Löbel, U. Schurath, W. W. Wendler, and A. Wiese. Untersuchungen über Smogbildung, insbesondere über die Ausbildung von Photooxidantien als Folge der Luftverunreinigungen in der BRD. Annual Report 1975. University of Bonn, May 1976.

GC-CHEMILUMINESCENCE METHOD FOR THE ANALYSIS OF AMBIENT TERPENES

R. L. Seila*

ABSTRACT

A method for the quantitative and qualitative analysis of ambient terpenes is described and evaluated. Samples of ambient air collected on a solid adsorbent are desorbed into a cryogenic trap for injection into a gas chromatographic column. After separation by the column, the sample is split for simultaneous detection by flame ionization and ozone chemiluminescence. The chemiluminescence detector is a modified commercial ambient nitrogen oxide-oxides of nitrogen monitor. Response data for a variety of terpenic hydrocarbons, and the results of some ambient analyses are reported.

INTRODUCTION

The contribution of natural hydrocarbons emitted from trees and other vegetation to the formation of photochemical oxidants is a continuing subject of debate and study. Rasmussen, et al. (1) report that monoterpenes and isoprene are the major compounds released to the atmosphere from plants. The research of Grimsrud et al. (2) indicate that terpenes are very reactive with short residence times in the atmosphere. These findings suggest that natural hydrocarbons may be important precursors for the reactions which form O_3 in rural atmospheres.

In order to more fully understand the relationship between biomass and rural O_3 concentrations, varied and reliable analytical methods for the identification and quantitation of terpenes are desirable. Gas chromatography (GC) with flame ionization detection (FID) has been the method used by most previous investigators (1, 3, 4, 5, 6). The inherent problem with this method is that the FID does not provide a definitive qualitative analysis, since it does not enable identification of specific organic compounds (7). Experience in the Environmental Protection Agency (EPA), Environmental Sciences Research Laboratory (ESRL) has been that the GC resolution of terpenes from the ever present very dilute automobile exhaust in rural air is very difficult. This problem has been overcome by the use of two detectors.

There is a problem of uncertainty concerning the results of detailed hydrocarbon analyses of relatively clean rural air samples collected in Tedlar bags due to contaminants from the polyvinyl fluoride film (11). Another problem of using bags for sampling rural air for terpene analysis is that the ambient O_3 in the bags reacts quickly with terpenes during the time interval between

*U. S. Environmental Protection Agency, Research Triangle Park, North Carolina.

collection and analysis. For these reasons and the fact that the concentration of large volumes of air is necessary for the analysis of low ambient terpene concentrations, it was decided to assemble and test a GC method which would employ a solid adsorbent for sampling large volumes and would simultaneously measure the FID and chemiluminescent responses of these samples.

Ozone chemiluminescence measurement of olefins has been performed by Quickert, et al. (8) who evaluated the direct response of a modified commercial O_3 monitor to several selected olefins but not to terpenes. Hilborn, et al. (9) used the same instrument as a total olefin monitor for ambient measurements. McClenny, et al. (10) measured the chemiluminescent response of various olefins with O_3 and demonstrated the feasibility for analysis of vinyl chloride and related compounds by using a combination of GC and O_3 chemiluminescence. A commercial instrument manufacturer under contract to EPA has produced a prototype vinyl chloride analyzer using this method.

EXPERIMENTAL

INSTRUMENTATION

A schematic of the flame ionization-chemiluminescence chromatographic system used for terpene analysis is provided in Figure 1. It consists basically of two components--a Perkin Elmer 900 GC with FID and a Bendix Model 8101-B NO_x chemiluminescence analyzer.

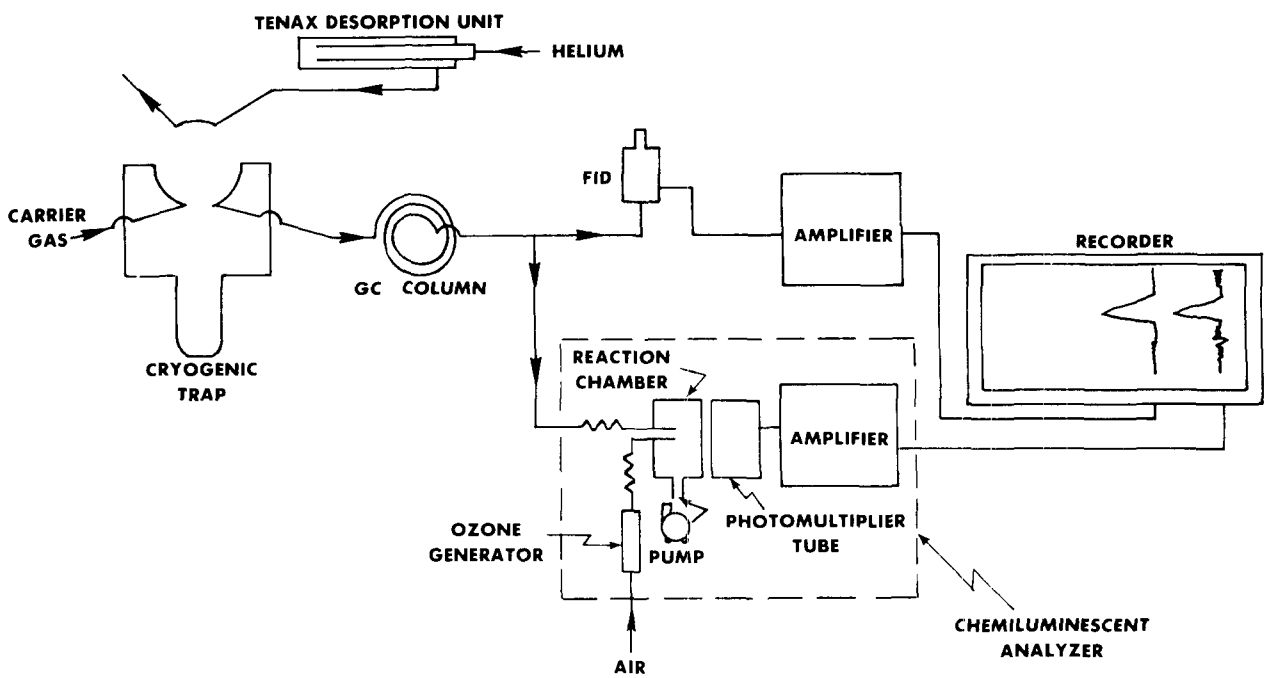

Figure 1. Schematic of FID-chemiluminescent gas chromatograph.

The NO_x analyzer used as a chemiluminescence detector was modified in several respects. The photomultiplier tube was replaced with one from a Bendix O_3 chemiluminescence analyzer. The red interference filter between the photo-

multiplier tube and the reaction chamber was replaced with a transparent glass window. The glass capillary which controls the flow of ambient air into the reaction chamber at a rate of approximately 150 ml min^{-1} was replaced with one identical to the one used to restrict the O_3 flow into the reaction chamber to 20 ml min^{-1}. This capillary gave a carrier gas inlet flow rate of 27 ml min^{-1}. The same pump which comes with the instrument was used to operate the reaction chamber at a pressure of 50 Torr. The O_3 air supply pressure switch used to energize the O_3 generator at 18 pounds per square inch gauge (psig) was adjusted to allow operation at a pressure of 8 psig. A 35 liter tank was placed in the vacuum line between the pump and the reaction chamber to act as a ballast.

The outputs from the FID amplifier and chemiluminescence analyzer were 1 mv and 10 mv respectively and were connected to a strip chart recorder operated at a chart speed of 1.27 cm min^{-1}.

CHROMATOGRAPHIC CONDITIONS

The GC column employed was 120 cm x 2.36 mm inside diameter (ID) ss OPN/Porasil C, 80/100 mesh (Waters Associates). The carrier gas was helium at a flow rate of 50 ml min^{-1}. The column and FID detector temperatures were 120°C and 160°C respectively. After splitting, the carrier flow rate to the FID was 23 ml min^{-1} and the flow rate to the chemiluminescence detector was 27 ml min^{-1}. The FID air and hydrogen flows were 472 ml min^{-1} and 49 ml min^{-1} respectively. A cryogenic trap, consisting of 0.5 ml of Chromosorb 750 in a 27 cm x 2.36 mm ID section of ss tubing, was used to trap the sample before injection onto the column. Liquid oxygen was the cryogen. A Seiscor six port gas sampling valve was used for flow diversions involved in sample trapping and injection. The valve was placed in the GC oven with the column at a temperature of 120°C.

SAMPLING

Tenax GC (2,6 diphenyl-p-phenyleneoxide polymer, Alltech Associates) 60/80 mesh was the adsorbent used for collecting ambient samples. Stainless steel tubes, 14 cm x 6.35 outside diameter (OD), containing 3.8 ml of Tenax and glass wool plugs were the sampling cartridges. Before use the cartridges were conditioned under helium flow at 350°C for at least 24 hours.

A Thomas pump connected to a two port manifold to which two Tenax cartridges could be attached for duplicate sampling constituted the sampling apparatus. The air flow rate was measured with a calibrated rotometer and adjusted as necessary when ambient samples were collected.

A special Tenax desorption unit was fabricated from a Perkin Elmer liquid injection port. This design has been described by Bellar, et al. (12). The exit of the desorption unit was connected to the sampling valve to which the cryogenic trap was attached. The valve plumbing was reverse that of common GC valve plumbing. In the valve off position, the carrier gas flows through the cryogenic trap to the column. Only when the valve is actuated does helium from the desorption unit flow through the cryogenic trap. This arrangement was used to prevent contamination of the cryogenic trap from a Tenax cartridge in the desorption unit. Samplers were desorbed at 250°C while purging the cartridge

with helium at 47 ml min^{-1} for 15 minutes.

CHEMICALS

Terpenes liquid samples were obtained from Glidden-Durkee, Aldrich and Chemical Samples Company.

RESULTS AND DISCUSSION

Before the instrumentation was assembled, a preliminary experiment was performed to determine if some terpenes would chemiluminesce when reacted with O_3. This work was done using the apparatus as described by McClenny, et al. (10). Bag samples of α-pinene, β-pinene, myrcene, γ-terpinene, and d-limonene were sampled and did provide chemiluminescent response. This suggested that a GC-chemiluminescence method for terpenes was feasible.

The chemiluminescent responses of selected terpenes were evaluated by injecting masses varying from 0.08 μg to 1.08 μg into the FID-chemiluminescence chromatograph. Samples were cryogenically trapped from bag standards prepared by microliter syringe injections into nitrogen. This gave initial terpene concentrations of 3 to 4 ppm. Lower bag concentrations were produced by withdrawing and adding nitrogen to the bags. The FID analyses of the diluted bags were used to calculate the terpene dilution concentrations by multiplying the FID response times the terpene FID response factors obtained from the initial known bag samples. Sample masses were also changed by varying the sample volume between 8 and 100 ml.

Figure 2 is a graphical representation of the results of the response study. The concentrations on the abscissa were calculated from the known samples masses and a presumed total sample volume of 15 liters. The chemiluminescent response was determined by measuring peak area by the height times width at half-height method. This area (mm^2) response was divided by 100 to give the relative response depicted by the ordinate of the graph. Most of the curves are not straight lines. Myrcene and β-pinene points appear to fall on a straight line, while the other compounds show a slight decrease of sensitivity with increasing concentration.

The chemiluminescence sensitivity varied considerably from compound to compound as can be seen by the curves in Figure 2. Sensitivities were measured by a linear regression calculation of the slope of the area response versus concentration for the straight portion of the curves--generally at concentrations below 5 ppb. The slopes were converted to the accepted sensitivity units of millivolt second/μg (7). The minimum detectable masses were calculated by dividing the minimum detectable area by the sensitivity for each compound. The minimum detectable area was the peak area for a recorder deflection of twice the noise level. The noise level was 0.008 mv and the minimum detectable area was 30 mm^2 or 0.57 mv · sec. The minimum detectable concentrations were calculated from the known minimum detectable masses and an assumed sample volume of 15 liters. Table 1 summarizes the sensitivity and detectability results.

The sensitivity of chemiluminescent detection was improved considerably (approximately 47 percent) by operating the chemiluminescent reaction chamber at

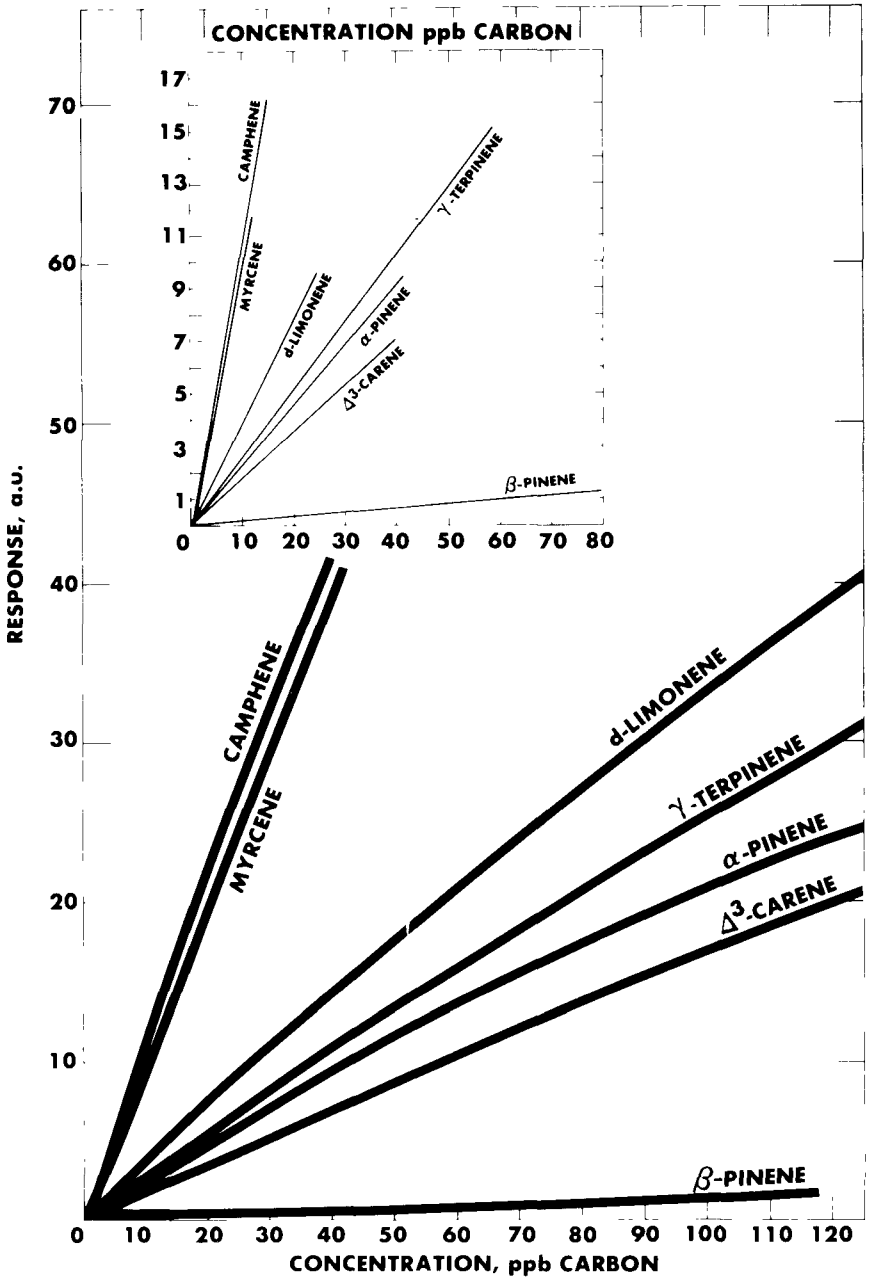

Figure 2. Chemiluminescent response versus concentration* for selected terpenes. (*A sample volume of 15 liters drawn through Tenax was assumed for the concentration calculations.)

reduced (50 Torr) rather than ambient pressure.

Table 2 is a comparison of terpene relative chemiluminescence sensitivities and their ozonolysis rates. There is a general positive correlation of increased sensitivity with increased ozonolysis rate (2).

The efficiency of the Tenax cartridges was evaluated by two methods. A bag of low concentration α-pinene, β-pinene, d-limonene, and myrcene was prepared.

TABLE 1. CHEMILUMINESCENCE SENSITIVITY, MINIMUM DETECTABLE MASS AND CONCENTRATION FOR SELECTED TERPENES

Compound	Sensitivity*	Minimum Detectable Mass	Minimum Detectable Conc.†
Camphene	256.9	0.0022 μg	.03
Myrcene	208.0	0.0027 μg	.03
d-Limonene	82.7	0.0069 μg	.08
γ-Terpinene	58.6	0.0097 μg	0.11
α-Pinene	50.7	0.0112 μg	0.13
Δ^3-Carene	37.0	0.0153 μg	0.18
β-Pinene	3.4	0.1665 μg	1.97

* Millivolt · second per microgram

† Parts per billion. Concentrations based on 15 liter sample volume

TABLE 2. CHEMILUMINESCENCE RELATIVE SENSITIVITES AND RELATIVE OZONOLYSIS RATE OF SELECTED TERPENES

Compound	Relative Sensitivity	Relative Ozonolysis Rate
Camphene	5.1	--
Myrcene	4.1	8.6
d-Limonene	1.6	4.4
γ-Terpinene	1.2	1.9
α-Pinene	1.0	1.0
Δ^3-Carene	0.73	0.83
β-Pinene	0.067	0.25

A 25 liter sample was drawn through two Tenax cartridges in series. These cartridges were analyzed. The analysis of a two liter cryogenic sample directly from the bag provided a measurement of the actual bag concentrations. Comparison of the cryogenic analysis and Tenax analyses responses gave the Tenax cartridge efficiency. A comparison of the responses of the front and back cartridges by the formula $\left(1 - \frac{\text{Response, back cartridge}}{\text{Response, front cartridge}}\right) \times 100\%$ also produced a trapping efficiency. The results of this experiment are presented in Table 3.

The fact that the Tenax adsorption efficiency for C_{10} terpenes is not

TABLE 3. COMPARISON OF TENAX ADSORPTION EFFICIENCY DETERMINED BY TWO METHODS FOR FOUR TERPENES OF VARYING SAMPLE SIZE

Compound	Bag Concentration, ppb	Efficiency, Tenax Versus Cryogenic Analysis	Efficiency, Front Cartridge Versus Back Cartridge
α-Pinene	.30	57%	74%
β-Pinene	.59	63%	70%
d-Limonene	.87	69%	64%
Myrcene	2.15	33%	28%

greater than 90 percent for a 25 liter volume is surprising and not what one would expect from reviewing some of the literature on Tenax (13-18).

A high efficiency of desorption (> 95 percent) of Tenax adsorbents was verified several times by trapping cryogenically a second consecutive 15 minute sample from a cartridge. Comparison of the first desorption analysis with the second indicated that practically all of the adsorbed species had been removed.

Chemiluminescence interference by aromatic hydrocarbons was evaluated by analyzing automobile exhaust. There was no interference in the terpene retention time region. This result agrees with the results of Hilborn, et al. (9) and McClenny, et al. that aromatic compounds do not respond to ozone chemiluminescence (10).

The major source of error of this method arises from a sampling technique which employs Tenax. The problems with Tenax are contamination and adsorption efficiency.

Three types of blank analyses were performed to check Tenax background. Cartridges were analyzed at the end of conditioning, after conditioning and cooling, and after sampling prepurified nitrogen (Linde). The analysis of a cartridge at the end of conditioning revealed zero background on both the FID and chemiluminescent responses at the amplifier attenuations used for ambient analyses (FID-16X, chemiluminescence - 2X). The cartridge was removed from the desorption unit and allowed to cool for 15 minutes while continuing the helium purge flow. The subsequent chemiluminescent response revealed two small peaks, comparable in magnitude to the minimum detectability. One peak retention time coincided with that of Δ^3-carene. The FID chromatogram revealed general contamination, but again of a magnitude corresponding to minimum detectable peaks. The 30 liter prepurified nitrogen sample displayed general FID contamination of low magnitude. The chemiluminescent response showed very small peaks at α-pinene and myrcene and two small

unknown peaks in the retention region of terpenes and three very significant peaks at retention time zero to one minute. The two small unknown peaks were major peaks in all the later ambient samples and were confirmed to be Tenax artifacts by their absence from cryogenic concentration analyses of two ambient bag samples.

The error due to the uncertainty of Tenax adsorption efficiency under ambient sampling conditions is difficult to access and will be more thoroughly investigated. The data of Table 3 indicate an efficiency of 60 to 70 percent.

The reproducibility error expressed as percentage standard deviation was calculated from peak height measurements of four peaks from eight duplicate ambient analyses. The average percent standard deviations were ± 20 percent and ± 22 percent for the FID and chemiluminescent responses respectively. The chemiluminescence and FID reproducibility of the chromatograph without Tenax adsorption and desorption were both ± 10 percent. The lack of any reproducibility difference between the chemiluminescent and FID responses and the large reproducibility discrepancy of the method with and without Tenax indicate that Tenax is a large source of reproducibility error.

Ten duplicate day time ambient samples were collected and analyzed. Six were from a small group of loblolly pines (*Pinus taeda L.*) behind the EPA/RTP Environmental Research Center. The other four were from an 18 year old, rural, homogeneous stand of loblolly pine. The chemiluminescence chromatograms of all of the samples showed only two peaks corresponding to previously analyzed known terpenes. The two peaks were α-pinene and myrcene, γ-terpinene. Their concentrations were all less than 2 ppb.

CONCLUSIONS

The method described herein has the advantage of simultaneous measurement of FID and O_3 chemiluminescent responses for GC samples. This double measure provides for a more confident identification and quantitation of terpenes in ambient air.

The disadvantage is that this method employs Tenax, which has been shown to have adsorption efficiency and contamination problems, as a solid adsorbent for concentrating ambient samples. If the use of Tenax proves to be too great a problem, direct ambient cryogenic sampling of smaller volumes can be used as the concentration technique.

ACKNOWLEDGEMENT

The author wishes to acknowledge the assistance of Dr. William McClenny of the U.S. EPA Environmental Sciences Research Laboratory.

REFERENCES

1. Rasmussen, R.A. What Do the Hydrocarbons from Trees Contribute to Air

Pollution? J. APCA, 22 (7): 537-543, 1972.

2. Grimsrud, E.P., Westberg, H.H., Rasmussen, R.A. Atmospheric Reactivity of Monoterpene Hydrocarbons, NO_2 Photooxidation and Ozonolysis. In: Proceedings of the Symposium on Chemical Kinetics Data for the Upper and Lower Atmosphere, International Journal of Chemical Kinetics Symposium No. 1, 1975. pp. 183-195.

3. Rasmussen, R.A., Went, F.W. Volatile Organic Material of Plant Origin in the Atmosphere. Proc. Nat. Acad. Sci., 53: 215-220, 1964.

4. Rasmussen, R.A. Isoprene: Identified as a Forest-Type Emission to the Atmosphere. Environ. Sci. Technol., 4(8): 667-671, 1970.

5. Rasmussen, R.A., Holdren, M.W. Analyses of C_5 to C_{10} Hydrocarbons in Rural Atmospheres. APCA 65th Meeting, paper # 72-19, June, 1972.

6. Tyson, B.J., Dément, W.A., Mooney, H.A. Volatilisation of Terpenes from Salvia Mellifera. Nature, 252 (5479): 119-120, 1974.

7. McNair, H.M., Bonelli, E.J. Basic Gas Chromatography. Varian Aerograph, Walnut Creek, CA, 1969, pp. 118, 87-89.

8. Quickert, N., Findlay, W. J., Monkman, J.L. Modification of a Chemiluminescent Ozone Monitor for the Measurement of Gaseous Unsaturated Hydrocarbons. The Science of the Total Environment 3(4): 323-328, 1975.

9. Hilborn, J.C., Findlay, W.J., Quickert, N. The Application of Chemiluminescence to the Measurement of Relative Hydrocarbons in Ambient Air. In: Proceedings of the International Conference on Environmental Sensing and Assessment, Las Vegas, Nevada, 1975, 24-2.

10. McClenny, W.A., Martin, B.E., Bumgardner, R.E., Stevens, R.K., O'Keeffe, A.E. Detection of Vinyl Chloride and Related Compounds by a Gas Chromatographic, Chemiluminescence Technique. Environ. Sci. Technol., 10(8): 810-813, 1976.

11. Seila, R.L., Lonneman, W.A., Meeks, S.A. Evaluation of Polyvinyl Fluoride as a Container Material for Air Pollution Samples. J. Environ. Sci. Health--Environ. Sci. Eng., A11(2): 121-130, 1976.

12. Bellar, T.A., Lichtenberg, J.J. Determining Volatile Organics at Micro gram-per-Litre Levels by Gas Chromatography. J. American Water Works Assn., 66(12): 739-744, 1974.

13. Bertsch, W., Chang, R.C., Zlatkis, A. The Determination of Organic Volatiles in Air Pollution Studies: Characterization of Profiles. J. Chromatog. Sci., 12(4): 175-182, 1974.

14. Pellizzari, E.D., Development of Method for Carcinogenic Vapor Analysis in Ambient Atmospheres. EPA-650/2-74-121, U.S. EPA, Research Triangle Park, NC, 1974, 148 pp.

15. Pellizzari, E.D., Development of Analytical Techniques for Measuring Ambient Atmospheric Carcinogenic Vapors. EPA-600/2-75-076, U.S. EPA, Research Triangle Park, NC, 1975, 187 pp.

16. Pellizzari, E.D., Bunch, J.E., Carpenter, B.H., Sawicki, E. Collection and Analysis of Trace Organic Vapor Pollutants in Ambient Atmospheres, Technique for Evaluating Concentration of Vapors by Sorbent Media. Environ. Sci. Technol. 9(6): 552-555, 1975.

17. Ibid, Thermal Desorption of Organic Vapors from Sorbent Media. Environ. Sci. Technol. 9(6): 556-560, 1975.

18. Pellizzari, E.D., Bunch, J.E., Berkley, R.E., McRae, J. Determination of Trace Hazardous Organic Vapor Pollutants in Ambient Atmospheres by Gas Chromatograph/Mass Spectrometry/Computer. Anal. Chem. 48(6): 803-806, 1976.

MEASUREMENTS OF SULFATE, INORGANIC GASEOUS NITRATE AND OTHER CONSTITUENTS IN THE ATMOSPHERE

T. Okita*

ABSTRACT

Measurements were made of sulfate, gaseous nitrate and other constituents in the atmosphere in Tokyo and its surrounding area. Gaseous nitrate concentrations were higher in summer than in winter and correlated closely with those of oxidants. Sulfate-to-sulfur dioxide concentration ratios did not appear to correlate with oxidant concentrations, and they varied with relative humidity.

INTRODUCTION

In photochemical air pollution various types of pollutants are produced, including oxidants. They exert adverse effects on human health, plants, etc.

In this report, results from measurements of sulfate, inorganic gaseous nitrate (probably nitric acid vapor) and other constituents, conducted in Tokyo and its surrounding area, are presented and compared with measurements of oxidants.

ANALYTICAL PROCEDURES

MEASUREMENT OF NITRATE

Ambient gaseous nitrate was measured by collecting it first on a Sodium Chloride (NaCl)-impregnated filter from which it was subsequently extracted and analysis was made for it. For preparation of the NaCl-impregnated filter, a circular Toyo 51A cellulose filter 5 cm in diameter was soaked with a 5% aqueous solution of NaCl, and was dried using an infrared lamp in a chamber free from nitrogen dioxide (NO_2) and nitric acid gases. The filter was then stored in a silica gel desiccator.

For ambient air sampling, either a Millipore FHLP Teflon filter or a Sumitomo FP Teflon filter 47 mm in diameter along with an NaCl-impregnated filter were placed in separate filter holders. They were connected in series, with the FHLP filter upstream from the NaCl-impregnated filter. The inside walls of the holders were coated with Teflon and the filter holders were heated by a 30-W tape heater wound around the holder. The air was sampled through the filters at

*Department of Community Environmental Sciences, the Institute of Public Health, Tokyo, Japan.

a metered flow rate of about 20 l min^{-1}. Particulate and gaseous nitrates were collected on the FHLP and NaCl-impregnated filters, respectively.

For measurement, the gaseous nitrate collected on the NaCl-impregnated filter was extracted into 30 ml of hot water. Then 20 ml of the extract was used for the nitrate measurement. The particulate nitrate collected on the FHLP filter was ultrasonically extracted into 30 ml of warm water. In either case the nitrate in solution was reduced to nitrite by hydrazine in alkaline solution. The resultant nitrite was determined by reacting it with Griess-Romijn reagent (1) as modified by the technique as described in Ota et al. (2).

Efficiency of nitric acid collection on the NaCl-impregnated filter was 90-100% (mean efficiency 96.6%) for sampling flow rate of 20 l min^{-1}. Interference from 0.1 ppm of NO_2 was equivalent to about 1 μgm^{-3} of nitrogen in the form of nitrate ion (NO_3^-). It was not enhanced by the presence of O_3. Interferences from peroxyacetylnitrate (PAN) and organic nitrates were negligible.

For particulate ammonium nitrate (deposited on the FHLP filter), ultrasonic extraction of nitrate from the filter in warm water was the most efficient extraction procedure, the efficiency being almost 100%. Loss of nitric acid vapor on the FHLP filter was kept low (1-4%) by heating the filter holder with a 30 W tape heater. Efficiency of particle collection by the FHLP filter has been reported at 99.99%, even for the size corresponding to the penetration maximum (3).

MEASUREMENT OF SO_2, NO_2, AND SULFATE (SO_4^{-2})

Ambient SO_2 and NO_2 were measured using automated electric conductivity and colorimetric (Saltzman) analyzers, respectively. Particulate sulfates were collected on fiber glass filters and measured nephelometrically.

RESULTS

CORRELATIONS BETWEEN NITRATES, NO_2, AND OXIDANT CONCENTRATIONS

During 1973-1976, measurements of ambient gaseous and particulate nitrates were conducted at the Institute of Public Health (IPH) and the Tokyo Metropolitan Institute of Environmental Control (TMIEC), located, respectively, in downtown Tokyo, and at Mt. Tsukuba (altitude 876 m) which lies about 80 km NNE of downtown Tokyo (4).

Figure 1 shows the relationship of gaseous nitrate concentrations (measured at the IPH between 10 a.m. and 5 p.m.) and daily maximum oxidant concentrations measured at the Meguro Air Monitoring Station located about 3.5 km from the IPH (during the period of July 25 to August 30, 1975). The data of Figure 1 indicate that the concentration of gaseous nitrate increases with increasing oxidant concentration. Such a correlation between gaseous nitrate and oxidant was also found by our measurements in the summer of 1973 (4). Figure 2 shows the relationship between the concentrations of gaseous nitrate and NO_2 measured by the sodium arsenite method (5). There was a tendency for high gaseous nitrate concentrations to occur with high NO_2 concentrations in downtown Tokyo, but at Mt. Tsukuba the gaseous nitrate concentrations were much higher than were those

of NO_2. As shown in Figure 3, there was no correlation between particulate nitrate and oxidant concentrations at the IPH site in the summer of 1975.

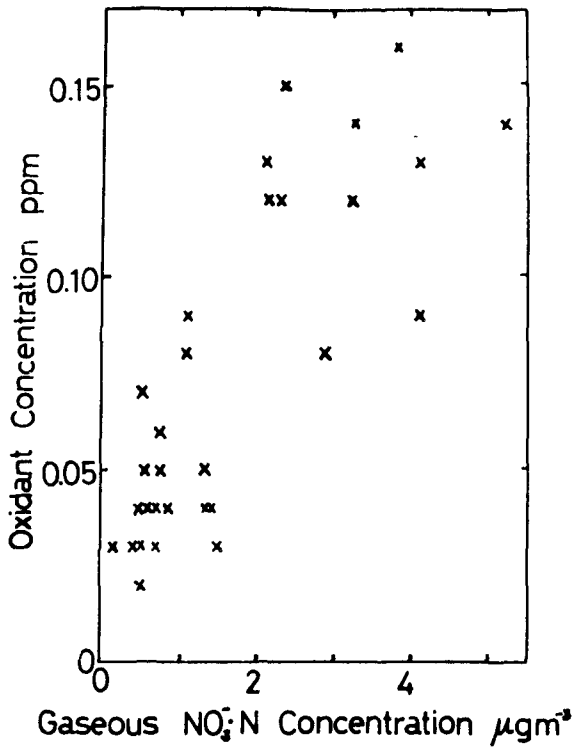

Figure 1. Relationship of gaseous NO_3 concentration at the Institute of Public Health versus daily maximum oxidant concentrations.

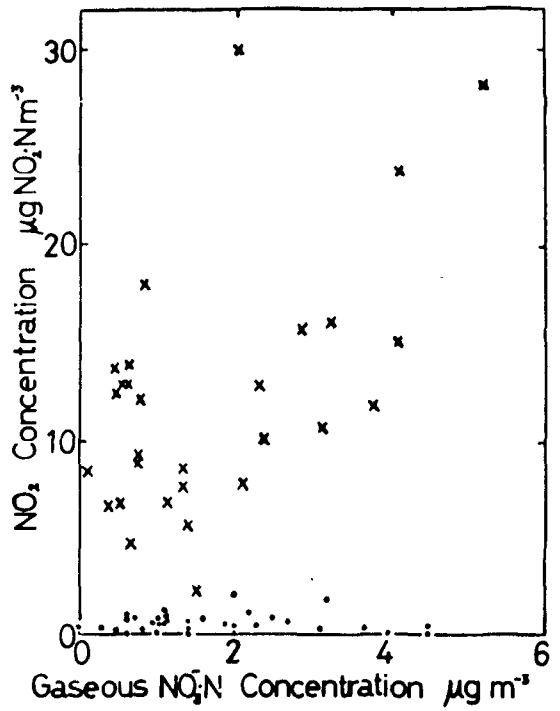

Figure 2. Relationship between NO and gaseous NO^- concentrations.
X IPH (July 25 - August 30, 1975)
● Mt. Tsukuba (June 25 - July 3, 1975)

Figure 4 shows the relationship between daily mean concentrations of gaseous and particulate nitrates measured at the IPH and TMIEC sites in January of 1976. Comparison of Figure 4 with Figures 1 and 3 indicates that, whereas there was only a small seasonal change of the concentration of particulate nitrate, the mean gaseous nitrate concentration in summer was about five times that in winter in downtown Tokyo. To further study the seasonal variation of gaseous nitrate concentration, additional measurements were made between October 13 and 17, 1975, at Mt. Tsukuba. These measurements indicated that the mean NO_2 and both the gaseous and particulate NO_3^- concentrations were 4.3, 0.4 and 1.5 μgm^{-3}, respectively. Comparison of these results with those shown in Figure 2 reveals that the gaseous nitrate concentrations were much lower in autumn than in early summer, whereas NO_2 showed an opposite pattern.

CORRELATIONS BETWEEN SO_4^{-2}/SO_2, NO_3^-/NO_2 AND OXIDANT CONCENTRATIONS

In the period June 25 to July 7, 1975 a survey of atmospheric constituents was conducted in a large area surrounding Tokyo (Figure 5). The data examined included measurements of SO_2, NO_2, SO_4^{-2} and NO_3^{-1}. Figure 6 indicates the day-to-day variation of daily mean values for SO_4^{-2}-S/SO_2-S, NO_3^--N/NO_2-N, oxidant concentration and relative humidity at Kumagaya, Ichihara and Kawasaki. These

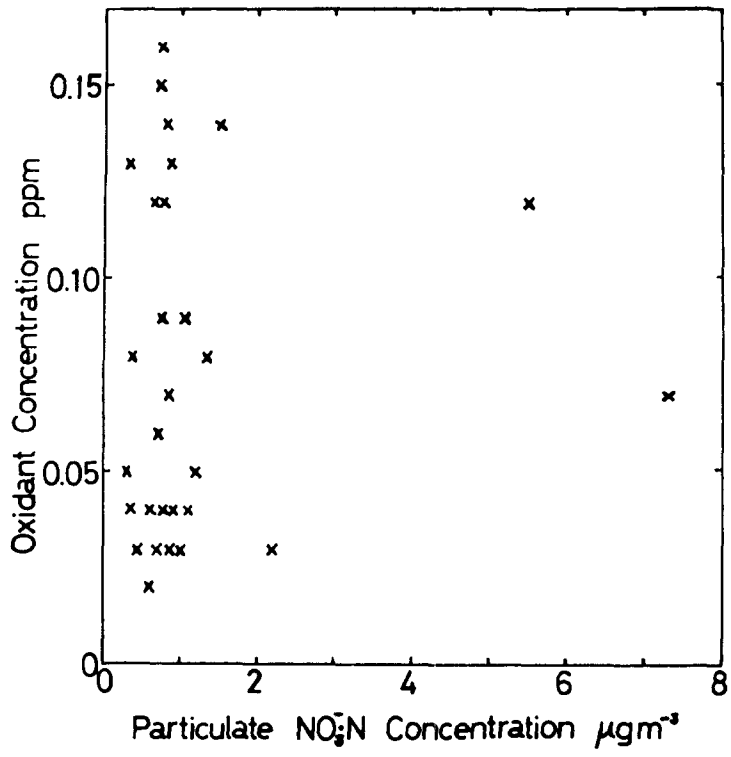

Figure 3. Relationship of particulate NO_3^- concentration at IPH versus daily maximum oxidant concentration.

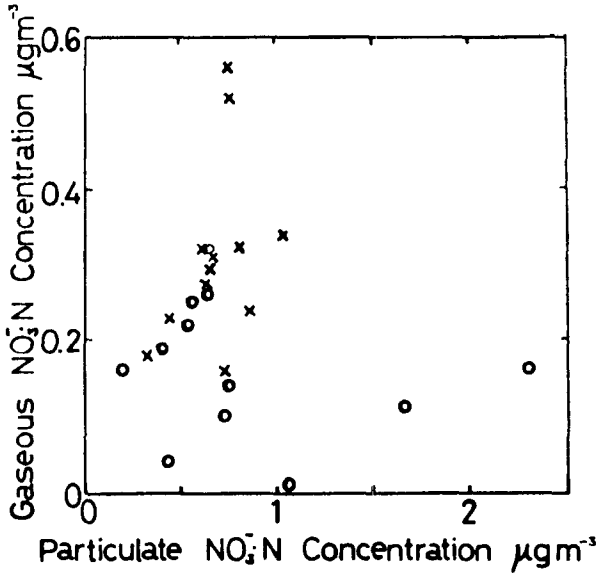

Figure 4. Relationship between daily mean concentrations of gaseous and particulate NO_3^- on January 1-24, 1976.
X IPH
o Tokyo Metropolitan Institute of Environmental Control

values show that SO_4^{-2}-S/SO_2-S correlates well with humidity rather than with oxidant level. The NO_3^--N/NO_2-N, on the other hand, shows some correlation with oxidant level. The author found that nitric acid vapor is collected on glass fiber filter and thus a portion of particulate nitrate comes from nitric acid vapor in the atmosphere.

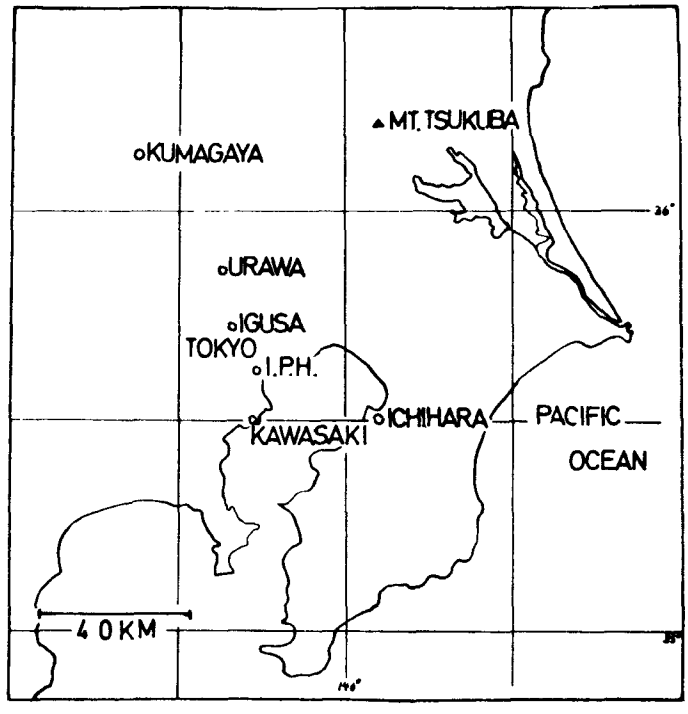

Figure 5. Area surrounding Tokyo where survey of atmospheric constituents was conducted June 25 - July 7, 1975.

REFERENCES

1. Mullin, J.B. and J. P. Riley. The spectrophotometric determination of nitrate in natural waters, with particular reference to sea water. Analyt. Chem. Acta 12, 1955. pp. 464-480.

2. Ota, T., R. Ishibashi and M. Osaki. Determination of nitrate ion using hydrazine reduction technique. J. Japan Soc. Air Pollution 1, 1970. pp. 72 (in Japanese).

3. Liu, B.Y.H. and K. W. Lee. Efficiency of membrane and nucleopore filters for submicrometer aerosols. Particle Technology Laboratory Publication No. 266, 1975.

4. Okita, T. and S. Morimoto. Measurement of nitric acid and particulate nitrate in the atmosphere. Preprint of Autumnal Meeting of Met. Soc. of Japan, 143, 1973 (in Japanese).

5. U. S. Environmental Protection Agency. Ambient air quality standards. Reference method for determination of nitrogen dioxide. Federal Register

38, 1973. pp. 15174-91.

6. Environment Agency of Japan, Study Committee of Contaminated Precipitation. Report of Study of Contaminated Precipitation in 1975, 1976. (in Japanese).

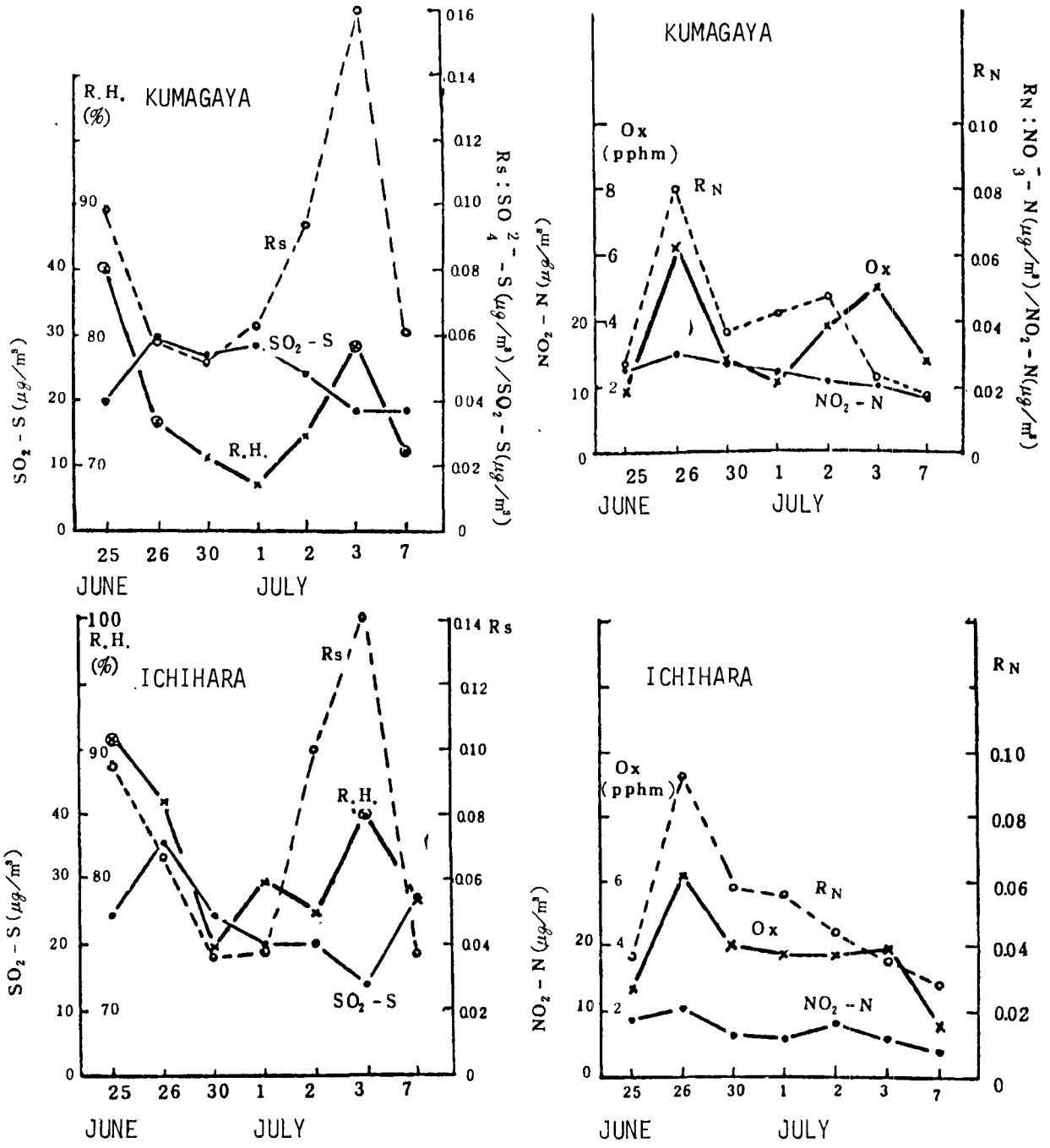

Figure 6. Day to day variations of R_s, R_n, oxidant concentration and relative humidity--Kumagaya and Ichihara.

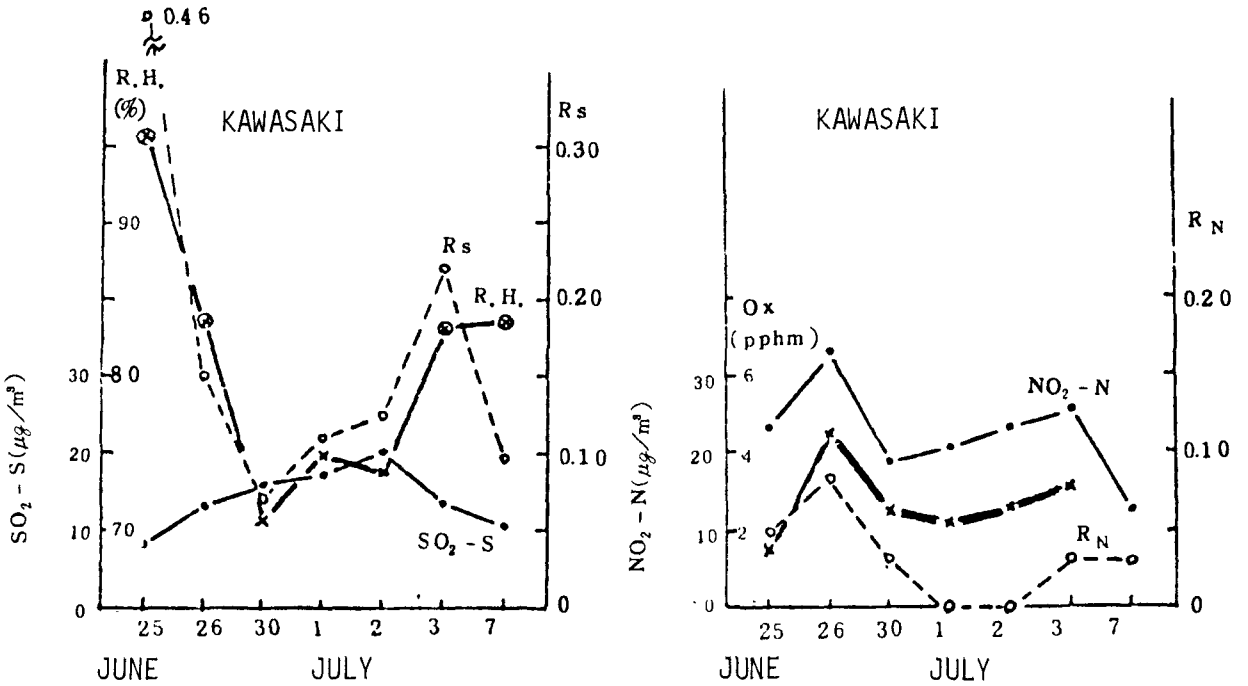

Figure 6. Day to day variations of R_s, R_n, oxidant concentration and relative humidity--Kawasaki.

A PORTABLE INSTRUMENT FOR THE CALIBRATION OF OZONE ANALYZERS BY OPTICAL ABSORPTION MEASUREMENTS

K. H. Becker, A. Heindrichs, and U. Schurath*

ABSTRACT

An instrument for rapid calibrations of ozone analyzers over the concentration range 10 ppb to several ppm is described. It includes a photochemical ozone source. The ozone concentration is calculated from the optical absorption of monochromatic 253.7 nanometer radiation, as measured in a tubular absorption cell. Due to its rapid response, the instrument is particularly suited for the calibration of chemiluminescent ozone analyzers with short time constraints.

INTRODUCTION

Ozone measurements in Europe indicated in 1973 that the ozone (O_3) concentration was frequently considerably higher than the natural background concentration of 20 to 40 ppb at ground level, and on some occasions exceeded the 200 ppb level above which health effects are manifest (1). This relevation initiated an international program for the investigation of the oxidant situation in a number of European countries with the aim of recommending control strategies. Since then the number of monitoring stations for O_3 in the German Federal Republic and other European countries was considerably increased. Nearly all O_3 analyzers in the stations are based on the chemiluminescent reaction of O_3 with ethylene which is particularly suited for continuous monitoring. Such analyzers are not by principle absolute detectors and must be calibrated. Furthermore, sensitivity changes must be anticipated under continuous operating conditions. These changes cannot be totally eliminated by re-calibrations with a built-in O_3 generator which can lack stability. In addition, O_3 losses can occur in the sampling line and dust filter.

Calibrations of O_3 analyzers are usually made by comparison with the hydrogen iodide (HI) method. The stoichiometry of this wet chemical reaction, at O_3 concentrations below 500 ppb, is approximately the following (2,3):

$$O_3 + 2\ I^- + 2\ H^+ \rightleftarrows I_2 + H_2O + O_2 \qquad (1)$$

The procedure, apart from its well known error sources (4), has all the disadvantages of an integrating method: the calibration is time consuming and must be performed with an O_3 source of highly constant output, whereas an advantage of chemiluminescent analyzers is, in particular, their short response time.

*Institut für Physikalische Chemie der Universität Bonn, Bonn, Germany.

This paper presents a reliable technique for the calibration of O_3 analyzers which eliminates the disadvantages of wet chemical methods. It measures optical absorption by O_3 using an ultraviolet means, a method frequently used in laboratory experiments (5,6).

THE PRINCIPLE OF MEASUREMENT

The highest absorption coefficient of O_3 in the Hartley band nearly coincides with the wavelength 253.7 nanometers (nm) of the mercury resonance line. The absorption obeys Beer's law, due to the continuous nature of the absorption spectrum in this region. The recommended value of the absorption coefficient at 253.7 nm is defined by Equation 2.

$$\log_{10}(I/I_0) = k \times p\ 273/T \qquad (2)$$

(T = temperature in K, x = absorption path in cm; p = ozone pressure in atmospheres), is $k = 133.9\ atm^{-1}cm^{-1}$ (7). This value obtains support from numerous determinations (8) and agrees well with $k = 134.5\ atm^{-1}cm^{-1}$ measured in this laboratory (5). At an optical path length of 3 m and 20°C, 100 ppb O_3 causes an intensity reduction of 0.89% relative to pure synthetic air. Weak intensity reductions can be measured reliably at 253.7 nm, provided a low pressure mercury lamp of sufficient stability is used. The suitable concentration range of 10 to 500 ppb O_3 can thus be covered.

EXPERIMENTAL

The experimental setup is shown schematically in Figure 1. Ozone is produced in synthetic air by means of a simple but efficient photochemical O_3 generator with an elliptical reflector. The sampling gas then flows through a light protected glass tube of 1500 mm length. Radiation from a low pressure mercury lamp (Oriel type C-13-61) in a brass housing is collimated along the axis of the tube through a metal capillary. The light is reflected at the far end of the glass tube by a quartz triple prism which has the advantage over a plane mirror that the angle of reflection is always 180°. Therefore no adjustment of the prism is necessary, and the intensity of the reflected light is nearly independent of the angle of incidence on the prism surface. The returning light beam is deflected 90° by a plane mirror through a quartz window and interference filter for 253.7 nm on the cathode of a photomultiplier tube (EMI 9665 B). The light reaching the photomultiplier is better than 99.9% monochromatic since 95% of the lamp output is at 253.7 nm, and the interference filter blocking ratio is $1:10^4$. The effective absorption path is 3100 mm. All metal parts exposed to the gas stream are teflon coated. The volume of the optical cell including both the entrance and the exit chambers is 180 ml, giving a residence time of 11 s at a typical flow rate of 1000 ml/min. Decay measurements in the absorption cell at stopped flow resulted in a lifetime of 70 min., increasing to 100 min. after 1 hour exposure to ozonized air. The systematic error due to heterogeneous decomposition of ozone in the cell is therefore less than 0.3%.

To determine O_3 in the concentration range below 500 ppb, intensity reductions below 4.35% must be measured. A well stabilized high voltage supply for the photomultiplier tube, and a stable light source are therefore needed. A selected low pressure mercury lamp of the above-mentioned type was found adequate after a short period of conditioning, and at a constant line voltage. Intensity changes below 5% are conveniently measured by compensating 95% of the voltage across the photomultiplier anode resistor at full intensity I_0 with a battery. The remaining signal is amplified and displayed on a strip chart recorder which is then deflected full scale at 5% optical absorption.

CALIBRATION OF A CHEMILUMINESCENT OZONE ANALYZER

A Bendix O_3 analyzer, Model 8002, was calibrated in the 500 ppb range and below. The coupling of the analyzer to the optical measuring cell is shown in Figure 1. Both instruments were run with time constants of 1 s. The synthetic air flow rate was 108 liter/hour. The calibration procedure is illustrated by the strip chart recordings of the signals from both instruments in Figure 2. Stepwise changes of the O_3 concentration in the sampling gas were achieved by shielding or unshielding part of the mercury lamp in the O_3 generator. The intensity I_0 was checked in between the measurements by completely shielding the mercury lamp in the generator. A drift of I_0 could thus be taken into account by linear interpolation. The calibration of the O_3 analyzer, as depicted by the recordings in Figure 2, was completed within 11 minutes. Figure 3 shows the resulting plot of chemiluminescent analyzer signal versus the optically measured O_3 concentration, as calculated from the recordings by means of Equation 2. The slope of the straight line gives the sensitivity of that particular analyzer as 1.88 V per ppm O_3, with a standard deviation of $\pm$ 2.5%.

COMPARISON WITH THE POTASSIUM IODIDE (KI) METHOD

The potassium iodide (KI) method is widely considered an absolute method for O_3 measurements, since, under suitable conditions, the stoichiometry given by Equation 1 is closely obeyed. In practice, however, the KI method often leads to serious errors, as was shown recently on occasion of a monitoring program in the U.S. (9). (One of the probable reasons for such errors is that the sensitivity of chemiluminescent analyzers is reduced by a factor of nearly 2 when oxygen is used as test gas instead of synthetic or purefied air (10).) The precision of the optical method for O_3 determination depends, in principle, only upon the reliability of the absorption coefficient at 253.7 nm used in Equation 2. Determinations of the absorption coefficient are based on elementary physical measurements such as the length of the absorption path, the pressure of O_3, and the temperature. The relatively wide error limits of the absorption coefficient, $\pm$ 1.5%, are mainly due to the difficulties inherent in the production and handling of pure O_3. The O_3 concentration is deduced from the pressure increase after complete decomposition into molecular oxygen.

A direct comparison between optically measured O_3 in synthetic air and measurements by the KI method resulted in good agreement between the two methods.

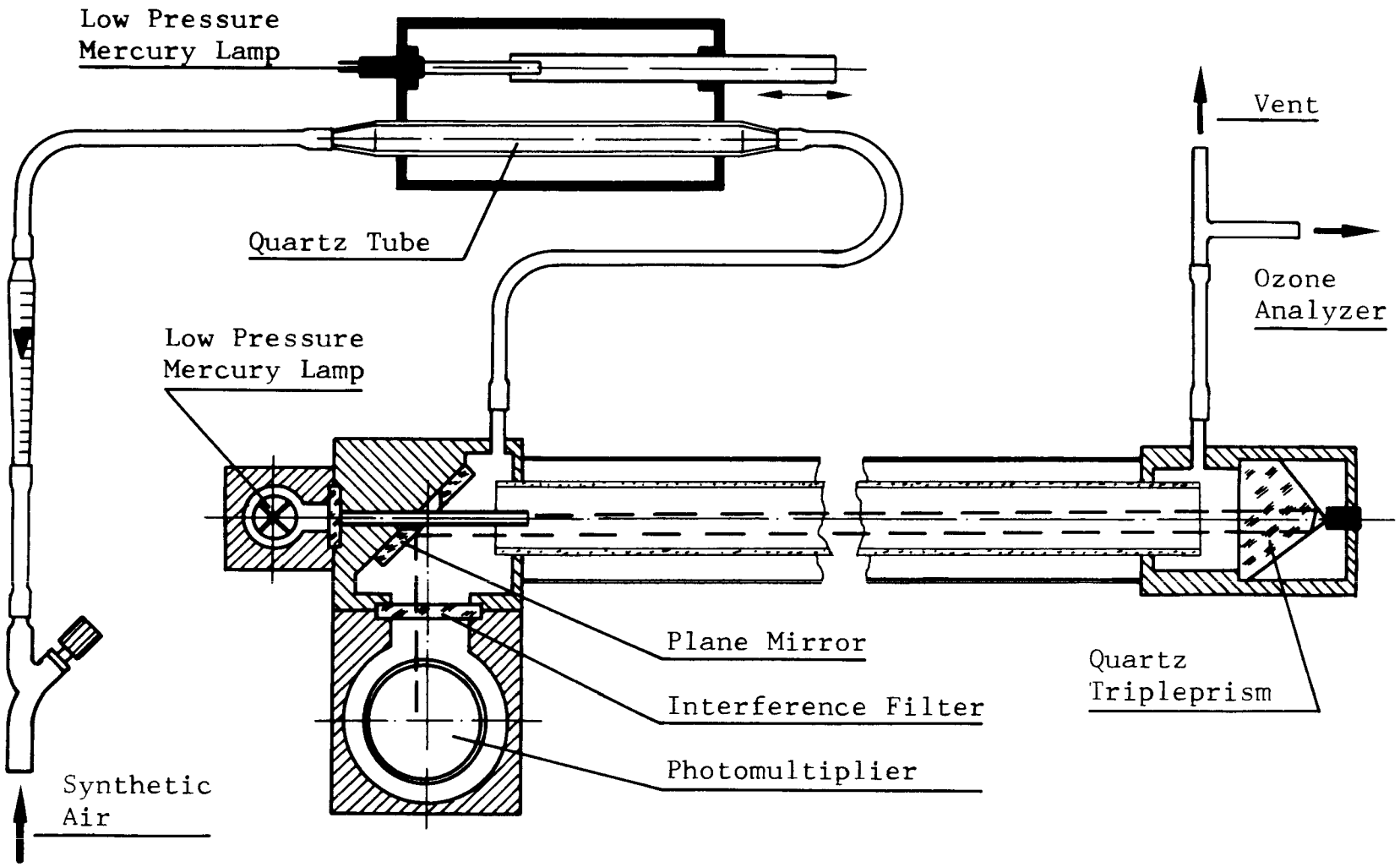

Figure 1. Schematic diagram of optical ozone meter.

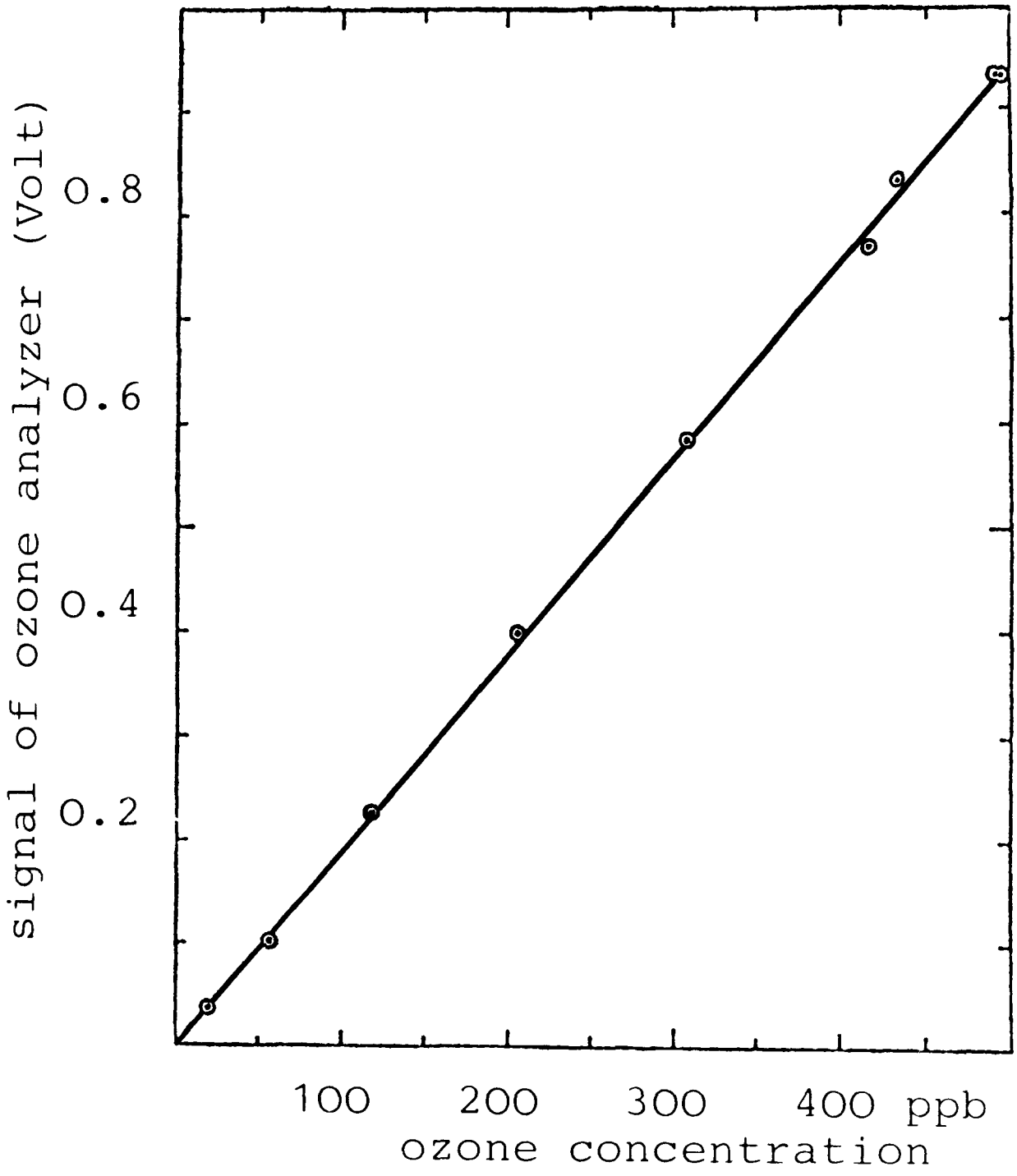

Figure 2. Calibration of a chemiluminescent ozone analyzer. (a) Absorption by ozone at 253.7 nm in the cell, (b) Corresponding signal of the chemiluminescent ozone analyzer in series with the cell.

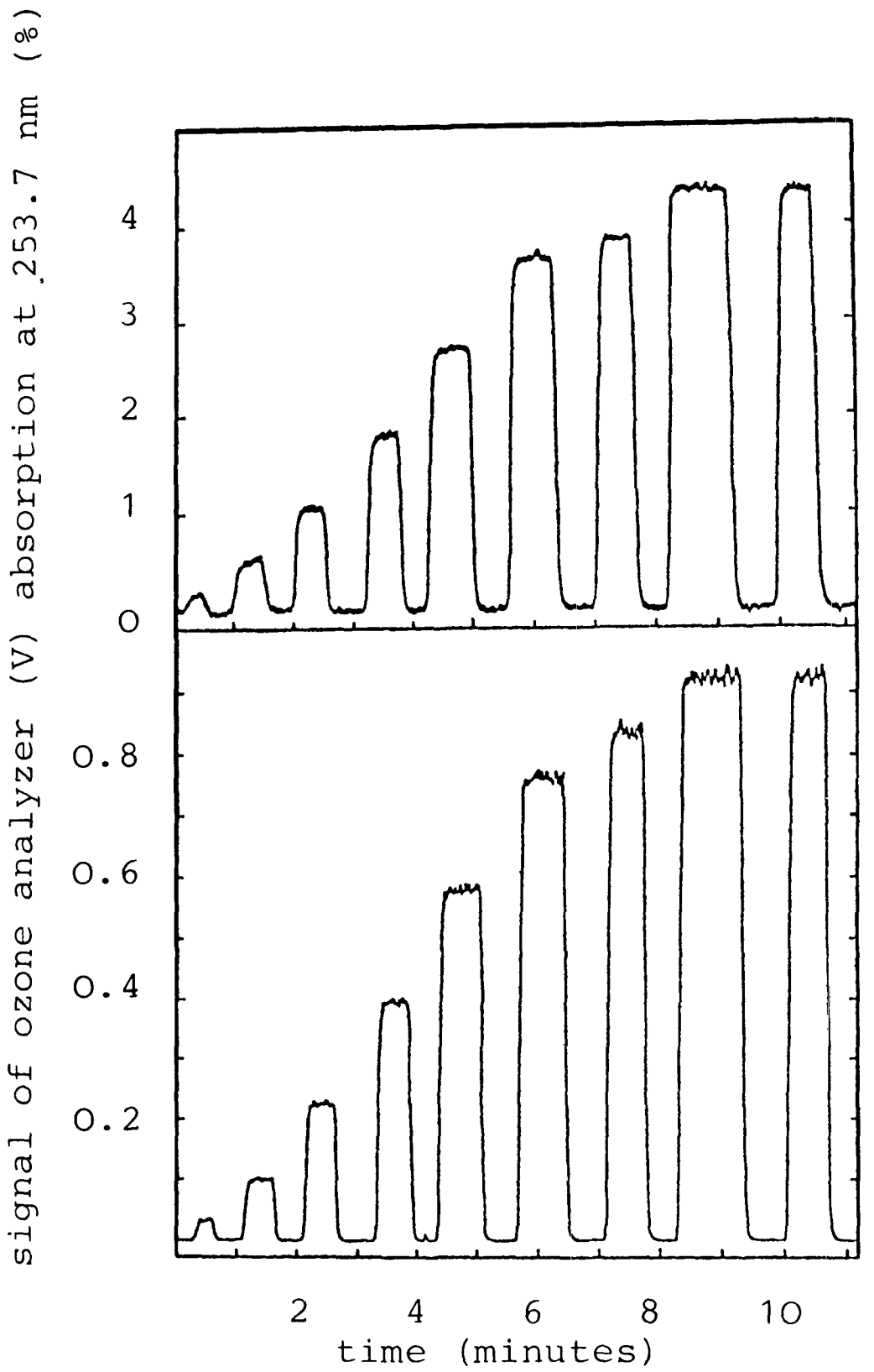

Figure 3. Calibration curve, calculated from the recordings in Figure 2.

ACKNOWLEDGEMENT

The authors express their thanks to J. Lobel and A. Wiese for their valuable assistance. The O_3 meter was developed as a part of a research programme on photochemical smog formation in the German Federal Republic, supported by the "Bundesministerium des Innern."

REFERENCES

1. Becker, K. H., and U. Schurath. Entsteht Photochemischer "Smog" in der Bundesrepublik Deutschland? Umschau 73:310, 1973.
2. Leithe, W. Die Analyse der Luft und ihrer Verunreinigungen in der freien Atmosphäre und am Arbeitplatz. Wissenschaftliche Verlagsgesellschaft mbH, Stuttgart, 1968.
3. Methods of Air Sampling and Analysis. Published by American Public Health Association, 1015 Eighteenth Street, N. W., Washington, D. C., 1972.
4. Perry, E. P., and D. H. Hern. Stoichiometry of ozone-iodine reaction: Significance of iodate formation. Envir. Sci. Technol. 7:65 and 647, 1973.
5. Becker, K. H., U. Schurath, and H. Seitz. Ozone-Olefin Reactions in the Gas Phase. 1. Rate Constants and Activation Energies. Int. J. Chem. Kinet. VI:725-739, 1974.
6. Hames, P. Thesis, Technische Universität München/DECHEMA Institut Frankfurt, 1975.
7. Hampson, R. F., Editor. Survey of photochemical and rate data for twenty-eight reactions of interest in atmospheric chemistry. J. Phys. Chem. Ref. Data 2:267-311, 1973.
8. Hudson, R. D. Critical review of ultraviolet photoabsorption cross sections for molecules of astrophysical interest. Rev. Geophys. Space Phys. 9:305, 1971.
9. Stephens, Edgar R., and Arthur M. Winer. The Oxidant Measurement Discrepancy. California Air Environment 6(1), 1975/76.
10. Schurath, U., and W. Wendler. Über die Verwendbarkeit von ozonhaltigem Sauerstoff zur Kalibrierung von Ozonanalysatoren. Staub-Reinhalt. Luft 35 (9):329-310, 1975.

STATUS OF CALIBRATION METHODS FOR OZONE MONITORS

R. J. Paur, R. K. Stevens, and D. L. Flamm*

ABSTRACT

The 1% neutral-buffered potassium iodide Federal Reference Method for calibrating ozone monitors has been widely criticized for its inconsistent results. The United States Environmental Protection Agency and other groups have examined other methods for determining ozone concentrations in calibrated atmospheres. The two most promising methods are ultraviolet photometry and gas phase titration. Ozone can be conveniently monitored by ultraviolet absorption photometry due to its strong broad absorption band in the 200-300 nanometer region. The gas phase titration technique relies on the well known reaction of nitrogen oxide with ozone. Gas phase titration and ultraviolet photometry yield comparable results over an ozone concentration range of 0.05 to 0.7 ppm. Recently, under Environmental Protection Agency sponsorship, a modified potassium iodide method has been developed. In preliminary studies, the new method appears to be accurate and precise over the ozone concentration range of 0.1 to 1.0 ppm.

INTRODUCTION

The Federal Reference Method for determining ozone (O_3) concentrations in synthetic atmospheres used to calibrate O_3 monitors is the 1% neutral-buffered potassium iodide (1% NBKI) procedure as described in the Federal Register 36 (228): 22384-22397, November 25, 1971. This calibration method is based on the spectrophotometric determination of iodine released from an NBKI absorbing solution of O_3.

The 1% NBKI method has been widely criticized for its inconsistent results. (See Figure 1.) In late 1973 it was discovered that state and local agencies in the Los Angeles area were obtaining significantly different estimates of O_3 concentrations in that area. These differences were traced to different KI calibration methods used by the various agencies. As a result of those findings, some half dozen studies have been carried out since mid 1974 to determine the accuracy of various KI methods. The results of some of these studies are summarized in Table 1.

*R. J. Paur, R. K. Stevens, Environmental Protection Agency, Research Triangle Park, North Carolina.
D. L. Flamm, Texas A&M University, College Station, Texas.

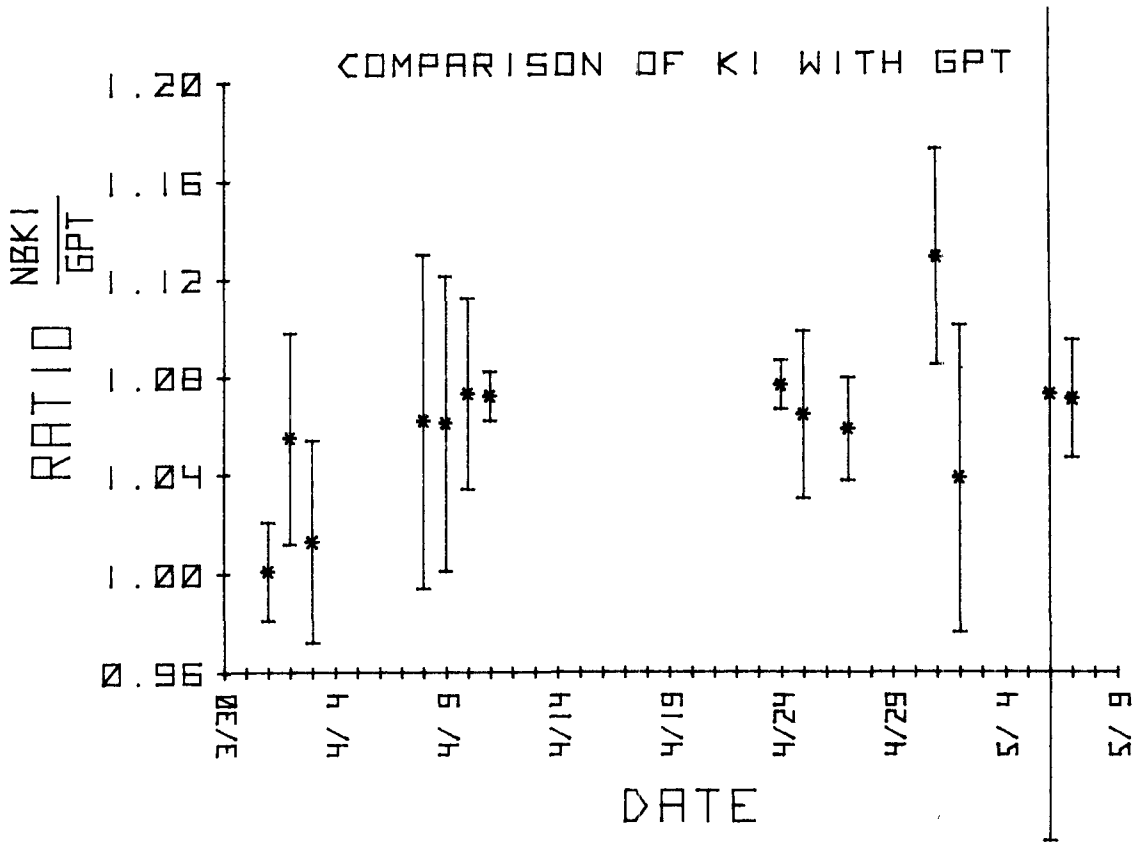

Figure 1. Comparison of potassium iodide with gas phase titration.

Table 1 illustrates that the 1% NBKI method run under dry conditions (i.e. the Federal Reference Calibration Method) gives results approximately 10% greater than ultraviolet (UV) photometry or gas phase titration (GPT). It should be remembered that all of these studies were run under ideal conditions, and that in normal usage the precision of the method may well be less than that indicated by the Table.

In addition to the KI studies, the U.S. Environmental Protection Agency (EPA) and other groups have examined several other methods for determining the O_3 content of calibration atmospheres. Two of these methods, UV photometry and GPT, have been in use for some time and are generally considered to be valid methods. A third method, 1% boric acid buffered potassium iodide (1% BAKI) is new and is in the preliminary stages of evaluation.

ULTRAVIOLET PHOTOMETRY

Ozone lends itself to UV photometry due to its strong broad absorption band in the 200 to 300 nanometer (nm) region. The peak of this band very nearly coincides with the 254 nm radiation of low pressure mercury (Hg) discharges. In spite of the high absorptivity of O_3 at 254 nm (133.9 cm^{-1} atm^{-1}, base 10), the UV photometer must have capability to resolve changes in transmittance of less than 1 part in 10^4 if ozone concentrations to within 5

TABLE 1. COMPARISON OF VARIOUS KI DETERMINATIONS WITH UV PHOTOMETRY OR GAS PHASE TITRATION

Study	KI Method	Reference Method	Ratio[c] $\frac{KI}{Reference}$	O_3 Conc. Range, ppm	Relative Humidity
Baumgardner, et al	1% NBKI	GPT	1.01 ± 0.04	0.1 - 0.5	0
Baumgardner, et al	2% NBKI	GPT	1.04 ± 0.03	0.1 - 0.5	0
Baumgardner, et al	2% NBKI	GPT	0.61 ± 0.04	0.1 - 0.5	0
Baumgardner, Paur	1% NBKI	GPT	1.05 ± .05	0.4	0
Baumgardner, Paur	1% NBKI	GPT	1.12 ± .07	0.4	40-60%
Baumgardner, Paur	2% NBKI	GPT	1.13 ± .03	0.4	0
Baumgardner, Paur	2% NBKI	GPT	1.18 ± .05	0.4	40-60%
CARB, El Monte	1% NBKI	UV	1.25 a	0.1 - 0.8	50%
	2% NBKI	UV	1.29 a	0.1 - 0.8	50%
	2% UBKI	UV	0.96 a	0.1 - 0.8	50%
Hodgeson	1% NBKI	UV	1.11 ± .01	0.05-10.1	0
Beard	1% NBKI	GPT	1.08 ± .035	0.08- 0.8	0
Smith	1% NBKI	GPT	1.11 ± .02	0.2 - 0.4	0
Hughes	1% NBKI	GPT	1.0 b	0.2 - 0.4	0

a. These workers also report intercept data which indicates a constant additive bias.
b. Variable depending on sampling time and color development time.
c. There is no absolute standard for ozone in the sub-part-per-million range. Therefore, precision of calibration procedures is determined by the reproducibility of measurements while the stability of the ozone concentration is monitored by ambient air ozone monitors. The accuracy of ozone calibration procedures at the sub-ppm level is estimated from the degree of agreement between two or more procedures that are accurate at ozone concentrations which can be monitored manometrically. UV photometry and gas phase titration are methods of high precision; they are accurate at high ozone concentrations; they agree well at sub-ppm ozone concentrations so they are assumed to be accurate at low concentrations. For these reasons the results of most potassium iodide studies are reported in terms of KI values relative to UV photometry or gas phase titration values.

ppb using a pathlength consistent with an easily portable instrument are to be measured. At least one such photometer, which with minor modifications appears to have the capacity for suitable accuracy, is commercially available.

GAS PHASE TITRATION

Gas phase titration techniques rely on the well known reaction of O_3 with nitric oxide (NO):

$$nNO + mO_3 \rightarrow mNO_2 + mO_2 + (n - m)NO$$

The reaction can be monitored by determining either the amount of NO consumed or the amount of nitrogen dioxide (NO_2) produced. Standard reference materials (SRM) for NO are available from the National Bureau of Standards (NBS) in the form of cylinders containing 50 to 100 ppm NO in nitrogen (N). A nitrogen dioxide (NO_2) SRM is available in the form of a permeation tube. In addition to NO and/or NO_2 standards of known accuracy, GPT methods generally require accurate flow measurements to determine the degree of dilution of the standard in the calibration system.

Figure 2 presents a typical comparison of O_3 concentrations determined by UV photometry and GPT. The slope of the curve is approximately unity and the small scatter about the curve attests to the precision of both analyses. Results similar to those in Figure 2 have been obtained in several laboratories and are summarized in Table 2.

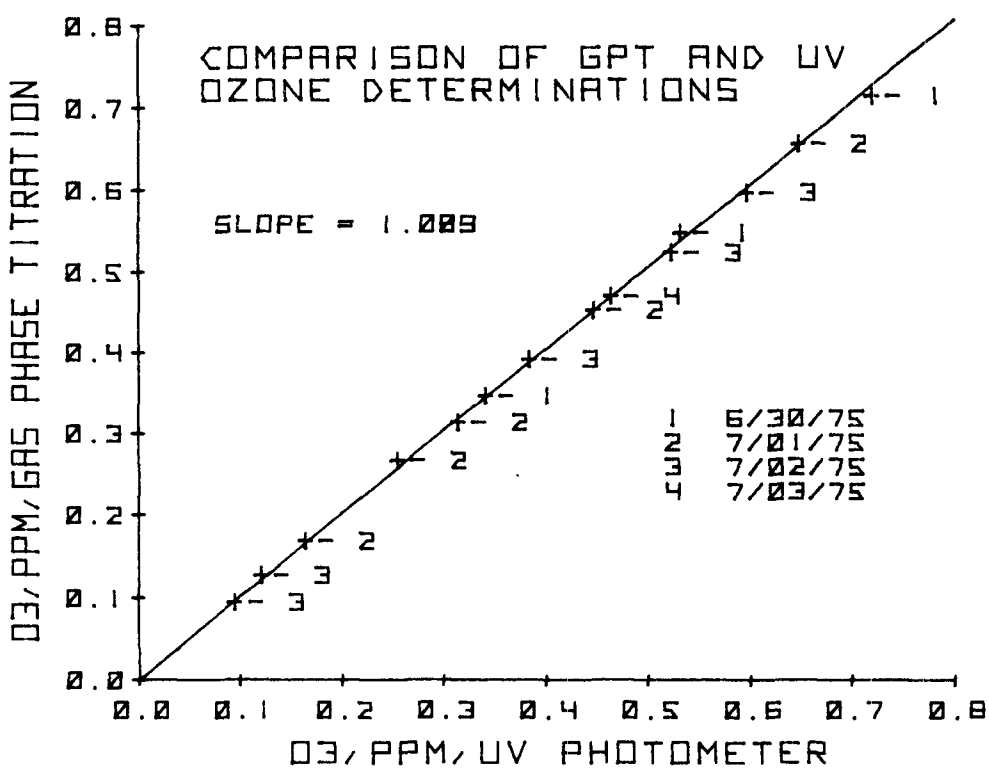

Figure 2. Comparison of gas phase titration and UV ozone determination.

TABLE 2. COMPARISON OF OZONE DETERMINATIONS BY GAS PHASE TITRATION WITH UV PHOTOMETRY

Study	O_3 Con. Range, ppm	Results
Paur*	0.06 - 0.7	$(O_3)_{GPT} = (1.009 \pm .004)\ (O_3)_{UV} - (0.002 \pm 0.002)$
		$(O_3)_{GPT} = (1.001 \pm .007)\ (O_3)_{UV} - (0.005 \pm 0.003)$
DeMore	0 - 1	$(O_3)_{GPT} = (1.00 \pm .02)\ (O_3)_{UV}$
Hodgeson	0 - 10	$(O_3)_{GPT} = (1.00 \pm .02)\ (O_3)_{UV}$
Stedman		$(O_3)_{GPT} = (1.0)\ (O_3)_{UV}$

* Two separate 4-day studies using different NO standards and different system flows.

BORIC ACID POTASSIUM IODIDE

The 1% boric acid potassium iodide (BAKI) method is similar to the 1% NBKI method except for replacing the phosphate buffer with 0.1 M boric acid. The results obtained from the BAKI method differ from the NBKI results in several important aspects.

The NBKI method yields results some 10 percent greater than the BAKI method at the 0.5 and 1.0 ppm levels. In studies conducted at Texas A&M University, the BAKI results were in good ($\pm$ 3 percent) agreement with a Dasibi O_3 monitor set up to run as an absolute photometer. This Dasibi instrument was later compared with an O_3 calibration system at EPA headquarters in Research Triangle Park, N.C. (EPA/RTP) and results agreed to within $\pm$ 2 percent.

The color development of the NBKI method continues for some 15-30 minutes or more after completion of sampling, and by the end of color development the NBKI results may be more than 20% greater than the photometer results. In contrast the BAKI color development appears to be stable by the time the absorbing solution can be transferred to curvettes. The change in absorbance in the NBKI method may be due to decomposition of an intermediate species formed during sampling. A preliminary study of this phenomena indicates that decomposition of hydrogen peroxide occurs at approximately the same rate as is required to explain the time dependence of the absorbance.

The Texas A&M studies also indicate that the BAKI method yields the same

results when using fritted bubblers as when using "midget impingers"; the NBKI method has been criticized for yielding different results with different kinds of absorber glassware.

A preliminary study of the BAKI method has been carried out in the EPA/RTP laboratories to compare BAKI results with an O_3 calibration system that utilizes both GPT and UV photometry to provide a reliable estimate of the O_3 concentration. For 50 data points (29 at ~500 ppb, 6 at ~250 ppb and 15 at ~120 ppb), the average ratio of BAKI results to photometric results was 1.016 with a standard deviation for the ratio of 3 percent.

The new BAKI method is currently being examined with respect to its stability under changes in relative humidity. Further studies will examine the sensitivity of the method to impurities in the reagents. This last point is of particular interest since the BAKI results were approximately 10% lower than the photometric results at the 0.1 ppm level in the Texas A&M study; the ratio of BAKI results to UV photometry results did not show any discernible concentration dependence in the EPA/RTP results.

SESSION 3

SOURCES OF TROPOSPHERIC OZONE - I

Chairman: R.A. Rasmussen
Washington State University

METEOROLOGICAL CONDITIONS CONDUCIVE TO HIGH LEVELS OF OZONE

T. R. Karl and G. A. DeMarrais*

ABSTRACT

Aerometric data are considered for two locations: Los Angeles and St. Louis. Numerous studies of photochemical oxidant, often called Los Angeles smog, are brought together to depict the meteorological effects on ozone concentrations. Recently obtained data from the Environmental Protection Agency's Regional Air Pollution Study are subjected to regression analyses to sort out the meteorological variables that are conducive to high levels of surface ozone.

INTRODUCTION

The ozone/oxidant problem, starting with a plant damage investigation (1), has been studied for 30 years. The photochemical aspects were partially understood a quarter-century ago (2). Beginning with specialized forecasts in 1952 and daily forecasts in 1953, the meteorologist was predicting when ozone concentrations [O_3] would be bothersome to people (3). By 1954, there was a compendium on the meteorological aspects of the ozone problem in Los Angeles (4) and a report on one of the largest field programs on the three dimensional variation of oxidant and meteorology in the LA Basin (5). Space limitations prevent the enumeration of all the field studies that have been conducted, but the spatial coverage and results indicate that high [O_3] are a nationwide affliction.

Observed levels of [O_3] are higher in California than in the rest of the nation. The literature on the meteorological aspects of the ozone problem in California, particularly in the LA Basin, is plentiful, but a composite picture does not exist. Such a picture, based on existing information, is presented in this paper and will be referred to as the Pipe-Mix Model.

A second major section of this report is an examination of various meteorological variables related to [O_3] for a 25-station network in St. Louis (STL). This data set was chosen for study because of the high quality and large quantity of aerometric data within an urban and rural environment outside the LA area.

THE PIPE-MIX MODEL OF THE LOS ANGELES OXIDANT PROBLEM

A review of the literature indicated that an understanding of various

*Environmental Protection Agency, Research Triangle Park, North Carolina. The authors are on assignment with EPA from the National Oceanic and Atmospheric Administration, U.S. Department of Commerce.

parts of the ozone problem in LA existed. There are two main meteorological processes contributing directly to the problem--horizontal transport and vertical mixing (abundant solar radiation away from the immediate coast is an everyday phenomenon in the Basin in the summer, so its contribution to $[O_3]$ does not vary). The horizontal transport aspect has been called the "pipe reactor effect" (6). Vertical mixing accounts for the mixing of air aloft with that at the surface. The detailed descriptions and pictorial presentations that follow are called the Pipe-Mix Model (July conditions are presented).

The basic elements in the Pipe Reactor Effect (Figure 1) are:

- The average wind speed in the Basin is 7 mph (7).
- Sunlight is of sufficient intensity to initiate photochemical reactions early in the morning (8).
- Production exceeds destruction of ozone in this contaminated layer during the period 2 to 7 hours after the photochemical reaction is initiated (9). The time when the production first exceeds destruction (in the summer) is around 8 a.m. (8).
- The daytime surface wind patterns are so persistent that the reactive air mass moving downwind under the subsidence inversion can be considered as moving in a pipe (6).

This pipe reactor effect means:

- Primary emissions in upstream locations result in problems further down the pipe, and
- The resulting $[O_3]$ are cumulative.

The basic elements in the Vertical Mixing Effect (Figure 2) are:

- There is a reservoir of ozone aloft that can be brought down by vertical mixing. In 1954, ozone aloft was restricted to the volume below the inversion base (5), but now the inversion is a major reservoir of ozone aloft (10, 11, 12).
- The reservoir extends from Coastal Ventura and Los Angeles County to the mountains north and east of Los Angeles. Its presence to the west and northwest of Los Angeles was shown by Lea (10). The movement from Los Angeles to Coastal Ventura County was shown to occur by Kauper and Niemann (13). Winds aloft data during nighttime hours for Santa Monica and Long Beach (14) show that this movement is a frequent occurrence. During the day the movement is in the opposite direction and the highest concentrations in the Basin are generally over the eastern part (11, 12).
- $[O_3]$ aloft remain relatively high throughout the night (10, 15, 16), as there is very little ozone destruction aloft.

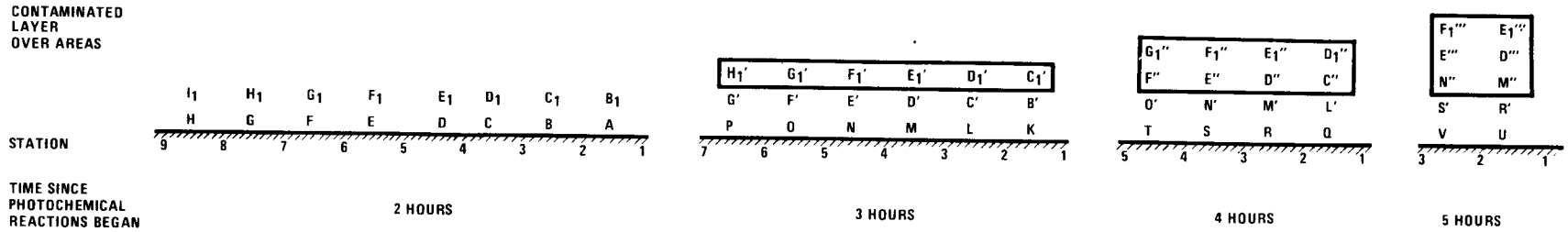

LEGEND

NUMBERS = STATIONS IN A DOWNWIND DIRECTION, 7 MILES APART, FROM 9 TO 1, WIND SPEED IS 7 mph.

LETTER = (WITHOUT SUBSCRIPT OR PRIME MARK) PRIMARY EMISSION DURING HOUR IN LAYER BETWEEN STATIONS

SUBSCRIPT = EMISSION FOR PRIOR HOUR (FIRST HOUR AFTER INITIATION OF PHOTOCHEMICAL REACTIONS) PLUS RESIDUE FROM EARLIER HOURS

PRIME MARKS = EACH MARK INDICATES AN ADDITIONAL HOUR OF PHOTOCHEMICAL REACTIONS

BOXED AREA = UPWIND CONTRIBUTION TO LOCAL OZONE CONCENTRATIONS

ASSUMPTION = OZONE PRODUCTION EXCEEDS DESTRUCTION WITHIN A LAYER STARTING AT 2 HOURS AFTER INITIATION OF PHOTOCHEMICAL REACTIONS

Figure 1. Pipe reactor effect (downwind transport in Los Angeles in July).

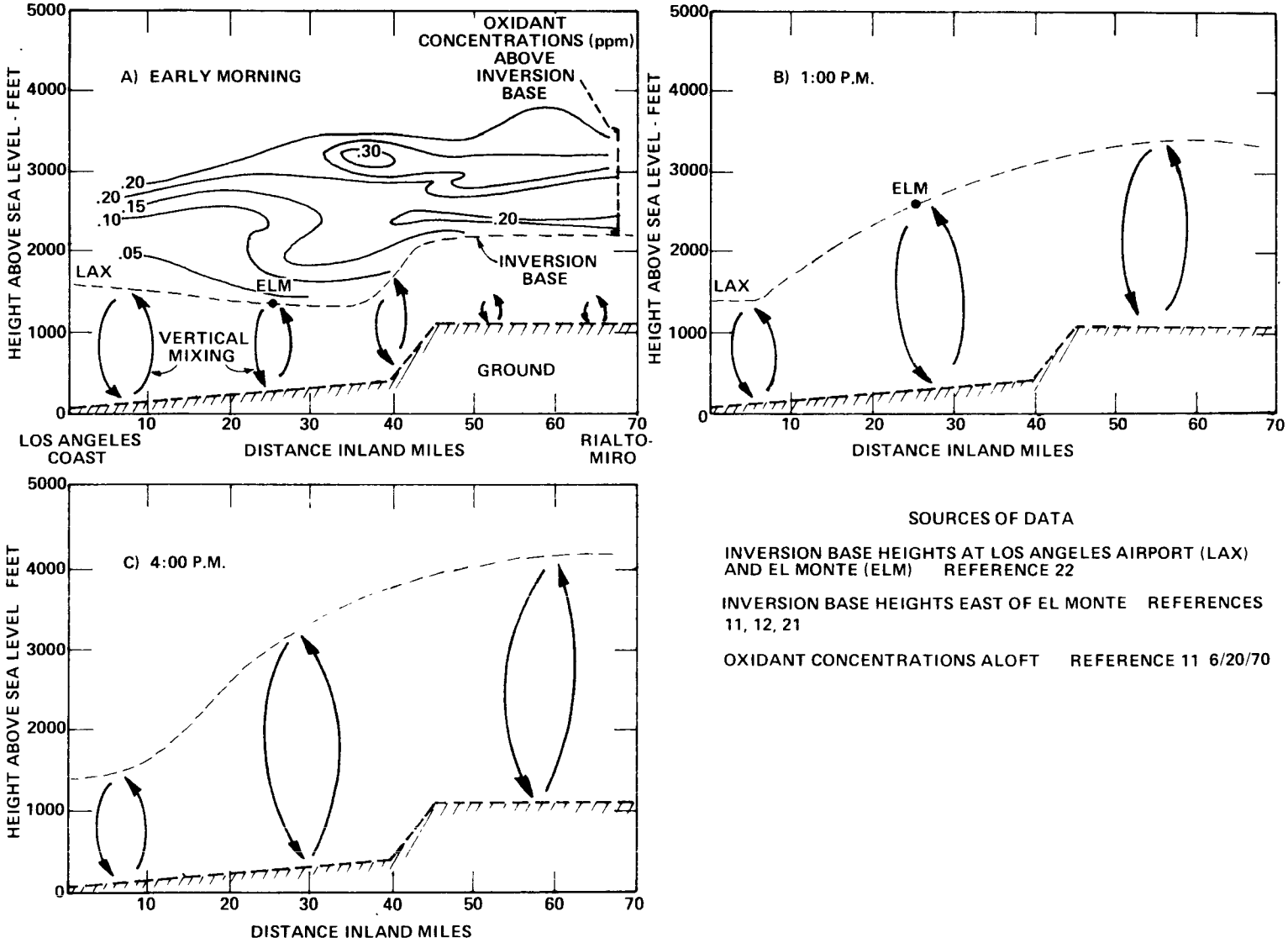

Figure 2. Daytime variations in inversion base heights and vertical mixing, summer day, Los Angeles coast to Rialto-Miro, July.

- $[O_3]$ aloft vary spatially and from day to day (10, 11, 12, 15). The spatial variations are due to the various methods and places through which the ozone gets into the layer aloft (10, 11, 17). Prediction techniques based on historical data (18, 19, 20) show that the highest ground level concentrations occur when the 500-mb level (on the average, about 5.6 km above the surface) is relatively high, is warm, and is marked by a weak pressure gradient. This condition would likewise mean that the air aloft is stagnant (ozone accumulates). Variations in rates of accumulation account for day-to-day differences in concentrations aloft.

- Vertical mixing extends to much greater heights over the eastern than over the western part of the Basin during the day (11, 12, 21). Climatological data (7) for the Basin show the average diurnal temperature ranges are 10° to 15°F in the western areas, whereas they are 30° to 38°F in a very large part of the eastern section. Surface-based inversions with negligible vertical mixing occur almost every night where the range of temperatures is large and are relatively infrequent in the west in July.

- Vertical mixing that gives a dilution benefit when it mixes surface air with cleaner air aloft is a detriment when the concentrations aloft are higher than those at the surface. In the western part of the Basin, because the increase in mixing height is small during the day (22) and because the $[O_3]$ in the affected volume aloft are relatively low, the ground level concentrations are not increased markedly in the typical situation (occasionally easterly winds aloft move the higher concentrations to the west and vertical mixing brings the high concentrations to the ground) (16). In the east, where the daytime mixing occurs to greater heights and the $[O_3]$ aloft are relatively high, the ground level concentrations can be increased markedly.

The combined parts of the pipe-mix model demonstrate the synergistic effect of the two meteorological parameters, horizontal transport and vertical mixing, in the observed levels of $[O_3]$ in the area.

METEOROLOGICAL CONDITIONS RELATED TO OZONE CONCENTRATIONS IN ST. LOUIS

DATA

As part of the Environmental Protection Agency's (EPA) Regional Air Pollution Study (RAPS) in St. Louis, a network of 25 Regional Air Monitoring Stations (RAMS) continuously record aerometric data. Surface measurements of $[O_3]$, wind direction and speed, and global radiation (global radiation is defined as the total of direct plus diffuse sky radiation received by a unit horizontal surface), as well as the vertical temperature gradient near the surface (5 to 30 meters), were derived from the RAMS network during the period July 1, 1975 through September 15, 1975. The locations of the stations in the network and their associated land use are shown in Figure 3.

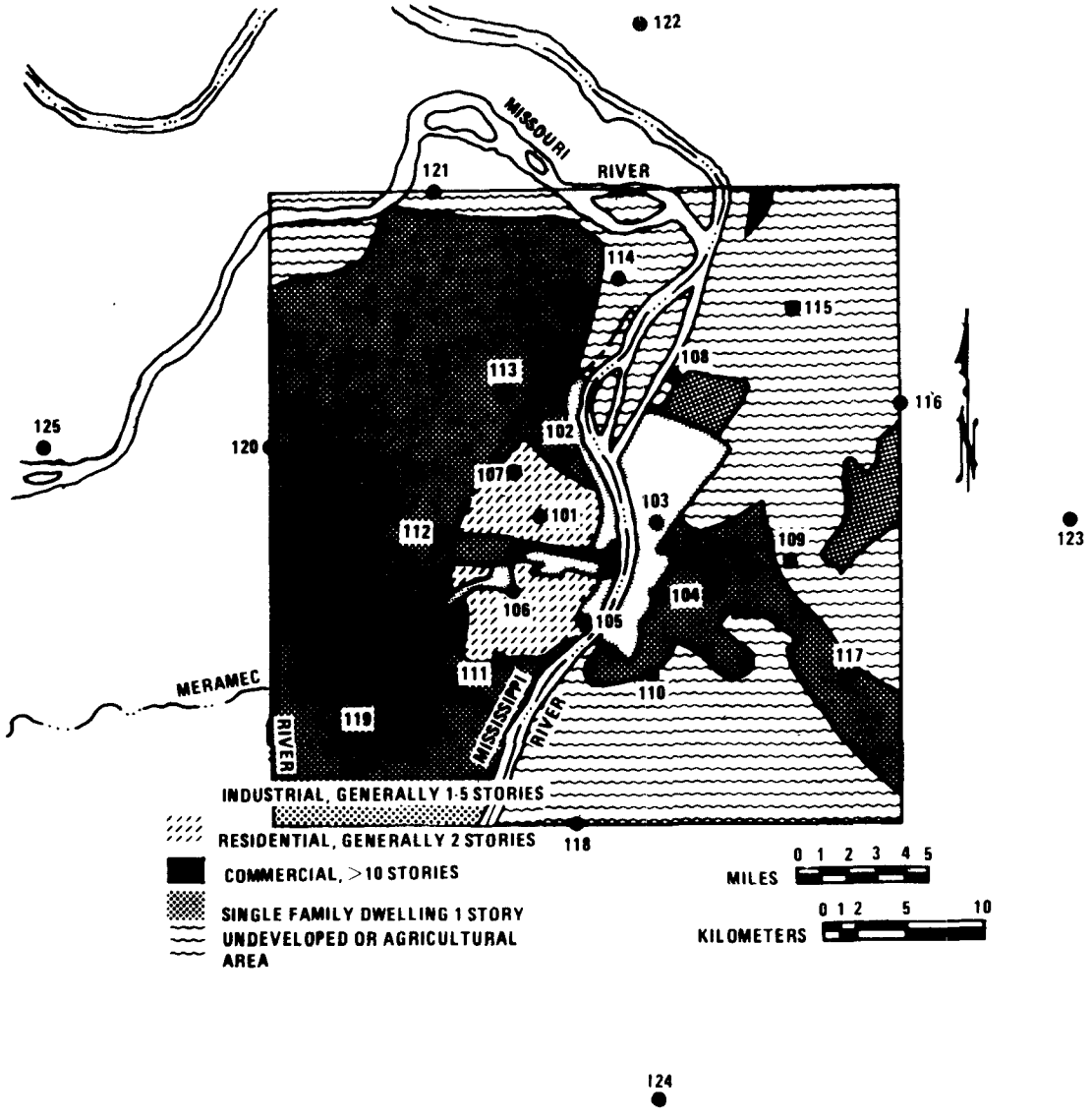

Figure 3. Station locations and land use in the St. Louis area (modified from Reference 23).

Additional data were acquired from the National Weather Service at Lambert Airport, which is approximately 5 km northeast of Station 120. Synoptic charts of various other meteorological variables, prepared by the National Meteorological Center, were also employed.

In the RAMS network each station was visited at least twice weekly for routine maintenance. The data from each station were checked by computer programs (24) and by visual inspection to eliminate erroneous values.

RESULTS OF THE ANALYSIS

A stepwise regression technique was employed as a means of sorting out the role played by various meteorological variables with regard to surface

$[O_3]$. At each station ozone concentration was used as the dependent variable. Table 1 lists all the variables subject to entry into the regression equations.

TABLE 1. VARIABLES SUBJECT TO ENTRY INTO THE REGRESSION EQUATION

$[\overline{O_3}]$ -- AVERAGE OZONE CONCENTRATION (ppb) BETWEEN 1000 AND 1500 LOCAL DAYLIGHT TIME (LDT).

TMAX -- DAILY MAXIMUM TEMPERATURE AT LAMBERT AIRPORT (°C).

WS -- AVERAGE SURFACE WINDSPEED (m/sec) ACROSS THE RAMS NETWORK BETWEEN 0800 AND 1500 LDT

$\sqrt{\text{PRECIP}}$ -- SQUARE ROOT OF THE NUMBER OF DAYS SINCE THE LAST MEASURABLE PRECIPITATION OCCURRED AT LAMBERT AIRPORT

$\sqrt{\text{RAD}}$ -- SQUARE ROOT OF 10 TIMES THE AVERAGE GLOBAL RADIATION (lang/min) BETWEEN 0800 AND 1500 LDT DETERMINED FROM STATIONS 103, 104, 107, 114, 118, AND 122.

$\sqrt{\text{FRONT}}$ -- SQUARE ROOT OF THE NUMBER OF DAYS SINCE THE LAST COLD FRONT PASSED ST. LOUIS

HT500 -- HEIGHT OF THE 500 mb SURFACE (FEET ABOVE SEA LEVEL) OVER ST. LOUIS AT 0700 LDT

ΔHT500 -- 24-HOUR CHANGE (FEET) IN THE HEIGHT OF THE 500-mb SURFACE FROM THE PREVIOUS 0700 LDT OBSERVATION.

ΔT -- TEMPERATURE (°C) AT 30 METERS MINUS THE TEMPERATURE AT 5 METERS AVERAGED ACROSS STATIONS 109, 111, AND 112 DURING THE PERIOD 1000 TO 1500 LDT.

YNRAIN -- REPRESENTS WHETHER OR NOT MEASURABLE PRECIPITATION FELL BETWEEN 1000 AND 1500 LDT. THE VARIABLE EQUALS 1 IF IT DID OCCUR AND 0 IF IT DID NOT OCCUR.

WD -- FRACTION OF TIME DURING THE PERIOD 0800 TO 1500 LDT WHEN THE SURFACE WIND BLEW ≥ 1 m/sec FROM THE EIGHT SECTORS LISTED BELOW. WIND DIRECTION WAS DETERMINED BY AVERAGING ALL 25 STATIONS.

VARIABLE	SECTOR (+22.5°)	VARIABLE	SECTOR (+22.5°)
N	360°	S	180°
NE	45°	SW	225°
E	90°	W	270°
SE	135°	NW	315°

CALM -- FRACTION OF TIME DURING THE PERIOD 0800 TO 1500 LDT WHEN THE SURFACE WIND SPEED IN THE RAMS NETWORK AVERAGED ≤ 1 m/sec.

VORT500 -- AVERAGE VORTICITY (sec^{-1}) AT 500 mb OVER ST. LOUIS BASED ON THE 0700 AND 1900 LDT 500-mb VORTICITY CHARTS.

ΔVORT500 -- 12-HOUR CHANGE IN VORTICITY (sec^{-1}) AT 500 mb BETWEEN 0700 AND 1900 LDT.

Table 2 lists the importance of each variable at the various stations as determined by their F ratios (25) in the final step of the regression technique. The F ratio associated with each independent variable is a measure of the additional variance explained by the variable not accounted for by the other variables already in the regression equation. In this technique, F ratios were computed for each variable and a step was made by the inclusion of a variable with a significant F ratio or the deletion of a variable when its F ratio had become insignificant due to the inclusion of other variables. The final step occurred when the remaining variables (those without ranks in Table 2) had F ratios that were statistically insignificant at the 1% significance level (25). The signs (+ or -) in Table 2 on top of each ranked variable indicate the sign of the coefficient in the final equation. For wind direction (WD) the significant sector is listed above the rank along with its sign. At some stations there are two significant wind directions. For these stations the rank is listed for the more significant of the two. It should be noted that for the three variables, global radiation ($\sqrt{RAD}$), the number of days since the last frontal passage ($\sqrt{FRONT}$), and the number of days since the last measurable precipitation occurred ($\sqrt{PRECIP}$), the square roots of the variables were found to be more effective predictors of average ozone concentrations [$\overline{O}_3$] than linear predictors. There are sound physical reasons for this type of an approach. In general, meteorological conditions change rapidly during and shortly after the passage of a front or a significant rainfall, as opposed to several days after their occurrence. One reason why the global radiation is not linearly correlated to [$\overline{O}_3$] in STL is because often the most intense global radiation occurs when dispersion is good, i.e., after a frontal passage.

TABLE 2. THE RELATIVE IMPORTANCE OF VARIOUS VARIABLES IN THE FINAL STEP OF THE REGRESSION EQUATION

STATIONS / VARIABLES	101	102	103	104	105	106	107	108	109	110	111	112	113	114	115	116	117	118	119	120	121	122	123	124	125
TMAX	+1	+1	+1	+1	+4	+4	+1	+1	+1	+1			+3	+1	+4	+1	+1		+2	+6	+1		-1		
WS	-4	-2	-2	-3	-3	-2	-2	-2	-3	-3	-3	-4	-5	-2	-2	-4	-3		-4	-2	-2		-5		
WD	-S 2		S 4				-S +NW 4	-S +SW 4		-S -SW 4	+NW +W 4	-SW 6	+SE 7	+SW 6	+SW 3	-S 2		+NE -S 3	+NE 1		-N +SE 4	+S 4	-S 3	+NW 2	+E 6
$\sqrt{PRECIP}$	+3		+3	+2	+2		+3		+2	+2			+4	+4		+3	+2	+1	+3	+5		+2			+3
HT 500				+5	+5	+1					+1	+1			+5			+2		+3		+1			+1
$\sqrt{RAD}$		+3	+5		+1	+3		+3			+2	+2	+1	+7	+1					+1					+4
CALM								+5	+4	+5	+5		-4	+5			+5								
VORT 500				+4														+5						-1	+2
$\sqrt{FRONT}$													+2					+4		+4			+2		
HT 500							+5					5		+3											
T					+6							-3	+6				+4								+5
YN RAIN																					-3	-3	4		
Δ VORT 500																									-7
VARIANCE EXPLAINED BY RANKED VARIABLES	59	64	80	77	75	65	71	67	64	71	69	84	68	69	75	67	65	87	66	88	69	68	85	40	81
SAMPLE SIZE	53	69	47	50	57	61	51	65	61	59	56	41	63	61	36	43	48	29	64	37	55	40	28	34	44

It is immediately apparent that the importance of each variable can vary considerably from station to station. Some of this variability can be attributed to the fact that data were available at some stations and not others on any given day. However, in general the maximum temperature (TMAX) and the wind speed (WS) are the most important predictors of $[\overline{O}_3]$ in the RAMS network. WS is important since it has the direct effect of diluting the pollutant. Looking more closely at Table 2, it appears that WS is of less importance as a predictor of $[O_3]$ at rural stations. However, at these stations the effects of dilution, low concentrations at high wind speeds, and high concentrations at low wind speeds are combined with the effects of advection from the city to give a non-linear relationship with $[\overline{O}_3]$.

There are several reasons for TMAX showing up as an important variable. Laboratory results have shown that ozone production is temperature dependent (26). However, the maximum temperature is a surrogate for various other meteorological variables. The most obvious one in the summertime is global radiation. There is a significant positive correlation between $\sqrt{RAD}$ and TMAX. The maximum temperature is also related to changes in air masses. For example, a cold frontal passage with its good dispersion characteristics and cleaner air is followed by several days with lower daily maximum temperatures. Additionally, lower maximum temperatures are observed with rain falling within the time span between 1000 and 1500 LDT, which is the time span used to obtain the $[\overline{O}_3]$. Rain occurring during these hours is associated with low $[\overline{O}_3]$. Furthermore, since high temperatures are not observed until several days after a cold frontal passage, there would be sufficient time for the build-up of ozone throughout the low troposphere, and the high surface temperature would be conducive to mixing this ozone down to the surface.

WD frequently appears as being significant in the regression equations. The effects of near-surface advection and the weather associated with the wind blowing from particular directions are combined here. In order to illustrate these effects, Figure 4 shows, for three representative stations, the correlation coefficients of WD with $[\overline{O}_3]$ and another curve that shows the approximate magnitude of the coefficients if transport from the city is not important. This last curve was obtained by considering the correlations of WD and $[\overline{O}_3]$ at all 25 stations. Because the stations are very nearly equally distributed around the city center, the unshaded curve on Figure 4 represents the correlation coefficients that can be attributed to "weather" or climate. This curve should be considered relative to the shaded curve in order to see if transport of ozone and/or its precursors from the city to outlying areas does occur. Figure 4 shows that the higher $[\overline{O}_3]$ at Stations 118 and 121 are associated with winds blowing from the city. Referring back to Table 2, it is not surprising to see WD ranked high in significance, because advection of ozone and/or it precursors from the city cannot be accounted for by any other variable. The sector of significant WD and the sign of the coefficients included in the regression equation on the final step can be explained in terms of advection from the city and "weather." However, Stations 101, 103, 107, and 108 elude explanation. At these stations, wind direction variables might have entered the equations by pure chance or local influences such as a nitrogen oxide plume could have influenced the $[\overline{O}_3]$.

Meteorological variables other than TMAX, WS, and WD that appear in the regression equations with about equal frequency and rank are HT500, $\sqrt{PRECIP}$,

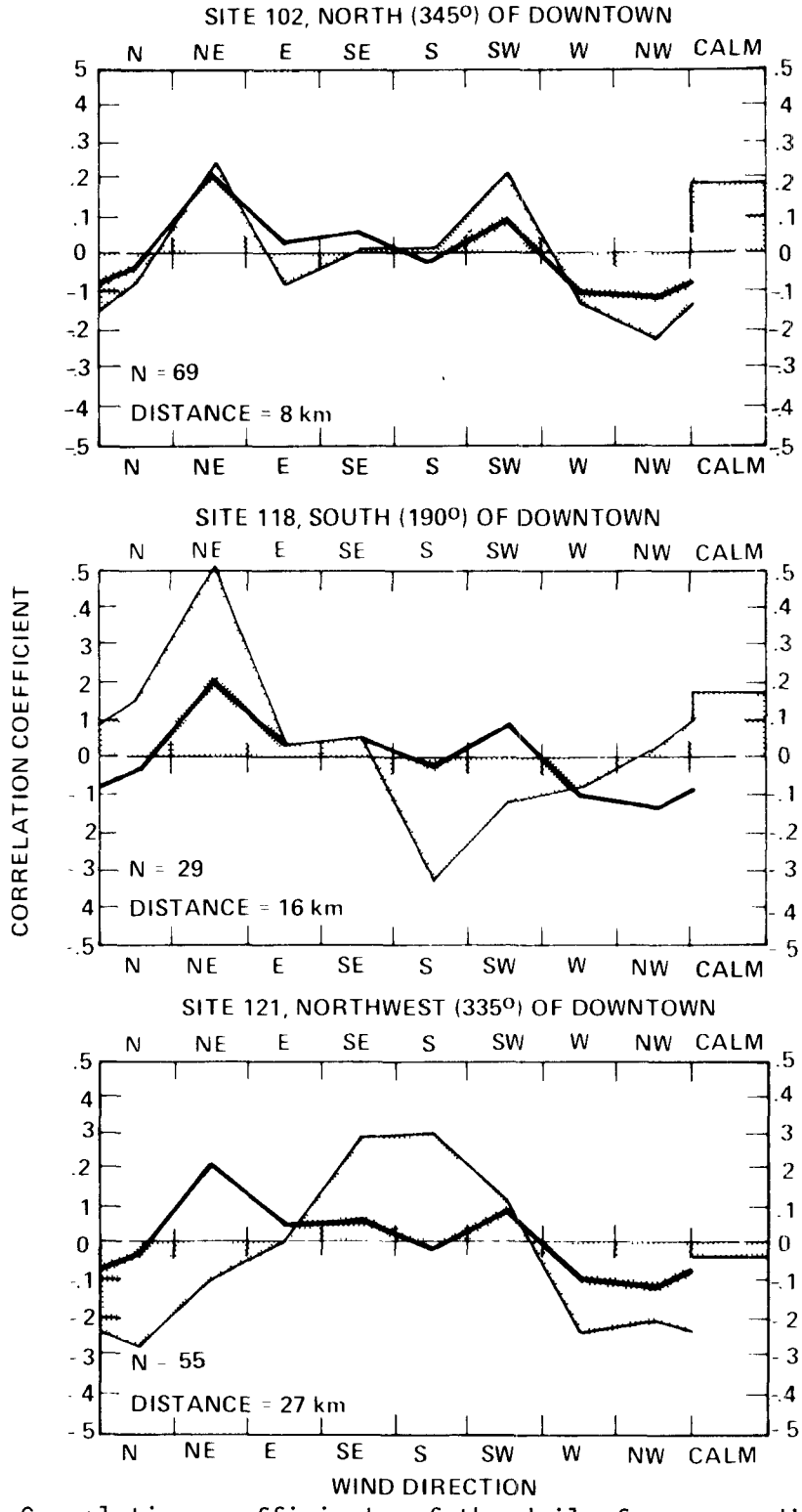

Figure 4. Correlation coefficients of the daily frequency distribution of wind direction (WD) and calm (CALM) with ozone concentrations - shaded; equally weighted average correlation coefficients derived from all 25 stations - unshaded. Distance is given from downtown St. Louis at Stations 102, 118, and 121.

and $\sqrt{RAD}$. The height of the 500-mb surface HT500 serves much the same purpose in explaining $[\overline{O_3}]$ as does TMAX. In fact, four out of five times when HT500 ranked as the most significant variable in the regression equation, TMAX did not even rank significantly as an important variable. It was somewhat surprising to see $\sqrt{PRECIP}$ rank high in significance so often. However, it should be noted that $\sqrt{PRECIP}$ shows a significant correlation with $\sqrt{RAD}$ (approximately 0.45). Upon further investigation of the results in Table 2, the question arises of why the variable YNRAIN, which represents whether or not measurable precipitation occurred (Table 1), ranked so few times as compared to $\sqrt{PRECIP}$. YNRAIN is even more strongly correlated with $\sqrt{RAD}$ (approximately -0.65) than is $\sqrt{PRECIP}$. In addition, both YNRAIN and $\sqrt{PRECIP}$ are significantly correlated with the same variables included in the regression analyses. These results suggest that $\sqrt{PRECIP}$ accounts for a process not accounted for by YNRAIN. A plausible explanation for this is: summertime rainfall in STL (which is mostly convective) inhibits ozone production during the daytime, but in addition, after the rainfall, several days must pass before the return of meteorological conditions that are conducive to high levels of ozone. The variable $\sqrt{RAD}$, which is the driving mechanism for ozone production, frequently takes a "back seat" to the various other meteorological variables. Many of the reasons for this have already been cited. Primarily, the day-to-day variance in the global radiation received at the surface is highly correlated with other meteorological variables, TMAX, HT500, $\sqrt{PRECIP}$, YNRAIN, but in addition, these variables also represent other meteorological factors that influence $[\overline{O_3}]$.

The remaining variables in Table 2 deserve brief comment. First, it should be noted that sometimes the variable CALM, representing near calm winds, was included in the regression equations even when WS was already in the equation. Second, the stability very close to the ground (ΔT) appears to play a minor role in explaining $[\overline{O_3}]$ when other variables are used in combination with this variable. Third, there is no apparent physical reason for the sign of the vorticity at 500-mb (VORT500) at Stations 107, 118, and 125 to be positive. Lastly, at Station 112, when HT500 and ΔHT500 were both in the same equation, the coefficient of ΔHT500 was negative. This indicates a tendency for higher concentrations as the 500-mb ridge begins to break down.

CONCLUSIONS

Data has been analyzed from two metropolitan areas of differing climates. In each area there was a dense network of high-quality data. The following conclusions were reached from our analyses.

The proposed Pipe-Mix Model shows there are two meteorological processes, horizontal transport and vertical mixing, contributing to the LA ozone problem. The horizontal transport involves fairly well-known sources and photochemical reactions, whereas the vertical mixing involves a source of "second-hand" ozone that varies in concentration.

In the STL area, the combination of a few meteorological variables can explain, on the average, about 70% of the day-to-day variance in average ozone concentrations during hours of peak concentrations. Various combinations of the following variables were effective in this regard: (a) the daily

maximum temperature, (b) the wind speed, (c) the wind direction, (d) the number of days since the last measurable precipitation occurred, (e) the global radiation, and (f) the height of the 500-mb surface. Furthermore, it was confirmed that the near-surface advection of ozone and/or its precursors from the city does contribute to high ozone levels downwind of the city.

REFERENCES

1. Middleton, J.T., J.B. Kendrick, and H.W. Schwalm. Injury to Herbaceous Plants by Smog or Air Pollution. Plant Disease Reporter, 34 (9): 245-252, 1950.

2. Haagen-Smit, A. J. Chemistry and Physiology of Los Angeles Smog. Ind. Eng. Chem. 44 (6): 1342-1346, 1952.

3. Kauper, E.K., R.G. Holmes, and A.B. Street. Meteorological Variables and Objective Forecasting Techniques Relating to the Air Pollution Problem in Los Angeles. Technical Paper No. 15, Air Pollution Control District, Los Angeles, California, 1955. 15 pp.

4. Neiburger, M. and J. Edinger. Meteorology of the Los Angeles Basin. Report No. 1, Southern California Air Pollution Foundation, Los Angeles, California, 1954. 97 pp.

5. Renzetti, N.A., Editor. Aerometric Survey of the Los Angeles Basin. August-November 1954. Report No. 9, Air Pollution Foundation, Los Angeles, California, 1955. 334 pp.

6. Tiao, G.C., G.E.P. Box, and W.J. Hamming. Analysis of Los Angeles Photochemical Smog Data: A Statistical Overview. J. Air Poll. Control Assoc., 25 (3): 260-268, 1975.

7. U.S. Weather Bureau. Climatography of the United States No. 86-4 (Decennial Census, California, 1951-1960). U.S. Dept. of Commerce, Washington, D.C., 1964. 216 pp.

8. Hamming, W.J., R.L. Chass, J.E. Dickinson, and W.G. MacBeth. Motor Vehicle Control and Air Quality The Path to Clean Air for Los Angeles. Presented at the Meeting of the Air Pollution Control Association, Paper No. 73-73, Chicago, Illinois, June 1973. 19 pp.

9. Middleton, J.T. and A.J. Haagen-Smit. The Occurrence, Distribution and Significance of Photochemical Air Pollution in the U.S., Canada, and Mexico. J. Air Poll. Control Assoc., 11 (3): 129-134, 1961.

10. Lea, D.A. Vertical Ozone Distribution in the Lower Troposphere Near an Urban Pollution Complex. J. Appl. Meteor., 7: 252-267, 1968.

11. Edinger, J.G. Vertical Distribution of Photochemical Smog in Los Angeles Basin. Environ. Sci. Technol., 3: 247-252, 1973.

12. Gloria, H.R., G. Bradburn, R.F. Reinison, J.N. Pitts Jr., J.V. Behar and L. Zafonte. Airborne Survey of Major Air Basins in California. J. Air Poll. Control Assoc., 24 (7): 645-652, 1973.

13. Kauper, E.K. and B.L. Niemann. Los Angeles to Ventura Over Water Ozone Transport Study. Report prepared for California Air Resources Board by Metro Monitoring Services, Covina, California, 1975. 54 pp.

14. DeMarrais, G.A., G.C. Holzworth and C.R. Hosler. Meteorological Summaries Pertinent to Atmospheric Transport and Dispersion Over Southern California. Technical Paper No. 54. U.S. Weather Bureau, Washington, D.C., 1965. 86 pp.

15. Blumenthal, D.L., W.H. White, R.L. Peace and T.B. Smith. Determination of the Feasibility of the Long-Range Transport of Ozone or Ozone Precursors. Final Copy (draft copy) prepared by the Environmental Protection Agency by Meteorology Research, Inc., Altadena, California, 1974. 86 pp. plus 2 appendices.

16. Air Resources Board. California Air Quality Data, April, May, June 1974. Vol. VI, No. 2. Sacremento, California, 1974. 83 pp.

17. Miller, A. and C.D. Ahrens. Ozone Within and Below the West Coast Temperature Inversion. Dept. of Meteorology Report No. 6, San Jose State College, San Jose, California, 1969. 74 pp.

18. Kauper, E. K., D. F. Hartman, and E. G. Roberts. Air Pollution Forecasts for Los Angeles, Using an Objective Method. Manuscripts of Los Angeles Air Pollution Control District, California, 1964. 16 pp.

19. Zeldin, M.D. Ozone Forecast Model. Manuscript of San Bernardino Air Pollution Control District, California, 1974. 4 pp.

20. Air Resources Board (2). California Air Quality Data, October, November, December 1974. Vol. VI, No. 4, Sacramento, California, 1974. 94 pp.

21. Lust, D. Semi-Annual Report on Operation of Environmental Meteorological Support Unit in Los Angeles. Inter-Office Communication of National Weather Service dated August 9, 1972.

22. Lust, D. Inversion Base Heights and Temperatures, Los Angeles Airport and El Monte. Manuscript of Weather Service Forecast Office, Los Angeles, California, 1976. 3 pp.

23. Auer, A.H. Metropolitan Land Use in the Metropolitan St. Louis Area. Report No. AS116, Dept. of Atmospheric Science, Univ. of Wyoming, 1975. 30 pp.

24. Jurgens, R. B. and R. C. Rhodes. Quality Assurance and Data Validation for the Regional Air Monitoring System of the St. Louis Regional Air Pollution Study. In: Proceedings of the EPA's Conference on Environmental Modeling and Simulation, Cincinnati, Ohio, 1976 (in press).

25. Panofsky, H.A. and G. W. Brier. Some Applications of Statistics to Meteorology. The Pennsylvania State University, University Park, Pennsylvania, 1958. 224 pp.

26. Alley, F.C. and L.A. Ripperton. The Effect of Temperature on Photochemical Oxidant Production in a Bench Scale Reaction System. J. Air Poll. Control Assoc., 11 (12): 562-565, 584, 1961.

27. Brooks, C.P. and N. Carruthers. Handbook of Statistical Methods in Meteorology. Her Majesty's Stationary Office, London, 1953. pp. 210-241.

OZONE IN RURAL AND URBAN AREAS OF NEW YORK STATE

PART I

P. Coffey, W. Stasiuk, V. Mohnen*

ABSTRACT

Ozone concentrations have been measured at rural and urban sites in New York State for the last several years. Most of the ozone found at these sites is the result of long range transport processes and not local photochemical generation. Periods of high ozone concentrations are regional in nature and are associated with high pressure weather systems. The nitric oxide and particulate matter produced in urban areas destroys ozone and thus these areas tend to experience fewer hours of ozone concentrations in excess of 80 ppb than do the rural areas. However, on occasion, ozone appears to be generated in the urban plume in excess of the prevailing background ozone concentrations. The magnitude of the contribution of ozone so generated to the overall ozone levels in the air mass associated with the high pressure system is both variable and uncertain.

INTRODUCTION

Several years ago, the Division of Air Resources of the New York State Department of Environmental Conservation and the Atmospheric Sciences Research Center of the State University of New York initiated a continuing study designed to investigate the sources of the ozone being found in New York State and the northeastern United States.

Quite frequently, starting in late spring and continuing throughout the summer, ozone concentrations in excess of the National Ambient Air Quality Standard (80 ppb not to be exceeded more than one hour per year) were being recorded at urban monitoring sites in New York State. While these urban sites usually recorded ozone concentration patterns which correspond to the classical diurnal cycle characteristic of local photochemical generation and subsequent distruction, there was evidence that the problem was more complex. Earlier studies by New York State (1) in the mid-1960's, using the cracking of rubber as an indicator of ozone, indicated that ozone concentrations were higher in the rural areas than in the urban areas. The results were reinforced by Johnston (2) and Richter (3) who, in the early 1970's, measured high concentrations of ozone in rural Maryland and West Virginia, respectively.

---

*Bureau of Technical Services, Division of Air Resources, New York State Department of Environmental Conservation, Albany, New York.

STUDY DESIGN

The ozone study was designed to collect and analyze ozone data over a large area from both stationary surface sites and instrumented aircraft. To supplement existing urban monitors situated in the larger cities of New York State, several sites were added.

The summit atmospheric physics laboratory at Whiteface Mountain (Elevation 4,980 feet) in the northern Adirondack Mountains of New York was chosen to be a permanent site. This laboratory, operated by the Atmospheric Sciences Research Center of the State University of New York, is situated in a very remote area of the Northeast well over 100 miles from the nearest sizable urban area. The elevation of the site, which is above the tree line, is sufficient to place it above the summertime nocturnal inversion layer, yet low enough so that it remains well within the daytime surface mixing layer.

A temporary rural elevated site was set up in a fire tower 40 feet above the summit of Mount Utsayantha (elevation 3,200 feet) located in Delaware County approximately 180 miles south of Whiteface Mountain. This site has the same meteorological characteristics as the Whiteface site.

A third temporary rural site was operated in a remote conifer forested valley area known as the "Pack Forest." This site (Elevation 800 feet) was approximately 55 miles south of Whiteface. Unlike the other two rural sites, the Pack Forest location was typically under the nocturnal inversion layer. The location of these rural sites and several urban sites used during the study is shown in Figure 1.

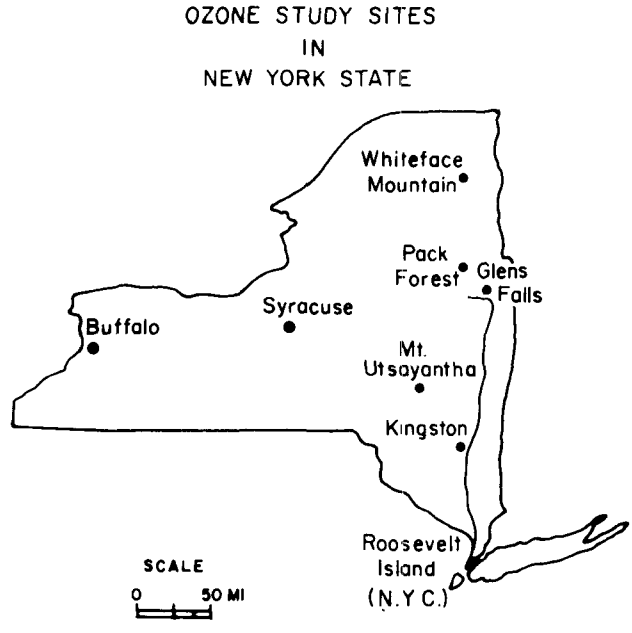

Figure 1. Locations of various sites in New York State.

In addition to the above mentioned fixed location sites, instrumented helicopter and airplane flights were made on both a local and long-range basis.

RESULTS

The Whiteface station, because of its isolation from urban areas, produced ozone data which was unperturbed by local anthropogenic sources. The monthly average ozone concentrations at this site for 1973 and part of 1974 are shown in Figure 2. The classical springtime rise is evident, as is the fall and winter low. While not evident in this figure, the month of highest ozone concentration is very dependent on year by year climate variations. For example, while the 1973 highest average ozone concentrations were measured for August, the highest month in 1974 was June. This coincided with a shift in 1974 climatic conditions producing winter-like weather patterns over the northeastern United States after June of that year.

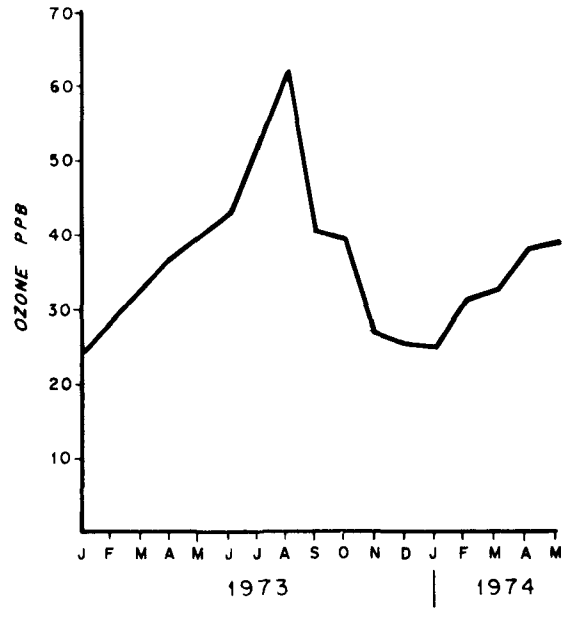

Figure 2. Average monthly ozone concentrations recorded at summit of Mount Whiteface.

EFFECT OF NOCTURNAL INVERSION

In Figure 3, ozone concentrations at the Whiteface site are compared with those at the Pack Forest site from August 6, 1973 to August 17, 1973. The Pack Forest valley site, which is under the nocturnal inversion, recorded distinct diurnal variations in ozone concentration which look very much like the classical case of local daytime photochemical ozone generation and subsequent nighttime destruction. However, the lack of local anthropogenic sources and the existence of high concentrations of ozone above the nocturnal

inversion layer as seen from the Whiteface data suggests a different mechanism (4). That is, the ozone seen at both sites is generated elsewhere and transported over long distances to these locations. The distinct diurnal variation at the Pack Forest site is caused by local nighttime destruction of ozone under the nocturnal inversion layer by reaction with gases such as nitric oxide and terpenes, by contact with the surface and by reaction with particulate matter. The daytime breakup of the inversion layer allows ozone replenishment from the ozone reservoir above this layer.

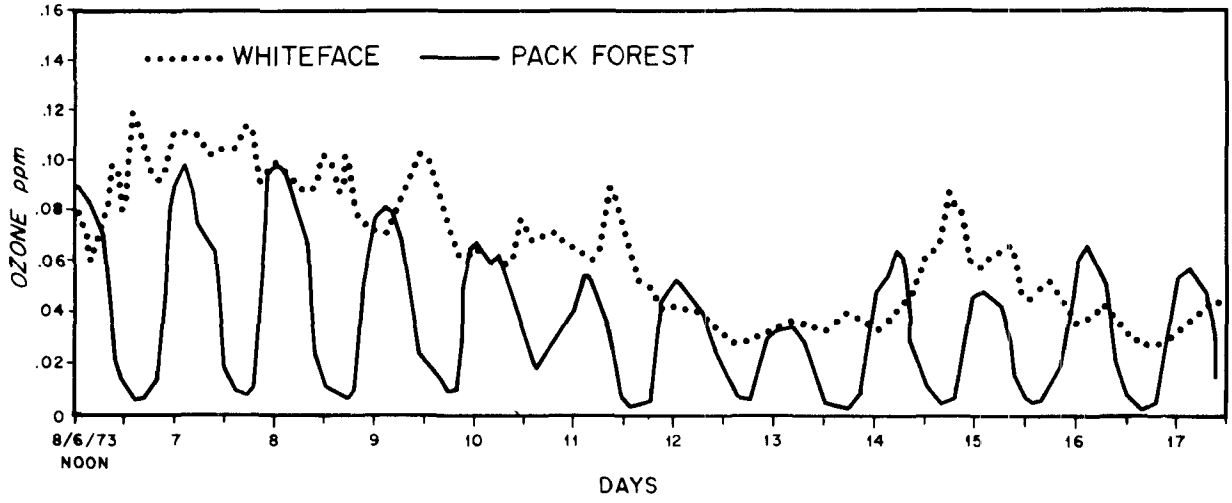

Figure 3. Ozone Concentrations at Whiteface and Pack Forest from August 6, 1973 to August 17, 1973.

That this mechanism is responsible for diurnal ozone fluctuations in urban areas can also be demonstrated.

Approximately 25 miles to the south and east of the Pack Forest is located the city of Glens Falls (population 18,500). Its ozone concentrations are almost identical to those found at the Pack Forest site. The relationship between these two sites is illustrated in Figure 4 on an hourly average basis for the month of July, 1973. Note also on this figure the Whiteface hourly average which exhibits a reverse diurnal. Evidently, the ozone concentration at Whiteface experiences a daytime minimum due to the influx of ozone depleted air from under the nocturnal inversion. During the winter months when the snow covered mountain summit is typically under the nocturnal inversion, the summit ozone diurnal fluxuation is reversed as would be expected.

LONG RANGE TRANSPORT

That long range transport of ozone occurs on a massive scale is suggested by Figure 5. In this figure, continuous ozone data from the Whiteface site for the first 17 days of August, 1973 is presented for comparison with the rural Utsayantha site and the urban site of Syracuse, New York. The missing ozone data is a result of malfunctions in the data transmission system of the continuous air monitoring network. Despite a separation of 180

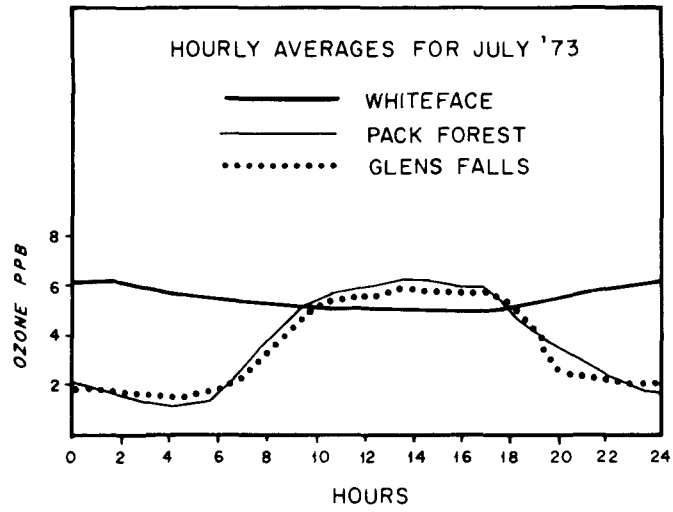

Figure 4. Hourly ozone averages at Whiteface, Pack Forest and Glens Falls sites for July, 1973.

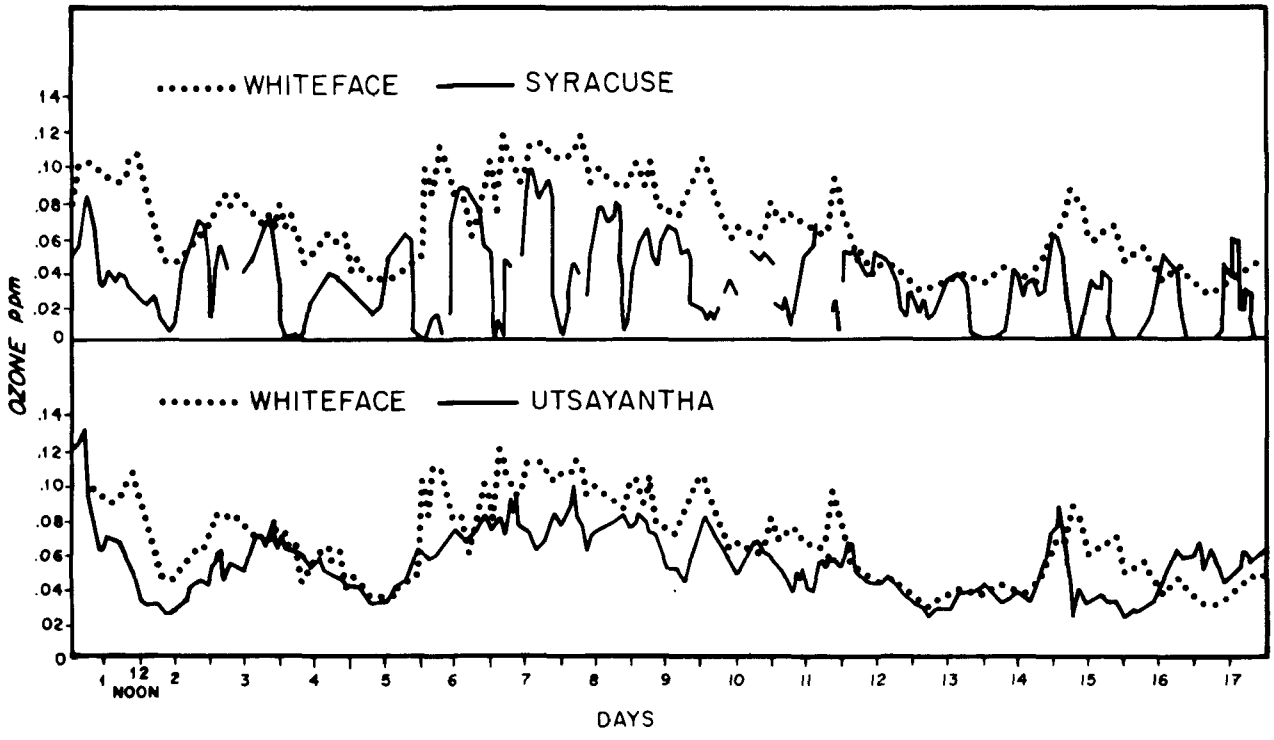

Figure 5. Comparison of ozone concentration at Whiteface site with that at Utsayantha and Syracuse sites for the first 17 days of August, 1973.

miles between the two rural stations (Utsayantha and Whiteface), the ozone levels at both sites are nearly equal and exhibit the same variations.

Of perhaps more interest are the comparisons of the urban ozone concentrations at Syracuse with the rural concentrations at Whiteface. The typical diurnal ozone pattern is seen in the urban areas with nighttime values usually reduced to zero by reaction with nitric oxide. A close examination of this figure shows that the urban daily maximum ozone values apparently are high when non-urban ozone values are high and are low when non-urban values are low. We have reported similar relationships for Whiteface, Glens Falls and Montreal, Canada (5). This strengthens the hypothesis that the urban ozone observed in New York State may be more the resultant of a physical process of transport and mixing than of local photochemical generation.

WEATHER

Episodes of high ozone concentrations are associated with high pressure systems. Ozone concentrations rise as the center of the high moves southeast of the area during which time the surface winds blow from the southwest quadrant. Elevated sulfate concentrations are also associated with these systems (5,6).

URBAN OZONE

It has been shown by Coffey and Stasiuk (7) that urban areas experience fewer hours in excess of the 80 ppb ozone standard than do rural areas. Figure 6 illustrates this point for the cities of New York, Mamaroneck, Buffalo, Glens Falls and the rural sites at Whiteface and the Pack Forest. Apparently, the destruction of ozone by nitric oxide tends to be greater than the photochemical generation of ozone within the urban area.

URBAN OZONE PLUME

Figure 6 is interesting in that all the sites but one experience ozone maximums of around 135 ppb. The site at Mamaroneck, however, experiences several hours of ozone concentrations significantly higher. This site is approximately 20 miles from New York City and typically downwind during an ozone episode. An explanation of these high ozone concentrations is that on occasion when reaching the Mamaroneck area, the urban plume from the New York City area has depleted its nitric oxide content and has become a net producer of ozone. This argument is reinforced by Figure 7 - an ozone concentration isopleth of the northeastern area drawn from data supplied by 95 ozone reporting stations in the region. Several ozone plumes are evident as is the regional nature of the ozone problem.

CONCLUSIONS

The diurnal fluctuations in ozone concentration observed at surface sites is largely the resultant of local meteorological parameters and not local photochemical generation. Above the nocturnal inversion ozone a high concentration persists throughout the night and serves to replenish the surface ozone

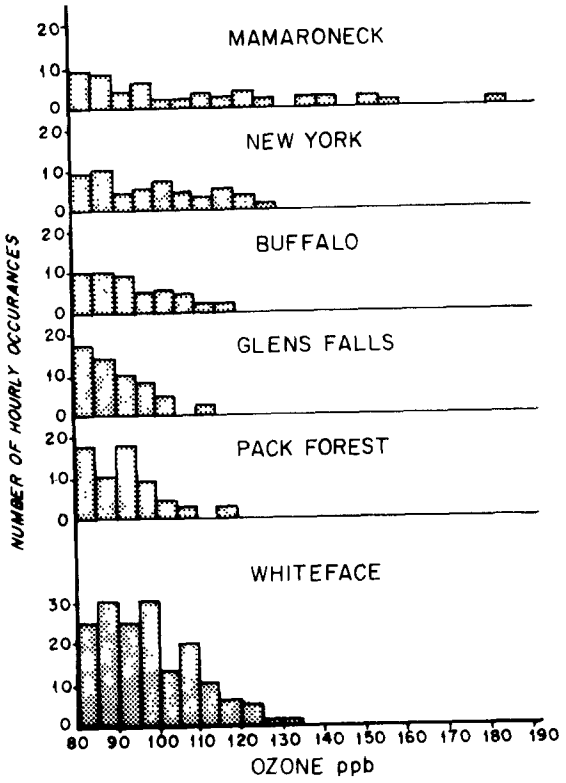

Figure 6. Frequency distribution of ozone concentrations in excess of 80 ppb from 7/1/73 to 8/22/73.

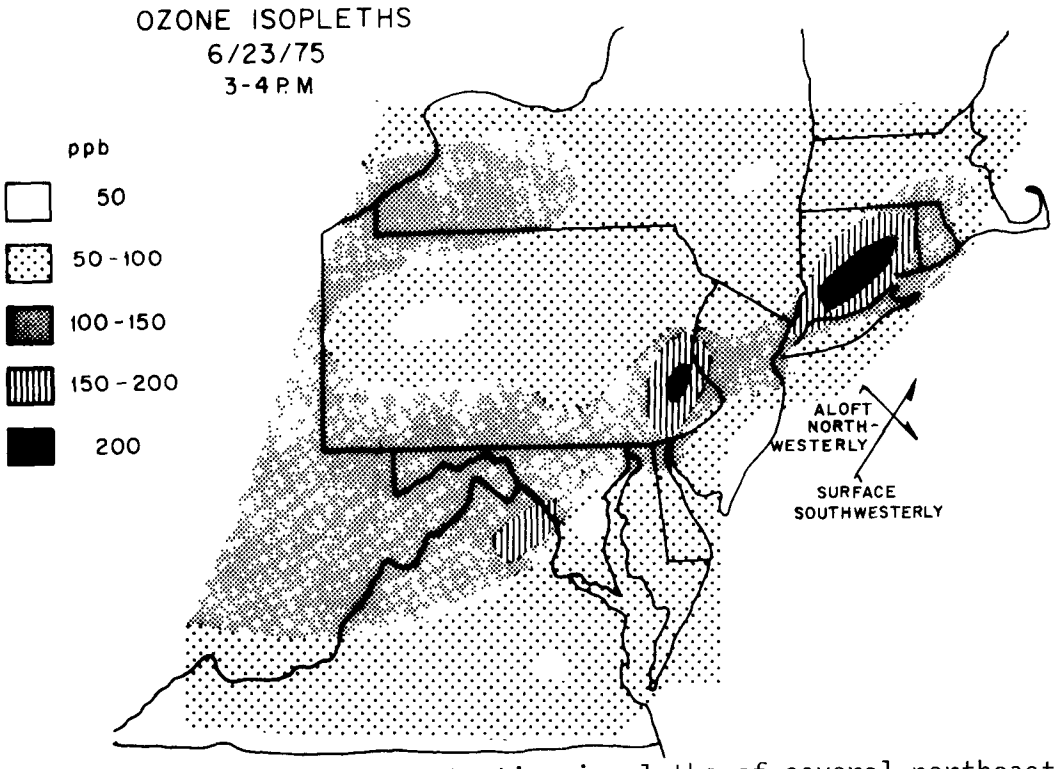

Figure 7. 3-4 P.M. ozone concentration isopleths of several northeastern states for June 23, 1975.

concentrations during the daylight hours.

The ozone problem is a regional one, episodic in nature associated with high pressure systems.

Urban areas tend to have less ozone than do rural areas, however, ozone plumes have been measured downwind of the larger urban areas. The relative contribution of ozone generated in urban plumes to the overall ozone concentrations associated with high pressure systems is unknown. Similarly, the relative contribution of ozone from the stratosphere and ozone produced from naturally emitted precursors is also uncertain. Resolution of the reasons for elevated ozone concentrations in these air masses is needed since the levels are greater than the federal ambient air quality standard.

REFERENCES

(1) Statistical Analyses of Data from Effects Stations in New York State, January-December, 1969. New York State Department of Environmental Conservation, Report No. BAQS 24.

(2) Johnston, et.al., "Investigation of High Ozone Concentrations in the Vicinity of Garrett County, Maryland and Preston County, West Virginia," Research Triangle Institute publication, January, 1973. NTIS #PB-218540.

(3) Richter, H.G., "Special Ozone and Oxidant Measurements in Vicinity of Mount Storm, West Virginia," Research Triangle Park, North Carolina, Research Triangle Institute, October, 1970.

(4) Coffey, P.E., Stasiuk, W.N., "Evidence of Atmospheric Transport of Ozone into Urban Areas," Environmental Science and Technology, Volume 9, No. 1, p. 59. January, 1975.

(5) Stasiuk, W.N., Coffey, P.E. and McDermott, R.F., "Relationships Between Suspended Sulfates and Ozone at a Non-Urban Site." Paper No. 75-62.7 presented at 68th National Annual Meeting of the Air Pollution Control Association, Boston, Massachusetts, June, 1975.

(6) Quickert, N., Wallworth, B. and L. Dubois, "Characterization of an Episode with Elevated Ozone Concentrations."

(7) Coffey, P.E., Stasiuk, W.N., "Urban Ozone: Its Local and Extraregional Components." Presented at the 79th National Annual Meeting of AIChe, Houston, Texas, March, 1975.

OZONE MEASUREMENT AND METEOROLOGICAL ANALYSIS OF TROPOPAUSE FOLDING

V. A. Mohnen, A. Hogan, E. Danielsen, and P. Coffey*

ABSTRACT

Ozone measurements made at several surface stations in New York and Massachusetts show typical continental diurnal variation; a mountaintop (850 mb) station in the same region experiences very little diurnal variation. The moutaintop ozone concentration always exceeds that of the surface stations, and this concentration trend is predictable by meteorological analysis. The results of these experiments indicate that the ozone source level lies above 850 mb. Flight experiments have verified that significant downward transport of ozone from the lower stratosphere accompanies a tropospheric fold, and that this ozone-enriched air may reach the surface and/or remain in the middle troposphere.

INTRODUCTION

Vertical profiles of ozone mixing ratio, averaged to remove the fluctuations, are consistent with a net production in the upper stratosphere and a net destruction at the earth's surface (1,2). From this results an average background concentration for the "natural" ozone. Ozone concentrations that far exceed this average, and that are not caused by a sudden increase in downward transport, are caused by photochemical production of ozone in the lower part of the troposphere from precursor gases of anthropogenic origin. Downward transport of ozone from the stratosphere to the troposphere occurs when the boundary between the stratosphere and the troposphere deforms, becomes vertical in the core of the jet stream, and then folds beneath the jet core. Danielsen (3) concluded after completing several case studies of large-scale cyclogenesis that "tropopause folding" was an integral part of cyclogenesis and that, therefore, the net seasonal and annual transport of mass could be estimated by multiplying the mass transport per cyclogenesis times the number of cyclogenetic events. This estimate of 4.3×10^{20} gm·year^{-1} implied that a mass comparable to the entire norther hemishperic stratosphere was exchanged in one year, the outflow being from the lower stratosphere on the cyclonic side of the jets, the inflow implied at higher elevation on the anticyclonic side of the jets. Table 1 summarizes the current estimates on globally averaged ozone

*V.A. Mohnen and A. Hogan, State University of New York at Albany, Atmospheric Sciences Research Center.
E. Danielsen, National Center for Atmospheric Research, Boulder, Colorado.
P. Coffey, New York State Department of Environmental Conservation, Albany, New York.

TABLE 1. SUMMARY

ESTIMATED STRATOSPHERIC OUTFLOW NORTHERN HEMISPHERE

(1959) 4×10^{20} gm/year

STRATOSPHERIC MASS

$$M_S = [4.5 + 0.5 \cos \frac{2\pi}{\tau} (t - \frac{1.5}{12})] \times 10^{20} \text{ gm}$$

(1964) OUTFLOW DERIVED FROM Sr^{90} DEPOSITION IN 1960 + 1963

$$\frac{dM}{dt}_{outflow} = [3.6 + 1.8 \cos \frac{2\pi}{\tau} (t - \frac{4.5}{12})] \times 10^{20} \text{ gm/year}$$

OZONE MASS MIXING RATIO IN LOWER STRATOSPHERE

$$\chi_{O_3} = [1.3 + 0.3 \cos \frac{2\pi}{\tau} (t - \frac{4.5}{12})] \times 10^{-6} \text{ gm/gm}$$

ANNUAL OUTFLOW OF OZONE

4.7×10^{14} gm O_3

5.8×10^{36} molecules

AVERAGE FLUX

7×10^{10} molecules cm^{-2} sec^{-1}

PAETZOLD 1955	FABIAN + JUNGE 1970	REGENER 1957
4×10^{10}	$(4 - 7.6) \times 10^{10}$	$(12 - 16) \times 10^{10}$

OZONE TRANSPORT IN SPRING 5 TIMES TRANSPORT IN FALL.

(Danielsen and Mohnen, 1976)

fluxes (4).

Taba (5) reviewed the World Meteorological Organization Congress on ozone observations, which concluded that in a major portion, daily and seasonal variations in ozone concentrations were due to meteorological phenomena. More recent reviews of the ozone literature (6-7) support this conclusion.

It is quite obvious that the average ozone concentration observed in the planetary boundary layer is governed by more than one mechanism:

- Cyclogenetic events and subsequent further transport of stratospheric air to the ground. (Depends on season and geographic latitude as far as the jet stream is concerned, and on atmospheric stability with regard to vertical transport.)
- Photochemical production within the planetary boundary layer or in the lowest troposphere. (Depends on season, geographic latitude, atmospheric stability and, most importantly, on the concentration of anthropogenic precursor gases such as oxides of nitrogen and reactive hydrocarbons.)
- Destruction on the earth's surface. (Depends strongly on the type of surfaces. Values between 0.01 to 2 $cm \cdot s^{-1}$ have been found for surface destruction rates; i.e., they can differ by a factor as high as two hundred.)

It can be expected, therefore, that the average ozone concentration differs from region to region. Background ozone measurements within the planetary boundary layer for the purpose of establishing realistic air quality standards must be made on a regional basis. The "region" is defined by climatology, geographic latitude, topography, type of surface, etc.

The Atmospheric Sciences Research Center (ASRC) and the New York State Department of Environmental Conservation have collaborated in operating a series of ozone observations in rural and urban New York State for several years. Station descriptions can be found in Coffey and Stasiuk (8). This analysis of ozone background concentration will be confined to the ASRC Whiteface Mt. (4860 ft.) and Schenectady County Airport stations, the Pittsfield, Mass. station operated by the Department of Public Health, Commonwealth of Massachusetts, and the Albany-Rensselaer station operated by the New York State Department of Environmental Conservation. The secular variation of ozone (1974 data) for these four stations is presented in Figure 1a.

The data are consistent with the classical concept of increased ozone transport from the stratosphere to the troposphere during the spring ("springtime rise" of ozone). Further mixing down to the ground is enhanced during the summer months, as indicated by the increase in afternoon mixing height measured at the Albany Airport (Figure 1b).

A positive correlation between afternoon mixing height and ozone concentration suggests ozone transport from aloft into the planetary boundary layer. It is also interesting to note that the monthly averaged ozone

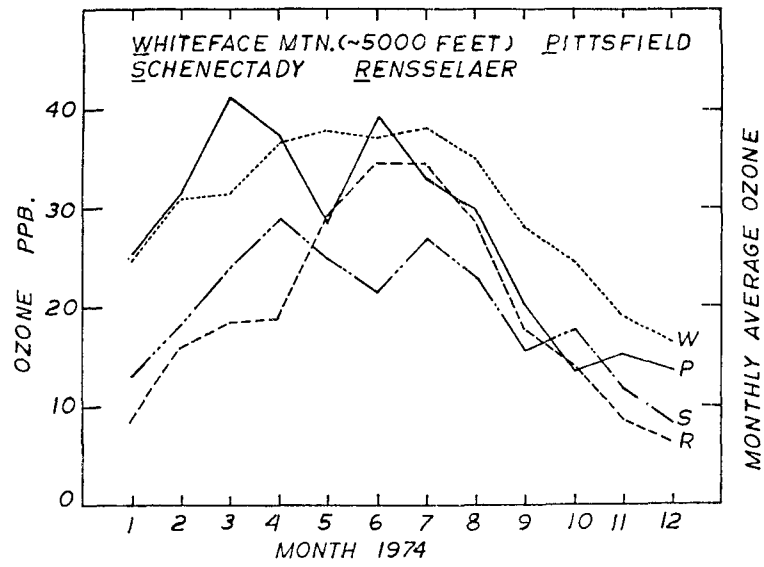

Figure 1a. Secular variation of ozone.

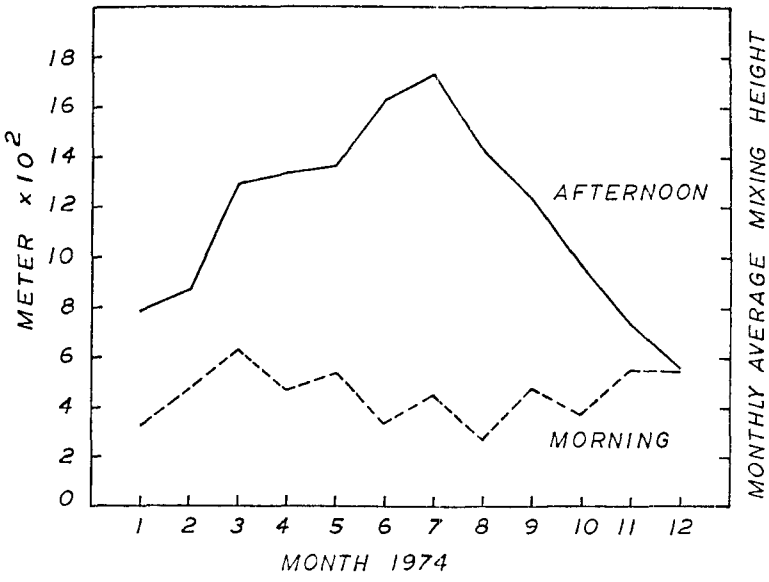

Figure 1b. Mixing height, Albany airport.

concentration for Whiteface Mt. (4860 ft. or 850 mb) was always highest (except March 1974 for the Pittsfield station; however, March is not a "photochemical" month) of all the stations. To further substantiate the transport mechanism from aloft as the main source of ozone for this region (versus the photochemical mechanism observed in other regions), we have plotted the "normalized" ozone diurnal in Figure 2a for the four stations.

Also plotted in Figure 2b are the normalized diurnal variation of (horizontal) windspeeds. Maximum wind speed results in maximum vertical

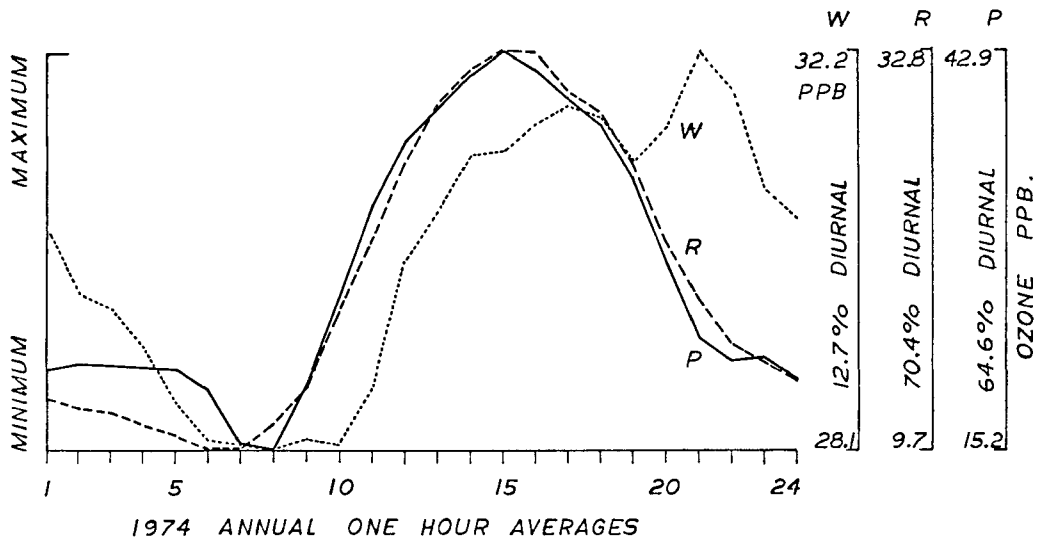

Figure 2a. Normalized diurnal variation of ozone, Whiteface Mtn. Rensselaer. Pittsfield.

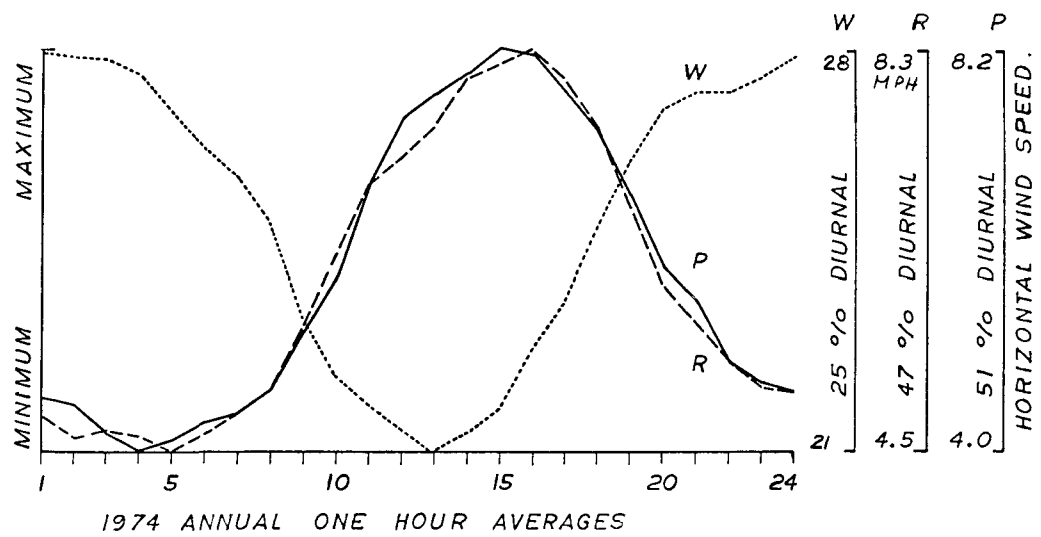

Figure 2b. Normalized diurnal variation of windspeed, Whiteface Mtn. Rensselaer. Pittsfield.

mixing. Both the ozone concentration and the wind speed peak at 15:00 for the surface stations Rensselaer and Pittsfield and show otherwise an identical trend. The Mountain station has a considerably lower diurnal variation (∿13%) and a second ozone maximum at 22:00. This can be explained by the specific local mountain micro meteorology (heating and cooling of the mountain resulting in katabatic wind situations). The diurnal variation of ozone is consistent with the "classical" concept of ozone destruction at the surface and replenishment from aloft, whereby the ozone downward flux to the surface is enhanced as turbulent mixing increases.

Figure 3 shows the mean hourly ozone concentrations observed at Whiteface Mt. and Schenectady County Airport during the period 21-31 July 1975. The 850 mb potential temperatures from the National Oceanic and Atmospheric Administration radiosonde at Albany Airport are noted on the same axis. This short data run is used to facilitate display of hourly values; daily or twice daily means suppress some important short-term trends in ozone concentration. Examination of Figure 3 shows an unmistakable parallel in the trends in ozone concentration at Whiteface Mt. (altitude ~850 mb) and in the 850 mb potential temperature reported for Albany, some 120 miles south of Whiteface Mt. At this level, an increase in air temperature (and/or potential temperature) would be indicative of subsiding air. A warming trend should then be accompanied by increasing ozone concentration, and a cooling trend should be accompanied by steady, or decreasing, ozone concentration. This is the general case for the Whiteface Mt. observations. It is again obvious that the Schenectady ozone concentration appears to approach, but never exceeds, the Whiteface Mt. ozone concentration. For the northeastern region of New York State, we can therefore reiterate the importance of meteorological mixing processes as the dominant parameter governing the diurnal behavior of surface ozone concentrations.

We have further substantiated these findings through occasional airplane flights (equipped with chemiluminescence ozone detectors) over New York State to levels up to 12,000 ft. While the source of ozone observed at the four stations must be "uniformly" distributed at elevated levels (certainly above the 850 mb level and therefore above the planetary boundary layer), we cannot yet establish a link between ozone-rich stratospheric air mass intrusions and high surface ozone concentrations.

However, the first large-scale experiments have been initiated in collaboration with the National Center for Atmospheric Research (NCAR). Data from three examples of tropopause folding have been collected and analyzed that demonstrate the vertical ozone transport. The measurements were made in Project DUSTORM during April 1975. Large scale cyclogenesis was predicted and the NCAR aircraft first traversed the folded tropopause at 21,000 ft., flying perpendicular to the wind. After the limits of the zone were determined, the plane turned back and reentered the zone. Three upwind-downwind sampling flights were made--one near the warm boundary, one in the center, and one near the cold boundary. Then the aircraft ascended to 25,000 ft. and this flight pattern was repeated. On the same day, an observer traversed the same storm system on a commercial aircraft, making ozone measurements at approximately 39,000-41,000 ft. Figure 4 shows the vertical cross-sections along Electra and commercial airline flight paths normal to folded tropopause and jet streams. Isotachs are drawn at 10 $m \cdot sec^{-1}$ intervals (solid lines). Folded tropopause (dashed lines) is also indicated in Figure 4.

Figure 5 shows the locations of jet and Electra flight paths at 0000 GMT on the 26th and 27th of April 1975. Dashed line denotes trajectory of ozone-rich air from 26th to 27th. Figure 6 shows the time profiles of ozone number mixing ratio, wind speed, and temperature measured along commercial flight path on 26 April 1975. Tropopause level (dashed line) is from conventional tropopause analysis charts (provided to us by P. Falconer, NOAA).

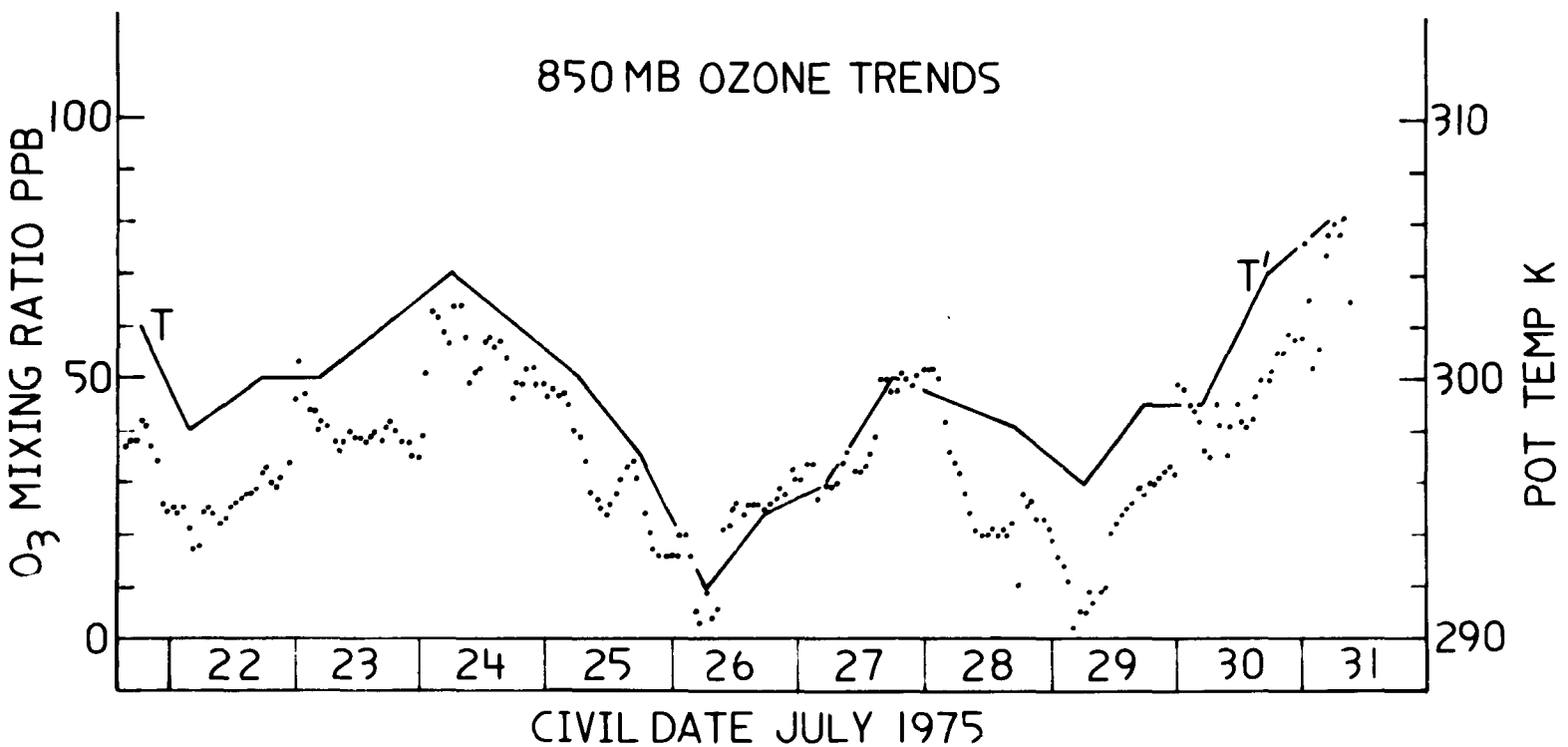

Figure 3. 850 mb ozone trends.

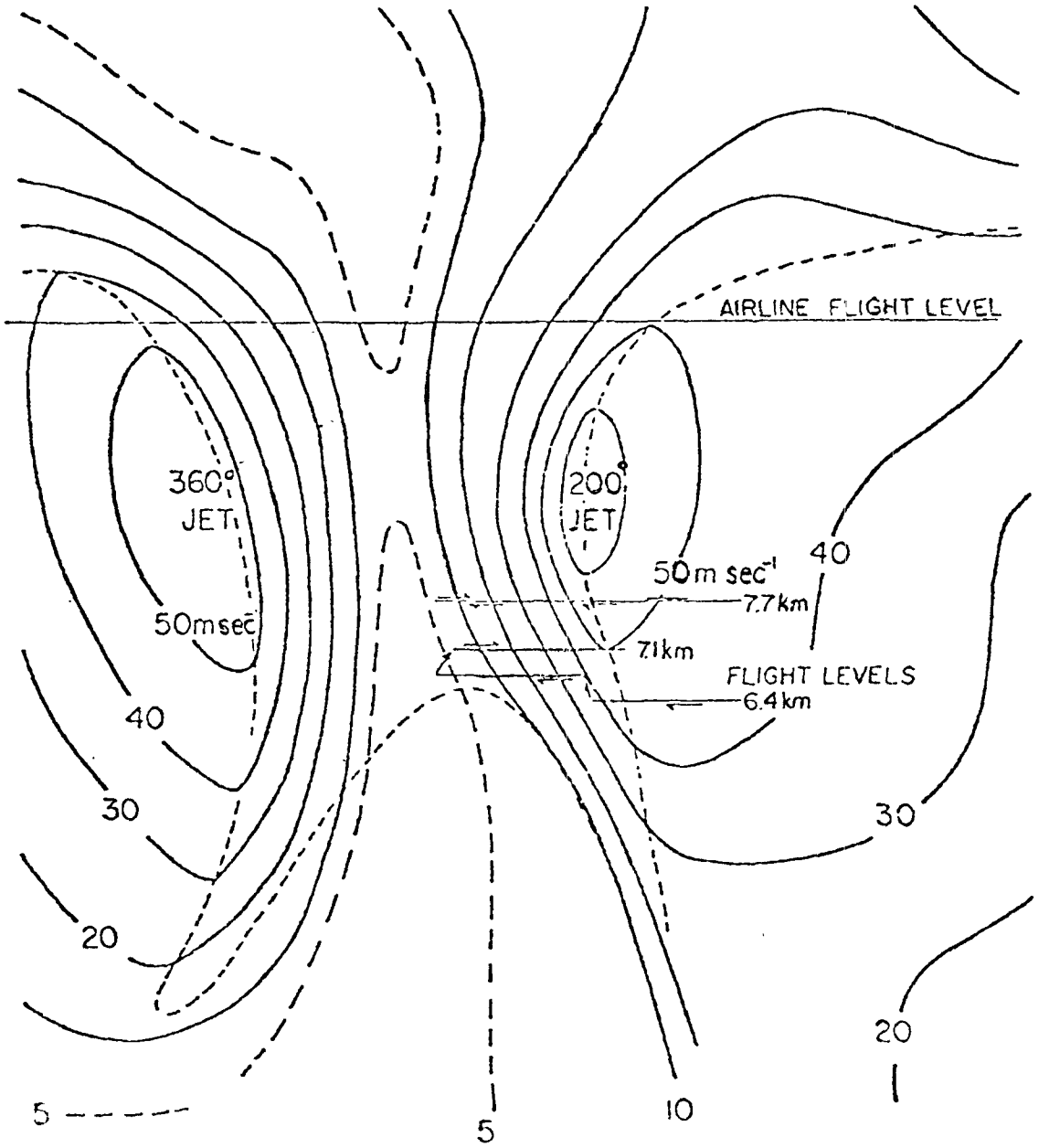

Figure 4. Vertical cross-sections along Electra and commercial airline flight paths normal to folded tropopause and jet streams.

The preliminary evidence presented here from the Electra and commercial flight data obtained during the operation of Project DUSTORM confirms the concept of tropopause folding and the assumption that ozone-rich air is transported into the troposphere with each major cyclonic development, and that this ozone-rich air, although diluted by mixing with tropospheric air, can reach the surface of the earth. The surface deposition pattern is strongly asymmetrical due to the narrowness of the folded structure and the strong deformations in the descending air. Some local regions may be

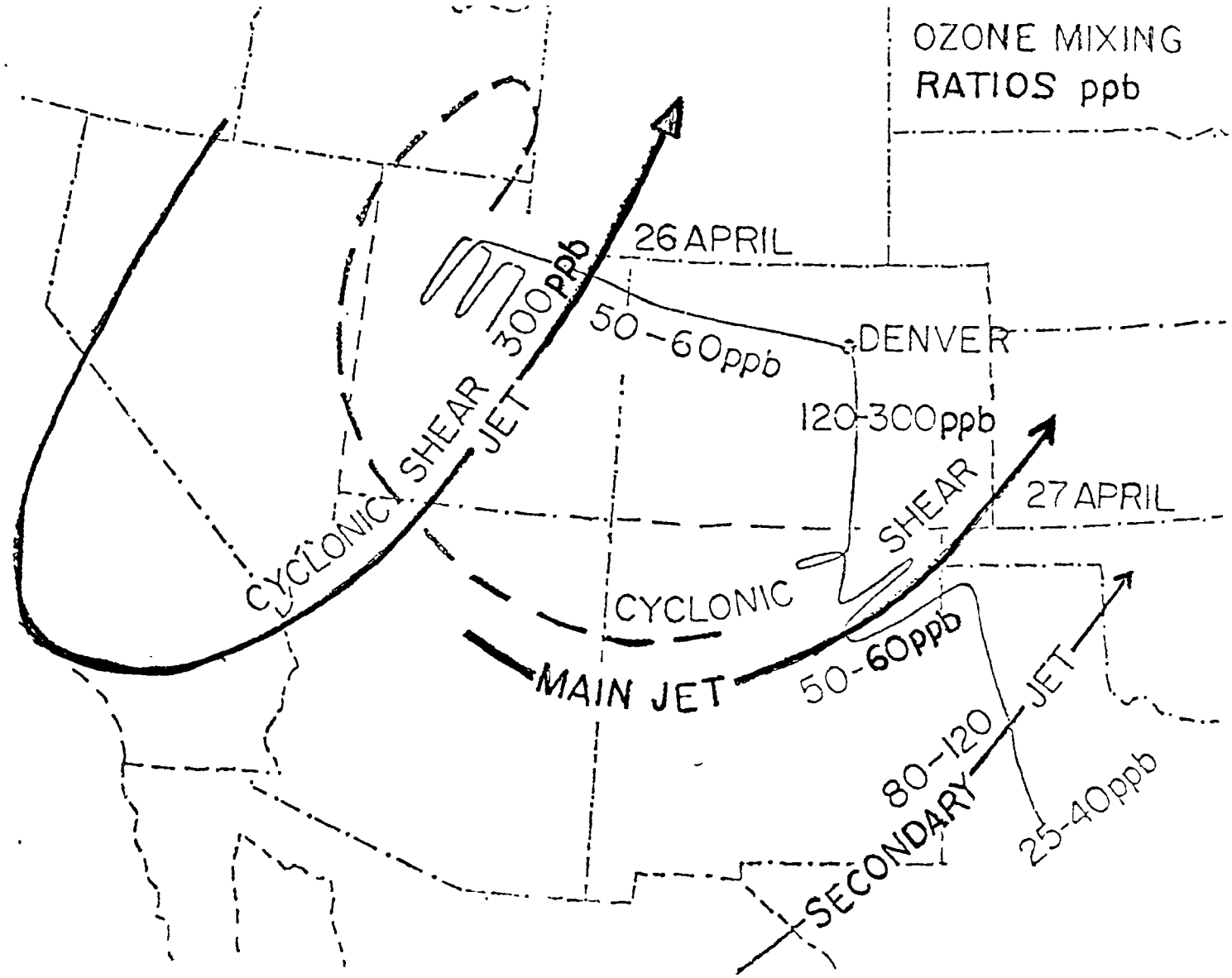

Figure 5a. Locations of jet and Electra flight paths, 0000 GMT, 26-27 April 1975.

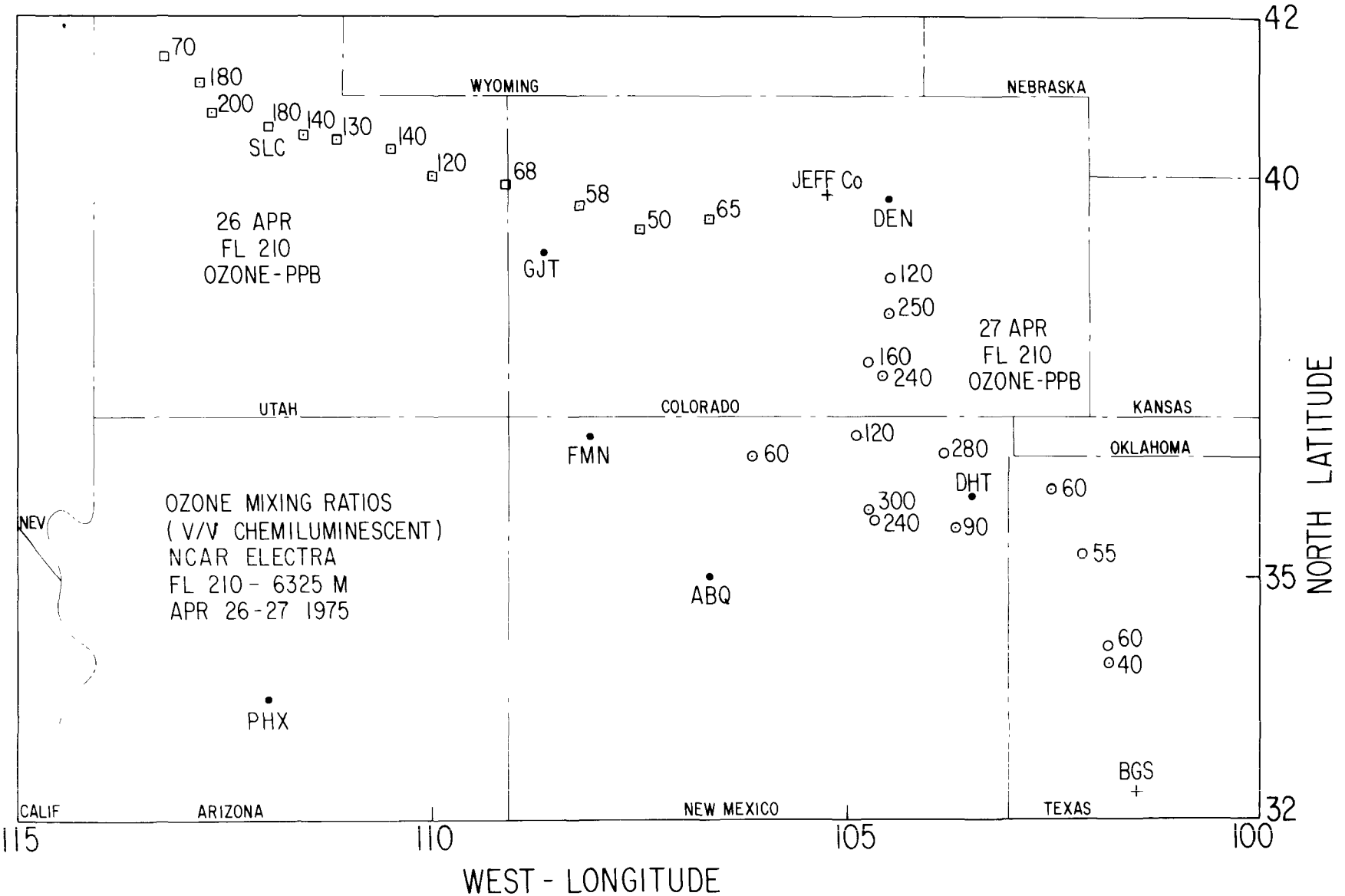

Figure 5b. Locations of jet and Electra flight paths, 0000 GMT, 26-27 April 1975.

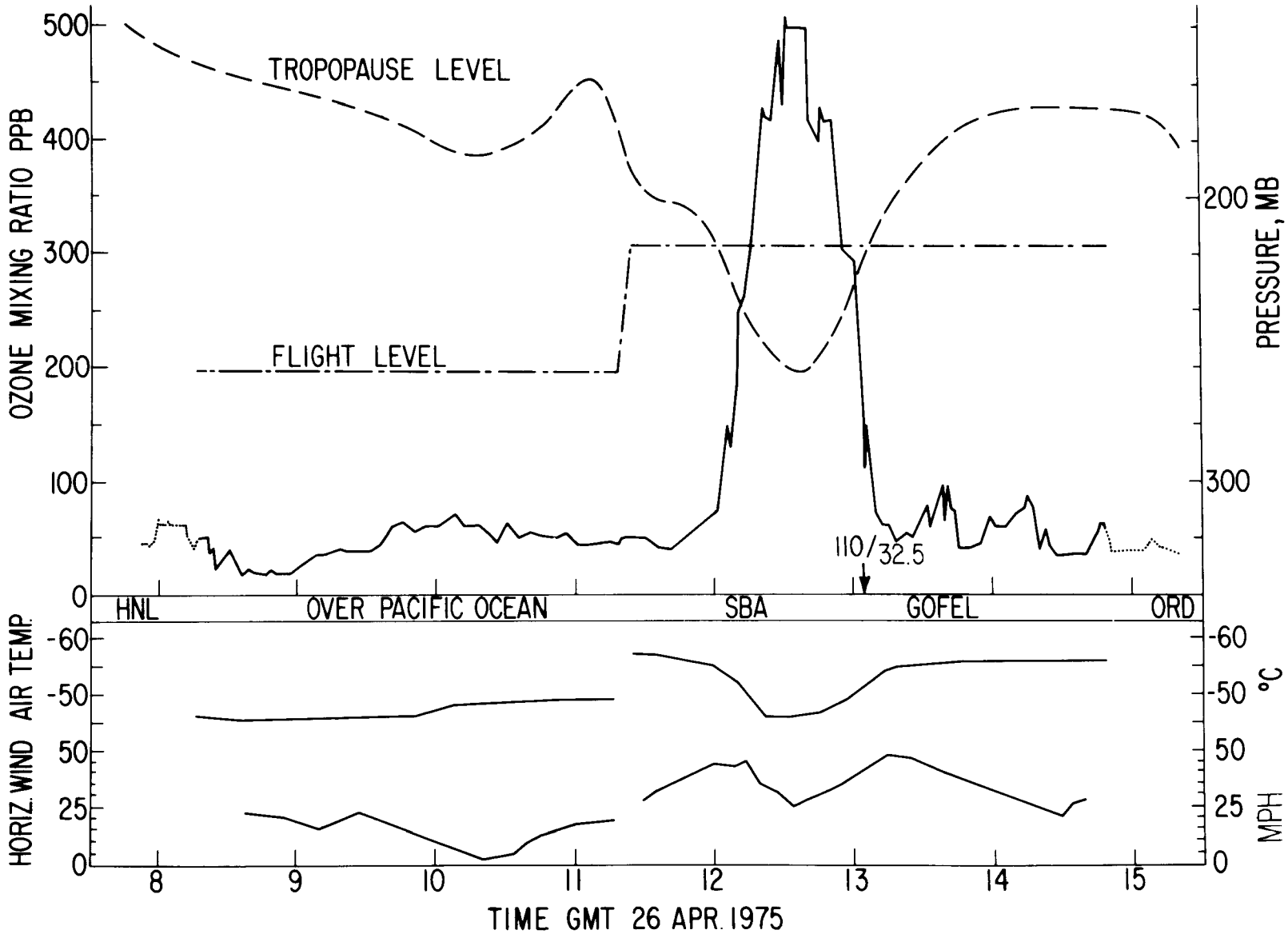

Figure 6. Time profiles of ozone number mixing ratio, wind speed, and temperature, measured along commercial flight path 26 April 1975.

influenced by this ozone-rich layer for just two or three hours, others for one or two days. More research is necessary to quantify the effects of this ozone source on the surface ozone chemistry.

REFERENCES

1. Junge, C.E., "Global ozone budget and exchange between stratosphere and troposphere." Tellus XIV, 363-377 (1962).

2. Fabian, P., "A theoretical investigation of tropospheric ozone and stratospheric-tropospheric exchange processes." Pure and Appl. Geophys., 106-108, 1027 (1973).

3. Reed, R.J. and E.F. Danielsen, "Fronts in the vicinity of the tropopause." Arch.Meteor.Geophys.Biobl., SA, B11, 1-17 (1959).

4. Danielsen, E.F. and V.A. Mohnen, "Ozone measurements and meteorological analysis of tropopause folding." International Symposium on Ozone, Dresden (Aug. 1976).

5. Taba, H., "Ozone observations and their meteorological applications." Technical Note No. 36, World Meteorological Organization, Geneva (1961).

6. Vassy, A., "Atmospheric ozone." Advances in Geophysics, Vol. 11, 115-173. Academic Press, N.Y. (1965).

7. Reiter, E.R., Atmospheric Transport Processes. Part 2: Chemical Tracers. AEC Div. of Technical Information (1971).

8. Coffey, P.E. and W.N. Stasiuk, "Evidence of tropospheric transport of ozone into urban areas." Environmental Science and Technology, Vol. 9, No. 1, p. 59 (Jan. 1975).

METEOROLOGICAL FACTORS CONTROLLING PHOTOCHEMICAL POLLUTANTS IN SOUTHEASTERN NEW ENGLAND

R. A. Dobbins, J. L. Nolan, J. P. Okolowicz, A. J. Gilbert*

ABSTRACT

The ozone measurements in southeastern New England from May to September 1975 were examined with the aid of data on ground level meteorology, not radiation, and nearby radiosondes. The ozone concentrations at seven sites in this region fluctuate essentially in unison as would occur if this pollutant was primarily transported into the region. The clear-weather diurnal cycle normally shows very low concentrations prior to sunrise and the daily maximum occurs during late afternoon. Occasional daily maximum readings are observed to occur after sunset if cloudiness is present and other conditions are favorable. A mechanism is offered in explanation of the diurnal cycle that is consistent with the observations reported by others.

INTRODUCTION

In this paper we examine the effect of transport and meteorological conditions on photochemical air pollution in southeastern New England during the period from May through September 1975. Ground level ozone (O_3) measurements at seven sites in Massachusetts, Connecticut and Rhode Island (Figure 1), along with the appropriate meteorological data, provide the basis for this study. The sites represent small cities (Providence, Fall River) and rural areas (Groton, Eastford, Scituate, Fairhaven, Medfield) on the northern terminus of the northeast corridor. The ozone measurements at the sites were made using the gas-phase chemiluminescence technique as prescribed by the U.S. Environmental Protection Agency (EPA) (1), and the quality assurance procedure was carried out for each instrument following the EPA guidelines (2). This quality assurance program in Rhode Island included daily a zero check, a single span point each week and a multipoint calibration once a month. From 20 May 1975 through 14 November 1975 the EPA Region I laboratory conducted monthly audits of Massachusetts, Connecticut, and Rhode Island sites including Eastford, Connecticut and Providence and Scituate, Rhode Island. Dr. Thomas Spittler, reporting on the results of these audits, concluded that the ozone data from the region was of good quality (3). Continuous nitrogen dioxide (NO_2) measurements were made in Providence using

*R. A. Dobbins, Brown University, Providence, Rhode Island.
J. L. Nolan, J. P. Okolowicz, State of Rhode Island, Department of Health, Providence, Rhode Island.
A. J. Gilbert, New England Consortium for Environmental Protection, Providence, Rhode Island.

the Lyschkow modification of the Saltzman method. The instrument was zeroed every day and standards were run once a month. Baseline drift was significant but linearly corrected when reducing the data; therefore, the data is of good quality.

1 - Eastford
2 - Groton
3 - Scituate
4 - Providence
5 - Medfield
6 - Fall River
7 - Fairhaven

Figure 1. Location of Regional Ozone Monitoring Sites.

Our examination of the ozone readings was facilitated by the use of a simple atmospheric total radiation meter. The device consisted of two flat stainless disks with copper-constantan thermocouples mounted to measure their temperature difference. One polished disk, which assumed air temperature, was shaded by three horizontal aluminum wafers that formed a radiation shield. The second disk was painted with flat black paint to achieve a high emissivity and was located on the top wafer so as to command a clear view of the sky. The temperature difference between the disks was controlled by both radiation and convection; therefore, the thermocouple output has no quantitative significance. Nevertheless, the record does provide excellent qualitative differentiation among the following types of atmospheric radiation histories: (a) strong insolation as indicated by a noontime deflection of about +15°C with a moderate turbulent noise component; (b) zero net radiation flux leading to neutral stability; and (c) a negative deflection of 2.5 to 4.0°C indicative of outgoing radiation from the earth's surface. The negative readings were found to correlate perfectly with the occurrence of either a surface-based or low level inversion as revealed by radiosonde observations at Chatham, Massachusetts.

Air parcel trajectories for the 500 meter level were calculated using the computer program developed by Heffter and Taylor (4). This program used observed winds to calculate the prior position at six-hour intervals of an air parcel located over Providence at a specified time. The winds used in the calculation apply to the 300 to 700 meter altitude band that is typical of the middle level of the daytime convective boundary layer in our region. The observed wind vector at a point on the surface or above the surface is assumed constant for six-hour time periods, and the parcel wind vector at each three-hour period is found by interpolation from all wind vectors observed

within 300 nautical miles. The individual wind observations are weighted in accordance with their distance and upwind/downwind locations from the time-dependent position of the specified air mass. The assumption of stepwise steadiness may not be suitable if, for example, a time-dependent pressure field is present or a frontal system traverses the region. The procedure involving weighting factors for the interpolation procedure is not known to have been tested. Therefore, we consider the trajectories to be estimates and, in this study, we applied two additional criteria. The estimated trajectory was considered valid only if (a) the number of available observed winds was greater than five and (b) the estimated trajectory was consistent with the surface wind observed at the National Weather Service at Warwick, Rhode Island.

OBSERVATIONS

The graph of the daily average ozone concentrations for five of the seven sites during the month of June 1975 (Figure 2) demonstrates the strong correlation of ozone concentrations throughout the region. This situation suggests that ozone concentrations in southeastern New England are, in large part, the result of advection into the region. On a daily basis, the transport mechanism results in ozone peaks occurring at approximately the same time and magnitude throughout the region, especially on days having high sustained wind speeds.

Air parcel trajectories were examined for those days having a daily ozone concentration greater than .055 ppm at Providence. The trajectories in Figure 3 have arrival times closely corresponding to the occurrence of the ozone peak at Providence. The trajectories indicate that 90 percent of the air flows in question arrive from the southwest quadrant traveling northeast. In examining the air flows from the southwest, we find that 60 percent of these trajectories are generated by relatively large Bermuda highs. The remaining 40 percent of the southwest flows are generated by more complex weather systems, such as approaching cold fronts and/or low pressure systems situated to the north of the New England region. The northeasterly air flow indicated in Figure 3 is actually the reversal of air flowing from the southwest through the region. The arrival of a "back door" cold front (from the northeast) results in this air, with a high O_3 concentration, being transported towards the southwest, again passing through the region. This may be an example of the inability of the trajectory model to deal with such discontinuities. In tracing the air flows back 48 hours prior to their arrival at Providence, we find that 73 percent of the trajectories lie along the "Northeast Corridor." These trajectories correspond to the occurrence of the highest concentrations of O_3 in the southeastern New England region during the period under study.

To demonstrate the variation of ozone increase in the morning hours, the 0300-0500 EST ozone average was plotted versus the 0800-1000 EST average at both Providence and Scituate for selected conditions. The 0300-0500 period was chosen to represent the ozone value just prior to sunrise, and the 0800-1000 interval was believed to be too early for any significant local ozone production. These data were plotted for mornings following low level or surface-based inversion (chosen with both radiosonde and radiometer data) and for mornings following cloudy nights (selected with climatological and radiometer data) for both Providence and Scituate. A least mean squares line was then fit to

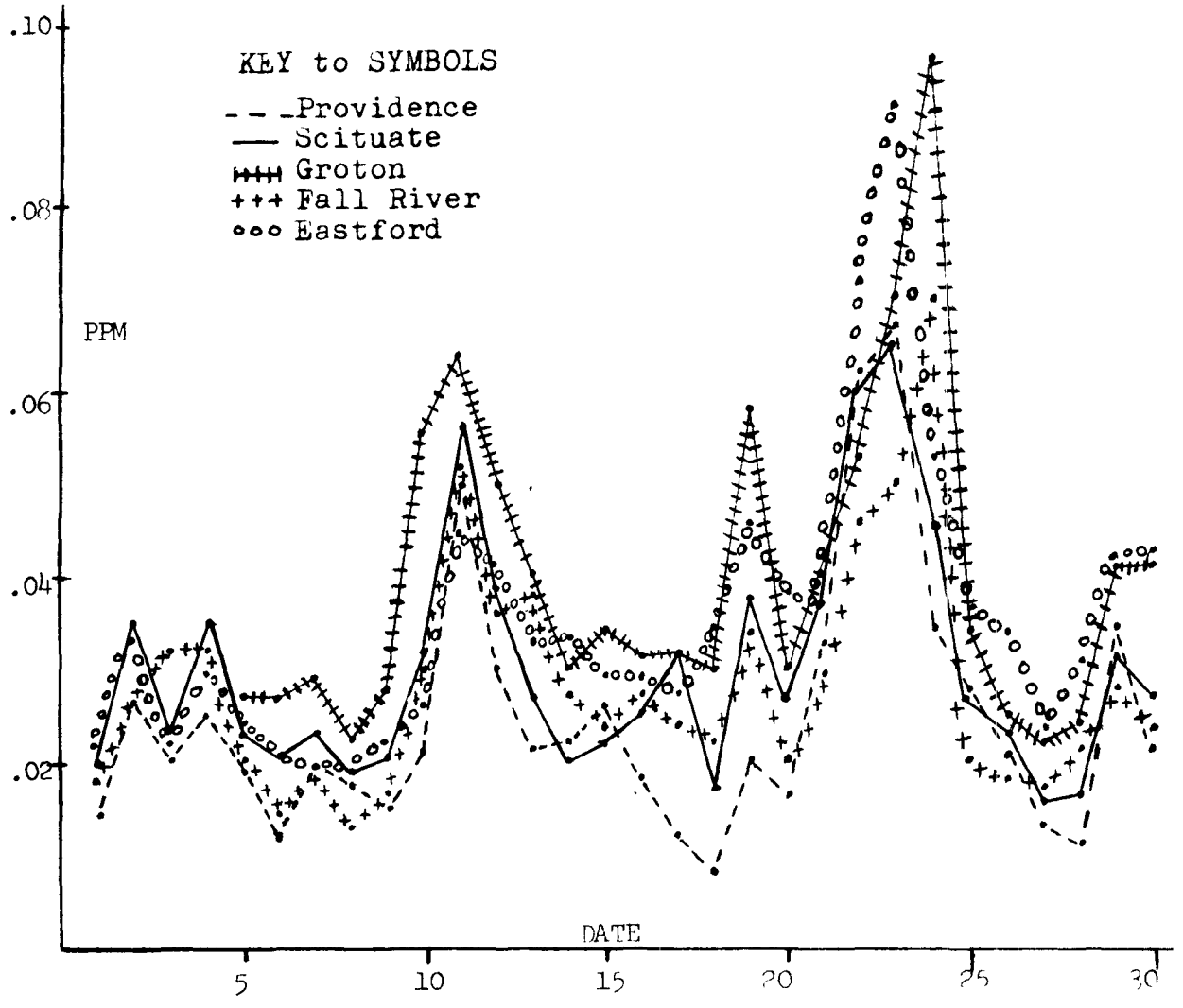

Figure 2. Daily O_3 averages, June 1975.

each set of data in Figure 4, with the slope of each line representing the average ratio of the pre-sunrise to post-sunrise O_3 reading. After sunrise there was very little change in O_3 concentration at either Scituate or Providence under the cloudy night condition. However, when radiation inversions were present prior to sunrise, the post-sunrise O_3 concentration at Scituate increased by a factor of three and at Providence by a factor of ten.

In figures 5a and 5b we have graphed several pollutant concentrations (hourly averages) on the same chart as the radiometer temperature difference. Figure 5a illustrates several features that are typical of a clear sky diurnal ozone cycle in our region. Ozone builds up during the first clear day to a level of 0.035 ppm and falls to zero soon after sunset. During the second sunny day the peak ozone reading of 0.055 ppm occurs at 1400-1500 hours EST and again decreases sharply after sunset. In Figure 5b the radiometer indicates a partly cloudy day, and the peak O_3 reading of 0.12 ppm at noon is followed by a long period during which the reading is 0.05 ppm. This level persists until midnight during the night, when the radiometer shows no temperature

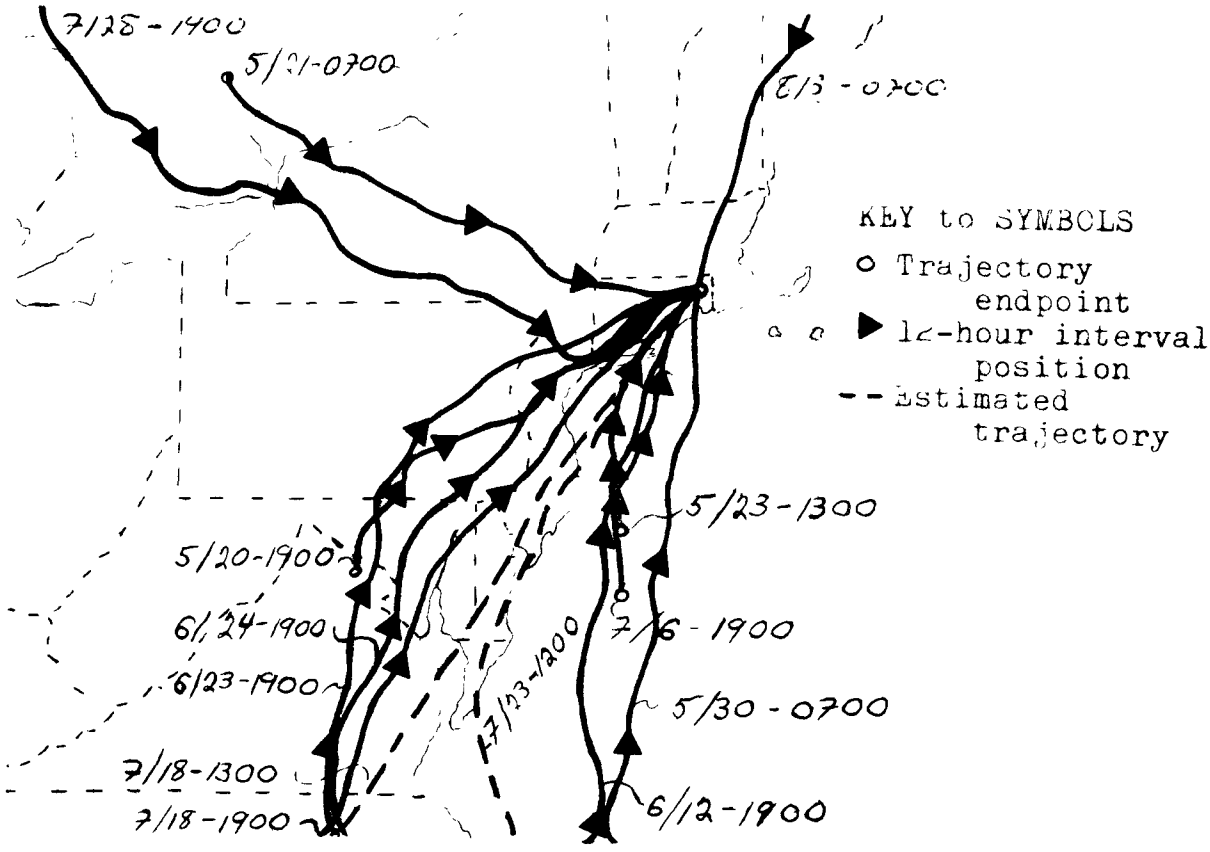

Figure 3. Air parcel trajectories daytime O_3 peaks, May - September 1975.

difference; the sky is therefore overcast. After midnight the ozone reading drops to 0.015 ppm and does not increase after sunrise, when cloudiness remains high. These O_3 concentration cycles are typical of clear and cloudy weather in our region. Note that in Figure 5b the NO_2 concentration remains low and does not decrease when the O_3 readings increase dramatically during the first partly cloudy day.

Table 1 is a list of seven dates on which ozone peaks occurred during the nighttime hours. In each case the daytime concentrations were significantly lower than the standard while the peak nighttime value was over or near the standard. A comparison of the trajectories (Figure 6) with the weather maps showed that on each occasion the trajectory originated in a clear area while the southeastern New England region was cloudy all day and evening. This seems to indicate that the ozone was formed in the sunny area and combined with clouds as it was advected into southeastern New England. This weather condition was commonly associated with the approach of a cold front to our region, but other more complex weather systems produced similar results. As was the case for the daytime peaks, the majority (85 percent) of the wind flows on these nights were from the southwest quadrant. Additionally, 70 percent of the trajectories were found to lie along the eastern seaboard.

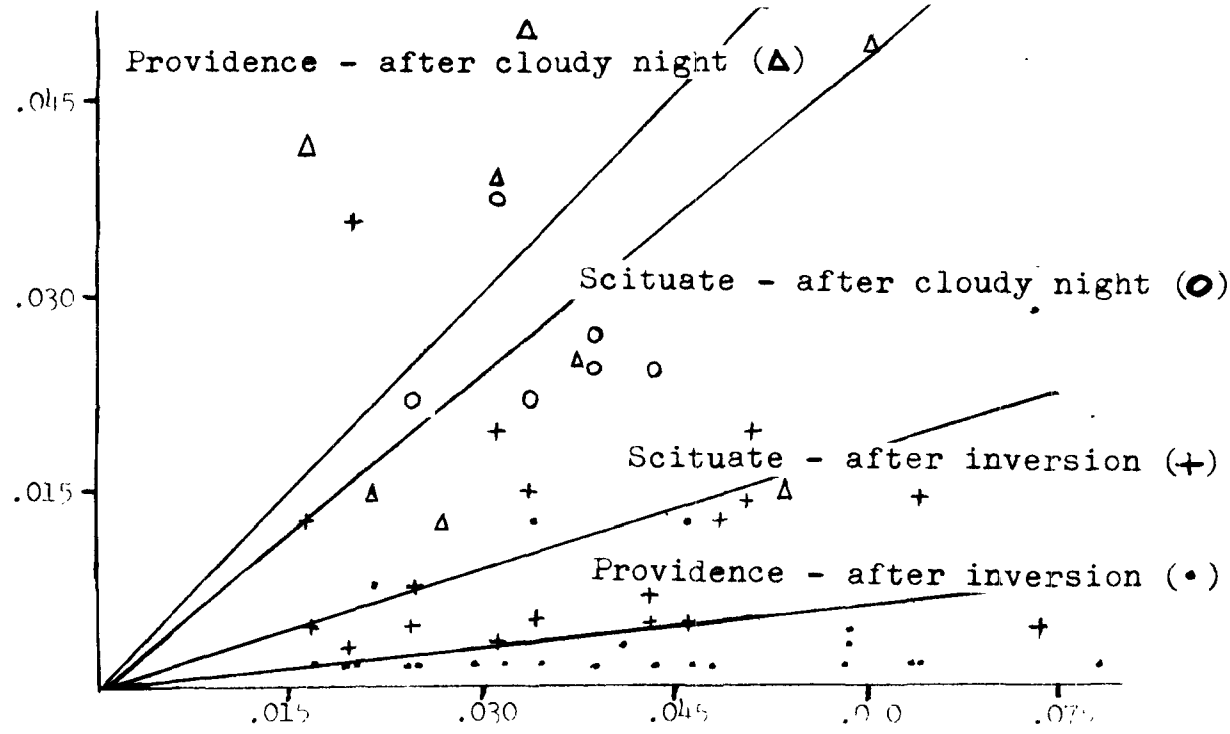

Figure 4. Average O_3 concentrations, ppm. Providence and Scituate pre- vs. post-sunrise.

DISCUSSION

The formation of ozone in the atmosphere over Los Angeles has been recently discussed by Calvert (5), who shows that the rate controlling reactions involve: (a) the photolysis (K_1) of NO_2 to form O and nitric oxide (NO) which is followed by the rapid formation of O_3, and (b) the recombination (K_3) of O_3 and NO to form NO_2 and O_2. Thus, Calvert shows that, within a given air parcel, the relationship for the concentration ratio is given by

$$\frac{[O_3]\,[NO]}{[NO_2]} \approx \frac{K_1}{K_3} \qquad (1)$$

between the hours of 0900 and 1400 local time. The increasing solar intensity during the daylight hours causes O_3 to reach peak levels in the afternoon hours because, in part, the radiation-dependent K_1 is then a maximum. We find many cases where there is a similarity between the O_3 diurnal cycle in our region and the Los Angeles Basin, suggesting that the above reaction sequence describes our O_3 concentrations. However, the basic mechanics that caused the diurnal O_3 in southeastern New England are entirely different. These mechanisms must also be consistent with the previous observations: the nearly coincident daily O_3 averages at five locations as shown in Figure 2; the occurrence of nighttime high levels of O_3 only under conditions of cloudiness; and finally, the occurrence of increasing daytime levels of O_3 under clear skies when the NO_2 concentrations are negligible.

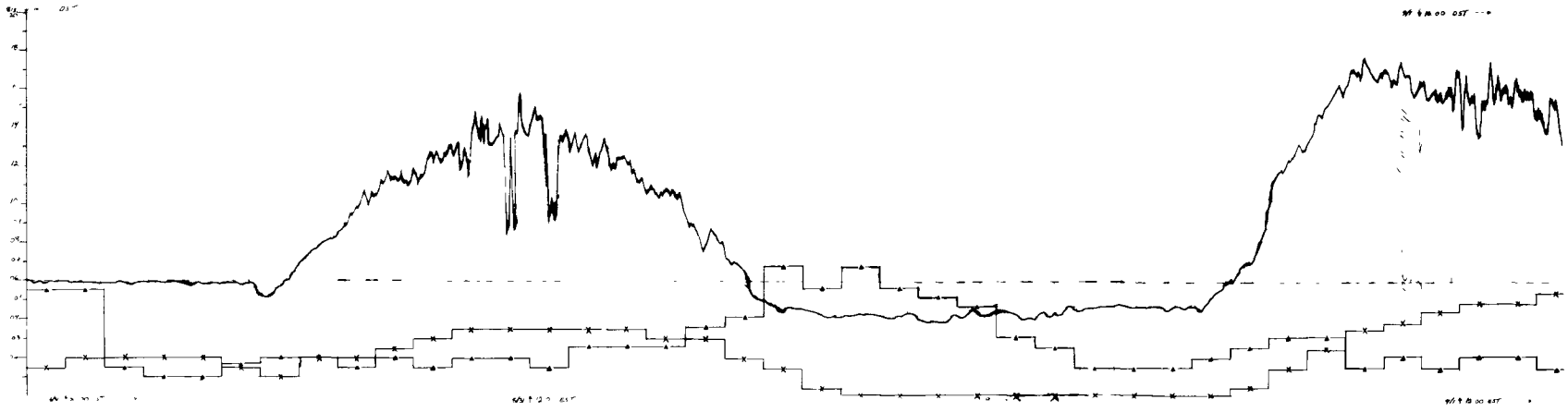

Figure 5a. Typical clear weather cycle August 31 and September 1.

× O_3
▲ CO

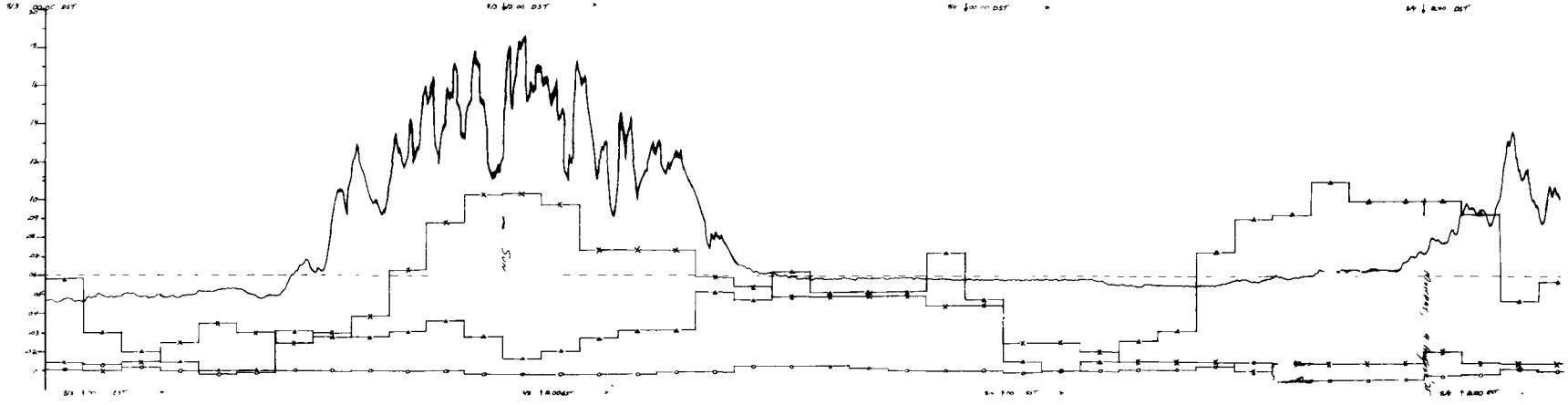

Figure 5b. Typical cloudy weather cycle August 3 and 4.

TABLE 1. CLOUDY NIGHTS WITH O_3 PEAKS: TIME AND MAGNITUDE OF PEAKS (ppm)

	Prov.	Scit.	Grtn.	F.R.	Estfd.	Fhvn.	Med.
May 12-13	0200 .059	No Data	2200 .070	2100 .071	No Data	No Data	No Data
June 3-4	2300 .074	2300 .054	0100 .070	2300 .079	2000 .045	No Data	No Data
June 29-30	2300 .054	0000 .049	0200 .070	2200 .057	0000 .061	No Data	No Data
July 4-5	0000 .113	2300 .088	No Night	0100 .121	No Data	No Data	No Data
Aug. 13-14	0000 .093	2200 .093	2000 .140	0000 .094	2000 .115	0100 .135	0000 .095
Aug. 21-22	0000 .098	2200 .084	2200 .130	1900 .099	2300 .100	1900 .125	0000 .100
Sept. 11-12	2000 .108	No Data	No Data	2000 .124	2100 .125	1900 .103	2100 .138

Based on these observations, we conclude that long distance transport is the major source of O_3 observed in our region. We further hypothesize that the depletion of ozone by reaction on the earth's surface with substances that are readily oxidized is an important factor that influences its concentration in the surface layer. These effects are the dominant factors that control ozone levels in our area and that account for a diurnal cycle that is strongly dependent upon the atmospheric stability. Some common sequences that we observe that are explained by this hypothesis are the following: (a) Clear Night Condition--Following a clear day, high concentrations of ozone may be advected into our region. During a cloudless night, strong outgoing radiation results in the formation of a nocturnal surface layer that is of depth equal to about 100 meters (6, 7). Within this confined layer, the ozone is reduced to marginally detectable levels by surface depletion reactions. Presumably high levels of ozone exist above the surface layer and then escape detection by the monitoring devices whose intake ducts are typically ten meters above the surface. Rural versus urban readings do differ because traffic-generated NO may be injected at ground level into the stable nocturnal surface layer by early morning traffic; thus urban O_3 readings will be generally lower than rural readings. Within two-three hours after sunrise, the nocturnal inversion is dispersed by solar heating of the earth's surface. Morning ozone readings rapidly increase when the O_3 above the disintegrating inversion is allowed to reach the ground through a fumigation process; (b) Cloudy Night Condition--A heavy layer of cloudiness present

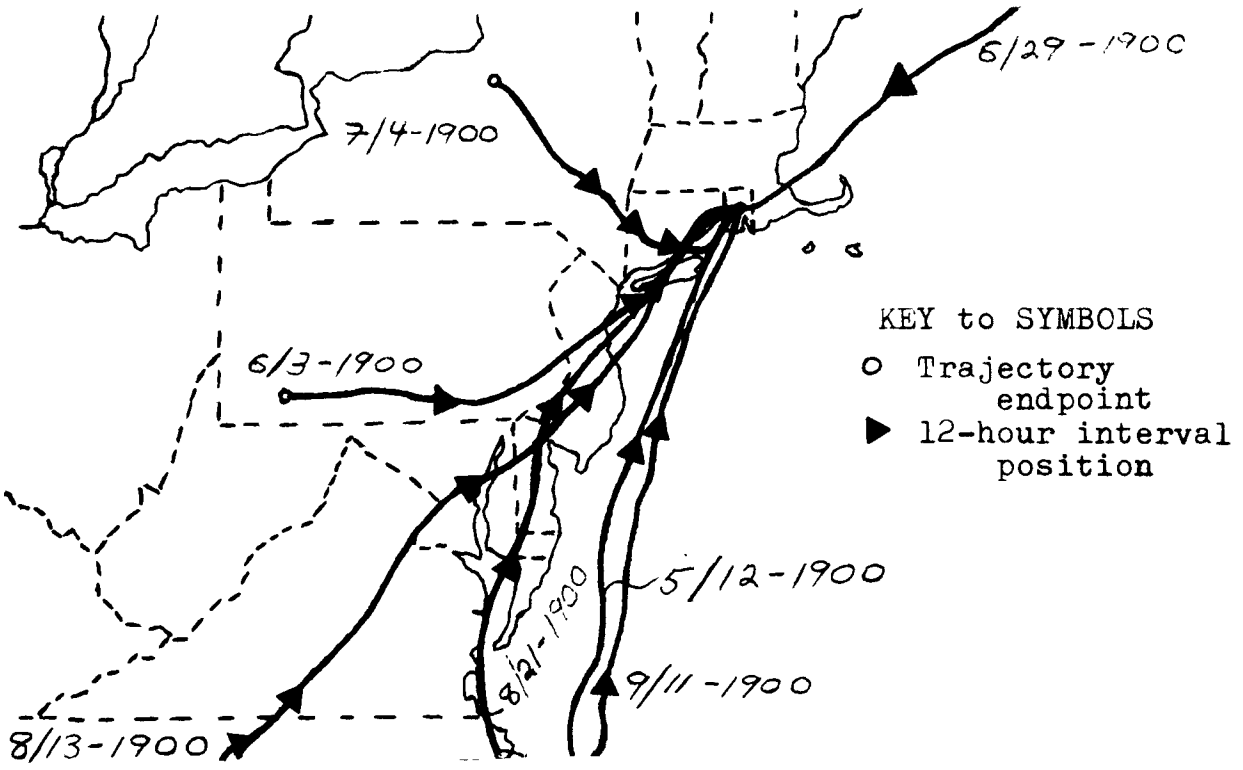

Figure 6. Air parcel trajectories nighttime O_3 peaks May - September 1975.

during nighttime hours results in a neutral atmosphere boundary layer whose typical height is 500-1000 meters. If the cloudiness follows a clear day, the O_3 levels at the surface can be high because of advection from sources outside our region. The O_3 concentration is totally controlled by the levels resulting from advection. Surface depletion reactions play a minor role because mixing from aloft is unimpeded by any stable layer near the surface. These two sequences are illustrated by the pre-sunrise/post-sunrise O_3 ratios in Figure 4 and by the correlation between the radiometer output and O_3 concentrations shown in Figure 5.

SUMMARY

We conclude that the ozone concentrations in southeastern New England result primarily from the transport of this pollutant into this region from distant sources. A study of air mass trajectories indicates that the ozone usually is transported from the southwest direction. The O_3 violations occur even when the morning NO_2 levels are low, suggesting that the local photolytic effect does not contribute to the O_3 peak.

We propose that under clear skies, surface depletion reactions occurring within the nocturnal inversion layer cause the low O_3 readings that are observed prior to sunrise. After sunrise, when the inversion is broken up by solar heating, the O_3 existing aloft is allowed to fumigate the surface, causing a rapid increase in ozone concentrations. Nighttime high levels of ozone directly reflect the influence of long distance transport under conditions when the cloudiness prevents the formation of a nocturnal inversion, and the

unimpeded mixing diminishes the relative importance of the surface depletion reaction.

This proposed mechanism involving surface depletion reactions is consistent with the observations of others. It may explain why Calvert found Equation 1 invalid during the early morning hours in the Los Angeles Basin and why he and others have observed O_3 concentrations increasing with altitude in the early morning hours under clear skies. The surface depletion reaction mechanism combined with transport is also consistent with the rural O_3 readings at Wilmington, Ohio, reported by Lonneman et al. (8); these readings increased dramatically during morning hours without a significant decrease of the very low level of NO_2 that was observed.

ACKNOWLEDGEMENTS

The authors wish to acknowledge the assistance of Larry Niemeyer and Dale Coventry of the U. S. Environmental Protection Agency, Research Triangle Park, North Carolina, in running the air parcel trajectories model; Marvin Rosenstein, U. S. Environmental Protection Agency, Region I, for providing the radiosonde data; and Arnold Leriche, U. S. Environmental Protection Agency, Region I, for the air quality data. Financial support was supplied by the New England Consortium for Environmental Protection for A. J. Gilbert and J. P. Okolowicz.

REFERENCES

1. Appendix D, "National Primary and Secondary Ambient Air Quality Standards," Federal Register, Vol. 36, No. 84, Part II, Friday, April 30, 1971.

2. EPA-R4-73-028c, Guidelines for Development of a Quality Assurance Program (Photochemical Oxidants), June 1973.

3. Spittler, T. M., "Report on Ozone Field Audits for 1975 Summer Ozone Study," N. E. Region APCA Monthly, Hartford, Conn., April 1976.

4. Heffter, J. L. and Taylor, A. D., "A Regional-Continental Scale Transport Diffusion and Deposition Model," NOAA Technical Memorandum, ERL ARL-50, June 1975.

5. Calvert, J. G., "The Theory of Ozone Generation in the Los Angeles Atmosphere," Environmental Science and Technology, Vol. 10, 1976, p. 248.

6. Yamada, T. and Mellor, G., "A Simulation of the Wangara Atmospheric Boundary Layer Data," Journal of Atmospheric Sciences, Vol. 32, 2309, 1975.

7. Shaw, N. A., "Acoustic Sounding of the Atmosphere," Ph.D. Thesis, University of Melbourne, Australia, 1971.

8. Lonneman, Buffalini & Seila, "PAN and Oxidant Measurements in Ambient Atmospheres," Environmental Science and Technology, Vol. 10, 1976, p. 374.

SESSION 4

SOURCES OF TROPOSPHERIC OZONE - II

Chairman: R.A. Rasmussen
Washington State University

AN ASSESSMENT OF THE CONTINENTAL LOWER TROPOSPHERIC OZONE BUDGET

R. Chatfield and R. A. Rasmussen*

ABSTRACT

Several different regimes of photochemistry and transport are necessary to describe the different patterns of diurnal ozone variation observed in rural areas of eastern North America. One chemical regime may govern ozone concentration for days then, within hours, it may be displaced by another regime as precursor concentrations, atmospheric mixing, and radiation change because of winds and weather. These regimes include: (a) exposure of the air's surface layer to tropospheric background ozone; (b) diurnal variation of ozone in clean, fair weather situations due to vertical mixing of background air and chemistry within the boundary layer; (c) production and transport of ozone within urban plumes; and (d) regional photochemistry acting on accumulated precursors to produce enhanced oxidant levels outside any individual urban plume.

These regimes are illustrated with case studies selected as archetypes of many days of intensive sampling in the midwest and northeast of the United States. Distinct patterns of ozone behavior are interpreted using fluorocarbon and hydrocarbon measurements. Detailed gas-chromatographic analysis of individual hydrocarbons describe oxidant precursor levels. Fluorocarbon measurements describe direct urban contamination and the degree of accumulation of anthropogenic emissions on a regional scale.

The tropospheric background appears to be about 60% greater than previously reported and there is evidence for east-west as well as north-south variations of the mean background across the continent. These conclusions arise from a reanalysis of the extensive ozone sounding programs of the sixties.

We present a brief assessment of the developments in other descriptions of the rural ozone budget over the last six years and suggest directions for future, more detailed modeling efforts.

INTRODUCTION

In 1970, the ozone budget of the nonurban troposphere seemed about to be expressed with reasonable numerical precision. Fabian and Junge in that year

*Washington State University, Pullman, Washington.

described a simple model, applicable outside urban areas, based on production of ozone in the stratosphere and on destruction at the earth's surface. On the basis of this model, all that seemed necessary to predict human exposure was better quantitation of boundary layer micrometeorology and surface reactivity. However, since 1970, a quantitative description of ozone concentrations, reactions, and fluxes has become much less definite—the ozone budget over and outside of the population centers of the mid-latitudes of the U.S. appears to be much less understood. Certain realizations have produced this indefiniteness:

- The long distance transport of oxidant pollution in urban and industrial plumes has been documented. For example, the work of Cleveland et al. (1976), Westberg (1976), and Spicer (1976) suggests that the plume of the New York City area may determine oxidant exposure in Boston, nearly 300 km distant.

- Measurements of high rural oxidant levels, outside the boundaries of distinct urban plumes, have repeatedly been reported. These levels have been described in terms of smog-like chemistry acting on regional accumulations of oxidant precursors (Robinson and Rasmussen, 1976; Ripperton, et al., 1974) or in terms of ozone of stratospheric origin (Coffey and Stasiuk, 1976).

- Levy (1971) has suggested that natural atmospheric processes produce radicals from methane oxidation even in clean environments. The details of this chemistry are still not adequately modeled; but, it is recognized that the process can produce or destroy ozone faster than transport to the earth's surface can destroy ozone (Crutzen, 1974). Chameides and Walker (1973, 1976) have suggested that this chemistry may produce much of the ozone of the troposphere.

- The prevalence of significant levels of non-methane hydrocarbons and other trace gases in rural areas has been demonstrated (Rasmussen, et al., 1976). It is not yet clear to what extent these gases may be responsible for modulating the surface ozone budget. Some compounds reduce ozone; others probably participate in free-radical chemistry processes that produce ozone.

- Our understanding of the natural range in the level of background tropospheric concentrations of ozone based on older methods of measurement has been questioned by the use of more accurate surface and airborne instruments. Chatfield and Harrison (1976c) have suggested that mid-tropospheric background ozone levels may be as much as 60% higher than estimated 1970.

This paper describes both the certainties and uncertainties of the tropospheric ozone budget. The following section sketches the photochemical and meteorological conditions affecting ozone transport and chemistry. Then observations characterizing mid- and lower-tropospheric ozone levels, which are free from boundary layer complexities, are presented. Three case studies of surface ozone variation with concurrent levels of hydrocarbon species and transport patterns are included. These case studies illustrate the alternate

importance of (a) vertical mixing of tropospheric air, (b) natural photochemical processes in the boundary layer, and (c) enhanced photochemical production of ozone due to anthropogenic emissions outside the boundaries of urban plumes.

OZONE CHEMISTRY AND TRANSPORT

In order to understand the variability of the concentrations of ozone observed near the earth's surface, we must appreciate the physical and chemical processes that govern its concentration in the boundary layer and the troposphere as a whole. Humans and plants, both sensitive to anomalously high ozone concentrations, have always lived within a few meters of the earth's surface. For this reason, our exposure to ozone has been within a very thin region of the atmosphere—the boundary layer. This layer is the region where ozone behavior is the most complex. Within the boundary layer (often considered equivalent to the "mixed layer") the chemistry and transport behavior of ozone is quite distinct from the rest of the troposphere.

First, within the limits of the boundary layer there are large sinks for atmospheric ozone. For three decades it has been apparent that the earth's surfaces, whether or not covered by vegetation, reduce ozone readily at various rates. Summaries of the importance of this sink may be found in Galbally (1974) and in Fabian and Junge (1970). The ocean's surface has much less ability to destroy ozone; its rate of destruction is still not well estimated (Regener, 1973). More recently, it has become apparent that trace gases emitted from natural biogenic sources and man's activities also effectively reduce ozone close to their surface sources. On the other hand, some of these gases, the hydrocarbons and nitrogen oxides, participate in reactions that resemble smog chemistry in great dilution. Many hydrocarbons, like isoprene, are measureable only within the earth's boundary layer, apparently indicating that they oxidize before they can travel far vertically. Others, like methane, appear to be distributed rather evenly throughout the troposphere (Ehhalt, 1972). Currently, the significance to the ozone budget of the photochemical reactions of these hydrocarbons is subject to considerable uncertainty. Levy (1972) and Crutzen (1974) have suggested that the oxidation of methane in the unpolluted lower atmosphere could contribute to or could destroy significant amounts of ozone. Chameides and Walker (1973) have taken the stronger position that photochemical oxidation of methane supplies the major source of tropospheric ozone. The ozone produced in their photochemical model dominates over transport and vertical diffusion in controlling ozone concentrations in the surface layer of the atmosphere (1976). Crutzen's (1974) description of the relevant reaction chains points out that various small changes in reaction rate coefficients and other model parameters change the destruction rate significantly and even allow for a net sink for ozone. Other hydrocarbons in addition to methane oxidize by means of radical-propagated reactions which may produce and/or destroy ozone via similar reaction pathways. While non-methane hydrocarbons are 3 to 4 orders of magnitude less concentrated in the boundary layer than methane, most of them are 2 to 4 orders of magnitude more reactive (Pitts, et al., 1976). The net result is that these species may contribute as significantly as methane to ozone formation. Graedel et al. (1976) have included isoprene and α-pinene in one reaction scheme; more ozone was generated from these hydrocarbons than from methane.

Three results of recent work stand out: (a) Chemical reactions produce or destroy ozone in the troposphere, (b) The variability of meteorology (sunlight, temperature, vertical mixing, and water vapor) and source strengths of precursors (hydrocarbons and nitrogen oxides) may vary so to allow both net production and destruction at different times, (c) Ozone-modulating chemistry is most active within the boundary layer; the boundary layer and the lower troposphere should be modeled as separate but interacting systems.

BACKGROUND TROPOSPHERIC OZONE

Systematic data on the variability of the ozone concentrations representative of the atmosphere above the boundary layer (90% of the troposphere) and away from densely populated areas are scarce. The data available until recently was incidental information obtained from programs designed to characterize surface ozone levels in urban air with little attention given to the ozone levels above the boundary layer. The ozone data available for mid-troposphere profiles was also peripheral since most of it came from ozone sounding programs designed to characterize stratospheric ozone. However, the latter programs provide an acceptable random sample of varying ozone levels characteristic of different weather situations and geographical locations obtained with instruments whose measurements are readily comparable.

Hering and Borden (1964a, 1964b, 1965, 1967) reported an extensive series of ozone soundings of the troposphere and stratosphere launched from 1963 to 1965. However they cautioned that errors in their method could be quite significant for the tropospheric portions of the soundings. Continuation of that ozone sounding program from 1966 to mid-1969 demonstrates the nature of one of these errors. Earlier ozone measurements used instruments based on the chemiluminescent reaction of ozone with rhodamine dye (CL instruments). The later ozonesonde studies used a Mast-type buffered KI electrochemical method (EC instruments). An analysis comparing the standardization of the instruments as well as the statistics of the ozone concentrations obtained from each type of instrument suggested that the EC instruments give more reproducible (precise) estimates of the tropospheric ozone. The better data obtained by the EC instruments in the second phase of the ozonesonde program are not very well known. This is unfortunate since the second data set apparently provides more information about the true variation of ozone in the mid-troposphere than does the first, larger data set. Chatfield and Harrison (1967c) reported that these EC instrument estimates may be more accurate estimates of free-tropospheric ozone. If Chatfield and Harrison's analysis of the two data sets is correct, estimates of tropospheric ozone based on Hering and Borden's earlier work should be raised by 50 to 60 percent.

Vertical profiles of ozone for the six stations that launched EC-type ozonesondes from 1966 to 1969 are shown in Figure 1. The ozone concentration profiles are the means of numerous soundings measuring the ozone above the stations named. The stations extended from the Canal Zone at 9°N to Goose Bay at 53.5°N. All of the stations are located within a few degrees longitude of the 75th meridian which passes through the East Coast of North America. The data analyzed are for the summer season. Consequently, the tropopause, above which ozone increases dramatically, is high, i.e., at Goose Bay, 9 km and, for

the tropical stations, over 14 km. For the three stations north of 30°N, the ozone profiles are nearly vertical. This constancy of ozone concentration suggests either that there is little net diffusive transport in the vertical or that the baroclinic eddies which produce the diffusive transport in mid-latitudes are not well modeled by K-theory. The vertical variation in the southern latitudes is a seasonal feature: in March for example, ozone is constant or decreases with height at these same stations. Transport by Hadley-cell motions and eddy motions described by Newell (1969) seems to be the most reasonable explanation.

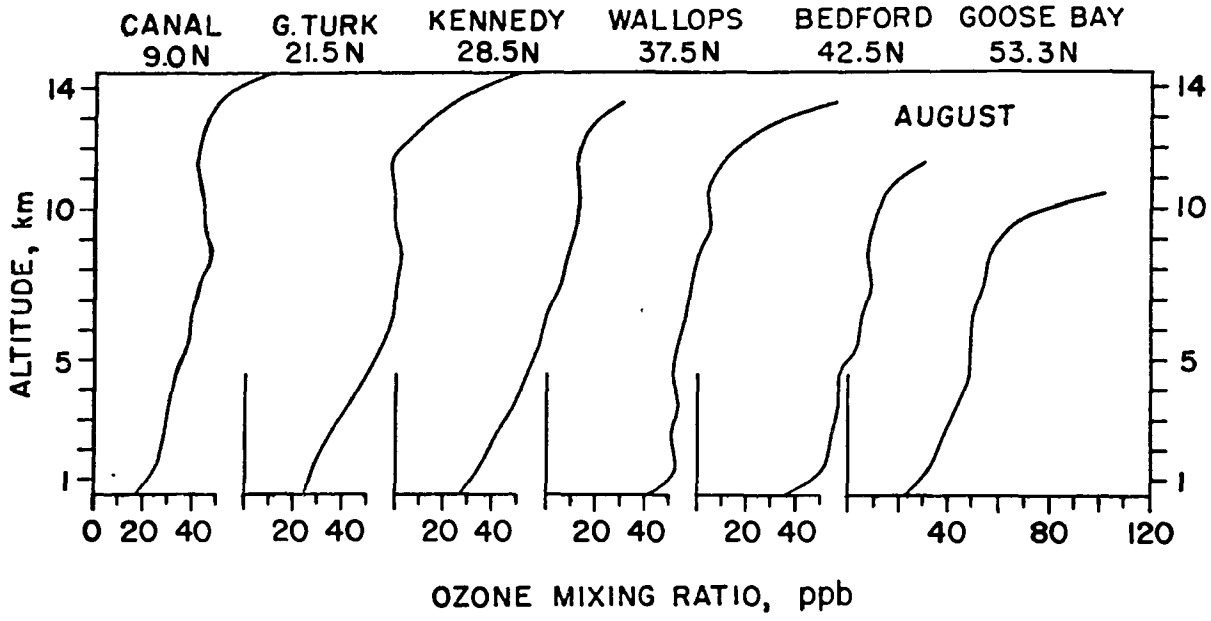

Figure 1. Averaged soundings of ozone concentration (in ppbv) above the listed stations. Electrochemical sondes launched during the summer seasons of the years 1966 through 1969 contributed to these means. The data for the lowest kilometer are not well estimated.

Figure 2 shows tropospheric ozone in a way that compares north-south variations among stations. The data used to generate this figure used EC ozonesonde reports for the layer 2 to 3 km above the earth's surface. The lower layers of the atmosphere are made more complex by boundary layer, local chemistry and transport features. Bedford, Massachusetts, 42.5°N, and Wallops Island, Virginia, 37.7°N, probably have additional complexities derived from large anthropogenic oxidant and SO_2 sources upwind (SO_2, for example, produced low instrument readings).

Certain aspects of Figure 2 argue persuasively that the stratosphere is the predominant origin of free-tropospheric ozone in the mid-latitudes. The left wall of Figure 2 shows a maximum ozone value at about 35°N in the month of January. As the year progresses, this maximum retreats northward to about 43°N, where it stays from March until September, and then advances to a lower latitude through the end of the year. The movement of this ridge of highest ozone values corresponds well to the retreat and advance of the mean position of the lower-tropospheric position of the polar front. It is this frontal region to which Danielsen's (1970) description of stratospheric injections into the troposphere applies. The value of the summer ozone maximum is also

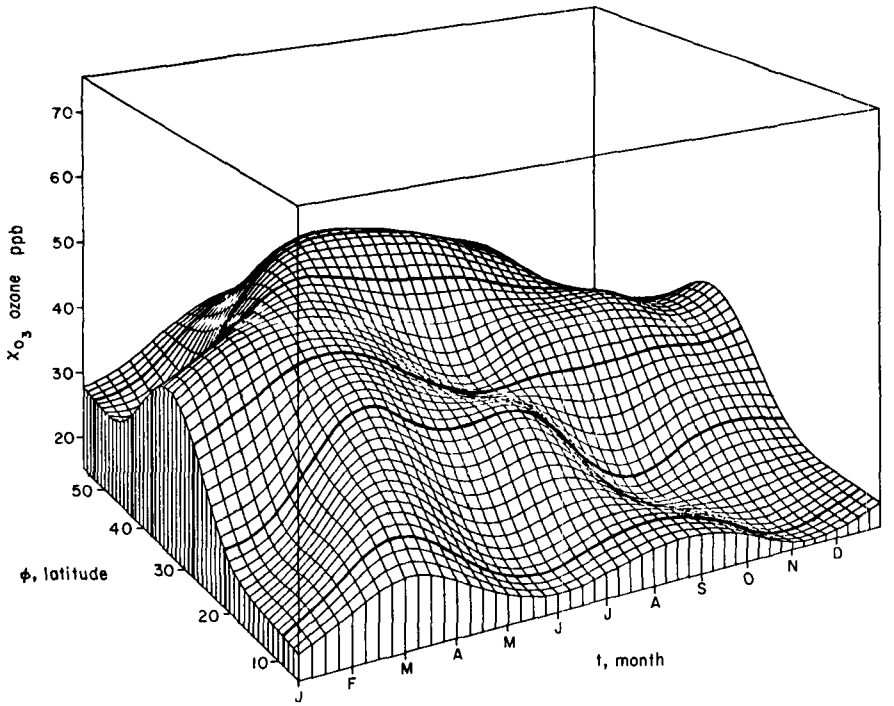

Figure 2. Time-latitude cross-section of ozone (ppbv) measured between 2 and 3 km by sondes launched from the stations listed in Figure 1. These stations lie within a north-south band running through the Eastern U.S.

reasonable in that only in the spring is the lower stratosphere in the mid-latitudes replenished with ozone from the tropical upper stratosphere. Injections from the stratospheric reservoir are also most likely to occur in the highly contorted tropospheric westerlies that are characteristic of spring weather.

Latitudinal variation is likely to be the most important type of variation, given the tendency of the winds to blow zonally. However, in Figure 3, contours of tropospheric ozone in the mid-troposphere, between 3 and 7 km, are drawn for all the stations reporting CL ozonesonde observations. The contoured ozone concentrations of ozone depicted have been raised by a factor of approximately 1.6 so as to agree with the results of the EC sonde data. The data seem to suggest an east-west variation in annual mean ozone. The chemical and dynamical explanations have been discussed by Chatfield and Harrison, (1967d).

TROPOSPHERIC BACKGROUND AS SAMPLED BY GROUND STATIONS

The deleterious effects of high ozone are most important near the ground; but, the complex chemistry and transport occurring within the boundary layer make ozone levels difficult to study. Aircraft and balloon soundings allow more extensive characterization of ozone formation and movement within this mixed layer, and have been quite useful in the past few years. However, another way to reduce the complexity of ozone behavior near the surface is intensive—that is frequent—measurement of ozone, hydrocarbon, and oxidant precursors, as well as tracers that give information about the origin of the

ozone sampled. For example, fluorocarbon tracers clearly identify the extent to which ozone may have had an urban origin.

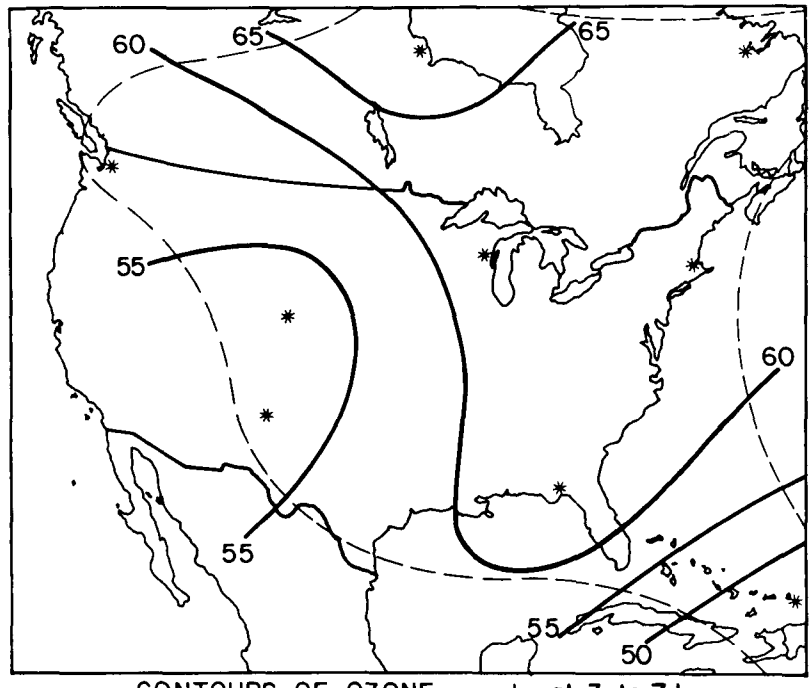

CONTOURS OF OZONE ppb at 3 to 7 km

Figure 3. Continental ozone background. Isopleths of ozone concentration (ppbv) derived from chemiluminescent ozonesonde ascents above the nine stations marked*. These isopleths are drawn for annual mean ozone; various seasons may exhibit somewhat different ozone climatology.

One such period during which a surface site was apparently exposed to clean tropospheric air is shown in Figure 4. The data were obtained at a farm site near Elkton crossroads in southwestern Missouri, just northwest of the Ozark Mountains. The fluorocarbon-11 (F-11) trace at the top of the figure is representative of uncontaminated urban emissions. Indeed, 115 ppt of F-11 was the minimum observable background level for surface air at that time period and altitude. As the radiation trace at the bottom of the figure shows, conditions were generally overcasted. The movement of warm Gulf air into the area during the afternoon resulted in showers in the early evening. One squall line thunderstorm (not associated with a deep 500-mb though) passed over the area at about 2200 CDT on the 25th. Intense stirring of clean middle tropospheric air to the surface occurred for the F-11 trace dipped to 105 ppt. The lack of any significant change in ozone level suggests that the ozone concentration overhead was similar to the concentration at the surface. The vertical ozone profiles shown in Figure 1 for stations north of 30°N latitude also suggest that the overhead ozone level does not normally change dramatically with altitude during the summer season. Total non-methane hydrocarbons also decreased during this period from 50 to 30 $\mu g\ m^{-3}$.

The ozone trace contained between August 25-26, 1976, is a typical pattern for windy, low-radiation situations in rural areas. The general ozone level varied irregularly between 30 and 47 ppb, and there was little indica-

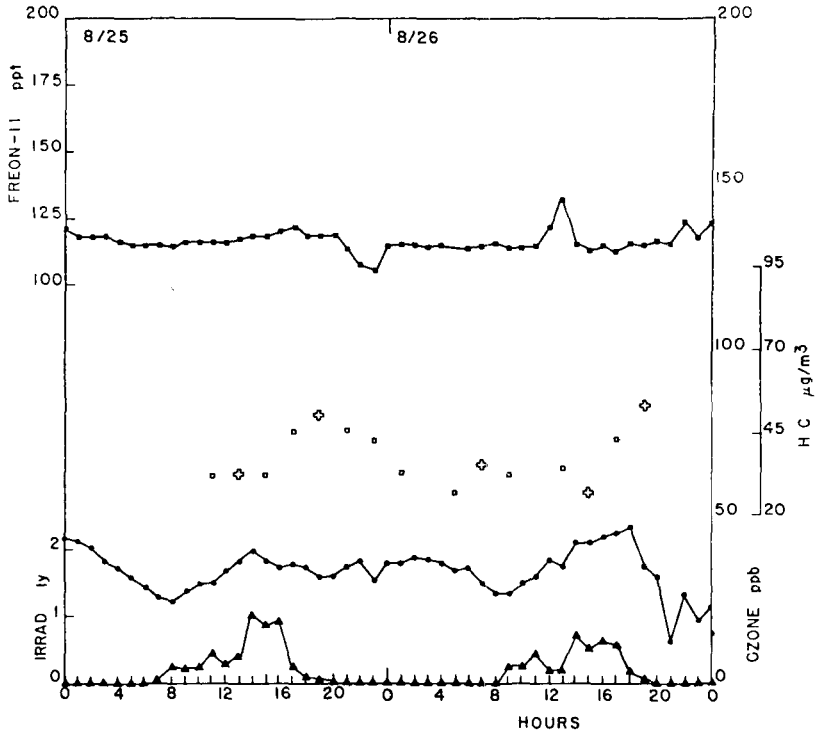

Figure 4. Variation in ozone, hydrocarbon, and fluorocarbon levels observed during stormy weather near Elkton crossroads in southwestern Missouri.

tion of a diurnal cycle.

How do these surface concentrations compare to the tropospheric ozone background illustrated in Figure 2? The latitude of Elkton, Missouri, is closest to Wallops Island, Virginia (37.5°N). The mid-tropospheric ozone concentration observed with the Wallops ozonesondes reported approximately 55 ppb of ozone in August and 50 ppb in September. Since Elkton is 17° west of Wallops Island, the evidence summarized in Figure 3 suggests that we should subtract approximately 5 ppb. In short, the agreement between sounding data and remote site data is consistent with the interpretation that the surface ozone observed at Elkton under windy, low radiation conditions is primarily derived from overhead replenishment of the ozone in the troposphere.

Such agreement is partly accidental since the standard deviation of the tropospheric ozone background at one location and season is 0.2 to 0.3 of the mean, as measured by the EC ozonesondes. The variability includes the range of true climatic variability of ozone as well as instrumental variability of the ozone data analyzed by Chatfield and Harrison (1967d). The variation on the ozone levels from the climatology of the lower atmosphere suggested by Figure 2 may persist for weeks, as observations at the same site in successive years indicate. That is to say, ozone displays "weather" just as do rain and temperature. Perhaps the most variation occurs in the spring, when the prevalence of blocking highs and cut-off lows create weather patterns which are conducive to stratospheric injections of ozone into the troposphere (Danielsen 1976). In certain cases, it appears that stratospheric injections followed by strong cumulonimbus downdrafts can produce hour-long periods when surface ozone concentrations are observed at levels of hundreds of ppb (Lamb, 1976)

and shorter periods when ozone can approach 600 ppb (Attmannspacher and Hartsmannsgruber, 1973). Davis and Jensen (1976) have recently summarized practical techniques for forecasting high ozone levels.

NATURAL PHOTOCHEMICAL OZONE IN THE BOUNDARY LAYER

The significance of the photochemical production of ozone within the lower troposphere has been a point of controversy in recent years (Chameides and Walker 1973, 1976; Chameides and Stedman, 1975; Fabian, 1974). Presumably, there is a greater likelihood of significant photochemistry occurring in the boundary layer with its higher concentrations of oxidant precursors than in the free troposphere. The evidence for significant photochemistry occurring in the mixed layer outside urban plumes in situations of relatively clean environments has been poorly documented.

Several days after the storms that characterized the August 25-27 weather at Elkton, Missouri, passed, the weather became sunny and the air relatively clean as shown in Figure 5. On the 30th, a weak cold front passed through the area in the early morning hours without bringing rain, although a few clouds persisted. Fluorocarbon levels gradually increased from 115 ppt in the afternoon although they remained below 125 ppt until midnight. Ozone showed a typical diurnal variation for clear weather with a broad maximum in the middle and late afternoon. The peak ozone hourly values reached 56 ppb, an increase of 28 ppb from that morning at 0900 CDT, which was about the time of the frontal passage.

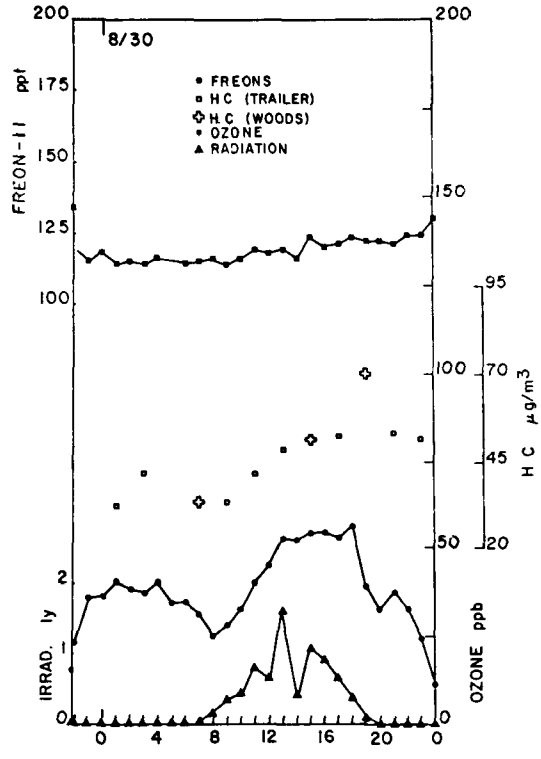

Figure 5. Fair weather diurnal variation pattern of ozone levels contrasted with hydrocarbon and fluorocarbon levels observed near Elkton, Missouri. The afternoon maximum in ozone may be due to local photochemistry.

The hydrocarbon composition of the atmosphere was consistent with unpolluted rural air with 30 to 50 $\mu g\ m^{-3}$. Total non-methane hydrocarbons (excluding oxygenated species) were usually about 50 $\mu g\ m^{-3}$ in the afternoon. A typical afternoon sample was composed of about 10 $\mu g\ m^{-3}$ of natural gas alkanes, 2.5 $\mu g\ m^{-3}$ aromatics, 2.0 $\mu g\ m^{-3}$ i-butane and n-pentane, 7.3 $\mu g\ m^{-3}$ of isoprene, and 6.5 $\mu g\ m^{-3}$ of four unknown but prevalent hydrocarbons of apparently rural origin and 20 $\mu g\ m^{-3}$ of other hydrocarbons, about half of which were statistically associated with rural unknown hydrocarbons. These identifications were made on the basis of gas chromatographic separations described in Rasmussen, Chatfield, and Holdren (1976). In summary, the hydrocarbon composition of the atmosphere was dominated by rural hydrocarbons with very dilute traces of some anthropogenic hydrocarbons.

The levels of hydrocarbons present were sufficient to produce the 28 ppb ozone increase observed during the day. Since it is theoretically possible to produce from each oxidized atom of carbon 3 or 4 radicals, and hence 3 or 4 ozone molecules, the 7.3 $\mu g\ m^{-3}$ of photochemically reactive isoprene could produce 28 ppb of ozone if it were to react completely. In addition, isoprene reacts so much more rapidly with hydroxide radicals than does methane that, at the concentrations observed, it creates almost twice as many radicals as methane (Pitts, et al., 1976). In reality, there are many reactions that destroy ozone and the necessary radical precursors. Also the flux of ozone into or out of the boundary layer, both with the free atmosphere and with the ground, are unquantified parameters affecting the resultant ozone concentrations. Only intricate photochemical modeling will be able to balance all of these effects.

While atmospheric chemistry processes within clean continental air can plausibly produce ozone, one of the authors has argued elsewhere that many pieces of evidence that seem to confirm photochemistry also confirm transport arguments (Chatfield and Harrison 1976a). Solar radiation, for example, governs meteorological processes (such as convective mixing) as well as photochemical rates. Conclusive observational evidence for photochemical ozone formation in rural atmosphere remains to be presented.

REGIONAL OXIDANT PHOTOCHEMISTRY

Perhaps the most problematic portion of the current understanding of the lower tropospheric continental ozone budget is assessing the extent to which urban and industrial hydrocarbon precursors may increase oxidant production on regional or sub-continental scales. Recently there has been considerable attention given to oxidant production in urban and industrial plumes. These studies show very clearly marked pollutant episodes occurring outside cities. Other contributors to this conference have described in greater detail the theoretical and observational features of these urban plumes. However, there is a larger problem of regional air pollution episodes. Our measurements at Elkton, a site specifically chosen to represent clean air in the far Midwest, suggest that the air within the boundary layer even at this very rural site is almost never entirely free of anthropogenic emissions.

Often, rural air is so well mixed horizontally that the plumes of small

to modest size (10,000 to 70,000 population) cities can not be distinguished 50 km downwind. Husar, et al. (1976) has noted the regional accumulation of visibility-degrading aerosol into regional "blobs" shifted by synoptic winds. Currently, such aerosol-haze is believed to be due to secondary heterogeneous photochemical reactions involving either hydrocarbons or sulfates, or both.

Our example of apparent regional air pollution episode comes from ground station studies conducted near Glasgow, Illinois, 104 km NNW of the St. Louis Gateway arch in July 1975. The studies at this site were conducted just prior to the Elkton studies.

The meteorology and trace chemistry conditions leading to this episode are shown in Figure 6. Both the time variation of the F-11 concentrations and total non-methane hydrocarbon (TNMHC) levels at the Glasgow site are shown. The correlation for F-11 spikes—indicators of urban plumes—and TNMHC spikes is very good, though not perfect. The line drawn at 115 ppt represents the minimum F-11 concentrations observed as Glasgow, Illinois, or Elkton, Missouri. The passage of urban air with higher levels of F-11 extend upward from this background level as spikes. Besides the minimum background representative of the cleanest air, there is a daily background suggested by the minimum concentrations attained each day when the site was most nearly free of urban plumes.

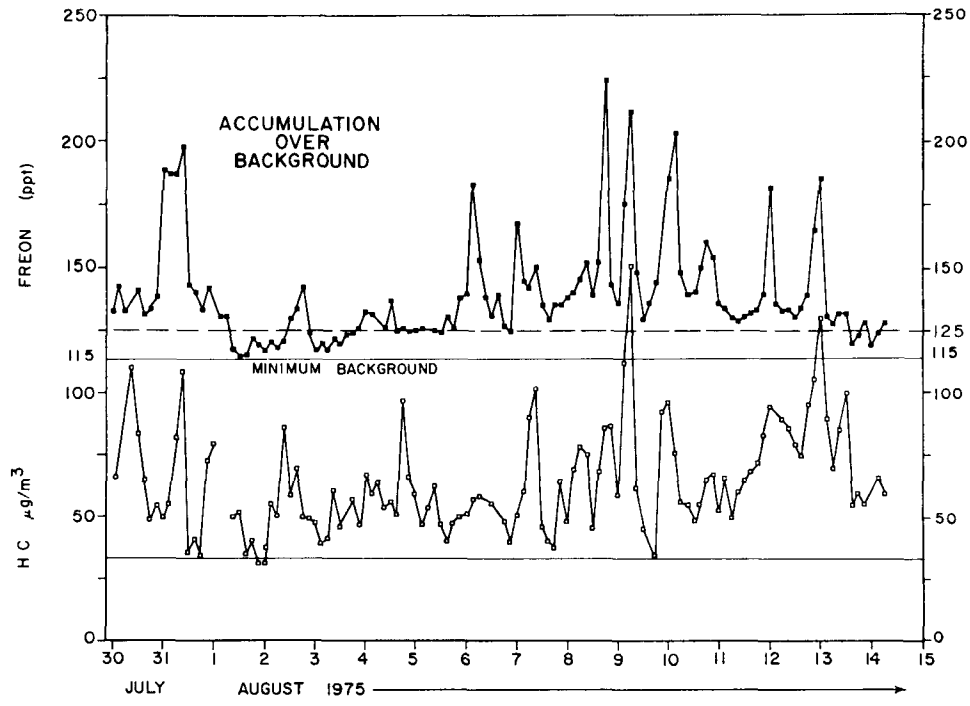

Figure 6. Regional accumulation of fluorocarbon-11 and non-methane hydrocarbon sampled on a farm 110 km north of St. Louis during the first two weeks of August 1975. The fluorocarbons spike to high levels when plumes of urban air are sampled; hydrocarbons show a similar behavior. There is also a gradual increase in minimum daily fluorocarbon concentrations from August 3 to August 13. On these dates, new high-pressure systems entered the area.

A subtle but important feature of the data gathered at Glasgow is the slow increase in this general level of the daily F-11 background from 117 ppt on August 2 to 130 ppt on August 12, and the subsequent more rapid decline to 118 ppt on August 13. The rise was not due to instrumental drift. Instead the rise in the F-11 background represents the accumulation of emissions in the air over the Midwest during this period. Of course, our site at Glasgow never sampled the same air parcel twice; but, the Eulerian description of the site portrays fluorocarbon buildup in a manner fairly representative of air parcels moving within a stagnant southward-drifting high-pressure system. The last frontal passage bringing in new air from the northwest was on August 2. During the following time lapse the air mass drifted from the industrial Midwest into the Glasgow site where it peaked August 12-14.

Somewhat similar accumulative behavior is evident for the TNMHC loading of the atmosphere shown in Figure 2, despite the greater variability that is evident for these reactive substances. It is likely that nitrogen oxides also increased during this period, but the Washington State University trailer did not measure them.

Figure 7 shows in detail the ozone, F-11, and TNMHC variations observed on August 12. About midnight, the St. Louis plume passed over the station according to the evidence of the surface winds and the F-11 readings monitored at the trailer site. The surface winds then swung south to the west-southwest from 0300 CDT until 1500 CDT; during this period it would have been nearly impossible for the site to be exposed to the St. Louis plume. By 1600 CDT, the wind turned again to flow from the south, and within 4 hours the sampling station was again directly exposed to St. Louis air. At 2000 CDT the plume-generated oxidant rose to over 100 ppb and then dropped quickly.

The interim period of west-southwest winds shows ozone behavior equally as interesting as the 100 ppb spike. During the interim period ozone reached 90 ppb for one hour, and remained at a level of over 85 ppb for 5 hours outside any identifiable urban plume.

The hydrocarbon chemistry of this day shows a mixture of anthropogenic and natural emissions. TNMHC averaged around 80 $\mu g\ m^{-3}$. Gas chromatographic analysis of the ambient air samples taken in the afternoon show about 17.4 $\mu g\ m^{-3}$ natural gas hydrocarbons, 6.4 $\mu g\ m^{-3}$ of aromatics, 4.4 $\mu g\ m^{-3}$ of automotive fuel vapors (e.g. pentane, octane), 4.3 $\mu g\ m^{-3}$ of automotive exhaust emissions (ethylene, propene, n-butane), 6.8 $\mu g\ m^{-3}$ of isoprene, 10.0 $\mu g\ m^{-3}$ of unknown compounds of suspected rural origin, and 29.0 $\mu g\ m^{-3}$ of other compounds.

Not all of the days during this interim period showed such high ozone levels outside of the plume episodes. The previous day showed only 60 ppb of ozone at maximum in conjunction with 60 $\mu g\ m^{-3}$ of hydrocarbons. Ozone levels might have risen further, but in the early afternoon clouds cut off the solar radiation, and ozone began to decline immediately. Also there were differences in the hydrocarbon concentration which may have affected oxidant production; i.e., there were lower concentrations of isoprene, and other rural unknown compounds, and natural gas alkanes. Other reports of elevated ozone distributions in the Eartern United States suggest the possibility of region-wide production of oxidant. One particularly interesting set of ozone meas-

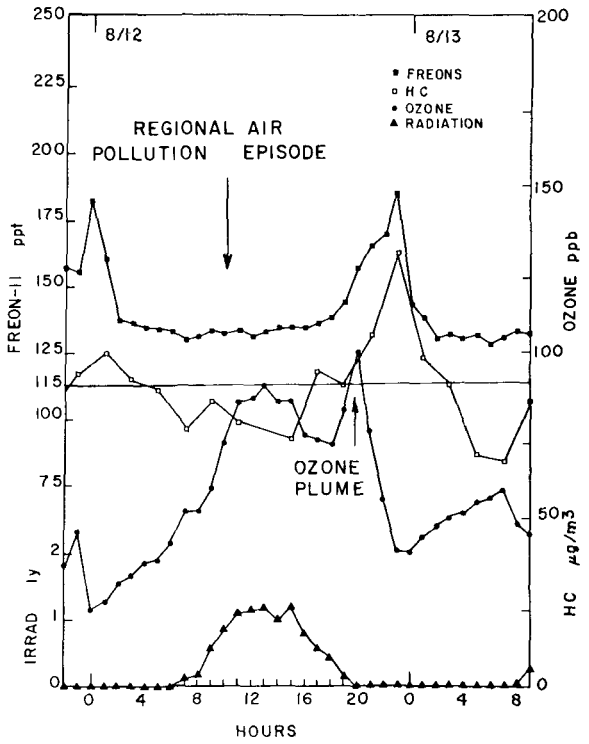

Figure 7. Elevated ozone levels related to regional accumulations of oxidant precursors by August 12 in Glasgow, Illinois. The F-11 spikes at 0 and 20 CDT indicate influx of urban air from St. Louis with accompanying increased ozone levels. Between these spikes, F-11 remains at levels significantly above the minimum background value of 115 ppt. It is suspected that similarly elevated levels of hydrocarbons and oxides of nitrogen may have produced the high midday ozone.

urements was made at 500 m above the ground between Canton, Ohio, and the Black Hills of South Dakota in the summer of 1974. The observed ozone concentration dropped from 70 ppb over the rural areas of Ohio early in the morning to 40 ppb over the rural Great Plains late in the evening on the same day. This measurement suggests a substantial east-west gradient in ozone, but other considerations prevent our accepting this gradient as representative of regional photochemistry acting solely on anthropogenic or natural emissions. The 70 ppb measurement was made early in the morning, and there is no data or estimate of the level to which it could have risen in the afternoon. Photochemical considerations would allow even larger ozone gradients due to anthropogenic emissions producing more ozone to add to the 70 ppb value. However, the distance scale is also a synoptic distance scale, so that ozone differences might be attributed to different ozone "weather": that is, the ozone gradient may reflect mid-tropospheric ozone variations or other weather effects rather than differing surface emissions. For these reasons it is important that measurements on this larger synoptic scale be repeated.

CONCLUSIONS

Substantial uncertainties exist in quantifying the significance of the

different sources of ozone or contributions of ozone precursors in the lower tropospheric ozone budget over continents. There is a clear need to model both transport and chemistry in the lowest few kilometers of the atmosphere. Both chemical and meteorological parameters for models on this scale are relatively uncertian. It appears that separate and interrelated models should be constructed for:

(1) The boundary layer. Emissions and photochemistry of non-methane hydrocarbons allow ozone levels to change significantly within a day, but other important precursor transport processes may occur over several days.

(2) The "free" lower troposphere. The interaction between local photochemistry and synoptic-scale transport must be qualified.

Verbal models of ozone variation near the surface may allow for different regimes of transport-dominated and photochemistry-dominated patterns of ozone concentration gradients or distributions to develop. In summary they are:

(1) Clean, strongly mixed troposphere. Ground level ozone from 15 to 70 ppb determined by the ozone concentration of mid-troposphere. This mid-tropospheric concentration may be summarized by latitude and season, as in Figure 3, but it is a "climatology" of ozone subject to ozone "weather."

(2) Clean, diurnally mixed troposphere. Both photochemistry and diurnal boundary-layer mixing give adequate descriptions of the ozone behavior. Models should incorporate both parameters quantitatively.

(3) Urban plumes. Individual urban plumes frequently modify ozone concentrations in the lowest kilometer of the troposphere of the Eastern United States. Large plumes may travel 200 to 300 km before losing their character. Their composition produces variations in the ozone pattern different than rural air; however, additions of rural hydrocarbons like isoprene may rekindle ozone production particularly in older plumes.

(4) Regional oxidant production. The trailing portions of slowly migratory high pressure systems accumulate ozone and oxidant precursors not attributable to a single urban area. There is a need for models of the photochemistry of these situations. The relationship of area wide production of oxidants with the development of photochemical aerosol-haze patterns described as "blobs" through the Midwest needs better study.

REFERENCES

Attmannspacher, W., and R. Hartmannsgruber. 1973. On Extremely High Values of Ozone Near the Ground. Pure and Applied Geophys. 106-108:1091-1096.

Chameides, W. L., and Donald H. Stedman. 1976. Ozone Formation from NO_x in Clean Air. Environ. Sci. Tech. 19(2):150-153.

Chameides, W., and J. C. G. Walker. Dec. 20, 1973. A Photochemical Theory of Tropospheric Ozone. J. Geophys. Res. 78:8751-8760.

Chameides, W., and J. C. G. Walker. 1976. A Time-Dependent Model for Ozone Near the Ground. J. Geophys. Res. 81(3):413-420.

Chatfield, R. B., and H. Harrison. 1976a. Tropospheric Ozone: Mixing vs. Photochemistry. J. Geophys. Res. 81(3):421-423.

Chatfield, R. B., and H. Harrison. 1976b. Proceedings of the Specialty Conference on Ozone/Oxidants - Interactions with the Total Environment. APCA.

Chatfield, R. B., and H. Harrison. 1976c. Tropospheric Ozone, I: Evidence for Higher Background Values. Submitted for publication in J. Geophys. Res.

Chatfield, R. B., and H. Harrison. 1976d. Tropospheric Ozone, II: Variations Along a Meridional Band. Submitted for publication in J. Geophys. Res.

Cleveland, W. S., B. Kleiner, J. E. McCrae, and J. L. Warner. 1976. Photochemical Air Pollution: Transport fron the New York City Area into Connecticut and Massachusetts. Science. 191:179-181.

Coffey, P. E., and W. N. Stasiuk. Jan. 1976. Evidence of Atmospheric Transport of Ozone into Urban Areas. Environ. Sci. Tech. 9:59-62.

Crutzen, Paul J. 1974. Photochemical Reactions Initiated by and Influencing Ozone in Unpolluted Tropospheric Air. Tellus. 26(1-2).

Danielsen, E. F., et al. 1970. Observed Distribution of Radioactivity, Ozone, and Potential Vorticity Associated with Tropopause Folding. J. Geophys. Res. 75:12.

Davis, D. R., and R. E. Jensen. March, 1976. Low Level Ozone and Weather Systems. Proceedings of the Specialty Conference Ozone/Oxidants - Interactions with the Total Environment. APCA.

Ehhalt, D. H. 1974. The Atmospheric Cycle of Methane. Tellus. 26(1-2):58-70.

Fabian, P. 1974. Comments on 'A Photochemical Theory of Tropospheric Ozone.' by W. Chameides and J. C. G. Walker, J. Geophys. Res. 79(27):4124-4125.

Fabian, P., and C. E. Junge. 1970. Global Rate of Ozone Destruction at the Earth's Surface. Arch. Met Geoph. Biokl. 19(Ser. A):161-172.

Graedel, T., and D. L. Allara. March, 1976. The Kinetic Photochemistry of Natural and Perturbed Remote Tropospheres. Submitted for publication.

Hering, Wayne S., and Thomas R. Borden, Jr. Ozonesonde Observations Over North America, AFCRL-64-30(I-IV), Air Force Cambridge Research Laboratories, Meteorology Laboratory Research Project 8631. Environmental Research Papers. No. 133:279.

Husar, R. B., N. V. Gillani, J. D. Husar, and C. C. Paley. March 1976. Hazy Air Masses Over the Continental United States. Submitted for publication.

Lamb, Robert G. 1976. Personal communication of an analysis of an ozone epi-

sode in Santa Rosa, California occurring in November, 1975.

Levy, H. H. 1971. Normal Atmosphere: Large Radical and Formaldehyde Concentrations Predicted. Science. 173:141.

Levy, H. H. 1974. Photochemistry of the Troposphere. Advances in Photochemistry. 370-524.

Newell, R. E., D. G. Vincent and J. W. Kidson. 1969. Interhemispheric Mass Exchange from Meteorological and Trace Substance Variations. Tellus. 21(5):641-647.

Rasmussen, R. A., R. B. Chatfield, and M. Holdren. 1976a. Hydrocarbon Levels Observed in a Midwest Rural Open-Forested Area. Report being submitted to the Coordinating Research Council. Contract No. CAPRAC-11.

Rasmussen, R. A., R. B. Chatfield, and M. Holdren. 1976b. Hydrocarbon and Oxidant Chemistries Observed at a Site near St. Louis. Report being submitted to the Environmental Protection Agency. Contract No. 68-02-2254.

Regener, V. H. 1974. Destruction of Atmospheric Ozone at the Ocean Surface. Arch. Met Geoph. Biokl. 23(Ser. A):131-135.

Ripperton, L. A., J. B. Tommerdahl, and J. J. B. Worth. 1974. Proceedings of the Annual Meeting of the APCA, Denver, Colorado, June 9-13, 1974.

Robinson, E., and R. A. Rasmussen. March 1976. Identification of Natural and Anthropogenic Rural Ozone for Control Purposes. Proceedings of the Specialty Conference on Ozone/Oxidants - Interactions with the Total Environment. APCA.

Spicer, Chester W. 1976. Ozone and Hydrocarbon Measurements by Batelle. Proceedings of the Northeast Oxidant Transport Symposium held at Research Triangle Park, North Carolina on January 20-21, 1976.

Westberg, H. H. 1976. Ozone and Hydrocarbon Measurements by W.S.U. Proceedings of the Northeast Oxidant Transport Symposium held at Research Triangle Park, North Carolina on January 20-21, 1976.

Westberg, H. H., K. J. Allwine, and D. Elias. March 1976. Vertical Ozone Distribution above Several Urban and Adjacent Areas across the U. S. Proceedings of the Specialty Conference on Ozone/Oxidants - Interactions with the Total Environment. APCA.

URBAN KINETIC CHEMISTRY UNDER ALTERED SOURCE CONDITIONS

L. A. Farrow, T. E. Graedel, and T. A. Weber*

ABSTRACT

The effect of altered source generation rates on ozone concentrations in northern New Jersey has been assessed by a series of detailed photochemical calculations. The Sunday Effect, in which measured Sunday ozone concentrations in certain urban areas are similar to those occurring on workdays despite markedly different motor vehicle emissions, is successfully reproduced. The concept of functional oxygen groups is introduced and used to show that the Sunday effect results form the tight balance between ozone production through nitric oxide photodissociation and oxygen scavenging by nitric oxide, from the advection of ozone from less urban areas, and from the incorporation of similar quantities of ozone preexisting above the morning mixed layer.

INTRODUCTION

The chemical generation and destruction of ozone in the urban troposphere is known to be inextricably connected with the atmospheric chemistry of hydrocarbons (HC) and oxides of nitrogen (NO_X). Despite this connection, however, ambient air quality data (Paskind and Kinosian, 1974) and smog chamber studies (Dimitriades, 1975) have not shown a simple relationship between ozone and its precursors. An example of the complexity of the problem is the Sunday Effect (the only altered source condition for which substantial quantities of air quality data are available), in which Sunday ozone concentrations in certain urban areas are similar to those occurring on workdays despite markedly different motor vehicle emissions (Bruntz, et al., 1974; Cleveland, et al., 1974).

This paper presents the results of detailed chemical kinetic computations representing workdays and Sundays in Hudson County, New Jersey. The computational techniques are applied to the Sunday Effect, which is shown to be a consequence of the chemistry and meteorology of the urban troposphere.

COMPUTATIONAL FORMULATION

Calculation of the diurnal chemical concentrations in the urban troposphere is based on a chemistry of 143 reactions in 76 species. Extensive

*Bell Laboratories, Murray Hill, New Jersey.

descriptions of the chemistry of oxides of nitrogen, hydrocarbons, and sulfur compounds are included in the reaction set, as is a representation of the heterogeneous interactions between gas phase radicals and the atmospheric aerosol. This chemical formulation is described in detail by Graedel, et al., (1976) (hereafter termed "Paper I"). As has been discussed previously (Paper I), no chemical set can be considered a complete representation of tropospheric photochemistry. The excellent agreement with data that results, however, indicates that our formulation, at the very least, captures the essential processes which control that chemistry.

The computational architecture that is utilized is based on a 3x1 matrix of geographical areas, in which each matrix element is rectangularized transformation of the dimensions of a county; those represented are (from west to east), Morris County, New Jersey, Essex County, New Jersey, and Hudson County, New Jersey. Since available emission inventories for the region are compiled on a county-wide basis, each of the counties is treated as a "reaction volume" with source terms corresponding to the emission data. Emissions attributable to mobile sources are varied in accordance with local traffic density functions and those for power plants in accordance with energy generation patterns. Other emissions are regarded as constant with time. For computations with varied source conditions, all sources are multiplied by the same reduction or enhancement factor; diurnal emission patterns are preserved.

The flow of gases from one matrix element to the next is controlled by the local wind velocity and direction. In the computations presented here, we utilize an average diurnal wind flow pattern derived from measurements at Newark Airport (Essex County) on summer days of normal convective mixing. The variations in mixing height are specified by a function derived from lidar measurements of the atmospheric aerosol. The chemical species within each reaction volume are assumed to be fully mixed.

Several differences exist between the workday and Sunday computations. The most important is the marked difference in motor vehicle emissions and power generation functions for Hudson County. Atmospheric aerosol concentrations are lower on Sundays and, perhaps as a result, the solar radiation at ground level is somewhat higher (Cleveland et al., 1974). In addition to its meteorological effects, the change in aerosol concentration reduces the heterogeneous interactions which have important effects on tropospheric chemistry (Farrow, et al., 1975; Graedel, et al., 1975). The increased solar radiation increases the rate of the photosensitive reactions included in the chemical set.

RESULTS OF SUNDAY EFFECT CALCULATIONS

Computations of the kinetic chemistry of the urban troposphere have been performed for Morris, Essex, and Hudson Counties, New Jersey, for both workdays and Sundays. The workday computations have been described in detail in Paper I, and the agreement with a wide variety of air quality data for Hudson County (across the Hudson River from Manhattan) have been judged to be good. For the Sunday computation, there are insufficient days with appropriate characteristics (i.e. full sun, summer, westerly wind direction, wind speed

within the central 50% of all values) to permit a direct comparison between data and computational results. It is possible, however, to make general comparisons with less stringently stratified data. Figure 1a shows the computed diurnal ozone (O_3) concentrations for workdays and Sundays. The Sunday computation reproduces two important characteristics of the Sunday ozone data illustrated by Bruntz, et al, (1974): the virtual equivalence of the afternoon ozone peak, and the higher ozone values on Sunday morning. The ozone computations show higher Sunday evening values not reflected in the data; this discrepancy may be a result of inadequate representation of the heavy traffic flow from New Jersey shore points to the metropolitan area that occurs on summer Sunday evenings.

The reduction in the ozone precursors nitric oxide (NO) and nitrogen dioxide (NO_2) on Sundays is snown in Figures 1b and 1c. Similar reductions occur in air quality data (Cleveland, et al., 1974), and are representative of concomitant reductions in other species such as carbon monoxide (CO) and nonmethane hydrocarbons.

The results can be succinctly summarized: The computations have succeeded in reproducing the ozone Sunday Effect, while simultaneously demonstrating the reduction in primary emittants known to occur on Sunday.

FUNCTIONAL GROUP ANALYSIS

The Sunday Effect is intriguing because of its defiance of the intuitively anticipated precursor-product relationship between ozone-producing species and ozone itself. Having duplicated the Sunday Effect computationally, we then proceeded to deduce a unifying analytical technique that not only demonstrates why the Sunday Effect occurs, but offers potential insight into a wide variety of other atmospheric chemical regimes. The initial step is to divide the oxygen-containing species into groups on the basis of the function of the incorporated oxygen in photochemical reactions. Four groups are distinguished: fixed oxygen (ϕO), accessible oxygen (αO), dissociative oxygen (δO), and odd oxygen ($\circ O$).

The chemical species assigned to each group depend on the chemical detail of the analysis. In this study, odd oxygen includes $O(^3P)$ (indicated throughout as O), $O(^1D)$, and O_3. Dissociative oxygen includes those species that photodissociate to produce odd oxygen; NO_2 and nitrous oxide (N_2O) comprise the δO subgroup in this study. Accessible oxygen species are those that can donate an oxygen atom to permit the formation of δO in a single reaction step; in our study this group comprises nine RO_2 radicals, nitric acid (HNO_3), HO_2, nitrogen pentaoxide (N_2O_5), and NO_3.

$$NO_2 \xrightarrow{h\nu} NO + O$$

$$N_2O \xrightarrow{h\nu} N_2 + O(^1D).$$

(We note that recent experimental results indicate that N_2O photodissociation does not occur in the lower troposphere [Stedman, et al., 1976]. The effect

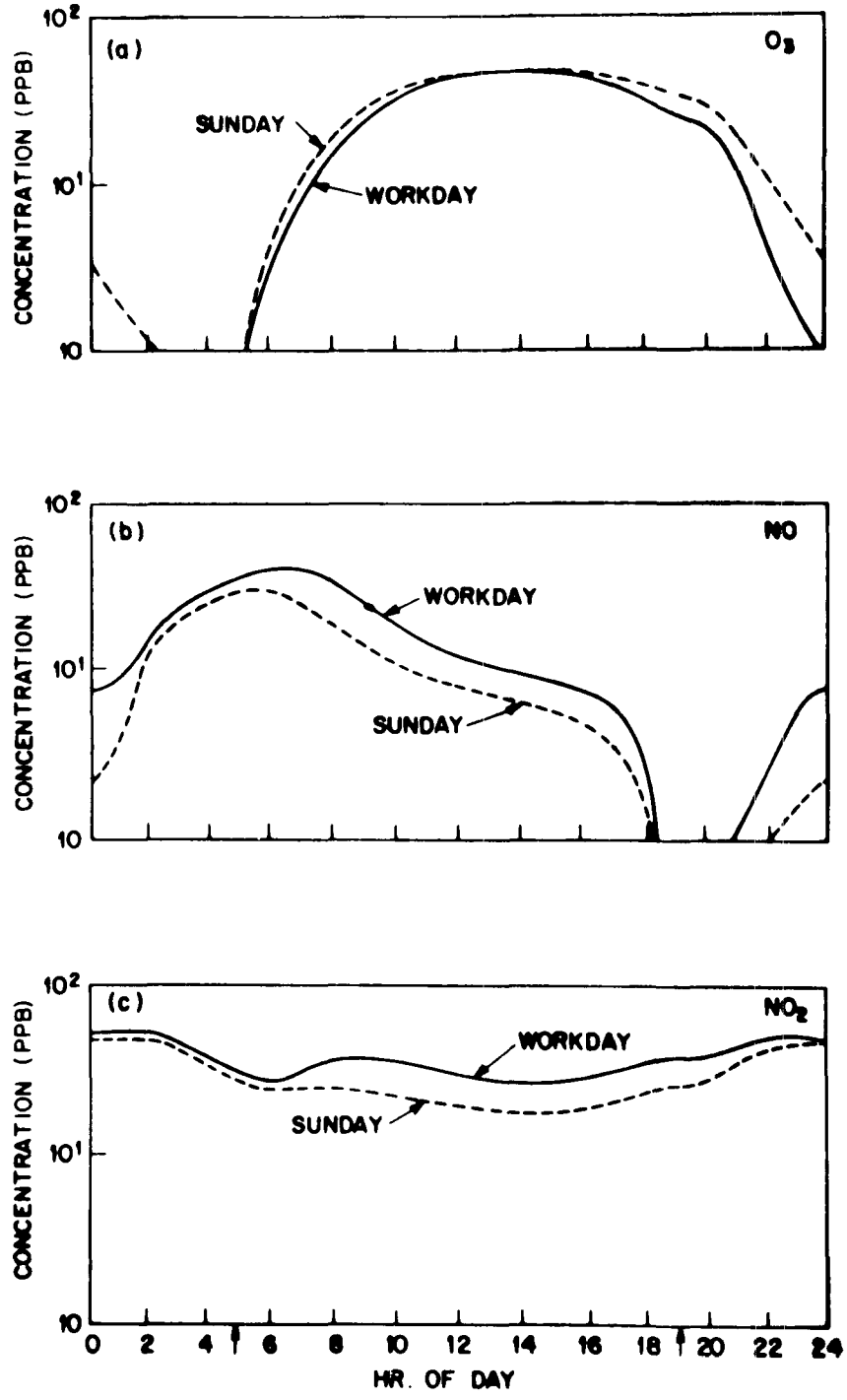

Figure 1. Computed diurnal concentration patterns for workdays and Sundays in Hudson County, New Jersey.

of its inclusion in the calculation at rates previously thought to be correct has negligible effect on any of the results discussed herein.) The triple letter designations in Figure 2 are group transition rates that are not the result of gas phase chemistry. Rates SMx represent the sums of all source emission and meteorological rates contributing to changes in the group concentration (note that rates SMx may be either positive or negative), and rates ARx represent group concentration changes because of heterogeneous reactions with atmospheric aerosols (Paper I). No triple letter rates are indicated in Figure 2 for ϕO, since oxygen (O_2) dominates the ϕO concentration and is negligibly affected by SMF or ARF processes; since we neglect heterogeneous processes for NO_2 and N_2O, rate ARD does not exist.

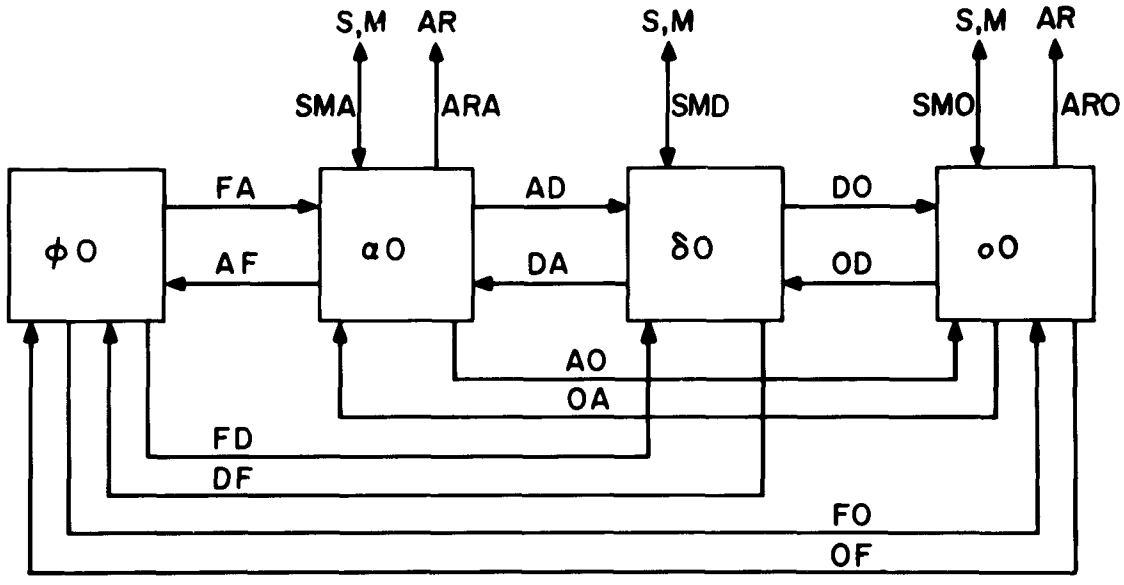

Figure 2. The functional oxygen group diagram. The symbol S refers to emissions sources. M to meteorological sources and sinks, and AR to removal by aerosol incorporation.

The relative magnitudes of the group transition rates are very different. Figure 3 presents functional group diagrams for workday and Sunday at 12 a.m. Several features are immediately apparent. The first is that the dominant rates are DO and OD, and that they balance to better than 1% for both calculations. Secondly, the net rates for group transition from ϕO to δO are clearly positive. Finally, while the magnitudes of the bypass group transition rates are less than those along the central "backbone" of the diagram, they are of potential significance in view of the net rates along the backbone. The same consideration applies to the SMx rates. (For this problem, sources furnish only fixed oxygen; the SMx rates are thus solely meteorological.) Aerosol effects are small relative to the other group transition rates. A general decrease in nearly all the rates is evident when comparing Sunday with workdays. This decrease results from the decreased emissions of NO, the building block compound that carries the oxygen from group to group, and of reactive hydrocarbons, the precursors of the radicals responsible for most of the group transitions. Despite the decreased rates, the strong feedback among the

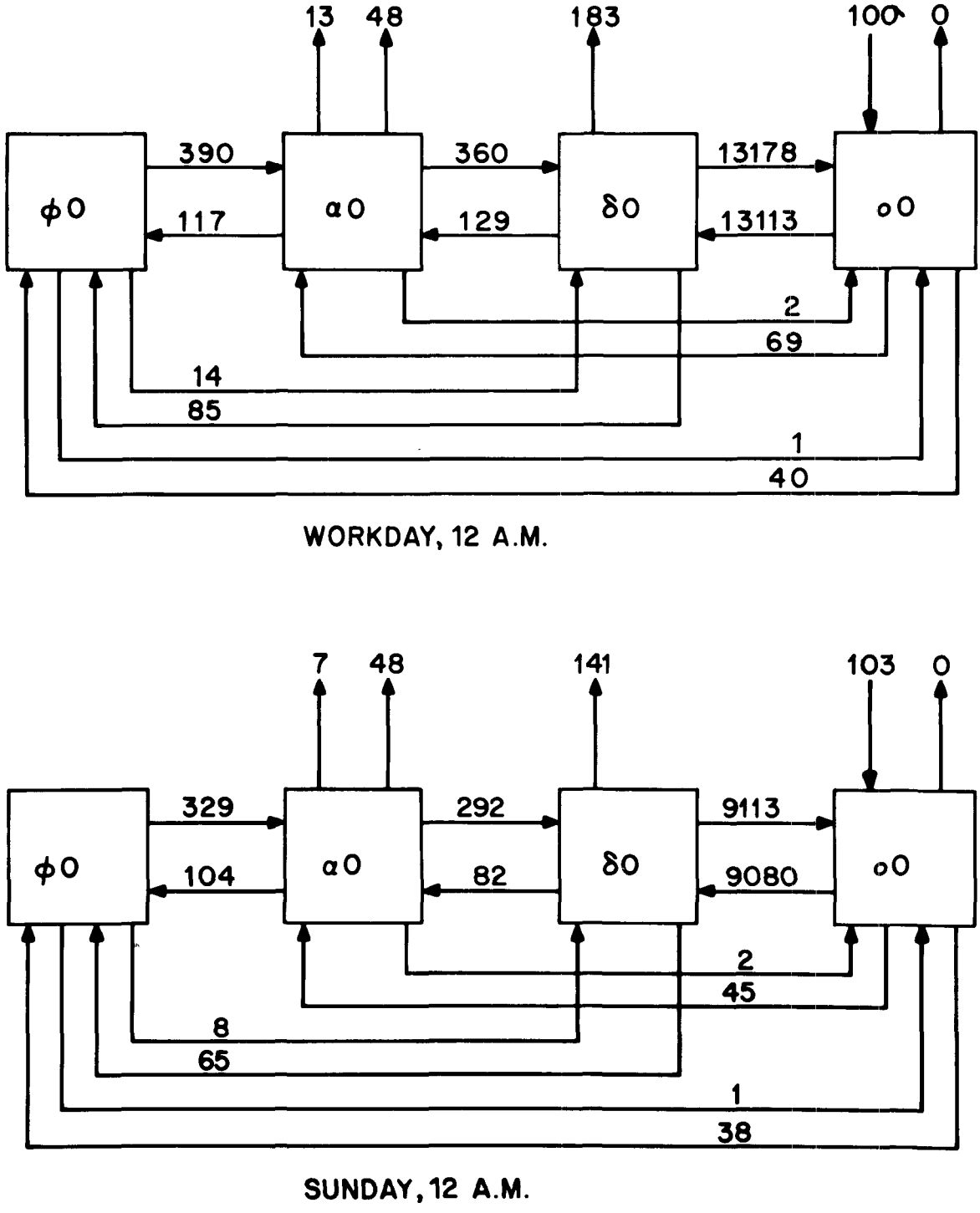

Figure 3. Functional oxygen group diagram at 12 a.m. for workdays and Sundays, Hudson County, New Jersey.

reactive atmospheric compounds enables the overall chemistry to retain its basic weekday structure.

It can be seen from Figure 3 that the group transition rates DO and OD, although markedly larger on workdays, have a similar net rate, which represents the close balance between

$$NO_2 \xrightarrow{h\nu} NO + O$$

$$NO + O_3 \rightarrow NO_2 + O_2.$$

The SMO rate is the largest of those remaining and is virtually identical weekdays and Sundays. This term represents not only the ozone advected into Hudson County from the less urban areas upwind, but also that which enters the "reaction volume" as the rising height incorporates preexisting "fossil" ozone (Ripperton, 1974) from above. This incorporation was shown in Paper I to be consistent with air quality data, and provides a vital carryover buffer against the day-to-day perturbations of ozone precursors.

The early morning excess in ozone concentrations on Sundays reflects the ozone reductions that occur when rush hour NO emissions enhance the rate of ozone scavenging by NO. These reductions, combined with the slightly higher solar flux levels present on Sundays, produce a somewhat higher value net rate of ozone production on Sunday mornings than on workday mornings. A further factor inhibiting net ozone production on workdays is the increased rate of the ozone scavenging reaction

$$NO_2 + O_3 \rightarrow NO_3 + O_2$$

caused by the higher NO_2 concentrations. The inhibitory factors are eventually overcome by the workday presence of δO (i.e. $NO_2 + N_2O$); the result is virtual equality of resulting peak ozone.

CONCLUSIONS

Functional group analysis of oxygen in the troposphere has demonstrated that the Sunday effect in urban areas results from the tight balance between ozone production through NO_2 photodissociation and ozone scavenging by NO, from the advection of ozone from less urban areas, and from the incorporation of similar quantities of ozone preexisting above the morning mixed layer. The higher levels of NO_2 on workdays increase the rates of the NO-NO_2-O_3 shuttle reactions, but do not significantly alter the similar behavior of odd oxygen on workdays and Sundays. The increased levels of NO_x on workdays have other consequences, however. The advective transport of NO_x is enhanced relative to Sundays (as seen in the increased group transition rate SMD), with a concomitant expansion of the downwind impact of the urban area. In addition, the rates of secondary reactions are higher on workdays, resulting in higher concentrations of organic and inorganic nitrates and concomitant increases in the potential of the atmosphere to cause lachrymation.

The success of the calculations and analysis performed thus far in deriving results consistent with field data for two cases of differing source conditions suggests further studies on the changes in ozone concentrations as anthropogenic emissions are varied over reasonable limits. Such work is now proceeding and will be reported subsequently.

REFERENCES

Bruntz, S. M., W. S. Cleveland, T. E. Graedel, B. Kleiner, and J. L. Warner. Ozone Concentrations in New Jersey and New York: Statistical Association with Related Variables. Science, 186, 257-259, 1974.

Cleveland, W. S., T. E. Graedel, B. Kleiner, and J. L. Warner. Sunday and Workday Behavior of Photochemical Air Pollutants in New Jersey and New York. Science, 186, 1037-1038, 1974.

Dimitriades, B. Chamber Studies, Scientific Seminar on Automotive Pollutants. EPA-600/9-75-003, Environmental Protection Agency, Washington, D.C., 1975.

Farrow, L. A., T. E. Graedel, and T. A. Weber. The Effect of Aerosols on the Free Radical Chemistry of the Lower Atmosphere. Removal of Trace Contaminants from the Air. ACS Symposium Series, 17, 17-27, 1975.

Graedel, T. E., L. A. Farrow, and T. A. Weber. Kinetic Studies of the Photochemistry of the Urban Troposphere. Atmospheric Environment (in press), 1976

Graedel, T. E., L. A. Farrow, and T. A. Weber. The Influence of Aerosols on the Chemistry of the Troposphere. Int. J. Chem. Kinetics Symp., 1, 581-594, 1975.

Paskind, J., and J. R. Kinosian. Hydrocarbon, Oxides of Nitrogen, and Oxidant Pollutant Relationships in the Atmosphere over California Cities. Paper presented at 67th Annual Meeting, Air Pollution Control Association, Denver, Colorado, June 9, 1974.

Ripperton, L. A., Eastern United States High Ozone Concentration: Chemical Aspects. Clean Air. 4, (16), 79-82, 1974.

Stedman, D. H., R. J. Cicerone, W. L. Chameides, and R. B. Harvey. Absence of N_2O Photolysis in the Troposphere. J. Geophys. Res., 81, 2003-2004, 1976.

THE EFFECT OF OZONE LAYERS ALOFT ON SURFACE CONCENTRATIONS

T. N. Jerskey, T. B. Smith, S. L. Marsh, and W. H. White

ABSTRACT

Pollutant layers aloft in the Los Angeles Basin were found to result from a variety of mechanisms including heating of mountain slopes, convergence zones, and plumes from stationary sources. Aged pollutants tend to accumulate aloft along foothills during the late afternoon. Under stagnant wind conditions these layers of ozone and other products of photochemical reactions may remain in the area and contribute to high surface ozone concentrations along the foothills on the following day. Examination of the chemistry of reentrainment suggests that the intermediate products of photochemical reactions (such as nitrous acid and aldehydes) can accelerate the rate of ozone formation. This entrainment process may contribute substantially to the ground-level ozone concentration under episode conditions.

INTRODUCTION

This paper presents evidence that, under the stagnant wind conditions that characterize episode periods, ozone layers aloft can account for a substantial portion of the surface ozone concentrations in the Los Angeles Basin. The data analyzed were obtained during the Three-Dimensional Gradient Study (Blumenthal et al., 1974). Below we discuss possible mechanisms for the formation of pollutant layers aloft and analyze their possible effects on surface concentrations.

SOURCES OF LAYERS ALOFT

An examination of a large number of layers aloft indicates that the following mechanisms may be responsible for their formation in the Los Angeles Basin: (a) convergence of the windfields, (b) flow up heated mountain slopes, (c) undercutting by the sea breeze, (d) plumes from stationary sources, and (e) formation of a radiative inversion. With the exception of the first two mechanisms, the layers formed are near the surface and can be incorporated readily into the mixed layer on the following day. When layers aloft form by convergence of the windfields, the pollutants are often carried far above the inversion base and generally have a low probability of becoming entrained on the following day. Also, layers formed by upslope flow often are carried far above the base of the inversion; but, because of the heating occurring on the mountain slopes on the following day, these layers can be entrained and affect surface concentrations along the foothills.

*Jerskey, Systems Applications, Inc., San Rafael, California.
Smith, Marsh, and White, Meteorology Research, Inc., Altadena, California.

Pollutants carried into elevated layers during the afternoon are subject to transport by the prevailing winds at those levels during the night. Depending on wind direction and speed, the pollutants in the layers aloft may be carried inland over the desert and diffused, may be carried toward the coastal areas, or may remain in the foothill areas until the next morning. The worst pollution episode conditions are associated with the lack of transport of the layers aloft away from the foothill areas. Under these conditions, the material aloft remains undiluted and is available for entrainment into the mixed layer on the following day.

IMPACT OF LAYERS ALOFT ON SURFACE CONCENTRATIONS

The object of this phase of our analysis was to determine the impact of the layers of pollutants aloft on concentrations within the mixed layer as the inversion rises to entrain the material aloft. In our approach we assumed that all the material aloft in the morning profile up to the midday inversion height was entrained.

For the eight days on which a sufficient overlap existed between the morning and midday measurement locations, we tabulated coefficients for the correlation between the mass of entrained pollutants and the change of the pollutant mass loadings between the morning and midday flights. The correlation coefficients varied considerably over the eight days. Furthermore a high correlation coefficient did not appear to be related to the quantity of pollutant entrained from aloft or the pollutant concentration on a particular day. Upon closer inspection of the data, we found that the entrained ozone did appear to be correlated with the difference between the mass loading in the morning and at midday. A similar conclusion could not be drawn for aerosol mass or carbon monoxide, even when the change in mass loading was modified to account for emissions into the air parcel. Instead of considering the mass entrained at individual locations, the average mass entrained for the entire basin can be calculated. By averaging the difference between the morning and midday loading over the basin, one can minimize the variation of measurements from location to location. Furthermore, averaging over all the measurements minimizes the effect of advection, particularly for a secondary pollutant like ozone, whose spatial variations in concentration are relatively small compared with those of primary pollutants. The mean values of the entrained ozone mass loading and the difference between the morning and midday mass loadings for the eight days studied are plotted in Figure 1. The correlation coefficient for the eight days was 0.78.

Because of the relative location of Cable and Rialto and the routes flown by the aircraft, the time delay between measurements made at the two locations (typically 90 minutes) was approximately the time required for an air parcel to be advected between them. For this portion of the data set we again calculated the mass entrained from aloft (using the vertical ozone distribution at the beginning of the trajectory measured at Cable) and the change of the mass loading in the mixed layer calculated for Cable and Rialto. Morning and midday trajectories between Cable and Rialto were available for eight days in 1973. Afternoon trajectories were not considered since the depth of the mixed layer generally decreased along the trajectory during this time period. By comparing the change in the ozone mass loading with the ozone entrained from aloft (see

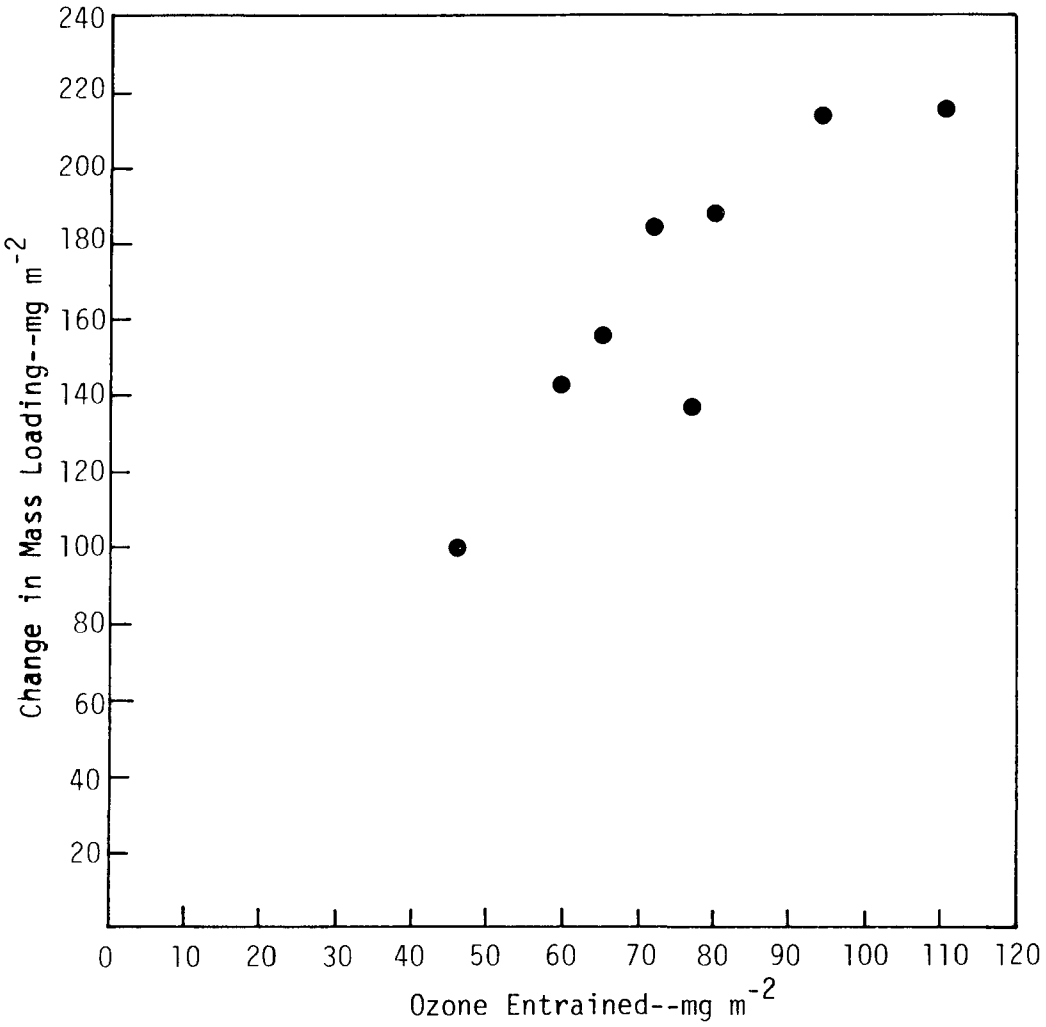

Figure 1. The change in ozone mass loading as a function of the mass of ozone entrained from the mixed layer.

Figure 2) we confirmed the observation that high ozone concentrations at Rialto are correlated with high ozone concentrations aloft.

Further evidence that the layers aloft have an impact on the concentration of ozone in the mixed layer is provided by an analysis of the surface concentrations for July 25, 1973, a day when ozone concentrations reached a level of 0.5 ppm at Upland (near Cable). Figure 3 shows the vertical sounding at Cable at about 0830 Pacific Daylight Time (PDT) on July 25. Substantial ozone concentrations were found aloft, peaking at over 0.2 ppm at a height of 2100 feet mean sea level (msl). The sounding also shows a rapid decrease in b_{scat} above 1800 ft msl, indicating a very shallow surface mixing layer. Figure 4a shows the surface ozone concentrations from the California Air Resources Board (ARB) pollution network for the period from 0900-1000 PDT on July 25. Peak values of 0.15 ppm in the basin occurred in the Upland area but generally high values existed along the entire foothill area from San Bernardino (SBD) to

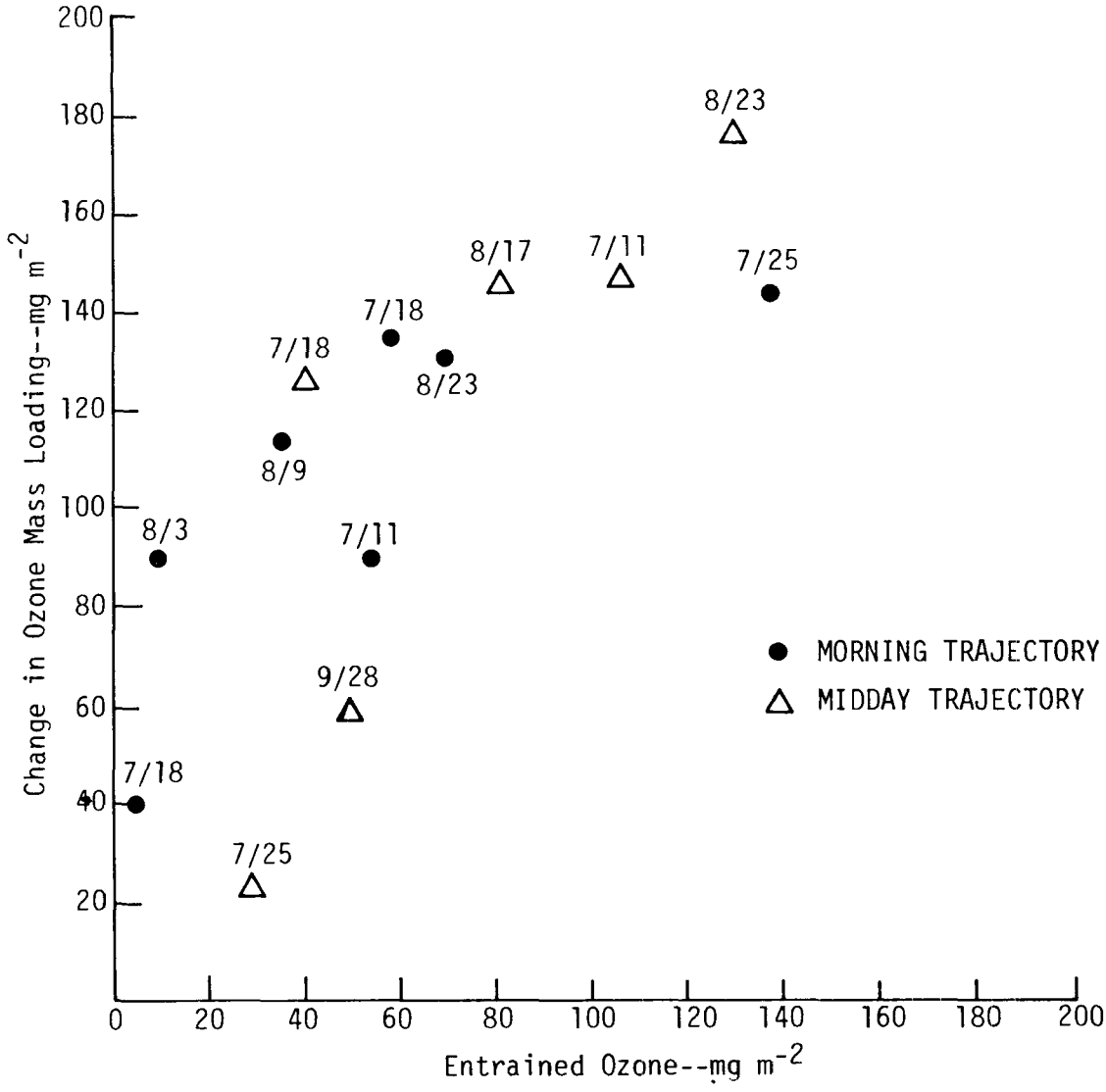

Figure 2. The change in ozone mass loading along the trajectory from Cable to Rialto as a function of the ozone entrained.

Burbank (BUR). By 1200-1300 PDT (Figure 4b) the ozone concentrations along the foothills had increased at a time when the mixed layer at Cable had increased to 2500 ft msl, incorporating much of the pollutants aloft. At this time there was also evidence of new ozone production in the central Los Angeles area (CAP). Subsequently these new ozone concentrations were carried northeastward to the foothill area and mixed with the existing high ozone concentrations to produce levels as high as 0.5 ppm at Upland during the hours from 1600 to 1700 PDT.

These data suggest that the high ozone concentrations observed along the foothills were influenced by the downward mixing of pollutants from aloft as surface heating caused the inversion base to rise and entrain these materials. Although ozone is mixed downward into the mixed layer, we believe that the intermediate products (such as aldehydes and nitrous acid) of the photochemical reactions are responsible for the high ozone concentrations observed along the

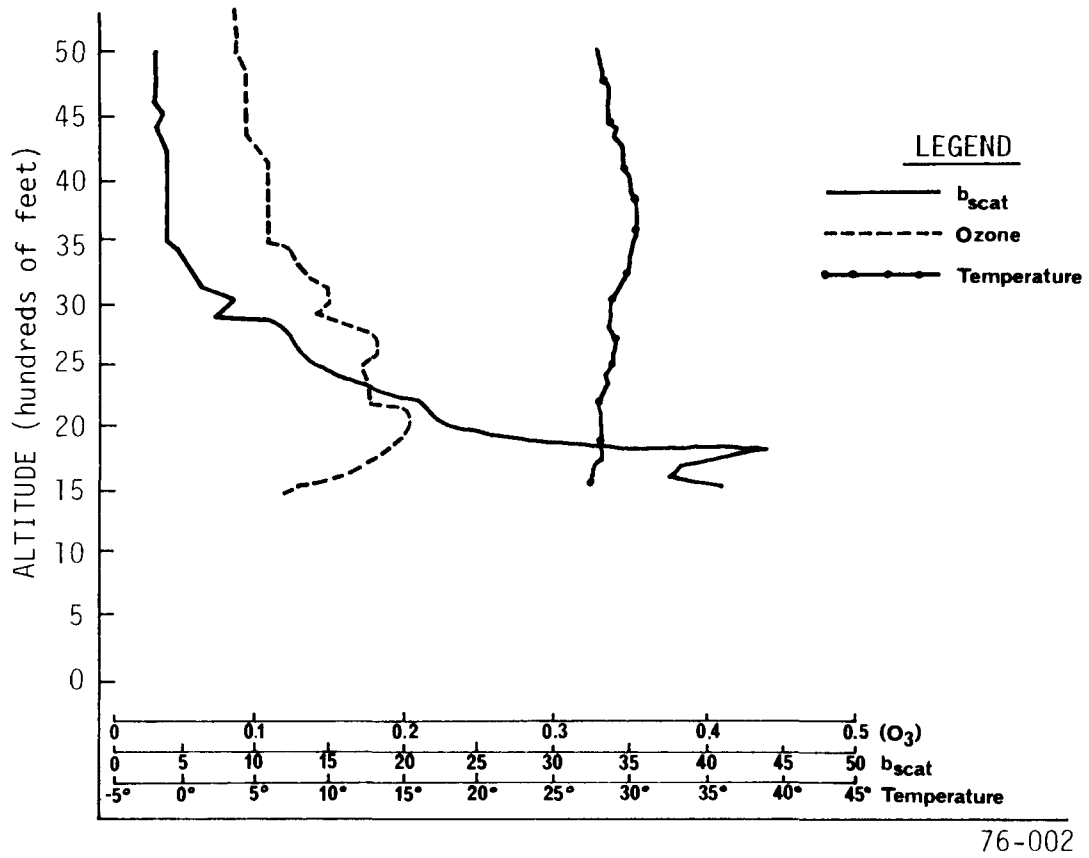

Figure 3. Vertical sounding at Cable Airport (Upland), July 25, 1973 (0830 PDT)

foothills. The effect of these intermediate products on the ozone formation rate is illustrated by the numerical simulation of a smog chamber experiment using the Hecht et al. (1974) kinetic mechanism (see Figure 5). In Case 1 (see Table 1) the simulation was performed without any initial ozone or aldehyde concentration. Case 2, with the initial ozone concentration at 0.42 ppm, showed little change in the final ozone concentration. However, when the aldehydes were carried over (Case 3), the ozone production rate was accelerated initially, leading to higher ozone concentrations at early times. The photolysis of aldehydes produces radicals that react with nitri oxide to give nitrogen dioxide (NO_2). Thus these intermediate products accelerate the formation of ozone by increasing the concentration of NO_2.

SUMMARY AND CONCLUSIONS

Layers of ozone aloft can be formed by one of several mechanisms. Once these layers are formed the impact they have on surface concentrations on the following day depends on the strength and direction of the winds aloft. Under stagnant conditions the layers can remain overnight where they were formed. On the following day surface heating causes these layers to be entrained into the mixed layer, where they can contribute a substantial fraction of the ozone concentration on that day. Hence, a knowledge of the winds aloft can serve as a forecasting tool for prediction episode conditions.

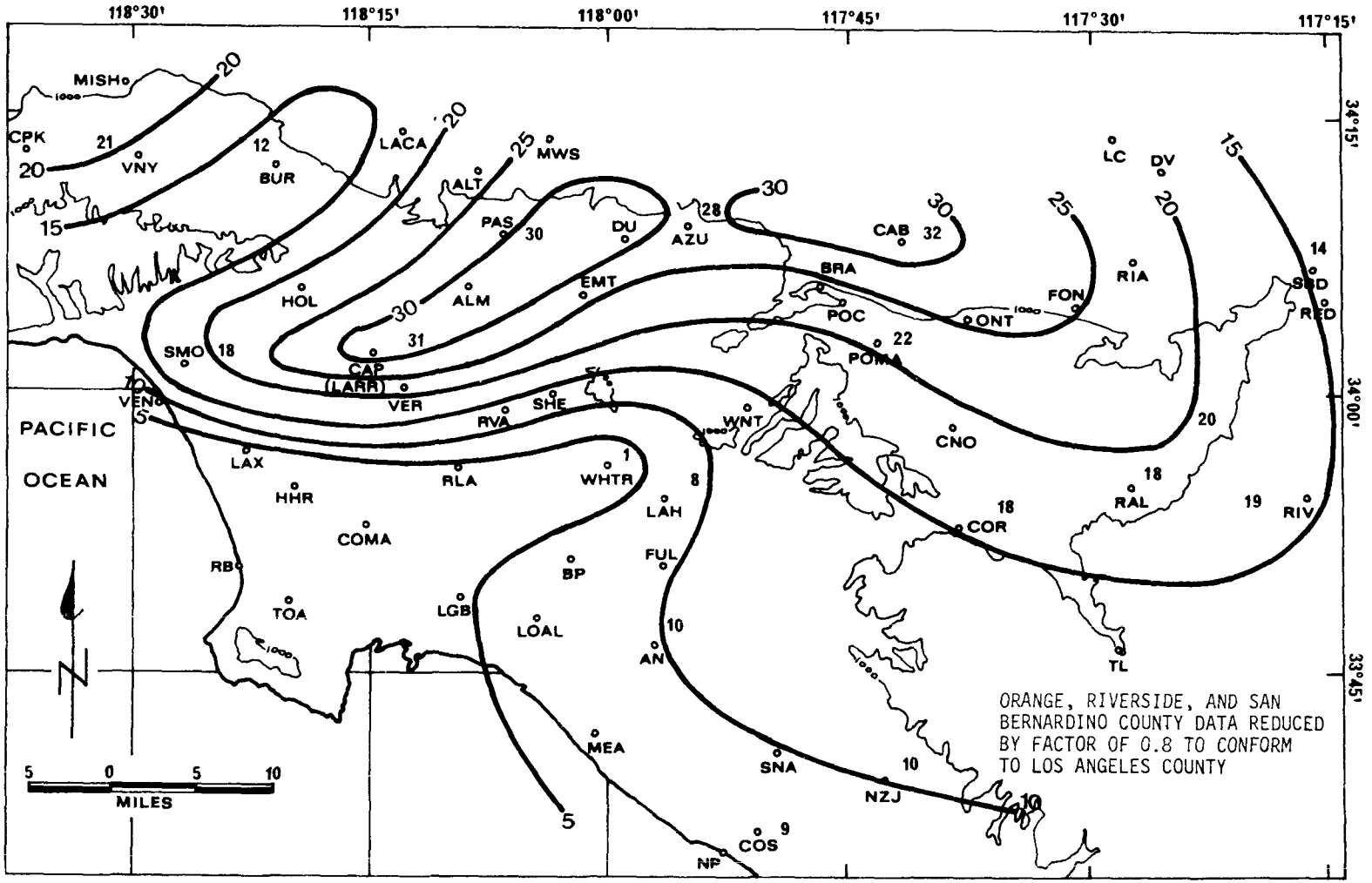

Figure 4a. Surface ozone concentrations (in PPHM), July 25, 1973 (1200-1300 PDT).

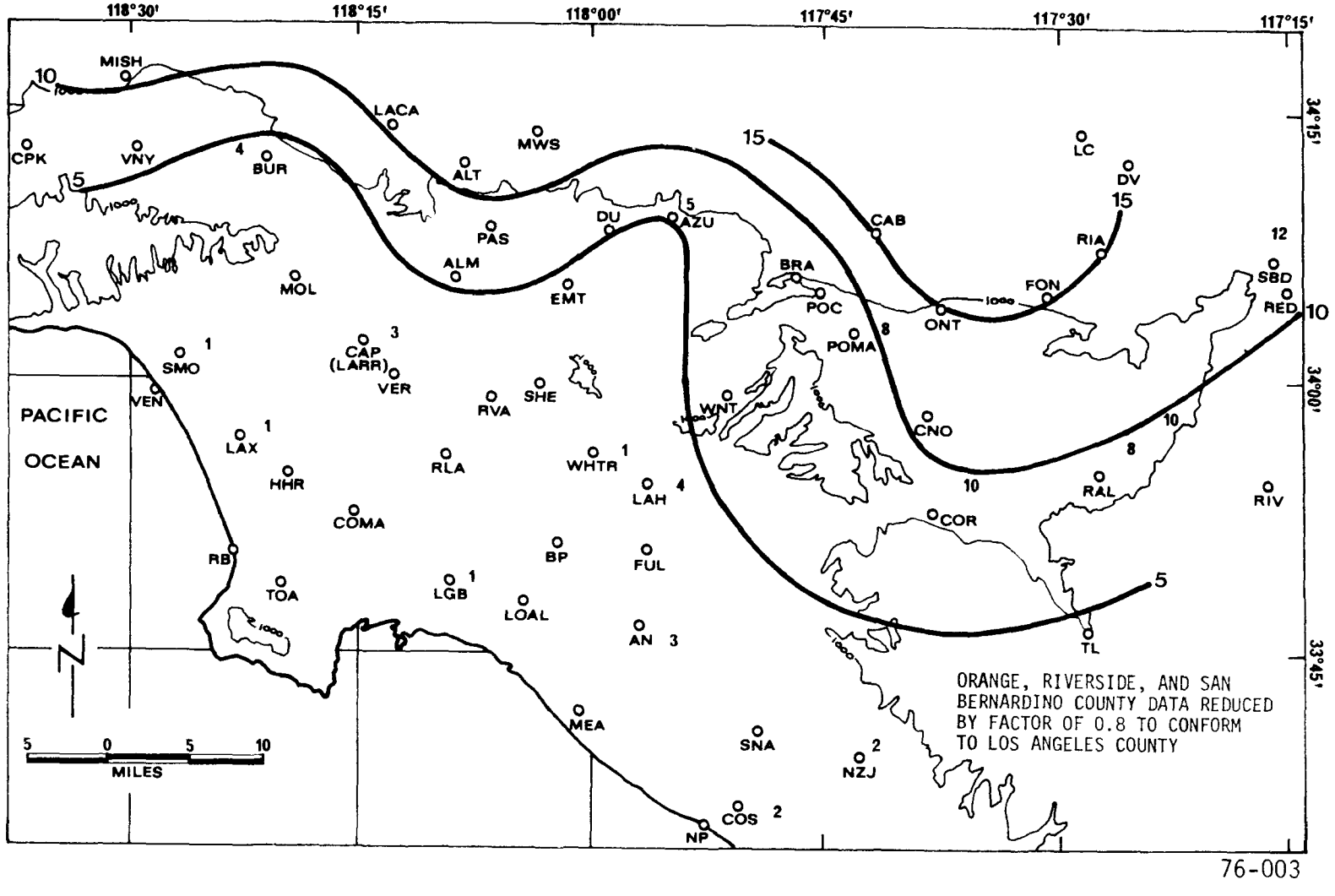

Figure 4b. Surface ozone concentrations (in PPHM), July 25, 1973 (0900-1000 PDT).

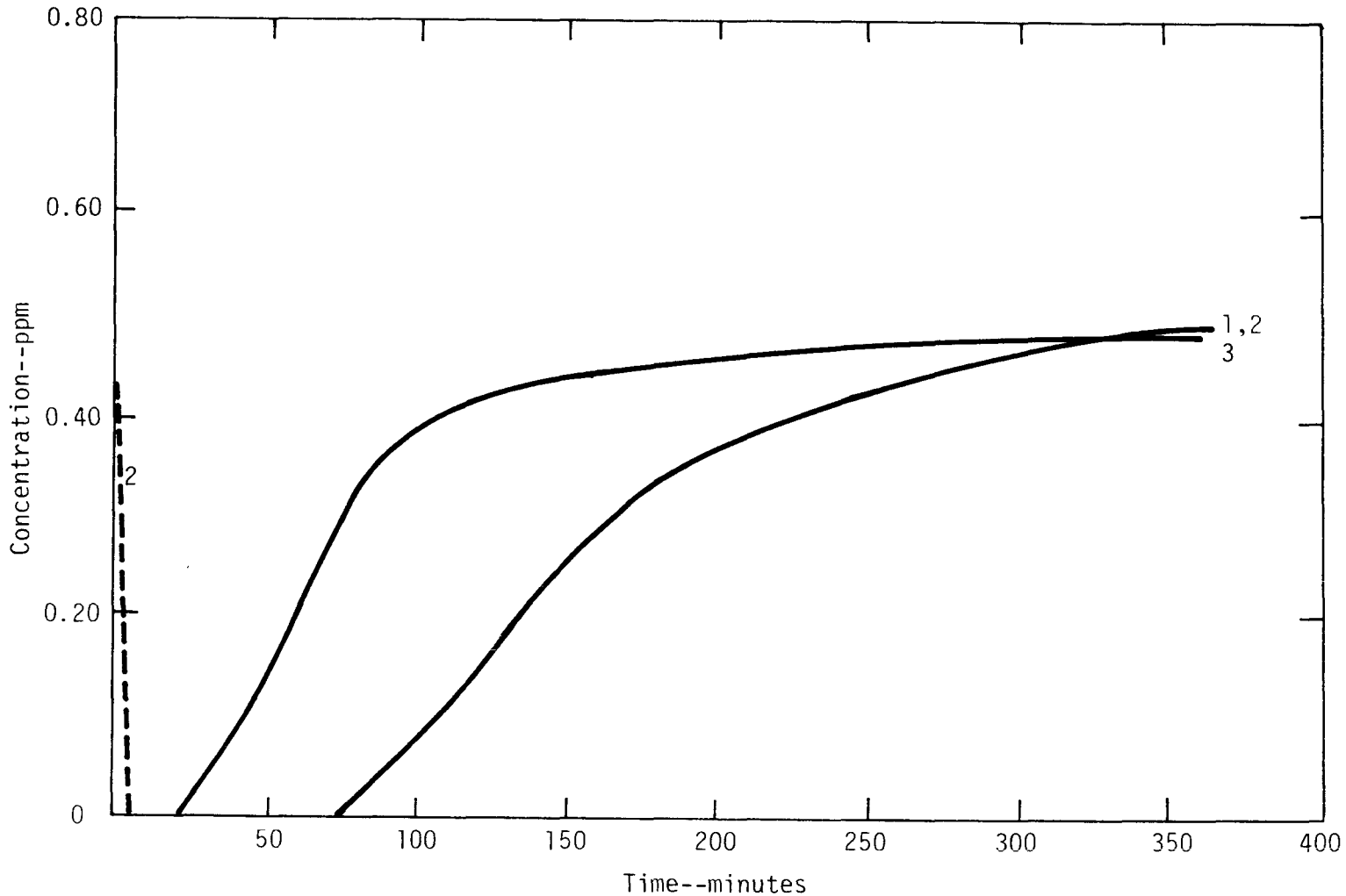

Note: The curves are numbered to correspond with the cases given in Table 1.

FIGURE 5. OZONE CONCENTRATION AS A FUNCTION OF TIME IN A BOX REACTOR

TABLE 1. INITIAL POLLUTANT CONCENTRATIONS (IN PPM) FOR THE RESULTS SHOWN IN FIGURE 5

Pollutant	Case 1	Case 2	Case 3
NO	0.94	0.94	0.94
NO_2	0.13	0.13	0.13
PAN	0	0	0
Ozone	0	0.42	0
Propylene	1.04	1.04	1.06
Formaldehyde	0.02	0.02	0.25
Acetaldehyde	0	0	0.17
Propionaldehyde	0	0	0.03

These results suggest that air quality simulation models must take into account the three-dimensional structure of pollutant concentrations in order to predict episode conditions.

ACKNOWLEDGMENTS

This study was carried out under the support of the California Air Resources Board (ARB) as part of a study to examine the data from the Three-Dimensional Gradient Study. Mr. Gary Palo and Mr. C. L. Bennett of the ARB served as contract monitors and contributed significant inputs in regard to the ARB problems and interests in the study.

REFERENCES

Blumenthal, D. L., et al. Three Dimensional Pollutant Gradient Study. 1972-1973 Program. MRI 74 FR-1262, ARB-631 and ARB-2-1245, 1974. Meteorology Research, Incorporated, Altadena, California.

Hecht, T. A., J. H. Seinfeld, and M. C. Dodge. Further Development of a Generalized Kinetic Mechanism for Photochemical Smog, Environ. Sci. Technol., Vol. 8, p. 327.

SESSION 5

SOURCES OF TROPOSPHERIC OZONE - III

Chairman: R.A. Rasmussen
Washington State University

OZONE CONCENTRATIONS IN POWER PLANT PLUMES: COMPARISON OF MODELS AND SAMPLING DATA

T. W. Tesche, J. A. Ogren, and D. L. Blumenthal*

ABSTRACT

Field measurements and modeling studies have been carried out to investigate reports that ozone may be generated in plumes from large power plants in concentrations exceeding ambient levels. Analysis of aerometric data from three Western power plants consistently revealed ozone depletion within the plume in the vicinity of the stack and a gradual increase in ozone concentration to approximately background levels far downwind. No ozone generation was observed in the plumes studied. Extensive model validation studies with the Reactive Plume Model were performed. Comparison of model predictions and measured plume concentrations indicated that the model is a useful tool for studying reactive plumes. To determine whether the model could be used to reveal conditions for which ozone might be generated in plumes, hypothetical scenarios involving different ambient hydrocarbon levels were investigated. For very high hydrocarbon concentrations (6 ppm as methane) the model does predict net ozone formation of approximately 6-12 percent above background levels. The limitations and implications of this result are discussed.

INTRODUCTION

The possibility of ozone formation above ambient concentrations in power plant plumes has recently been raised by several investigators (1,2). To better understand the factors affecting the behavior of ozone in power plant plumes, the Electric Power Research Institute (EPRI) contracted with Meteorology Research, Inc., (MRI) and Systems Applications, Inc., (SAI) to perform at three Western United States power plants to determine the behavior of ozone in the plumes, and to support a validation study of the Reactive Plume Model (RPM), originally developed to study reactive power plant plumes under various environmental conditions. Because the results of the EPRI study are presented in greater detail elsewhere (3,4), only the essential findings are reviewed here. The primary emphasis of this paper concerns the modeling results obtained with RPM.

*T. W. Tesche, Systems Applications, Inc., San Rafael, California. J. A. Ogren and D. L. Blumenthal, Meteorology Research, Inc., Altadena, California.

FIELD MEASUREMENT PROGRAM

Airborne plume sampling was conducted in August and October 1975, primarily with the MRI Cessna 206, which was instrumented to measure and record continuously ozone (O_3), nitric oxide (NO), nitrogen oxides (NO_X), sulfur dioxide (SO_2), light scattering coefficient, condensation nuclei, temperature, dew point, turbulence, pressure (altitude), and position. Sulfate aerosol and hydrocarbon (HC) samples were obtained for later chemical analysis. Supporting ground-based measurements included winds aloft (using pibals) and ultraviolet solar radiation. In addition, a Douglas B-23 (operated by the University of Washington), instrumented similarly to the Cessna 206, was used to collect supplemental plume data during part of the program.

Aerometric measurements were made at the following power plants: Four Corners, Farmington, New Mexico (coal-fired, dry environment); Cunningham, Hobbs, New Mexico (gas-fired, dry environment); and Wilkes, Longview, Texas (gas-fired, humid environment). Data from coal-and oil-fired plants in humid environments were also analyzed along with the data from the plants listed above to provide a comprehensive basis for studying the behavior of ozone in power plant plumes. In all of the cases studied, ozone depletion within the plume occurred near the plant, followed by a gradual increase to background levels as ambient air was entrained in the plume.

A typical ozone profile is shown in Figure 1. The plume is readily identified by the elevated SO_2 concentrations. High values of NO, NO_X, and b_{scat} were also associated with the plume. Ozone concentrations in the plume were well below background levels. Depletion of ozone relative to background was observed wherever the plume was distinguishable from background concentrations, although the deficit was very small at far downwind distances. Another example of plume concentration data is presented in Figure 2. This plume isopleth characterization is based on ozone measurements at five altitudes. The plume contained high NO and NO_X concentrations, and a pronounced ozone deficit. However, an ozone layer with high concentrations was observed above the plume. Analysis of the data collected on this day revealed that the ozone layer was not associated with the plume, and was probably caused by the advection and aging of pollutants emitted upwind of the sampling area. Clearly, without supporting measurements upwind of the plant and well outside of the plume, it would be possible to misinterpret some of the ozone profiles used to create Figure 2 as evidence of ozone formation on the edges of the plume.

MATHEMATICAL MODELING OF POWER PLANT PLUMES

Recently, the California Air Resources Board sponsored the development of a package of three numerical models to characterize both the physical and chemical transformations of power plant plumes (5). One of these — the Reactive Plume Model (RPM) — was an integral part of the EPRI study.

THE REACTIVE PLUME MODEL (RPM)

RPM was developed to study the complexities of plume photochemistry in detail; transport and dispersion are treated in a less rigorous fashion. The

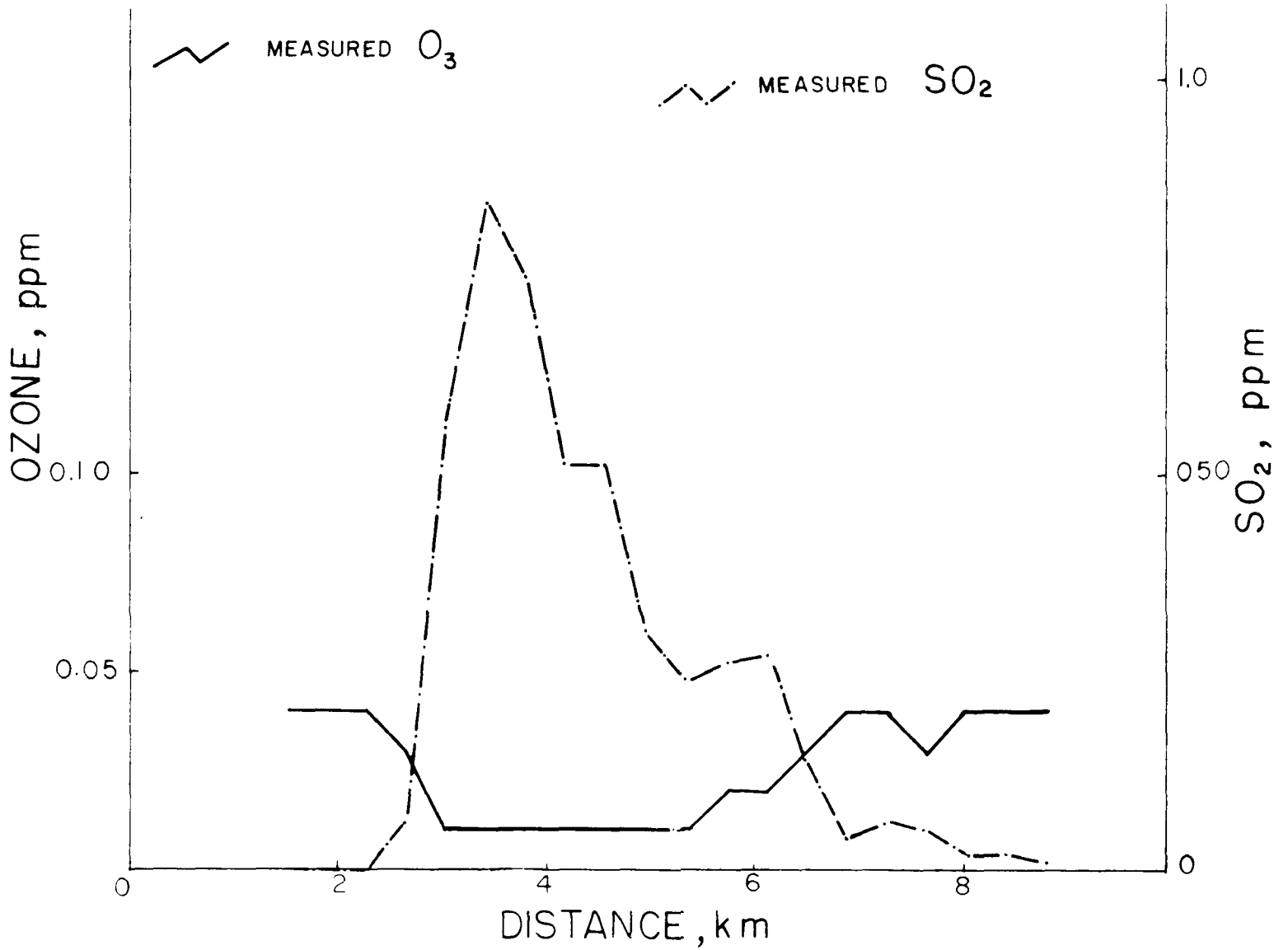

Figure 1. SO_2 and O_3 profiles, Four Corners Plant plume, 21 km downwind, August 28, 1975, 1768 M MSL.

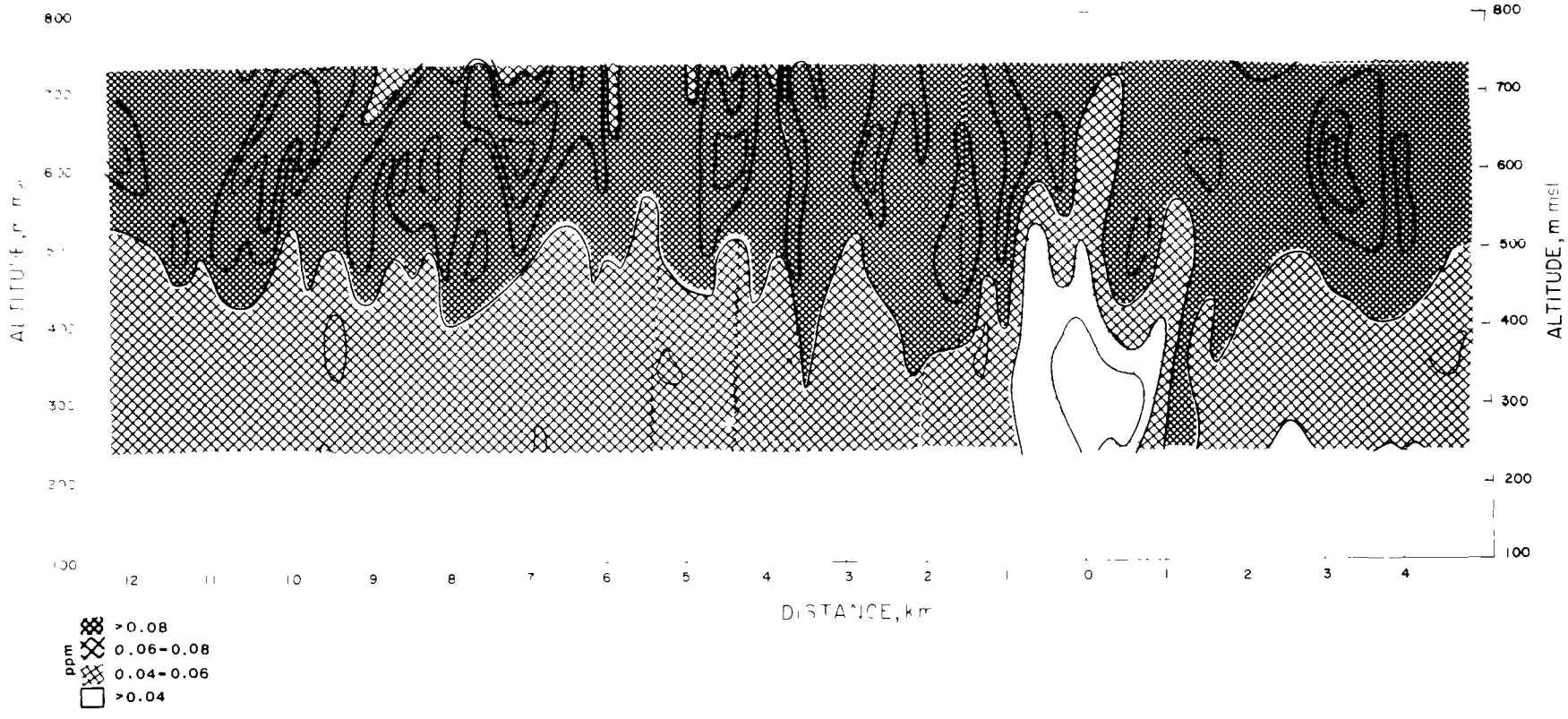

Figure 2. O_3 isopleths 10 km downwind of Wilkes Plant, October 11, 1975, distances are given from plume centerline.

model employs a refined version of the lumped-hydrocarbon, Hecht-Seinfeld-Dodge photochemical mechanism (6). For generality, the kinetic mechanism has been augmented with a set of provisional sulfur oxidation reactions in order to simulate the environment of power plant plumes contain sulfur emissions. The model is based upon a mass balance for pollutant species involved in plume photochemistry. Within a Lagrangian air parcel moving downwind, photochemical reactions are modeled by accounting for:

- The mass of a given pollutant emitted from the stack — initial conditions
- The mass of a given pollutant entrained from the ambient air as the plume expands — boundary conditions
- The mass of a given pollutant created or destroyed due to reactions within the air parcel — chemical reactions.

Plume dilution is prescribed in RPM either from measurement or theory. Estimates of dilution rates can be based on measured plume widths and mixing depths; alternatively, the model can compute the dilution of pollutants by a Gaussian formula using dispersion coefficients estimated from either the standard Pasquill-Gifford method (7), the modified Bowne scheme (8), or a recent method based upon similarity theory (5). The speed at which the parcel is transported downwind is specified from wind measurements aloft via pibal records. Reliance is placed upon aircraft measurements to determine the pollutant concentrations as close to the stack as possible (the initial conditions) and to record the temporal and spatial variation in background pollutant concentrations (boundary conditions). Finally, average concentrations of pollutants measured by aircraft within the plume are used for comparison with model predictions.

RPM VALIDATION STUDIES

One objective of the EPRI program was to provide a data base suitable for determining RPM's accuracy in simulating the behavior of reactive power plant plumes. Consequently, a large number (sixteen) of model verification studies were carried out with the EPRI field data. One set of comparisons between predictions and measurements is presented here.

On August 28, 1975, the Four Corners plume was sampled by the MRI aircraft. At distances of 5, 21, 60, and 87 km downwind of the plant, the plume was characterized with horizontal traverses at three different altitudes and with vertical spirals. Concentrations of SO_2 in the Four Corners plume were identifiable at all four sampling distances. Maximum SO_2 concentrations within the core of the plume exceeded 1 ppm at 5 km and declined with increasing distance from the plant, falling to 0.04 ppm at 87 km. The observed SO_2 concentrations outside the plume were 0.01 ppm or less.

Ozone concentrations outside the plume were in the 0.04 to 0.05 ppm range, increasing slightly with the increase in solar insolation during the morning. While ozone concentrations within the plume were depressed relative to those

outside at all distances, the absolute ozone concentrations in the plume increased with distance downwind, from a minimum of 0.01 ppm or less at 5 km to 0.04 ppm at 87 km. Background reactive HC levels were estimated to be 0.027 ppm by volume (approximate 0.16 ppm as methane). The mean wind speed ranged from 1.2 to 5.0 meters per second.

The RPM simulation for this day was carried out for a distance of 100 km from the stack. Predicted NO, NO_2, O_3 and SO_2 concentrations, designated by the symbol "O", are presented in Figures 3 through 6. Background and plume measurements, designated by "B" and "M" respectively, are also plotted in the figures. Nitric oxide predictions (Figure 3) exhibit excellent agreement with the data. After approximately 24 km, NO levels in the plume are depressed to approximately background levels. In addition, NO_2 predictions (Figure 4) are also in good agreement with the data. On the other hand, ozone predictions exceed measured values by approximately 30 percent far downwind of the stack. As may be seen in Figure 5, the measured concentrations increase gradually; at 84 km the measured plume ozone is just slightly less than the background. In Figure 6 very good agreement exists between predicted and measured SO_2 concentrations over a relatively wide range of values.

Based on the RPM validation studies conducted to date, it is possible to make a preliminary assessment of the model's validity and utility. RPM is capable of predicting the dilution of conservative pollutants and tracer material quite well. For reactive primary pollutants such as NO and SO_2, predictions are generally in good agreement with measurements. Model predictions of secondary pollutants such as NO_2 and O_3 are strongly influenced by the concentrations of reactive HC in the ambient atmosphere. There appears to be a tendency for the model to overpredict NO_2 and O_3 concentrations when high background HC concentrations are present. However, at present, it is not clear whether there are factors involved in the NO_2 and O_3 overpredictions other than high HC estimates. From RPM simulations for which the assumed HC concentrations are believed to be reasonably accurate, we estimate that the accuracy of the Model for O_3 predictions at large downwind distances is within $\pm$ 25 percent. In general, the overall predictive capability of the model appears to be commensurate with the ability of present sampling methods (9) to characterize the unsteady nature of power plant plumes.

OZONE FORMATION IN POWER PLANT PLUMES

To determine if RPM is capable of identifying conditions for which ozone in excess of background concentrations may be formed in plumes, two basic simulations were carried out. First, the photochemical model CHEMK was used to predict initial background concentration variations throughout the day.* Then, with the predicted background concentrations as inputs, RPM was exercised to study how the predicted plume ozone levels varied relative to the predicted

*Due to numerical instabilities in the integration algorithm, it is not possible to conduct a "background simulation" with RPM. Instead, another model, CHEMK, incorporating the same kinetic reaction steps as RPM, was used to simulate the temporal changes in the background pollutant concentration (10).

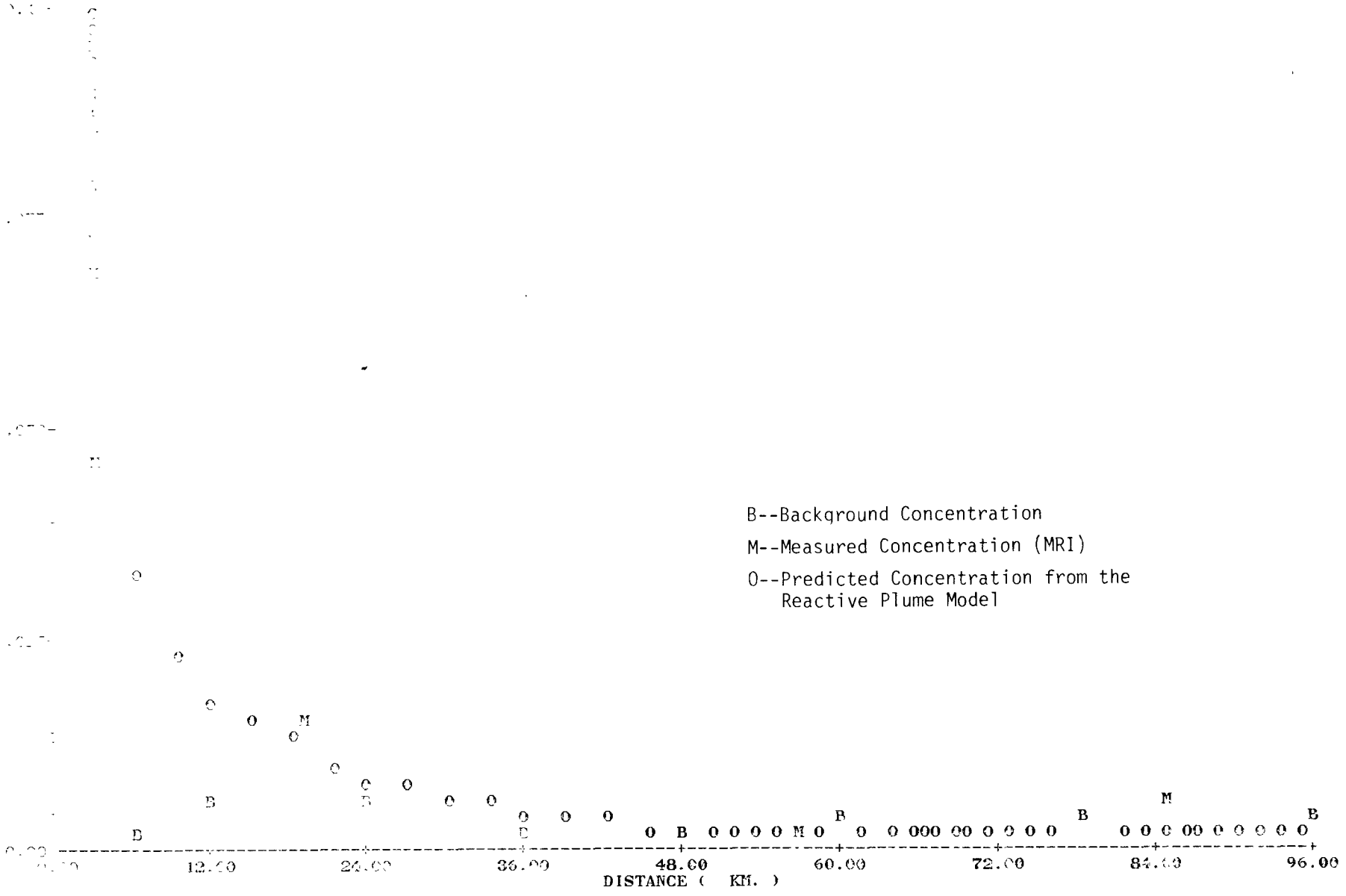

Figure 3. Predicted and measured NO concentrations in the Four Corners power plant plume on August 28, 1975.

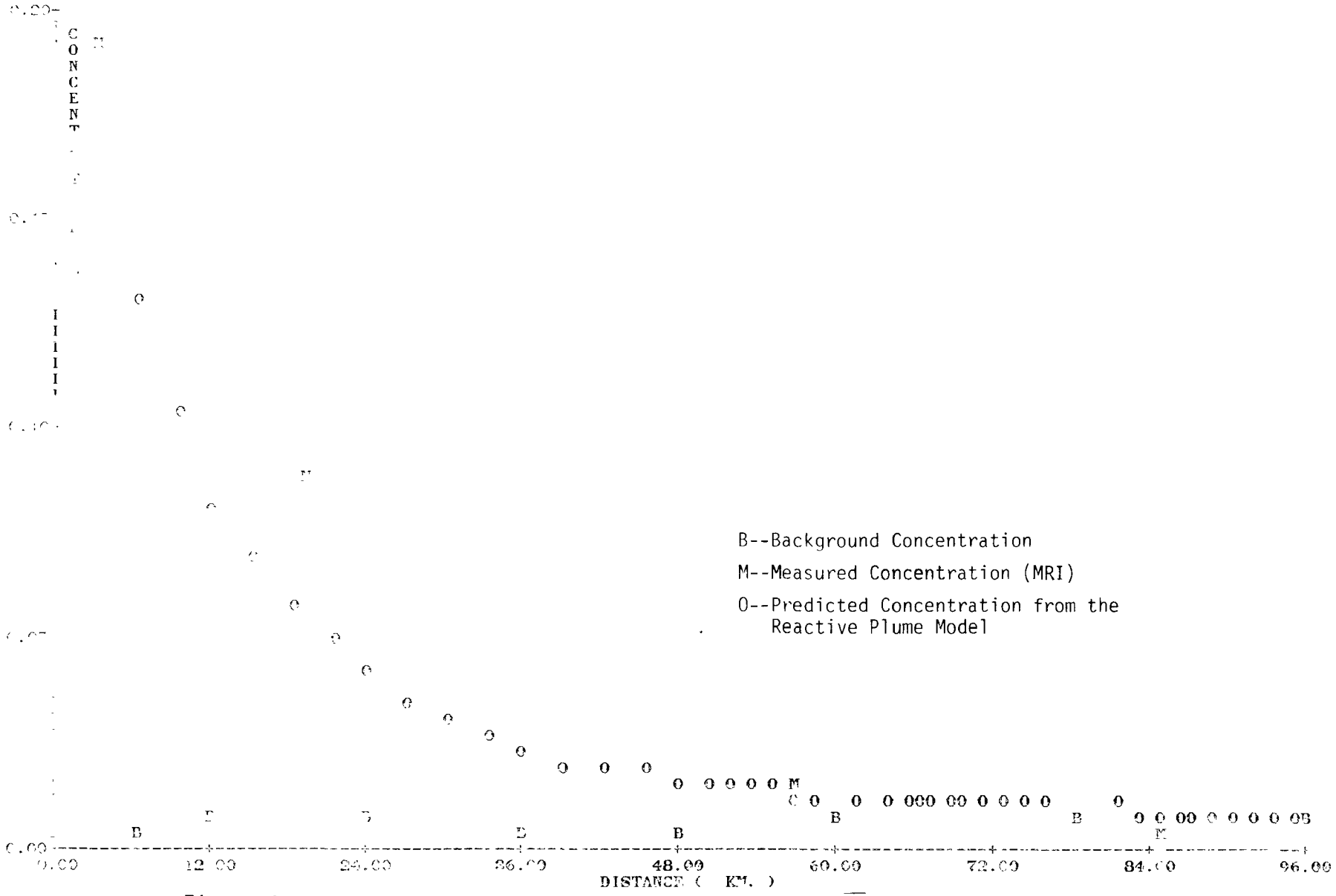

Figure 4. Predicted and measured NO_2 concentrations in the Four Corners power plant plume on August 28, 1975.

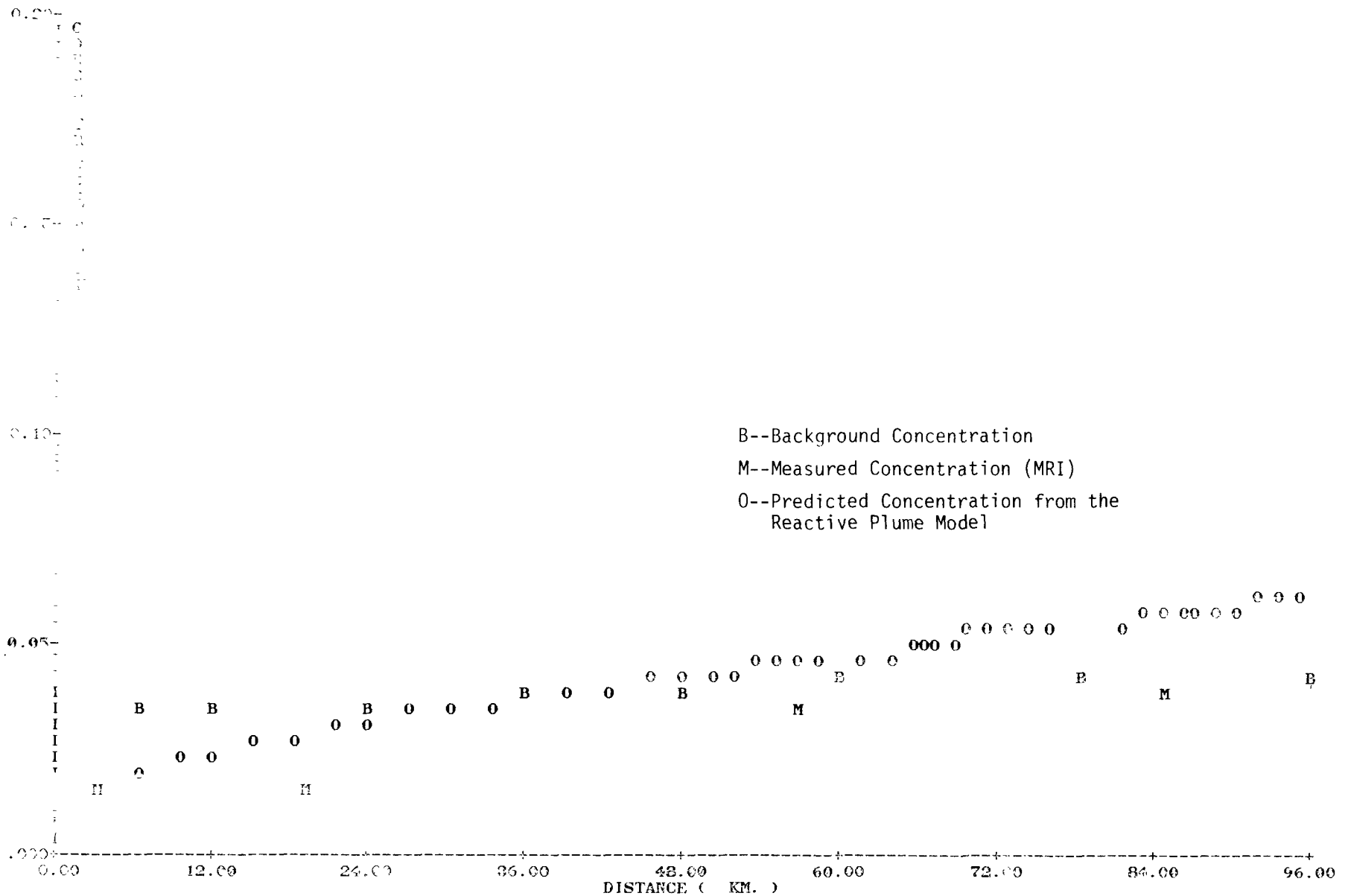

Figure 5. Predicted and measured O_3 concentrations in the Four Corners power plant plume on August 28, 1975.

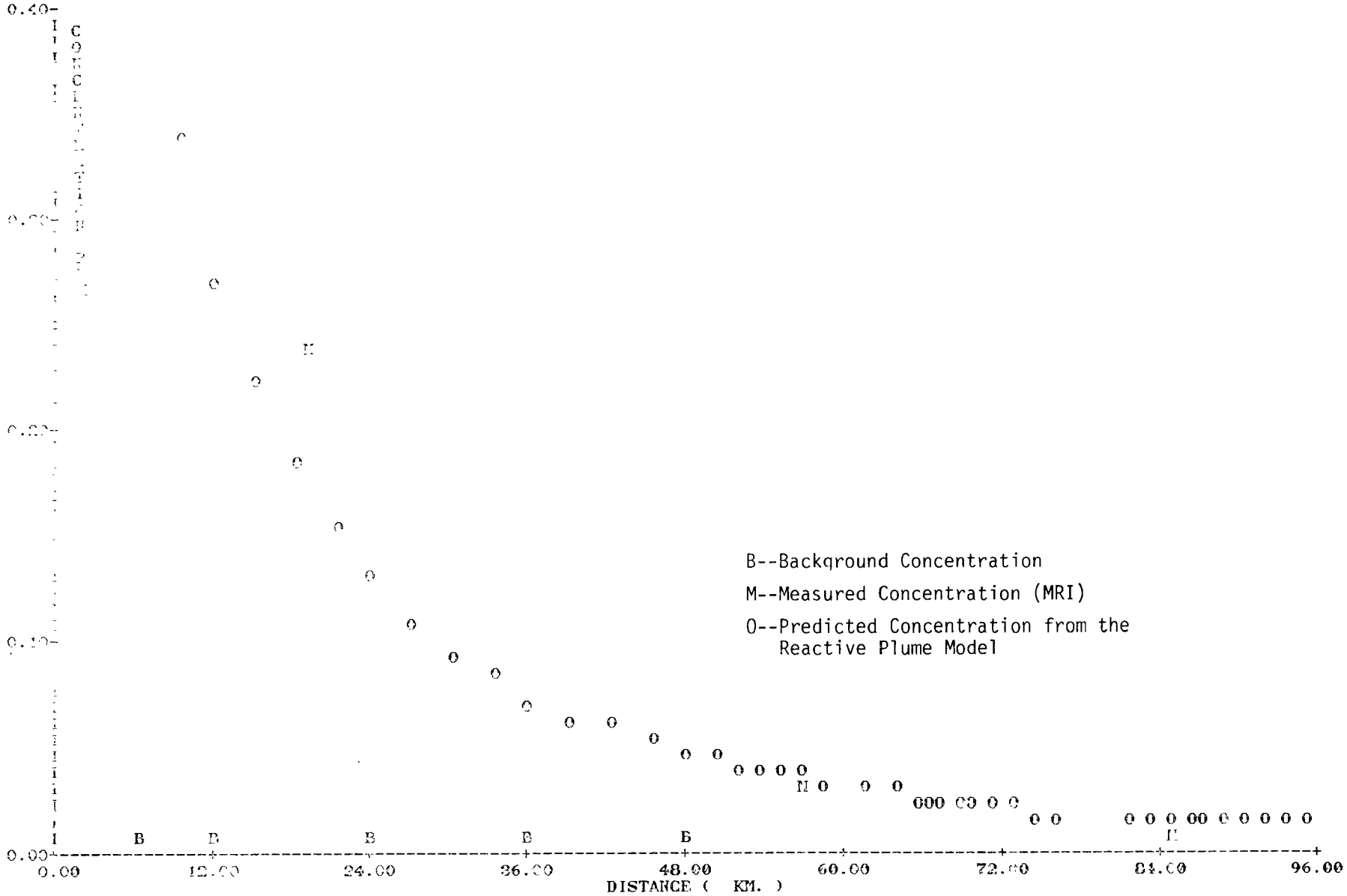

Figure 6. Predicted and measured SO_2 concentrations in the Four Corners power plant plume on August 28, 1975.

background. If the plume concentrations exceed background levels, this would suggest that the model is simulating a condition for which ozone generation in the physical environment might occur.

Two hypothetical scenarios involving different ambient HC concentrations were investigated. In one case HC was approximately 6.0 ppm as methane; in the other HC was reduced to 0.6 ppm as methane. Initial conditions similar to what might be expected in an urban air atmoshpere were chosen for the simulations. Dispersion characteristics and initial pollutant concentrations were chosen to be identical to those observed for the Four Corners Plume on August 28, 1975. Wind speeds varied between 1.2 and 5.0 meters per second.

The following simulations were carried out for both scenarios:

- Using the CHEMK photochemical model, the initial ambient concentrations reacted for 6 hours leading to a predicted variation in background concentrations.

- RPM was exercised using as inputs the time-varying background concentrations of NO, NO_2, O_3, olefins, paraffins, aldehydes, aromatics, and SO_2 predicted by CHEMK.

Results of the simulations are presented in Figures 7 and 8. The curves in the figures give the background ozone concentrations predicted by CHEMK and the plume ozone concentrations predicted by RPM using computed CHEMK backgrounds for NO, NO_2, O_3, SO_2, and the four lumped HC groups — olefins, aldehydes, aromatics, and paraffins. In Figure 7, the low HC case, predicted plume ozone concentrations exceed predicted background levels by about 0.005 to 0.010 ppm between simulation times of 60 and 180 minutes. Before and after this period the plume is observed to have an ozone deficit relative to the background. On the other hand, the case of highly reactive HC backgrounds (Figure 8) is associated with an ozone bulge of 0.030 ppm (approximately 12 percent above background) occurring midway through the simulation. In fact, with the exception of the ozone deficit occurring in the first 20 minutes of the simulation, the plume ozone levels exceed predicted ambient levels by 0.015 to 0.030 ppm (6 to 12 percent above ambient) throughout the simulation. Thus, for the initial and background conditions used in the high HC background example, RPM predicts net ozone generation in the plume relative to the predicted background ozone level given by CHEMK.

From this case study it appears that for ambient reactive HC concentration levels on the order of 6.0 ppm as methane, RPM predicts plume ozone concentrations approximately 6 to 12 percent higher than the predicted background concentrations derived from a smog chamber photochemical model. While this result suggests that for high background HC conditions the models do predict slight ozone formation, the results of this case study are too limited to confirm or refute an ozone formation hypothesis in the real environment because important phenomena that affect background and plume pollutant concentrations (e.g., emissions from other sources, surface pollutant removal processes) were not included in the simulations. One way to include these phenomena and perhaps to derive a more general result would be to use a more sophisticated photochemical model that treats plume and background reactions simultaneously,

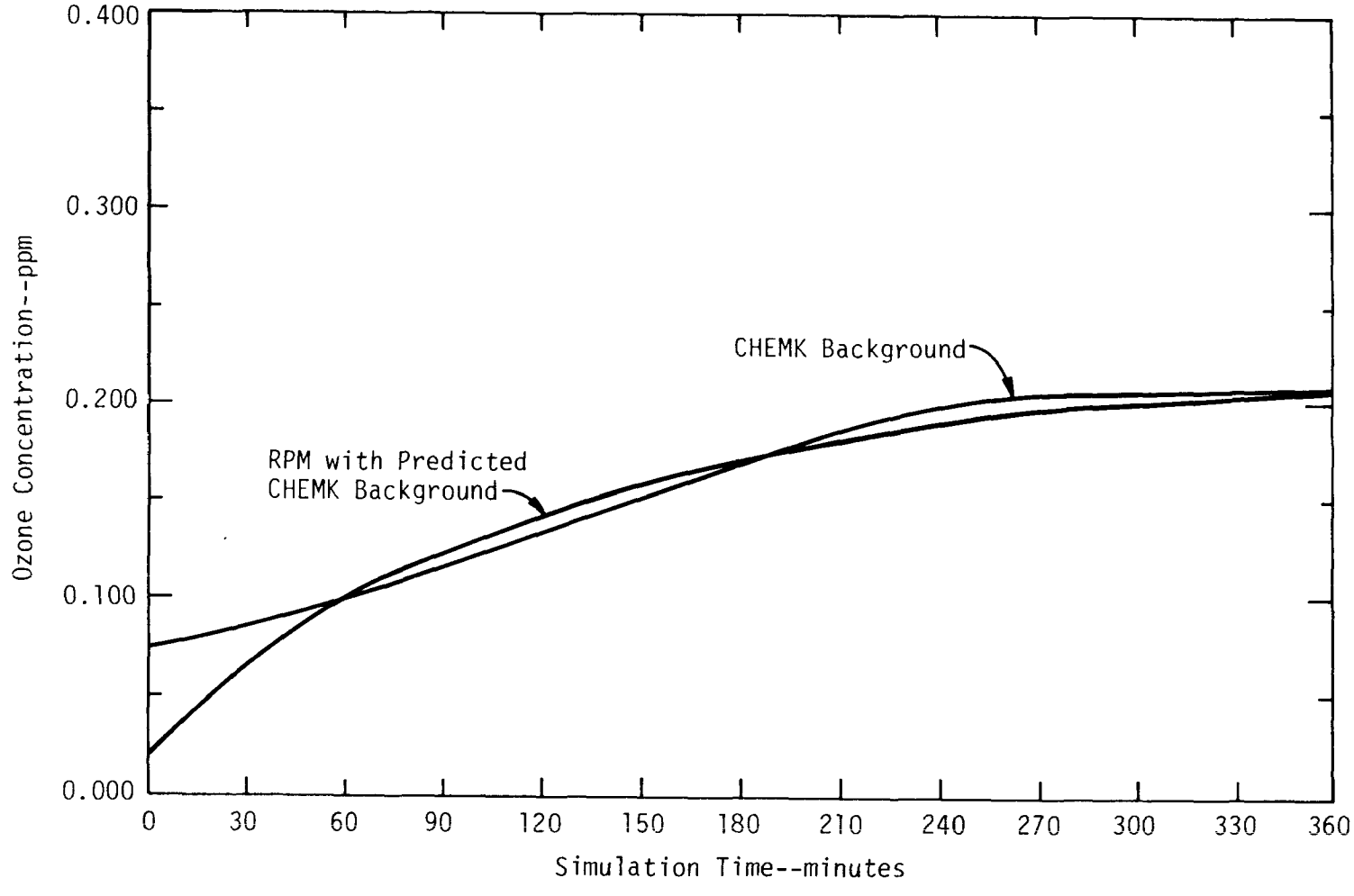

Figure 7. Comparison of predicted plume and background ozone concentrations: low hydrocarbon concentration case.

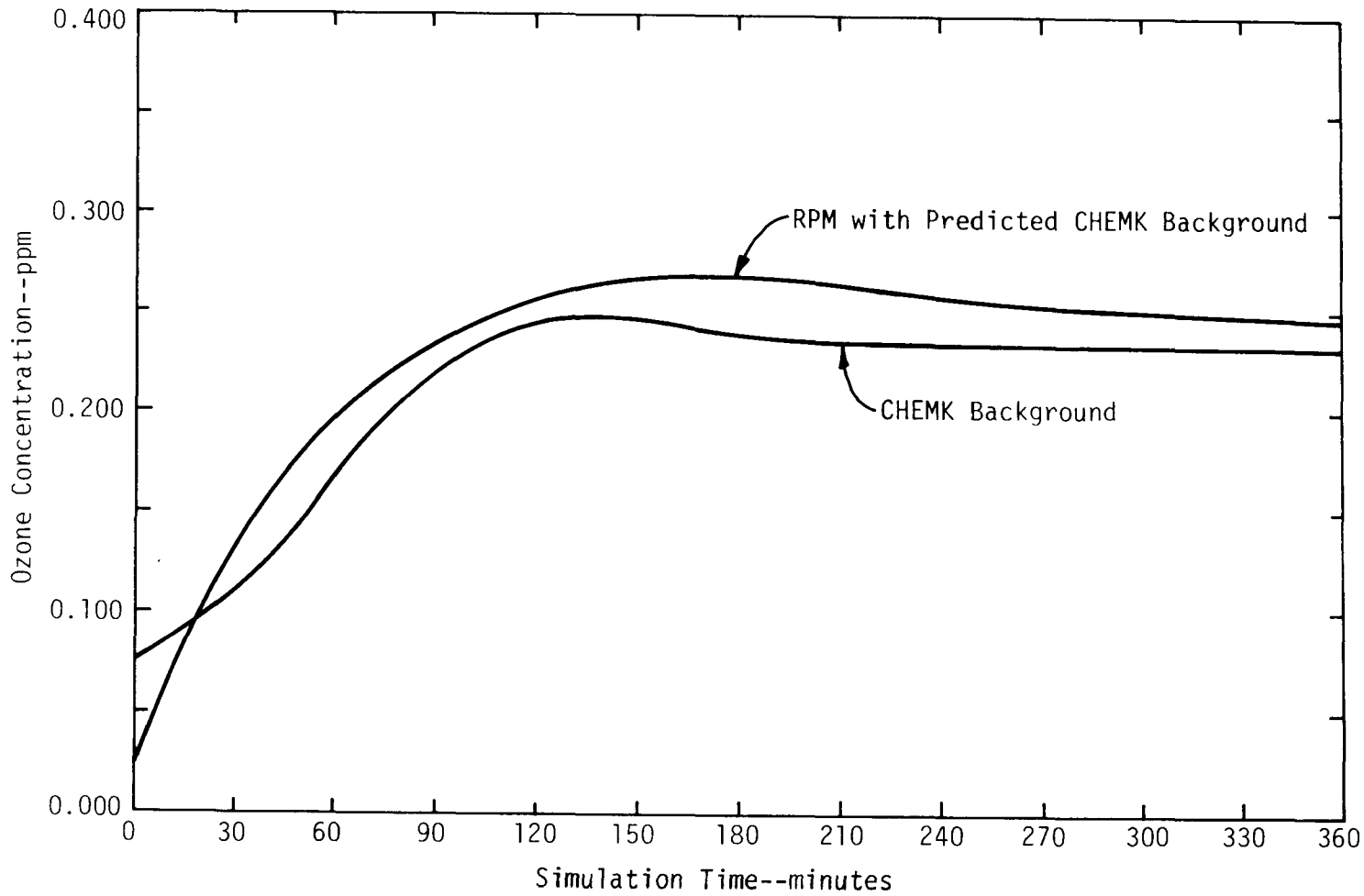

Figure 8. Comparison of predicted plume and background ozone concentrations: high hydrocarbon concentration case.

and accounts for source emissions and pollutant removal processes.

CONCLUSIONS

From the results of field studies, data analysis and a review of the literature, we conclude that formation of ozone in power plant plumes above ambient concentrations is not a common occurrence if it occurs at all. In all of the plumes studied during the EPRI program the ozone observed in the plume can be explained by entrainment of ambient ozone and ozone precursors.

It appears that for certain special conditions RPM does predict plume ozone concentrations slightly in excess (6 to 12 percent) of background levels. These conditions involve the entrainment of high ambient reactive HC concentrations (6.0 ppm as methane). However, the computer simulations yielding this result are only the first step in examining the ozone formation hypothesis.

In attempting to determine the contribution of a given power plant to regional ozone concentrations, one should examine the plume and the plant site for conditions that may be conducive to ozone formation. These include a major HC source in the immediate vicinity of the plant or high HC emissions from the plant itself. If conditions potentially conducive to ozone formation in the plume are encountered, models capable of predicting photochemical reactions may be of value in assessing the situation.

ACKNOWLEDGEMENTS

The authors express their sincere thanks to the many individuals who contributed to various aspects of this program, particularly Dr. W. H. White and Mr. J. Anderson (MRI) and Drs. M. K. Liu, G. Z. Whitten, and P. M. Roth, and Mr. M. A. Yocke (SAI). This study was supported by the Electric Power Research Institute under Contract No. RP-572, under the direction of Mr. Charles Hakkarinen.

REFERENCES

1. Davis, D. D., G. Smith, and G. Klauber, Trace Gas Analysis of Power Plant Plumes Via Aircraft Measurement: O_3, NO_x, SO_2 Chemistry, Science, Vol. 186, 1974, pp. 733-736.

2. Buffington, P. D. and E. A. Bartczak, Ozone: Chemical Action and Reaction in the Lower Level Transport Winds, Presented at the 68th Annual Meeting of the Air Pollution Control Association, Boston, Massachusetts, June 1975.

3. Ogren, J. A., D. L. Blumenthal, and W. H. White, Study of Ozone Formation in Power Plant Plumes, Presented at the Ozone/Oxidants: Interactions with the Total Environment meeting, Air Pollution Control Association II-5 Committee, Dallas, Texas, March 10-12, 1976.

4. Determination of the Feasibility of Ozone Formation in Power Plant Plumes, Report to the Electric Power Research Institute prepared by Systems Applications, Inc., and Meteorology Research, Inc., contract No. RP-572, May 1976.

5. Liu, M. K., D. Durran, P. Mundkur, M. Yocke, and J. Ames, The Chemistry, Dispersion, and Transport of Air Pollutants Emitted from Fossil Fuel Power Plants in California: Data Analysis and Emission Impact Model, Report EF76-18 to the California Air Resources Board by Systems Applications, Inc. San Rafael, California, May 1976.

6. Hect, T. A., J. H. Seinfeld, M. C. Dodge, Further Development of a Generalized Kinetic Mechanism for Photochemical Smog, Environ. Sci. Tech., Vol. 8, 1974, pp. 237-339.

7. Slade, D. H., ed., Meteorology and Atomic Energy 1968, U.S. Atomic Energy Commission Publication TID-24190, 1968.

8. Bowne, N. E., Diffusion Rates, Journal of the Air Pollution Control Association, Vol. 24, No. 9, September 1974.

9. Tesche, T. W., G. Z. Whitten, M. A. Yocke, M. K. Liu, Theoretical Numerical, and Physical Techniques for Characterizing Power Plant Plumes. Report EC-144 to the Electric Power Research Institute by Systems Applications, Inc., San Rafael, California, October 1975.

10. Whitten, G. Z., Rate Constant Evaluations Using a New Computer Modeling Scheme, Paper presented at the 167th National Meeting of the American Chemical Society, April 1974.

OZONE AND NITROGEN OXIDES IN POWER PLANT PLUMES

D. Hegg, P. V. Hobbs, L. F. Radke, and H. Harrison*

ABSTRACT

Results are presented of airborne measurements taken in the plumes of two coal- and two gas-fired power plants. Measurements were made of the concentration of nitric oxide, nitrogen dioxide, ozone and sulfur dioxide, temperature, relative humidity, and ultraviolet radiation. Ozone concentrations exceeding those of the surrounding ambient air were not found in these plumes, which were observed out to distances of 90 km (4 hours travel time) from the stacks. Analysis of the plume chemistry suggests that, over distances and time scales within which plumes are differentiable from background (the near-field), the chemistry is generally controlled by the rates at which the plumes mix with the ambient air rather than by chemical kinetics. Consequently, on these scales, the rates of conversion of nitric oxide to nitrogen dioxide is slow and the nitrogen dioxide/nitric oxide ratios are small (the highest ratio measured was 4.3). This analysis is consistent with the absence of observable ozone generation in the near-fields of the power plant plumes studied.

INTRODUCTION

The possibility of ozone (O_3) formation, perhaps in excess of federal standards, in the near field plumes (the distance over which the plume is differentiable from the background) of fossil-fueled power plants has been suggested by the observations of Davis et al. (1974) at the Morgantown, Maryland, coal-fired power plant. However, in other studies, ozone at concentrations above the ambient background levels has not been detected in power plant plumes (Teshe et al., 1976).

In this paper we present the results of field studies of the plumes from two coal and two gas-fired power plants. The two coal-fired plants were the Pacific Power and Light Plant at Centralia, Washington, and the Four Corners Plant at Farmington, New Mexico. The gas-fired plants were the Cunningham Plant at Hobbs, New Mexico, and the Wilkes Plant at Longview Texas. Airborne measurements were made of the concentrations of nitric oxide (NO), nitrogen dioxide (NO_2), O_3, and sulfur dioxide (SO_2), temperature, relative humidity, ultra-violet radiation, and condensation nucleus concentrations. Data were collected in thirty flights over an 8-month period and parameters needed to specify the nitrogen oxides (NO_X)-ozone chemistry of the plumes were derived. The data consisted primarily of ambient and plume O_3 concentrations, plume

*University of Washington, Seattle, Washington.

center-line and plume average NO_2/NO ratios, plume center-line and plume average NO to NO conversion rates, and the correlations of NO_2/NO with NO_x across the plume. We conclude that at the spatial resolution of our measurements ($\gtrsim$ 150 m) the NO_x-O_3 chemistry is commonly controlled by the rate of mixing of a plume with the ambient air, rather than by kinetic rate constants. Consequently, the macroscopic conversion rate of NO to NO_2 is slow and the NO_2/NO ratios remain too low to permit ozone generation in the near-field plume. A full account of the work summarized in this paper, including all field data, has been given by Hegg et al. (1976).

INSTRUMENTATION

The University of Washington's (U.W.) B-23 aircraft was used for most of the sampling, but some data were gathered by a Cessna 206 operated by Meteorology Research, Inc. (Ogren et al., 1976). In addition to an extensive set of meteorological and aerosol sizing instruments (Hobbs et al., 1976), the U.W. sampling aircraft also carried a Meloy 160-2A sulfur analyzer, a Monitor Labs 8440 chemiluminescent NO_x analyzer, a Monitor Labs 8410A ozone analyzer and an Eppley untrviolet radiometer. The sulfur analyzer was periodically calibrated against a Meloy CS10-2 calibration source (permeation tube), and the NO_x and ozone analyzers were calibrated against a Monitor Labs 8500 calibration source (which was ultimately calibrated against gas-phase titration for NO_x and against buffered potassium iodide for ozone).

FIELD RESULTS AND ANALYSIS

Ozone concentrations higher than in the surrounding ambient air were never observed in the power plant plumes that we studied. We did observe three episodes (on October 10, 11, and 13, 1975) of very high O_3 levels ($\sim$120 ppb) in the plume of the Wilkes plant at Longview, but detailed analysis (Hegg et al., 1976) of the background O_3 field, including its vertical structure, revealed that the high concentrations in the plume on these occasions were caused by the advection of high ambient blobs of O_3 into the plume.

The amount of O_3 that can exist in photochemical steady-state with a given quantity of NO_x is directly related to the ratio of NO_2/NO (Steadman and Jackson, 1974). For a system of either NO_x plus hydrocarbons (HC), or NO_x plus HC plus SO_2, it has been shown experimentally that O_3 generation will not occur to any appreciable extent until the NO_2/NO ratio rises to about 10 (Kocmond et al., 1975). Therefore, the ratios of NO_2/NO in power plant plumes give an indication of the near-field ozone generating capability. Since the NO_x emitted from power plants is mostly NO, the conversion rate of NO to NO_2 is also an important parameter.

In the above discussion, we have tacitly assumed that the plumes are close to photochemical steady-state. This, at first glance, appears to be plausible because the fast rate constants of the NO_x-O_3 system result in a very short relaxation time to steady-states, about 1 minute at typical plume concentrations of NO (0.050 ppm and O_3 (0.015 ppm) for typical temperatures and UV radiation levels. Indeed, the NO_x-O_3 system has been shown to be in

photochemical steady-state for well-mixed ambient air (Steadman and Jackson, 1974). However, a diffusing plume may not be in macroscopic photochemical equilibrium because diffusive mixing times over the spatial scale of the plume may be short compared to the chemical relaxation times. Indeed, over a small enough spatial scale, the mixing times do become short compared to chemical relaxation times. The relative size of this sub-scale to the plume mixing scale determines the extent to which a plume is macroscopically in a steady-state. We must therefore consider this problem in more detail.

A plume of NO_x, initially mostly NO, interacting with ambient air containing O (or any other species of comparable reactivity with NO) may be viewed as a bimolecular reaction, with initially unmixed reactants, in a turbulent fluid. This problem has been treated theoretically with some success; also, some laboratory results are available (O'Brian, 1974; Hill, 1976). Assuming that the bimolecular reaction is fast compared to mixing times over the scale of the plume (for $NO + O_3 \rightarrow NO_2 + O_2$, $\tau_{O_3} \simeq 1$ minute for typical NO concentrations near 0.05 ppm), the reactant species become spatially segregated with the reaction occurring entirely within a relatively narrow reaction zone between the two spatial regions. Figure 1 illustrates this view of the plume. The width of the reaction zone is essentially the spatial sub-scale over which the mixing time is comparable to the chemical relaxation time. The well known ozone deficits associated with power plant plumes are, in fact, manifestations of spatial segregation of reactant species. Figure 2 shows an example of this effect which suggests that the width of the reaction zone is indeed small compared to the plume radius. Thus, over the spatial scale of the plume, the mixing time is long compared to the chemical relaxation time and most of the volume of a plume should be in local photochemical steady-state.

The time required to mix the initially separated reactants (NO and O_3) over the whole plume is longer than that required for reactions between NO and O_3 to take place in the sub-scale. Therefore, the macroscopic rate of reaction is controlled by the rate of mixing of the plume with the ambient air, rather than by the kinetic rate constant for the reaction. The plume chemistry is therefore diffusion controlled.

Evidence for the diffusive control of the plume chemistry can be obtained by considering the spatial distribution of the NO_2/NO ratio in the plume. Since NO_2 is the product of the reaction of NO and O_3, the ratio of NO_2/NO should be highest at the reaction zone; for a biomolecular diffusion-controlled reaction, this zone should be located at the edge of the plume between the regions of high NO and O_3 (Figure 1b). Assuming this to be the case, the ratio of NO_2/NO should then be negatively correlated with the total concentration of NO_x (which we employed as a plume tracer and assumed to be conserved in the plume).

Table 1 shows the results of a correlation analysis of NO_2/NO with NO_x in the power plant plumes we have investigated. In fourteen out of eighteen cases there was a negative correlation between NO_2/NO and NO_x indicating that the plumes were indeed generally diffusion controlled. However, on three occasions there were significant positive correlations between NO_2/NO and NO_x,

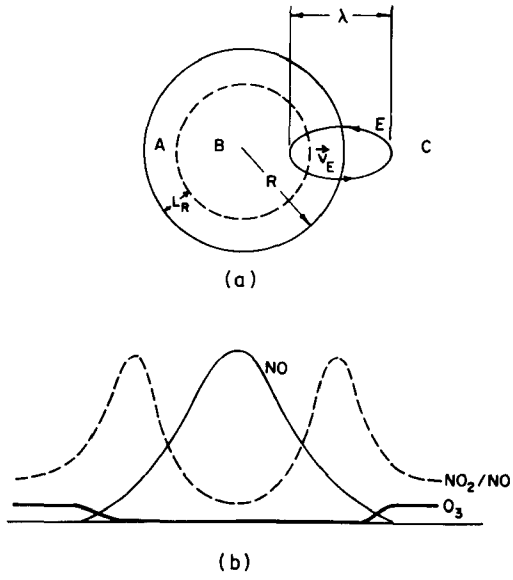

Figure 1. Diagrams for a bimolecular reaction in a turbulent plume: (a) shows a cross-sectional view of the plume. The reaction zone is an annulus of area A and width L_R. The interior of the plume, where the concentration of NO is high, has area B. Area C is the exterior region of ozone. E is a mixing turbulent eddy of velocity V_E and scale λ. (b) shows concentrations of the gases across section (a).

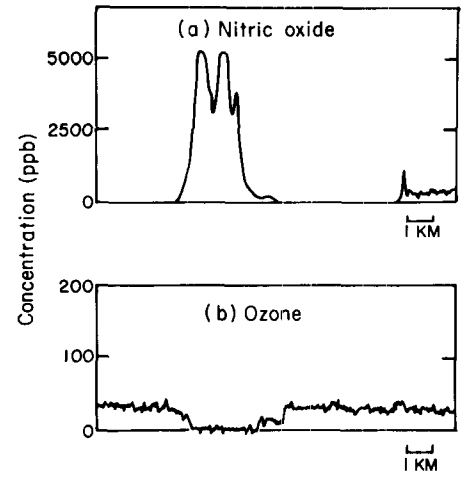

Figure 2. Profiles of nitric oxide and ozone across the plume of the Four Corners coal-fired power plant on 16 October 1975. The range was 1 km downwind from the stack and the altitude was 1950 m.

which indicates that in some situations the plume chemistry may be chemically controlled. This is not surprising in view of the variability in the time scales for atmospheric mixing, and it is to be expected when concentration gradients of NO_x become small over both the spatial scale of the measurements and the macroscale of the plume.

The degree to which the plumes are in chemical steady state may be considered in terms of the three fast reactions:

$$NO + h\nu \xrightarrow{k_a} NO + O \qquad (1)$$

$$O + O_2 + M \xrightarrow{k_2} O_3 + M \qquad (2)$$

$$NO + O_3 \xrightarrow{k_3} NO_2 + O_2 \qquad (3)$$

where the k's are rate constants and $k_a = 8.0 \times 10^{-3}$ ($\lambda < 400$ nm), $k_2 = 1.1 \times$

TABLE 1. CORRELATION OF NO_2/NO WITH NO_x IN POWER PLANT PLUMES

Date	Power Plant	Range (km)	Correlation Coefficient (Vxy)	Significance Level (%)	Data Source
6/16/75	Centralia*	0.8	-0.75	> 90	Hegg et al. (1976)
"	"	1.6	-0.92	> 90	"
"	"	4.8	-0.94	> 98	"
7/29/75	"	0.8	-0.87	> 95	"
"	"	1.6	-0.90	> 99	"
8/20/75	"	0.2	-0.57	> 75	"
"	"	3.2	-0.51	> 50	"
10/10/75	Longview †	5.0	+0.98	98	"
"	"	3.0	+0.10	< 50	Ogren et al. (1976)
10/11/75	"	3.0	-0.76	> 90	"
"	"	10	+0.99	99	"
10/17/75	Farmington*	20	-0.91	> 90	Hegg et al. (1976)
"	"	40	-0.91	> 95	"
"	"	70	-0.54	> 50	"
"	"	10	+0.80	80	Ogren et al. (1976)
10/30/75	Centralia*	8.0	-0.74	> 80	Hegg et al. (1976)
10/31/75	"	2.4	-0.80	80	"
"	"	5.6	-0.69	> 80	"

* Coal-fired
† Gas-fired

10^{-34} exp(500/T), and $k_3 = 1.7 \times 10^{-12}$ exp(-1310/T) (Crutzen, 1974). If the system is in the photostationary state, then:

$$\psi = (NO_2)\ k_a/k_3(NO)(O_3) = 1 \tag{4}$$

(Steadman and Jackson, 1974). Because values for all of the parameters in Equation (4) can be determined from our airborne measurements, departures of the measured ψ from unity are indicators of departure from chemical steady state at the spatial scales of the measurements. Moreover, departures of ψ from unity are explicable in terms of the relative size of the reaction ozone compared to the size of the plume.

Before displaying these departures, however, we wish to consider the dependence of ψ on the width of the reaction zone (expressed in terms of the ratio of the time scale of the chemical kinetics to the time scale of plume mixing). Consider a simple bimolecular reaction:

$$A + B \xrightarrow{k} C\ . \tag{5}$$

where k is the chemical rate constant. Then,

$$\frac{d\overline{A}}{dt} = K_r \frac{\partial^2 \overline{A}}{\partial r^2} - k(\overline{AB} + \overline{A'B'}) \tag{6}$$

where K_r is an eddy diffusion coefficient along the radius of a cylindrical plume, and the bars indicate the effect of correlated concentration fluctuations. If the effect of correlated concentration fluctuations on the chemical kinetics is negligible for fast chemistry, Equation 6 can be approximated as:

$$\frac{d\overline{A}}{dt} = \frac{\beta \overline{A}}{\tau_D} - \frac{\overline{A}}{\tau_C} \tag{7}$$

where τ_C is the kinetic time scale and τ_D is a diffusive time scale defined by:

$$K_r \frac{\partial^2 \overline{A}}{\partial r^2} = K_r \frac{\overline{A}}{r^2} = \frac{\overline{V'^2}\,\tau_T \overline{A}}{\overline{V'^2}\,\tau_D{}^2}\ . \tag{8}$$

τ_D is a time scale characteristic of the mixing over some sub-scale (L_R) of the plume, τ_T is the turbulent time scale over the spatial scale R (Figure 1a) and V' is the turbulent velocity fluctuation. The value of β is given by;

$$\beta = \frac{\overline{V'^2}\,\tau_T}{\overline{V'^2}\,\tau_D} \tag{9}$$

Integrating (7) over the chemical time scale:

$$\ln \frac{\overline{A}}{A_o} = \beta \frac{\tau_C}{\tau_D} - 1 \tag{10}$$

and

$$\overline{A} = A_o \exp\{\beta \tau_C/\tau_D + 1\} . \tag{11}$$

Hence,

$$\psi = \frac{k_a}{k_3} \frac{\overline{C}}{\overline{AB}} = \alpha \exp\{-\beta \tau_C/\tau_D + 1\} \tag{12}$$

Values of ψ and τ_C/τ_D from our field data are listed in Table 2. The value of τ_C was determined from the formula of Steadman and Jackson (1974), namely:

$$\tau_C = \{k_a + k_3(NO) + k_3(O_3)\}^{-1} \tag{13}$$

The value of τ_D was approximated as:

$$\tau_D = R/2V_E \tag{14}$$

where R is the radius of the plume, $V_E \simeq 0.4\ \overline{U}$ and $\overline{U}$ is the mean wind velocity (Pasquill, 1974). The data in Table 2 were fitted to Equation 12 and α and β determined as regression coefficients. The values were found to be stable with values of: $\alpha = 0.2 \pm 0.03$ and $\beta = 4 \pm 1$. The multiple correlation coefficient of the regression was found equal to 0.61. We conclude that observed departures from the photostationary state can indeed be explained by the relative size of a plume reaction zone and that the plume chemistry is, in fact, diffusion controlled.

If the plume chemistry is diffusion controlled, the net conversion rate of NO to NO_2 will be considerably slower than that inferred from chemical kinetics. Furthermore, the value of the ratio NO_2/NO should, and does, remain low. Conversion rates of NO to NO_2 were calculated for the plume centerline and for the plume as a whole using the formula

$$\frac{(NO_2)_i + \gamma(NO)_i}{(1 - \gamma)\ (NO)_i} = \frac{(NO_2)_f}{(NO)_f} \tag{15}$$

where γ is the fraction of NO converted to NO_2 and the subscripts i and f refer to the initial and final times, respectively, that the concentrations were measured. (Note that Equation 15 assumes that NO_x is conserved.) Measured values for the 50% conversion times of NO to NO_2 are shown in Table 3. The 50% NO to NO_2 conversion times for the centerline of the plume are plotted in Figure 3, where it can be seen that the conversion rate decreases approximately inversely as the square of the travel time from the stack; this result is consistent with our previous conclusion that the plume chemistry is diffusion controlled.

Ratios of NO_2/NO measured during this study are quite low (Tables 4 and

TABLE 2. VALUES OF τ_C/τ_D AND CORRESPONDING VALUES OF ψ

Date	Power Plant	Range (km)	τ_C/τ_D	R (m)	$\overline{U}$ (m s^{-1})	ψ (observed)	ψ (calculated)
10/17/75	Farmington	20	0.034	2,860	6	0.60 ± 0.19	0.47
"	"	40	0.002	3,718	9	0.64 ± 0.11	0.43
10/31/75	Centralia	2.4	1.17	429	9	0.13 ± 0.05	0.01
"	"	5.6	0.44	1,215	9	0.14 ± 0.03	0.12
10/11/75	Longview	3	0.17	721	7	0.13 ± 0.02	0.30
"	"	10	0.18	648	7	0.12 ± 0.02	0.29
10/31/75	Centralia	21	0.39	1,200	9	0.17 ± 0.05	0.14
10/30/75	"	0.8	0.88	358	10	0.15 + 0.03	0.03
10/16/75	Farmington	17	0.005	13,700	5	0.54 ± 0.06	0.52
"	"	30	0.010	16,300	5	0.37 ± 0.05	0.51
10/30/75	Centralia	18	0.45	1,144	10	0.18 ± 0.03	0.12

TABLE 3. TIMES REQUIRED FOR 50% OF NO TO BE CONVERTED TO NO_2 IN POWER PLANT PLUMES

Date	Power Plant	Travel Time (min)	50% Conversion Time Along Centerline (min)	Average 50% Conversion Time for Plume (min)
6/16/75	Centralia	5.0	5.9 - 7.6	3.6 - 4.3
"	"	14	Indeterminate	Indeterminate
7/29/75	"	23	"	"
8/20/75	"	30	366 - 1002	"
10/11/75	Longview	18	24 - 53	48 - 82
10/17/75	Farmington	96	119 - 160	93 - 126
10/31/75	Centralia	7.9	11.6 - 120	Indeterminate
11/4/75	"	14	29 - 320	---
11/5/75	"	2.3	2 - 3.4	3.3 - 16.7

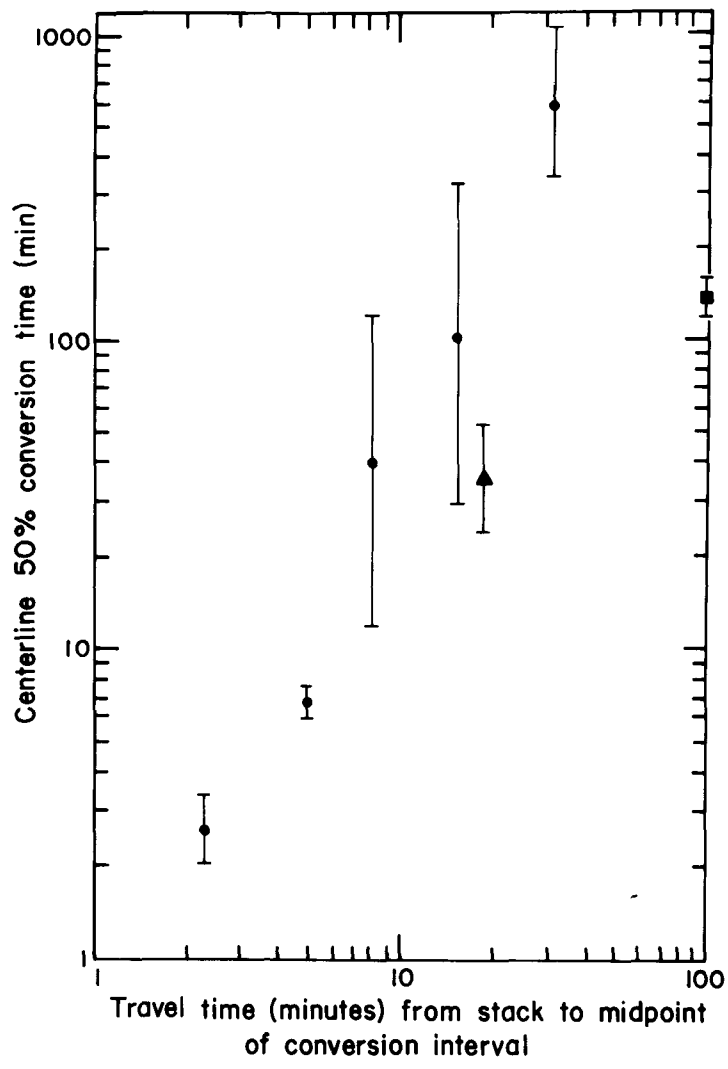

Figure 3. 50% conversion times for NO to NO_2 versus travel time from the plant. The circles indicate data from the Centralia coal power plant, the triangle and square are for the Longview gas power plant and the Farmington coal power plant, respectively.

5). The highest ratio observed during the entire study was 4.3. Because laboratory experiments have shown that the NO_2/NO ratio must reach a value of at least 10 before appreciable O_3 generation can occur, our field-measured ratios are consistent with our observations that O_3 was not generated in the near-field plumes.

CONCLUSIONS

Analysis of the NO_x-O_3 chemistry of four power plant plumes has revealed that the chemistry of the plumes was generally diffusion controlled over the distances measured in our study (90 km) and for travel times up to 4 hours. The NO to NO_2 conversion rates and NO_2/NO ratios were consequently slower than

TABLE 4. NO_2/NO RATIOS ALONG THE CENTERLINE OF THE PLUME FROM THE CENTRALIA COAL POWER PLANT ON 30 OCTOBER 1975

Range (km)	Travel Time (min)	NO_x (ppm)	NO_2/NO
0.8	1.4	0.42	0.33
8.0	14	0.099	1.3
17.6	22	0.065	1.9
22.4	39	0.055	4.3*
38.4	65	0.039	2.6

*Highest ratio observed in study.

TABLE 5. PLUME AVERAGE NO_2/NO RATIOS WITH CORRESPONDING TRAVEL TIMES FOR VARIOUS FLIGHTS AT THE CENTRALIA COAL POWER PLANT

Date	Travel Time (min)	NO_x (ppm)	NO_2/NO
7/29/75	15	0.13	0.25 ± 0.03
"	30	0.07	0.27 ± 0.05
6/16/75	3.3	0.27	0.24 ± 0.02
"	6.7	0.11	1.14 ± 0.07
"	20	1.05	1.08 ± 0.14
8/20/75	3.5	0.38	0.27 ± 0.01
"	60	0.06	0.26 ± 0.03
11/5/75	1.5	0.07	0.47 ± 0.07
"	3	0.05	0.70 ± 0.10

would be inferred from chemical kinetics. The highest value of NO_2/NO was 4.3, which is consistent with our observation that ozone was not generated in the power plant plumes that we studied.

ACKNOWLEDGEMENTS

This research was supported by contracts RP572-3-1 and RP330-1 from the Electric Power Research Institute.

REFERENCES

1. Crutzen, P. J. 1974. Photochemical Reactions Initiated By and Influencing Ozone in Unpolluted Tropospheric Air. Tellus. 26: 47-56.

2. Davis, D. D., G. Smith and G. Klauber 1974. Trace gas analysis of Power Plant Plumes via Aircraft Measurement. Science. 186: 733-735.

3. Hegg, D. A., P. V. Hobbs and L. F. Radke 1976. Reactions of Nitrogen Oxides, Ozone and Sulfur in Power Plant Plumes. Final Report Under Contract RP 572-3-1 And Interim Report Under Contract RP 330-1 prepared for the Electric Power Research Institute, 3412 Hillview Avenue, Palo Alto, California 94304.

4. Hill, J. C. 1976. Homogeneous Turbulent Mixing with Chemical Reaction. Ann. Rev. Fluid Mech. 8: 135-161.

5. Hobbs, P. V., L. F. Radke and E. E. Hindman II 1976. An Integrated Airborne Particle-Measuring Facility and Its Preliminary Use in Atmospheric Aerosol Studies. J. Aerosol Sci. 7: 195-211.

6. Kocmond, W.C., D.B. Kittelson, J.Y. Young and K.L. Demerjian, 1975. Study of Aerosol Formation in Photochemical Air Pollution. EPA Report No. 65013-75-007.

7. O'Brian, E. E. 1974. Turbulent Diffusion of Rapidly Reacting Chemical Species. Adv. in Geoph. 18b: 341-348.

8. Ogren, J. A., S. A. Muller, M. E. Thistlewaite, J. A. McDonald, W. R. Kiruth, M. E. Drehsen, J. A. Nuebuck and S. B. Bristow 1976. Data Volume, Determination of the Feasibility of Ozone Formation in Power Plant Plumes. Meteorology Research Inc. Report MRI 76-FR-1388.

9. Pasquill, F. 1974. Atmospheric Diffusion. 2nd Ed., Halstad Press, New York.

10. Steadman, D. H. and J. O. Jackson. 1974. The Photostationary State in Photochemical Smog. Paper presented at CODATA Chemical Kinetics Meeting, Detroit, Michigan.

11. Tesche, K. W., G. Z. Whitten, M. A. Yoche and M. K. Liu. 1976. Theoretical Numerical and Physical Techniques for the Characterization of Power Plant Plumes. Electric Power Research Institute, Topical Rpt. EC-144.

THE ANALYSIS OF GROUND-LEVEL OZONE DATA FROM NEW JERSEY, NEW YORK, CONNECTICUT, AND MASSACHUSETTS: DATA QUALITY ASSESSMENT AND TEMPORAL AND GEOGRAPHICAL PROPERTIES

W. S. Cleveland, B. Kleiner, J. E. McRae, and R. E. Pasceri*

ABSTRACT

Hourly, ground-level ozone measurements from 41 sites in eastern New York, northern New Jersey, Connecticut, and Massachusetts from May 1, 1974 to September 30, 1974, are analyzed. Various techniques for assessing data quality and uniform calibration show the data to be of high reliability for yielding information on the ozone problem in the region. Statistical analyses show that nighttime concentrations, relative to those during the day, are highest in Massachusetts. The sites distribution of daily maximum concentration are highest in the Stamford-Greenwich region of south Connecticut and next highest in a region to the east and northeast of Stamford-Greenwich. These results, together with other analyses, demonstrate that photochemical air pollution resulting from primary emissions in the New York City metropolitan area is transported by prevailing winds on a 300 km northeast trajectory through Connecticut as far as northeastern Massachusetts.

INTRODUCTION

This paper presents an analysis of ambient ground-level ozone measurements from a region of the northeastern United States covering eastern New York, northern New Jersey, Connecticut, and Massachusetts. The data consist of hourly averages from May 1, 1974, to September 30, 1974, at 41 sites. Their quality and uniform calibration assessed, their diurnal behavior is analyzed, and the geographical variation in concentrations over the region is described.

The ozone data, gathered at monitoring site locations shown in Table 1 and Figure 1, were provided by the following agencies: New Jersey sites — New Jersey Department of Environmental Protection; New York sites (except Yonkers) — New York State Department of Environmental Conservation; Yonkers — Boyce Thompson Institute; Connecticut sites — Connecticut Department of Environmental Protection; Massachusetts sites — Massachusetts Department of Public Health.

---

*W. S. Cleveland, B. Kleiner, J. E. McRae, J. L. Warner, Bell Laboratories, Murray Hill, New Jersey. R. E. Pasceri, New Jersey Department of Environmental Protection, Trenton, New Jersey.

TABLE 1. SUMMARY OF OZONE DATA AT 41 SITES IN THE NORTHEASTERN UNITED STATES FOR 1974. ALL OZONE CONCENTRATIONS ARE IN PPB.

Column	Description
1	Site name
2	State (J = New Jersey, Y = New York, C = Connecticut, and M = Massachusetts).
3	Site letter (the site letter together with the state allows identification of the location in Figure 1).
4	Maximum hourly reading from May to September with suspect values shown by a *.
5	Number of days from May to September with valid daily maxima (i.e., maximum hourly concentration from 0800 to 2400 EST).
6	Median of the daily maxima for June to August.
7	Upper quartile of daily maxima for June to August (one site omitted).
8	Ratio of upper quartile of readings at 1500 hours EST from May 15 to August 15 to upper quartile of readings at 0100 hours EST from May 15 to August 15.

Name	State	Code	Maximum	Days	Median	Quartile	Ratio
Asbury Park	J	A	176	121	59	82	2.2
Somerville	J	S	196	114	58	81	5.5
Chester	J	C	170	90	90	110	1.7
Bayonne	J	B	208*	122	80	100	4.8
Elizabeth	J	E	98	95	50	64	4.7
Newark	J	N	140	125	47	63	5.6
Welfare Island	Y	W	185	115	81	102	5.3
Yonkers	Y	Y	132	148	56	80	3.4
Eisenhower Park	Y	E	154	48	55		4.5
Babylon	Y	B	207*	109	72	111	3.5
Mamaroneck	Y	M	165	120	62	89	8.3
Greenwich	C	G	270	133	100	140	3.7
Stamford Farms	C	S	250	63	97	145	3.1
Stamford Trailer	C	s	240	136	91	134	5.6
Bridgeport	C	B	250	137	80	116	4.1
Danbury	C	D	270	89	81	120	4.8
New Haven	C	N	302	94	76	127	3.7
Waterbury	C	W	252	76	75	112	5.1
Morris	C	M	225	90	85	99	2.9
Deep River	C	d	202	57	94	117	2.6
Middletown	C	m	365	105	80	122	3.1
New Britain	C	n	240	119	82	124	2.5
Groton	C	g	244	110	74	113	2.7
Hartford	C	H	306	135	68	103	2.9
Windsor	C	w	234	103	60	82	4.8
Eastford	C	E	197	56	85	96	2.7
Springfield	M	S	108	131	34	48	1.9

(continued)

TABLE 1. (continued)

Name	State	Code	Maximum	Days	Median	Quartile	Ratio
Worchester	M	W	250	128	66	86	1.8
Fitchburg	M	F	174	136	65	87	2.1
Fall River	M	f	214	94	73	109	1.5
Lowell	M	L	145	135	63	86	2.5
Quincy	M	Q	173	102	62	79	2.0
Boston	M	B	136	84	36	56	2.0
Cambridge	M	C	130	95	54	74	1.9
Waltham	M	w	116*	92	42	59	2.4
Medford	M	M	166	76	52	79	3.1
Kingston	Y	K	159	123	64	91	3.0
Pittsfield	M	P	166	109	65	84	2.2
Rensselaer	Y	R	128	106	60	78	2.9
Schenectady	Y	S	128	116	56	72	2.4
Glens Falls	Y	G	127	115	64	84	2.5

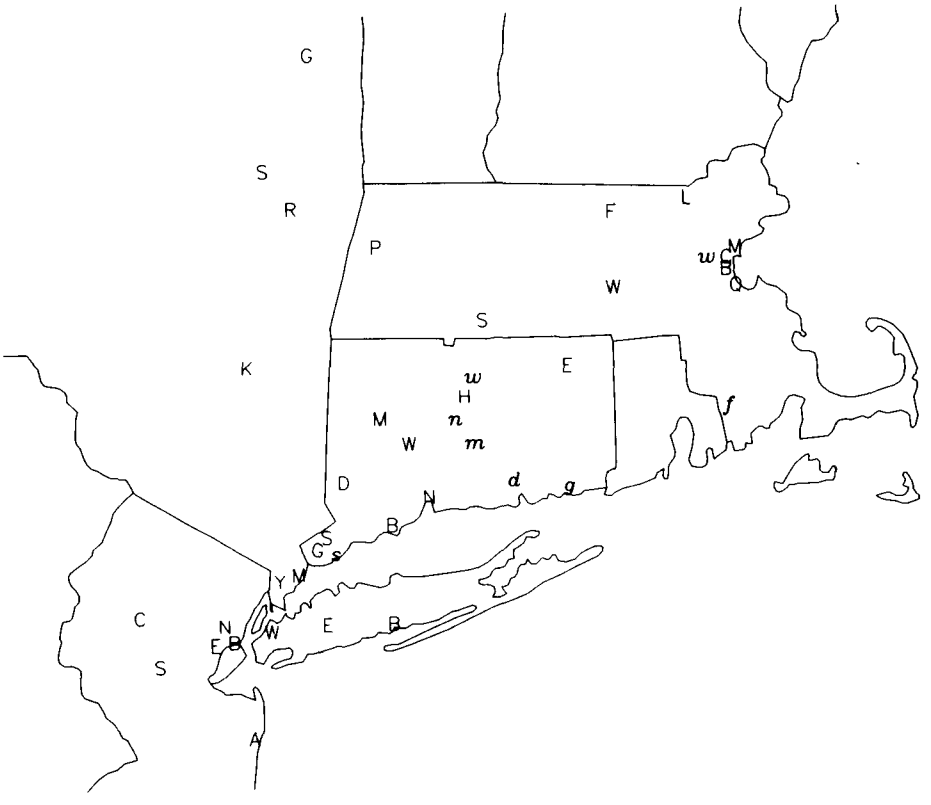

Figure 1. Site letters in column 3 of Table 1 are shown at site locations.

With the exception of the Boyce Thompson Institute unit, all monitors were of the gas phase, ozone-ethylene type. Some of the commercial types used (Bendix, REM) have been recently examined by Clark, et al., who also briefly reviewed the development history of the ozone-ethylene detector (1). Field tests of various ozone and oxidant analyzers have been reported by Stevens, et al. (2,3). The cooperating agencies have found that the various commercial brands of analyzers are equivalent with regard to the accuracy needed for air monitoring networks. Boyce Thompson Institute employed the colorimetric method for oxidants determination with a dichromate scrubber to avoid sulfur dioxide interference (4).

Each monitoring agency, operating independently, utilized a variety of analyzers, field calibration techniques and schedules. Generally, however, all field calibrations were referred to the federal reference method utilizing the reaction of oxidants with neutral, buffered potassium iodide (5). In addition, the Connecticut, New Jersey, and New York agencies participated with their EPA Region II laboratory in a joint ozone calibration on June 21, 1974 (6). Previously, on June 14-17, the EPA laboratory had calibrated their Bendix 016059 calibrator at the National Bureau of Standards, Washington, D. C., which utilized the federal reference method. Efforts toward standardizing ozone calibration techniques have been reported by Hodgeson, et al (7).

DATA QUALITY AND CALIBRATION

No detailed investigation of ambient air quality data can omit the important consideration of data quality (8). A number of nonstatistical considerations make it plausible that the data are of high quality. The first is the reliability and relative ease of maintenance of the chemiluminescent monitors (3). The second is the high frequency of site visits by agency personnel and the data review programs carried out by all agencies. Third, the uniformity of calibration was greatly enhanced among the New Jersey, New York, and Connecticut agencies by the joint calibration program of June 21, 1974, described in the introduction. While such considerations inspire confidence in the data, it is still desirable to use statistical methodology for further verification. In this section the particular techniques that have been used in assessing the ozone data are described.

Bad data, particularly if caused by transmission errors, often have little regard for the measurement scale. Thus, the first step in our data quality assessment was to calculate the largest hourly reading at each site and inspect the data for a time interval containing the maximum. In a number of cases, transmission errors were detected; in a few cases, correctly transmitted numbers were discarded as unlikely because of a lack of validation from other sites. In three cases, suspicion was raised but there was no proof of bad data. These values were retained with the notation that something might be wrong. A typical example was recorded in Waltham, Massachusetts, on August 7, 1974; 24-hourly values in ppb starting at 0100 hours EST were 0, 10, 20, 10, 20, 30, 40, 50, 50, 100, 120, 100, 80, 70, 40, 40, 50, 40, 40, 40, 30, 30, 20, 10. The readings were not terribly unusual; but, in comparison with measurements for the day at other sites, were atypical. At other sites, there was relatively little photochemical activity measured; the highest reading being 70 at Cambridge.

Table 1 lists the maxima for the 41 sites to show the highest concentrations of ozone in the region. The three suspect values are indicated. For these sites, the second highest readings in ppb are 167 (Bayonne), 112 (Waltham), and 201 (Babylon).

If the data at a particular site contains an undue amount of measurement noise, then it is to be expected that the variation of the measurements through time will not correspond well with those at other sites. For each day, the maximum of the hourly averages from 0800 to 2400 was calculated for each site. Correlation coefficients, with 5% trimming at points along the two principal components, between all pairs of sites were computed for the square roots of these daily maxima (9). The trimming is a statistical device which prevents a small fraction of the data having an undue influence on the correlations, which are meant to summarize the general behavior. The sample distribution of the square roots is approximated well by a normal probability plots for each of the 41 sites (10). Although in a few cases, such as Bridgeport, the square root maxima are skewed to the right, the square roots provide a more satisfactory plot than logs or the untransformed data.

Since distance between sites must be taken into account in assessing the levels of the correlations, correlations between all pairs of sites are plotted against inter-site distances in Figure 2. Moving statistics have been superimposed on the plot to summarize the behavior of the plotted points. The middle curve summarizes the middle of the distribution of correlations given distance, the upper curve summarizes the upper tail of the distribution, and the lower curve summarizes the lower tail. The correlations tend to be quite large for small distances, and, as has previously been observed, tend to decrease with increasing distance (11). The only site with unusually low values, given distance to other sites, is Asbury Park. In fact, all correlations below 0.2 involve this site. A careful study of the Asbury Park data led to the conclusion that the site location, and not data quality, was responsible for the low values. This conclusion is discussed further in the final section of this paper.

One of the most elusive questions for statistical methodology to investigate is that of uniform calibration, particularly between different agencies. Despite the joint calibration described earlier, it was desirable to use the data to conduct further checks. The distributions of daily maxima at pairs of sites were compared by an empirical quantile-quantile (EQQ) plot (12, 13). This analysis was complicated, however, because even if two sites are located within a few miles of one another and even if calibration is exactly the same, the two sites do not have to have the same ozone concentrations, since local primary emissions can substantially influence ozone levels (14). However, the philosophy invoked is that if there is a major discrepancy between two close sites for which an explanation cannot be found, then the calibration is questioned.

To eliminate distortions due to missing data, the distributions of daily maxima at two sites were compared only for days when both sites have all daily maxima. X_i, for $i=1,\ldots,n$, is the ordered daily maxima (X_1 is the smallest, X_2 is the next smallest, etc.) from one site, and Y_i the ordered maxima for the second site. The EQQ method of comparing the ozone levels at the two

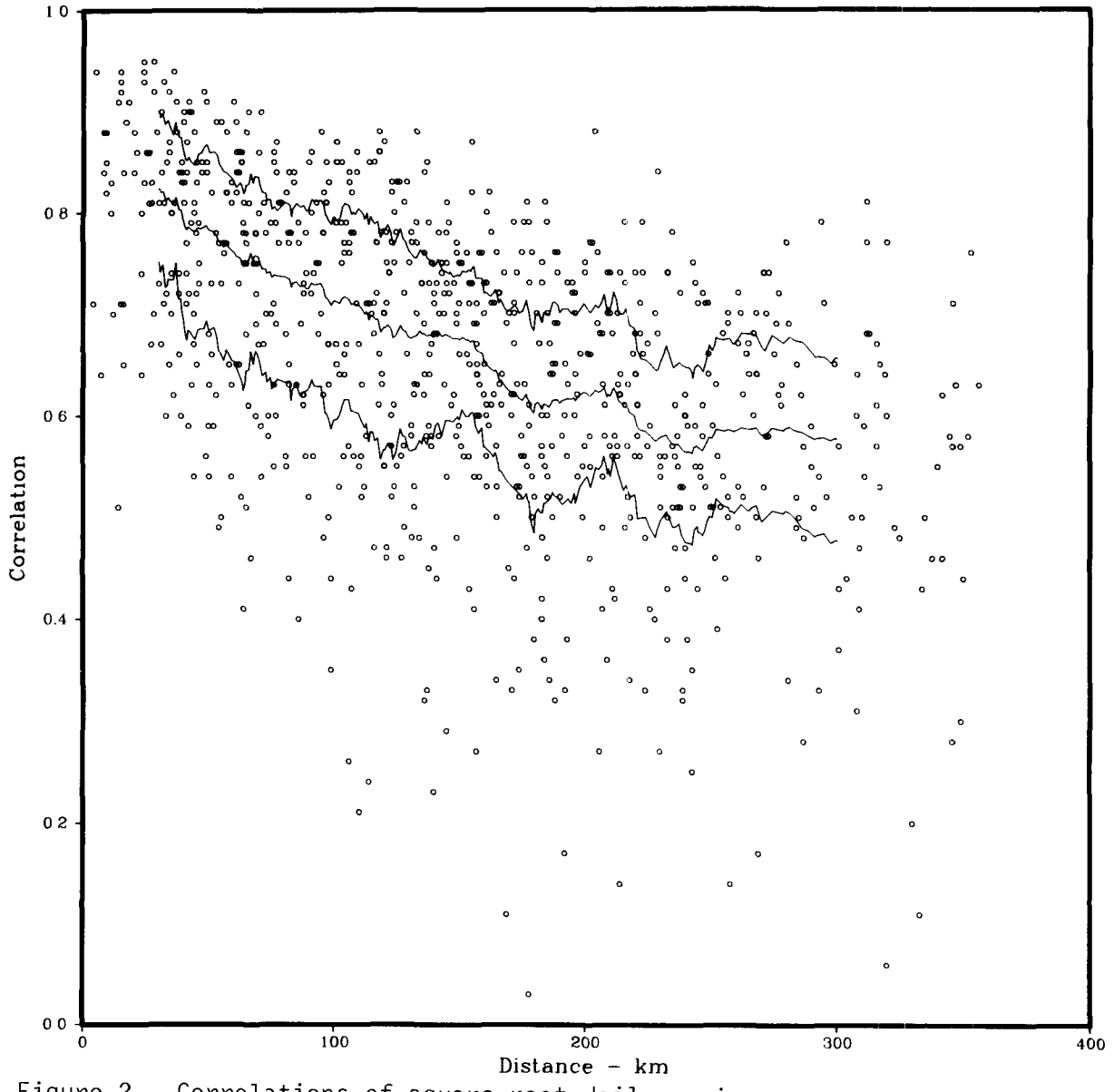

Figure 2. Correlations of square root daily maximum ozone concentrations between all pairs of the 41 sites are plotted against the distances between sites. Moving statistics have been superimposed to summarize the information on the plot.

sites consists of plotting Y_i versus X_i. If the plotted points lie near the line Y=X, the two distributions are nearly the same. These plots were made for a large number of pairs of nearby sites and only one major discrepancy was found. Figure 3 shows the EQQ plot for Mamaroneck, maintained by the New York State Department of Environmental Conservation, and Stamford Trailer, which is 24 km from Mamaroneck and is maintained by the Connecticut Department of Environmental Protection. The points on the EQQ plot lie well below the line Y=X, indicating that Stamford has considerably higher ozone levels. The result in the next section that ozone measurements in the region are highest in Connecticut carries with it important conclusions about the nature of the

photochemical air pollution problem in the region. It is, therefore, important to investigate further whether the recorded Connecticut concentrations are too high as a result of faulty calibration.

An important factor for consideration is that Mamaroneck is in the vicinity of strong automobile emissions of nitric oxide, which would tend to reduce the ozone concentrations (14). An example of the effect of these emissions is, as shown in the next section, that Mamaroneck has the lowest nighttime ozone concentrations of the 41 sites. In order to compare the Connecticut data in other ways, EQQ plots have been made in Figure 3 comparing Fall River, Massachusetts, with Groton, Connecticut; and Babylon, New York, with Bridgeport, Connecticut. Groton, located in eastern Connecticut appears to agree quite well with Fall River. Babylon, like many of the Connecticut sites, lies in a region where prevailing winds reach after crossing the center of the New York City metropolitan area and has ozone concentration distributions much like

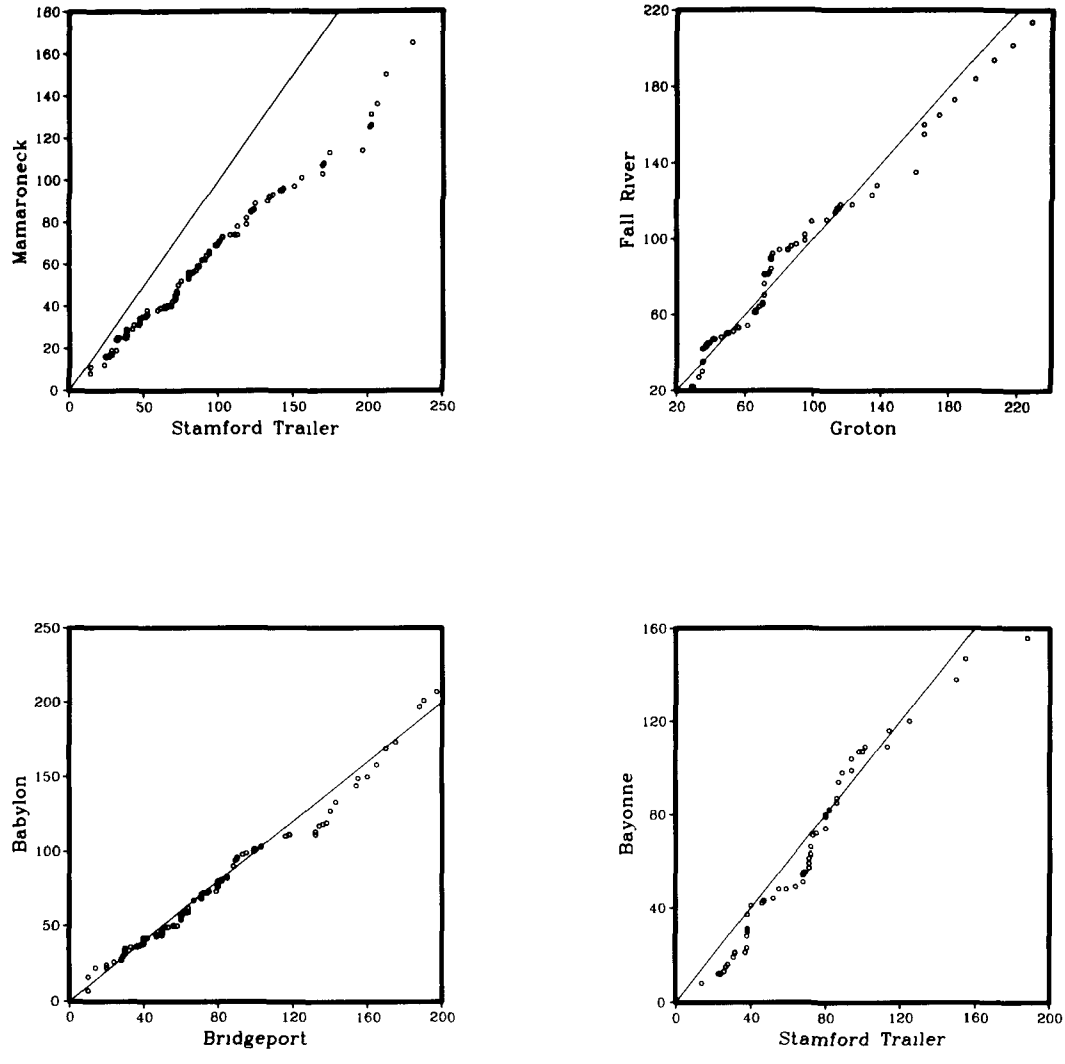

Figure 3. Empirical quartile-quartile plots of daily maximum ozone concentrations (ppb) for four pairs of sites.

that of many of the Connecticut sites. Levels in Babylon agree quite well with those in most of Connecticut, and are only slightly lower overall than the levels in the Stamford-Greenwich region, which, as will be shown, are the highest in the state of Connecticut. For example, the EQQ plot in Figure 3 comparing Babylon and Bridgeport shows the two sites to have very similar distributions. The fourth EQQ plot in Figure 3 compares the distributions of daily maxima at Bayonne, New Jersey, and Stamford Trailer for all days from May to September when the resultant wind direction at 1000 and 1300 hours EST at La Guardia Airport is between 0° and 180°. The two sites have very similar concentration distributions for such days which lends credence to uniform calibration between new Jersey and Connecticut.

A final verification for the Connecticut data comes from an aircraft flight on August 1, 1974, in which ozone was measured over the state of Connecticut (15). The aircraft measurements gave no indication of Connecticut ground station measurements being too high. For example, at 1606 hours EST the aircraft 1000 ft. over Bridgeport was measuring 135 ppb while the ground station average from 1600-1700 hours EST was 110 ppb.

DIURNAL VARIATION OF OZONE CONCENTRATIONS

The diurnal variation at each of the 41 sites was studied by calculating and plotting the upper quartiles for each hour of the day from May 15 to September 15. One noticeable feature was the reduction in the amount of diurnal variation in the upper quartiles at the Massachusetts sites. In Table 1 the ratios of the upper quartiles at 1500 divided by the upper quartiles at 0100 are given. The ratio tends to decrease with increasing distance from the New York City metropolitan region. In particular, the Massachusetts values appear to be the lowest. One site, Mamaroneck, has an unusually large ratio, caused, presumably, by local sources of primary emissions which appear to reduce the ozone levels overall, but which have a particularly strong influence on nighttime levels. Mamaroneck has the lowest upper quartile at 0100 for all 41 sites.

GEOGRAPHICAL VARIATION OF OZONE CONCENTRATIONS

A detailed comparison of the 41 ozone concentration distributions at the sites would be easier if there were not missing values. Missing data can lead to distortion in the comparison of distributions unless special care is taken. To illustrate this, consider two nearby sites with nearly the same ozone concentration distributions. Suppose the first has all data from May through September; but, for the second, the data is missing for the first two weeks in May when the maxima are at their lowest for the season. Then a comparison of all data at site one with all data at site two would leave the false impression that site two has a higher ozone distribution. In a previous section, each comparison of distributions to check calibration involved only two sites. But in this section, the goal is to compare the 41 distributions simultaneously. The number of days with no missing data at all sites is extremely small, so it is necessary to compare distributions of values over different sets of days. Thus a statistical technique was developed to determine which

aspects of the daily maxima at each site were reliable for all sites, except for the upper quartile at Eisenhower Park. Thus these values, given in Table 1, are regarded as valid for comparing the dependence of ozone levels on geographical location. One result, somewhat unexpected before this analysis was carried out, is that Eastford and Deep River, despite having only about one month of data, are usable in the geographical comparison. However, it was found that the largest reading at each site could not be used for comparing ozone concentration distributions at different sites.

Analysis of the data revealed that the ozone levels taper off at the beginning and end of the May to September period. Since data at a site tends to be missing in stretches of several days, rather than isolated days, and since a number of sites have missing data for large stretches of days at the beginning and end of the season, it makes comparison of distributions even more difficult if the whole period May-September is included. For this reason only the months June-August were used in computing the medians and upper quartiles.

In Figure 4 the upper quartiles are plotted against geographical location. The region of highest ozone concentrations is in the Greenwich-Stamford region of southwestern Connecticut, while the next highest are in a belt which spreads out from there to the east and northeast. The five sites with the lowest upper quartiles and medians are Boston, Waltham, Springfield, Newark, and Elizabeth.

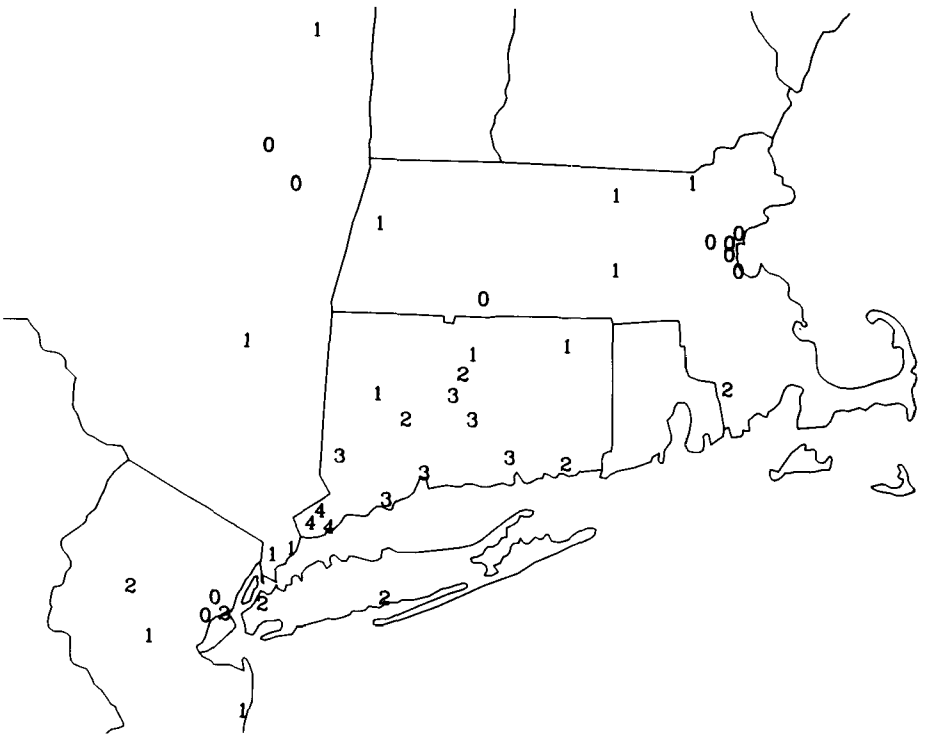

Figure 4. Upper quartiles of daily maximum ozone concentrations from June to August at each site are plotted against geographical locations. The values are coded by numbers: 0=79 ppb or less; 1=80-99 ppb; 2=100-114 ppb; 3=115-129 ppb; 4=130 ppb or more.

SUMMARY

Hourly average, ground-level ozone measurements from 41 sites in eastern New York, northern New Jersey, Connecticut, and Massachusetts for the time period May 1, 1974, to September 30, 1974, have been analyzed. The quality and uniform calibration of the data were assessed by several statistical procedures. In a few cases short stretches of data were invalidated. A discrepancy between the Mamaroneck and Stamford Trailer sites, which brought the uniformity of calibration between New York and Connecticut into question, was resolved by the conclusion that local primary emissions were reducing the ozone concentrations in Mamaroneck substantially. The general conclusion is that the ozone data are of high quality and reliable for examining the problem of ozone pollution.

An analysis of diurnal behavior revealed that diurnal variation tends to decrease (i.e. nighttime values are closer to daytime values) with increasing distance from the New York City metropolitan region. Nighttime values, relative to the daytime values, were particularly high in Massachusetts.

An analysis of the geographical variation in ozone concentrations showed that the lowest concentrations are in Boston, Waltham, Springfield, Newark, and Elizabeth. All five sites are located next to high traffic density arteries, and therefore have large emissions of nitric oxide that reduce the ozone levels. Since this depression of the levels drastically reduces the information content in data from such areas, it is recommended that future placement of ozone monitors not be immediately adjacent to high traffic density roadways.

The highest ozone concentrations are in the Stamford-Greenwich region of Connecticut while the next highest are in a region to the east and northeast of Stamford-Greenwich.

CONCLUSIONS

This paper and other publications directly dealing with transport of photochemical air pollution provides strong evidence that photochemical air pollution resulting from primary emissions in the New York City metropolitan area is transported by prevailing winds on a 300 km northeast trajectory through Connecticut and as far as northeastern Massachusetts (16,17). This occurrence accounts for southwestern Connecticut having the highest ozone concentrations in the region. Thus, it would appear that, similar to the Los Angeles Basin, the chemistry of ozone production is such that areas downwind of strong precursor emissions have the highest ozone concentrations (18,19).

The phenomenon of transport provides the explanation for the low correlation of ozone daily maxima at Asbury Park with those at other sites. Asbury Park is the only site which is both south to southeast of the New York City metropolitan area and in a region which is downwind of the area on a significant number of days. Thus Asbury Park has its highest ozone concentrations when the wind is from the northwest and north, while the majority of other sites, which lie to the east and northeast, have their highest ozone concen-

trations when the wind is from the west and southwest.

Transport also provides the explanation for the high nighttime ozone concentrations in Massachusetts relative to those during the day. The distance between the New York City metropolitan area and eastern Massachusetts is such that the effects of transport, in the form of high ozone concentrations, often occur in eastern Massachusetts during the time period from 1900 to 2400 hours.

REFERENCES

1. Clark, T. A., R. E. Baumgardner, R. K. Stevens, and K. J. Krost. Evaluation of New Ozone Monitoring Instruments by Measuring in Non-Urban Atmospheres. Instrumentation for Monitoring Air Quality. ASTM STP 555. American Society for Testing and Materials, Philadelphia, Pennsylvania, 1974.

2. Stevens, R. K., J. A. Hodgeson, L. F. Ballard, and C. E. Decker. Ratio of Sulfur Dioxide to Total Gaseous Sulfur Compounds and Ozone to Total Oxidants in the Los Angeles Atmosphere — An Instrument Evaluation Study. Determination of Air Quality, G. Mamantov and W. O. Shults, eds., Plenum Publishing Co., New York, 1972.

3. Stevens, R. K., T. A. Clark, C. E. Decker, and L. F. Ballard. Field Performance Characteristics of Advanced Monitors for Oxides of Nitrogen, Ozone, Sulfur Dioxide, Carbon Monoxide, Methane, and Nonmethane Hydrocarbons. APCA Meeting, Miami, Florida, June 1972.

4. Jacobson, J. S. and G. D. Salottolo. Photochemical Oxidants in the New York-New Jersey Metropolitan Area. Atmos. Env. 9, 1975, pp. 321-322.

5. U. S. Environmental Protection Agency. National Primary and Secondary Air Quality Standards, Federal Register 36, 1971, pp. 8186-8201.

6. Brown, R. M., G. Wolff, and J. A. Spatola. Results of the Cooperative Ozone Calibration. Environmental Protection Agency Region II, Edison, New Jersey, July 21, 1974.

7. Hodgeson, J. A., R. K. Stevens, and B. E. Martin. A Stable Ozone Source Applicable as a Secondary Standard for Calibration of Atmospheric Monitors. ISA Transactions, II, No. 2, 1972, pp. 161-167.

8. Nehls, G. J. and G. G. Akland. Procedures for Handling Aerometric Data. J. Air. Poll. Control Assoc., 23, 1973, pp. 180-184.

9. Gnanadesikan, R., and J. R. Kettenring. Robust Estimates, Residuals, and Outlier Detection with Multiresponse Data. Biometrics, 28, 1972, pp. 81-124.

10. Kempthorne, O. and L. Folks. Probability, Statistics, and Data Analysis. Iowa State University Press, 1971, pp. 220-221.

11. Bruntz, S. M., W. S. Cleveland, T. E. Graedel, B. Kleiner, and J. L. Warner. Ozone Concentrations in New Jersey and New York: Statistical Association with Related Variables. Science 186, October 18, 1974, pp. 257-259.

12. Wilk, M. B. and R. Gnanadesikan. Probability Plotting Methods for the Analysis of Data. Biometrika, 55, 1968. pp. 1-17.

13. Cleveland, W. S., T. E. Graedel, B. Kleiner, and J. L. Warner. Sunday and Workday Variations in Photochemical Air Pollutants in New Jersey and New York. Science, 186, December 13, 1974. pp. 1037-1038.

14. Graedel, T. E., and L. A. Farrow. Ozone: Involvement in Atmospheric Chemistry and Meteorology. Ozone Chemistry and Technology. Franklin Institute Research Laboratories, Philadelphia, 1975.

15. Wolff, G., W. Stasiuk, P. Coffey, and R. Pasceri. Aerial Ozone Measurements Over New Jersey, New York, and Connecticut, presented at APCA Annual Meeting, Boston, 1975.

16. Cleveland, W. S., B. Kleiner, J. E. McRae, and J. L. Warner. Photochemical Air Pollution: Transport from the New York City Area into Connecticut and Massachusetts. Science, 19, 1976. pp. 179-181.

17. Cleveland, W. S., B. Kleiner, J. E. McRae, and J. L. Warner. The Analysis of Ground-Level Ozone Data from New Jersey, New York, Connecticut, and Massachusetts: Transport from the New York City Metropolitan Area. Proceedings of the Fourth symposium on Statistics and the Environment. American Statistical Association, Washington, D. C., 1976.

18. Altshuller, A. P. Evaluation of Oxidant Results at CAMP Sites in the United States. J. Air. Pollut. Control Assoc., 25, 1975. pp. 19-24.

19. Tiao, G. C., G. E. P. Box, and W. J. Hamming. Analysis of Los Angeles Photochemical Smog Data: A Statistical Overview. J. Air. Pollut. Control Assoc., 25, 1975. pp. 260-268.

CHEMICAL AND METEOROLOGICAL ANALYSIS OF THE MESOSCALE VARIABILITY OF OZONE CONCENTRATIONS OVER A SIX-DAY PERIOD

W. D. Bach, Jr., J. E. Sickles, II, R. Denyszyn and W. C. Eaton*

ABSTRACT

The Research Triangle Institute conducted low altitude aircraft flights over east Texas, most of Louisiana, and adjacent areas of the Gulf of Mexico to investigate the areal extent of high ozone concentrations. Ozone concentrations were continuously measured along the flight paths and at ground stations at Corpus Christi, Port O'Connor, Austin, Houston, and Port Arthur, Texas and at DeRidder, Louisiana.

On October 19, 1975, a high pressure system developed over the area and subsiding motion began to develop a stable layer of air aloft. Ozone concentrations in excess of 160 μg/m³ were found over east Texas and over western Louisiana. As the pressure system developed and moved eastward the next day, the highest ozone was measured over western Louisiana. Ozone concentrations remained above 160 μg/m³ at 300 meters over the Gulf of Mexico and inland, but decreased to 110 μg/m³ above the stable layer. Ozone measurements at the ground monitoring locations agreed with the trends of the airborne measurements.

Air parcel trajectories arriving at ground stations or at significant points along the flight tracks were computed to describe the horizontal motion of the atmospheric boundary layer. Time-altitude cross sections of potential temperature at Lake Charles, Louisiana, showed a dynamic atmospheric boundary layer.

The occurrences of high ozone concentrations and ozone gradients within this episode were examined considering the ozone precursor emissions and the meteorological situation. Ozone precursor emissions in the study area and limited ventilation are primarily responsible for maintaining the high ozone concentrations until cleaner air is transported into the region.

INTRODUCTION

Until about ten years ago, ozone (O_3), a principal constituent of photochemical smog, was thought to occur in high concentrations only in urban areas where the precursor materials – hydrocarbons (HC) and oxides of nitrogen (NO_x) – were abundant in automotive exhaust. Nonurban ozone concentrations typically ranged from 40 to 120 μg/m³, below the present National Ambient Air Quality

*Research Triangle Institute, Research Triangle Park, North Carolina.

Standard (NAAQS) of 160 $\mu g/m^3$ (1). Recent measurements have shown that ozone concentrations frequently exceed the NAAQS at numerous nonurban locations in different parts of the United States (2-5). In most instances, the evidence indicates that horizontal transport of ozone and the in situ generation/destruction cycle of ozone are primary contributors to the high concentrations.

Hydrocarbon emission densitites in several counties along the northern Gulf Coast are in the 95th to 98th percentile of all counties in the United States, due in large to the petrochemical industry of the area (6). The abundance of hydrocarbons in the atmosphere suggests that generation of photochemical oxidants may be a problem in and downwind of the urban industrial centers.

In studies conducted by the Texas Air Control Board (7-9), hourly ozone concentrations greater than 160 $\mu g/m^3$ were measured in nonurban areas of east and southeast Texas and along the coast of the Gulf of Mexico. High ozone concentrations were found upwind of urban areas, in onshore flow from the Gulf of Mexico, and in pine forests a hundred miles or more from the principal hydrocarbon emissions areas. Neither the spatial extent of the region of high ozone concentration nor the sources of high ozone concentrations were determined.

In response to the Environmental Protection Agency's interest in developing strategies to control urban oxidants including ozone, the Research Triangle Institute conducted a field program of surface and airborne measurements to investigate and document the occurrences and the areal extent of regions of high ozone concentration in the northern Gulf Coast area of Texas and Louisiana. The program began June 25 and continued through October 31, 1975.

This analysis considers one episode of high ozone concentration at the ground and aloft that shows a strong dependence of the observed ozone concentrations upon slowly changing meteorological conditions. Some of the measured concentrations are not identified with urban precursors and may represent a natural event, further complicating the problems of oxidant control.

DATA ACQUISITION AND ANALYSES

GROUND STATION MEASUREMENTS

RTI established a base station at the Beauregard Parrish Airport, DeRidder, Louisiana, a nonurban location 50 miles north of Lake Charles. Ozone, oxides of nitrogen, sulfur dioxide, and total suspended particulate (TSP) were continuously monitored. Grab samples were taken for later analysis of selected hydrocarbon and halocarbon species. The Texas Air Control Board provided hourly ozone data measured at their Nederland (Port Arthur-Beaumont), Houston (Aldine), Austin, and Corpus Christi, Texas locations. These locations are generally considered more urban-industrial than nonurban since they are near large hydrocarbon emission areas (Figure 1). Ozone measurements at Port O'Connor, Texas, were provided by the DuPont Company. All of these locations were routinely audited by EPA and RTI as a part of an independent quality assurance program.

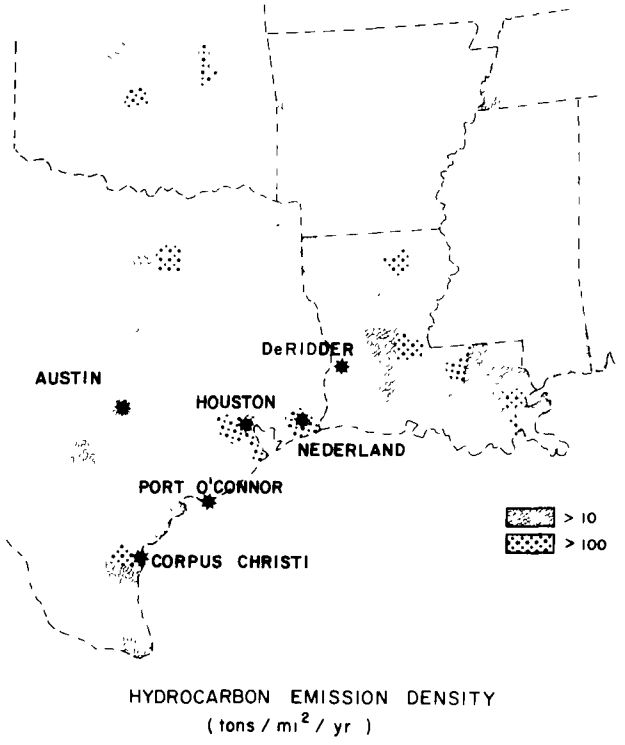

Figure 1. Hydrocarbon emission density by county.

AIRCRAFT MEASUREMENTS

RTI operated a twin engine aircraft from the DeRidder base station. The ozone, oxides of nitrogen, air temperature, and dewpoint temperature were continuously monitored and the data digitized at 30-second intervals. Similar measurements were made aboard the EPA B-26 research aircraft. These aircraft provided spatial coverage unavailable from any other source.

Flight plans were designed to investigate specific problems of the Gulf Coast area, including a pair of areal survey flights. The survey flights were conducted on successive days when similar meteorological conditions were expected. Additional flights were designed during the field program to investigate specific situations that developed or were indicated by meteorological conditions or air quality data. Flight protocols called for a low pass over the DeRidder ground station after takeoff and again before landing to cross-check the aircraft and ground-based measurements. When directed, the aircraft were used to obtain vertical profile data in 1000 to 2000 feet vertical increments during both ascent and descent over a given location.

AIR PARCEL TRAJECTORIES ANALYSES

Approximate trajectories were computed for air parcels arriving at selected positions along the flight track when the aircraft was in the vicinity. Those computations used 12-hourly wind data from the regular rawinsonde network, averaged vertically over the lowest 2 km of the atmosphere. Parcel displacements were integrated at 2-hour intervals over a 48-hour period to give the trajectories.

CROSS SECTION ANALYSES

Time-altitude cross sections of potential temperature, θ, and the southerly wind component, v, were developed for the Lake Charles rawinsonde location, which is typical of the conditions in the coastal area during the period. Potential temperature is conserved in adiabatic processes, and it is a good indicator of atmospheric changes. Descending θ-isopleths with increasing time indicate descending motion and/or advection of cooler air. Furthermore, as the vertical gradient of θ increases, atmospheric stability increases, and the vertical mass transfer is inhibited.

FLIGHT ANALYSES

Altitude corrections were applied to airborne ozone measurements in accordance with test results in the EPA-Las Vegas Environmental Test Chamber. The corrected ozone data showed excellent continuity of trends at 2-minute intervals, so the concentrations at 10-minute intervals along the flight track were plotted. Concentrations of oxides of nitrogen were seldom above the detectability of the chemiluminescent instruments, so those numerical data were of little value.

CASE STUDY

OVERVIEW

On October 16, a tropical storm moved inland about 150 miles east of De Ridder. Over the next two days a ridge of high pressure moved southeastward causing clearing skies, cooler temperatures, and a northwesterly flow of air. By the evening of October 18, the ridge had expanded and covered much of the coastal area. The atmosphere at Lake Charles was well-mixed to approximately 1.7 km (Figure 2). Above that, a large-scale subsiding motion associated with the ridge had begun to develop a stable layer. An anticyclonic circulation pattern of a high pressure system began to develop on the morning of October 19. The subsidence continued, lowering the mixing height and inversion layer to 1.0 km on the morning of October 21. Thereafter, the subsidence diminished and warmer air returned with a southerly flow. The stable layer began to rise, but its intensity did not diminish until the afternoon of October 22. By the morning of October 23, the stable layer was effectively broken and vertical mixing was no longer confined. This sequence of events is typical of transient anticyclonic systems.

During this period the maximum afternoon hourly ozone concentrations were generally high at urban and nonurban locations until the high pressure ridge or center passed eastward (Table 1). Thereafter, the afternoon ozone concentrations

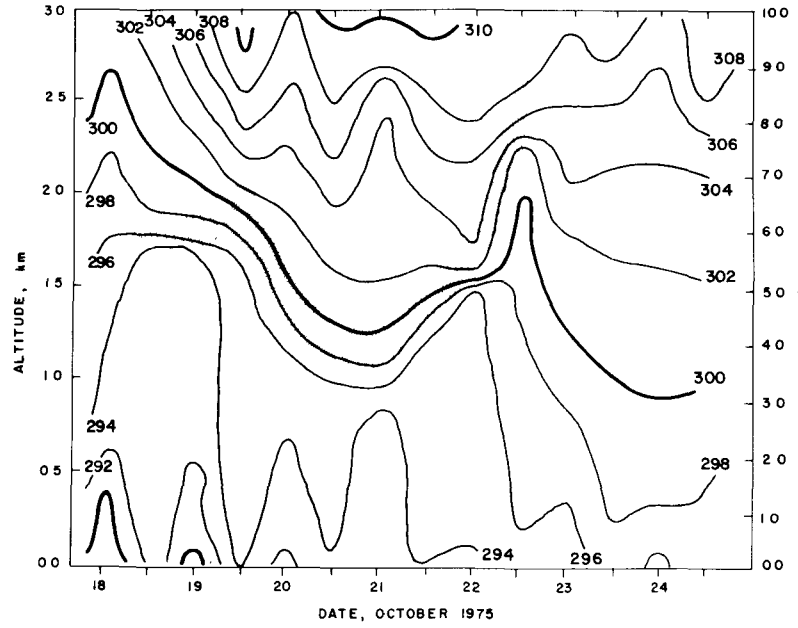

Figure 2. Time-altitude cross section of potential temperature at Lake Charles, Louisiana. Temperature inversion is stippled.

TABLE 1. MAXIMUM AFTERNOON OZONE CONCENTRATIONS ($\mu g/m^3$)

Location	October 18	19	20	21	22	23	24
Corpus Christi	112	224	140	112	88	64	50
Port O'Connor	106	151	133	98	76	22	30
Austin	128	154	156	124	108	88	62
Houston	M*	M	136	138	90	84	64
Nederland	M	M	156	182	120	78	60
DeRidder	109	122	256	210	76	22	30

*Missing Data

were perceptably lower as the onshore, well-mixed flow developed and prevailed. An eastward migration of higher ozone concentrations with the pressure system is also apparent.

The concentrations measured at Corpus Christi and Port O'Connor on October 19, at Austin on October 19 and 20, and at DeRidder on October 20 and 21, are among the highest recorded at those locations during the study period.

OCTOBER 19

On the morning of October 19, a weak high pressure center developed within the ridge in southeastern Texas and western Louisiana. The western half of a 2-day survey flight was initiated to investigate the gradient of ozone which might occur with the predominently northerly flow of air. By mid-afternoon, the high pressure center was located to the south-southeast of Lake Charles, but the pressure gradient was weak.

Air flow in the mixed layer had been northerly and was turning westerly during the day (Figure 3). The predominance of a northerly flow even in a developing anticyclone indicates an unusual situation. Anticyclonically-curved trajectories are expected with the transient high pressure system. These trajectories had cyclonic curvature, suggesting that the high pressure system was being formed and had only recently begun to establish its influence in the flow regime.

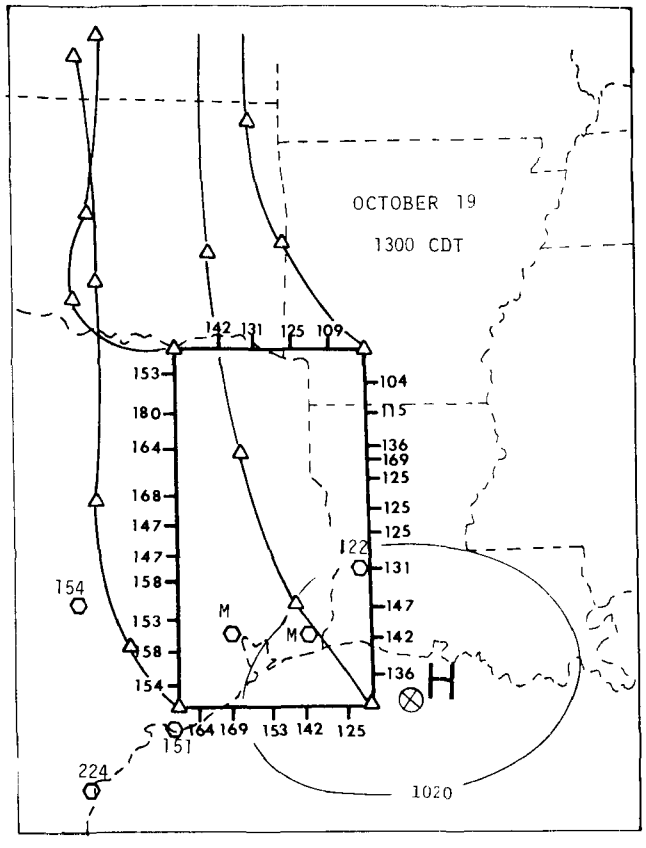

Figure 3. Ozone concentrations along flight track (—⊥—), the daily maximum of hourly ozone concentrations (⬡), air parcel trajectories with 12-hour positions (—△—), and surface pressure isobars (———) for October 19, 1975.

The flight began at 1000 CDT, proceeded clockwise around the rectangular pattern at 650 m (∿2000 ft MSL) before returning to DeRidder at 1700 CDT. All measurements were made within the well-mixed boundary layer, capped by the inversion layer.

Ozone concentrations measured during the eastern half of the flight were of the order of 130 $\mu g/m^3$, while in the western half, concentrations were mostly at or above the NAAQS. Cleraly, the western half of the flight shows an area-type distribution rather than a plume-type distribution of ozone developing from a localized source of precursors.

The substantial decrease of ozone from the northwest to the northeast corner of the flight does not seem related to hydrocarbon source areas along those trajectories. The air arriving in the northwestern corner had a path roughly over the Oklahoma City area 24 to 36 hours before the aircraft reached this point. The air arriving in the northeastern corner passed over the Tulsa, Oklahoma, area, also an oil refining area, 24 hours before. On the southbound leg of the flight, the aircraft apparently passed through a narrow plume southwest of the Shreveport, Louisiana, area and measured ozone concentrations as high as 169 $\mu g/m^3$ for a brief period.

Upon return to DeRidder, the ozone concentrations and their gradients were quite similar to those measured upon departure 7 hours previously. This suggests that the ozone existed in a quasi-steady state in the afternoon boundary layer. The higher ozone concentration of east Texas are not associated with specific ozone precursor source regions. The urban-industrial regions make no discernable contribution to those concentrations.

OCTOBER 20

By the afternoon of October 20, the high pressure center had moved to a position just north of Mobile, Alabama. Central pressures increased to 1023 mb as the circulation system developed. A high pressure ridge extended southeastward from the high center to the south of the flight area. For the previous 24 hours, southerly winds were reported at all of the ground monitoring stations. Further away from the high pressure center more air movement had occurred at Austin and Houston than at DeRidder and Nederland.

Of the ground stations, only DeRidder (256 $\mu g/m^3$) showed ozone concentrations above NAAQS. Surface trajectories showed that air arriving at DeRidder in the late afternoon had been in transit from the Nederland area for the past 24 hours. Concentrations measured at DeRidder were among the highest encountered.

The eastern portion of the area survey blocks was flown at 650 m ($\sim$2000 feet) counterclockwise along the path (Figure 4). The subsidence inversion covered the Gulf Coastal plain from southern Texas to central Alabama. Consequently, vertical motion probably was restricted to 1.5 km ($\sim$5000 feet) or less but above flight level. The area coverage was reduced from the previous day for operational reasons.

Ozone concentrations near 160 $\mu g/m^3$ were encountered on all legs of the flight and were persistent in the northern, western, and southern portions of the flight. Again, eastern portions of the flight were lower than the other portions, but were higher by about 30 $\mu g/m^3$ than on the previous day. Concentrations and concentration gradients over 4-hour intervals at DeRidder were continuous.

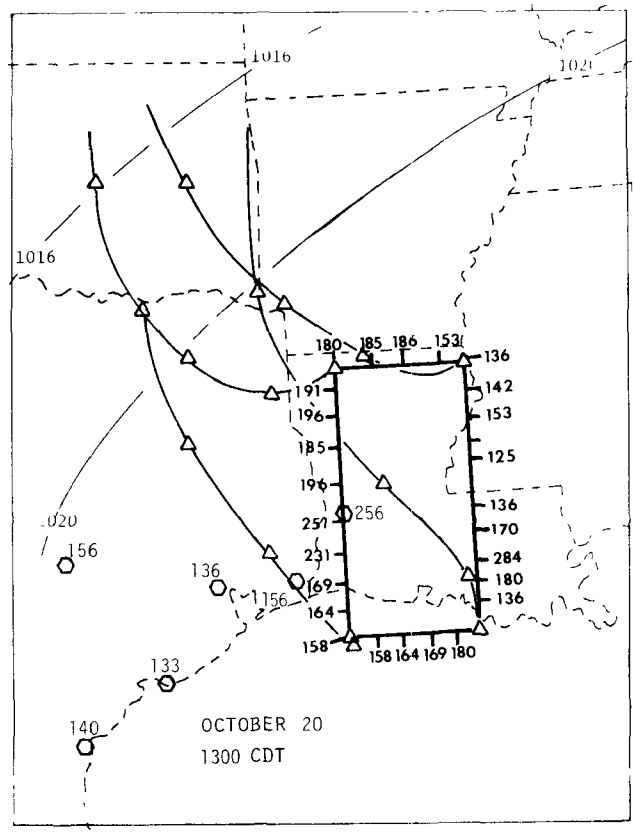

Figure 4. Ozone concentrations along flight track (——┴——), the daily maximum of hourly ozone concentrations (⬡), air parcel trajectories with 12-hour positions (——△——), and surface pressure isobars (———) for October 20, 1975.

High ozone concentrations persisted during the period of north and westerly flow across areas of low emission densities. The influence of precursor emission areas is not apparent. Since flights remained below the subsidence inversion, downward transport of ozone into the boundary layer is unlikely. The air parcels arriving in the northeastern corner of the flight suggests an increase of concentration with time. Twenty-four hours previously the parcel was near the Arkansas-Louisiana border, roughly in the area where ozone concentrations on the order of 110 $\mu g/m^3$ were sampled. At flight altitude 24 hours later, concentration on the order of 145 $\mu g/m^3$ were encountered. Air parcels arriving in the northwestern corner on this evening came from areas of east Texas where ozone concentrations were about equal to the NAAQS. Upon arrival, these concentrations increased to about 190 $\mu g/m^3$, an increase of 30 $\mu g/m^3$.

In the southwestern corner of the flight path, the trajectory shows flow across Nederland to the sample point where it had remained nearly stagnant for about 12 hours. Ozone concentrations at flight level were just below the NAAQS but were the lowest measured during this part of the flight.

The pattern of high ozone in the western part of the flight and lower in the eastern part persisted. Concentrations were generally higher throughout the flight. The ground stations near the flight area indicate increasing ozone concentrations while Corpus Christi and Port O'Connor indicate a reduction in the maximum concentration as onshore flow returned there.

OCTOBER 21

On October 21, the high pressure center had proceeded further eastward leaving only a ridge line with a northeastward axis. The air had begun to flow northward. The mixing depth of Lake Charles rose from 1.2 km in the morning to 1.45 km in the afternoon. The potential temperature associated with the mixing depth, however, did not change, suggesting that overall ascent of the air was occurring. Measurements of high ozone concentrations on the previous day at DeRidder, and the high concentrations already observed in the afternoon indicated that a flight was necessary. The RTI aircraft left Lake Charles for Nederland then went 160 km south out over the Gulf of Mexico before returning to Lake Charles via Nederland and DeRidder, where a vertical profile was flown (Figure 5).

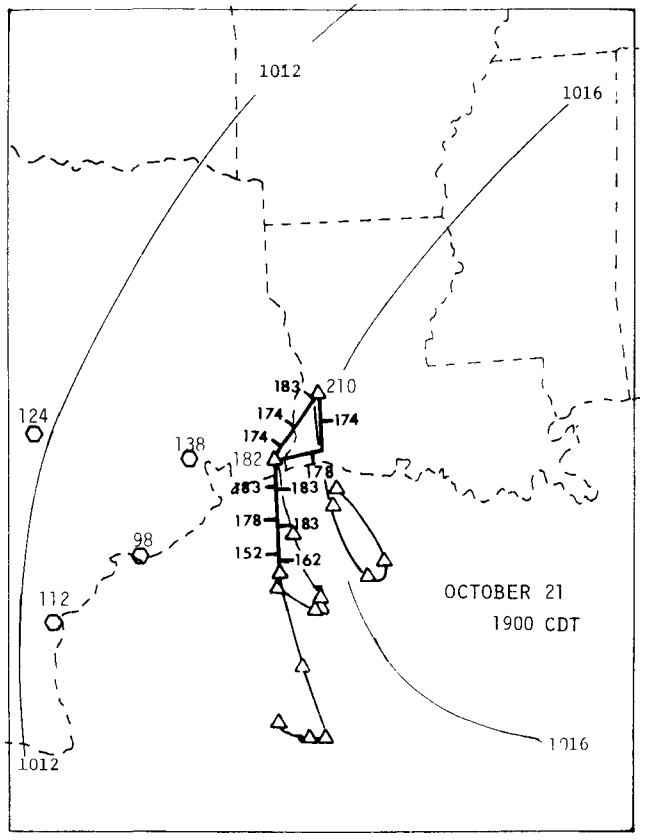

Figure 5. Ozone concentrations along flight track (——⊥——), the daily maximum of hourly ozone concentrations (⬡), air parcel trajectories with 12-hour positions (——△——), and surface pressure isobars (———) for October 21, 1975.

Ozone concentrations exceeded the NAAQS throughout the flight except at the southern tip of the flight, where ozone briefly decreased by about 20 $\mu g/m^3$. The over-water flight was made along the axis of the wind into Nederland outbound at 100 m and returning at 425 m (∿1400 feet). Trajectories suggest that advection of air having lower ozone concentrations into the Nederland area might have been expected within about 12 hours. The ground level concentration in Nederland decreased over the next 12 hours; but probably more in response to local nocturnal ozone destruction than in advection. On the following day,

the maximum ozone concentration was 62 μg/m^3 lower, indicating a change of air mass characteristics.

Trajectories also indicate that the air reaching Nederland had been carried out to sea, approximately 24 hours before a reversal of wind initiated a return flow into the Nederland area. Though initially it might appear that the high ozone concentrations were associated with air flow from the Gulf of Mexico, the trajectories analysis clearly shows that the air is only returning after having passed over land-based sources of ozone and ozone precursors.

In the vertical profile to approximatly 3 km at DeRidder (Figure 6), ozone concentrations increased with altitude to 1.2 km. Above 1.6 km, ozone concentrations decreased and remained constant, thereafter, to the top of the sounding. The ambient temperature decreased with altitude to 1.6 km. Over the next 300 m, the temperature was isothermal and the dewpoint temperature decreased by 11.2°C. During descent, ozone concentrations remained below 110 μg/m^3 above 1.5 km. In the next 300 m of descent, ozone doubled to 216 μg/m^3 and slowly decreased to 178 μg/m^3 in the lowest 300 m of the air. The aircraft temperatures agree closely with the late afternoon soundings taken at Lake Charles. On the return trip from DeRidder to Lake Charles, ozone concentrations also remained above the NAAQS between 300 and 600 m above the ground.

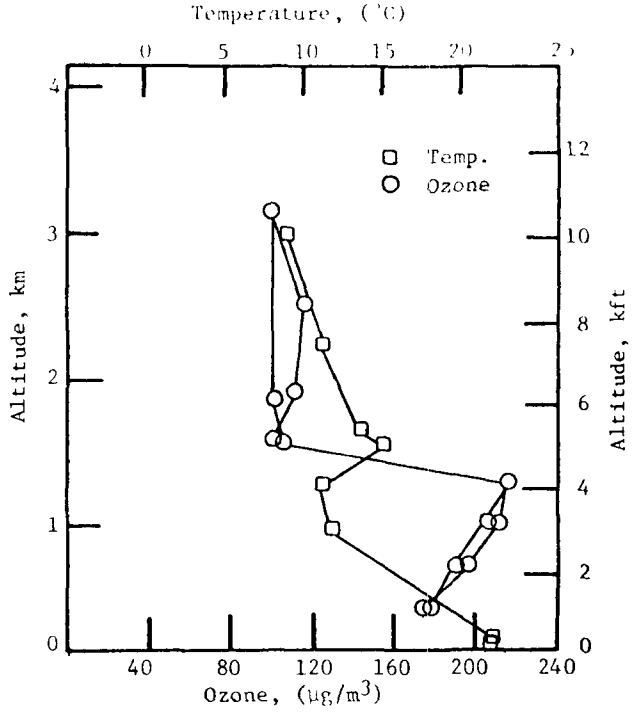

Figure 6. Vertical profiles of ozone and temperature at DeRidder at 1900 CDT October 21, 1975.

On this day, trajectories arriving at Houston and Austin showed a well-developed southerly flow, having been on the side of the high pressure system

for a longer time. Afternoon concentrations in the Houston area were 137 μg/m^3, a fairly low value for that station, and concentrations at Austin had decreased to 124 μg/m^3 from 159 μg/m^3 on the previous day.

OCTOBER 22

By the afternoon of October 22, the influence of the high pressure ridge had weakened through the area. The pressure gradient had increased and a strong onshore flow had developed through all levels of the atmosphere. Ozone concentrations between 99 and 122 μg/m^3 were measured during the EPA aircraft flight with no particular pattern to the concentrations measured (Figure 7). Ground level ozone concentrations at the four stations were comparable to those measured aloft indicating a relatively uniform distribution of ozone in the onshore flow.

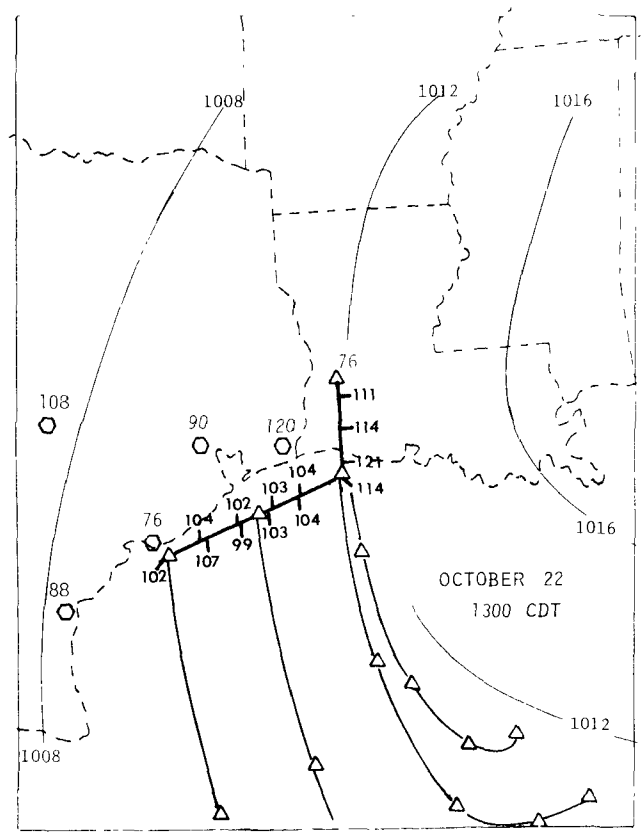

Figure 7. Ozone concentrations along flight track (—|—), the daily maximum of hourly ozone concentrations (⬡), air parcel trajectories with 12-hour positions (—△—), and surface pressure isobars (———) for October 22, 1975.

The air parcel trajectories indicate a long fetch over water preceded by turning from a northeasterly flow into a southeasterly to southerly flow. The ozone concentrations were slightly higher than background concentrations. The turning of the trajectories from a northeastern into a southerly flow suggests that the air might have had an earlier origin over the Gulf Coast region.

Mixing depth increased to about 1.8 km in the morning. By afternoon the stable layer had risen to 2.2 km; but, the afternoon mixing depth reached only about 1.8 km. Warm air associated with the increased onshore flow left a relatively unstable column of air within the mixed layer. The ventilation of the near coastal area had increased substantially and ozone concentrations decreased.

OCTOBER 23, 24

For the next two days, October 23 and 24, strong onshore winds persisted exceeding 10 m/s through most of the first 2 km. The lowest maximum ozone concentrations reported during the measurement program occurred at Nederland and Houston. The increased wind speeds reduced the local residence time of injected ozone precursors, increased the turbulence of the atmosphere giving better dispersion, and probably inhibited development of the oxidant potential on the Texas Gulf Coast.

Ozone concentrations between 68 and 93 $\mu g/m^3$ were measured during an EPA flight on October 24 (Figure 8. These values were consistent with concentrations found onshore at ground measurement stations. The strong southerly flow at this time gave no indication of having had any recent history over any continental areas.

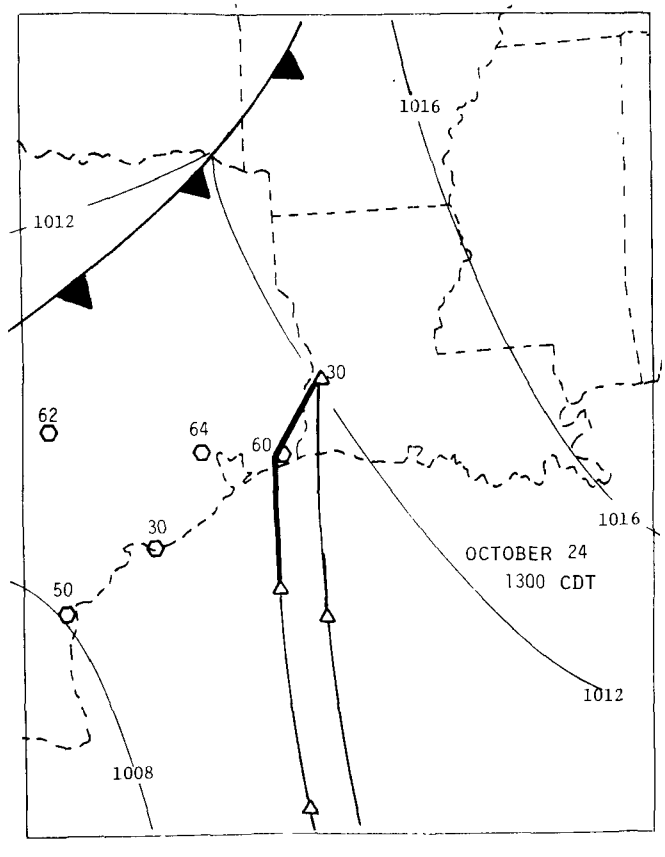

Figure 8. Ozone concentrations along flight track (—|—), the daily maximum of hourly ozone concentrations (⬡), air parcel trajectories with 12-hour positions (—△—), and surface pressure isobars (———) for October 22, 1975.

CONCLUSIONS

The single episode of high, nonurban ozone clearly demonstrates that ozone concentrations exceed the NAAQS and persist for several days over a large ($\sim$50,000 mi^2) area that has a low precursor emission and does not have an identifiable source region. That area apparently expands with increased concentrations and moves with the high pressure cell where vertical mixing is inhibited and horizontal transport is limited.

The local changes of ozone concentrations in the northern Gulf Coast area are strongly affected by transient high pressure systems and the history of the arriving air.

These findings are consistent with findings of other investigations that lead to the concept of a spent photochemical system developing in a slow-moving high pressure cell. Therefore, in at least one case, the same concept applies to the northern Gulf Coast area.

ACKNOWLEDGEMENTS

This research was performed under Contract No. 68-02-2048 with the Office of Air Quality Planning and Standards, Environmental Protection Agency, Research Triangle Park, North Carolina.

DISCLAMER

The opinions expressed herein are those of the authors and are not necessarily those of the sponsoring agency.

REFERENCES

1. Federal Register, National Primary and Secondary Ambient Air Quality Standards, April 30, 1971.

2. Research Triangle Institute, Investigation of Ozone and Ozone Precursor Concentrations at Nonurban Locations in the Eastern United States, Phase I, EPA-450/3-74-034, May 1974.

3. Stasiuk, W. N. and P. E. Coffey, Rural and Urban Ozone Relationships in New York State, JAPCA, 24, 564-568, 1974.

4. Research Triangle Institute. Investigation of Rural Oxidant Levels as Related to Urban Hydrocarbon Control Strategies, EPA-450/3-74-035, March, 1975.

5. Muller, P. R., M. H. McCutchan, H. P. Milligan, Oxidant Air Pollution in the Central Valley, Sierra Nevada Foothills and Mineral King Valley of California, Atmos. Environ., 6:603-633, 1972.

6. Personal Communication from Dr. E. L. Meyer, OAQPS, Environmental Protection Agency.

7. Texas Air Control Board, Yellow Pine Study, 1975.

8. Johnson, D. J., Texas Ambient Air Quality Continuous Monitoring Network, Texas Air Control Board, Air Quality Evaluation Division, 1973.

9. Wallis, R., J. H. Price, G. K. Tannahill, and J. P. Grise, Ozone Concentrations in Rural and Industrial-Urban Cities in Texas, Texas Air Control Board, Air Quality Evaluation Division, 1975.

OZONE AND HYDROCARBON MEASUREMENTS IN RECENT OXIDANT TRANSPORT STUDIES

W. A. Lonneman*

ABSTRACT

In recent years, field studies were undertaken to investigate ozone and ozone-precursor transport. In these studies samples were collected and analyzed for hydrocarbon concentration. The analytical results indicate that rural ambient air downwind of urban centers consists largely of diluted urban mix, with loss of the more reactive hydrocarbon components. Hydrocarbon and nitrogen oxides analyses at Wilmington, Ohio, indicate that high ozone concentrations are probably due to transport processes and are not the result of local photochemical formation.

INTRODUCTION

In recent years field studies were conducted to investigate the extent of ozone (O_3) and O_3-precursor transport downwind of urban areas. These studies were designed to provide better assessment of the oxidant transport problem and to furnish a data base for planning future oxidant control strategies. The study sites were located near large industrial and highly populated areas since the anthropogenic origin of high levels of tropospheric O_3 is expected to be the most significant and the only controllable source.

In 1974, EPA and EPA contractors conducted a study in Ohio. A network of ground sampling sites for O_3 was established, principally in Ohio but also in neighboring states. Some of these sites, mainly those operated by RTI, were equipped with other instrumentation for more detailed pollutant analysis. These other activities included the collection of bag samples for subsequent analyses of detailed hydrocarbons (HC) by the Environmental Sciences Research Laboratory (ESRL) mobile labs. An aircraft was used to follow urban plumes downwind of several metropolitan areas. In addition to O_3 and temperature measurements, the aircraft collected Tedlar bag samples for detailed HC analysis. Clinton County airport, an abandoned U. S. Air Force base, near Wilmington, Ohio, was used as the base station for these studies. The airport had very little air traffic and was ideally situated to sample urban plumes originating from nearby Dayton, Cincinnati, and Columbus. The EPA-ESRL mobile laboratory which was located at this site, measured continuous diurnal profiles of several pollutants. In addition, gas chromatographic analysis of the collected air sample bags was performed for detailed HC composition.

*U.S. Environmental Protection Agency, Research Triangle Park, North Carolina.

In 1975, a similar field study was conducted in the northeast. This study was undertaken in order to explain the high nighttime O_3 concentrations observed at several sampling sites throughout EPA Region I. The northeast area, including New York and New Jersey, represents the most highly populated and industrialized section of the United States. Needless to say, this area provides a critical testing ground for transport phenomena and constitutes the extreme test of present oxidant control strategy. The sampling network included several O_3 sampling sites located throughout EPA Region I. EPA contractors installed and operated additional sampling sites, at Battelle facilities located in Simsbury, Connecticut, and Washington State University located in Groton, Connecticut. The ESRL-EPA laboratory was located south of Boston, Massachusetts. In addition to these ground station laboratories, three aircraft were used to provide more extensive coverage of O_3 and HC precursor concentration, including the transport of urban plumes over the Atlantic.

Detailed reports of the 1974 study are presently available as EPA reports (1, 2). Reports of the 1975 study should be completed in the near future. The purpose of this paper is to present some results from these studies.

EXPERIMENTAL

The instruments employed in the ESRL mobile laboratory are listed in Table I. Calibration procedures were used frequently to ensure the quality of the data collected. Also for quality control, the calibration of the O_3 monitors was checked on a day-to-day basis, often by an audit team.

TABLE 1. MOBILE LABORATORY INSTRUMENT ARRAY

Pollutant/detection objective	Instrument
Nitrogen oxides	TECO 14B
Total hydrocarbon, methane, carbon monoxide	Beckman 6800
Total sulfur	Meloy SA-120
Ozone	Bendix model 8000
PAN	G.C.-Electron capture
Freon-11, carbon tetrachloride	G.C.-Electron capture
Visibility	MRI-Integrating Nepholometer
UV-Visible radiation	Eppley radiometer
Wind speed and direction	Bendix Aerovane system
Temperature and relative humidity	Hydrothermograph

The gas chromatographic procedures for detailed HC analysis are published elsewhere (3). A modification of the published cryogenic trapping procedure was used to concentrate larger air volumes and is graphically illustrated in Figure 1.

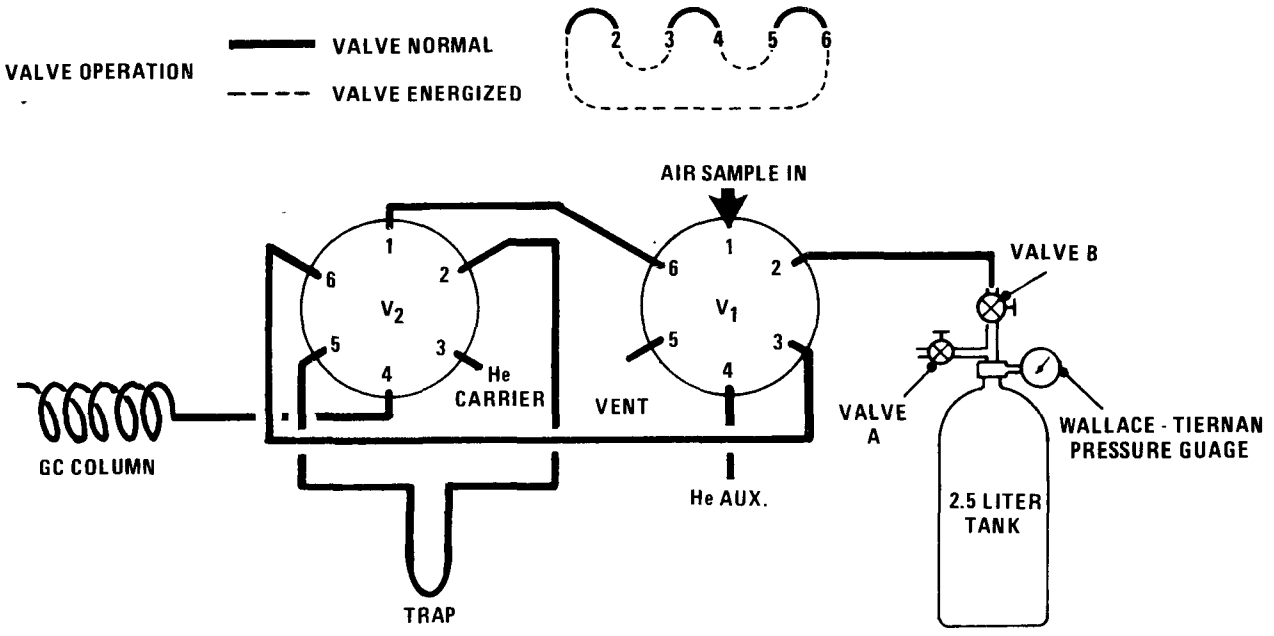

Figure 1. Trapping system.

For HC trapping we used the dual valve system illustrated in Figure 1. The vacuum gauge is a 0-200 torr Wallace-Tiernan gauge. Valve A is connected to a high-speed rotary vacuum pump and is opened to evacuate the 2.5-liter tank to 10-torr pressure (about a 30-second operation). At this point, valve A is closed. A bag sample is connected to port No. 1 of valve V_1. The trap is immersed in liquid O_2. Valve B is opened, and sample from the bag is pulled through the system at a rate of about 150 cm^3/min. When the pressure setting on the vacuum gauge reaches 20 torrs, valve V_1 is energized, routing the air sample into the trap. Samples are collected over a pressure differential of 20-170 torrs. This calculates to be (150/750) (2500 C) or about 500 C of air sample. Therefore, when the pressure on the gauge reaches 170 torrs, valve V_1 is deenergized. To inject the sample, the cyrogen is removed, and valve V_2 is energized. As illustrated in Figure 1, the trapped contents are front flushed onto the column; however, the trap can be easily modified to back flush the trapped contents onto the G.C. column.

RESULTS AND DISCUSSION

The location in Wilmington, Ohio, proposed to be an ideal rural sampling site, since it is surrounded by three major metropolitan areas. The site is downwind of a major city regardless of wind direction. The ground-level HC concentration of Wilmington was determined by collecting 30-minute-to-one-hour integrated bag samples during morning, afternoon, and evening periods. On occasion, 24-hour diurnal studies were conducted for a more complete investigation of HC compositional and concentration variations. This task involved the use of an automated bag sampler to collect 12 2-hour integrated samples.

A comparison of HC between urban and downwind rural areas involves the use of frequency plots of sample concentration versus the number of sample observations. Unfortunately, during these studies, ground-level urban samples were not collected in Cincinnati, Dayton, or Columbus; however, the HC concentration at these sites is expected to be similar to other urban sites sampled in previous studies. Frequency plots for Wilmington and for several urban areas previously studied are given in Figure 2.

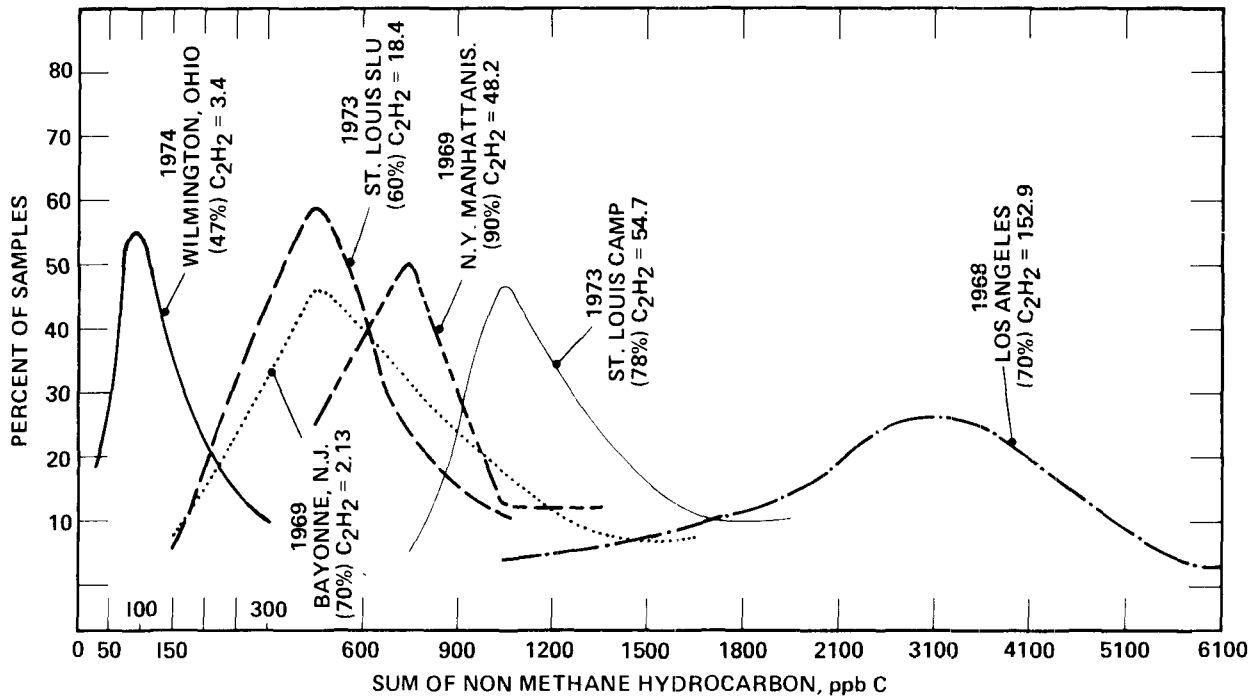

Figure 2. Distribution of the sum of nonmethane hydrocarbons at various sampling sites during the 600-900 a.m. time period.

If plots were available for these Ohio cities, they would probably be similar to that shown for the St. Louis SLU profile, since the size of the St. Louis metropolitan area is comparable to these Ohio cities. The profiles for Wilmington and St. Louis SLU are similar except for an approximate 5-6 fold dilution. A similar dilution factor may be observed by comparing average acetylene concentration between the two sampling sites.

The percentage value given in parenthesis in Figure 2 for each sampling site represents an estimate of total nonmethane HC as vehicular tailpipe emissions. This estimation was established from an average total nonmethane hydrocarbon/acetylene (TNMHC/C_2H_2) factor of 15.5, determined from previous tunnel or roadway samples collected in New York, St. Louis, Denver, and Boston. The value of 15.5 was calculated by averaging published factors of 13.9 for New York tunnels (3) and 15.0 for St. Louis roadways (4), with unpublished values of 16.0 for Denver roadways and 17.0 for Boston tunnel samples. The percentage calculation involved the ratio of the estimated vehicular emissions (average C_2H_2 X 15.5) to the average of the observed TNMHC. The difference between the percentage of vehicular emission and 100 represents HC from other urban HC sources, such as gasoline evaporative, spillage emission and industrial contribution.

No new or unidentified HC peaks, except those resulting from bag outgassing, were observed on our G.C. systems during the analysis of bag samples collected during the study. Naturally emitted HC, such as the C_{10} terpenes, are resolved on our G.C. systems; however, none of these compounds were ever observed, at least at the sensitivity of our instruments (1 ppbC). The frequency distribution plots for these sampling sites were established from as few as 25 sample points and may not be exactly representative; however, a large sample size would probably not significantly change the dimensions of these curves.

The analysis of bag samples collected at McConnelsville (another sampling site operated by RTI during the 1974 Midwest study, located 100 miles east and somewhat north of Wilmington) resulted in a distribution of TNMHC similar to that observed at Wilmington. Typically, the average TNMHC concentrations were higher during the morning hours than during the late afternoon sampling periods. These results are given in Figure 3. This dilution effect between morning and afternoon samples was observed in every urban area previously studied and is likely to be the result of improved vertical mixing resulting from surface heating during afternoon hours.

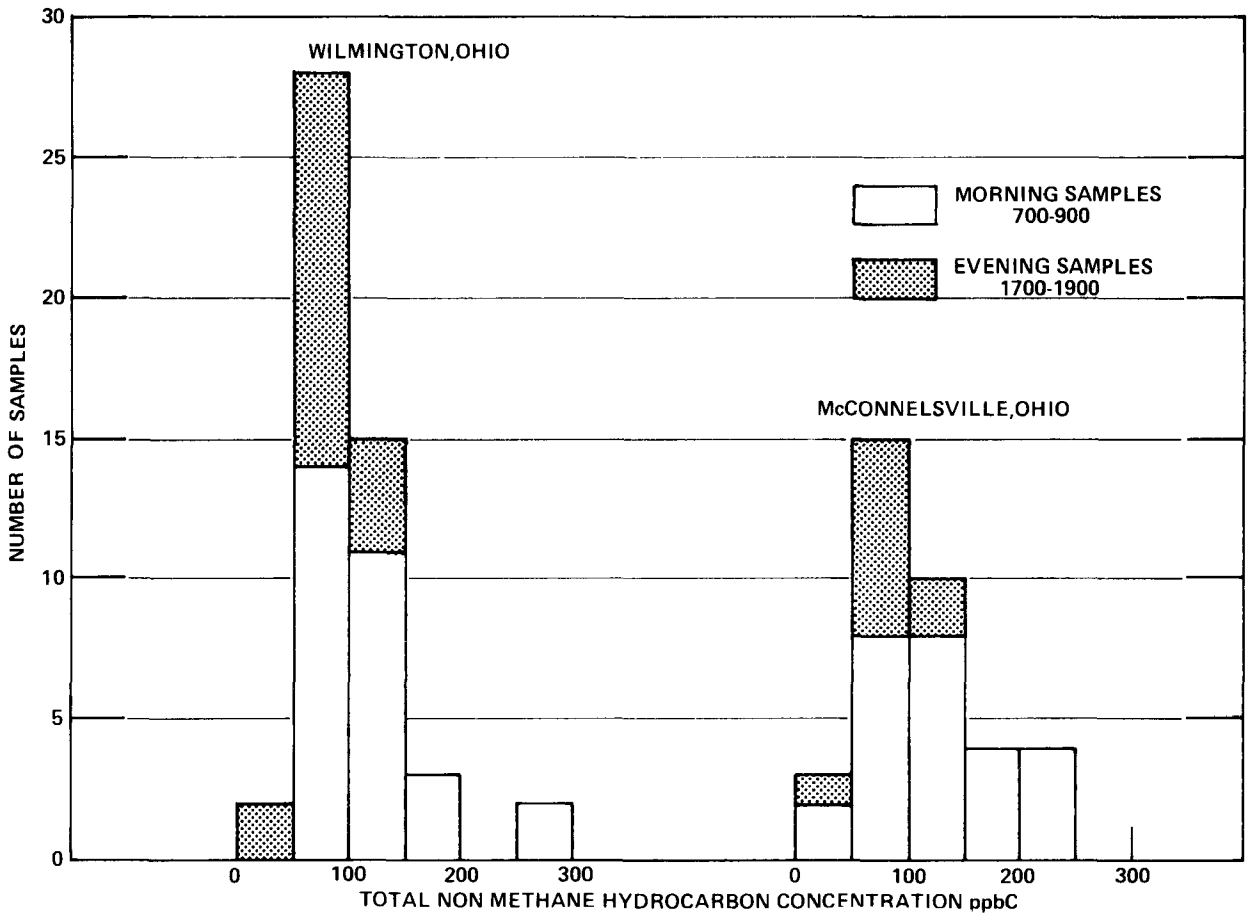

Figure 3. Sum of nonmethane hydrocarbon versus number of samples for two ground sites used in the 1974 Midwest Oxidant Transport Study.

The composition of HC in samples collected at Wilmington and McConnelsville, as well as at other ground sites, and in aircraft samples collected downwind of urban areas generally indicated reduced olefin and aromatic content. Figure 4 illustrates this for total olefin content for a diurnal study of the Wilmington site on July 18, 1974. The dashed line in the figure represents the average olefin content of the TNMHC concentration for 42 samples of less than 10 ppbC C_2H_2 concentration observed at St. Louis, Denver, and New York sampling sites. At each sample period, the sample bag collected at Wilmington during the diurnal study showed lower olefin content. The graph also illustrates reduced olefinic content during afternoon, undoubtedly the result of photochemical activity.

A different illustration of olefin loss is shown in Figure 5. In this figure, the estimated percent of olefin reacted was plotted, versus time. The percent of olefin reacted was determined by ratioing the observed sum of olefin concentration in the sample to the estimated original olefin concentration. The estimated original olefin concentration was determined by a calculation similar to one described earlier for vehicular TNMHC that uses C_2H_2 concentration and an averaged olefin/C_2H_2 factor of 3.4 obtained from tunnel and roadway samples. This calculation indicates that as much as 70 percent of the original olefin concentration has reacted by the late afternoon.

Similar observations, differing in magnitude, were made for other diurnal studies conducted at Wilmington. The results shown in Figures 2, 4, and 5 suggest that the ambient air sampled in Wilmington was a diluted urban HC mix, with associated photochemical loss of the more reactive compounds during the transport process.

It was stated earlier that low araomatic content of the TNMHC was also observed in Wilmington samples. The G.C. elution of these aromatic compounds was interfered with by unknown peaks later identified as outgassing components from Tedlar bag surfaces. These interfering peaks present serious problems for the accurate measurement of aromatic content and is an area we are presently investigating in our laboratories by evaluating alternate air sample containers. These unknown peaks were not included in any of the TNMHC summations. Acetaldehyde and acetone also were peaks identified as outgassing from Tedlar bag surfaces. It is likely that both acetone and acetaldehyde are both components of these rural ambient atmospheres; however, quantitative evaluation of these ambient levels is impossible because of this inconsistant outgassing contribution.

Ozone concentrations at Wilmington often exceeded the National Air Quality Standard of 80 ppb during the late afternoon and evening hours. The late evening levels of ozone suggests transport; however, the possibility that morning levels of TNMHC and nitrogen oxices (NO_X) at Wilmington are responsible for afternoon O_3 concentrations was investigated. Figure 6 shows a plot of morning concentrations of TNMHC and NO_X. The solid line in the figure represents the 0.08 ppm O_3 isopleth, determined by computer simulation of an atmospheric model developed by Dodge (5). The model is based on a mixture of n-butane-propylene-NO_X. The 0.08 ppm isopleth was determined from the worst possible case of limited vertical mixing and no horizontal transport.

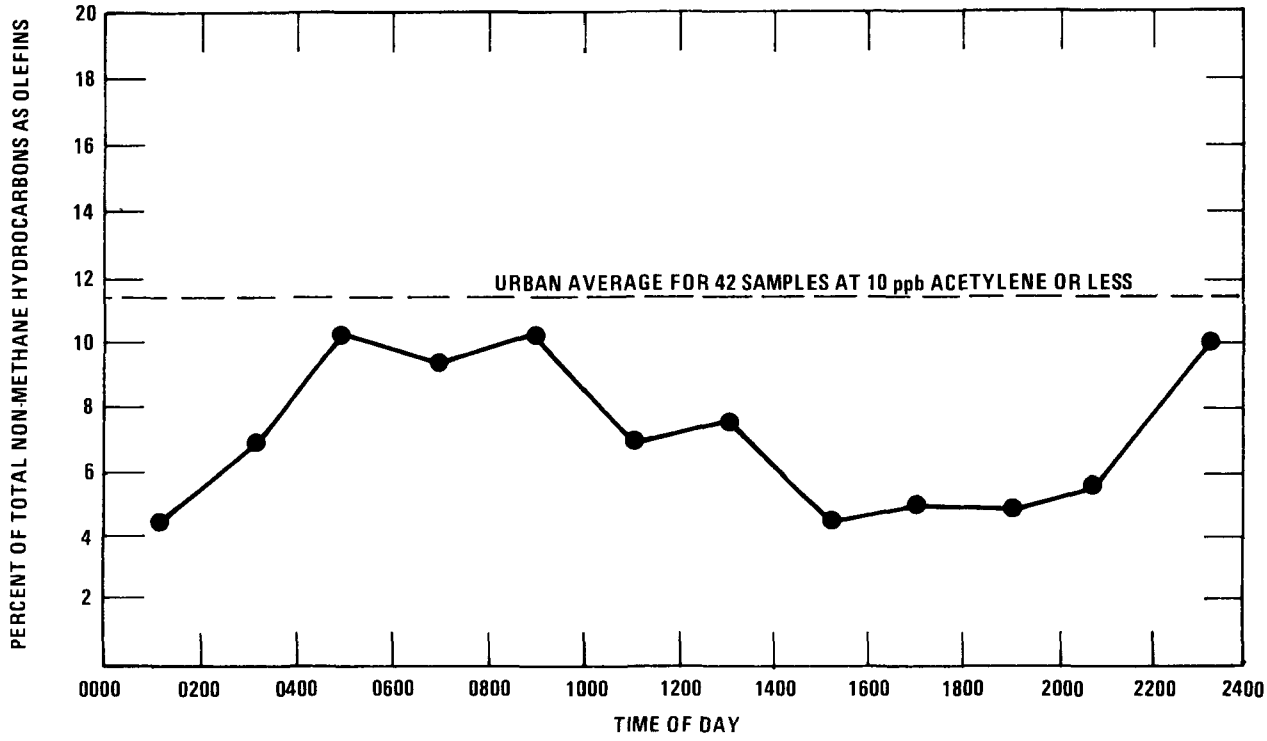

Figure 4. Diurnal variation of average olefinic fraction of total nonmethane hydrocarbon, Wilmington, Ohio, July 18, 1974.

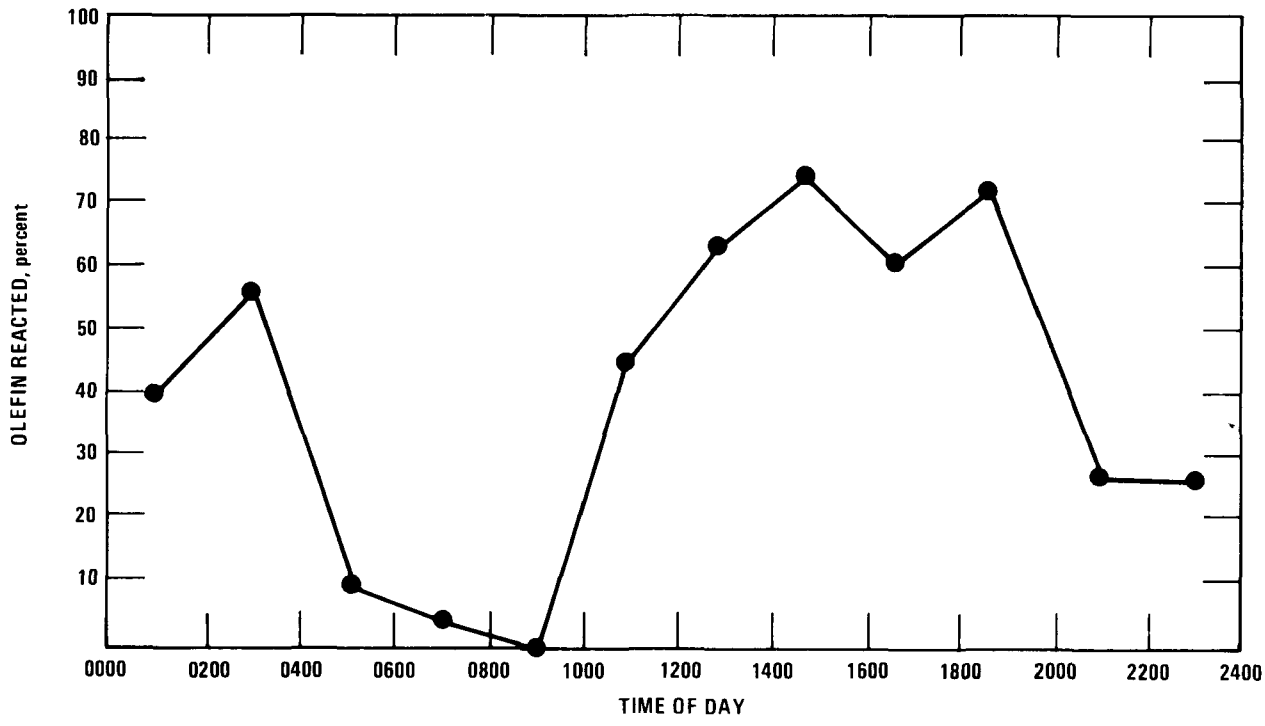

Figure 5. Diurnal variation of the fraction of olefins reacted, Wilmington, Ohio, July 18, 1974.

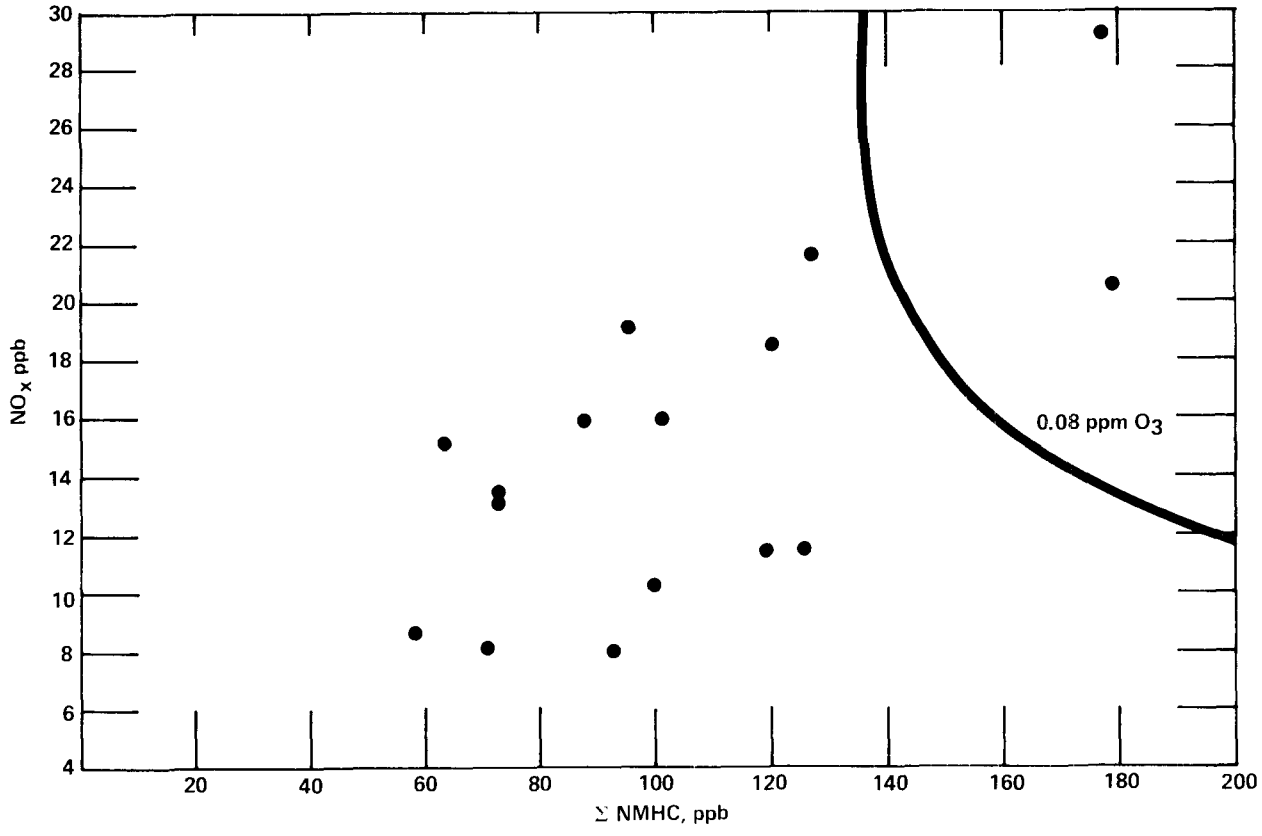

Figure 6. Wilmington, Ohio, 1974 sum of nonmethane hydrocarbon versus NO_x (600-900 a.m.).

Of the 16 data pairs available for the month of August, only two pairs fell on the right-hand side of the 0.08 ppm O_3 isopleths, meaning that these HC and NO_x levels were capable of producing O_3 at or above 0.08 ppm. Ozone maximums observed on these days are shown in Table 2.

TABLE 2. OZONE MAXIMUMS FOR AUGUST, 1974, DAYS WHERE MORNING NMHC AND NO_x CONCENTRATIONS ARE KNOWN IN WILMINGTON, OHIO

DATE	OZONE MAXIMUM, ppb	DATE	OXONE MAXIMUM, ppb
5	63	19	69
6	66	20	93
8	63	21	90
X 9	73	24	94
10	70	25	93
14	77	27	96
16	85	X28	45

The dates of the two data points falling on the right-hand side of the 0.08 ppm isopleth were August 9 and 28. On these two days, the O_3 standard was not exceeded. On 7 of the other 14 days, however, the O_3 standard was either approached or exceeded. These results suggest that local HC and NO_x levels do not account for all local O_3 observed and that a considerable portion of this O_3 is transported from upwind sources.

Other indications of the urban influence on downwind O_3 air quality are shown in Figures 7 and 8. These figures were constructed from aircraft flights upwind and downwind of Columbus. Figure 8 represents a square wave plume flight by RTI downwind of Columbus on July 21, 1974. The acetylene profile was established from bag samples collected along perpendicular paths to the urban plume. The ozone profile was drawn by averaging continuous O_3 concentrations measured along these paths. This figure, demonstrates, in effect, a net 15 to 20 $\mu g/m^3$ increase in O_3 as far as 40 miles downwind of Columbus.

Figure 8 represents a double-box type pattern as flown on July 9, 1974, during very stable atmospheric conditions. The solid line was constructed from C_2H_2 measurements of bag samples collected parallel to wind direction. The dotted line represents C_2H_2 profile constructed from C_2H_2 measurements of bag samples collected at locations perpendicular to the wind direction. On this day, the downwind urban effect on O_3 air quality is even more significant.

Results from the 1975 northeast study also show the effect of transported O_3 and O_3 precursors. The purpose of this study was not to investigate the transport of O_3 from urban to rural sites, but to study the transport of O_3 and its precursors from one urban area into other urban areas. In general, the study was concerned with the implementation of an effective transportation control plan designed to lower the O_3 concentration when the O_3 levels were already high upwind of the urban areas. A complete analysis of the data is not presently available. The ESRL mobile laboratory was located on Chickatawbut Hill, 10 miles south of Boston. Typical profiles of O_3 and other pollutants at the site are shown in Figure 9. Ozone transport is evident by the observation of increasingly high O_3 concentrations during nighttime hours. The evidence for urban origin of this O_3 is a corresponding increase in the concentrations of C_2H_2 and peroxyacetylnitrate (PAN). Similar results were observed on other days.

Aircraft measurements of O_3 and precursor concentrations were made over the eastern coastal regions of Massachusetts. Often, an urban plume containing high levels of O_3 was followed hundreds of miles out over the Atlantic Ocean. In an effort to investigate urban tracer relationships, C_2H_2 and corresponding O_3 data were assembled for comparison. On the basis of an analysis of samples collected over the Atlantic during late afternoons and evenings, there appeared to be a linear relationship between these two pollutants. Linear regression equations were determined for the data of three flights and for all the data points collected during these flights. The results are recorded in Table 3.

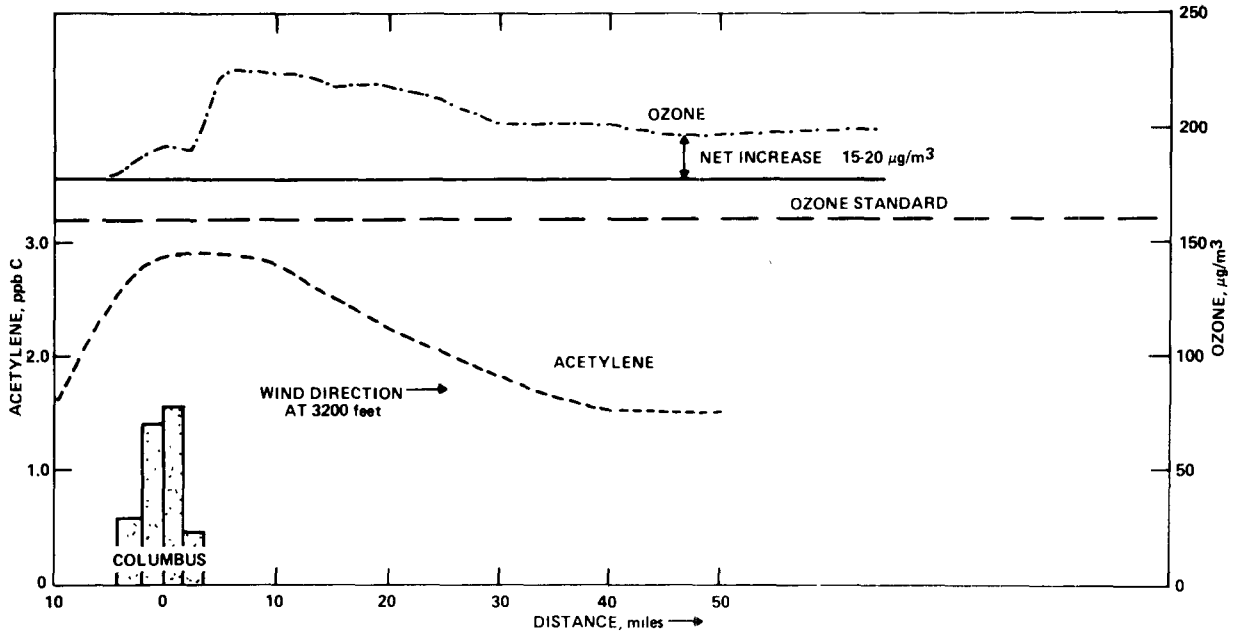

Figure 7. Air flight of 7/21/74, traverse pattern over Columbus, Ohio.

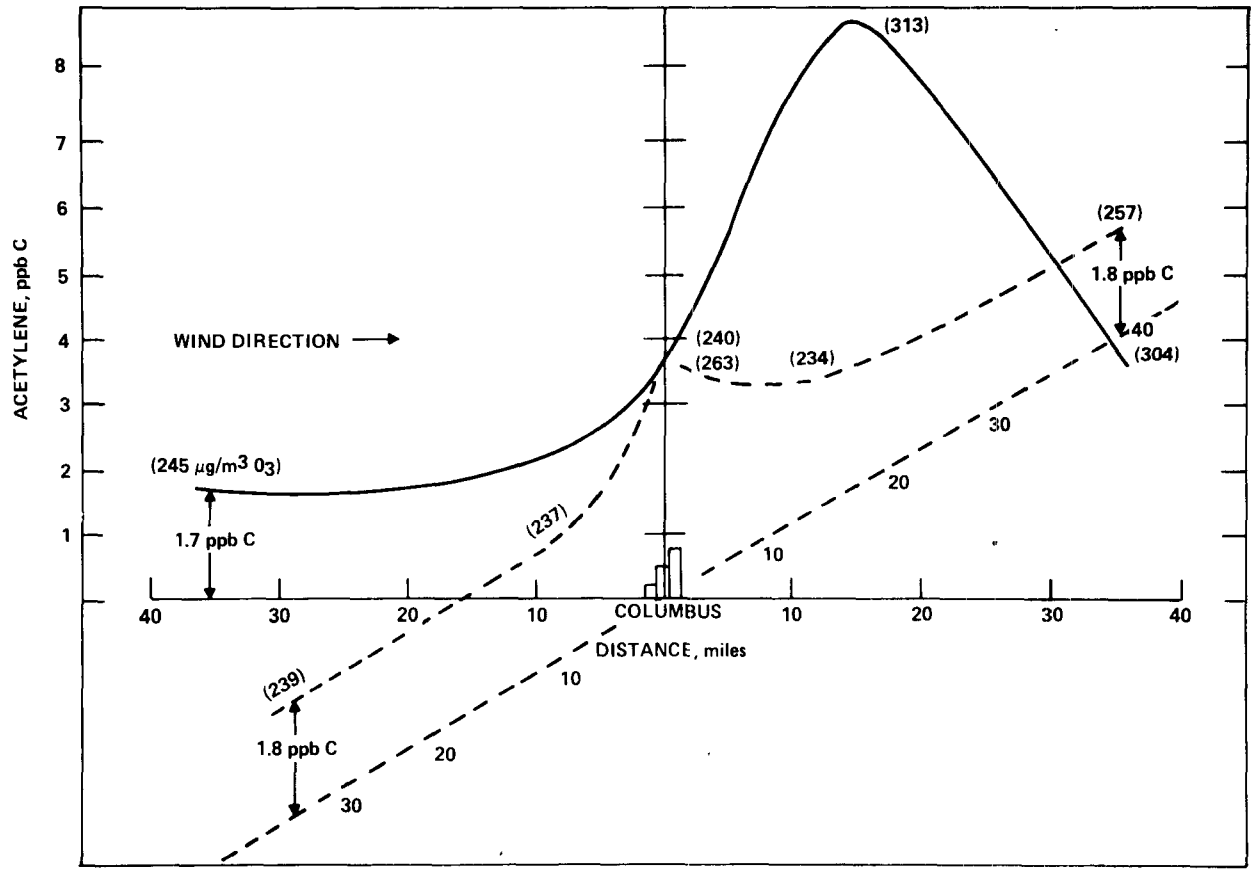

Figure 8. Air flight of 7/9/74, box pattern over Columbus, Ohio.

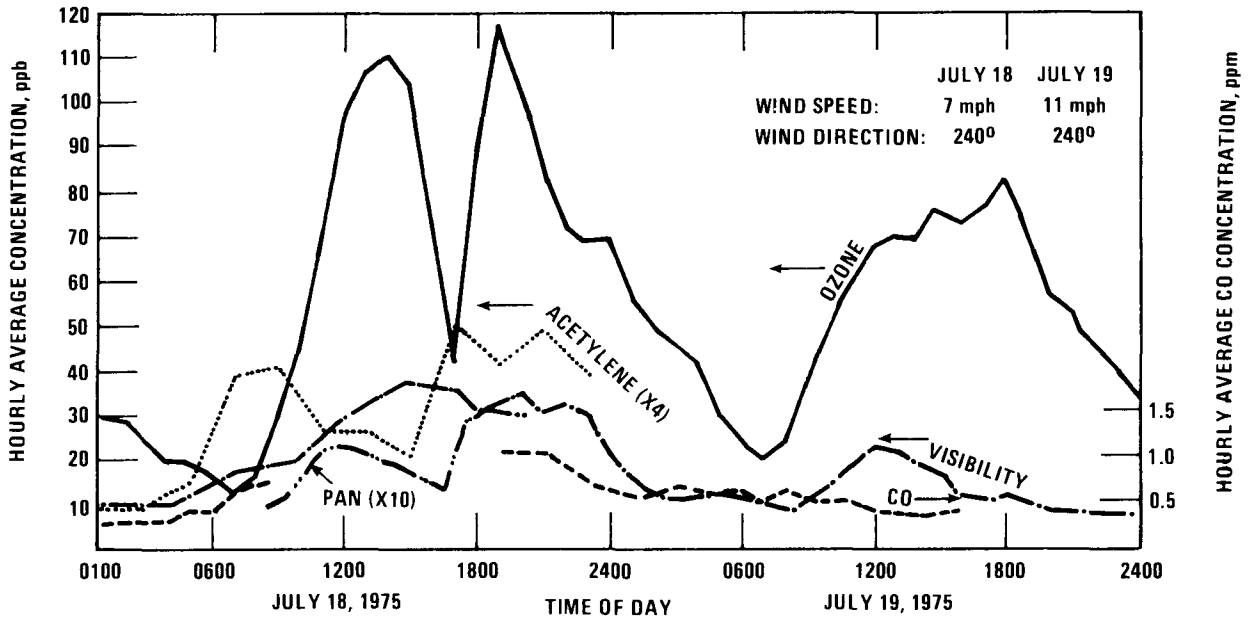

Figure 9. Diurnal hourly concentrations of O_3, CO, acetylene, and visibility, Chikatawbut, July 18 and 19, 1975.

TABLE 3. CORRELATION OF OZONE VERSUS ACETYLENE OFR EPA-LV AIRCRAFT SAMPLES BOSTON OXIDANT STUDY, 1975

Sample Period	Observations	P	Slope	Intercept	O_3 Range ppb	C_2H_2 Range, ppbC
August 14	7	0.91	19.6	46.1	53-186	1.0-7.1
August 20	7	0.95	15.9	38.1	40-69	0.3-1.5
August 27	6	0.94	14.6	32.0	58-99	1.6-2.6
All samples	66	0.85	19.4	31.0	29-186	0.2-7.1

The correlation coefficients between O_3 and C_2H_2 for these data sets are quite high, suggesting a significant relationship. The comparison of slope and intercept for the data sets is quite interesting. A bold interpretation of these results would suggest that the variation of the slope values for these data sets may be the result of variable chemical physical and chemical parameters such as initial concentration of HC and NO_X, HC/NO_X ratios, ambient temperature, and sunlight intensity.

On the other hand, the intercept could represent background O_3 when the C_2H_2 concentration is zero; or, in other words, the vehicular contribution is absent. The O_3 concentration represented by the intercept could be due to natural and industrial sources of HC and NO_X. Caution must be exercised when

making such interpretation. However, the values for the intercepts interestingly compare to background measurements of 30 ppb of ozone made over Maine on August 28, 1976.

In recent months, we have commenced a study of natural HC emissions at a forested area west of Durham, North Carolina. The vegetation at the site consists primarily of loblolly pine and has been used to perform micrometeorological measurements to estimate mass and energy balance. The purpose of our sampling program is to determine the composition of natural HC emissions.

In preliminary studies to determine detailed HC composition, O_3 bag samples were collected at various vertical heights below, within, and above the tree canopy. Additional samples were collected at ground level, upwind and downwind of this forested area. In some bag samples α- and β-pinene at times myrcene and Δ-carene were observed, most frequently in samples collected within or below the tree canopy. In these studies, a maximum of 87 ppbC α-pinene, 19 ppbC β-pinene, 3.3 myrcene, and 4.8 ppbC Δ-carene were observed at ground level, suggesting that perhaps pine needle litter was the principal source. Concurrent O_3 measurements indicated a 40 ppb O_3 level above the tree canopy and 30 ppb O_3 within or below the canopy. The reduced level of O_3 in the canopy suggests O_3 removal by either surface deposition or terpene-ozonolysis mechanisms. Samples collected upwind and downwind of the forested area showed no difference in O_3 concentration and only trace levels of terpene compounds in downwind samples. These studies also suggested that terpene emissions and ambient temperature were directly related.

More recently, simultaneous diurnal studies for HC and O_3 were performed at two vertical heights, one within and one above the tree canopy. The results of these studies are not presently available. Ultimately, we plan to determine vertical fluxes of these terpene hydrocarbons in an effort to evaluate emission strength.

CONCLUSIONS

Field studies conducted in recent years to investigate rural O_3 have indicated that the high levels of O_3 are of anthrophogenic origin, transported from upwind sources. The HC composition at rural Wilmington, Ohio, was similar to the HC composition at urban sampling sites. In fact the HC sampled in these rural areas appeared to be a diluted urban HC mix depleted to some extent of the reactive olefinic hydrocarbons. This loss of olefinic HC was probably the result of photochemical degradation.

Acetylene and corresponding O_3 measurements showed significant correlation in aircraft sampling programs of urban plumes over ocean bodies during the 1975 Northeast Study.

REFERENCES

1. Investigation of Rural Oxidant Levels as Related to Urban Hydrocarbon Control Strategies, U. S. Environmental Protection Agency, Publication EPA-450/3-75-036, 1975.

2. Transport of Oxidant Beyond Urban Areas, U. S. Environmental Protection Agency, Publication EPA-600/3-76-018, 1976.

3. Lonneman, W. A., S. L. Kopczynski, P. E. Dorley, and F. D. Sutterfield, Environ. Sci. Technol. 8, 229, 1974.

4. Kopczynski, S. L., W. A. Lonneman, T. Winfield, and R. Seila, J. Air Poll. Control Assoc., 25, 255 (1975).

5. Dodge, M. Combined Use of Modeling Techniques and Smog Chamber Data to Derive Ozone-Precursors Relationships, these proceedings.

SESSION 6

OZONE/OXIDANT TRANSPORT - I

Chairman: A.P. Altshuller
Environmental Protection Agency

TRANSPORT OF OZONE BY UPPER-LEVEL LAND BREEZE - AN EXAMPLE OF A CITY'S POLLUTED WAKE UPWIND FROM ITS CENTER

E. K. Kauper and B. L. Niemann*

ABSTRACT

A series of aircraft soundings and traverses, measuring ozone and the atmosphere temperature structure between the coastal portions of Los Angeles and Ventura County to the northwest were made during the summer of 1975. Winds aloft were simultaneously obtained, and the movement of upper level ozone layers were deducted by means of trajectory analyses using three-hourly streamline charts. The upper level flow, in the layers containing the ozone maxima, indicated that the ozone was brought over the Ventura County coastline from the Los Angeles Basin, even though surface wind reports, if used in a trajectory analysis, would show that no Los Angeles connection was involved.

INTRODUCTION

Questions regarding the origin of high ozone values in areas of southern California assumed to be upwind of the Los Angeles Metropolitan area have long been asked (1). Answere, using surface wind flow maps, indicate that such occurrences either were due to local sources in the Ventura County area northwest of Los Angeles, or came from off the Pacific Ocean (2). A second path, that through the San Franando Valley to the interior valleys of Ventura County, has also been postulated.

Recently, more detailed analyses of ozone episode cases in Ventura County have suggested the importance of ozone transport aloft and subsequent fumigation to the ground as a causative mechanism (3). However, these analyses have been seriously hampered by lack of wind, temperature and ozone profiles in Ventura County and air mass trajectories of high ozone concentration parcels aloft leaving the Los Angeles area.

To document the three-dimensional situation off the southern California coast, the California Air Resources Board funded a study of the over-water transport of ozone in 1975 from which the data used for this paper were derived (4).

GEOGRAPHICAL AND METEOROLOGICAL SETTING

The project area of concern involved the coastal portion of southern California, between West Los Angeles - Santa Monica and the Ventura County coastline to the north and west of the Los Angeles Basin.

*E. K. Kauper, Metro Monitoring Services, Covina, California.
B. L. Niemann, Teknekron Inc., Berkeley, California.

Flights were conducted during the summer of 1975 under what would be considered typical summer conditions. A marine layer, usually capped by a stratus cloud deck, was present during all operations. The height of the inversion and its strength varied during the study, with high inversions the rule during the June 2-4 study period, moderately low inversions during the period of July 10-11, followed by a period with a deepening marine layer, July 14-18.

EQUIPMENT

The airborne sampling was conducted from a Piper PA28-140, with the temperature and ozone sampling intake located on the left side of the fuselage, away from the engine exhaust outlet.

The sampling line, of 0.6 cm teflon, was kept short (1.2 m) to reduce the possibility of ozone loss due to wall effects. The ozone monitor was a Dasibi 1003AH, factory modified to provide reading update every 13 seconds, recorded on a Hewlett-Packard 680M strip chart recorder.

The ozone sensor, together with the recording system, was calibrated by the California Air Resources Board at its El Monte, California, facility.

Winds aloft were measured by means of optical tracking, using theodolites, of 30 gram pilot balloons. The balloons were inflated to a standard free-lift condition which gave a rate of rise averaging 600 ft/min (3 mps) from the surface to 5000 ft (1.5 km).

OPERATIONS

The aircraft followed the flight path shown in Figure 1, starting from Santa Monica Airport (SMO), climbing to 5000 ft (1525 m) and then descending for a touch-and-go landing at Ventura County Airport, Oxnard (OXR). The return trip to SMO was generally along the coast during good weather (VFR conditions); but when cloud cover required instrument flight, the path was along an inland route shown in Figure 1.

These flights were performed every three hours during the day, with one flight near midnight to monitor the nighttime conditions.

An aircraft observer recorded temperature and altitude information during the climbing and descending phases of the flights, with ozone being recorded continuously throughout the flight.

With the Dasibi instrument obtaining a reading every 13 seconds, the sampling rate in horizontal flight, corresponding to the aircraft's cruising speed of 120 mph, was one sample every 0.4 miles (0.6 km). During climb and descent, the rate of altitude change was 300 feet per minute, giving an ozone reading at 65 ft (20 m) intervals.

Winds aloft were measured at three locations, Los Angeles International Airport (LAX), Point Dume (DUM), and OXR, and were scheduled on the same time basis as the aircraft flights.

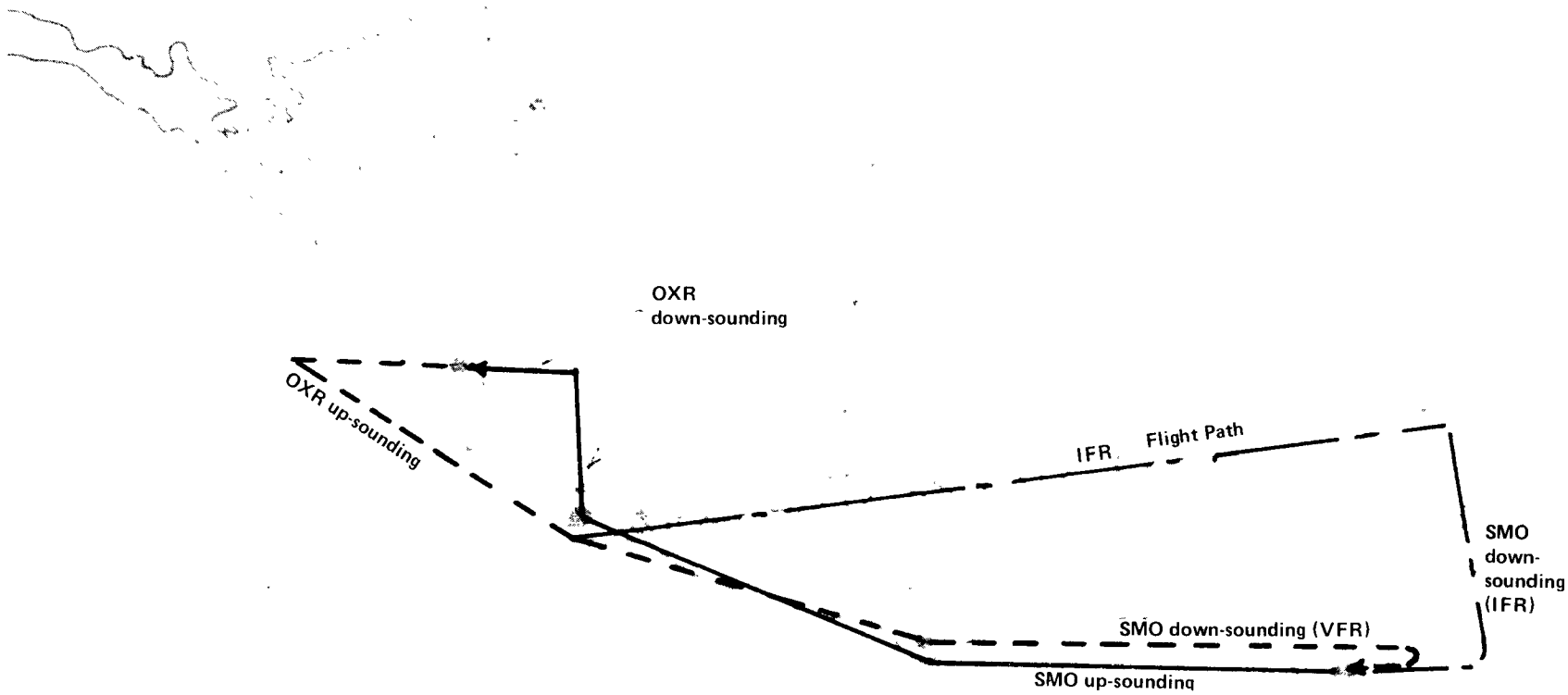

Figure 1. Aircraft flight paths and station location map.

RESULTS

The data obtained by the aircraft and the wind observation stations were plotted as vertical soundings, and placed on vertical cross-sections covering the route from Santa Monica to Oxnard. Figure 2 presents soundings of temperature and ozone at these two locations for a specific time. There is some question regarding the ozone values as recorded between 1000 and 2000 ft over SMO; but the other data points appear to be valid.

Cross sectional analysis of these data indicates that layers of ozone-rich air exist aloft over the coastal route between the Los Angeles Basin and the Ventura County area. These layers are mainly found just above the base of the main subsidence inversion, but also can be located within the stable layer of the inversion itself, as seen in Figure 2.

Trajectory analysis was carried out, using the winds aloft data from the pilot balloon network, plus winds aloft data taken by the Navy at Point Mugu (NTD). Wind flow streamline maps for the various altitudes with the maximum ozone were used in this work. Figure 3 represents the trajectory of the air parcel found over Oxnard with a concentration of 0.45 ppm at 900 ft (0.3 km) when the ozone maximum over Santa Monica was 0.31 ppm, at a similar height.

For comparison, the trajectory taken by a surface air parcel arriving at OXR at the same time as the upper air parcel is also shown in Figure 3. Its track into the coast at OXR from the west is characteristic of trajectories derived from the surface wind reports.

To provide some sort of climatology of upper air flow, trajectories of air containing the maximum ozone aloft over Oxnard were constructed daily for the 1200 PDT time period. Nine such trajectories were prepared, five of which followed a track along the coast between Santa Monica Bay and the Ventura coastline, similar to that shown in Figure 3. Three others were located along a San Fernando Valley - Thousand Oaks path, while only one could not be traced into the Los Angeles source region.

Inspection of the conditions associated with the individual trajectories indicates that the over-water trajectory from Los Angeles is more likely when the marine layer is shallow. The trajectories which indicated movement into Ventura County from the San Fernando Valley were associated with the deeper marine layer conditions.

A similar climatological approach to the ozone concentrations aloft, averaged for the project period, is shown in Figure 4. The ozone values increase aloft during the day over both SMO and OXR, but stay near 0.10 ppm during the night, rather than decreasing to near zero as is the case for surface measurements.

The most frequent winds aloft are shown in Figure 5, again for the project period. It is evident that the easterly winds dominate the flow, especially at levels aloft above the surface. For example at 1200 PDT, while the westerly sea breeze is blowing in the layer between the surface and 1000 ft at LAX and OXR, the flow aloft is easterly. At Point Dume (DUM), midway between the Los

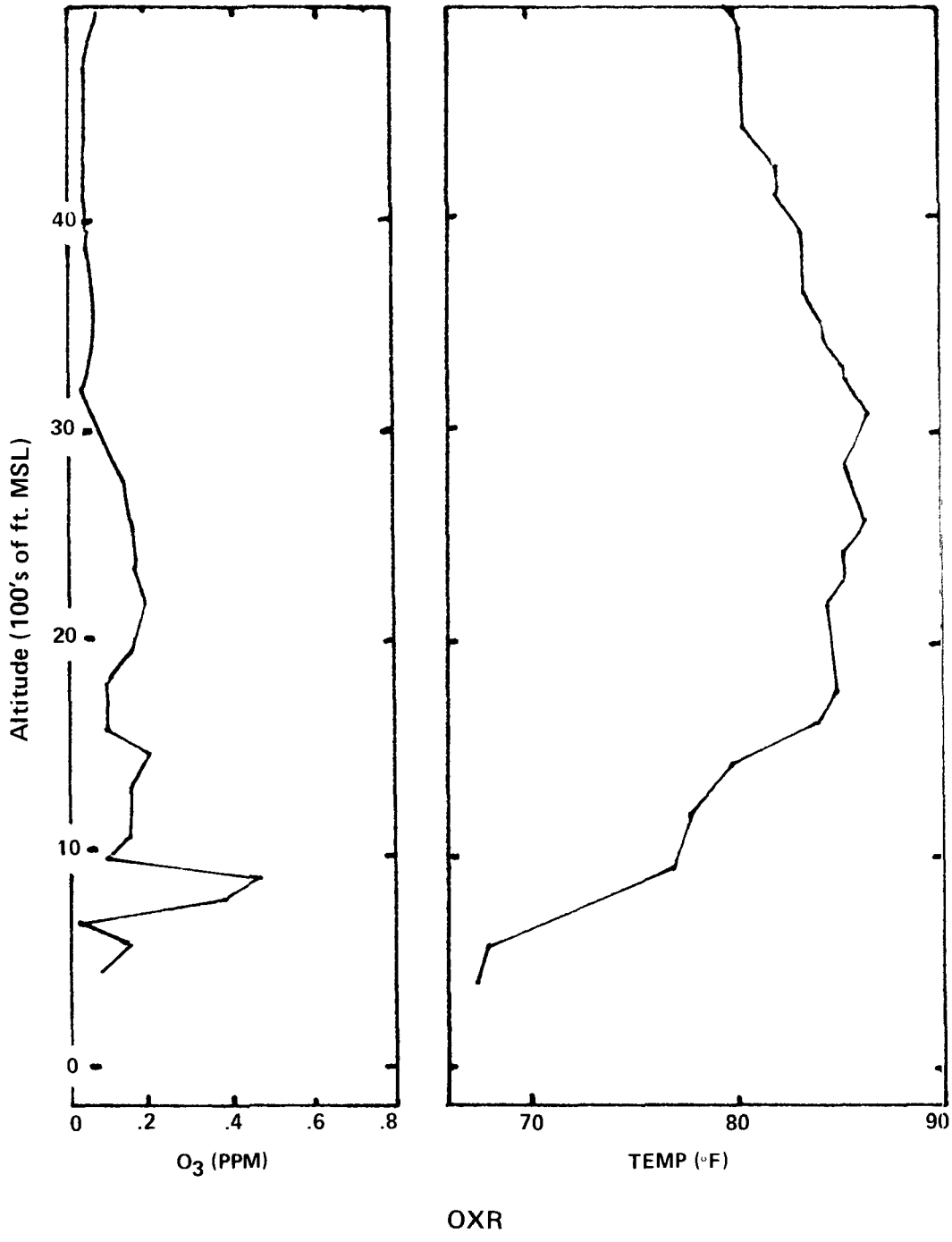

Figure 2a. Temperature and ozone sounding (OXR), July 10, 1975, 1500 PDT.

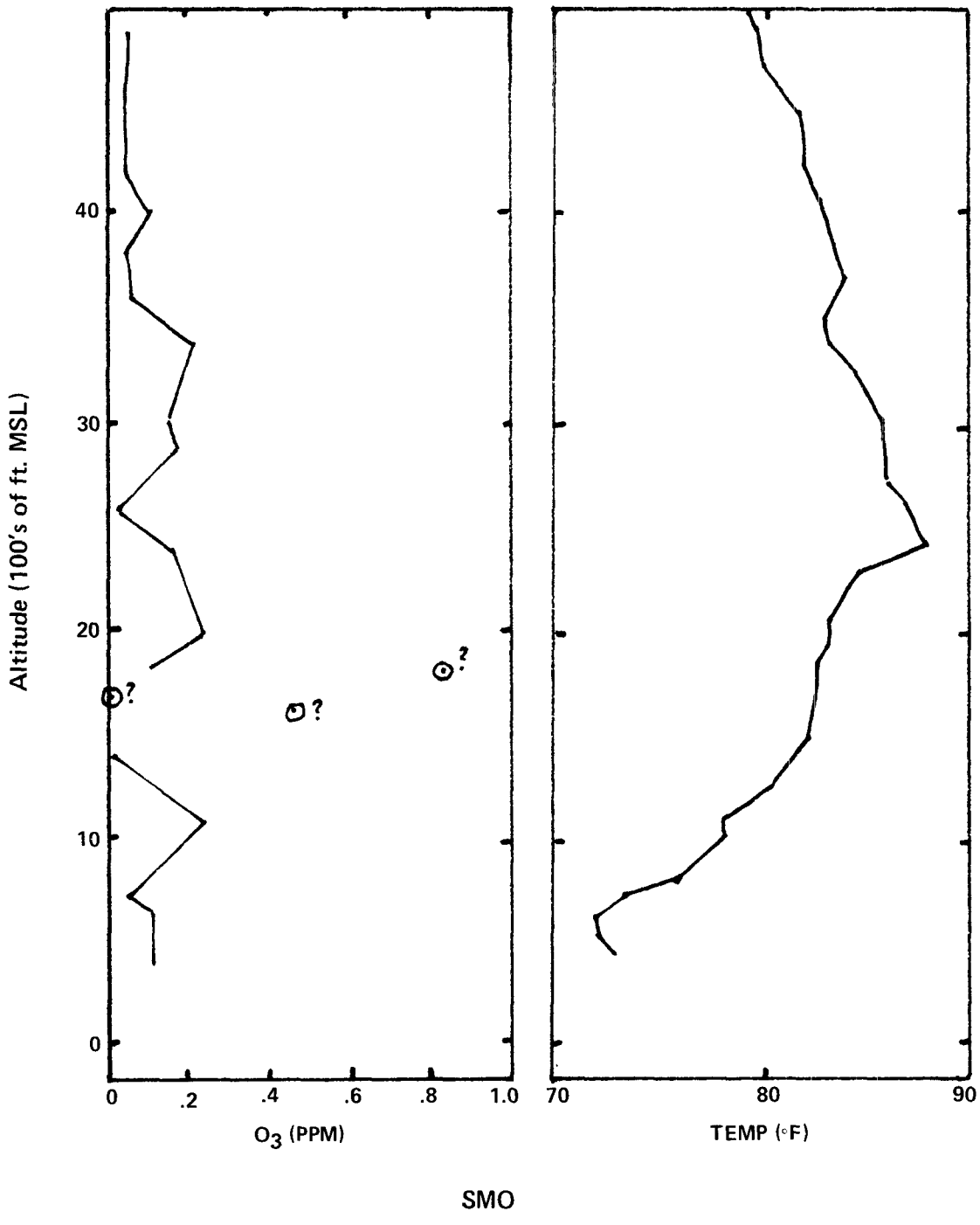

Figure 2b. Temperature and ozone sounding (SMO), July 10, 1975, 1500 PDT.

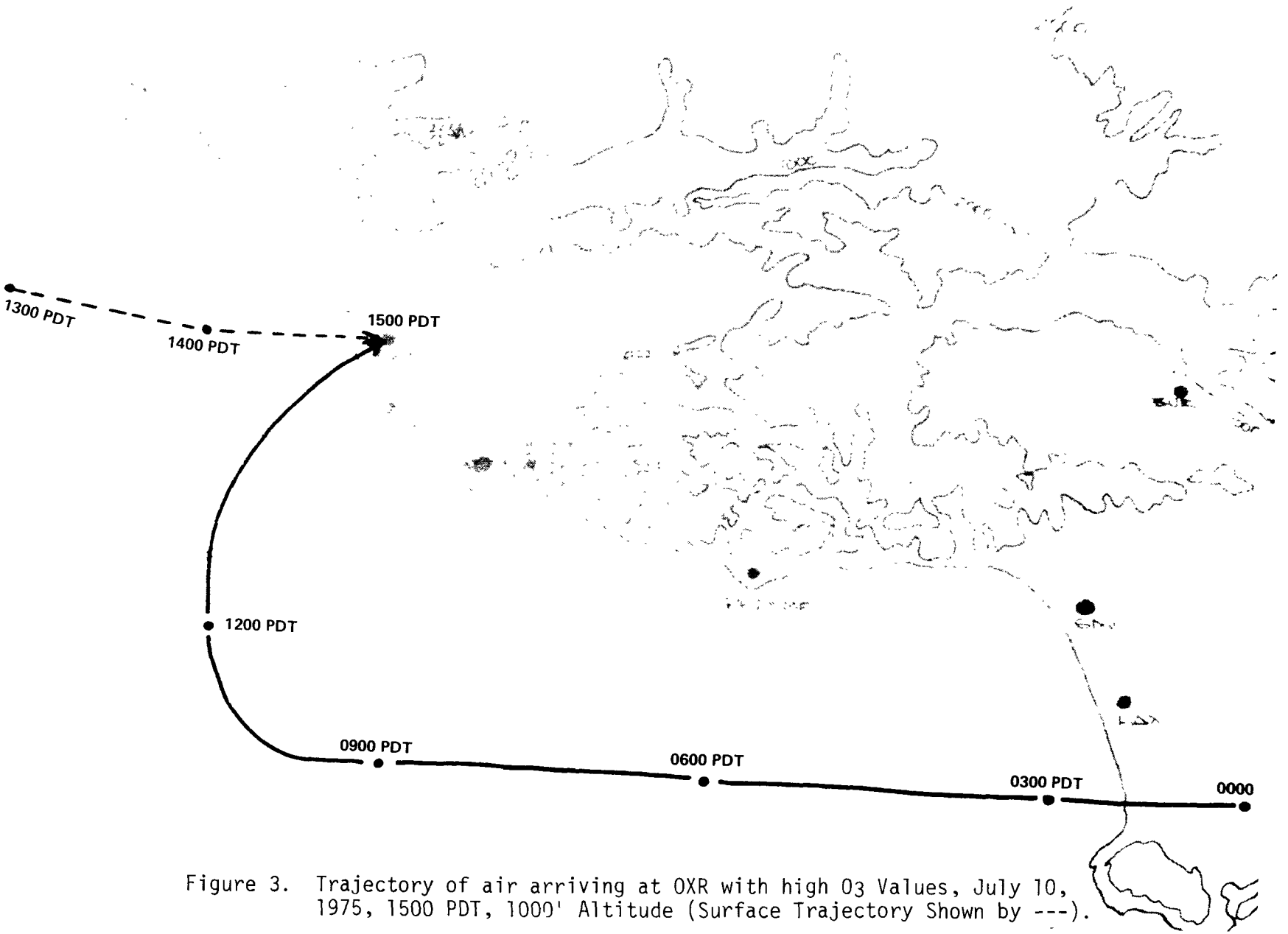

Figure 3. Trajectory of air arriving at OXR with high O_3 Values, July 10, 1975, 1500 PDT, 1000' Altitude (Surface Trajectory Shown by ---).

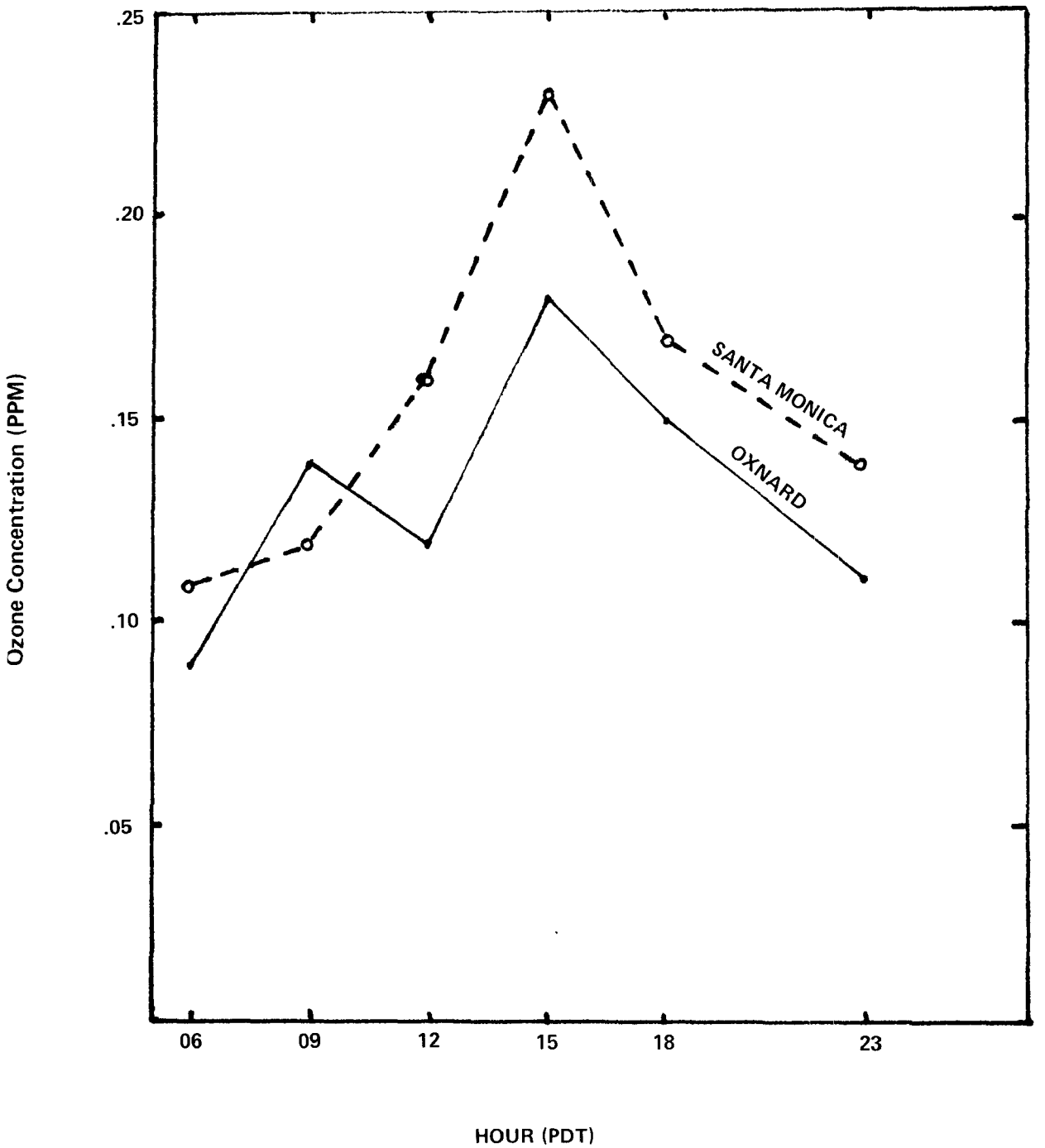

Figure 4. Average maximum ozone above inversion base, July 9-18, 1975.

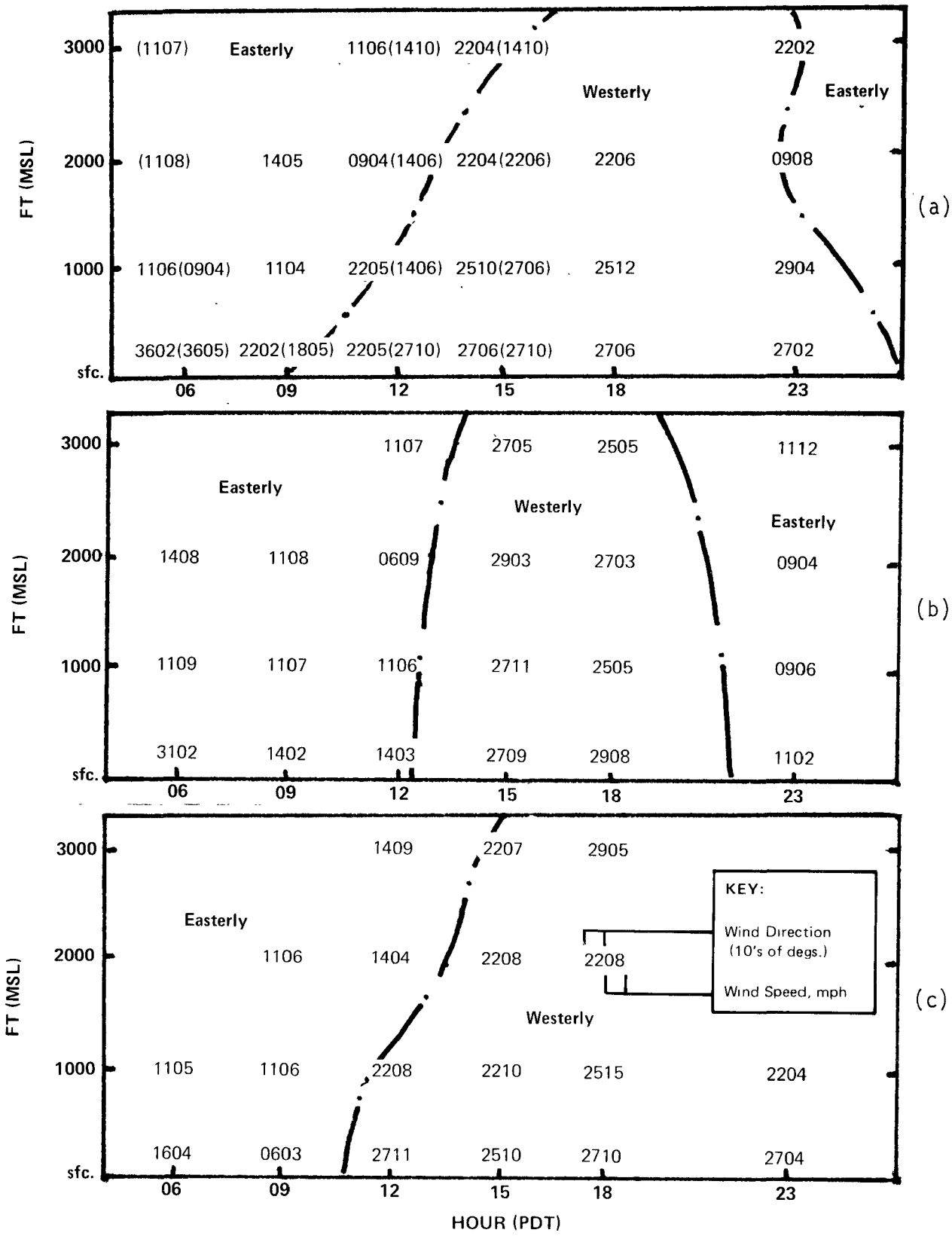

Figure 5. Most frequent winds aloft, June-July 1975; (a) OXR, NTD in (); (b) DUM; (c) LAX.

Angeles coastline and Ventura area, the westerly winds are not noted until well after 1200 PDT, even at the surface.

Conditions shown in Figure 5 reinforce the idea that ozone layers aloft can easily be transported from the east (from Los Angeles) to the Ventura County coast.

CONCLUSIONS

On the basis of a three-dimensional study of wind flow and ozone between the coastal portion of Los Angeles and Ventura County to the northwest, it is concluded that ozone rich layers exist aloft, and may be tracked as entities over the length of the study area.

The most persistent ozone layer was found just above the base of the subsidence inversion characteristic of the southern California summer season.

Trajectories of air containing the ozone aloft indicated a prior history over the Los Angeles Basin. (Surface wind-derived trajectories, on the other hand, give the impression that such a transport did not occur.)

The persistence of the ozone layers aloft, and the upper flow indicating transport from the Los Angeles area during what is considered normal summer conditions, leads to the conclusion that such is the common situation, and that the reported high ozone values at surface locations in Ventura County may well be the result of the surfacing of the aged photochemical pollution cloud from Los Angeles.

REFERENCES

1. Tubbs, D. Photochemical Oxidant Air Pollution in Ventura County, 2nd edition, 1965-1974, Report by the Ventura County Air Pollution Control District, 1975, 115 pp.

2. Chaplin, A.S. and R.R. Russell. A Report on the Impact of the Proposed Camarillo Airport on the Air Quality of the Oxnard Plain, Environmental Systems Div. Litton Systems, Inc., Camarillo, CA., 1970, p. 3.9.

3. Sklarew, R.C., and A.S. Chaplin. Analysis of Formation of High Ozone Concentrations in Ventura County, Report by the Environmental Systems Division, Xonies Corporation, to Ventura County Air Pollution Control District, 1975, 54 pp.

4. Kauper, E.K. and B.L. Niemann. Los Angeles to Ventura Overwater Ozone Transport Study, Report to California Air Resources Board, Sacramento, CA, #ARB4-1126, 1975.

OZONE FORMATION IN THE ST. LOUIS URBAN PLUME

W.H. White, D.L. Blumenthal, J.A. Anderson, R.B. Husar and W.E. Wilson, Jr.*

ABSTRACT

The pollutant emissions of metropolitan St. Louis can cause violations of the Federal Ambient Standard for ozone 160 km or more downwind. The apparent ozone yield of the estimated hydrocarbon emissions from the metropolitan area is close to the theoretical stoichiometric upper limit. These conclusions are drawn from detailed observations of the St. Louis urban plume made by instrumented aircraft during the summers of 1973, 1974, and 1975.

INTRODUCTION

Metropolitan St. Louis is a major urban-industrial center, encompassing coal-fired power plants with a combined capacity of 4600 megawatts (mw), oil refineries with a combined capacity of 4.4 x 10^5 barrels/day, various other industry, and a population of about two million. It is surrounded by flat, predominantly agricultural terrain, the nearest neighboring city of 50,000 or more people being 135 km distant. Due to its isolation, the impact of St. Louis on ambient air quality is relatively easy to determine; air that has been modified by the aggregate emissions of the metropolitan area forms a 30-50 km-wide urban plume downwind. The Fate of Atmospheric Pollutants Study (FAPS) showed that the aerosol burden of this plume is often identifiable 80 to 120 km from the city (1, 2, 3, 4).

As part of Project Midwest Interstate Sulfur Transformation and Transport (MISTT), pilot balloons and instrumented aircraft were used during the summers of 1973, 1974, and 1975 to quantify the three-dimensional flow of aerosols and trace gases in the St. Louis urban plume (5). The primary sampling platform for the program was the MRI Cessna 206 (6). In addition to extensive aerosol and meteorological instrumentation, this single-engine plane carried continuous monitors for ozone (O_3) (chemiluminescence), nitric oxide (NO) and nitrogen oxides (NO_x) (chemiluminescence), and sulfur dioxide (SO_2) (electrochemical). The flight pattern of the sampling aircraft was designed to characterize cross wind sections of the plume at discrete distances downwind of the city, and was established with the aid of an instrumented

*W.H. White, D.L. Blumenthal, J.A. Anderson, Meteorology Research, Inc., Altadena, California.
R. B. Husar, Washington University, St. Louis, Missouri.
W. E. Wilson, Jr., U.S. Environmental Protection Agency, Research Triangle Park, North Carolina.

scout aircraft operated by Washington University (7). Airborne operations were supported with half-hourly observations of winds aloft obtained by mobile pilot balloon units operating in the sampling area.

The use of a highly-mobile fixed-wing aircraft as the primary sampling platform led to an improved understanding of pollutant transport and dispersion at scales of 100 km or more. In addition, the design of the experiment made possible the study of transformations undergone by pollutants in the atmosphere at dilutions and time scales which are difficult to simulate in the laboratory. The formation of aerosols and loss of sulfur dioxide in the St. Louis urban plume are discussed elsewhere (7, 8). In this paper, we will present some results on the formation and transport of ozone, and discuss their implications for a control policy.

RESULTS

A plume of ozone concentrations well above background levels was encountered directly downwind of St. Louis on most sampling days. Ozone concentrations within this plume often exceeded 0.2 ppm, and concentrations in excess of 0.3 ppm were recorded. Net production of O_3 and/or nitrogen dioxide (NO_2) was often apparent less than 15 km downwind of major hydrocarbon (HC) sources near Wood River (chemical industry) and downtown St. Louis (motor vehicles). Figure 1 shows profiles of ozone and oxidant (O_3 + NO_2) concentrations measured immediately downwind of the metropolitan area under different wind regimes.

The geometry of the urban plume strongly depended on the prevailing wind direction. Under northwesterly or southeasterly conditions, parallel plumes from Wood River and St. Louis could be distinguished in traverses immediately downwind of the metropolitan area. The combined initial width of the two plumes was about 50 km. Under southwesterly or northeasterly flow, the two plumes tended to overlap and merge into one. The highest ozone concentrations were measured under these conditions, when the individual plumes reinforced each other. On two days in 1975, the wind held steady from the southwest all day long and the combined urban plume was mapped from St. Louis out to distances greater than 150 km.

Figure 2 shows ozone and aerosol light-scattering coefficient (b_{scat}) profiles recorded by the sampling aircraft during selected cross-wind traverses downwind of St. Louis on July 18, 1975. Each traverse path was flown at three different altitudes, starting just downwind of St. Louis at 0900 Central Daylight Time (CDT) and finishing near Decatur, Illinois, at 1900 CDT. These horizontal traverses, together with vertical soundings such as that shown in Figure 3, documented a broad, shallow pollutant plume extending from St. Louis out past Decatur, 170 km to the northeast. Outside the plume, ozone concentrations were fairly uniform and generally below the 0.08 ppm Federal Ambient Standard. Within the plume, ozone concentrations exceeded the Federal Ambient Standard even at 160 km from the St. Louis Arch. At this distance, where concentrations outside the plume were 0.07 ppm or less, concentrations in the center of the plume remained as high as 0.12 ppm.

The July 18 plume was mapped under hazy skies, with some scattered thunder-

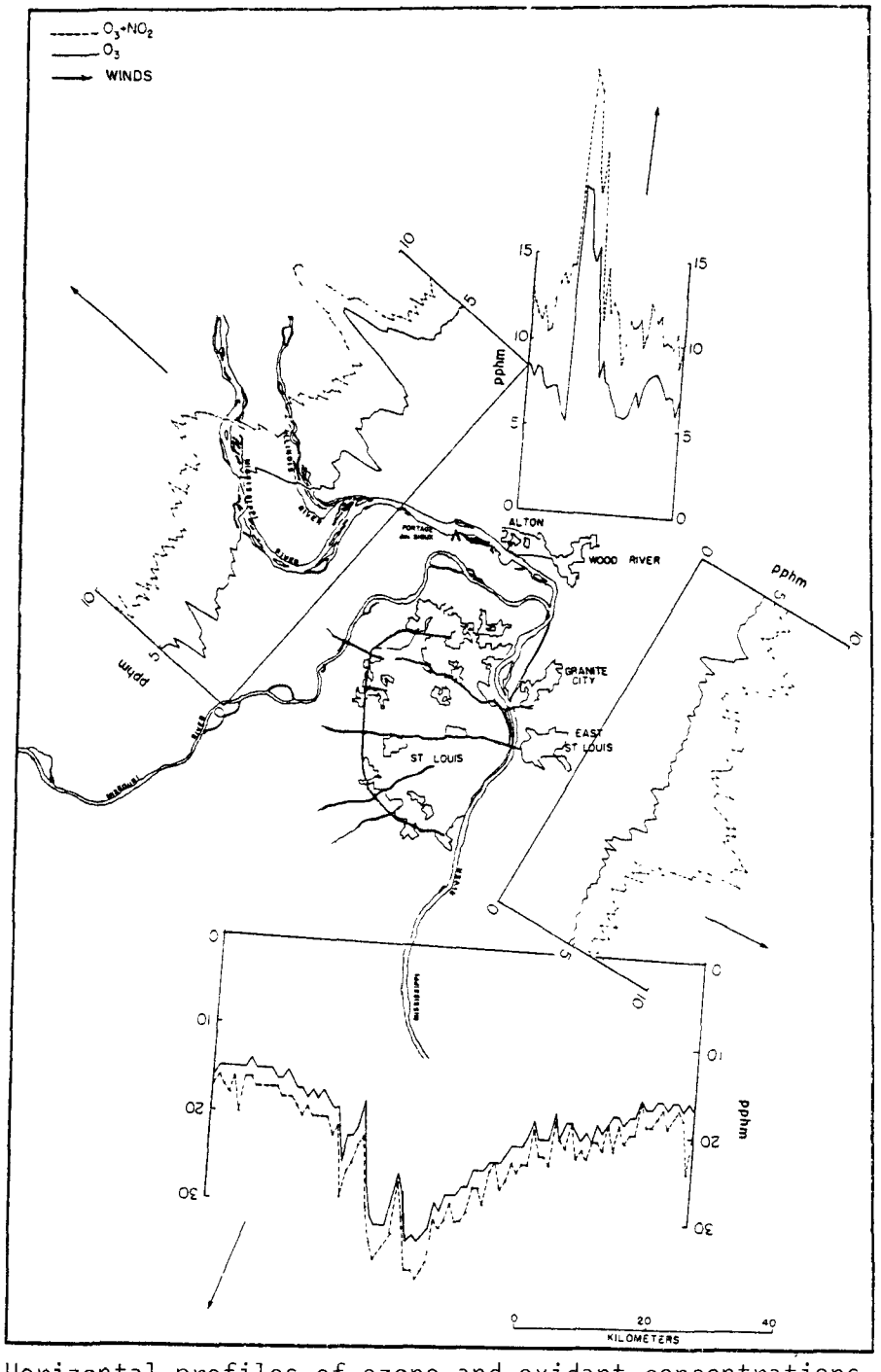

Figure 1. Horizontal profiles of ozone and oxidant concentrations downwind of metropolitan St. Louis under four different wind regimes. Profiles were recorded during traverses along profile baselines at the following altitudes and times: (clockwise from top) 610 m MSL, 1145-1152 CDT, 12 August 1974; 455 m MSL, 0933-0952 CDT, 30 July 1974; 760 m MSL 1451-1512 CDT, 28 July 1975; 455 m MSL, 1027-1048 CDT, 15 August 1974. Arrows show average winds measured in mixing layer during sampling period; their lengths equal distance covered in one hour at average wind speed.

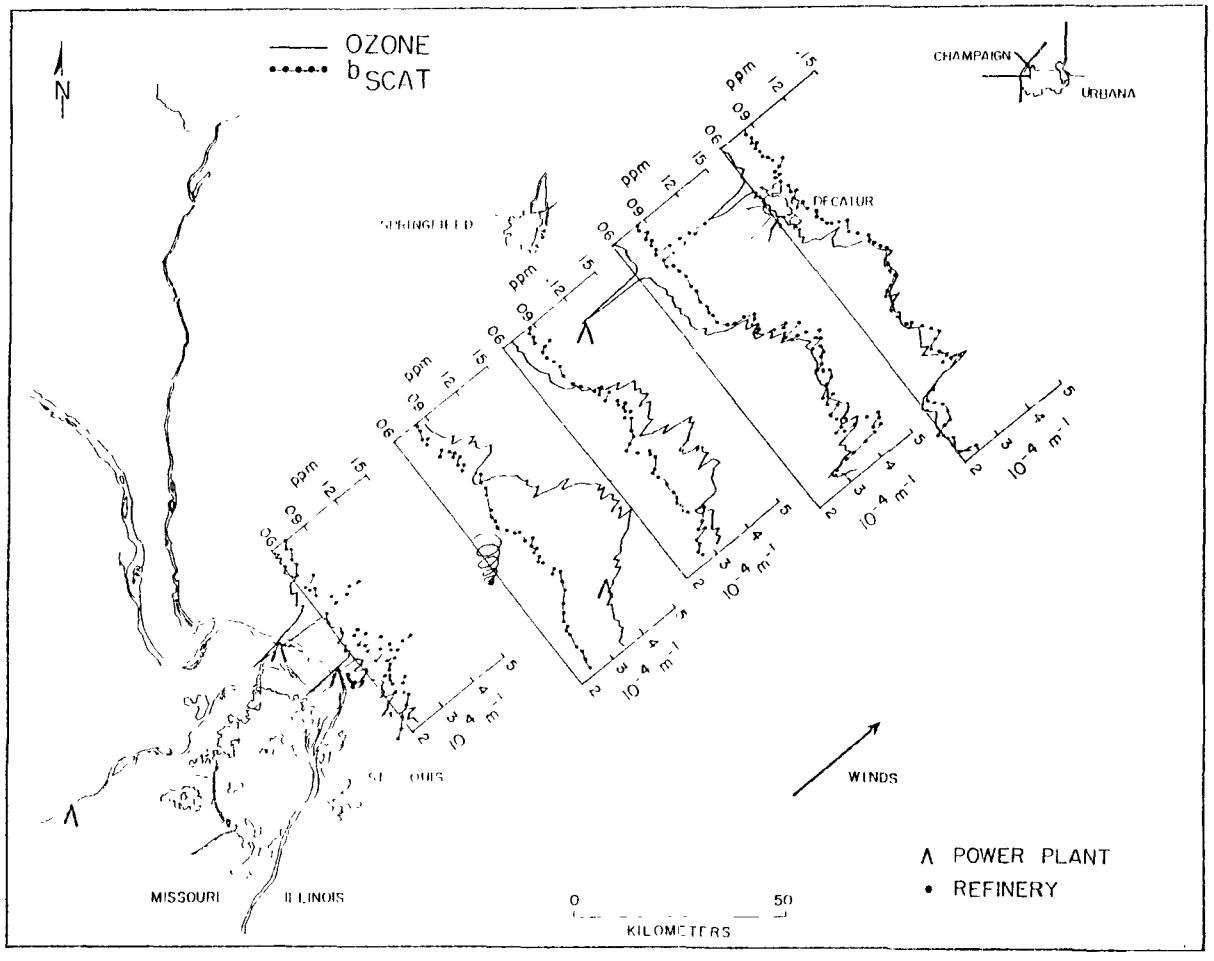

Figure 2. Selected horizontal profiles of ozone concentration and light-scattering coefficient (b_{scat}) downwind of St. Louis on 18 July 1975. Profiles were recorded during traverses along profile baselines at the following altitudes and times: (starting near city) 455 m MSL, 0849-0907 CDT; 455 m MSL, 1157-1220 CDT; 610 m MSL, 1348-1410 CDT; 760 m MSL, 1631-1656 CDT; 760 m MSL, 1804-1834 CDT. Spiral indicates location of vertical sounding shown in Figure 3.

showers appearing toward evening. The depth of the mixed layer, which was 0.3 km at 0900 CDT, increased rapidly during the morning, and exceeded 1.0 km by early afternoon. The continuing presence of a low pressure trough over the western plains produced strong southwesterly flow over the Missouri and upper Mississippi valleys, which was documented in the sampling area by a total of 36 pilot balloon observations carried out as part of Project MISTT. The mean transport vector (1) lay between 230° and 243° during the middle of the day, at speeds of 20-36 km/hr. At these speeds, among the highest encountered during the program, emissions from the city would have aged roughly 5-7 hours by the time they were sampled in the farthest passes.

The general direction of the airflow was corroborated by the alignment of power plant plumes in successive traverses. All of the major (greater than 1,000 mw capacity) power plants lying in and immediately upwind of the

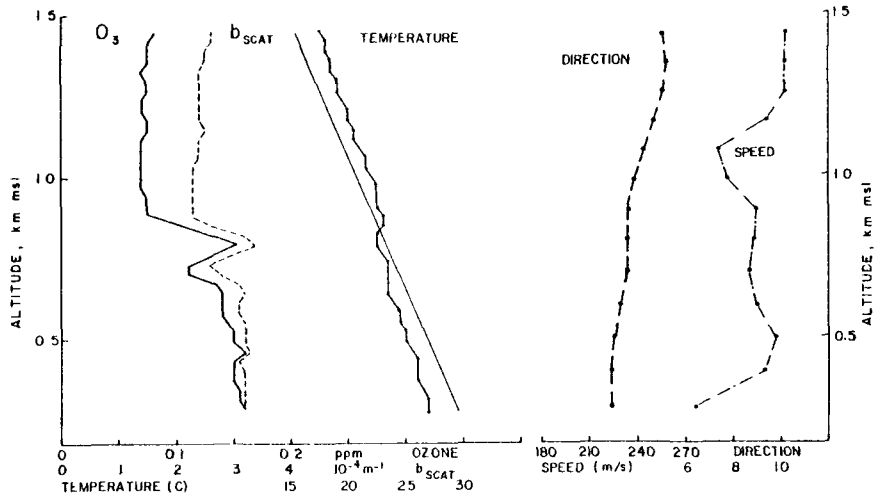

Figure 3. Vertical profiles of ozone concentration, (b_{scat}), temperature, and wind, measured in late morning on 18 July 1975. Profiles of ozone, b_{scat}, and temperature were recorded during spiral descent over Mt. Olive, Illinois (identified by spiral in Figure 2), 1130-1143 CDT. Straight line with temperature profile shows dry adiabatic lapse rate. Wind profiles were derived from pilot balloon released from Sorento, Illinois, 15 km from Mt. Olive, at 1200 CDT.

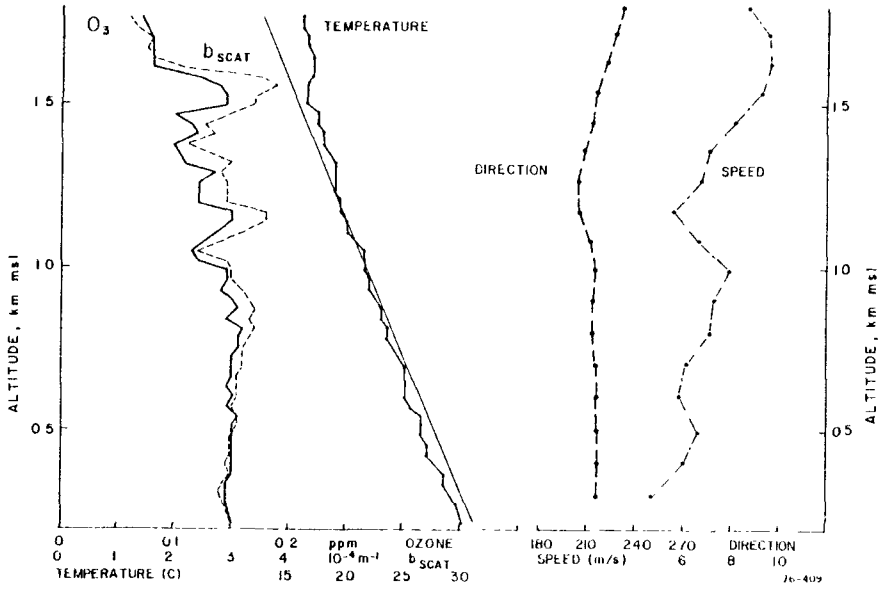

Figure 4. Vertical profiles measured in early afternoon on 11 August 1975. Profiles of ozone, b_{scat}, and temperature were recorded during spiral descent over Butler, Illinois (identified by spiral in Figure 5), 1329-1343 CDT. Wind profiles were derived from pilot balloon released from Taylorville, Illinois, 40 km northeast of Mt. Olive, at 1330 CDT.

area are noted in Figure 2. The plumes from some of these plants can be identified in Figure 2 by their ozone deficits, which result from the scavenging of the ambient ozone by plume NO (9). The Coffeen plant, 85 km WNW of St. Louis, is the only major downwind pollutant source known to the authors which lies within the July 18 urban plume.

Figure 5 shows selected ozone and b_{scat} profiles recorded on August 11, 1975. Sampling began upwind of St. Louis at 0800 CDT and continued downwind of the city until a line of thunderstorms moved into the sampling area at about 1600 CDT. At this time, the sampling aircraft had just completed a set of passes 145 km from the Gateway Arch, and the scout aircraft, which was not instrumented for ozone, had identified the aerosol plume 100 km further downwind. In all sampling passes downwind of the city, ozone concentrations outside the urban plume were below the 0.08 ppm Federal Ambient Standard, while concentrations within the plume were substantially above. Near Hillsboro, Illinois, 85 km from St. Louis, the ozone concentration reached 0.2 ppm in the middle of the day.

Skies on August 11 were partly cloudy, with scattered cirrus present during the morning and early afternoon. The mixing depth was about 0.3 km at 1000 CDT and reached 1.4 km by 1330 CDT (Figure 4). A weak low in western Nebraska triggered southwesterly flow in the lower atmosphere, at speeds somewhat below those of July 18. The mean transport vector lay between 221° and 243° during the middle of the day, at speeds in the range 16-30 km/hr. At these wind speeds, the sampling aircraft was progressing downwind at roughly the same rate as the air.

A distinctive feature of the MISTT program was the characterization of pollutant concentrations and winds over complete cross-sections of the urban plume. From the measurements at a given cross-section, the horizontal mass flow rate of a pollutant across that cross-section can be calculated directly:

$$\text{FLOW RATE} = \int u_x(x,z) \int (C(x,y,z) - C_0(x,z))\, dy\, dz,$$

where x is distance downwind, y,z are cross-wind and vertical coordinates, u_x is wind speed (from pilot balloon observations), C is pollutant concentration (from aircraft measurements), and C_0 is average pollutant concentration outside the plume (from aircraft measurements). Figure 6 shows ozone flow rates from three different days, plotted against distance downwind of the city. The quantities plotted are the flow rates of ozone in excess of background, and thus represent the specific contribution of metropolitan St. Louis to atmospheric loadings.

The measurements for Figure 6 were not, in general, made in the Lagrangian mode. Moreover, the measurements at less than 50 km from the city were all made in the morning, while the measurements at greater distances were all made in the afternoon. It is, therefore, difficult to distinguish between the contributions of solar elevation and atmospheric residence time to the increase in the ozone flow rate over the first 100 km. Nevertheless, it is of interest that the flow rates at 50 km or more from the city cluster in the range 95-125 T/hr. These numbers may be taken as a rough estimate

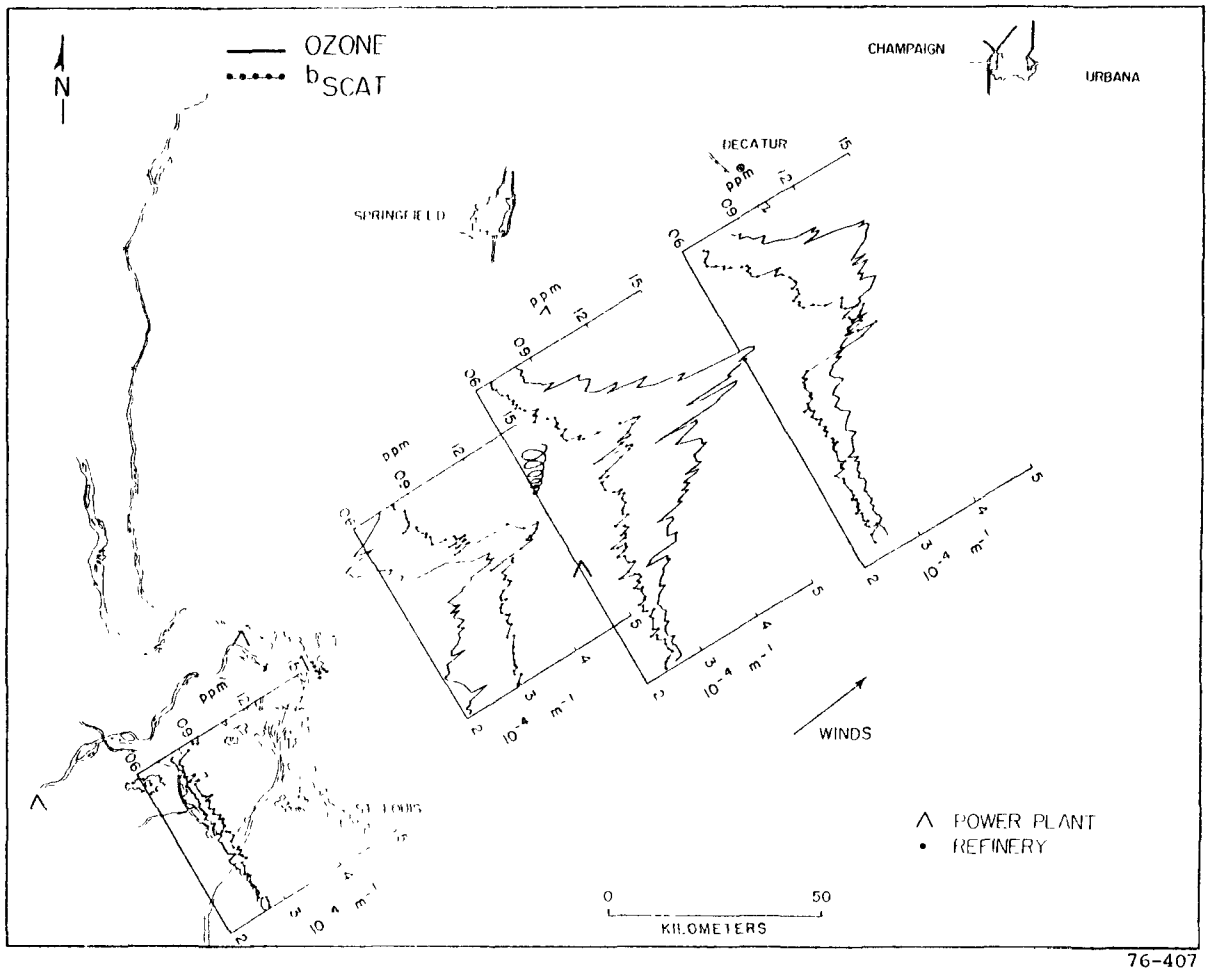

76-407

Figure 5. Selected horizontal profiles of ozone concentration and b_{scat} downwind of St. Louis on 11 August 1975. Profiles were recorded during traverses of profile baselines at the following altitudes and times: (starting upwind of city) 455 m MSL, 0744-0758 CDT; 425 m MSL, 1019-1036 CDT; 610 m MSL, 1245-1310 CDT; 760 m MSL, 1442-1508 CDT. Spiral indicates location of vertical sounding shown in Figure 4.

for the rate at which ozone was formed in the atmosphere from the emissions of metropolitan St. Louis.

DISCUSSION

The St. Louis urban plume was mapped on a total of eight days during the July 15-August 15, 1975, MISTT experiment, and ozone was a conspicuous indicator of the plume during this period. Daytime ozone concentrations within the plume generally exceeded the 0.08 ppm Federal Ambient Standard, even on the most distant sampling runs. Peak concentrations in the plume were typically twice those in the unmodified background air, and surpassed 0.15 ppm on most sampling days. (It should be noted that the object of Pro-

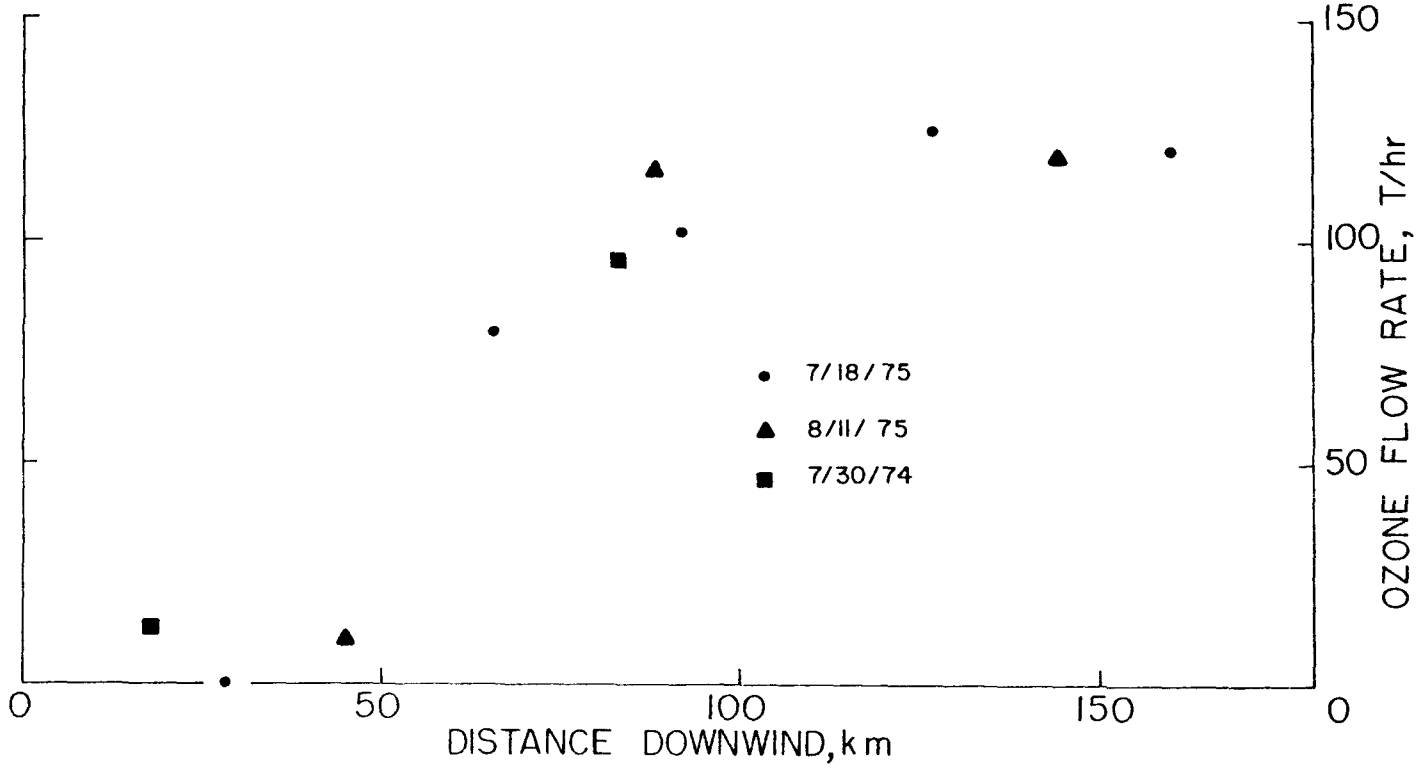

Figure 6. Ozone flow rates (in excess of background) in St. Louis urban plume on three different days. Values are calculated from winds within the plume and the difference between ozone concentrations inside and outside the plume. Downwind distances are measured from St. Louis Gateway Arch.

ject MISTT was not to develop a climatology of the urban plume, but to measure it in detail under conditions favorable for doing so, and sampling days were chosen according to this criterion.) Earlier measurements by FAPS had also found excess ozone in the St. Louis urban plume on two days in April, 1973 (3).

While upwind sources undoubtedly contribute to regional backgrounds at St. Louis, they clearly do not account for the excess concentrations of the urban plume, which were consistently found downwind of the city regardless of the wind regime. On the two days discussed in detail in this paper, the nearest upwind city of any size was Springfield, Missouri, over 300 km from St. Louis with only about 100,000 people. Nor is a stratospheric origin for the excess ozone any more likely; this would not explain the restriction of high concentrations to the mixed layer, and their alignment with the wind. Moreover, Figures 2 and 5 show that the excess ozone in the plume is associated with light-scattering aerosols, which would not be expected in a clean airmass subducted from the stratosphere. The excess ozone concentrations downwind of St. Louis must be attributed directly to the emissions of the metropolitan area.

The most obvious policy implication of the MISTT data is that ozone control strategies must, to be effective, be formulated on a regional scale. The 1975 experiment documented, in air 160 km from St. Louis, violations of the Federal Ambient Standard for ozone which were traceable to emissions from the metropolitan area. Between 125 and 160 km downwind there was no significant decay in the flow rate of ozone and no significant increase in the crosswind and vertical dimensions of the urban plume, so that violations of the standard probably extended much farther out. None of the ground-level ozone monitors operated by the State of Illinois were situated in the path of the observed ozone plume, so that the airborne measurements can be compared with the standard network measurements only in the background air, where they were consistent (10). Aircraft soundings in the plume (Figures 3 and 4) showed ozone concentrations to be quite uniform through the mixed layer, however, and it is probable that the high plume concentrations encountered aloft were experienced near the surface as well.

The elevated ozone concentrations within the St. Louis urban plume were superimposed on background ozone levels which were themselves substantially above those associated with clean air (11). On most sampling days, midday ozone levels outside the urban plume lay in the range 0.07-0.12 ppm. It is clear that if the emissions of St. Louis can contribute to the ozone backgrounds of cities far downwind, then much of the ozone background of St. Louis itself may not be natural, but instead due to cities and industry far upwind of St. Louis. There is some evidence that the composition of the upwind background strongly affects the chemistry of the downwind plume. For example, unusually high (for St. Louis) peak ozone concentrations were observed on July 28, 1975, a day of unusually high (for St. Louis) ozone backgrounds (Figure 1).

The annual emissions of non-methane HC in metropolitan St. Louis are estimated at about 1.6×10^5 tonnes (10, 12, 13). This corresponds to an average of 18-36 tons/hr, depending on whether emissions are spread out through

the day or concentrated in the daylight hours. H. M. Walker has pointed out that if these figures are accurate then the formation of 120 tons/hr of ozone in the St. Louis urban plume corresponds to a yield of one to two parts (by volume) ozone for each part (by volume as C) emitted HC (13). This would be a much higher yield than is typically found in smog chamber studies (14). Possible explanations for the high apparent yield would include enhanced production at low concentrations in the absence of wall losses, and the participation of incompletely-reacted HC products contributed by the background air. Hydrocarbon measurements taken during the recently-completed 1976 MISTT experiment may help to resolve this point.

Whatever its origin, the high apparent ozone yield of HC in the St. Louis urban plume carries important implications for photochemical simulation models. If most of the ozone produced in the plume is attributable to free radicals and unreactive HC advected into the city from upwind sources, then the composition of the background air is a critical input to a simulation model. This means that successful simulation on the mesoscale is dependent, via initial and boundary conditions, on successful simulation on the synoptic scale. Alternatively, if most of the ozone produced in the plume is attributable simply to the efficient utilization of HC emitted in metropolitan St. Louis, then the ozone yield of these HC is near the theoretical stoichiometric upper limit of two to one (15) or four to one (13). This means that the chain lengths of the reactions involving the more reactive HC species are determined primarily by the size of the initial HC molecule, and not by a competition between chain-propagating and chain-terminating reactions as in present lumped kinetic photochemical models (16).

ACKNOWLEDGEMENT

This research was supported by the U.S. Environmental Protection Agency, Environmental Sciences Research Laboratory, Aerosol Research Branch.

REFERENCES

1. Haagenson, P. L. and A. L. Morris. J. of Applied Meteorology 13:901, 1974.

2. Stampfer, J. F. and J. A. Anderson. Atmospheric Environment, 9:301, 1975.

3. Breeding, R. J. , P. L. Haagenson, J. A. Anderson, J. P. Lodge, Jr. and J. F. Stampfer, Jr. J. of Applied Meteorology 14:204, 1975.

4. Breeding, R. J., H. B. Klonis, J. P. Lodge, Jr., J. B. Pate, D. C. Sheesley, T. R. Englert and D. R. Sears. Atmospheric Environment 10:181, 1976.

5. Wilson, Jr., W. E., R. J. Charlson, R. B. Husar, K. T. Whitby, and D. L. Blumenthal. Proc. 69th Annual Meeting Air Pollution Control Assoc., Paper #76-30-06, June 1976.

6. White, W. H., J. A. Anderson, W. R. Knuth, D. L. Blumenthal, J. C. Hsiung and R. B. Husar. Final Report to U.S.E.P.A. on contract number 68-02-1919 by Meteorology Research, Inc., Altadena, California, 1976.

7. Husar, R. B., J. D. Husar, N. V. Gillani, S. B. Fuller, W. H. White, W. M. Vaughan and W. E. Wilson, Jr. Proc. of the Div. Environmental Chemistry, 171st National ACS Meeting, New York, April 1976.

8. White, W. H., J. A. Anderson, D. L. Blumenthal, R. B. Husar, N. V. Gillani, J. D. Husar and W. E. Wilson, Jr. Science, 1976 (in press).

9. Ogren, J. A., D. L. Blumenthal, W. H. White, T. W. Tesche and M. K. Liu. Proc. Int'l. Conf. on Photochemical Oxidants and its Control, Raleigh, North Carolina, 1976.(in press)

10. Illinois E.P.A. 1976.

11. Blumenthal, D. L., T. B. Smith, W. H. White, S. L. Marsh, D. S. Ensor, R. B. Husar, P. S. McMurry, S. L. Heisler and P. Owens. Final Report to California Air Resources Board on contract number ARB 2-1245 by Meteorology Research, Inc., Altadena, California, 1974.

12. U.S.E.P.A. 1976.

13. Walker, H. M. Proc. of the Conf. on Ozone/Oxidants, Air Pollution Control Assoc., Dallas, March 1976.

14. Wilson, W. E., Jr., D. F. Miller, A. Levy and R. K. Stone. J. Air Pollution Control Assoc. 23:949, 1973.

15. Klauber, G. M., Ph.D. thesis, Johns Hopkins University, 1975

16. Hecht, T. A., J. H. Seinfeld and M. C. Dodge. Environmental Science and Technology 8:327, 1974.

LONG RANGE AIRBORNE MEASUREMENTS OF OZONE OFF THE COAST OF THE NORTHEASTERN UNITED STATES

G. W. Siple, C. K. Fitzsimmons, K. F. Zeller, and R. B. Evans*

ABSTRACT

The Environmental Protection Agency participated in a study of oxidant and oxidant precursor transport in the northeastern United States in the summer of 1975. An instrumented aircraft was used to measure ozone and nitric oxide, and to take bag samples, among other parameters. Air trajectory analyses indicate that the air mass containing high ozone concentrations monitored over the Atlantic Ocean 250 kilometers east of New York City passed over that metropolitan area on the morning of the day the measurements were made.

INTRODUCTION

Atmospheric oxidants have been the subject of a variety of research investigations in recent years. The role of oxides of nitrogen (NO_x) and organic hydrocarbons (HC) as oxidant precursors has been documented within the framework of these studies. Although metropolitan areas have long been recognized as major contributors to the atmospheric burden of these precursor compounds, rural areas have also been implicated as origins of oxidant precursors. The internal combustion engine is a major source of oxidant precursors and, for that reason, states experiencing elevated oxidant concentrations have promulgated Transportation Control Plans (TCP) to aid in achieving air quality within the oxidant standard (0.08 ppm annual maximum). However, conditions conducive to local and broad area oxidant production and enhancement are quite complex; the physical and photochemical history of an air parcel before it enters an area can have a significant influence on the pollutant burden within that area. Recent reports of air quality studies in the northeastern U.S. (Cleveland et al., 1976) and the western U.S. (Blumenthal et al., 1974) appear to confirm the likelihood of the transport of oxidant and oxidant precursors over long distances. The Northeast Oxidant Transport Study (NOTS) was conducted during the summer of 1975 to identify and quantitate oxidant and oxidant precursor transport from New York-New Jersey metropolitan areas into and through the southern New England area.

*U.S. Environmental Protection Agency, Las Vegas, Nevada

INSTRUMENTATION

A field team from the U.S. Environmental Protection Agency's Environmental Monitoring and Support Laboratory at Las Vegas, Nevada, (EMSL-LV) participated in the NOTS gathering extensive air quality data with the Long Range Air Monitoring Aircraft (LORAMA) during August of 1975. The aircraft, a Monarch B-26, was modified to operate as an air monitoring platform. The instrumentation on board the aircraft is listed in Table 1. Oxidant, measured as ozone (O_3), was monitored during each flight by a gas-phase chemiluminescent Bendix 8002, an instrument which has proven reliable and precise for field data collection. Nitric oxide (NO) was measured with a TECO 14B single-channel gas-phase chemiluminescent analyzer, modified for high sensitivity and low noise. This particular instrument is designed to reliably measure NO_X in the range of 5 parts per billion (ppb) fullscale; but, this instrument was not used to monitor total NO_X or nitrogen dioxide (NO_2) at any time during the study. Other data routinely collected included coefficient of light scattering (b_{scat}), outside ambient temperature, dewpoint temperature, altitude, and navigational position. Bag samples were taken at strategic points on most flights for subsequent HC analysis by gas chromatography.

There are several important considerations with regard to air pollution data collected by means of an airborne platform. However, these are discussed in the literature (Hester et al., 1976) and are not specified here. It should be mentioned that detailed quality control procedures were an integral part of the field work; instrument calibration was performed on all instruments before and after each day's flights, checking both zero and one span level. During flight, periodic zero input checks were made. These calibration data, along with altitude correction factors derived from environmental chamber tests (Siple et al., 1976), were used to process the data into useable engineering units.

TABLE I. LORAMA INSTRUMENTATION

Parameter	Method/Instrument
O_3	Chemiluminescence/Bendix 8002
NO	Chemiluminescence/TECO 14B modified for low noise/high sensitivity
Outside Ambient Temperature	Integrated circuit/LX5700
Dewpoint Temperature	Hygrometer/Cambridge 13F-C3
Particulate Light Scattering	Integrating nephelometer/MRI 1550
Altitude	Integrated circuit/LX 3702A
Location	Digital DME/Collins DME-40
Hydrocarbons	Bag Samples (Tedlar)

MONITORING STRATEGY

The report of Cleveland et al. (1976), based on ground-level ozone data, seems to strongly indicate the reality of the pollutant transport phenomenon in the northeastern U.S. However, one might generally expect micro- and meso-scale geographical, meteorological, and anthropogenic irregularities within the study path to adversely affect conclusions concerning broad area phenomena such as pollutant transport over terrestrial areas. In contrast, air quality monitoring over oceanic areas offers unique opportunities for experimental design and data interpretation; the relatively smooth ocean surface provides simplified conditions for the study of pollutant dispersion. The ocean is not recognized as a significant source of, or a sink for, photochemical oxidant activity. Although complex interactions between oxidant and the ocean surface probably do occur, the exact nature of such interactions is not well-defined.

Without such knowledge, and for the sake of simplicity, it can be assumed that transport and dispersion of oxidant and oxidant precursors by meteorological means are primarily responsible for the ambient pollutant concentrations over marine areas. Under these simplified conditions, the fate of pollutants originating in littoral areas can be described confidently.

This report examines ozone data collected by the LORAMA over portions of the Atlantic Ocean off the northeastern seaboard. Perhaps the most significant flight was #9, performed on the afternoon of August 14, between 1430 and 1745 Eastern Daylight Time (EDT).

RESULTS AND DISCUSSION

Figure 1 shows the flight path for flight #9, which departed the Naval Air Station at South Weymouth (NZW) at about 1430 EDT on August 14. The flight turned south, to begin a spiral over Vineyard Bay, between the Elizabeth Islands and Martha's Vineyard. Figure 1 shows instantaneous ozone concentrations in ppb every two minutes, as a function of position, time, and altitude.

Figure 2 presents the vertical profiles of all data parameters measured continuously; the spiral began at 2135 meters above mean sea level (m MSL) and descended to 60 m MSL. One can notice two shallow temperature inversions; the base of the higher one is at approximately 1525 m MSL, the base of the lower is at approximately 1220 m MSL. The ozone profile, the humidity profile, and the light scattering coefficient profile indicate distinct patterns related to these inversions. However, one can note the rapid increase in ozone between 200 m MSL and 60 m MSL. This increase would not appear to be related to a trapped polluted layer since the temperature profile indicates a near adiabatic lapse rate at these lower altitudes. Similar measurements on numerous other flights over the ocean corroborate this observation. This might signify that the air within the mixing layer over the ocean is not necessarily well-mixed. Unfortunately, the TECO 14B was

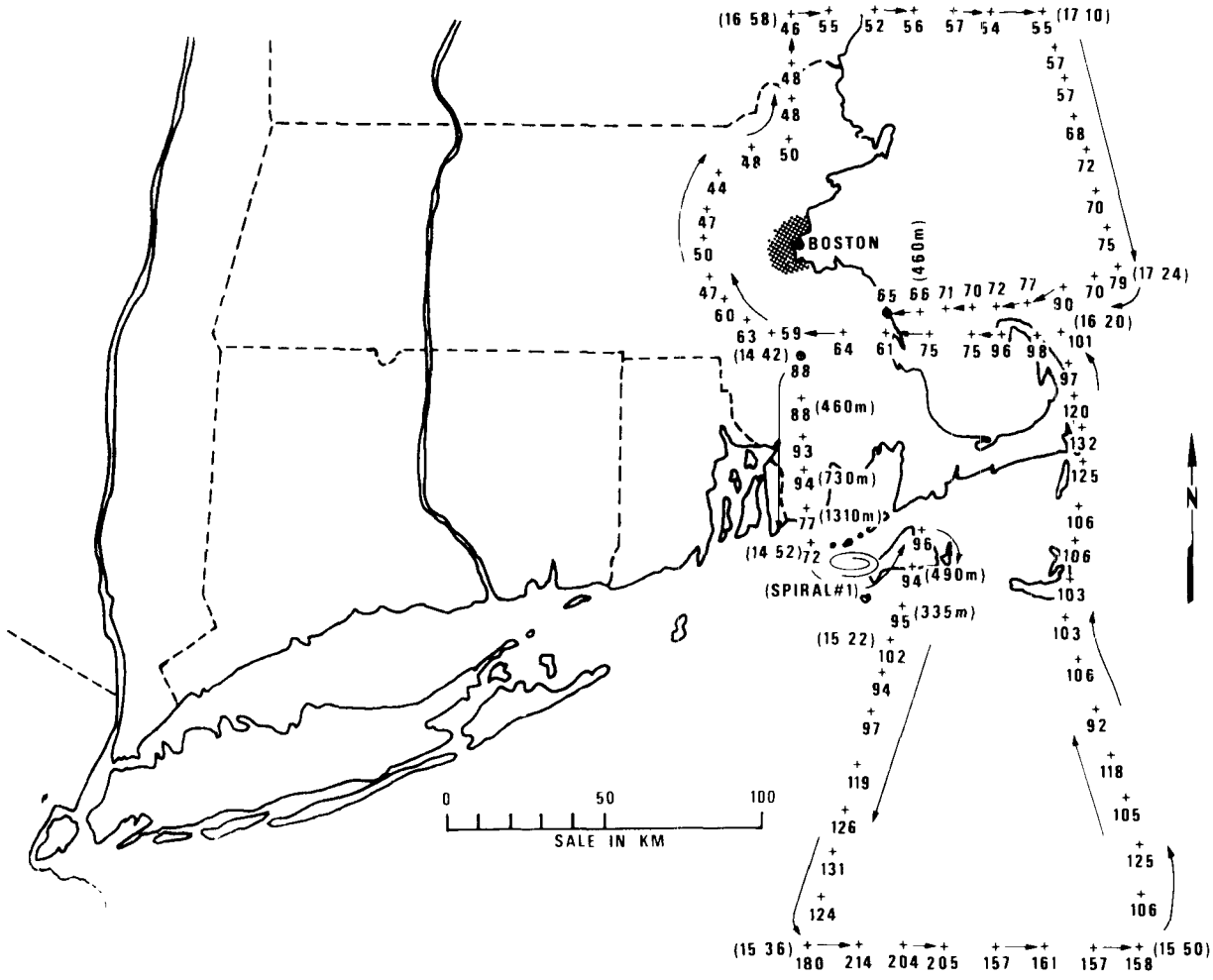

Figure 1. Flight #9 (August 14, 1975): Flight pattern and ozone distribution map.

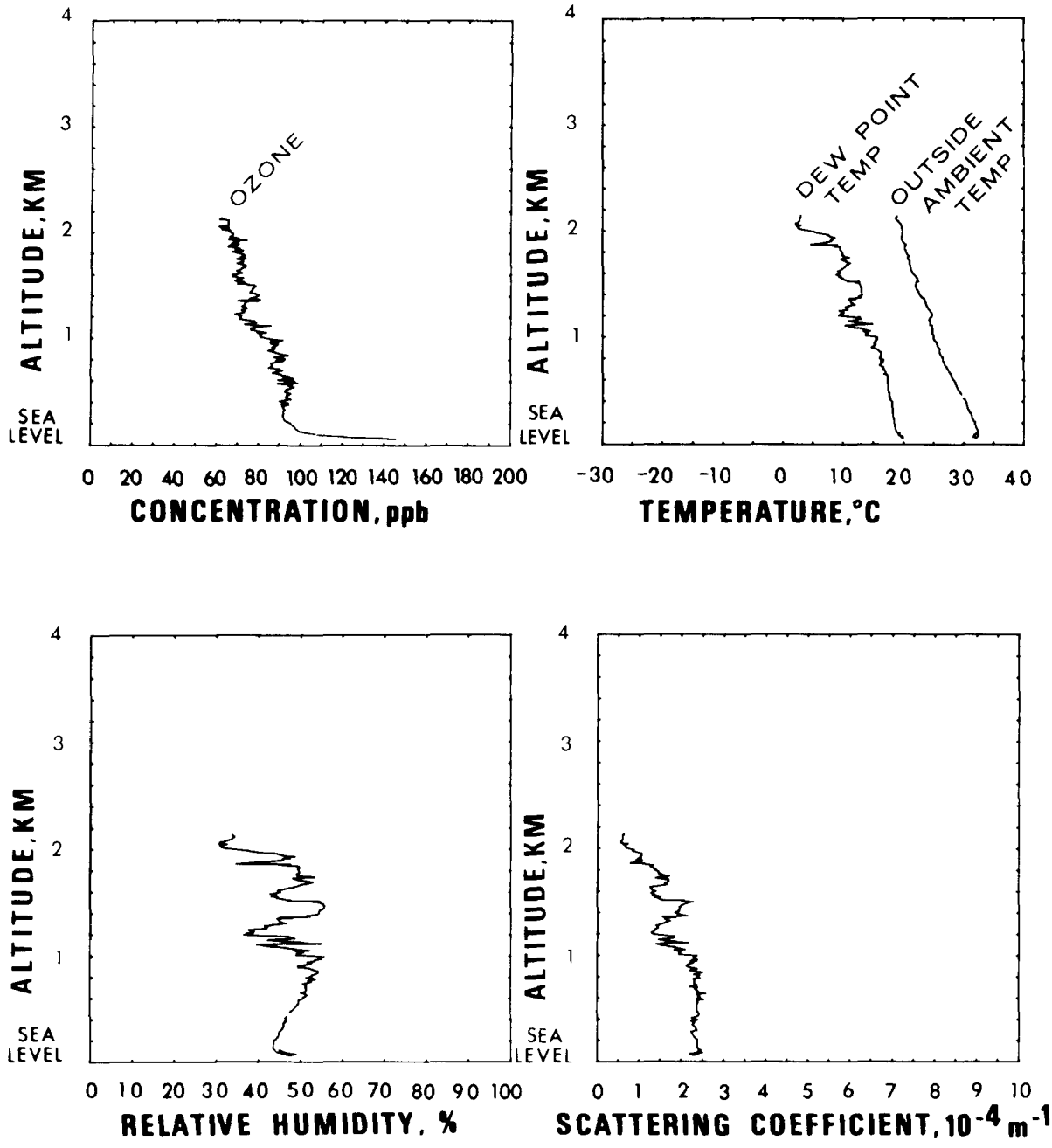

Figure 2. Flight #9 (August 14, 1975): Vertical profiles of parameters for spiral #1.

non-operational on this particular day so there is little indication as to the NO precursor values at this point.

At the completion of the spiral, the aircraft flew over Martha's Vineyard then headed southward again at an altitude of 335 m MSL. The ozone concentration continued to increase at this altitude and, at a point about 130 km south of Martha's Vineyard, the aircraft turned east. The ozone values continued to rise for a short distance, peaking at 214 ppb, then decreasing again. Bag samples taken in this area showed relatively high concentrations of acetylene (Environmental Protection Agency, 1976). The aircraft traveled about 110 km in an easterly direction, then turned northward. The ozone concentration continued to decrease, although there were several minor maxima and minima along the way. After passing the northern point of Cape Cod, the aircraft turned west, climbed to 490 m MSL and made a large circuit of eastern Massachusetts and the ocean just to the east of Boston, returning to NZW at about 1745 EDT.

The ozone concentrations in the northern circuit (50 ppb to 80 ppb) were lower than in the southern circuit (100 ppb to 200 ppb). In terms of ozone concentration, the air monitored in the southern circuit would appear to have a different history than that monitored in the northern circuit. If the spiral data taken near the beginning of the flight is a good indicator of the vertical profiles throughout the flight path (i.e., considering the time difference during the flight), the altitude difference between the two circuits is of little consequence.

Figure 3 illustrates a trajectory analysis calculated backwards in time from the coordinates of the southwest corner of flight #9 (bull's-eye). This is the area where the highest ozone concentrations were recorded. The aircraft was in this locality at approximately 1530 EDT. Three individual trajectories are represented on the figure by the letters A, C, and D. (These trajectories were prepared using the USAF ETAC trajectory program.) The letter C represents the trajectory of an air mass between the altitudes of 300 m above ground level (AGL) and 600 m AGL, terminating at the bull's-eye at 0700 EDT on August 14. The letter D represents the trajectory of an air mass between the same altitudes terminating at the bull's-eye at 1300 EDT. Finally, the letter A represents the trajectory of an air mass between the same altitudes terminating at the bull's-eye at 1900 EDT. The numbers associated with these letters indicate the number of 6-hour periods backward in a given trajectory.

It should be noted before any further analysis is forthcoming that any such trajectory is not solely definitive; there is necessarily an error margin which brackets the calculated path, compounding the error the further the trajectory recedes in time from the starting point. The program which generates these positions attempts to provide macroscale behavior based on a collection of widespread microscale observations.

Nonetheless, one can say that, in general, the air arriving at the bull's-eye portion of the flight path before and after flight #9 was from the northwest through west-northwest. The indicated trajectories C and A pass over southern New York state and northern New Jersey; all trajectories pass over portions of Long Island.

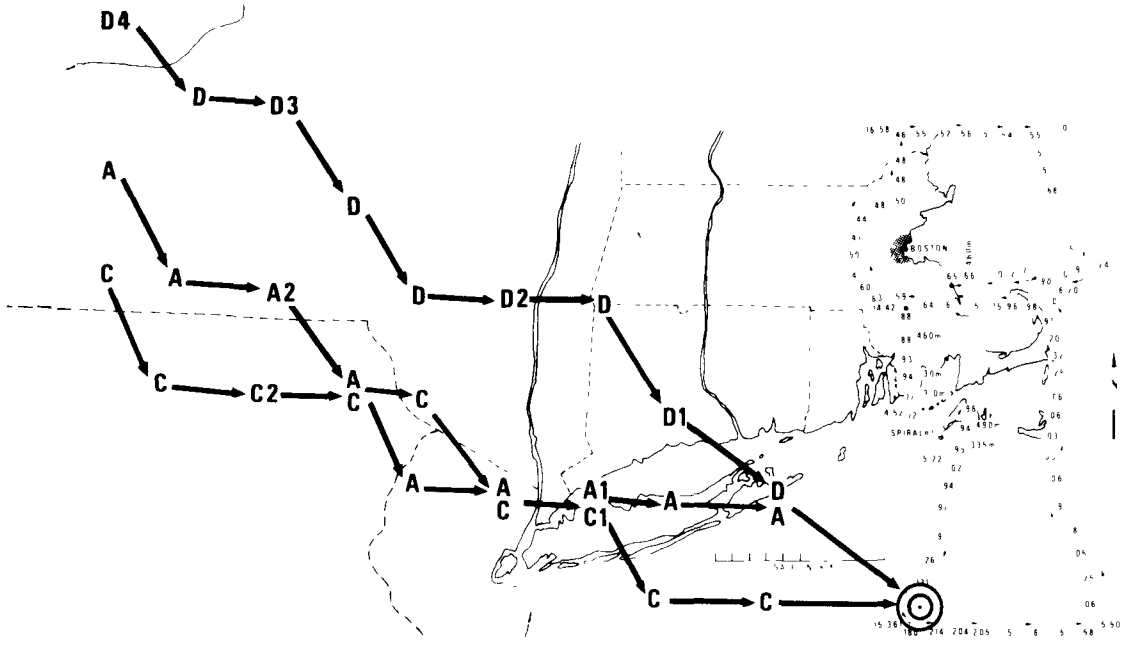

Figure 3. Computer trajectories for air parcel between 300 m AGL and 600 m AGL for August 14, 1975: A terminates at ◎ at 1900 EDT; C terminates at ◎ at 0700 EDT; D terminates at ◎ at 1300 EDT.

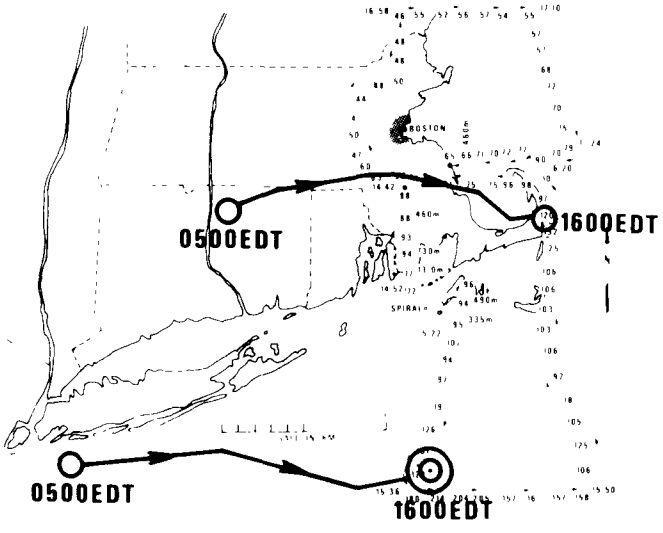

Figure 4. Hand-drawn trajectories for air parcels at surface level by time and space, terminating at 1600 EDT August 14, 1975.

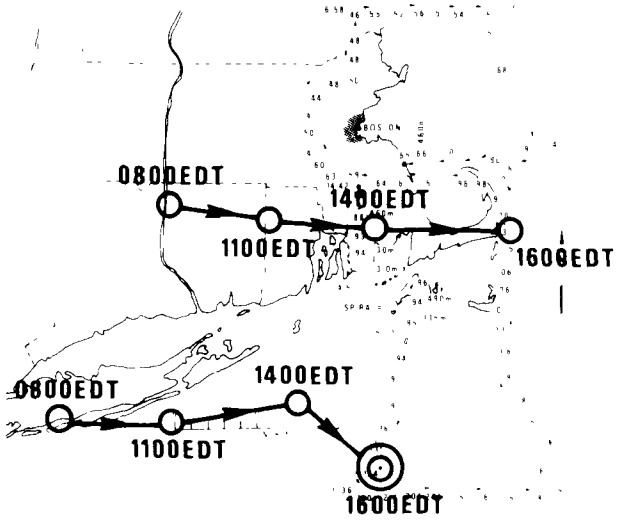

Figure 5. Hand-drawn trajectories for air parcels at 305 m AGL, terminating at 1600 EDT August 14, 1975.

Figures 4 through 7 were prepared by hand by our staff meteorologist and represent a best judgment air trajectory analysis. The basis for these trajectories is the extensive pibal and radiosonde data collected during the NOTS. The trajectories in Figure 4, at surface level, indicate generally westerly flow from early in the morning until late afternoon. Figure 5, at 305 m AGL, shows air flow generally from the west-southwest through west-northwest. The trajectories in Figure 5, at 610 m AGL, show a more north-westerly component for the air at this altitude. These figures appear to offer a rationale for the divergence of measured ozone concentrations in the different sectors of the flight. These air masses appear to have passed over land areas with different precursor emission potential; e.g., New York City vs. upstate Connecticut.

Figure 7 is a combination of the surface trajectory of Figure 4 and the 305 m AGL trajectory of Figure 5. Figure 7 represents a backward trajectory from points on the flight pattern, suggesting the ground area swept by the column of air from the surface to 305 m AGL from 0800 EDT to 1600 EDT. Although this is a subjective analysis neglecting vertical motion and based only on limited data, it can be concluded that a sizeable percentage of the air arriving at these points at 1600 EDT came from somewhere in the shaded areas between the surface and 305 m AGL.

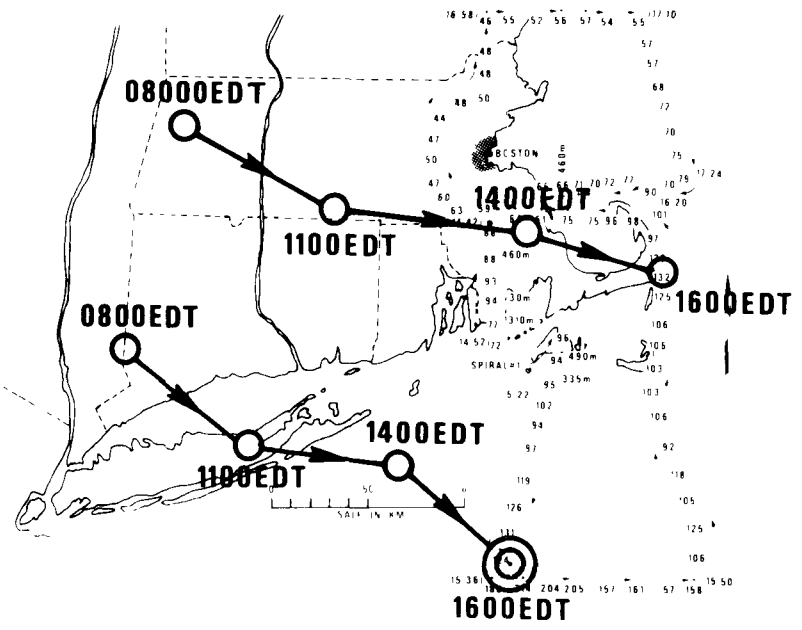

Figure 6. Hand-drawn trajectories for air parcels at 610 m AGL, terminating at 1600 EDT August 14, 1975.

These subjective trajectories compare favorably with the computer-generated trajectories, and are consistent with the hypothesis that the high ozone air was influenced by urban sources of ozone and ozone precursors (e.g., New York City, Newark), while the low ozone air was influenced by more rural sources of these air contaminants (e.g., upstate New York). The paucity of wind data over marine areas and the inherent errors of trajectory analysis limit definitive conclusions regarding ozone and ozone precursor transport.

With due regard for these limitations and the assumption of non-interaction of the ozone-ocean interface, the present analysis indicates that elevated ozone values were measured 250 km downwind of the New York City area.

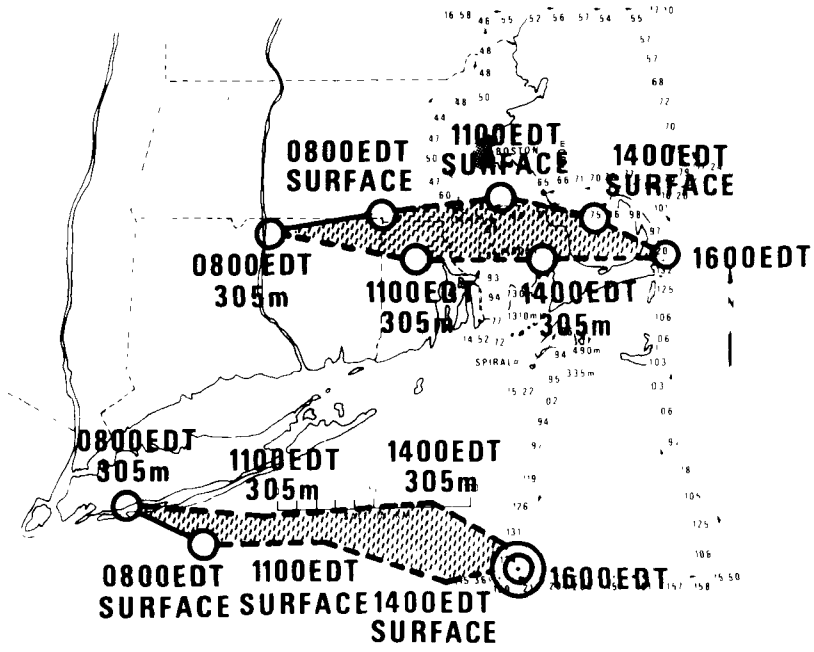

Figure 7. Combination of surface and 305 m AGL trajectories showing ground area swept by air arriving at the bull's-eye at 1600 EDT August 14, 1975.

CONCLUSIONS

Ozone data collected from an airborne platform over a wide area off the northeastern seaboard on August 14, 1975, show two basic regimes: high ozone (>0.08 ppm) in the southern sector of the area, low ozone (<0.08 ppm) in the northern sector. Vertical profile information suggests that ozone may not be well-mixed throughout the mixing depth over the ocean. Two separately-generated air parcel trajectories imply that the high ozone air measured in the southern flight sector passed over highly urbanized areas of New York and New Jersey on the morning of August 14, whereas the low ozone air measured in the northern flight sector was over rural areas of southern New England on the same morning. This suggests that ozone and/or ozone precursors have been transported at least 250 km downwind from a large source area.

Transport of air parcels over land surfaces will undoubtedly have a greater dispersive effect on air concentrations of air parcel constituents than transport over marine surfaces. However, under suitable meteorological conditions, transport winds could clearly carry an air parcel from the New York Metropolitan area as far as the Boston Metropolitan area, the oxidant burden of which exceeds the National Ambient Air Quality Standard.

REFERENCES

Blumenthal, D.L., W.H. White, R.L. Peace, and T.B. Smith. Determination of the Feasibility of the Long-Range Transport of Ozone or Ozone Precursors. Meteorology Research, Inc. Prepared for the U.S. Environmental Protection Agency, EPA-450/3-74-061, November 1974.

Cleveland, W.S., B. Kleiner, J.E. McRae, and J.L. Warner. Photochemical Air Pollution: Transport from the New York City Area into Connecticut and Massachusetts. Science, 191:179-181, 1976.

Environmental Protection Agency, Northeast Oxidant Transport Symposium, Research Triangle Park, North Carolina, January 20-21, 1976 (to be published).

Hester, N.E., R.B. Evans, D.T. Mage, J.L. Pierett, G. W. Siple, and J. J. van Ee. Some Considerations in Collecting Valid Data with Airborne Platforms. Proceedings of Specialty Conference on Air Pollution Measurement Accuracy as It Relates to Regulation Compliance, Air Pollution Control Association, Pittsburgh, 1976.

Siple, G.W., C.K. Fitzsimmons, J.J. van Ee, and K. F. Zeller. Air Quality Data for the Northeast Oxidant Transport Study, 1975: Final Data Report. U.S. Environmental Protection Agency (to be published).

AIRBORNE MEASUREMENTS OF PRIMARY AND SECONDARY POLLUTANT CONCENTRATIONS IN THE ST. LOUIS URBAN PLUME

N. E. Hester, R. B. Evans, F. G. Johnson, and E. L. Martinez*

ABSTRACT

Helicopters instrumented with air pollution monitors were used to characterize the urban plume of metropolitan St. Louis, Missouri. Maximum oxidant and particulate concentrations were found well downwind of the city and over rural areas. The maxima for both ozone and particulate were usually found to coincide. A parcel of air, characteristic of a period of high emissions due to morning rush hour traffic, was discovered within the urban plume. Power plant plumes superimposed on the urban plume were found to decrease the concentration of ozone in the urban plume for distances as great as 60 kilometers.

INTRODUCTION

Several studies during the last 5 years have shown ozone (O_3) concentrations that exceeded the federal standards in rural areas. A recent study by the United States Environmental Protection Agency of the phenomena concluded that these high ozone values could not be attributed to natural sources (EPA, 1975). The high ozone levels seemed to be related to a combination of local man-made sources and the transport of ozone and ozone precursors into rural areas from upwind urban areas.

As part of the Regional Air Pollution Study (RAPS) personnel from the Environmental Monitoring and Support Laboratory, Las Vegas, Nevada, made a number of flights with instrumented helicopters to measure ozone and related parameters in the St. Louis, Missouri, urban plume during the summer of 1975 (Allen 1973). These measurements were requested by the EPA Office of Air Quality Planning and Standards to aid in developing better criteria for the siting of monitoring stations for the reactive pollutants nitrogen oxides (NO_x, i.e., NO, NO_2) and ozone. In this report, the results of five flights made during July and August are discussed. Further flights in this program were conducted during the summer of 1976; however, the data have not yet been analyzed.

*N.E. Hester, R.B. Evans, F.G. Johnson, U.S. Environmental Protection Agency, Las Vegas, Nevada 89114.
E. L. Martinez, U.S. Environmental Protection Agency, Research Triangle Park, North Carolina 27711. (On assignment from National Oceanic and Atmospheric Administration, U. S. Department of Commerce.)

A close examination of the data from the 1975 flights provides insight into the chemical transformations which occur in urban plumes, and reveals the contribution of the city to the pollution problems of the surrounding rural areas.

EXPERIMENTAL

INSTRUMENTATION AND TECHNIQUE

The helicopters used in this study were instrumented to measure ozone (O_3), nitric oxide (NO), total oxides of nitrogen (NO_x), sulfur dioxide (SO_2), temperature, dewpoint, particulate light scattering, pressure altitude, air speed, compass heading, and navigational position. A more detailed description of the helicopters' capabilities, limitations, and instrumentation, and a description of the data collection and processing techniques have been published previously (Hester et al., 1975a, 1975b).

The wind data used in this study were obtained from four stations which were operated continually by RAPS during the time the helicopter flights were made. Wind measurements were taken by pilot balloons at approximately one-hour intervals. The locations of these four stations, indicated as Pibal 141, 142, 143, and 144, are plotted on the map shown in Figure 1. The wind data reported in Table 1 represent the mean and standard deviation of the speed and direction readings taken between 0600 and 1800 Central Standard Time (CST) at all four pibal stations on the days of the experiments.

TABLE 1. MEAN WIND SPEED AND DIRECTION BY DATE

Date	Altitude (MSL)	Wind Speed (Mean ± Std. Dev.)	Direction (Mean ± Std. Dev.)
July 15, 1976	200M	5.7 MPS ± 2.3	198° ± 36
	250M	5.9 MPS ± 2.5	200 ± 37
	300M	5.8 MPS ± 2.6	205 ± 40
	350M	5.7 MPS ± 2.7	208 ± 43
July 18, 1975	200M	8.0 MPS ± 3.3	229 ± 21
	250M	8.6 MPS ± 3.7	231 ± 18
	300M	9.2 MPS ± 4.1	232 ± 16
	350M	10.0 MPS ± 4.7	232 ± 15
August 3, 1975	200M	5.9 MPS ± 2.3	10 ± 16
	250M	6.0 MPS ± 2.2	12 ± 16
	300M	6.3 MPS ± 2.3	12 ± 16
	350M	6.5 MPS ± 2.5	12 ± 16
August 6, 1975	200M	7.0 MPS ± 2.9	30 ± 18
	250M	7.1 MPS ± 2.8	31 ± 17
	300M	7.1 MPS ± 2.8	31 ± 17
	350M	6.9 MPS ± 2.9	32 ± 17

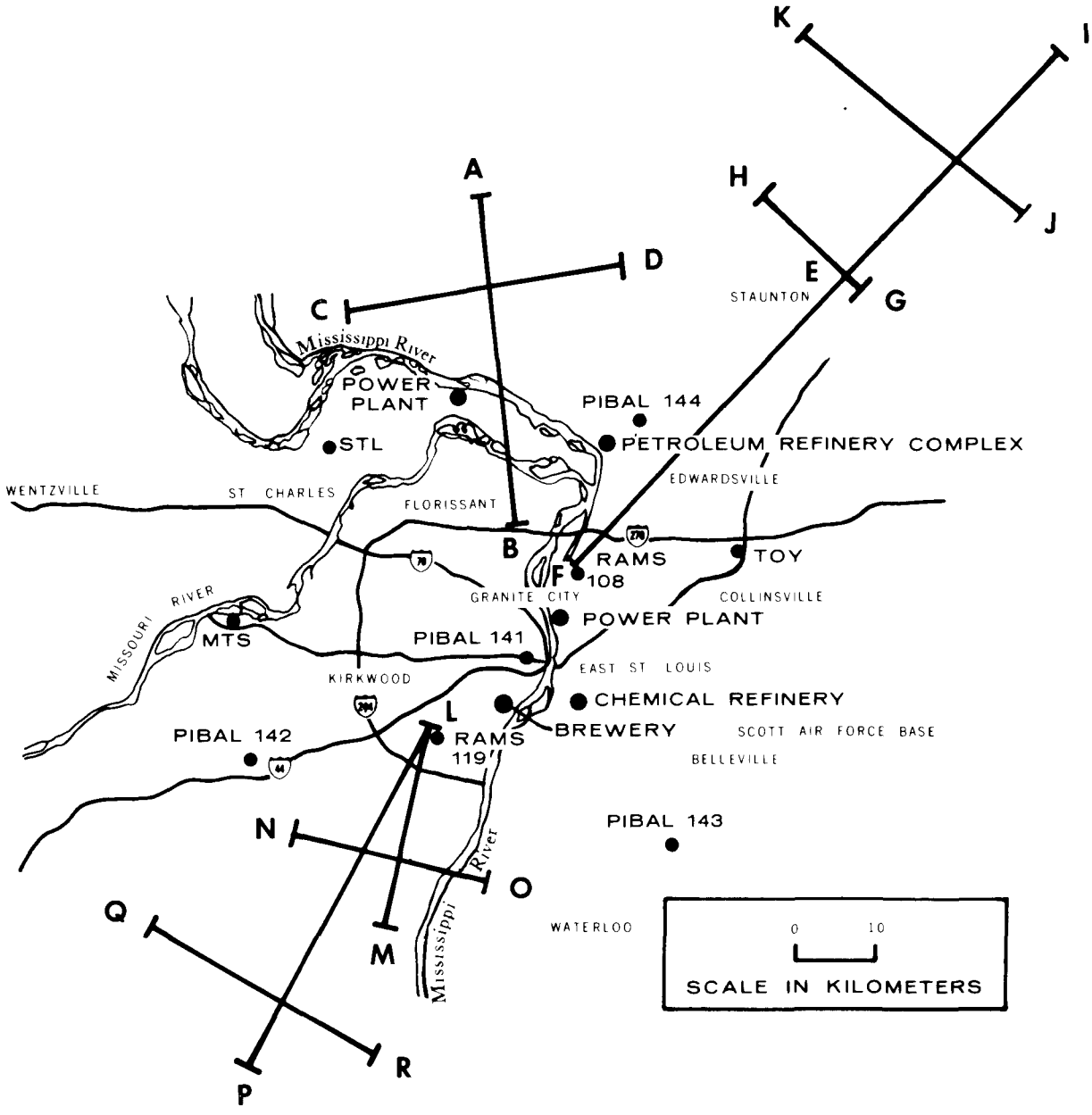

Figure 1. St. Louis map with aircraft flight patterns superimposed.

Flight patterns for each experiment were planned based on the most recent forecast of wind speed and direction coupled with the most recent pibal measurements from one or more of the four pibal stations. The point chosen to begin each day's sampling flight was, by best estimate, along the centerline of the urban plume, and near the outer edge of the metropolitan area. The first leg of each flight proceeded with the wind away from the city at an altitude of 305 m (1,000 feet) mean sea level (MSL). Ground elevations in the St. Louis area are typically 120 to 180 m MSL. The helicopter maintained a constant air speed of 111 kilometers per hour (60 knots). A maximum was sought in

pollutant concentration as the aircraft proceeded. On morning flights, the maximum in NO concentration was sought, and on afternoon flights, the maximum in ozone concentration was sought. The first leg of each flight proceeded past the point of the pollutant maximum until pollutant levels had ceased to fall sharply. At this point, a 180° turn was made. In some flights, where it was desired to better define the plume, the return leg proceeded all the way back to the starting point. However, most of the flights returned directly to the point of maximum pollutant concentration along the flight path, and then proceeded to fly a cross section of the urban plume.

The cross sections were determined by flying flight legs at 90° to the wind direction at 305 m MSL until the outer boundaries of the plume were defined. In some cases, the cross section revealed that the estimates of the position of the plume centerline had been somewhat in error, and higher pollution levels were found.

After the cross section was completed, the aircraft returned to the position of the maximum ozone or NO concentration and performed a vertical distribution of pollutants.

RESULTS BY DATE

July 15, 1975 (Afternoon)

On this date, the wind was steady from the south (see Table 1) and the flight patterns shown on Figure 1 as AB and CD were flown. The data from these flight patterns and from the vertical spiral are shown in Figures 2a, 2b, and 2c.

The data in Figure 2a from the flight down the plume axis, AB, revealed that the maximum ozone concentration (approximately 0.14 ppm) was 25 km downwind of B, the point closest to the city (approximately 40 km downwind of center of the city). The ozone maximum corresponds with the maximum light scattering coefficient (B_{scat}) reading, and with NO and SO_2 levels that were so low that they were at the noise level of the instruments. Near the furthest point out on the flight, point A, a sudden rise in SO_2 concentration and a sharp drop in ozone concentration were observed. This observation was attributed to wind direction, and the plume from the Portage des Sioux power plant (indicated in Figure 1, just north of the city) intersected the flight path. The power plant plume could be followed visibly to this general area.

The data in Figure 2b from the cross section flight (CD) shows that the width of the urban plume looking at O_3 levels was about 20 km and had a skewed shape. Evidence for mixing of the urban plume with the power plant plume was not evident in the cross section data. It is possible that the power plant plume was elevated above the flight altitude and did not descend to flight levels until it reached the vicinity of point A.

The vertical profile through the urban plume (Figure 2c) shows that there were three temperature inversions over the area at the time of the flight, at about 400 m, 500 m and at 900 m. The inversions did not have a strong effect on the pollutant profile with the exception that the NO levels showed

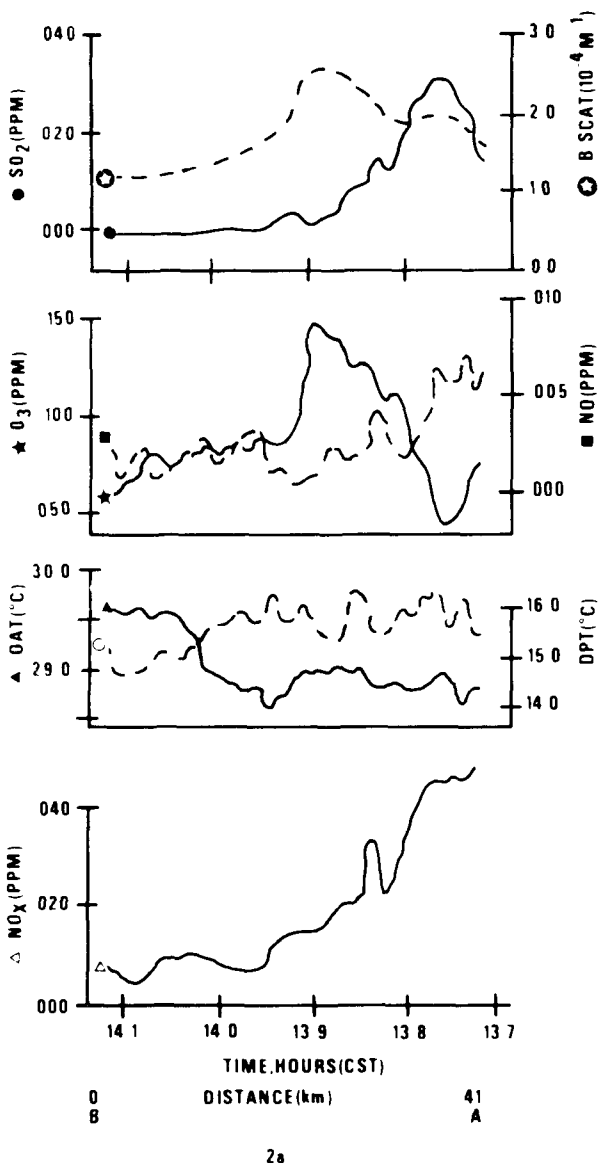

AXIAL PATTERN

Figure 2a. Data, collected July 15, 1975, from flight pattern AB (Figure 1).

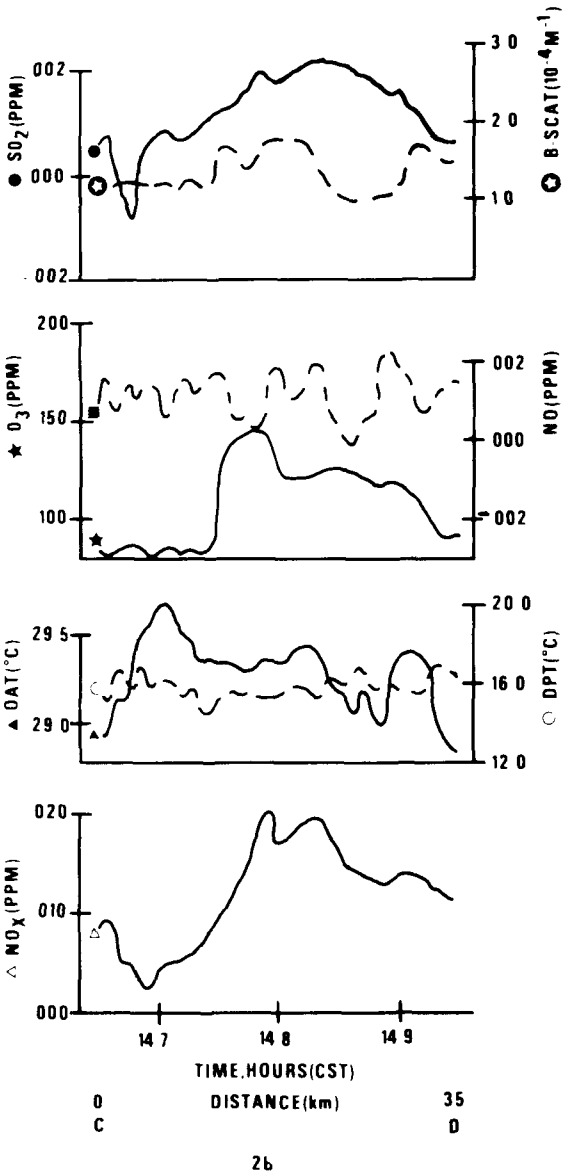

CROSS-SECTION PATTERN

Figure 2b. Data, collected July 15, 1975, from flight pattern CD (Figure 1).

a drop below the lower inversion. The pollutant profiles generally indicated a trend of decreasing concentrations with increasing altitude, with the exception of SO_2 whose concentration was too low to measure accurately.

July 18, 1975 (Morning and Afternoon)

A steady wind from the southwest (see Table 1) determined the flight pattern shown in Figure 1 for this date. Two sets of flights were made, one in the morning and one in the afternoon. The morning set of flights sought

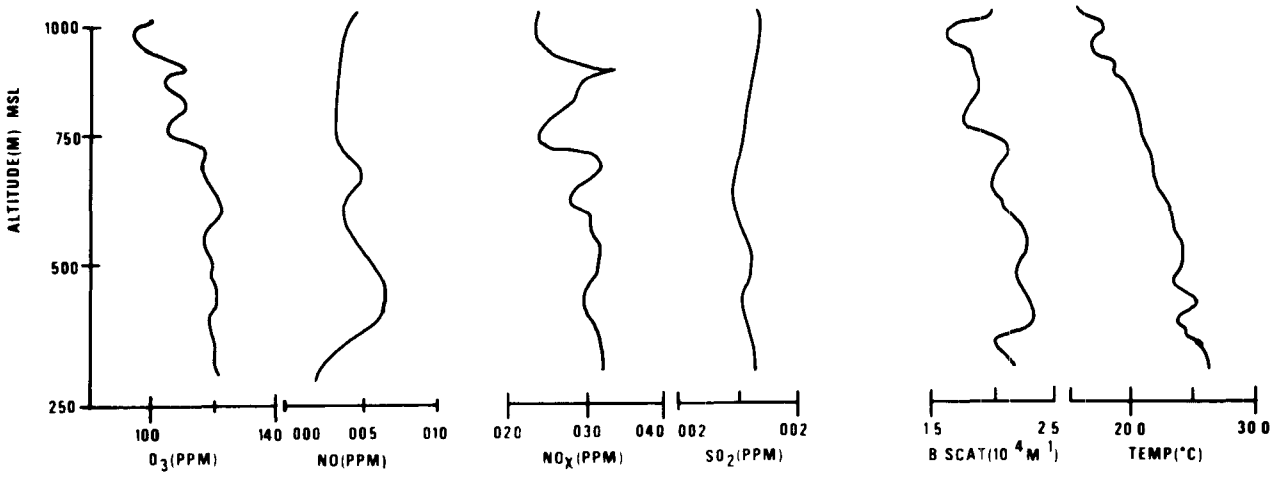

Figure 2c. Pollution data collected July 15, 1975, vertical spiral through urban plume (15:23-15:43 CST).

data on the maximum NO concentration in the urban plume, and the afternoon set of flights sought data on the ozone maximum.

The morning flight followed the patterns shown in Figure 1 as EF and GH. The data from these flight patterns and from a vertical spiral are shown in Figures 3a, 3b, and 3c. Maxima for NO and B_{scat} occurred approximately 30 km downwind from point F; however, operator misjudgment resulted in the cross section of the plume being measured approximately 10 km downwind of where the morning NO maximum occurred. By judging where sharp changes occur in pollution levels in Figures 3a and 3b, particularly B_{scat} readings, it is possible to see that there is a parcel of air with higher primary pollutant levels within the urban plume that is approximately 44 km long and 15 km wide. The existence of such a parcel could be explained by assuming that the city produces a large pulse of NO and particulate during the morning traffic rush, and that the parcel of air containing these pollutants moves downwind more or less intact.

The morning vertical profile, Figure 3c, revealed a great deal of temperature variability. Two low-level inversions were present at approximately 400-500 m and a series of inversions occurred above 750 m. The pollutant profiles did not appear to be correlated to the temperature profiles, and in general did not show a consistent pattern.

Patterns FI and JK in Figure 1 were followed on the afternoon flight of July 18. The data from these flights are plotted in Figure 4a, 4b, and 4c. The ozone concentration in the urban plume reached a maximum approximately 50 km downwind of the starting point of the flight, point F. At this maximum, the ozone concentrations reached a level that was twice that seen in the morning flight at the positions of highest NO and B_{scat} and was above the federal standard of 0.08 ppm. The maximum B_{scat} occurred at the same location as the maximum ozone readings; and the maximum B_{scat} level was approximately the same as seen in the morning flight. The NO and NO_x maximum concentrations were about one-half to one-third lower than morning levels, and it was no longer possible to define distinct boundaries for the parcel of air which was seen

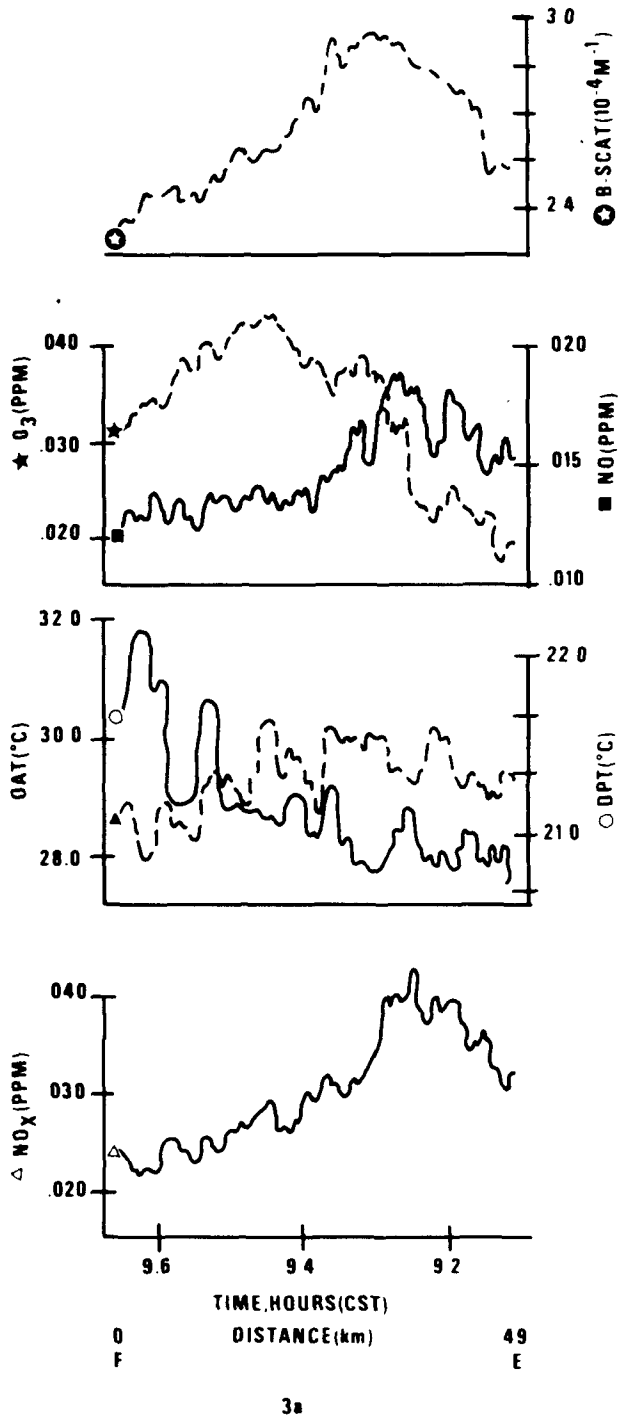

3a

AXIAL PATTERN

Figure 3a. Data, collected the morning of July 18, 1975, from flight pattern EF (Figure 1).

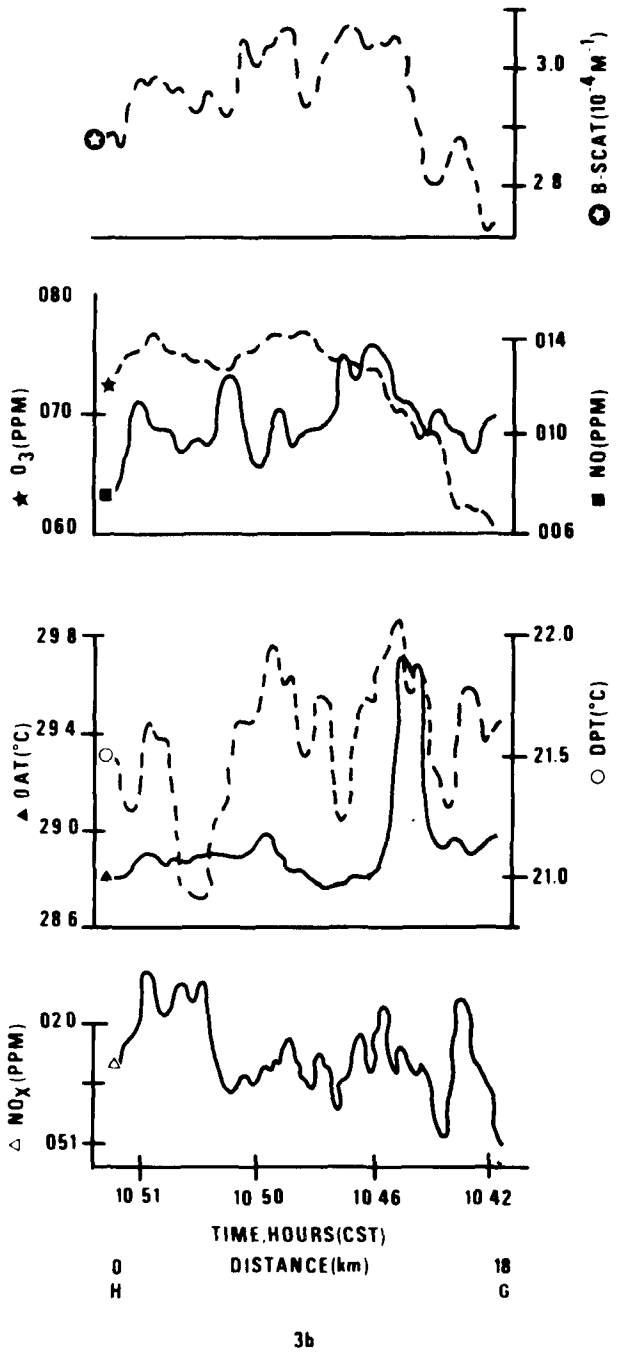

3b

CROSS-SECTION PATTERN

Figure 3b. Data, collected the morning of July 18, 1975, from flight pattern GH (Figure 1).

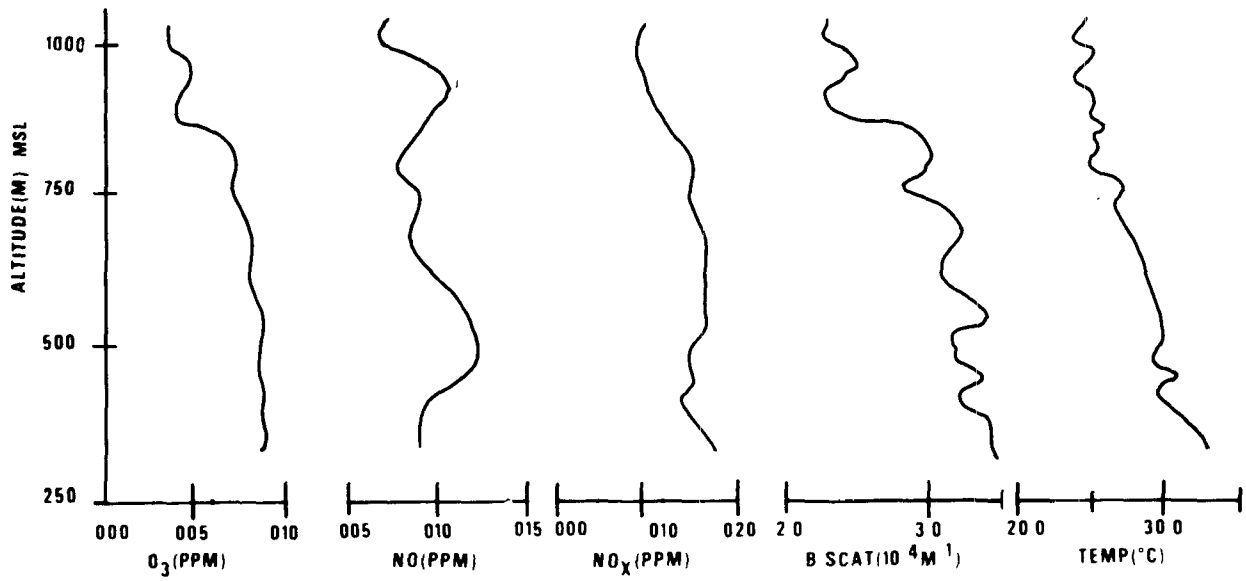

Figure 3c. Pollution data collected the morning of July 18, 1975, vertical spiral through urban plume (10:77-10:88 CST).

during the morning flight.

Comparing the maxima for individual pollutants can be misleading. The pollutant burden can provide a better understanding of the quantities of pollutants that have been produced. For example, the maximum B_{scat} readings were about the same in the morning and afternoon flights; however, the volume of air in which these concentrations were distributed was much larger in the afternoon, as indicated by the difference in plume widths shown in Figures 3b and 4b, and the difference in vertical profiles shown in Figures 3c and 4c. These differences indicate that there had in fact been a large production of particulate matter in the plume as it has moved away from the city. Similar consideration should be applied to the other pollutants in order to get a proper picture of the plume impact on the surrounding rural area.

The vertical temperature profile through the plume during the afternoon showed none of the temperature inversions present in the morning. The vertical pollutant profiles from the afternoon study were similar to the morning profiles in that they revealed little in the way of a definable pattern.

August 3, 1975 (Afternoon)

The wind on this date was from the north-northeast (Table 1) and the patterns shown in Figure 1 as LM and NO were flown during the early afternoon. The data are presented in Figures 5a, 5b, and 5c. August 3 was a Sunday, and this set of data provides a picture of the weekend urban plume which can be compared to the weekday plume characteristics in the other studies. The maximum ozone concentrations in the plume (again levels above the federal standard) were found 17 km downwind from the flight starting point, point L. As seen in previous studies, the position of the maximum B_{scat} readings generally corresponds to the position of the maximum ozone readings. The NO readings on

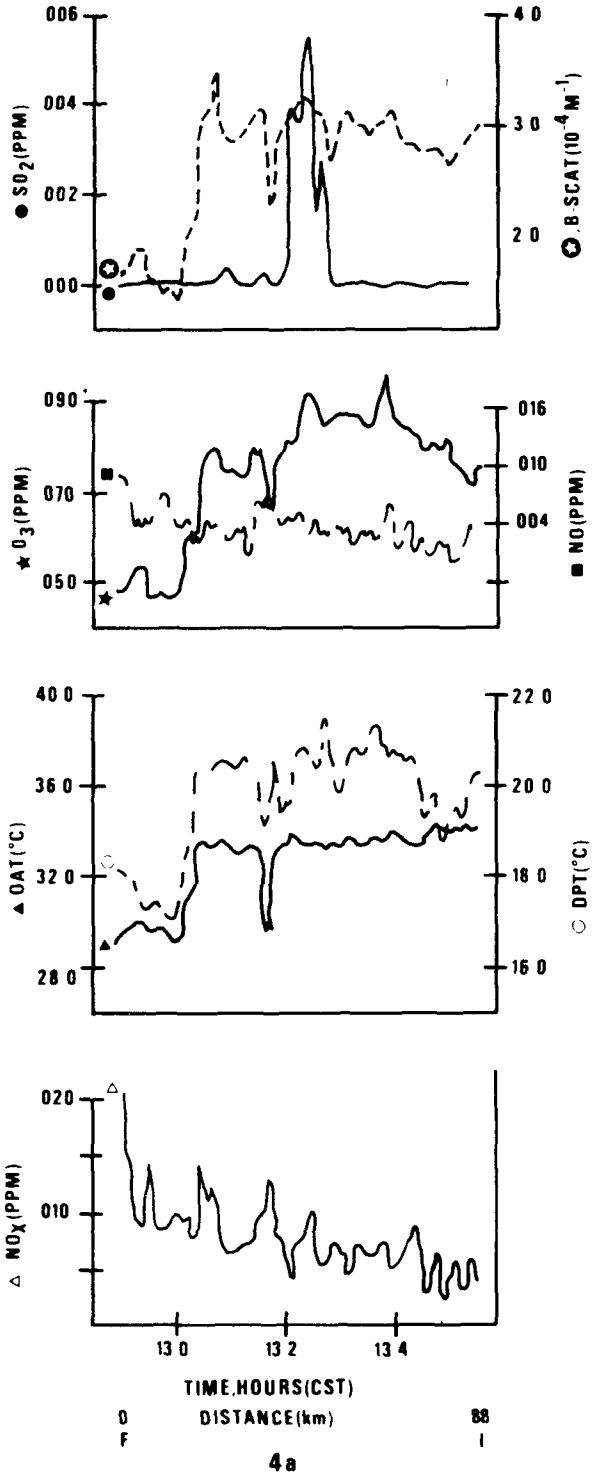

4a

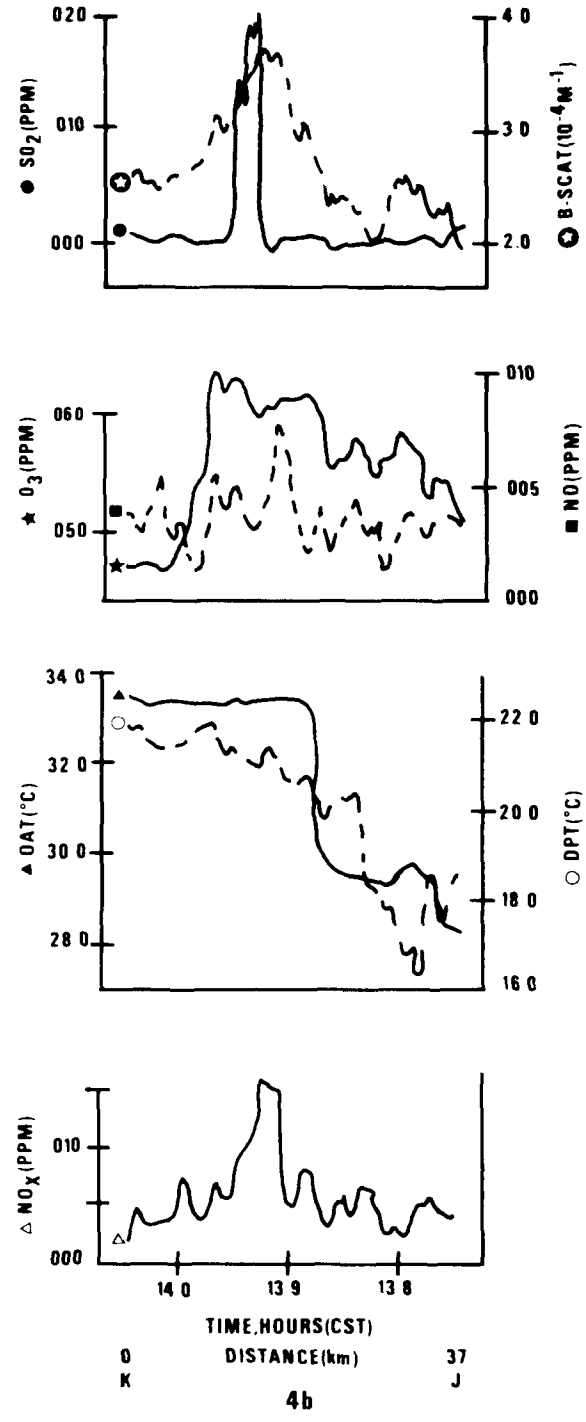

4b

AXIAL PATTERN

Figure 4a. Data, collected the afternoon of July 18, 1975, from flight pattern FI (Figure 1).

CROSS-SECTION PATTERN

Figure 4b. Data, collected the afternoon of July 18,1975, from flight pattern JK (Figure 1).

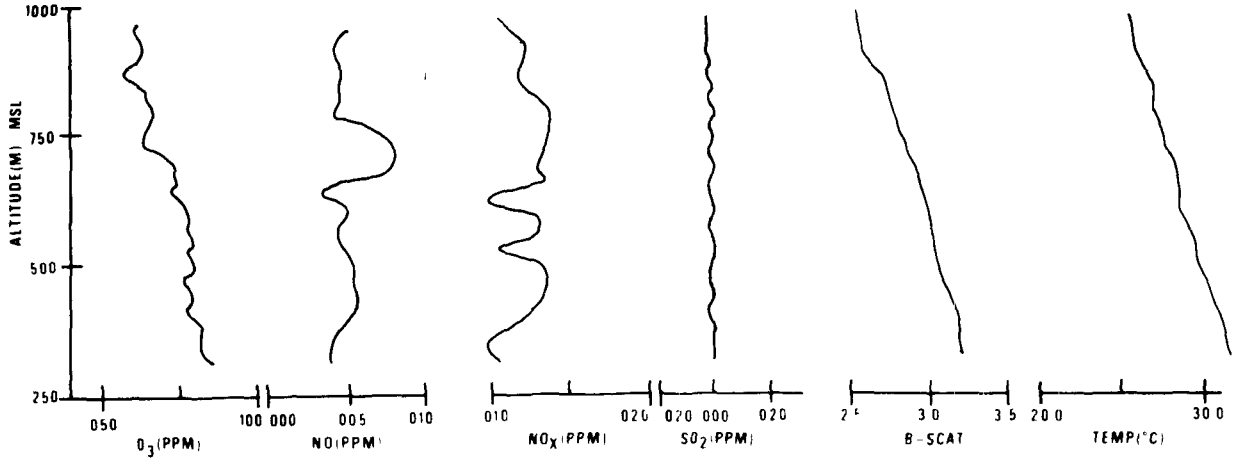

Figure 4c. Pollution data collected the afternoon of July 18, 1975, vertical spiral through urban plume (14:27-14:45 CST).

flight pattern LM were at the noise level of the instrument. The NO_x readings were somewhat elevated in the plume, and remarkably consistent throughout the entire flight. The SO_2 readings were elevated near the farthest point on the flight pattern, point M. These high SO_2 levels are probably due to the point sources along the Mississippi River whose full impact is better seen in the cross section flight pattern.

The cross section of the plume is extremely interesting in that it not only provides insight into the character of the urban plume, but also insight into the effects of large point source plumes superimposed on the urban plume. The data collected near point N (Figure 5b) show high SO_2 and NO_x readings. The most probable source of the SO_2 is the Portage des Sioux power plant located north of the city and approximately 60 km from the point where the measurements were made. The Portage des Sioux plume could be observed visually over the city approximately 30 km from the source heading toward the area where the measurements were made. Further, there are no other point sources upwind capable of producing a plume with the measured concentrations and with a plume width of approximately 6-7 km (Figure 5b). At the other end of this cross section flight pattern, point O, high SO_2 levels were again observed, as well as high B_{scat}, and the highest ozone readings. These high readings can be attributed to a number of point sources along the Mississippi River. The refinery complex at Wood River, Illinois, the power plant near Granite City, Illinois, and a brewery in St. Louis, Missouri, were all upwind of point O. All of the listed sources could contribute to the SO_2 and particulate levels. The refinery is a large source of hydrocarbons and NO_x which could have acted as precursors for the photochemical production of ozone and additional particulates.

The vertical profile of the plume, Figure 5c, showed a temperature inversion layer at 850 m. The inversion seemed to have little effect on the pollutant profiles. The pollutant levels remained fairly uniform with altitude.

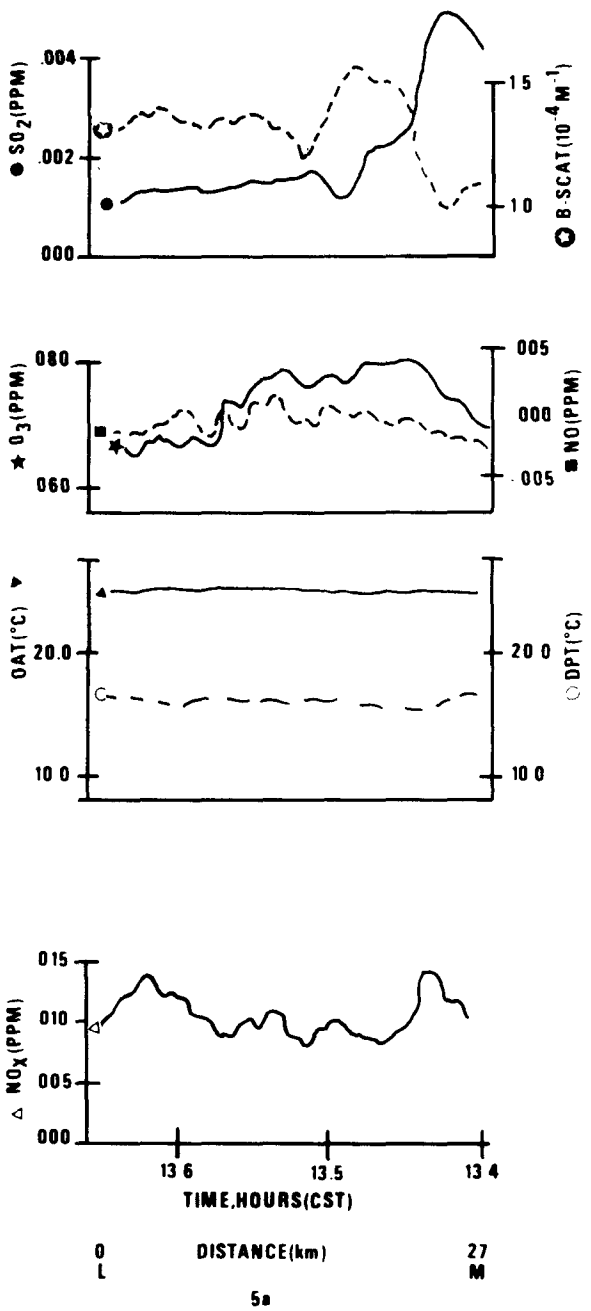

5a

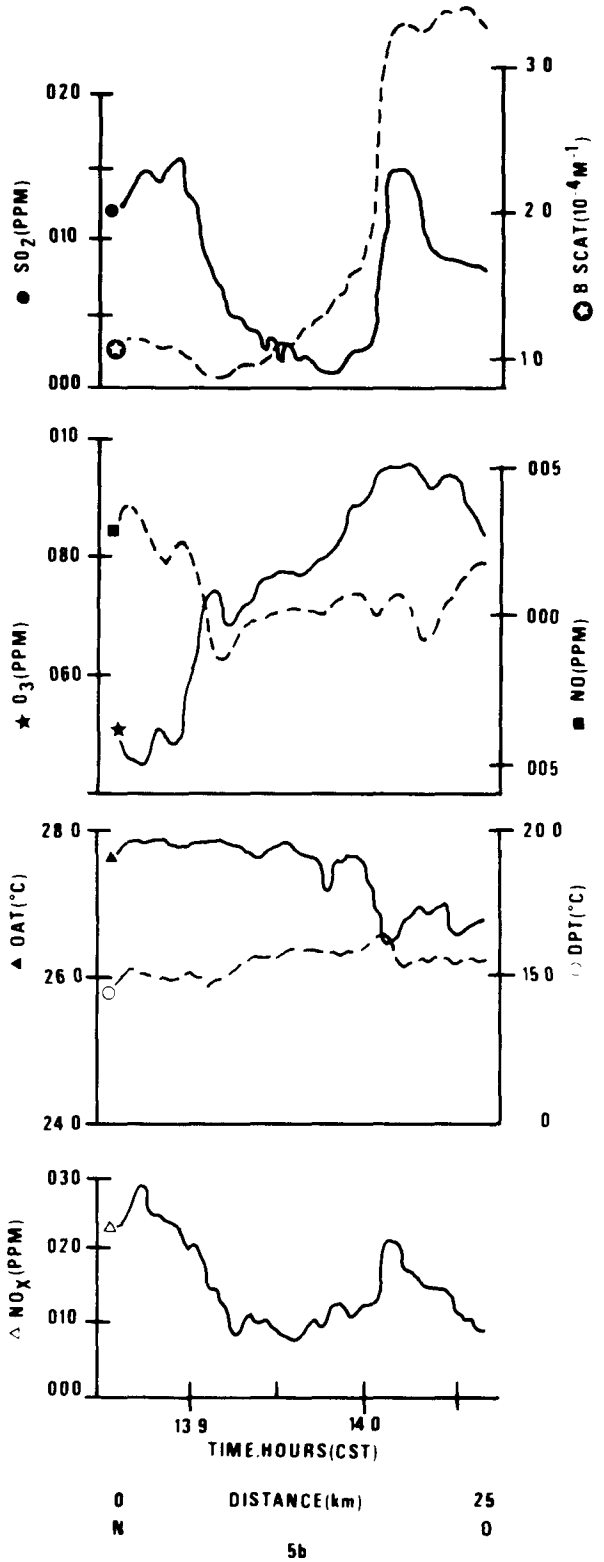

5b

AXIAL PATTERN

Figure 5a. Data, collected August 3, 1975, from flight pattern LM (Figure 1).

CROSS-SECTION PATTERN

Figure 5b. Data, collected August 3, 1975, from flight pattern NO (Figure 1).

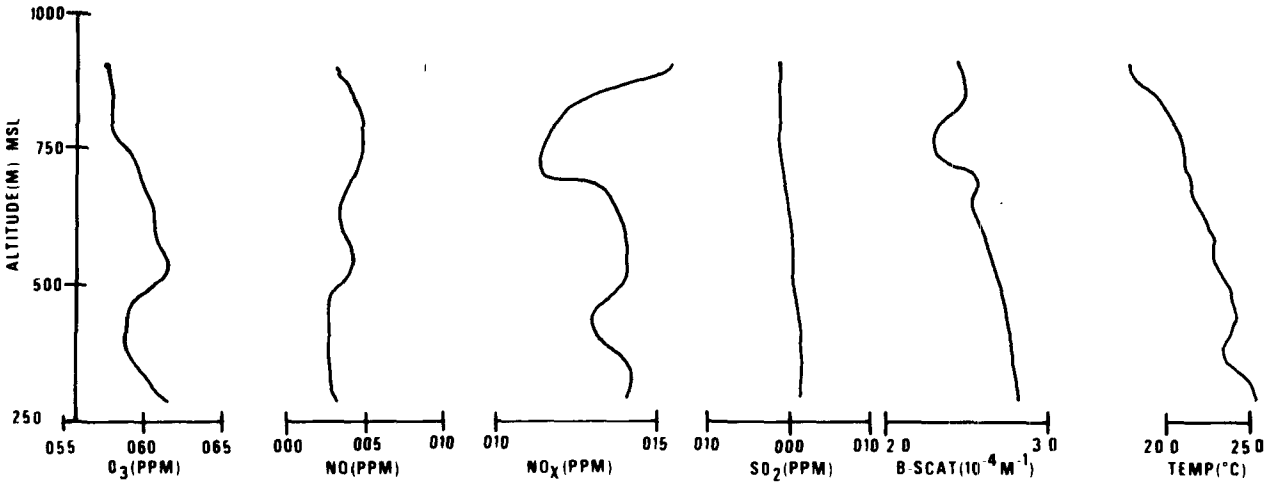

Figure 5c. Pollution data collected August 3, 1975, vertical spiral through urban plume (14:65-14:97 CST).

August 6, 1975 (Afternoon)

Winds from the north-northeast caused pattern LP and QR to be flown. The pattern with the plume, LP, showed that the maximum ozone concentration was 45 km downwind of the flight starting point (Figure 6a). The highest B_{scat} values again occurred with the highest ozone levels.

The cross section of the plume, pattern QR, revealed a well-defined urban plume with a width of about 30 km (Figure 6b). A slight depression in ozone concentration was seen near point R. Correspondingly high concentrations of oxides of nitrogen occurred at the same location as the depression in ozone. The NO_x were probably produced by a point source along the Mississippi River.

The vertical profile, Figure 6c, showed a low level temperature inversion at 365 m. A slight elevation in ozone and NO_x concentration is seen below the inversion but such a tendency was not apparent for the other pollutants.

CONCLUSIONS

This paper has reported the results of studies of the St. Louis urban plume on four days during the summer of 1975. Although the studies were done under a variety of meteorological conditions, several general conclusions can be made.

- The St. Louis metropolitan area produces a well-defined urban plume that could be easily traced 100 km downwind of the city.
- The St. Louis urban plume causes significant degradation of the air quality extending into rural areas downwind of the city. On July 15 and 18 and August 3, 1975, maximum ozone readings in excess of the

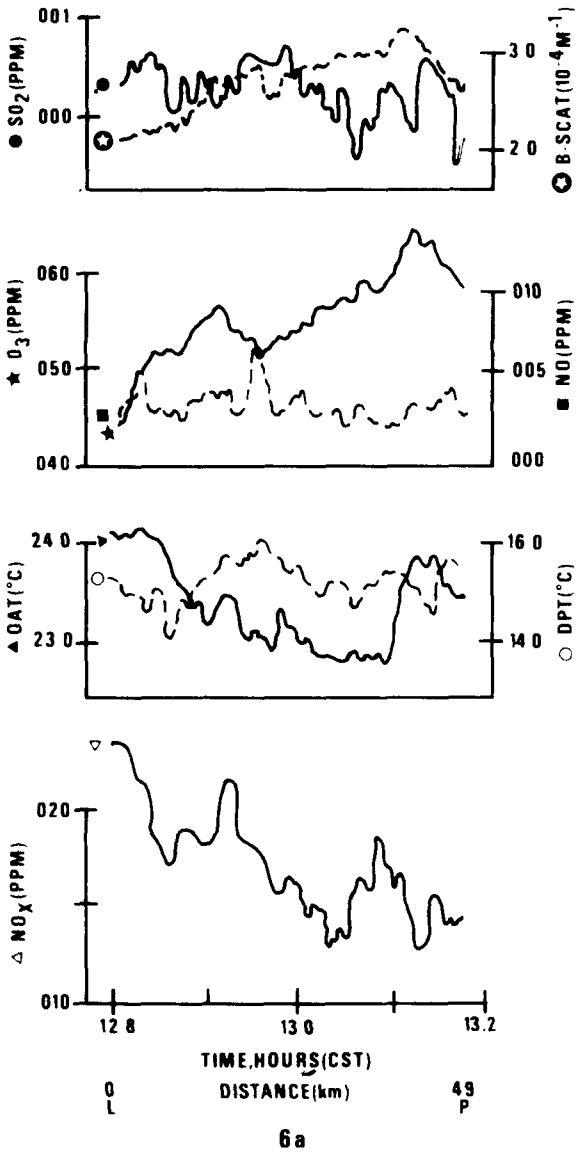

6a

AXIAL PATTERN

Figure 6a. Data collected August 6, 1975, from flight pattern LP (Figure 1).

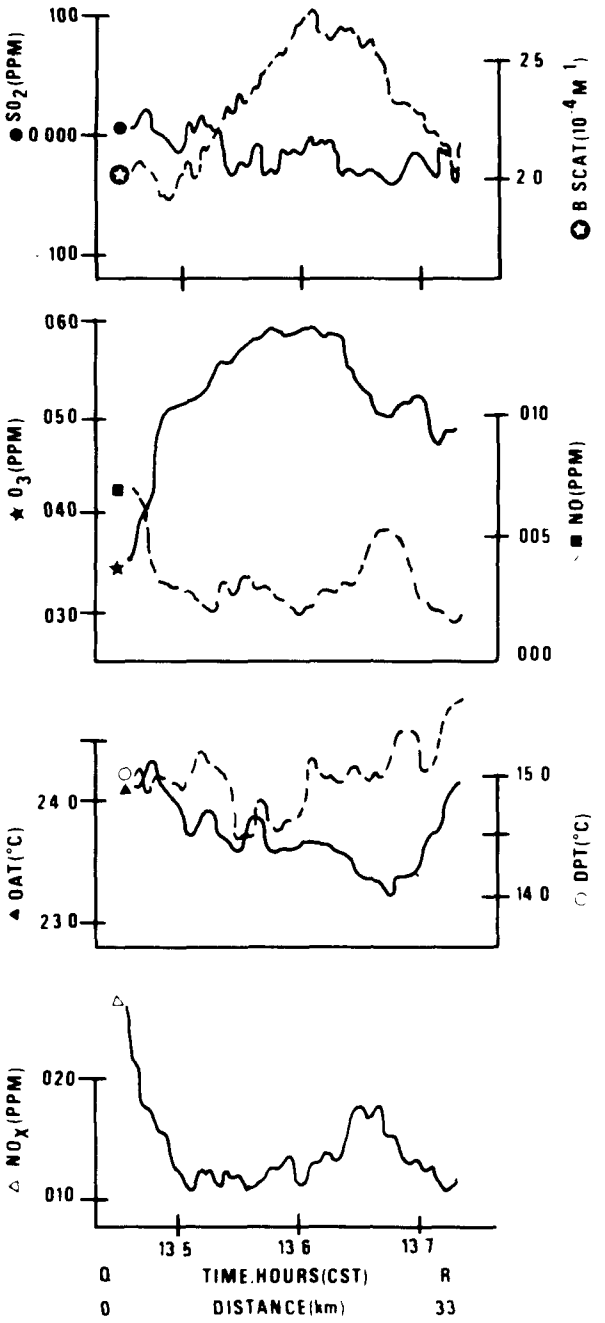

6b

CROSS-SECTION PATTERN

Figure 6b. Data collected August 6, 1975, from flight pattern QR (Figure 1).

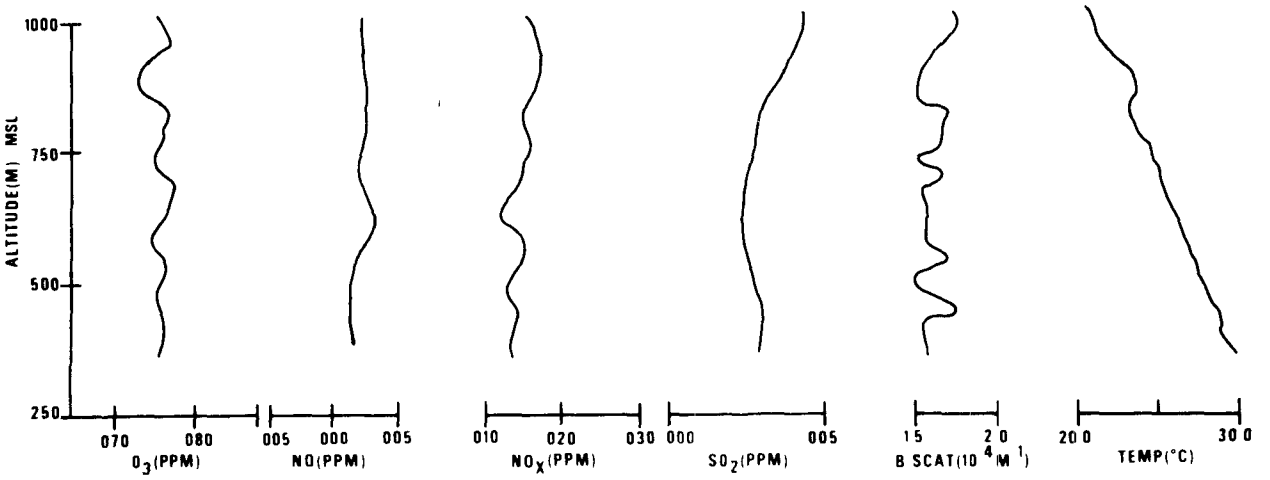

Figure 6c. Pollution data collected August 6, 1975, vertical spiral through urban plume.

federal 1 hour ambient standard were found at distances downwind from the edge of the city of 25 km, 50 km, and 17 km respectively. The measurements of high ozone readings were observed in the early afternoon, and there is a likelihood that higher levels at greater distances from the city may have occurred. This possibility was explored during the 1976 measurements.

- Downwind concentration maxima in ozone and particulate light scattering tended to coincide in each of the four afternoon plume studies. There are at least two possible explanations for this pehnomenon. The first explanation is that the production of ozone and the production of a large portion of particulate loading have a common chemical or photochemical reaction step that is rate-determining, and thus maximum levels occur in close proximity both temporally and spatially. The second explanation is that each time the urban plume was studied, the flight pattern passed through a parcel of air in the plume that was simply more polluted than the rest of the plume (e.g. a parcel of air from the morning rush hour traffic), and the high values of ozone and B_{scat} occurred together because of generally high precursor levels and not necessarily because of a common chemical or photochemical production step. The data from the morning flight on July 18 showed the existence of a distinct parcel of air with higher pollutant levels within the urban plume, and this result would support the second explanation. However, such a parcel would not have been expected in the Sunday data, and the maxima still correlated. Thus, further studies seem warranted to fully characterize the phenomena.

- Secondary pollutants, formed as the urban plume moved away from the city, seem to be the most significant components of the plume by early afternoon. The primary pollutants NO and SO_2 are, in general, depleted quite rapidly by dilution, chemical reactions, and other removal mechanisms as the plume proceeded away from the city, while

ozone and B_{scat} readings reached their highest values well downwind of the city.

- Power plant plumes within the urban plume appeared to cause depletion of ozone in the area of impaction on the urban plume. The plume from the Portage des Sioux power plant was observed impacting within the St. Louis urban plume on two separate days, July 15 and August 3, 1975. Depletion of ozone was observed at distances up to 60 km from the power plant.

DISCUSSION

Davis et al. (1974) reported studies of the effects of power plants on ambient air quality in the Washington, D. C., area. Depletion of ozone in plumes downwind of the power plants was found by Davis at distance $\leq$ 24 km, and a net increase in ozone concentration relative to air surrounding the plume was found beyond 24 km. The results reported in this work show depletion of ozone at 20 km from a power plant on July 15. This agrees with Davis' work. However, the data reported for August 3 revealed that the ozone depletion occurred to distances of 60 km, a significantly greater distance than reported by Davis. The Portage des Sioux power plant investigated in this study burns only coal in a cyclo burner system which emits fairly high concentrations of NO. The plant studied by Davis burned a fuel mixture of 75% oil and 25% coal. It is probable that the difference in combustion characteristics of these two plants could possibly explain the differences in effects of the power plant plumes. The Portage des Sioux plant probably emits higher levels of NO than the plant studied by Davis and causes depletion effects of the plume to be seen for greater distances.

White et al. (1976) reported results of measurements of ozone and light scattering aerosols in the St. Louis plume on one of the same days covered in this report. The results and conclusions reported in this work are in essential agreement with those of White with one major exception. White assumed that a quasi-Lagrangian interpretation could be made on the urban plume, and that transport and emission parameters changed so slowly that neighboring points in the plume could be reasonably compared. Flux measurements were calculated based on this assumption. It is felt that their assumption is in error and validity of such flux calculations is open to question. It is generally known from ground-based measurements that urban areas produce relatively high levels of pollutants during the morning and evening rush traffic periods.

Demerjian et al. (1974) recently discussed this phenomenon in their review of photochemical smog formation. The data in this report, collected during the morning of July 18, indicate that the St. Louis metropolitan area emitted a pulse of highly polluted air during the morning traffic period, as expected, and that this pulse was moving downwind within the plume. Given that such a parcel of air existed within the plume, it cannot be assumed that adjacent points in the plume are comparable. Quasi-Lagrangian assumptions cannot be made unless the size and position of such a parcel of air is carefully documented during the time period when the plume was studied. White et al. made no such documentation.

REFERENCES

Allen, P. W. 1973. Regional Air Pollution Study - An Overview. Paper No. 73-21, Proceedings of the 66th Annual Meeting, Air Pollution Control Association.

Davis, D. D., G. Smith, and G. Klauber, 1974. Trace Gas Analysis of Power Plant Plumes via Aircraft Measurement: O_3, NO_x, and SO_2 Chemistry. Science 186, 733-736.

Demerjian, K., J. Kerr, and J. Calvert. 1974. The Mechanism of Photochemical Smog Formation. Advances in Environmental Science and Technology Vol. 4, 1-262, John Wiley and Sons, New York.

EPA. 1975. Control of Photochemical Oxidants-Technical Basis and Implications of Recent Findings. EPA-450/2-75-005.

Hester, N., R. Evans, C. Fitzsimmons, D. Mage, and M. Price 1975a. Helicopter Platform Air Pollution Data, I. The RAPS Program. Paper No. 75-40.4, Proceedings of the 68th Annual Meeting, Air Pollution Control Association.

Hester, N., R. Evans, D. Mage, S. Pierett, G. Siple, and J. van Ee. 1975b. Some Considerations in Collecting Valid Data with Airborne Platforms. Proceedings, Speciality Conference on Air Pollution Measurement Accuracy as Relates to Regulation Compliance, Speciality Conference, Air Pollution Control Association, New Orleans, Louisiana, October, 1975, pp 73-86.

White, W., J. Anderson, D. Blumenthal, R. Husar, N. Gillani, S. Fuller, W. Wilson. 1976. Formation and Transport of Secondary Air Pollutants: Ozone and Light Scattering Aerosols in St. Louis Urban Plume. Proceedings, 171st National Meeting, American Chemical Scoiety, New York, New York. (In Press)

OZONE IN HAZY AIR MASSES

R. B. Husar, D. E. Patterson, C. C . Paley and N. V. Gillani*

ABSTRACT

A case study of high ozone concentrations in a synoptic scale hazy air mass (blob) over the eastern half of the U.S. is reported. The data base includes (a) U.S. Weather Service Network for hourly visibility observations (300 stations); (b) the National Air Sampling Network for daily sulfate (60 stations in eastern U.S.); and (c) the SAROAD data base of EPA for daily peak ozone concentration (90 stations in eastern U.S.). Contour plots of visibility and sulfate concentrations show close spatial and temporal correspondence between haziness and high sulfate levels, and reveal the existence and transport of a synoptic scale hazy blob. Contour plots of ozone also reveal large areas with elevated ozone levels, whose location and spatial extent correspond roughly with those of the hazy blobs. Long term observations of ozone and haziness at a single station in St. Louis show the prevalence of high ozone levels on hazy days. Based on this case study, it is not possible to conclude whether sulfate formation is enhanced by the presence of elevated ozone levels.

INTRODUCTION

In this paper, we report a case study of an episode of high ozone concentrations in synoptic-scale hazy air masses over the eastern half of the United States. In recent years, ozone concentrations well in excess of the ambient air quality standard (0.08 ppm) have been observed in rural areas at distances of several hundred kilometers from known sources of ozone precursor gases (Coffey and Stasiuk, 1975). Rural ozone may be a product of atmospheric reactions involving anthropogenic (White et al., 1976) as well as biogenic emissions, and may also be due to the downward mixing of stratospheric ozone. The relative contributions of the various sources of rural ozone, and the role of synoptic meteorology, are not quantitatively established. High rural ozone concentrations, however, have been observed most frequently inside large slow-moving high pressure cells in midwestern and eastern U.S. (Ripperton and Worth, 1973).

The occurrence of large hazy air masses containing sulfate concentrations in excess of 20 $\mu g/m^3$ have also been reported recently (Hall et al., 1973; Husar et al., 1976). The present work was initiated to examine whether synoptic scale hazy air masses with high sulfate levels also contain high levels of ozone. It was hoped that certain relationships could be found between

*Washington University, St. Louis, Missouri.

these two noxious secondary pollutants which would shed some light on their origins.

The method of analysis is based principally on inspection of contour plots of sulfates, ozone and ground visibility data over the eastern half of the U.S. Air parcel trajectory analyses, surface wind data and local measurements of the pollutants in St. Louis are also consulted. The spatial and temporal density of the data base for national sulfate distribution is sparser than that for ozone. However, hourly surface visibility observations reported routinely from several hundred weather stations have been used previously as an effective surrogate for sulfate data during air pollution episodes (Husar et al., 1976).

DATA BASE FOR THE ANALYSIS

The following three sources of data have been utilized in this work.

U.S. WEATHER SERVICE NETWORK FOR HOURLY OBSERVATIONS (SERVICE A)

Values of ground level visual range and other weather parameters are recorded every hour at several hundred stations distributed over the U.S. The data from about 300 of these stations (Figure 1a) are available on magnetic tapes supplied by the National Climatic Center, National Oceanic and Atmospheric Administration (NOAA). The high spatial density of this network permits the meaningful use of computer contour plotting techniques. Using the visibility data, the spatial extent, the temporal evolution and the transport of hazy blobs* may be followed for several days by inspection of chronological visibility contour maps (Husar et al., 1976). Noon visibilities were chosen to minimize the effect of early morning high humidities. The noon relative humidity for inland stations ranged between 50 and 80%.

THE NATIONAL AIR SAMPLING NETWORK (EPA) FOR SULFATE

Hi-volume filter samples collected over 24-hour periods by this network are routinely analyzed for sulfate. The samples are collected every 12 days, simultaneously at all sampling locations. For the present analysis, we were able to obtain sulfate data for about sixty NASN locations in the eastern half of the U.S. The spatial distribution of these stations is shown in Figure 1b. Isopleths of sulfate concentrations are plotted manually from the available data at 12-day intervals.

THE SAROAD DATA BASE (EPA) FOR OZONE AND TOTAL OXIDANT

Ozone and oxidant concentrations are recorded regularly at aerometric monitoring stations reporting to the U.S. EPA. Hourly average values are obtained from EPA's SAROAD data bank for 89 sites located in the eastern half of the U.S. (Figure 1c). For each station, the diurnal ozone pattern

*In the context of this report, "blob" is used synonymously with "hazy air mass."

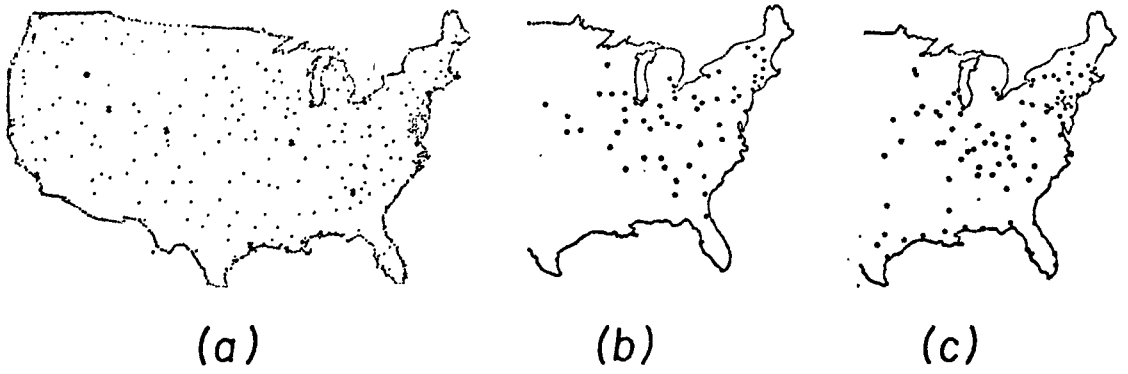

Figure 1. Geographical distribution and density of network stations: (a) National Weather Service Network for visibility; (b) National Air Sampling Network for sulfate; (c) EPA/SAROAD network for ozone.

was inspected and the daily peak concentration was chosen as the ozone level of the air mass. Subsequently, contour plots were prepared for each day of the episode based on these peak observations. Examples of data obtained by SAROAD stations are shown in Figure 6. In the upper part of the figure, the hourly average ozone concentrations are shown at station No. 7 of the St. Louis city-county monitoring network. The data exhibit the typical diurnal pattern consisting of near-zero readings overnight and in the early morning, rising to a peak in the early afternoon followed by a drop in the evening hours.

Although it is not clearly documented in the literature, it is reasonable to assume that the low overnight concentrations are the direct consequence of physical and chemical removal processes that tend to scavenge ozone from the atmospheric surface layer. It has been shown that the ozone concentration above the surface layer does not exhibit this diurnal pattern (Coffey and Stasiuk, 1975). Coffey and Stasiuk (1975) also gave evidence that ozone measurements near the surface obtained during the convectively active noon hour are representative of the ozone concentrations in the air mass in the absence of positively or negatively interfering local sources. Thus, the ozone concentration of the mixed layer air mass may be estimated from the envelope of the daily peak concentrations.

RESULTS

The relationship between ozone and haze is examined through a case study of a large hazy air mass that resided over the eastern U.S. for an estimated two weeks. Successive contour maps of noon visibility (Figure 2) are plotted for every second day from June 25 through July 5, 1975. Inspection of the sequence of maps reveals that multi-state regions are covered with a haze layer in which the noon visibility is less than 6 miles. From long range trajectory calculations and surface wind information, it was determined that the air mass of June 25 within which the visibility was less than 6 miles was of maritime origin in the Gulf of Mexico. This air mass had been transported in a northerly flow across Louisiana, Arkansas,

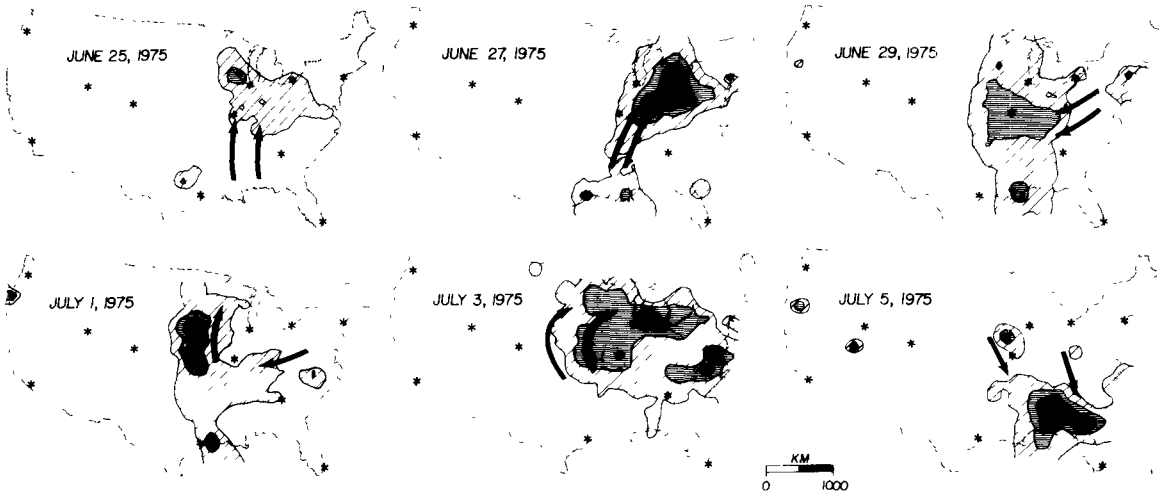

Figure 2. Sequential contour plots of ground visibility at 1200 CST (b_{ext} = 3.92/visibility range).

Illinois and Indiana. Between June 25 and 27, a NNE trajectory prevailed in the southern states; but, relative stagnation prevailed in the Great Lakes region. During this stagnation, the air mass became increasingly hazy. Thereafter, an easterly flow developed causing the hazy blob to drift slowly westward, passing over St. Louis, Missouri, on June 28-29, and continuing across Missouri and Kansas (June 30), and then drifting into Iowa and Minnesota (July 1,2).

The surface wind pattern at noon of June 30 is shown in Figure 3. Observe the clockwise circulation in the Great Lakes region. By July 3, the blob had circled over Lake Michigan continuing its residence over the high pollutant emission density regions of the northeast. In the next two days, however, a cold Canadian front advanced southward at a relatively rapid pace, sweeping the hazy air mass ahead of it. St. Louis once again experienced substantially reduced visibility on July 3-4 as the hazy air mass passed over it. By July 5, visibility deteriorations to less than 4 miles were experienced in Atlanta, Georgia, Birmingham, Alabama, and Tallahassee, Florida. Air trajectory analysis confirmed this southward motion of the blob.

During the above episode, sulfate data were obtained and plotted for June 23 and July 5, 1975. A close relationship has been observed between the spatial extent of the hazy air mass and high sulfate concentrations as shown in Figure 4. On June 23, the blob was located east of Lake Erie where sulfate concentrations over 30 $\mu g/m^3$ were measured. On July 5, both the haziness and high sulfate levels were reported in the southeastern U. S. (Georgia and Alabama). The coincidence of hazy air masses and high sulfate concentrations on these two days confirms the utility of visibility observations as a qualitative surrogate for sulfates.

Contour plots of the daily maximum ozone concentrations are shown in

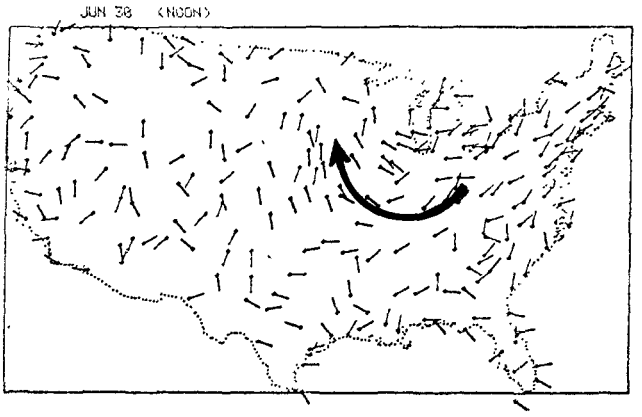

Figure 3. Surface wind direction pattern at weather stations for 1200 CST on June 30, 1975.

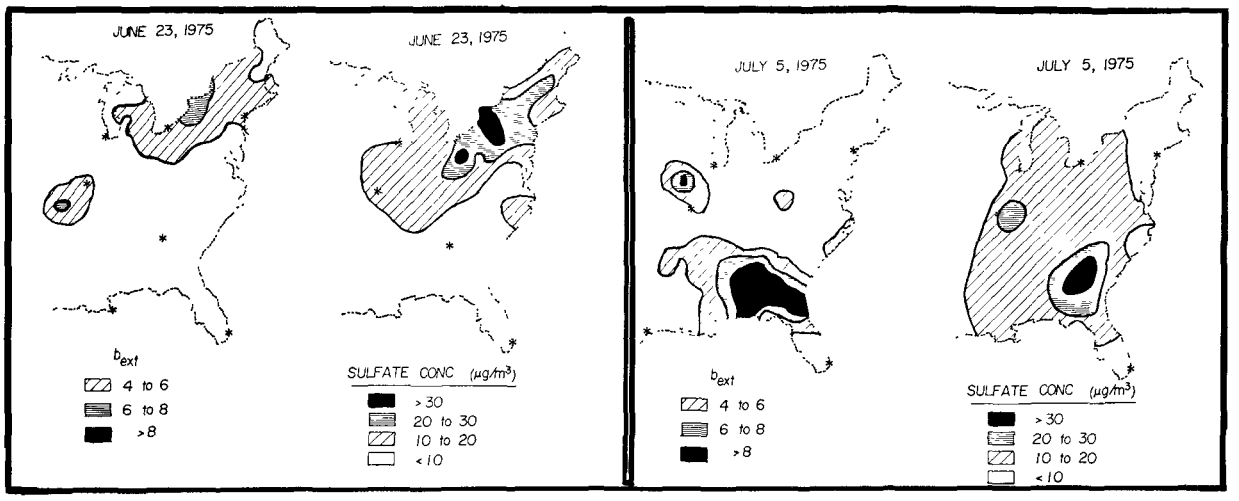

Figure 4. Comparison of contour plots of noon visibility and daily average sulfate concentration for June 23 and July 5, 1975.

Figure 5. Inspection of the corresponding contour plots for ozone and visibility (Figures 5 and 2, respectively) reveals that the geographical location of high ozone concentrations roughly corresponds to the areas of low visibility (and high sulfate). As may be anticipated, however, the correlation with haziness (low visibility) is much better for sulfate than for ozone.

Contours of daily maximum ozone concentration for June 25, 1975, show that an area of approximately 1000 square kilometers, located halfway between the Gulf of Mexico and the Great Lakes, had ozone concentrations in excess of .08 ppm. The air parcel trajectory followed a northerly course during that day. It is worth noting that, on that day, the haziness (Figure 2) developed somewhat farther north (i.e. later along the trajectory) compared to the area of high ozone levels. The spatial extents of ozone and

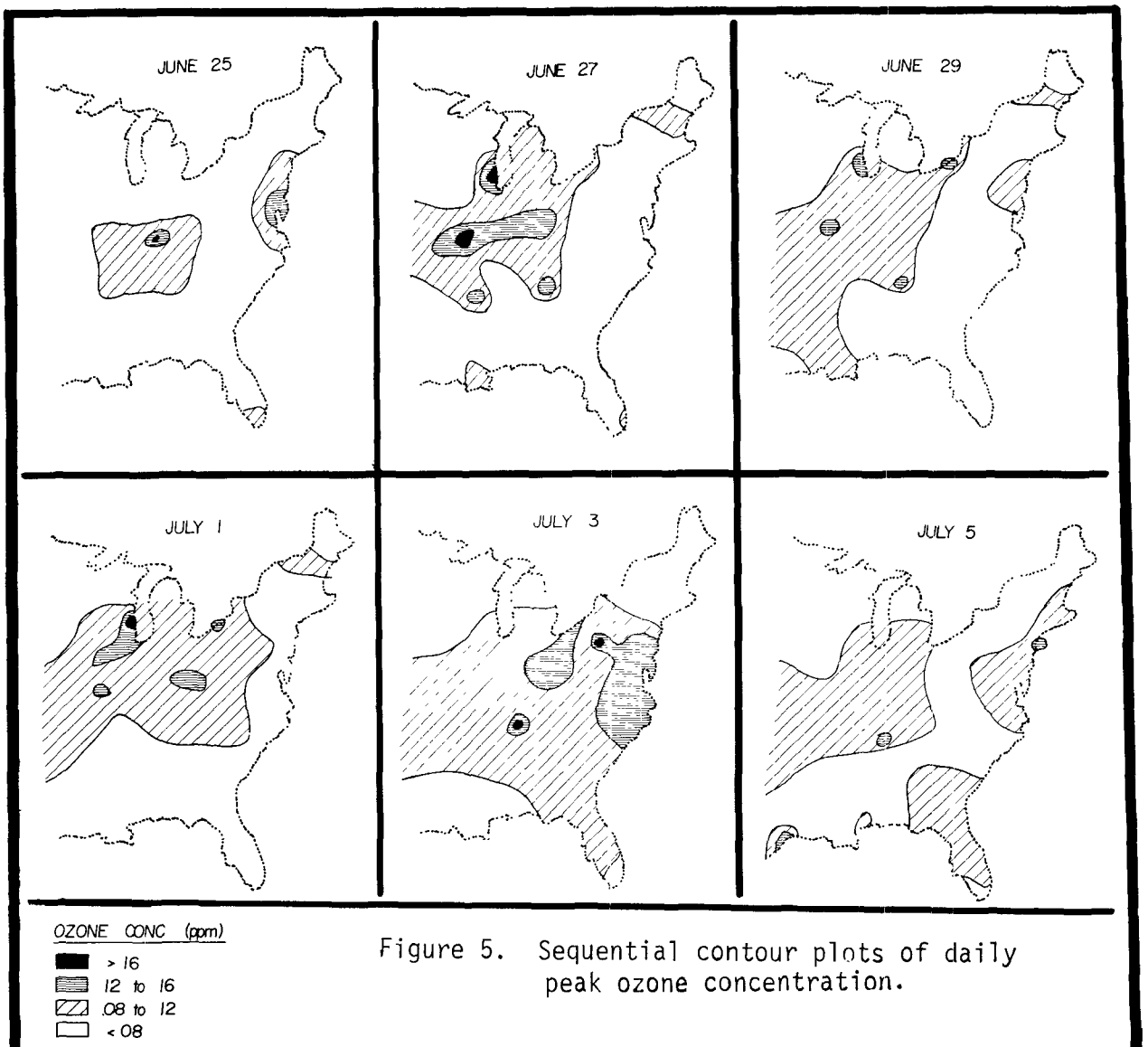

Figure 5. Sequential contour plots of daily peak ozone concentration.

haze areas roughly coincided on June 27 as the air mass stagnated. During the following days of the episode, high ozone levels (>0.08 ppm) continued their presence in the same approximate region of the U.S. where the haziness predominated. As the hazy air mass moved to the south by July 5, elevated ozone levels were comparatively suppressed immediately behind the front, but continued to be over .08 ppm farther to the north and west.

The possible relationship between hazy air masses and high ozone concentrations may also be studied by the analyses of long-term observations of visibility and ozone at fixed locations. The lower part of Figure 6 shows the three-month variation of the extinction coefficient (b_{ext} = 3.92/visual range). The visibility data were recorded at a St. Louis airport. The passage of the hazy blob observed previously over St. Louis is

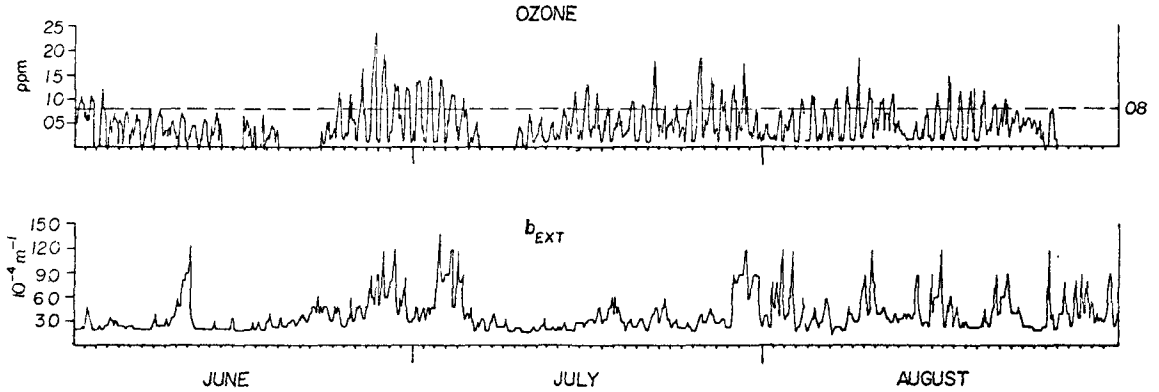

Figure 6. Comparison of long term observations of ozone and light extinction coefficient, b_{ext} = 3.92/visibility, at an air monitoring station in St. Louis, Missouri.

clearly shown by the two peaks of June 28-29 and July 3-4. Comparison of peak ozone concentrations and visibility data for June, July, and August 1975 shows that ozone levels above the standard roughly coincide with haziness corresponding to b_{ext} greater than 5.

DISCUSSION

The above data analysis provides some evidence that synoptic scale hazy air masses also contain elevated ozone concentrations. This evidence is based on only one case study, and is weaker than the observed correspondence between sulfate levels and haziness. A possible explanation for the simultaneous occurrence of high ozone-haze-sulfate levels may be given on simple meteorological grounds: in stagnant or slow-moving air masses, precursor gases for ozone and light-scattering aerosol are emitted and mixed, leading to an accumulation of these secondary pollutants due to the low ventilation coefficient. It is likely that this mechanism is the primary cause of synoptic scale air pollution phenomena. A more intriguing question is whether these two pollutants have a synergistic effect upon each other's development. Does the presence of high ozone concentrations promote the oxidation of sulfur dioxide to sulfate?

ACKNOWLEDGEMENT

This research was supported by the U.S. Environmental Protection Agency, Environmental Sciences Research Laboratory, Research Triangle Park, North Carolina. We wish to express our thanks to W.E. Wilson, Jr., N. Turcu, and the St. Louis County Health Department.

REFERENCES

1. Coffey, P.E. and W.N. Stasiuk. Evidence of Atmospheric Transport of Ozone into Urban Areas. Environmental Science and Technology 9(1):59-62, Jan. 1975.

2. Hall, F.P. Jr., C.E. Duchon, L.E. Lee and R.R. Hagan. Long-Range Transport of Air Pollution: A Case Study. Monthly Weather Review 101:404, Aug. 1970.

3. Husar, R.B., N.V. Gillani, J.D. Husar, C.C. Paley and P.N. Turcu. Long-Range Transport of Pollutants Observed Through Visibility Contour Maps, Weather Maps and Trajectory Analysis. Preprint, Third Symp. Atmos. Turb., Diff, and Air Quality, American Metrological Society, Raleigh, N.C., Oct. 1976.

4. Ripperton, L.A. and J.J.B. Worth. Interstate Oxone Studies. Second Joint Conf. on Sensing of Environmental Pollutants, Washington, D.C., Dec. 1973.

SESSION 7

OZONE/OXIDANT TRANSPORT - II

Chairman: A.P. Altshuller
Environmental Protection Agency

THE TRANSPORT OF PHOTOCHEMICAL SMOG ACROSS THE SYDNEY BASIN

R. Hyde and G. S. Hawke*

ABSTRACT

A classification of ozone traces and surface wind records for Sydney shows that high concentrations can occur in both morning drainage flow and afternoon seabreezes. Surface wind trajectories during the morning confirm the importance of cold air drainage in advecting oxidant precursors from inland sources towards the coast. Afternoon trajectories show that polluted air is transported back inland across the basin into areas designated as major industrial and population growth centres.

Measurements of the vertical structure of wind and temperature over Sydney indicate that the formation of photochemical smog during the morning is influenced by three distinct layers below the top of the subsidence inversion. These consist of a shallow local drainage flow approximately 100 m deep, which later merges with a regional drainage flow and forms a well-mixed layer 200-300 m deep. This layer is capped by an inversion and maintains an approximately constant depth for several hours below the gradient wind flow. Over this period, ozone concentrations continue to increase and only decrease with the arrival of a seabreeze or when surface heating destroys the capping inversion allowing the gradient wind to reach the ground.

INTRODUCTION

Sydney is located within a coastal basin at latitude 35°S on the east coast of Australia. Details of the topography, given in Figure 1, show the overall basin bounded by a plateau 150 m high to the north and another in the south, with the Blue Mountains to the west. Minor ridges, extending north from Campbelltown and northwest from Botany Bay, divide the region into the Hawkesbury Basin to the west, the Liverpool Basin to the southwest, and the Parramatta River Valley to the east.

Unlike Los Angeles, Sydney does not experience semi-permanent maritime inversions, but comes under the influence of subsidence inversions associated with migratory anticyclones moving from west to east across Australia. On some occasions, the passage of these high-pressure systems is blocked and they remain stationary over the Tasman Sea east of Sydney, causing high oxidant

*Macquarie University, North Ryde, N.S.W., Australia, 2113.

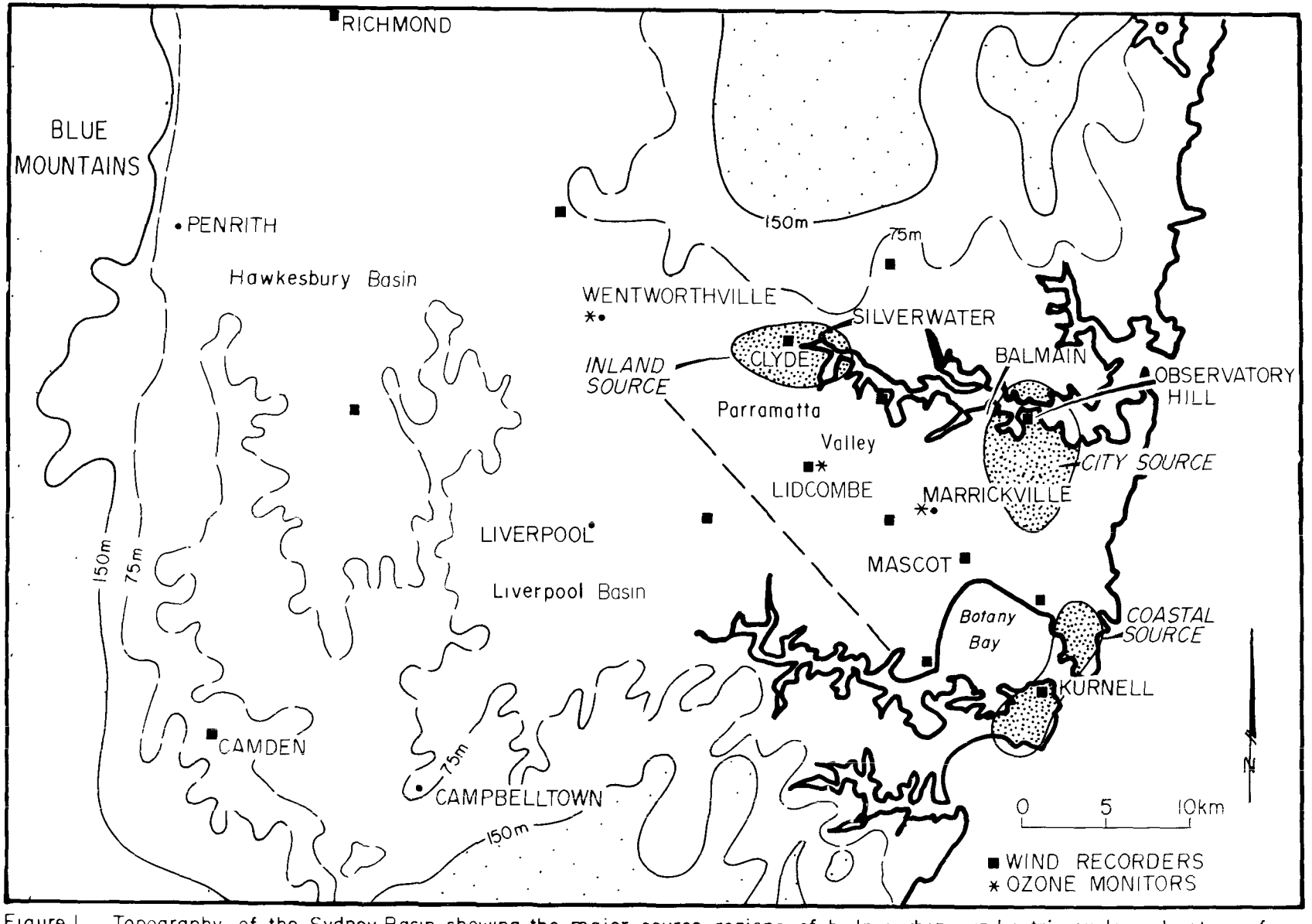

Figure 1. Topography of the Sydney Basin showing the major source regions of hydrocarbons and nitric oxides, location of wind recorders and ozone monitors (after Hawke and Iverach, 1974)

episodes. But in general each anticyclone causes high oxidant concentrations only on one or two days at a time. During the oxidant season, from October 1974 to April 1975, hourly-mean ozone concentrations exceeded 0.10 ppm in Sydney on approximately one day in six (Hyde & Hawke, 1976).

The two dominant mesoscale wind systems affecting the Sydney region are, firstly, nocturnal and early-morning drainage flows and, secondly, afternoon seabreezes. A preliminary examination of wind and temperature data, for some days when high oxidant concentrations were measured, indicated that ozone could occur in either the drainage flow or seabreeze systems (Hawke and Iverach, 1974). This was later confirmed by Hyde and Hawke (1976).

This work is being continued as part of the contribution of Macquarie University to the Sydney Oxidant Study, a multi-disciplinary project investigating the formation of photochemical smog in the Sydney Basin, funded by the New South Wales State Pollution Control Commission. Our present paper is divided into two parts; the first section presents a climatology of surface-wind trajectories within drainage flows and seabreezes on days with high oxidant concentrations and classifies variations in ozone concentrations throughout the day in terms of the meso-meteorological conditions. The second part of the paper deals with the vertical structure of the atmosphere above Sydney and its relationship to concentrations of ozone during the morning.

SURFACE WINDFLOW AND CONCENTRATIONS OF OZONE

In our earlier paper we showed that high concentrations of ozone occurred predominantly during the morning drainage flow. However, some of the days studied in that paper had maximum concentrations of ozone occurring within or after the arrival of the afternoon seabreeze. The analysis has now been extended in order to determine the influence of meteorological conditions on the transport of oxidants and their precursors across the Sydney Basin.

CLASSIFICATION OF OZONE CONCENTRATIONS

The 69 days when hourly concentrations of ozone were at least 0.10 ppm between January 1974 and June 1975 have been divided into three main categories according to the variations of ozone concentrations throughout the day. Characteristics of the different categories are briefly described below and an example of each is given in Figure 2.

Type A1 - morning increase in ozone concentrations terminated by the onset of the gradient wind at ground level.

Type A2 - morning increase in ozone concentrations terminated by the arrival of the seabreeze.

Type B - as for type A1 but followed by an abrupt increase in ozone concentrations coinciding with the arrival of the seabreeze.

Type C - ozone concentrations continued to increase for up to two hours after the arrival of the seabreeze.

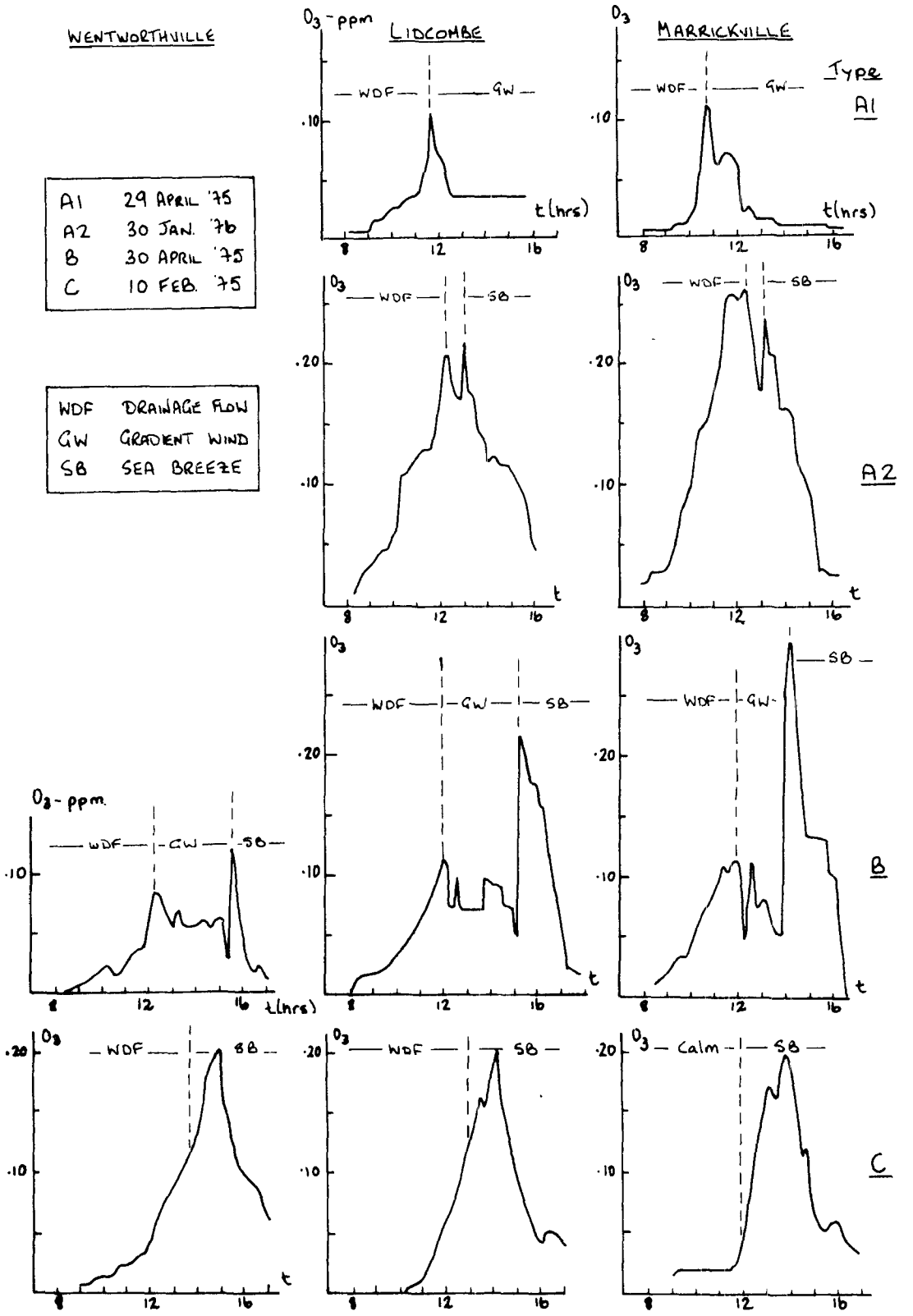

Figure 2. Variation in ozone concentrations during the day in the Sydney Basin in four categories.

The frequency of occurrence of these different categories at the three monitoring stations in the Sydney region, given in Table 1, shows that maximum ozone concentrations occur more frequently during the morning, especially near the coast. An explanation of meteorological conditions associated with this type of ozone pattern is given in the next section. Type C days occur relatively infrequently and have not yet been analyzed in detail. However, Type B days do occur on a significant number of occasions, especially inland.

TABLE 1. NUMBER OF DAYS WHEN MAXIMUM OZONE CONCENTRATIONS WERE AT LEAST 0.10 PPM, IN FOUR CATEGORIES, FOR JAN. 1974 - JUNE 1975

TYPE	LOCATION AND DISTANCE INLAND (KM)		
	Marrickville, 10	Lidcombe, 21	Wentworthville, 29
A1	21	8	5
A2	16	12	13
B	14	18	16
C	5	2	2
TOTAL	56	40	36

The exact cause of high concentrations of ozone within afternoon seabreezes has not yet been investigated but may be caused either by:

- a slowly moving seabreeze-front, with ozone forming within the seabreeze circulation as a result of precursor emissions near the coast (Lyons and Olsson, 1973);
- air containing oxidant precursors moving out to sea in the morning drainage flow, undergoing photochemical reactions and then being advected back inland with the seabreeze (Anlauf et al., 1975); or
- air advected from the Botany Bay region.

SURFACE WIND TRAJECTORIES

Although the above categorization of ozone concentration changes describe only conditions at the three fixed monitoring sites, surface-wind trajectories through these stations can be used to identify both source and receptor regions for photochemical smog in the Sydney Basin. Surface-wind trajectories through both Marrickville and Lidcombe on the 69 days described in the preceding subsection were calculated using the method of Wendell (1972) as follows:

(1) backwards in time until midnight the previous day for hours when the ozone concentration reached at least 0.10 ppm before the onset of strong gradient winds or arrival of the afternoon seabreeze, and

(2) forwards in time until midnight or until the trajectory moved outside the Sydney region for hours when ozone concentrations were at least 0.10 ppm in the afternoon seabreeze.

The Sydney region was divided into 5 km grid squares and the number of trajectories passing through each square was counted and converted into a percentage frequency of the total number of trajectories. The results of this analysis for (1) and (2) above at Marrickville and Lidcombe are given in Figure 3. The 5 per cent frequency category for trajectories backwards from Lidcombe has been omitted here because of the small number of trajectories involved.

At the moment we do not know what proportion of pollutants within the morning drainage flow are subsequently incorporated into the overall seabreeze circulation. Angell et al. (1976) found that tetroons released within the morning drainage flow in the Los Angeles Basin were subsequently advected back inland with the afternoon seabreeze. Whether or not a similar recirculation occurs in the Sydney basin is not yet known, and for this reason forward and backward trajectories in Figure 3 have been considered separately.

This analysis of surface wind trajectories confirms that polluted airmasses arriving at both Marrickville and Lidcombe during the morning have been advected there by westerly drainage flow from source regions to the northwest. The most common afternoon trajectory of polluted air within seabreezes is towards the southwest of the Sydney Basin, including the Liverpool-Campbelltown region. Unfortunately this region is designated as the major population growth centre for the next few decades (State Planning Authority of N.S.W., 1968, 1973). Several papers which discuss the advection of ozone across the Los Angeles basin show that the highest concentrations occur 50 km downwind of the major source regions within air advected inland with the afternoon seabreeze (Hanna 1975, Tiao et al., 1975, Blumenthal, 1976). The possible implications for Sydney are clear and illustrate the need to consider the incursion of photochemical smog when planning future growth centres.

VERTICAL STRUCTURE OF THE LOWER ATMOSPHERE OVER SYDNEY

The other part of our work in the Sydney Oxidant Study concerns the vertical structure of wind and temperature on days with high concentrations of ozone. This information is necessary to explain variations in oxidant concentrations on different days and as meteorological input for photochemical smog models.

Wind profiles are obtained using a recording single-theodolite pilot-balloon system developed by Hawke, and temperatures up to 300 m using a low-level tethersonde (Linacre 1976). These systems have been developed because it is not possible to obtain a resolution of less than 300 m from routine six-hourly pilot-balloon ascents at Mascot and the nearest routine radiosonde stations are approximately 130 km away to the north and south of Sydney.

OBSERVATIONS ON APRIL 29, 1975

During the 1975-76 oxidant season most of our wind and temperature profiles were obtained between sunrise and noon, in order to examine the influence of drainage and gradient wind flows on the morning increase of oxidant concentration. One such set of observations was made on April 29,

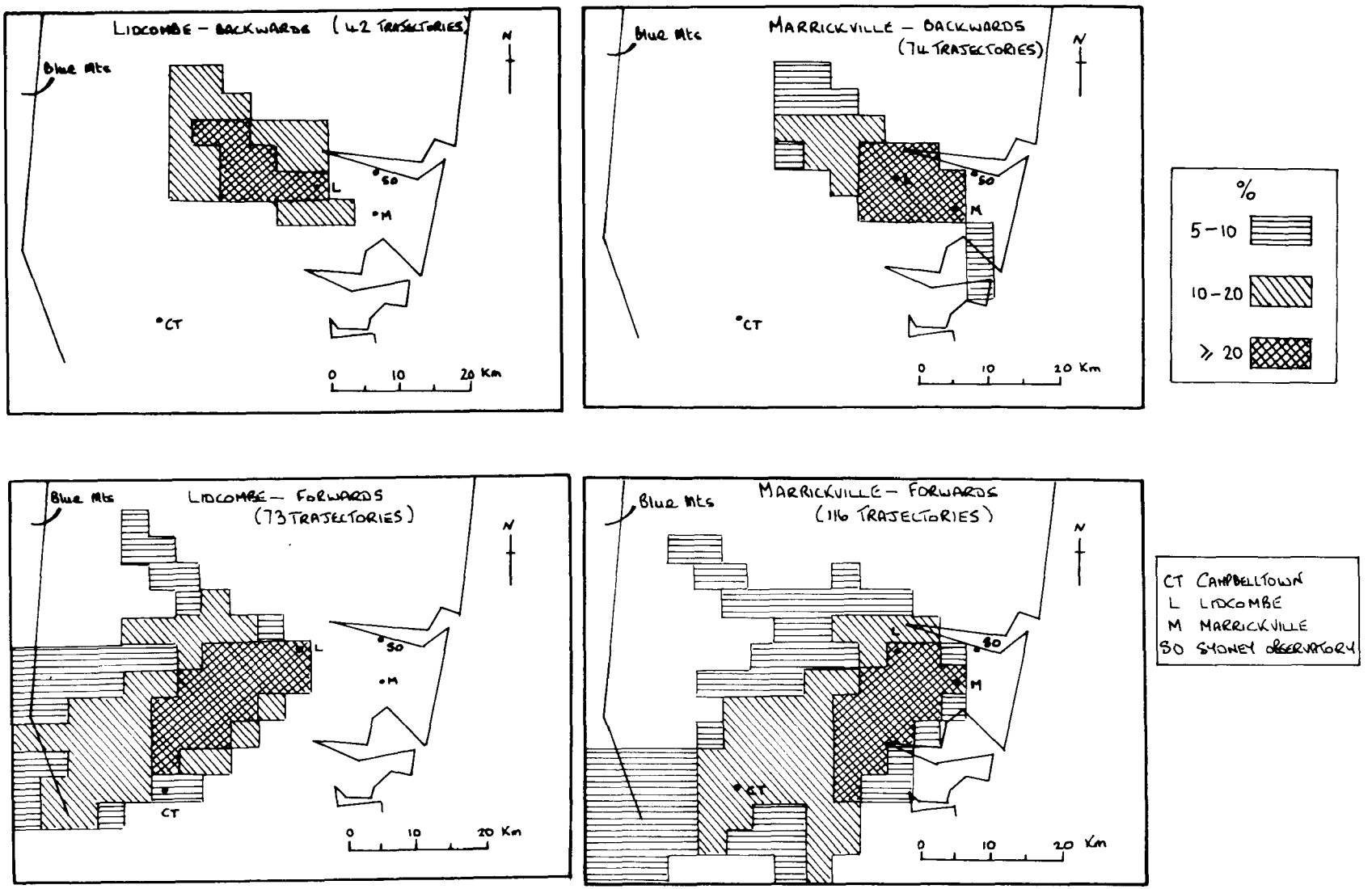

Figure 3. Source and receptor regions of air passing over Lidcombe and Marrickville with concentrations of ozone of at least 0.10 ppm. These are presented as a percentage frequency of surface-wind trajectories crossing 5 km grid squares, calculated backwards before the onset of gradient winds and seabreezes and forwards within seabreezes.

1975, and shows stratification typical of the atmosphere over Sydney during the morning on high oxidant days. On that occasion, simultaneous wind and temperature profiles were obtained at least every thirty minutes between 0500 and 1000 and are given in Figure 4. Details of the synoptic situation, ozone concentrations at Lidcombe and Marrickville, and the 0900 radiosonde ascent from Williamtown (130 km to the north) are given in Figure 5.

Macroscale Wind and Temperature Structure

The synoptic map is typical of many high oxidant days in Sydney, with a high pressure system centred over the Tasman Sea (Hawke and Iverach, 1974). At Williamtown the temperature profile shows a well-defined structure below 700 m with:

- a slightly stable layer between the surface and 250 m (a-b),
- a strong inversion layer between 250 m and 400 m (b-c), and
- a weaker inversion layer between 400 m and 700 m (c-d).

Wind profiles in Figure 4a have been divided into three periods of time corresponding to changes in thermal structure within the lower atmosphere. However certain features are common to each set of measurements and are listed below:

(1) a surface layer approximately 200 m deep, with a wind speed of 2-3 ms^{-1} from the north to northwest,

(2) a region of marked wind direction shear above the surface layer with a turning point at 250 m, and

(3) a layer between 250 m and 700 m having a 6 ms^{-1} northerly wind and turning points in wind direction shear at 400 m and 700 m.

Layer (1) above has approximately the same height at layer a-b in Figure 5c and the turning points at 400 and 700 m in (3) occur at similar heights to points c and d. These features describe the broadscale vertical structure and form part of the model to be developed below.

Mesoscale Wind and Temperature Structure

On a smaller scale Figures 4a and 4b show that the low-level wind and temperature structure on this day can be divided into three stages of development, as follows:

(1) Before sunrise (0635 a.m.) - during this period there was a strong surface inversion below 250 m with a westerly flow between 60 m and 200 m, above a shallow northwesterly flow,

(2) 0635 to 0845 a.m. - over this period the surface northwesterly layer heated up and formed a well-mixed layer approximately 100 m deep,

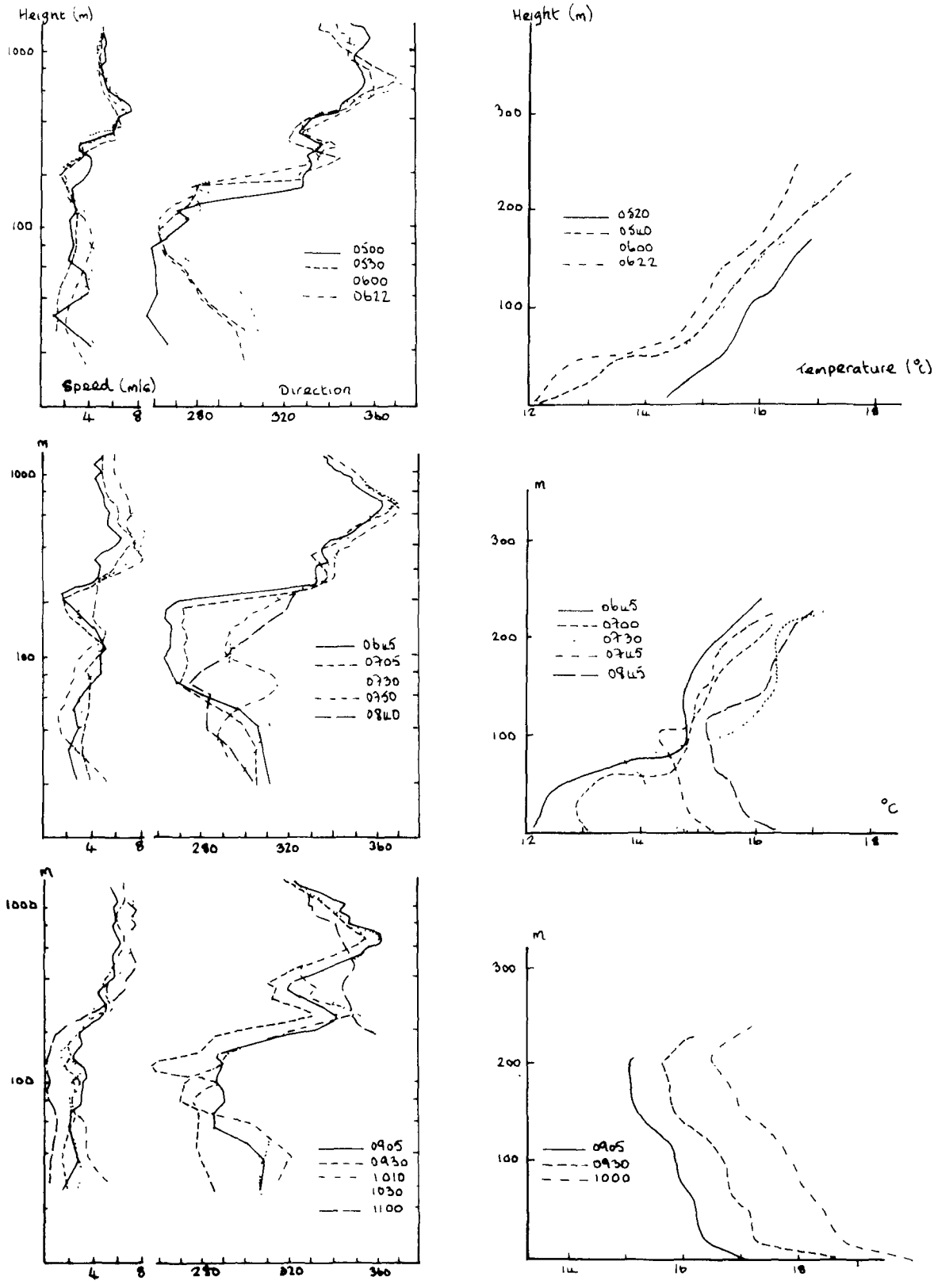

Figure 4. Wind and temperature profiles at Silverwater on April 29, 1975.

(3) 0845 to 1000 a.m. - between 0845 and 0900 a.m. the depth of the well-mixed surface layer increased from 100 m to 200 m. Subsequent wind and temperature profiles show this layer remaining 200 m deep until at least 1000.

No temperature profiles were made after 1000, but wind profiles at 1030 and 1100 show that the region of wind shear at the top of the surface layer had gone. Surface wind records over the Sydney region on this day show a change in wind direction from northwesterly to northerly and increase in wind speed between 1030 and 1130, and correspond to the period when ozone concentrations at Lidcombe and Marrickville started to decrease (Figure 5b).

MODEL

Vertical Structure

The structure of wind and temperature profiles on April 29, 1975, (and many other similar observations over a wide range of gradient wind velocities obtained during the past two years) suggests that during the morning there can be three distinct layers over Sydney, below the top of the subsidence inversion. These are shown schematically in Figure 6 where:

- 'a' is a local drainage flow down the Parramatta River valley, typically 80-150 m deep and contained by the region of high ground to the north of the river, and is a sub-layer of
- 'b', a regional drainage flow 200-300 m deep over the whole Sydney Basin.
- 'c' is the gradient wind flow below the top of the subsidence inversion.

Time Development

Before sunrise on a cloudless morning, drainage flow occurs within a ground-based inversion, caused partly by radiative cooling and partly by the advection of cold air from the Blue Mountains to the west. After sunrise (at time t_1 in Figure 6), surface heating allows the local drainage-flow to form a well-mixed layer underneath the still thermally-stable region. Then at time t_2 there is a sudden increase in mixing depth, signifying the end of local drainage-flow to form a well-mixed layer 200-300 m deep. Dividing the drainage wind into local and regional flows can explain a characteristic feature of many wind profiles measured at Silverwater. These show a surface layer about 100 m deep suddenly doubling in depth sometime during the morning. Observations show that after this deepening the regional drainage flow maintains a constant depth during subsequent surface heating and is separated from the gradient wind above by a sharp inversion layer. The gradient wind will reach the surface once surface heating has eroded this inversion (at time t_3). When this occurs, there is usually an increase in mixing depth and a change in windspeed and wind direction. This causes the sudden reduction in ozone concentrations typical of type A1 days.

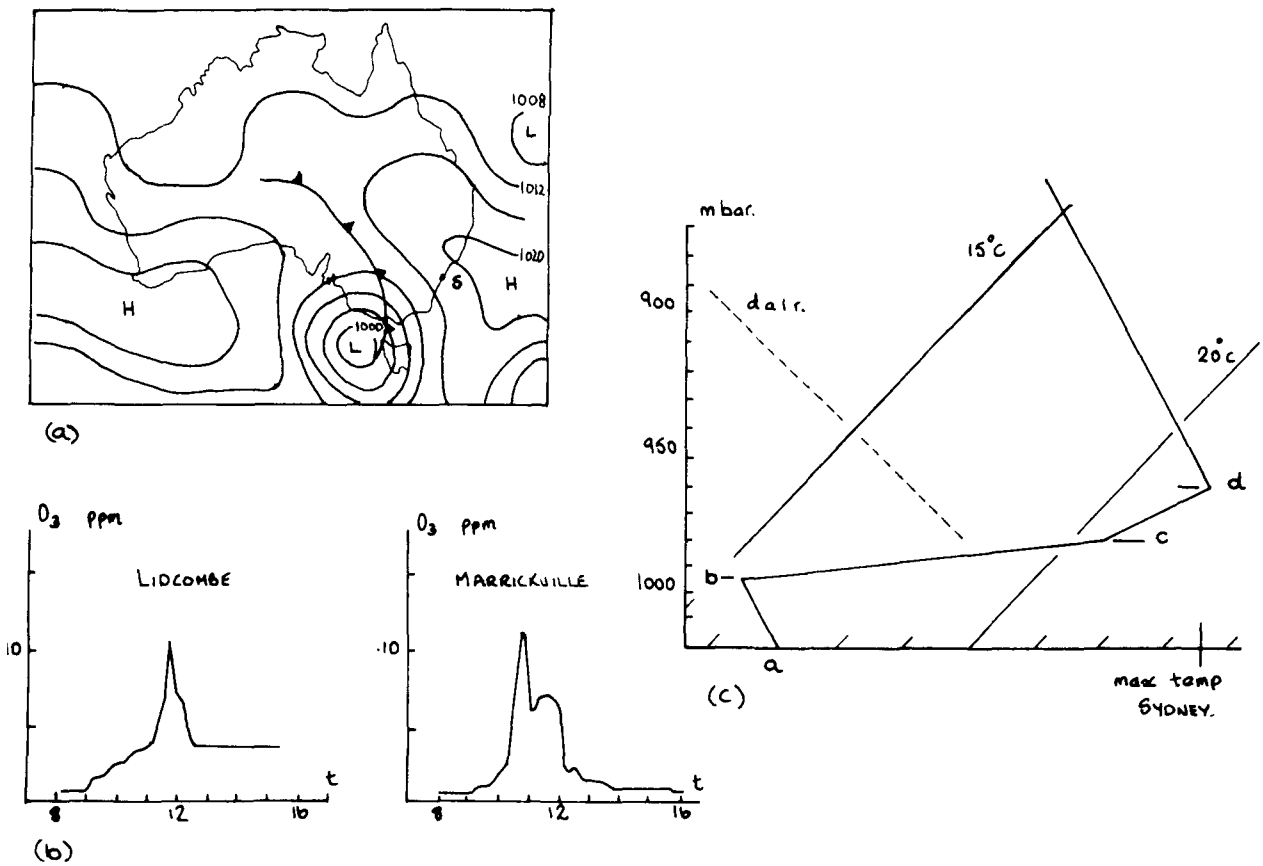

Figure 5. April 29, 1975: (a) Surface synoptic weather map. (b) Concentrations of ozone at Lidcombe and Marrickville. (c) 0900 temperature soundings from Williamtown, plotted on a T-O diagram.

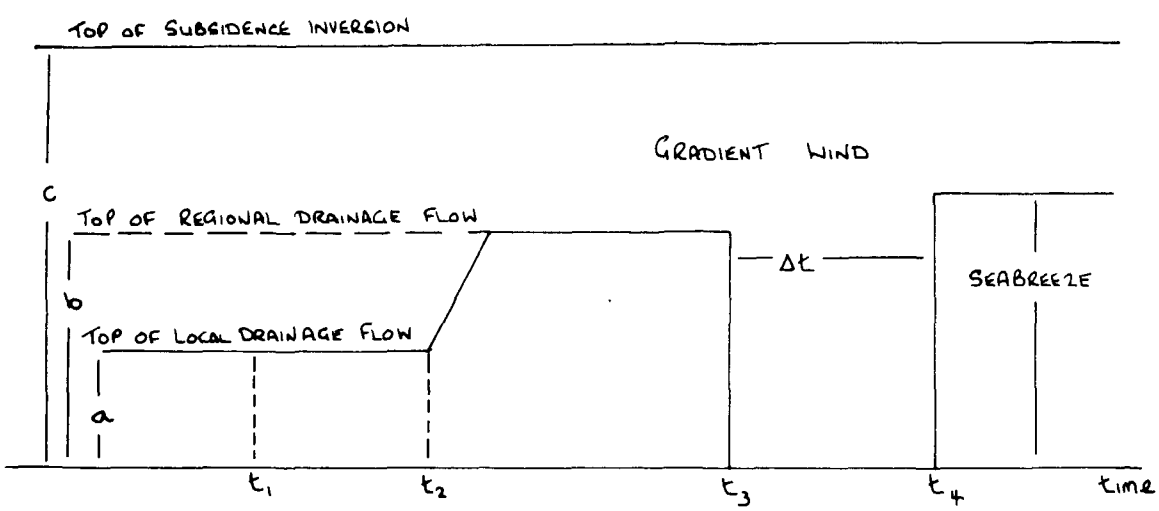

Figure 6. Schematic representation of the vertical structure of the lower atmosphere over Sydney on days having high oxidant concentrations.

Figure 6 also shows the seabreeze onset at time t_4, separated from t_3 by a period of time Δt which will depend on both surface heating and the gradient-wind speed and direction. Δt is an important variable, which equals zero if the seabreeze arrives at a location before the breakdown of regional drainage-flow. Under these conditions the day would become type A2.

Implications for the Formation of Oxidants in the Sydney Basin

The partition of drainage-flow into two types has important implications on the dispersion of oxidant precursors emitted into the atmosphere during the morning. Between sunrise and time t_2, precursors emitted close to the ground are advected towards the east in the well-mixed local drainage-flow. At the same time, precursors emitted from higher chimneys will be carried downwind in a stable layer and not experience much lateral or vertical diffusion. On occasions when the gradient wind inhibits regional drainage-flow, these emissions from elevated sources are often advected in a direction different from that taken by the surface emissions. After time t_2, precursors from both surface and elevated sources undergo photochemical reactions within a well-mixed layer 200-300 m deep. So subsequent concentrations of ozone during the morning largely depend on the time interval between t_2 and t_3. This time interval in turn depends on the strength of the inversion layer b-c in Figure 5c and would be influenced by the presence of any cloud during the morning which can reduce the rate of surface heating and so delay the breakdown of regional drainage flow. Therefore, although the right synoptic conditions may be present, the concentrations of ozone on any particular day may be very sensitive to variations in the length of time between the breakdown of the local drainage flow and the onset of either the gradient wind or afternoon seabreeze.

CONCLUSIONS

The material presented in this paper is intended to illustrate the importance of both horizontal transport and vertical structure of the lower atmosphere in the photochemical smog problem in Sydney. A knowledge of the vertical structure of wind and temperatures is necessary to identify the characteristic depths of layers which can inhibit the vertical diffusion of pollutants. This information can then be used in the future for forecasting days with high concentrations of ozone and as meterological input to photochemical smog models. The horizontal transport of photochemical smog within mesoscale wind systems must be considered when planning future urban growth centres so as to avoid sitting them downwind of major oxidant source regions.

ACKNOWLEDGEMENTS

The authors are grateful to the State Pollution Control Commission for permission to publish ozone data appearing in this paper, to the Bureau of Meteorology for access to meteorological observations, and to Associate Professor E. T. Linacre for his comments during the preparation of the paper. Thanks are also due to Mrs. Campbell Gibson who typed the manuscript.

This work was carried out under a grant from the State Pollution Control Commission as part of the Sydney Oxidant Study. The purchase and

maintenance of 3 anemometers in the Botany Bay region was funded by a grant from the Botany Bay Project Committee.

REFERENCES

ANGELL, J. K., C. R. DICKSON, AND W. H. HOECKER. Tetroon Trajectories in the Los Angeles Basin Defining the Source of Air Reaching San Bernadino-Riverside Area in Late Afternoon. J. Appl. Met., 15:197-204, 1976.

ANLAUF, K. G., M. A. LUSIS, H. A. WIEBE, AND R. D. S. STEVENS. High Ozone Concentrations Measured in the Vicinity of Toronto, Canada. Atmos. Environ., 9:1137-1139, 1975.

BLUMENTHAL, D. L. Distribution and Transport of Ozone in the South Coast Air Basin. Calif. Air Environ., 6 (1):4-10, 1975.

HANNA, S. R. Modelling Smog Along the Los Angeles-Palm Springs Trajectory. N.O.A.A. Environ. Res. Lab., Atmos. Turbulence and Diffusion Lab., Contribution No. 75/4, 1975.

HAWKE, G. S. AND D. IVERACH. A Study of High Photochemical Pollution Days in Sydney, N.S.W. Atmos. Environ., 8:597-608.

HYDE, R. AND G. S. HAWKE. A Preliminary Analysis of the Influence of Meteorology on Ozone Levels in Sydney. Smog '76 Conference, Clean Air Soc. of Aust. and N. Z., N.S. W. branch, Sydney, February 1976.

LINACRE, E. T. Low-Level Temperature Soundings with a Radiosonde on a Tethered Balloon. 1976. (in preparation)

LYONS, W. A. AND L. E. OLSSON. Detailed Mesometeorological Studies of Air Pollution Dispersion in the Chicago Lake Breeze. Mon. Wea. Rev., 101:387-403, 1973.

STATE PLANNING AUTHORITY OF N. S. W. Sydney Region: Outline Plan 1970-2000 A.D., March 1968.

STATE PLANNING AUTHORITY OF N. S. W. Population Projections for N. S. W. 1971 to 2000, November 1973.

TIAO, G. C., G. E. P. BOX, AND W. J. HAMMING. Analysis of Los Angeles Photochemical Smog Data: A Statistical Overview. J. Air Poll. Control Assoc. 25:260-268, 1975.

WENDELL, L. L. Mesoscale Wind Fields and Transport Estimates Determined from a Network of Wind Towers. Mon. Wea. Rev. 100:565-578, 1972.

OXIDANT LEVELS IN ALBERTA AIRSHEDS

H. S. Sandhu*

ABSTRACT

Some of the air quality and meteorological data gathered in Alberta during the past two years for selected days and time of the year is reported. Comparison between the observed and calculated values of ozone has revealed the occurrence of photochemical reactions. Possible sources contributing to ozone formation and transport are briefly discussed.

INTRODUCTION

Most of the information available to date on photochemical oxidant pollution and its control is derived from the laboratory and field studies carried out in the United States (1-3). Over the years attempts have been made to apply this knowledge to northern climates. It has been argued that photochemical oxidants should not pose a pollution problem at higher latitudes because of reduced solar radiation and lower temperatures. There is evidence now that these generalizations are in error (4,5).

In Canada, no other cities of a size comparable to Edmonton (53° 34'N 113° 35'W, elevation 676 m) and Calgary (51° 17'N 114°W, elevation 1080 m) with a population of about 500,000 each are situated as far north. The Province of Alberta, Figure 1, is one of the richest natural resource provinces in Canada. Because of mankind's dependence on energy, large resource developments such as the recovery of oil from Alberta Oil Sands are taking place or will take place farther to the north in the coming years. It is essential for environmental information to be gathered and analysed. Predictions should be made at the extremes of the meteorological conditions prevalent in the area instead of using conclusions based on different climatic conditions. Some aspects of photochemical air pollution in Alberta are briefly discussed in this paper.

RESULTS AND DISCUSSION

Alberta Department of the Environment expanded the monitoring network from one to three stations in each of the two cities in 1974 and started using instruments that employ the chemiluminescence method for detecting nitric oxide (NO), nitrogen dioxide (NO_2), and ozone (O_3), the flame ionisation technique for detecting hydrocarbons (HC) and the infrared absorption

*Alberta Department of the Environment, Edmonton, Canada.

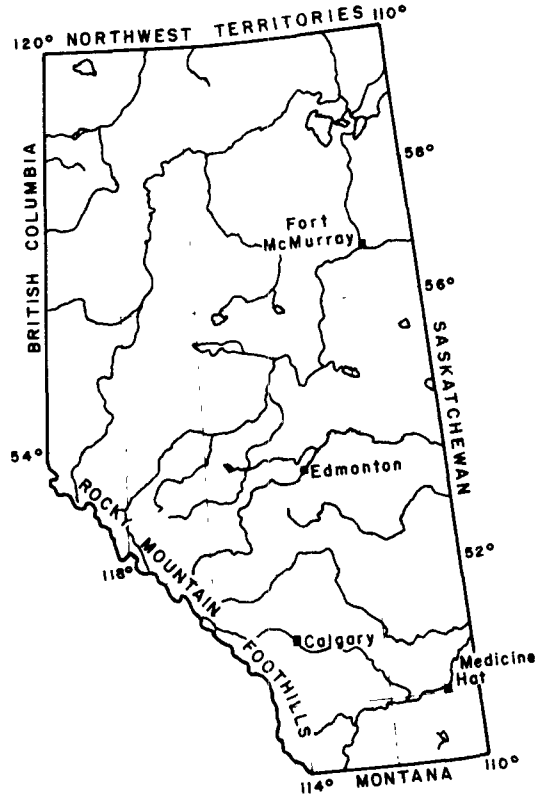

Figure 1. The Province of Alberta.

method for carbon monoxide (CO). Meteorological observations are made by Atmospheric Environment Service, Environment Canada, employing standard instruments at various stations in Alberta. Air monitoring reports for Edmonton and Calgary for the year 1974 have been published (6).

Temperature and air pollutants recorded on a typical cold day in spring (sunny, 7.5 cm of snow) are given in Table 1. Average wind speeds stayed around 16 km per hour (10 miles per hour). Observed O_3 values given in this table are a clear indication of its photochemical production and transport at these latitudes under reduced temperatures. Rawinsonde observations recorded at an upper air sounding station 49 km outside the city showed that the morning temperature inversion top was partially lifted by solar heating as the day progressed. Steady-state concentrations of O_3 were computed from the mechanism,

$$NO_2 + \text{sunlight} \rightarrow NO + O$$

$$O + O_2 + M \rightarrow O_3 + M$$

$$O_3 + NO \rightarrow O_2 + NO_2$$

using theoretical values of k_1 (clear sky approximation) for these latitudes,

$$k_2 = 1.7 \times 10^{13} \ (\text{cm}^6 \ \text{mole}^{-2} \ \text{sec}^{-1}) \ \exp \ (+2100 \ (\text{cal mole}^{-1})/RT) \quad (7)$$

TABLE 1. TEMPERATURE AND AVERAGE AIR POLLUTANT CONCENTRATIONS MEASURED AT THE EDMONTON DOWNTOWN MONITORING STATION ON APRIL 1 1975

Variable	Hour	09	10	11	12	13	14	15	16	17
Temp. (°C)		-16	-14	-13	-13	-11	- 9	- 8	- 8	- 8
NO_2 (pphm)		5	3	4	3	3	3	3	5	6
NO (pphm)		9	4	3	4	3	3	3	4	7
O_3 (pphm)		2	5	5	6	6	7	7	6	5

and

$$k_3 = 6.0 \times 10^{11} \text{ (cm}^3 \text{ mole}^{-1} \text{ sec}^{-1}) \exp(-2460 \text{ (cal mole}^{-1})/RT \quad (8).$$

These values are lower by a factor of two when compared to midday values of O_3 given in Table 1. This discrepancy could be due to the combined effects of factors such as advection of background O_3 increased albedo of the surface, production of O_3 through other precursors or the production of O_3 through heterogeneous reactions. A preference for any one factor would be misleading at this time. The observed peak value of 7 pphm is above the Alberta Standard and Canadian Objective (maximum desirable) which is 5 pphm. Though rare, such situations could prevail up to three or four days at this time of the year depending on the intensity and dynamics of the air mass.

During summer months in 1975, O_3 levels above 5 pphm were recorded on almost all sunny days in Edmonton. Levels observed on three days during July 1975 are given in Table 2. Since non-urban O_3 measurements are not available for this time period it is premature to interpret these data.

Central Alberta, the area between Edmonton and Calgary, is a region of high convective cloud activity and it experiences many thundershowers and hailstorms during summer months. To date, no one has made measurements of surface O_3 present in rural areas during summer months. A monitoring program is planned to observe non-urban O_3 levels and estimate O_3 produced through this natural phenomenon.

To obtain information on the background levels of reactive pollutants at these northern latitudes, a three week monitoring study was carried out in Edmonton in September 1975. A typical set of data is given in Table 3.

TABLE 2. AVERAGE OZONE CONCENTRATIONS (PPHM) OBSERVED AT THE EDMONTON DOWNTOWN MONITORING STATION DURING JULY 1975

Day	Hour	08	09	10	11	12	13	14	15	16	17	18	19
4		1	3	10	7	10	11	16	9	4	5	5	5
24		1	3	5	6	7	7	7	8	6	6	7	10
28		6	6	6	7	8	11	13	19	18	10	7	6

TABLE 3. TEMPERATURE, WIND SPEED AND AVERAGE AIR POLLUTANT CONCENTRATIONS MEASURED AT THE EDMONTON DOWNTOWN MONITORING STATION ON SEPTEMBER 24, 1975*

Hour	Temp (^{o}C)	NO_2 (pphm)	NO (pphm)	O_3 (pphm)	Reactive Hydrocarbons (pptm)
07	11	6 (2)	40 (2)	0 (1)	11
08	12	6 (2)	55 (2)	0 (1)	24
09	14	7 (2)	16 (2)	0 (1)	11
10	18	6 (2)	11 (1)	1 (2)	6
11	20	6 (2)	6 (1)	3 (2)	6
12	22	5 (1)	5 (1)	4 (3)	6
13	24	7 (1)	6 (1)	4 (3)	6
14	23	7 (2)	5 (1)	5 (3)	6
15	24	7 (2)	5 (1)	5 (3)	4
16	24	9 (2)	5 (1)	5 (3)	5
17	23	9 (2)	5 (1)	4 (3)	6
18	23	11 (2)	12 (2)	2 (2)	7
19	21	15 (3)	24 (2)	0 (2)	5
20	18	15 (2)	23 (3)	0 (2)	6

* The values in parenthesis are measured at Kavanagh, 45 km south of Edmonton city limits.

Average wind speed on this day was 6.5 km per hour (4 miles per hour). To the author's knowledge, background air pollutant levels shown in this table are the first reliable measurements outside a major urban center in Canada that is this far north. During this period background O_3 levels varied between 1-3 pphm on sunny days, peaking around midday. The levels of reactive HC in Alberta cities are relatively small compared to those in other major cities at the present time. The relationship of NO to O_3 (Table 3) in the urban and non-urban air is quite interesting in that NO is the main molecule that reacts with urban O_3.

Meteorological and air quality data for the summer of 1976 is not available yet in the reduced and manageable form. However, monitored data for Edmonton, Calgary, and Medicine Hat (50° 01'N, 110° 43'W, elevation 719 m) on July 25, 1976, are given in Tables 4 and 5. July 25 was a typical hot summer day with more than 14 hours of sunshine. The values of O_3 recorded at Medicine Hat are typical background O_3 values. Residential monitoring stations in both Edmonton and Calgary recorded generally higher O_3 concentrations as compared to downtown monitoring stations. The hourly NO_2/NO ratio around midday is higher in Calgary than in Edmonton, but O_3 values are higher in Edmonton. A complete analysis will be carried out after all the data for 1976 becomes available.

TABLE 4. SOME METEOROLOGICAL VARIABLES OBSERVED AT THREE MONITORING STATIONS IN ALBERTA ON JULY 25, 1976

Variable	Edmonton	Calgary	Medicine Hat
Sunshine (hours)	14.7	15.2	14.3
Max. Temp. (°C)	26.7	28.7	28.4
Max. Windspeed (km/hour) and Direction	19 Southwest	20 North	-
Precipitation (mm)	0	0	trace

CONCLUSIONS

Ozone is formed through photochemical reactions of air pollutants present in the major urban airsheds of Alberta. Typical background O_3 concentrations are in the range 1-3 pphm. Some observations suggest that the precursors for O_3 production are advected to the cities. Oxidant/ozone concentrations are expected to stay below the provincial standard of 5 pphm in winter months, but will exceed the standard during summer months on sunny days.

ACKNOWLEDGEMENTS

The author thanks the Research Secretariat staff for helpful discussions and the Air Quality Branch staff for the help in acquiring the needed data.

TABLE 5. AVERAGE CONCENTRATIONS (PPHM) OF NO_2, NO AND O_3 MEASURED IN THREE ALBERTA CITIES ON JULY 25, 1976

Hour	Edmonton*			Calgary*			Medicine Hat		
	NO_2	NO	O_3	NO_2	NO	O_3	NO_2	NO	O_3
06	2	3	4(4)	2	1	1(1)	-	-	1
07	2	2	5(5)	2	1	1(2)	-	-	1
08	2	3	5(6)	3	1	1(3)	-	-	1
09	2	3	6(7)	2	2	2(4)	-	-	2
10	3	3	6(7)	2	1	3(5)	-	-	3
11	3	4	7(8)	2	1	3(5)	-	-	3
12	4	3	7(9)	2	0	3(5)	-	-	3
13	4	3	8(11)	2	0	3(6)	-	-	3
14	4	4	8(12)	2	0	3(6)	-	-	3
15	4	4	9(13)	2	1	2(5)	-	-	3
16	3	5	9(14)	2	0	2(5)	-	-	3
17	4	4	8(14)	2	1	2(6)	-	-	3
18	4	5	8(14)	2	1	2(6)	-	-	3
19	4	5	8(13)	3	1	2(5)	-	-	3

* These are the values observed at the DOWNTOWN station. The values observed at the RESIDENTIAL station are in parentheses.

REFERENCES

1. Altshuller, A. P. and J. Bufalini. Photochemical Aspects of Air Pollution: A Review. Environ. Sci. Technol. 5:39, 1971.

2. Pitts, J. N., Jr. and B. J. Finlayson. Mechanisms of Photochemical Air Pollution. Angewandte Chemie. 14:1, 1975.

3. Demerjian, K. L., J. A. Kerr and J. G. Calvert. The Mechanisms of Photochemical Smog Formation. Adv. Environ. Sci. Technol. 4:1, 1975.

4. National Research Council of Canada, Associate Committee on Scientific Criteria for Environmental Quality Report NRCC No. 14096. Photochemical Air Pollution: Formation, Transport and Effects, 1975. 224 pp. Also note other references in this report.

5. Sandhu, H. S. A Study of Photochemical Air Pollutants in the Urban Airsheds of Edmonton and Calgary. Alberta Environment, Edmonton, 1975. 155 pp.

6. Annual Air Monitoring Reports for the Cities of Edmonton and Calgary. Alberta Environment, 1974. 33 pp. each.

7. Johnston, H. S. Gas Phase Reaction Kinetics of Neutral Oxygen Species. National Bureau of Standards Report NSRDS 20, 1968.

8. Clyne, M. A. A., B. A. Thrush and R. P. Wayne. Kinetics of the Chemiluminiscent Reaction between Nitric Oxide and Ozone. Trans. Farad. Soc. 60:359, 1964.

AN INVESTIGATION OF LONG-RANGE TRANSPORT OF OZONE ACROSS THE MIDWESTERN AND EASTERN UNITED STATES

G. T. Wolff, P. J. Lioy, G. D. Wight, R. E. Meyers, and R. T. Cederwall*

ABSTRACT

Long-range transport of ozone across the midwestern and eastern U. S. was investigated by analyzing daily ozone isopleth maps and comparing them to meteorological maps and air parcel trajectories for the period April 12-23, 1976. This period was characterized by the presence of a large high-pressure system which produced widespread violations of the ozone standards as well as record breaking maximum springtime temperatures over much of the study area. Daily maximum ozone values from the state networks were used to produce the daily ozone maps. Movement of areas of high ozone concentrations corresponded to the movement of the high pressure system. Actual transport across these areas is supported by trajectory analysis. Daily visibility maps were also prepared and they suggest that areas of low visibility generally coincide with areas of elevated ozone under certain conditions.

INTRODUCTION

A considerable amount of data suggesting the importance of long-range ozone transport has been generated over the past few years (1,2,3). Several investigators have characterized ozone generation and subsequent transport within urban plumes (2,4,5,6). Transport of this nature, however, is on a relatively small scale and does not account for the high concentrations observed upwind of the urban plume source.

In 1976, Wolff et al. showed the additive contributions of multiple urban plumes on ozone concentrations as air parcels traveled northeastward through the Washington, D. C.-Boston, Massachusetts Corridor (8). Prior to the onset of the southwesterly flow, the authors pointed out that the air parcels entering this corridor from the west already contained ozone concentrations in excess of 0.10 ppm. Since these levels could not be directly associated with any particular urban plume, they were assumed to be background levels associated with the particular air parcels entering the Corridor. The data further indicated that the ozone levels associated with the air parcels were dependent upon the previous path and rate of travel of the air parcels. Since trajectory analysis demonstrated that these

*G. T. Wolff and P. J. Lioy, Interstate Sanitation Commission, New York, New York.
G. D. Wight, Connecticut Department of Environmental Protection, Hartford, Connecticut.
R. E. Meyers and R. T. Cederwall, Brookhaven National Laboratories, Upton, New York.

parcels had passed over industrialized and urban areas of the midwest, the authors suggested that the midwest could be a significant source region for the ozone entering the Corridor. The data presented in this paper examine this hypothesis. In addition, daily maps containing visibility isopleths are compared to the ozone isopleths. Husar, and Tong et al. attempted to use visibility as tracers for sulfates (9,10). The study reported in this paper employed this technique in an attempt to track the movement of areas containing high concentrations of ozone.

METHODOLOGY

In September 1975, Connecticut hosted a meeting for state officials from EPA Regions I, II, III, and V on ozone transport and hydrocarbon control strategies. At this meeting, a task force was established to gather, disseminate, and analyze ozone data from the monitoring networks of the participating states. The ozone data presented in this paper were obtained through the task force.

Selection of individual sites for inclusion in this analysis was based on obtaining a uniform geographical distribution and avoiding the presence of local interferring sources. In some cases, it was impossible to satisfy the second criteria and local anomalies in ozone concentrations resulted. For most of the states near the East Coast, this problem was eliminated by employing smoothing techniques. In the western sections of the study area, this was not possible because many of the sites are located in downtown urban areas. As a result, the ozone concentrations surrounding these areas may actually be higher. In addition, anomalies may occur due to calibration variations. The task force, however, has established a quality assurance program to minimize these variations.

Weather maps were obtained from the National Weather Service. The air parcel trajectories were developed at Brookhaven National Laboratories, and the method has been discussed previously (8).

Visibility isopleth maps were developed from data obtained every three hours by the National Weather Service. Husar, in his analysis, used noontime visibility readings (9). This approach resulted in local inconsistencies due to the occurrence of isolated storms and ground fog which produced visibilities not representative of the surrounding areas. In an attempt to overcome these difficulties, the isopleths presented here were based on the lowest recorded daily visibility in the absence of ground fog, precipitation, and a dew point depression of two degrees Fahrenheit or less. If these conditions persisted throughout the day at a particular site, the data were not used.

RESULTS AND DISCUSSION

A high pressure system, which moved out of Canada on April 10 and 11, was centered over Lake Michigan on the morning of April 12 (Figure 1a). On the afternoon of April 12, the first ozone readings within the high pressure system in excess of the National Ambient Air Quality Standard (NAAQS=0.08 ppm) were detected in Indiana and Ohio. Ozone levels in excess of 0.06

ppm were generally confined to these two states also.

By the morning of the 13th, the high was centered over the Ohio-West Virginia border (Figure 1b). Ozone levels exceeding 0.06 ppm now extended from western Indiana eastward into New Jersey and areas exceeding 0.08 ppm were observed in Ohio and New Jersey. This was in contrast to only one area being above the NAAQS on April 12 (Ohio). Air parcel trajectories terminating on April 13 indicate that the air over Ohio and Indiana on April 12 was advected to the East Coast of the Mid-Atlantic states by the afternoon and evening of April 13 (Figure 2b).

From April 14 to April 16, the center of the high pressure system continued to move southeastward and by the morning of April 16, it was centered off the coast of North Carolina (Figures 1c-e). The trajectories for the same period indicate that air parcels in the western Midwest (Illinois) were moving north-northeastward (Figures 2b-d). During this time, the 0.06 ppm isopleth moved northward from northern Illinois on April 13 to northern Wisconsin on April 16. The 0.08 ppm isopleth now extended in a band from Indiana to New Jersey. Trajectories from the Ohio area during the same period exhibited a more defined westerly component toward New Jersey. As a result, by April 16, the 0.06 ppm and 0.08 ppm isopleths covered most of the northeast from Maine to Virginia and Massachusetts to Virginia, respectively.

On April 17 (Figures 1f and 2f), both the 0.06 ppm and the 0.08 ppm isopleths began to contract in the western Midwest as a cold front over western Illinois began to move eastward. In the eastern sections, the trajectories on April 16 continued to move east-northeastward and, on April 17, the 0.06 ppm isopleth extended through northern New Hampshire.

The pattern observed on April 17 changed little on April 18 (Figure 1g). The cold front moved slowly eastward into Indiana. Continued northward movement of the isopleths ceased, however, as a stationary east-west front prevented it from moving into northern Maine. Trajectories from Richmond, Virginia, on April 17 and April 18 (Figures 2f-g) indicated that little horizontal advection occurred over the Middle Atlantic States. The same pattern persisted into April 19 as the cold front moved into Ohio and contraction of the 0.06 ppm isopleth continued (Figures 1 and 2h).

The eastward movement of the cold front across the northern part of the region greatly increased between April 18 and 19 (Figure 1h). Over southern sections, the front was considerably slower and by the morning of April 20, it was oriented on a southwest-northeast plane from southern Indiana to southern Maine. The northern edge of both of the isopleths generally corresponded with the position of the front. Trajectories on April 20 (Figure 2h) further illustrate the air flow resulting from the frontal movement.

Cyclogenesis on April 20 and 21 changed the flow patterns considerably by April 21 (Figure 1j). As the low pressure system intensified over the Great Lakes, the predominantly westerly flow across the East Coast shifted to a southeasterly flow. This shift was demonstrated by the trajectories

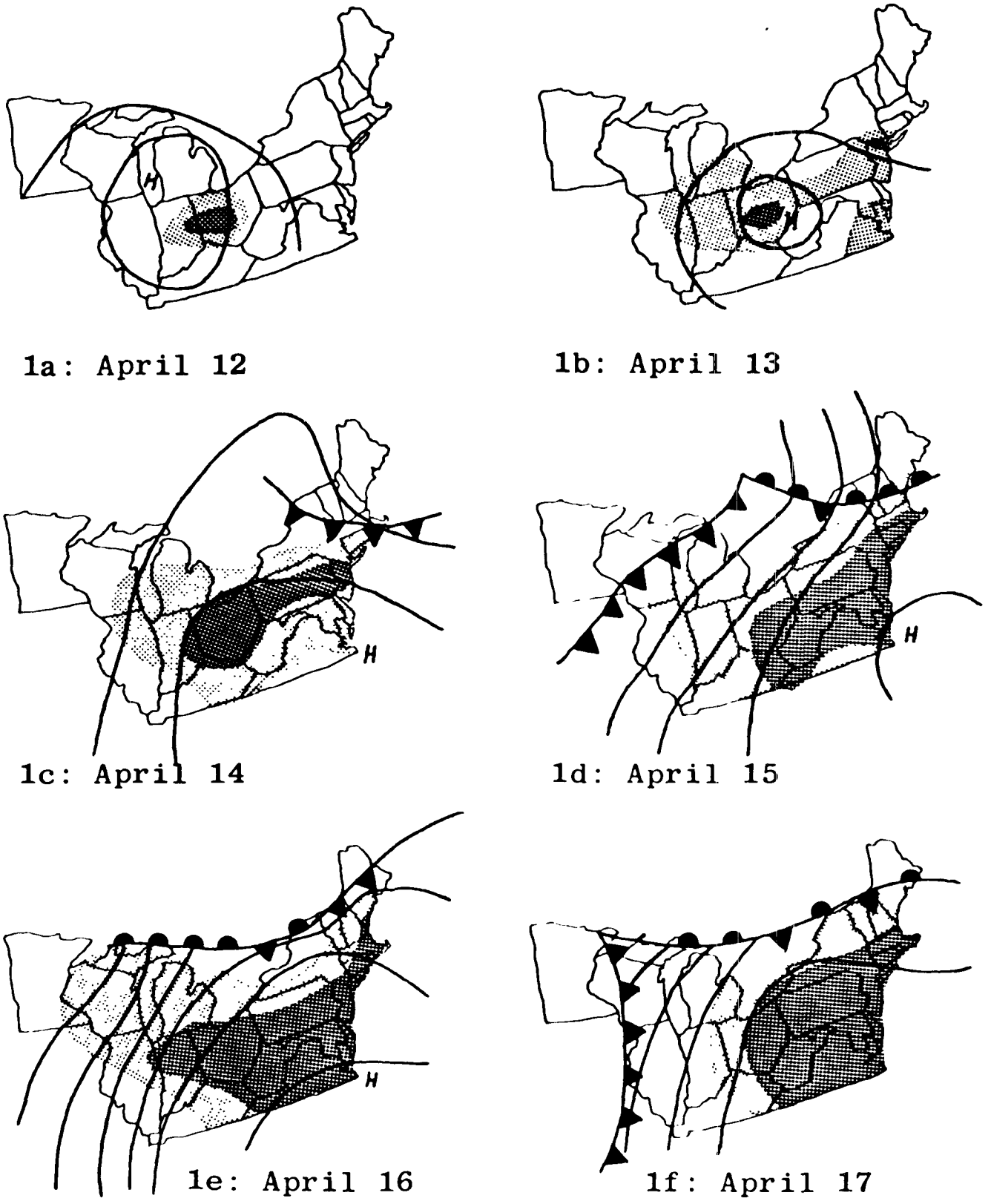

Figure 1 a-f. The accumulation and transport of ozone, April 12-17.

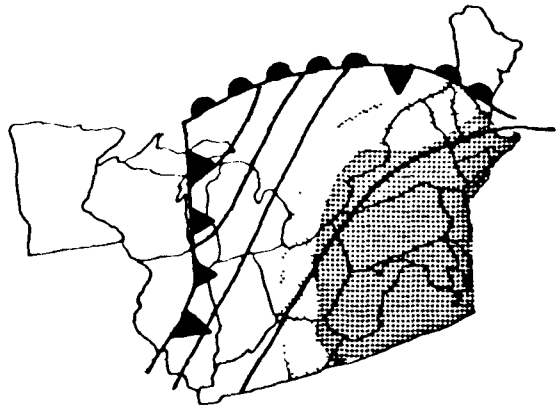

1g: April 18

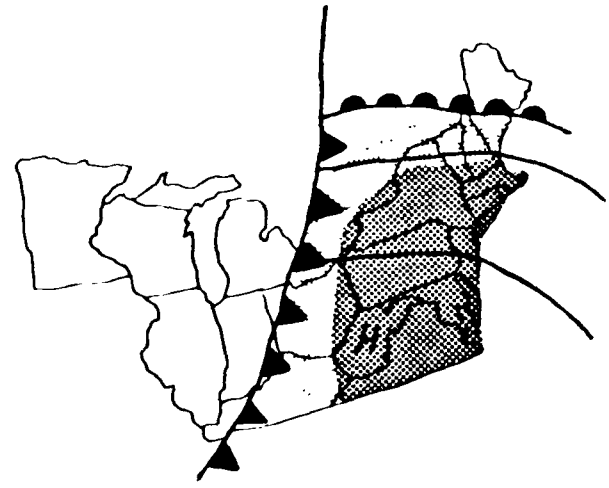

1h: April 19

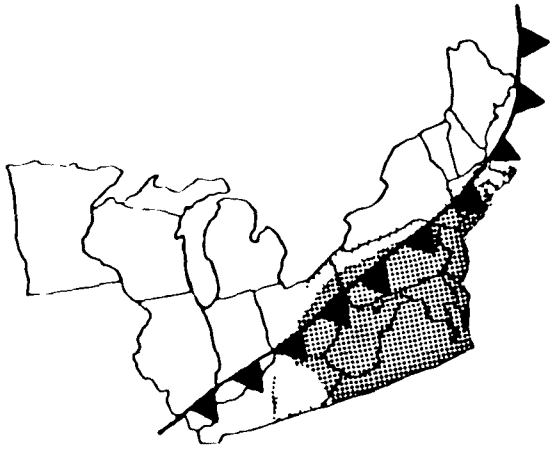

1i: April 20

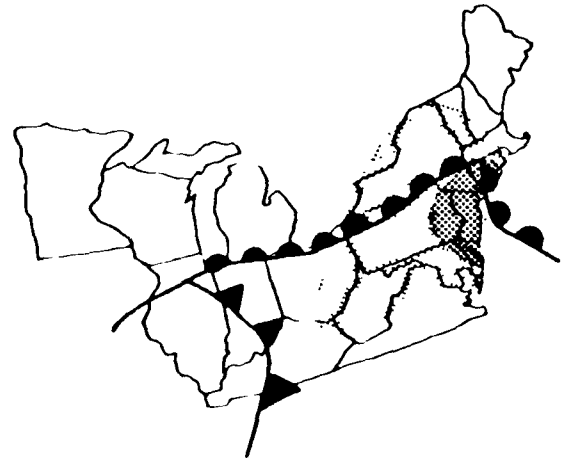

1j: April 21

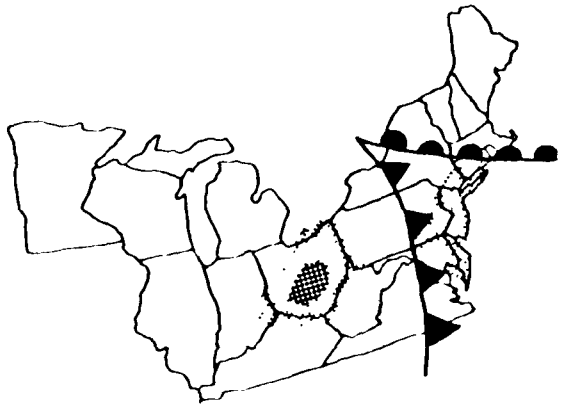

1k: April 22

≥ 0.06 ppm

≥ 0.08 ppm

Figure 1 g-k. The accumulation and transport of ozone, April 18-22.

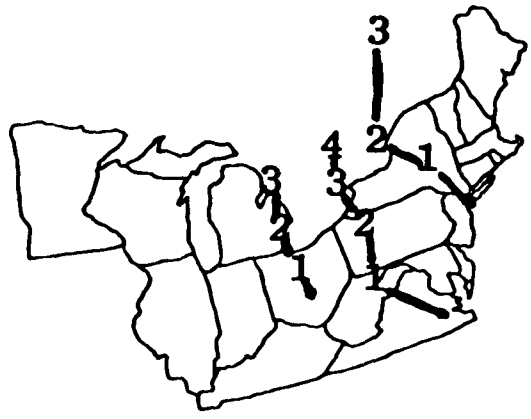

2a: April 12

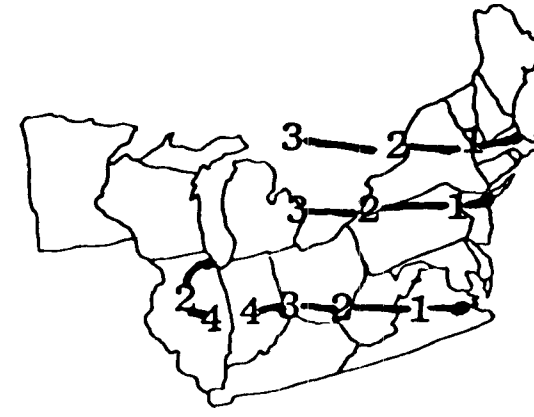

2b:April 13 at 1900

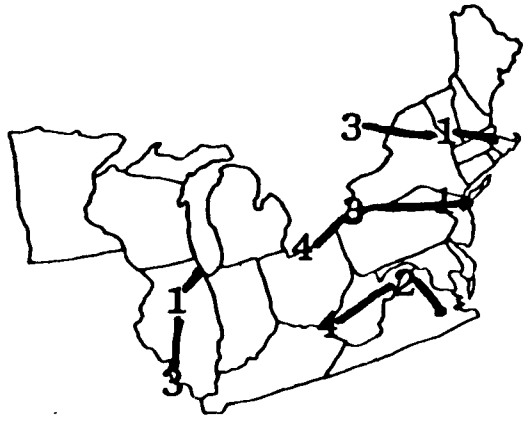

2c: April 14 (Chi.=0700)

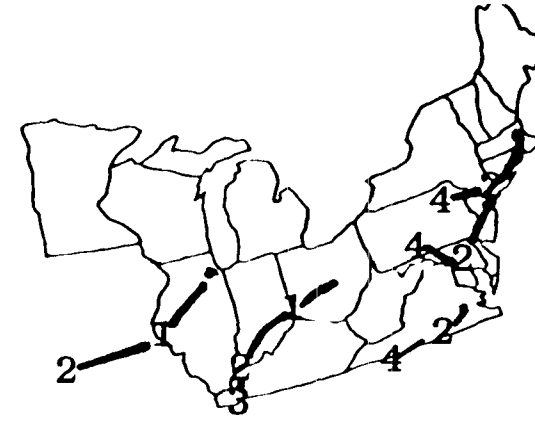

2d:April 15 (Rich.=0700)

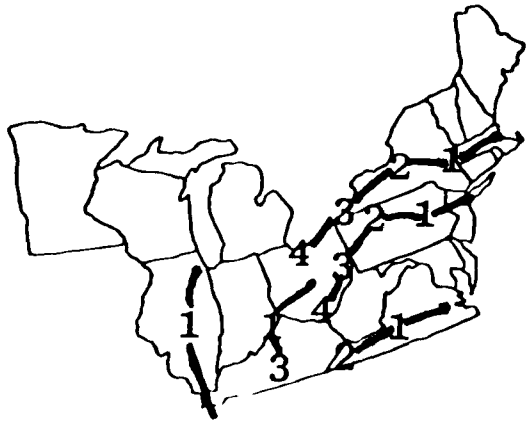

2e: April 16

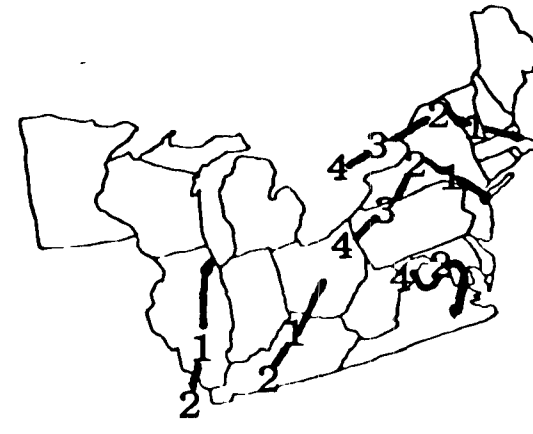

2f: April 17

Figure 2 a-f. Backward air parcel trajectories for Chicago, Columbus, Boston, Richmond, and New York, April 12-17. All trajectories terminate at 1300 hours unless otherwise stated. (Position key: 1 = position 6 hours ago, 2 = position 12 hours ago, 3 = position 18 hours ago, and 4 = position 24 hours ago.)

2g: April 18

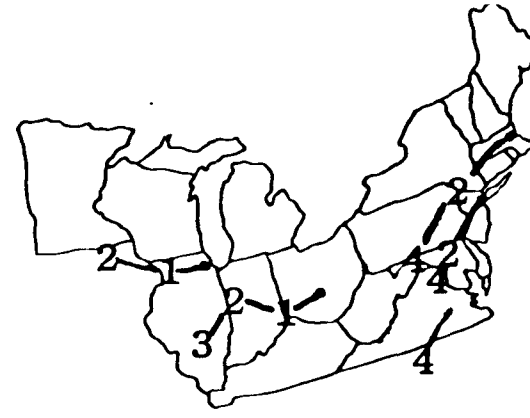

2h: April 19

2i: April 20

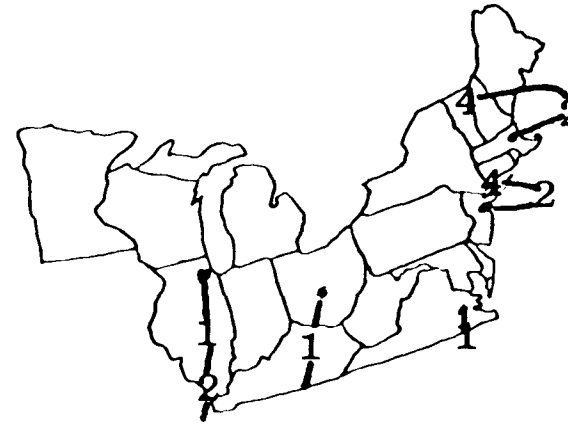

2j: April 21

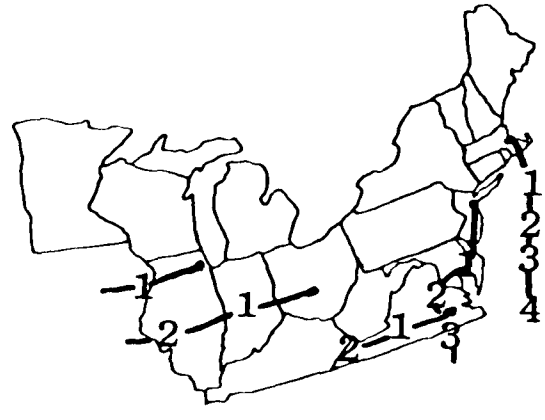

2k: April 22

Figure 2 g-k. Backward air parcel trajectories for Chicago, Columbus, Boston, Richmond, and New York, April 18-22. All trajectories terminate at 1300 hours unless otherwise stated. (Position key: 1 = position 6 hours ago, 2 = position 12 hours ago, 3 = position 18 hours ago, and 4 = position 24 hours ago.)

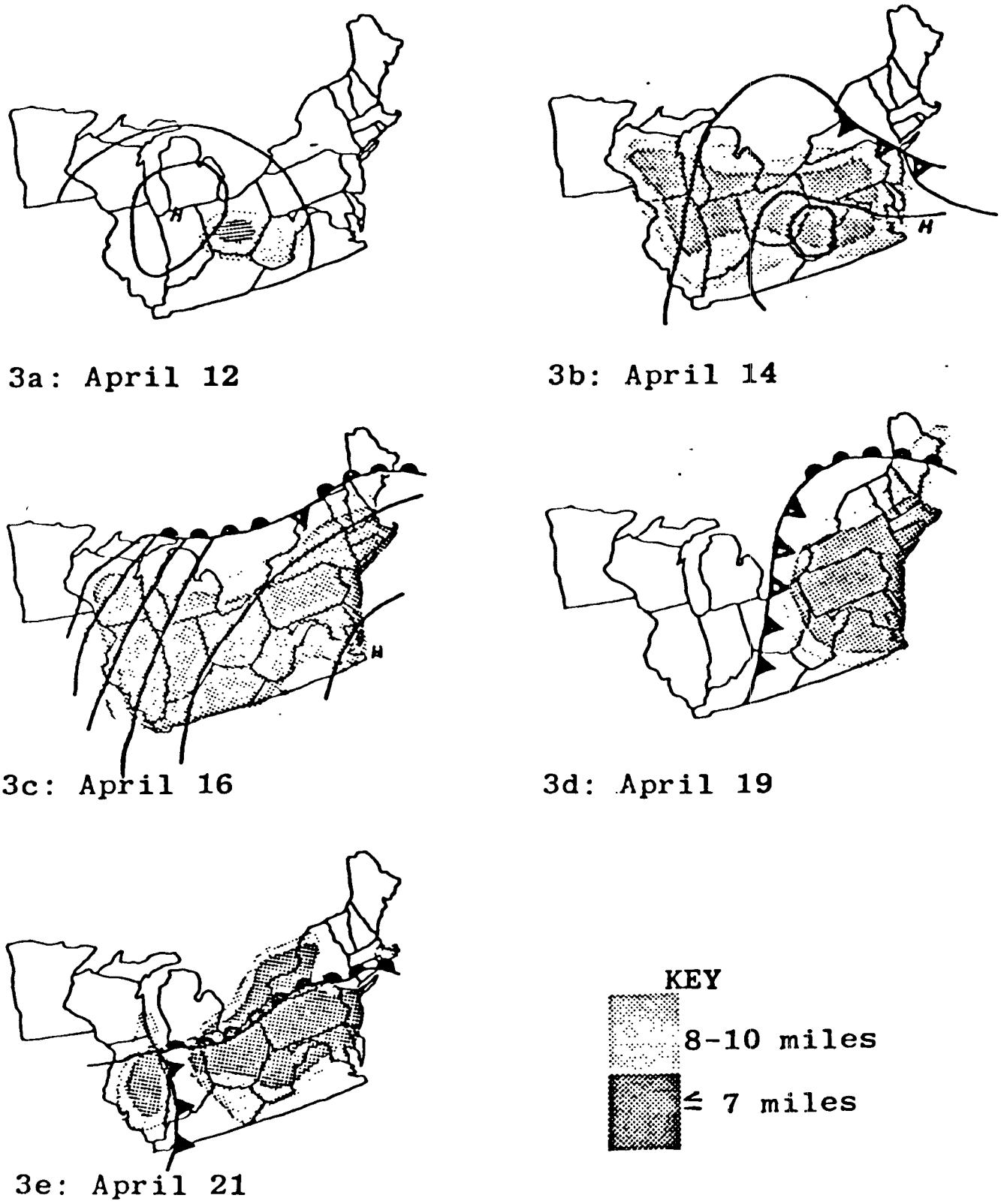

Figure 3 a-e. Visibility recorded during the high ozone concentration period of April 1976.

on April 21 while the trajectories on April 22 showed a pronounced southernly flow (Figures 2i and j). This shift resulted in advection of the 0.06 ppm isopleth northward, but because of the cloud cover and precipitation associated with this flow, the 0.08 ppm isopleth remained confined to an area with partly sunny skies centered around New Jersey.

On April 22, the low continued to move northeastward, while the cold front moved rapidly toward the Atlantic Ocean (Figure 1b). The trailing edge of the 0.06 ppm isopleth is shown moving off the Coast.

The visibilities for the same period are shown in Figures 3a-f. There are considerable geographical similarities between the areas of low visibility and high ozone from April 12-19. However, as the winds shifted on April 20 and 21 and the ozone levels decreased, the visibilities did not change substantially. This was probably due to the moisture associated with the southeasterly flow.

CONCLUSIONS

The above analysis illustrates transport of photochemical air pollution from the midwestern United States to the East Coast. Trajectory analyses also suggest that transport of photochemical air pollution from the Southern states (south of Virginia and Kentucky) to the Mid-Atlantic States also occurred between April 17 and 19.

The movements of the area of high ozone concentrations corresponded extremely well with the movements of the high pressure system as well as with the advance and retreat of frontal systems near the perimeter of the high pressure system.

Visibility maps may be a valuable technique in tracing ozone transport under certain conditions. A significant correspondence between the areas of high ozone and the areas of low visibility occurred during most of the study period. Toward the end of the period, as the high pressure system weakened and moisture was advected into the area via an on-shore circulation, the relationship became less established.

At the present time, daily ozone isopleth maps are being developed for the entire summer of 1976. The techniques used in this report will be employed on this data. Current efforts are also being undertaken to refine the selection and presentation of the visibility data. In the present research we have only examined the daily maximum ozone concentration, subsequent studies will include analysis of ozone during other time periods. In addition, the possibility of stratospheric injection of ozone is being investigated by employing isentropic analysis (11).

ACKNOWLEDGEMENTS

The authors wish to express their gratitude to all of the members of the Moodus Data Sharing and Analysis Committee for providing the ozone data used in this report. The authors also thank Messrs. Michael Anderson,

James Oliver, William Simpson, Jerry Bujancius of the Connecticut Department of Environmental Protection, Richard Taylor of the New York State Department of Environmental Control, and Konrad Wisniewski and William Edwards of the Interstate Sanitation Commission for their assistance in data collection and analysis.

REFERENCES

1. Coffey, P.E. and W.N. Stasiuk, Jr. Evidence of Atmospheric Transport of Ozone into Urban Areas. Environmental Science and Technology., 9(1):59-62, 1975.

2. Wolff, G.T., W.N. Stasiuk, Jr., P.E. Coffey and R.E. Pasceri. Aerial Ozone Measurements over New Jersey, New York and Connecticut. In: Proceedings of the 68th Annual Meeting of the Air Pollution Control Association, Boston, Mass., 1975. paper 75-586.

3. Bach, Jr., W.D. Investigation of Ozone and Ozone Precursor Concentrations at Non-Urban Locations in the Eastern U.S. - Phase II: Meteorological Analysis. EPA-450/3-74-034-a, U.S. EPA, Research Triangle Park, N.C., 1975. 144 pp.

4. Wolff, G.T. Preliminary Investigation of the Photochemical Oxidant Problem in the N.J.-N.Y.-Conn. A.Q.C.R. Interstate Sanitation Commission N.Y., N.Y., 1974. 69 pp.

5. Rubin, R.A., L. Bruckman and J. Magyar. Ozone Transport. In: Proceedings of the 68th Annual Meeting of the Air Pollution Control Association, Boston, Mass., 1975. paper 75-07.1.

6. Cleveland, W.S., B. Kleiner, J.E. McRae and J.L. Warner, Photochemical Air Pollution: Transport from the New York City Area into Connecticut and Massachusetts. Science, 191:179-181, 1976.

7. Wolff, G.T., P.J. Lioy, G.D. Wight and R.E. Pasceri. An Aerial Investigation of Photochemical Oxidants over the Eastern Mid-Atlantic States. In: Proceedings of EPA Symposium on Ozone Transport, Research Triangle Park, N.C., 1976(In Press).

8. Wolff, G.T., P.J. Lioy, R.E. Meyers, R.T. Cederwall, G.D. Wight R.E. Pasceri and R.S. Taylor. Anatomy of Two Ozone Transport Episodes in the Washington, D.C. to Boston, Mass. Corridor. Presented at the 10th Annual Meeting of the Mid-Atlantic Amer. Chem. Soc., Phil., Pa., 1976 (also submitted for publication).

9. Husar, R.B., J.D. Husar, N.V. Gillani, S.B. Fuller, W.H. White, J.A. Anderson, W.M. Vaughan and W.E. Wilson, Jr. Pollutant Flow Rate Measurements in Large Plumes: Sulfur Budget in Power Plant and Area Source Plumes in the St. Louis Region. Presented at the 172nd National Amer. Chem. Soc. Meeting, N.Y., 1976.

10. Tong, E.Y., G.M. Hidy, T.F. Lavery, and F. Berlander. Regional and Local Aspects of Atmospheric Sulfate in the Northeast Quadrant of the U.S. In: Reprints 3rd Symposium on Atmospheric Turbulence Diffusion and Air Quality, American Meteorological Society, Raleigh, N.C., 1976.

11. Danielson, E.F. Transport and Diffusion of Stratospheric Radioactivity based on Synoptic Hemispheric Analyses of Potential Vorticity. NYO-3317-3, Atomic Energy Commission, Washington, D.C., Nov. 1967.

OXIDANT AND PRECURSOR TRANSPORT SIMULATION STUDIES IN THE RESEARCH TRIANGLE INSTITUTE SMOG CHAMBERS

J. E. Sickles, II, L. A. Ripperton, and W. C. Eaton*

ABSTRACT

The generation of ozone under simulated conditions of pollutant transport was studies in a system of four, 27 cubic meter, outdoor smog chambers. Chamber construction was of 5 mil FEP Teflon® on an aluminum frame. Simulation of transport was accomplished by irradiating reactants for three days with sunlight and by diluting the contents of the chambers. The initial charge of nonmethane hydrocarbon was 1 to 10 parts per million carbon of a surrogate urban mixture; the initial nitrogen oxides' charge was 0.10 to 1.0 ppm. This resulted in initial nonmethane hydrocarbon to oxides of nitrogen ratios of 7 to 20. Without the addition of reactants after the initial charge, the second- and third-day chemical systems in the chambers generated ozone concentrations greater than the National Ambient Air Quality Standard for photochemical oxidant. The analogy between the chemical behavior of chamber simulations and nonurban high ozone (>0.08 ppm) systems measured in the field is good.

INTRODUCTION

The Research Triangle Institute's outdoor smog chamber facility is shown in Figure 1. The system is composed of 4 outdoor chambers (each 27 cubic meters in volume) made of 5 mil FEP Teflon on aluminum frames. Each chamber has its own air cleaning system to oxidize hydrocarbons (HC) and remove oxides of nitrogen (NO_x).

The study reported here was conducted during July and August of 1975 under Environmental Protection Agency sponsorship. The purpose was to study the behavior of ozone (O_3) concentration under simulated conditions of transport of oxidants and their precursors downwind from urban environs. To simulate movement from the cities, chemical pollutant systems were irradiated for multiple daylight periods and subjected to a period of dilution with clean air. Data are reported for the three 24-hour dilution rates: 0.0% (i.e., batch), 77.5%, and 95%. After 24 hours of dilution, the chambers were operated in a batch mode with no additional dilution.

Initial reactant charges were 1 to 10 parts per million carbon (ppmC) of a surrogate urban mixture and 0.1 to 1.0 ppm of NO_x of which 20% was nitrogen dioxide (NO_2). The nonmethane hydrocarbon (NMHC) to NO_x ratios were chosen to be from 7 to 20.

*Research Triangle Institute, Research Triangle Park, North Carolina.

Figure 1. RTI Smog Chamber Facility.

DISCUSSION

The results of the study have been summarized in a series of tables similar to Table 1. The first 4 columns after the data and chamber number provide information about the behavior of the system on the first day. For this series of runs, the 24-hour dilution rate was 95% and it was begun at the time of NO_x crossover (at about 0830). In chamber 1, the NMHC charge was about 7 ppmC and the NO_x was about 1.0 ppm with a ratio of 7. Maximum O_3 concentration in Chamber 1 was about 1.1 ppm the first day. The next column indicates whether the following data are from the second or third day of irradiation. The NO_x concentrations at sunrise were in the parts per billion (ppb) range. The second- and third-day NMHC/NO_x ratios were high; for the whole set of experiments they ranged from 22 to over 250. Gas chromatographic analysis of the HC remaining on the second and third day showed a preponderance of alkanes and aromatic compounds with alkenes virtually exhausted except for a few tens of ppb of ethylene that usually remained.

The maximum O_3 concentrations obtained on the second and third days were in most cases (in all cases in Table 1) above the National Ambient Air Quality Standard (NAAQS) for photochemical oxidant. The net O_3 concentrations generated (i.e., the difference between the morning minima and the afternoon maxima) were also almost always greater than the NAAQS despite extremely low NO_x concentrations.

Table 2 represents another type of summary and analysis of the O_3-generative data from the second and third days of irradiation. Both the NO_x data and the NMHC/NO_x ratios have been stratified by numerical range and the net O_3 concentrations associated with a particular combination have been listed in the appropriate cell. Averages of individual cells, vertical columns, and horizontal rows, are indicated. Although not presented, the same treat-

TABLE 1. SELECTED RESULTS FROM THE JULY 28-30 THREE-DAY CHAMBER RUNS

Date / Chamber No.	Percent Dilution, Time of Dilution Initiation	Initial NMHC/NO_x Concentrations ppmC/ppm	NMHC/NO_x Ratios	Maximum O_3 First Day ppm	Subsequent Days	Precursors (ppm) at Sunrise NO_x	Precursors (ppm) at Sunrise NMHC	NMHC/NO_x Ratios	Min O_3 ppm	Max O_3 ppm	Net O_3 ppm	Σ Solar Rad. at O_3 Max (Langley's)
Chamber No. 1 July 28-30	95 % @ 0830	7.02/.967	7.3	1.062	2	0.007	0.84	120.0	.023	.286	.263	515.4
					3	0.009	0.85	94.4	.050	.240	.190	421.2
Chamber No. 2 July 28-30	0840	4.24/.235	18.0	0.604	2	0.003	0.77	256.7	.006	.212	.206	535.2
					3	0.005	0.76	152.0	.035	.190	.152	420.6
Chamber No. 3 July 28-30	0840	3.95/.715	5.5	0.667	2	0.005	0.48	96.0	.013	.214	.201	534.6
					3	0.005	0.55	110.0	.037	.190	.153	397.8
Chamber No. 4 July 28-30	0850	1.15/.105	10.8	0.325	2	0.002	0.55	275.0	.003	.175	.172	541.2
					3	0.003	0.63	210.0	.042	.167	.125	427.2

ment was also afforded the maximum O_3 concentrations. The net O_3 and maximum O_3 concentrations were then examined at various combinations of NMHC concentration range and NMHC/NO_x ratios. Ranges of NO_x and NMHC concentration were arbitrarily selected to provide a spread of ratios. These indicated comparisons are plotted in Figure 2, 3, and 4.

In Figure 2 it can be seen that maximum, minimum, and net O_3 concentration increased with increasing NO_x. As the maximum O_3 concentration increased, so did the minimum. The divergence between maximum and net O_3 concentrations as the NO_x concentration increased was due to O_3 left over from the previous day. Similar behavior with increasing NMHC concentration can be seen in Figure 3.

In Figure 4, O_3 concentration was plotted against NMHC/NO_x ratios. Ozone concentrations (both maximum and net) were maximized at NMHC/NO_x ratios of 55 to 99.

The data suggest a so-called dilution effect on O_3 generation. It has been noted by others that a reduction in initial concentrations of reactants (at the same ratio) does not produce a proportional reduction in the subsequent O_3 maximum. Similar phenomena have been observed under dynamic dilution in this study. An example of this, employing second-day data, is illustrated in Figure 5. Similar initial concentrations and conditions of solar irradiation existed in the three cases. A 95% dilution of the system over 24 hours (ending about 0830 on the second day) produced only a 40% reduction in maximum O_3. The net O_3 generated with 95% dilution (0.26 ppm) was actually greater than the net generated in the batch system (0.20 ppm). The efficiency of O_3 generation (per NO_x molecule) was increased by dilution. This dilution effect may be one of the processes helping to deliver high O_3 concentrations to nonurban areas.

TABLE 2. NET OZONE GENERATED ON SECOND AND THIRD DAYS OF IRRADIATION AS A FUNCTION OF OXIDES OF NITROGEN AND NONMETHANE HYDROCARBON/OXIDES OF NITROGEN RATIO

NMHC/NO_x ppmC/ppm Range	NO_x Range ppb	1 - 5		6 - 8	9 - 14		15 - 53	
0-49					.195	.164	.181	.168
					.115	avg.	.154	avg.
					*.182			
.165								
50-99	.201	.201	*.124	.128	.312	.214	.365	.315
		avg.	*.131	avg.	.256	avg.	.300	avg.
					.230		.197	
					.214		.371	
					*.190		*.344	
					*.119			
					*.177			
.235								
100-199	*.152	.140	.263	.189	.123	.134	.150	.188
	*.217	avg.	*.250	avg.	.094	avg.	.135	avg.
	*.153		*.105		.033		*.238	
	*.123		*.257		*.285		*.228	
	*.054		*.068					
.163								
>200	.076	.147						
	.206	avg.						
	.172							
	.173							
	.129							
	*.125							
Avg. .147	Avg. .149		Avg. .171		Avg. .180		Avg. .241	

* Indicates 3rd-Day Values

A term, fossil O_3, has been coined to denote O_3 generated in urban environs which is transported over unspecified distances downwind. To investigate this phenomena, the decay of O_3 in spent, non-O_3-generating systems was examined from both chamber and field studies. Nighttime half-lives of O_3 were calculated for non-dilution chamber operation and are presented in Table 3. Maximum O_3 levels of the previous day are shown and half-lives assuming first

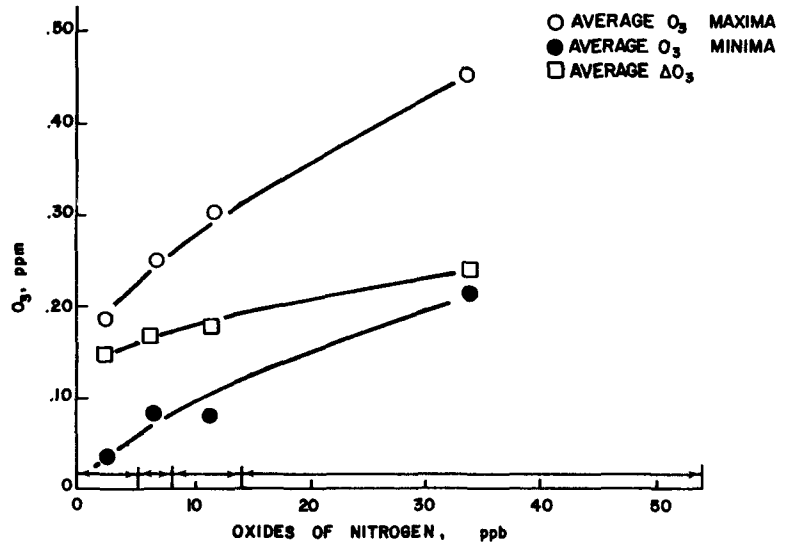

Figure 2. Average maxima, minima, and ΔO_3 concentrations as a function of NO_x concentrations at sunrise on the second and third days of irradiation.

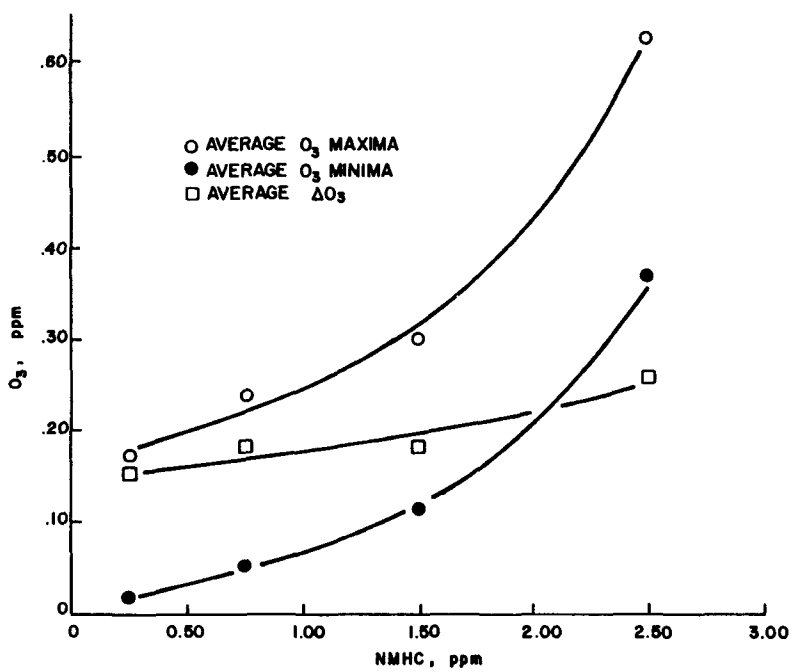

Figure 3. Average maxima, minima, and ΔO_3 concentrations as a function of nonmethane hydrocarbon concentrations on the second and third days of irradiation.

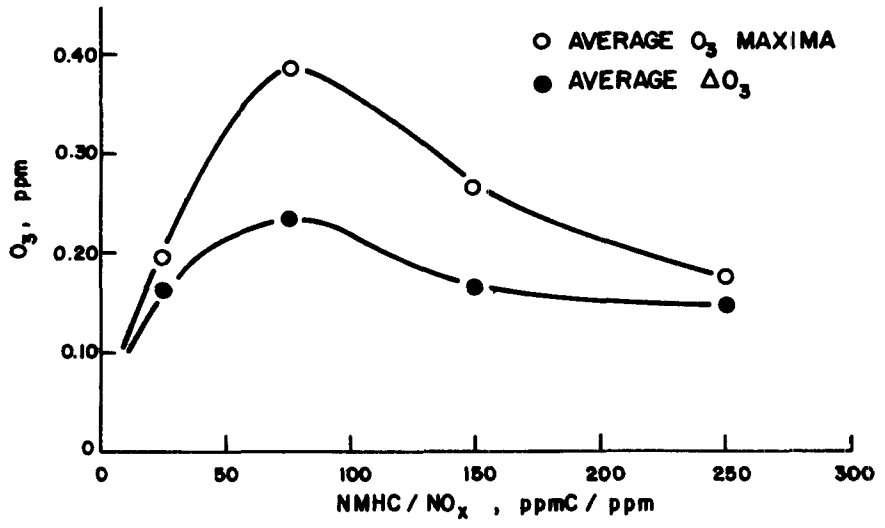

Figure 4. Average maxima and ΔO_3 as a function of nonmethane hydrocarbon to oxides of nitrogen ratio.

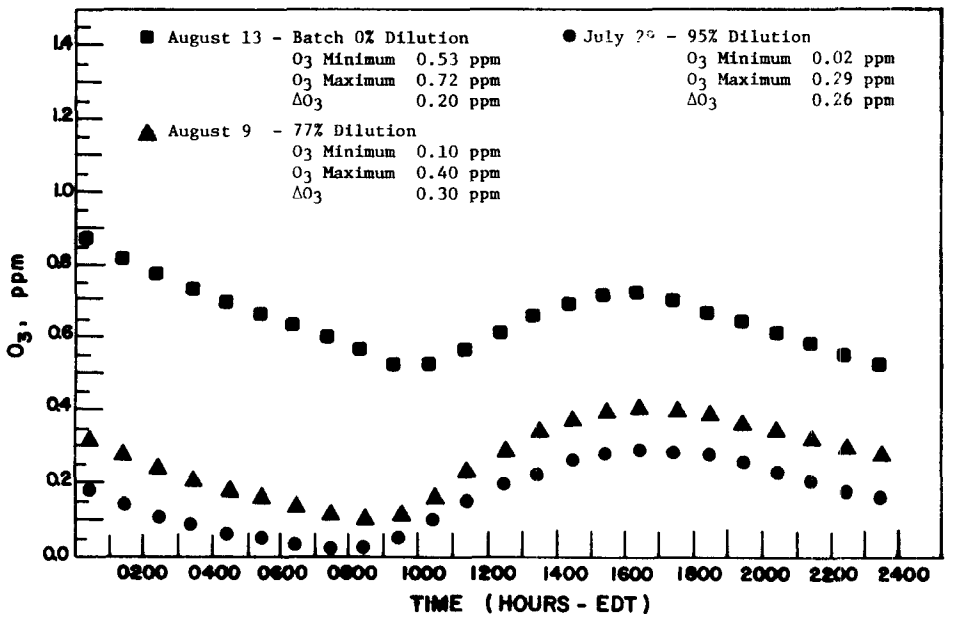

Figure 5. Ozone profiles over second-day irradiations for same initial conditions and different dilutions in Chamber 1.

order decay were calculated using the 0200 and 0500 hours concentrations. The table shows the 0200 hours concentrations and the calculated half-lives. The tabulated half-lives have been corrected for dark-phase clean chamber O_3 decay. Of the values calculated, 17 are below 20 hours, 5 are below 60 hours, and two are rather large, 265 and 450 hours. Data from two field studies may be used to obtain rough estimates of the dark phase O_3 half-life. A series of vertical O_3 concentration profiles taken with an aircraft on August 1, 1974, at Wilmington, Ohio, are shown in Figure 6. If it is assumed that the profile at 0700 on August 2 was the same as that at 0700 on August 1, then an assumed first-order decay from 1700 August 1 to 0700 August 2 suggests an O_3 half-life of 29.5 hours. Ozone measurements collected aloft (from 1800 June 8, 1976, to 0200 June 9, 1976) during the second flight of the DaVinci balloon suggest a half-life of 16 to 34 hours.

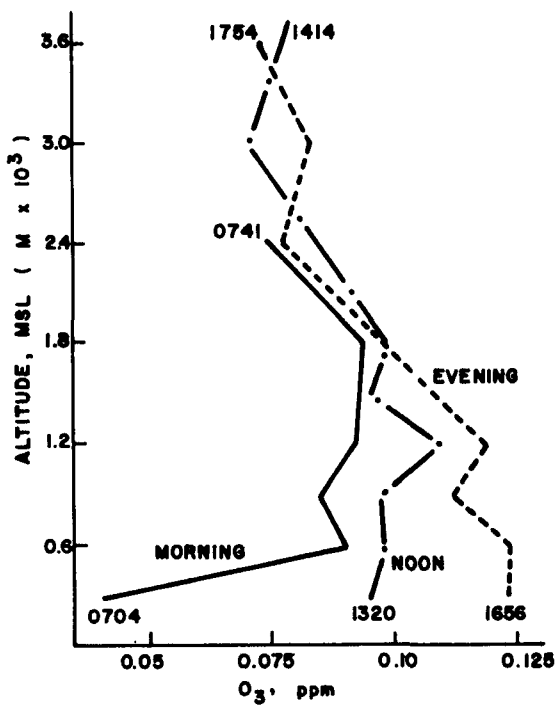

Figure 6. Vertical ozone soundings, August 1, 1974, Wilmington, Ohio.

With half-lives of 20 to 30 hours, the amount of O_3 left over on the following morning can provide a high minimum on which to build a high maximum for the first day. With half-lives of 20 to 30 hours, however, a parcel of fossil O_3 cannot maintain high concentrations for more than a day or two without augmenting synthesis.

Figures 7, 8, and 9 may be employed to compare field measurements with second- and third-day smog chamber data. Figure 7 depicts diurnal curves drawn from hourly O_3 averages at three Ohio stations in the summer of 1974. The maxima are between 0.07 and 0.08 ppm, indicating that many of the indi-

TABLE 3. DARK PHASE OZONE HALF-LIVES IN SMOG CHAMBER RUNS

Date	Experimental Type	Chamber Number	Max $[O_3]$ Previous Day ppm	$[O_3]$ at 0200 ppm	Half-Life ($t_{1/2}$) hrs
July 24	Dilution 95% * Initiated at 1700	1	0.185	0.066	4.3
		2	0.138	0.048	3.6
		3	0.119	0.038	11.6
		4	0.089	0.025	13.3
July 30	Dilution 95% Initiated at NO_x Crossover	1	0.286	0.102	6.4
		2	0.212	0.085	6.2
		3	0.214	0.076	7.4
		4	0.175	0.083	7.8
August 6	Dilution 77% Initiated at NO_x Crossover	1	0.479	0.311	14.9
		2	0.366	0.243	11.6
		3	0.350	0.213	10.0
		4	0.214	0.109	7.1
August 10	Dilution 77% Initiated at NO_x Crossover	1	0.400	0.218	16.6
		2	0.293	0.175	14.2
		3	0.288	0.150	19.2
		4	0.179	0.109	14.2
August 13	Batch	1	1.378	0.776	33.5
		2	0.886	0.561	42.9
		3	0.997	0.567	50.3
		4	0.549	0.415	265.4
August 14	Batch	1	0.724	0.422	19.9
		2	0.525	0.333	27.2
		3	0.786	0.352	54.5
		4	0.336	0.252	449.6

*Mechanical dilution had been terminated prior to the time periods chosen for half-life calculations.

vidual concentrations making up the hourly averages were over the NAAQS. The time of maxima at these rural stations was shifted more toward sundown than that typically observed in an urban atmosphere. Also the slope of the build-up side of the diurnal rural O_3 curve is steeper than the O_3-destructive side. Generally, this is not the case in urban atmospheres where freshly emitted pollutants (e.g. auto exhaust in evening rushhour traffic) act as O_3-destructive agents and cause the sharp drop on the destructive side of the diurnal urban O_3 profile.

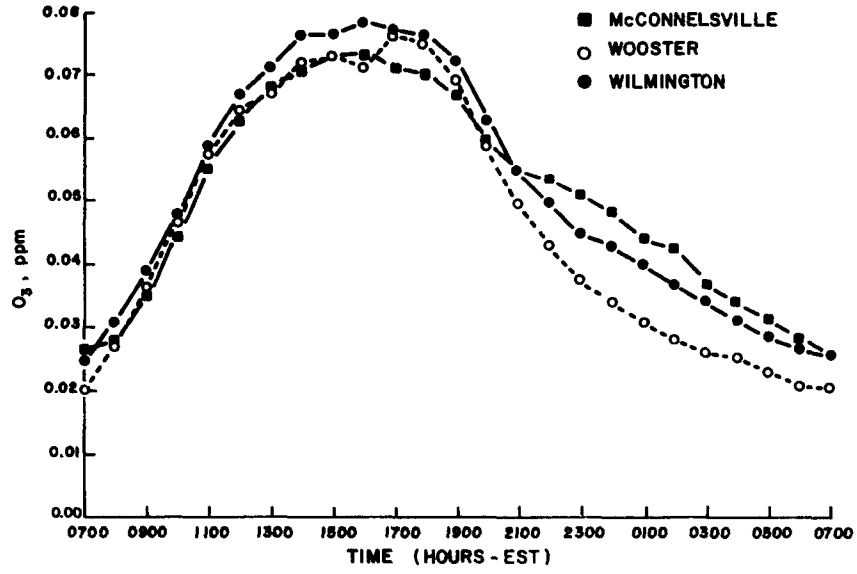

Figure 7. Mean diurnal O_3 concentration at Wilmington, Wooster, and McConnelsville, Ohio, from June 14-August 31, 1974.

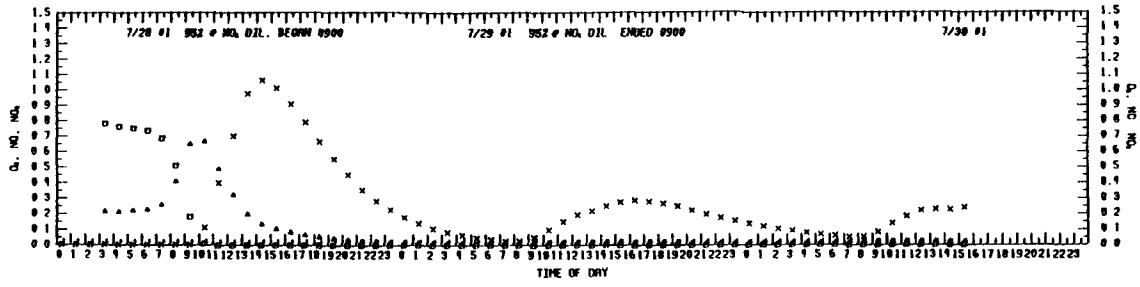

Figure 8. Typical three-day profiles for NO (□), NO_2 (Δ), and O_3 (×).

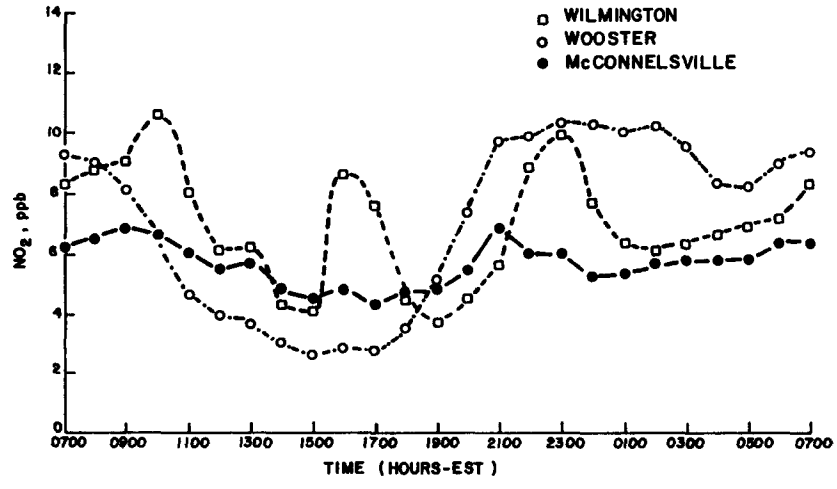

Figure 9. Mean diurnal NO_2 concentration at Wilmington, Wooster, and McConnelsville, Ohio, from June 14-August 31, 1974.

Concentration profiles for the previously discussed (Table 1) July 28-30 three-day run are presented in Figure 8. In this run, there was a 95% dilution of the system in 24 hours starting at the time of NO_x crossover. The NO_x became virtually undetectable, and the second- and third-day maximum O_3 and net O_3 concentrations were in excess of the NAAQS. Note also that the O_3-destructive side of the second-day O_3 profile is less steep than that typically observed for urban air.

Figure 9 depicts the hourly averages of NO_x from the field obtained at the same time and in the same areas as the O_3 data in Figure 7. The NO_x concentrations ranged from about 2 to 12 ppb. Smog chamber second- and third-day values were 1 to 53 ppb. Calculated from average data, the NMHC/NO_x ratios ranged from 27 to over 300 for field data and ranged from 22 to over 250 for second- and third-day smog chamber data.

Chamber data of the second and third day are remarkably similar to field data. In making comparisons between field data and chamber data the following caveats should be observed. No additional reactants were added to the chambers after the first day, whereas there is continuous addition of reactants to the ambient air. The so-called "dirty chamber effect" was also observed in the chamber. Direct comparisons and control strategy decisions based on these data are therefore difficult.

CONCLUSIONS

In partially spent simulated urban photochemical systems, O_3 was generated in concentrations above the NAAQS with low concentrations (ppb) of NO_x and high NMHC/NO_x ratios.

The smog chamber data also suggest that the role of fossil O_3 is to provide a high minimum upon which to build a high maximum on the next day. The fossil O_3, unaugmented by subsequent synthesis, probably cannot provide concentrations over the NAAQS for more than a day or two.

The smog chamber data indicate that the dilution effect (i.e., more efficient O_3 generation per molecule of NO_x with dilution) is an important process in delivering high O_3 atmospheres.

The atmospheric chemical problems in general and the high rural O_3 problem in particular will yield to a three-faceted approach: field measurements, experimentation in smog chambers, and mathematical modeling. Each single facet has its limitations but iterative studies using the combined approach should yield useful information and solutions to current problems of atmospheric chemistry.

OZONE EPISODES ON THE SWEDISH WEST COAST

P. Greenfelt*

ABSTRACT

Ozone measurements have been performed in Gothenburg on the Swedish west coast since 1972. On several occasions every summer increased levels of ozone were observed. The highest recorded 1-hour mean was 110 ppb. The high ozone levels coincided in time with increased concentrations of particle-borne sulphur both in and outside Gothenburg and of soot outside Gothenburg. Trajectory studies showed that most of these episodes were associated with transport of air masses from remote industrial areas.

INTRODUCTION

Long-distance transport of air pollutants over western Europe has been the object of extensive research in these countries since around 1970. This work has been focussed mainly on sulphur compounds and their role in the acidification of lakes, running waters and soil. The study of other essential air pollutants such as heavy metals, chlorinated hydrocarbons and nitrogen oxides has been very limited. However, as regards photochemical oxidants a few reports of investigations are available (1,2). This paper presents results of measurements of ozone and associated parameters performed on the Swedish west coast.

OZONE MEASUREMENTS IN GOTHENBURG

Continuous ozone measurements according to the chemiluminescent ozone-ethylene method have been carried out in Gothenburg on the Swedish west coast since January 1972. Gothenburg is a highly industrialized city (e.g. two oil refineries), with a population of half a million. Initially, the purpose of the measurements was to investigate the possible occurrence of locally produced photochemical ozone. Once the results were obtained, the measurements were extended to include long-range transport of oxidants and their precursors.

Only two months after the measurements were started, on the 16th of March, the ozone level in Gothenburg rose to above 90 ppb (Figure 1). Although higher peaks have been observed later, this one was remarkable because it occurred so early in the year. March is considered to be a winter month in Sweden; the monthly mean temperature in Gothenburg is +0.7°C. The meteorological conditions and the concentration of other pollutants on this day are shown in Table 1. The data clearly indicate that this ozone peak could not be associated with any natural sources. This is particularly obvious from the concentrations of soot and particle-borne sulphur as well as from the visibility data.

*Swedish Water and Air Pollution Research Laboratory (IVL), Gothenburg, Sweden.

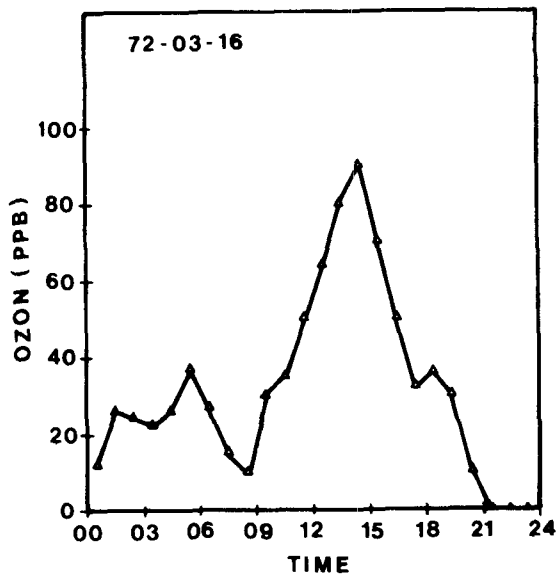

Figure 1. Ozone concentrations in Gothenburg, 16 March 1972.

TABLE 1. METEOROLOGICAL CONDITIONS AND CONCENTRATION OF AIR POLLUTANTS IN GOTHENBURG ON 16 MARCH 1972

Wind direction		SSE
Wind velocity		3 m/s
Temperature		+11.5°C
Relative humidity	at 13.00 hrs	54%
Visibility		7 km (4 miles)
Overcast		No
Ozone	max. 1-hour	180 μg/m³
SO_2		114 μg/m³
Soot (OECD-method)	daily mean	57 μg/m³
Particle-borne sulphur (X-ray fluorescence)		40 μg/m³

In the following months (March-August) of 1972, several similar peaks in ozone concentration above the natural background level were observed. These occurred mostly in the afternoons and early evening hours. However, peaks were observed also at other hours of the day, e.g. early morning. For this period, 1-hour concentrations above 80 ppb occurred on a total of 16 days; the highest

value recorded was 110 ppb. In subsequent summers (1973-76) similar ozone episodes were not as numerous as in 1972, and on no occasion did the ozone level exceed 110 ppb within Gothenburg.

The episodes have been evaluated on the basis of meteorological conditions and the concentration of other pollutants. The meteorological conditions during days with high ozone levels showed large variations. For example, the daily maximum temperatures during episodes in 1972 and 9173 ranged from +11.5°C to 31.5°C. The wind velocity also varied considerably (episodes could occur at wind velocities of up to 13 m/s), whereas there was a clear pattern with respect to wind direction: During nearly all episodes winds were blowing from the sector SE-W. Mostly low or moderate values for visibility were recorded. All meteorological observations were made at Torslanda Airport, 10 km west of Gothenburn (Figure 2).

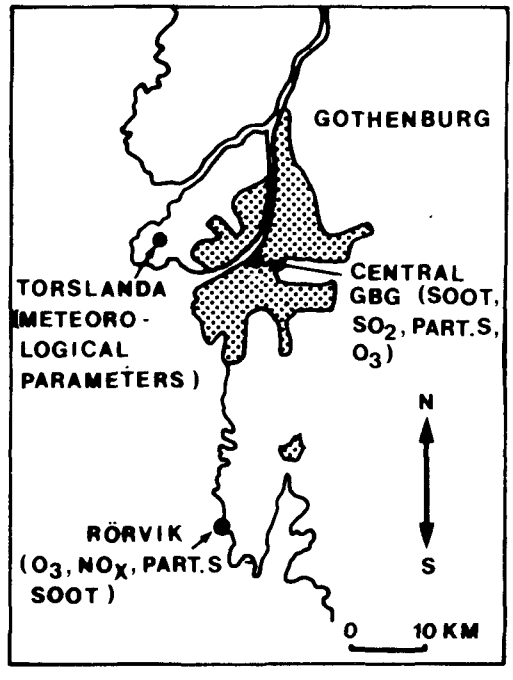

Figure 2. Location of sampling stations for air pollution monitoring and meteorological measurements

Sulphur dioxide, soot and particle-borne sulphur are measured in Gothenburg in a routine network. To determine the origin of the ozone episodes observed in Gothenburg, comparisons were made between daily mean concentrations of these pollutants and peak ozone concentrations. Correlation coefficients were calculated for each month with more than 10 comparable data in the periods March-August 1972 and 1973. No significant covariations for sulphur dioxide and soot were found, but a clear positive relationship was observed for particle-borne sulphur. The correlation coefficients between daily maximum 1-hour ozone mean values and daily mean values of particle-borne sulphur were in the range of 0.30-0.80 in nine out of ten months (Table 2). As examples of the covariations, plots from August 1972 and 1973 are shown in Figure 3.

TABLE 2. CORRELATION BETWEEN DAILY MAXIMUM 1-HOUR CONCENTRATIONS OF OZONE IN GOTHENBURG (GBG) AND SOOT, PARTICLE-BORNE SULPHUR IN GOTHENBURG AND RÖRVIK. MARCH - AUGUST 1972 AND 1973.

	Ozone vs. soot Gbg		Ozone vs. soot Rörvik		Ozone vs. part. S Gbg		Ozone vs. part. S Rörvik	
	r	n	r	n	r	n	r	n
1972 March	0.31	22	0.13	24	0.48	22	0.38	24
May	-0.21	27	-0.17	27	-0.15	27	0.01	27
June	0.04	22	0.68	26	0.30	23	0.69	24
July	0.36	25	0.43	28	0.65	25	0.60	28
Aug.	0.01	17	0.48	17	0.80	17	0.30	13
1973 April	-0.23	13	0.30	13	0.50	13	0.67	13
May	0.50	31	0.50	31	0.63	31	0.51	31
June	0.28	30	0.34	30	0.62	30	0.54	30
July	0.08	31	0.42	28	0.31	31	0.31	31
Aug.	0.25	26	0.51	26	0.65	26	0.63	26

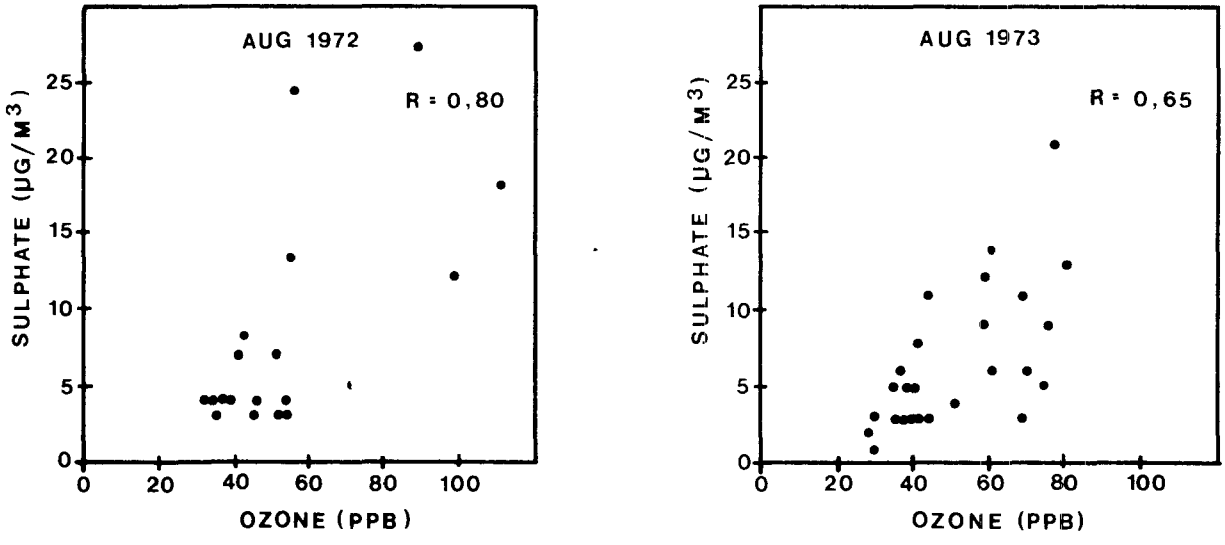

Figure 3. Daily mean concentration of particle-borne sulphur in Gothenburg plotted against maximum 1-hour concentration of ozone in Gothenburg for the months of August 1972 and 1973

From other measurements on the Swedish west coast it is known that the concentration of particle-borne sulphur within Gothenburg is mostly a product of long-range transported sulphur. The daily ozone peak concentrations in Gothenburg were therefore compared to the concentrations of soot and particle-borne sulphur samples at a non-urban coastal station (Rörvik) about 40 km south of Gothenburg (Figure 2). This station is primarily used for long-range transport studies. Soot and particle-borne sulphur have proven to be very useful tracers for long-range transport of air pollutants. Positive correlations for particle-borne sulphur and for soot were observed at this station (Table 2). These results indicated that the observed ozone episodes were not associated with pollutants produced in Gothenburg, but were a result of long-range transported pollutants. To confirm this, 48-hour trajectories were calculated for the days with high ozone concentrations in 1972 and 1973 (3). It was found that in 28 out of 33 cases, the air masses came from the sector E-S-W, having passed over heavily industrialized areas in Great Britain or on the Continent. As an example, the trajectory for March 1972 is plotted in Figure 4.

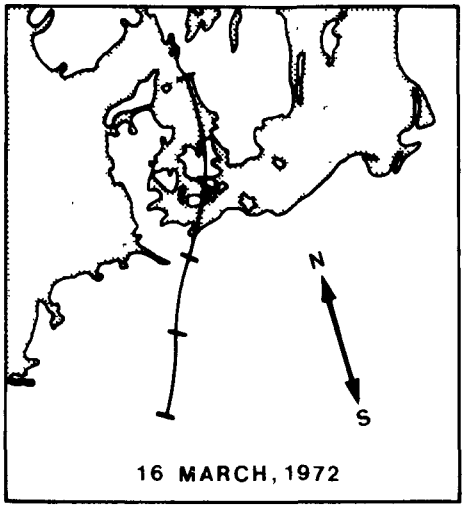

Figure 4. 48-hour trajectory for 16 March 1972.

Comparisons were also made between daily maximum concentration of ozone and particle-borne strong acid measured according to Brosset (4). However, acid has not as yet been measured on a routine basis comparable to ozone monitoring and no statistical evaluation is therefore possible. Nevertheless, an examination of the data will show that most of the strong acid episodes are associated with ozone peaks (Table 3).

In the summer of 1975 ozone measurements were also performed at the non-urban station (Rörvik). There, high ozone levels were observed on several occasions. The 1-hour ozone concentration exceeded 120 ppb on 11 days in that period; the maximum hourly concentration was 210 ppb.

There was mostly a close covariation between the ozone levels observed in

TABLE 3. COMPARISON BETWEEN CONCENTRATION OF STRONG ACID ON PARTICLES SAMPLED AT RÖRVIK AND MAXIMUM OZONE CONCENTRATIONS DURING THE FIVE MOST ACID EPISODES IN THE SUMMER OF 1975

	H^+ n mole/m^3 Rörvik	NH_4^+/H^+ mole/mole Rörvik	O_3 ppb Gothenburg	O_3 ppb Rörvik
May 19	225	2.8	66	76
29	62	2.4	45	75
Aug. 5	77	1.3	54	130
7	21	2.8	84	151
29	56	3.6	47	-

Rörvik and Gothenburg. However, for most of the time, the level was higher at Rörvik. This indicates that there is no local contribution to the ozone level in Gothenburg. Instead, other pollutants emitted locally partly destroy the incoming ozone. Figures 5 and 6 give examples of ozone episodes.

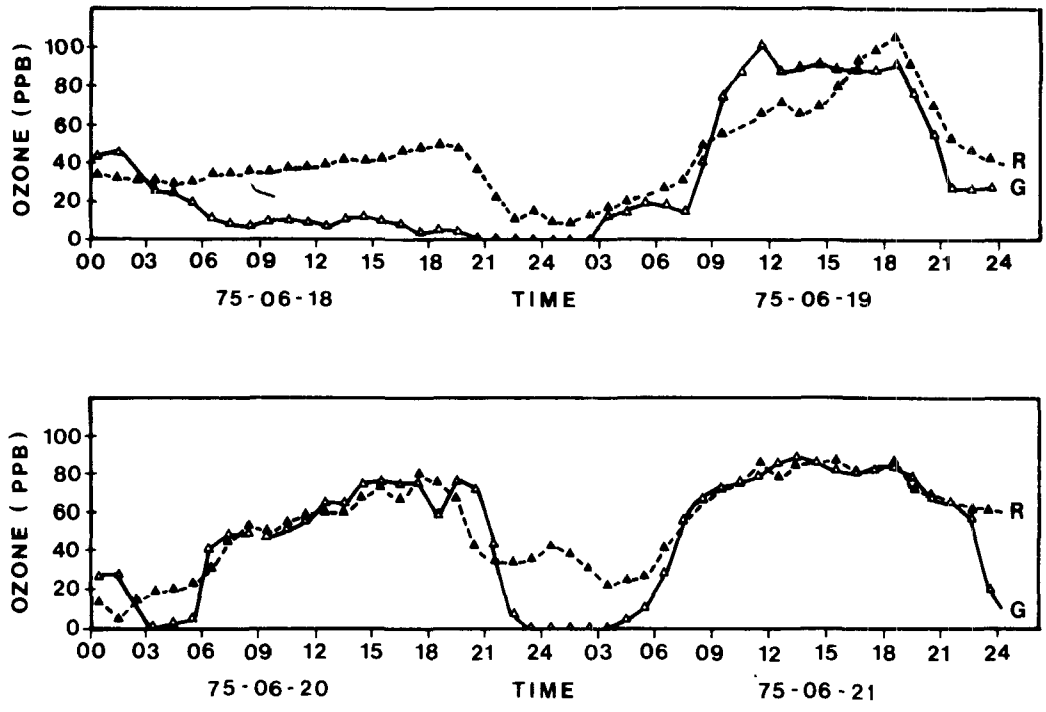

Figure 5. Ozone concentration in Gothenburg and Rörvik, June 18-21, 1975.

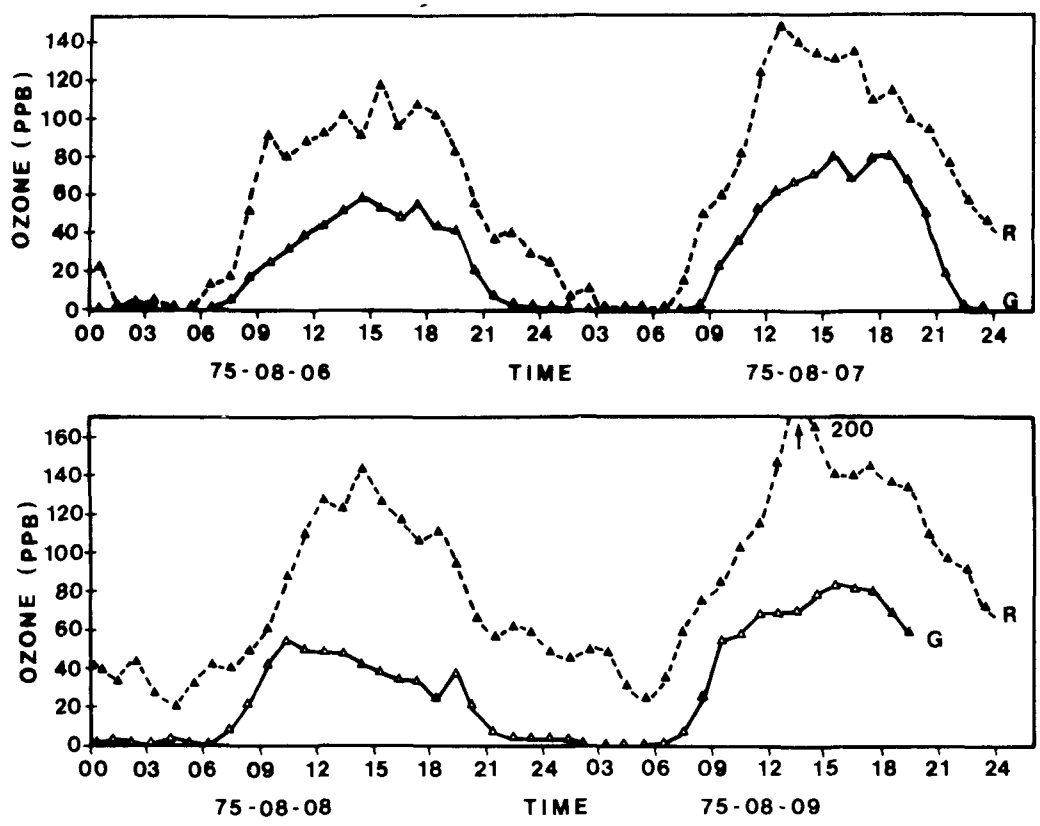

Figure 6. Ozone concentration in Gothenburg and Rörvik, August 6-9, 1975.

In a further investigation of the cause of the ozone episodes, continuous measurements of nitrogen oxides were carried out during the summer of 1975 at Rörvik. The levels of nitrogen monoxide as well as nitrogen dioxide were in the range of 1-10 ppb. Despite the small variations in concentration, positive relationships could be seen between the early morning concentrations of nitrogen oxides and maximum ozone levels. Figure 7 is an example of the variation pattern.

DISCUSSION

From our measurement data as well as from those collected in other countries in western Europe, it is clear that several ozone episodes occur every summer over large areas in Europe. The impact of these episodes is not known and no investigations have as yet been carried out in Sweden to clarify this. It is very likely that these ozone peaks cause damage to vegetation, but no such effects have as yet been observed. One reason for this may be that plant injuries on the Swedish west coast are often assumed to be caused by sea spray.

As regards effects on human health, complaints about photochemical smog were made on one occasion (28 May 1973) in Gothenburg to the local Board of Health. The highest concentration of ozone in Gothenburg that day was 80 ppb. No data from areas outside the city are available. This episode was associated with very high concentrations of an aerosol consisting of sulphuric acid and ammonium sulphate (5,6).

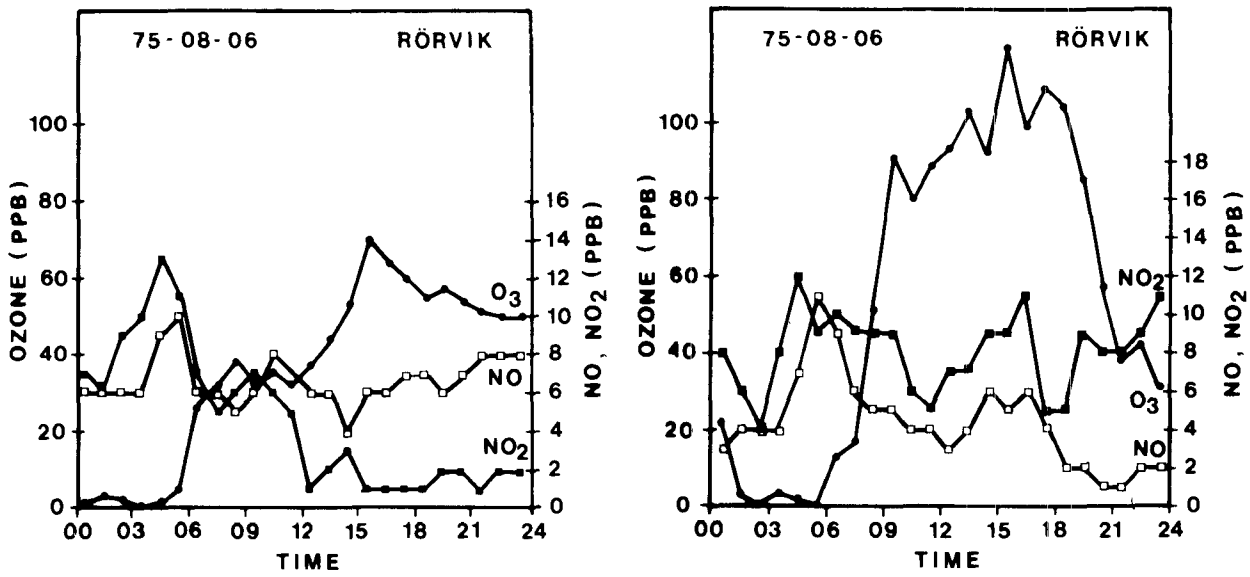

Figure 7. Variations in concentrations of ozone and nitrogen oxides at Rörvik, 2 July 2975 and 6 August 1975.

One question that arises when studying the simultaneous occurrence of high ozone levels and high concentrations of acid sulphate aerosols is: Does ozone play any role in the oxidation of sulphur dioxide in the long-range transported air masses? The question is very justified considering the correlations observed between ozone and sulphate. In winter, the sulphate in the frequent episodes resulting from long-range transported pollutants is formed through catalytic oxidation. In summer, this process is less likely because of, among other things, low relative humidities. The summer aerosols also differ from the winter aerosols in several other respects, e.g. size distribution and acidity. These differences indicate that sulphates are formed by different mechanisms and that ozone or oxidants are compounds that might play a role in sulphate formation.

It is well known that the reaction between ozone and sulphur dioxide in the gas phase is a very slow reaction and of minor importance for the oxidation of sulphur dioxide. However, according to experiments by Penkett, oxidation by ozone in the liquid phase might be possible (7). The acid aerosols normally occurring in connection with ozone episodes contain a water phase even at rather low relative humidities. Research on this reaction mechanism is in progress.

REFERENCES

1. Cox, R. A., A. E. J. Eggleton, R. G. Derwent, J. E. Lovelock, and D. H. Pack. Long Range Transport of Photochemical Ozone in North-Western Europe. Nature, 225 (5504): 118-121, 1975.

2. Grennfelt, P. Measurements of Ozone in Gothenburg, January 1972 - August 1973 and Studies of Co-Variations Between Ozone and Other Air Pollutants. Internal publication B221, Swedish Water and Air Pollution Research Laboratory (IVL), Gothenburg, January 1975.

3. Henrikson, A. B. An Investigation of the Accuracy in Numerical Computations of Horizontal Trajectories in the Atmosphere Meteorologi, 27. Swedish Meteorological and Hydrological Institute, Stockholm, 1971.

4. Askne, C., and C. Brosset. Determination of Strong Acid in Precipitation, Lake Water and Air-Borne Matter. Atm. Environ. 6: 695-696, 1972.

5. Brosset, C., K. Andréasson, and M. Ferm. The Nature and Possible Origin of Acid Particles Observed at the Swedish West Coast. Internal publication B189, Swedish Water and Air Pollution Research Laboratory (IVL), Gothenburg, 1974.

6. Brosset, C. Acid Particulate Air Pollutants in Sweden. Internal publication B 222, Swedish Water and Air Pollution Research Laboratory (IVL), Gothenburg, 1975.

7. Penkett, S. A. Oxidation of SO_2 and Other Atmospheric Gases by Ozone in Aqueous Solution. Nature Physical Science, 240 (101): 105-106, 1972.

SESSION 8

IMPACT OF STRATOSPHERIC OZONE

Chairman: R. Guicherit
IGTNO, Netherlands

OZONE OBSERVATIONS IN AND AROUND A MIDWESTERN METROPOLITAN AREA

G. D. Huffman, G. W. Haering, R. C. Bourke, P. P. Cook, M. P. Sillars*

ABSTRACT

A series of ground level and altitude measurements of ozone have been carried out in the Indianapolis area from 1974 to 1976. The major results of the ground level studies are reviewed and interpreted in terms of transport and generation processes. In addition, an extensive series of altitude surveys of ozone have been conducted. Typical results of both horizontal and vertical flight paths are presented. Again these results are described in terms of long range convection, turbulent mixing, photochemical generation and stratospheric transport. The diversity of the test results indicates that under given meteorological conditions any one or more of the above processes may occur. In summary, ozone generation and transport in an urban environment is extremely complex, and additional data is required prior to an in-depth understanding of the phenomena involved. Such an understanding would then hopefully lead to an effective control strategy.

INTRODUCTION

The Environmental Protection Agency (EPA) issued regulations in 1971 (1) stating that oxidant levels were to be maintained at values less than 0.08 ppm. This was predicated upon oxidant levels of 0.01 to 0.05 ppm in rural areas (2) and the presumption that values exceeding these levels were generated in urban centers.

In actuality, the oxidant level existing at a given location is the result of a complex interaction between meteorological, transport and generation (or destruction) processes and can be described--to first order accuracy --by the following relations (3, 4, 5):

$$\frac{\partial \overline{U}_i}{\partial \tau} + \overline{U}_{i,j}\overline{U}_j + \overline{(u_i u_j)}_{,j} = -\frac{1}{\rho_o}\overline{P}'_{,i} + \nu \overline{U}_{i,jj} + \frac{g}{T_o}\overline{T}'\delta_{i3} \qquad [1]$$

$$\overline{U}_{i,i} = o \qquad [2]$$

$$\frac{\partial \overline{T}'}{\partial \tau} + \overline{T}'_{,i}\overline{U}_i + \overline{(tu_i)}_{,i} = k\overline{T}'_{,jj} \qquad [3]$$

*G. D. Huffman, G. W. Haering, Indianapolis Center for Advanced Research (ICFAR) and Purdue University School of Science, Indianapolis, Indiana.
R. C. Bourke, P. P. Cook, Indianapolis Center for Advanced Research and Detroit Diesel Allison Division, General Motors, Detroit, Michigan.
M. P. Sillars, CWS, Inc., Flint, Michigan.

$$\frac{\partial \overline{c}^{(i)}}{\partial \tau} + \overline{U}_j \overline{C}^{(i)}_{,j} - \overline{(c^{(i)} u_j)}_{,j} = \alpha \overline{C}^{(i)}_{,jj} - F^{(i)} \exp(-E^{(i)}/R\overline{T}) \quad [4]$$

where Cartesian tensor notation has been used with 1 and 2 denoting the horizontal coordinates and 3 the vertical direction. A repeated subscript indicates a summation while ,i indicates differentiation. T' and P' represent the deviation from the adiabatic temperature and pressure conditions with the velocity, temperature, and concentration divided into a time mean, $\overline{U}_i$, $\overline{T}'$, and $\overline{C}^{(i)}$, and instantaneous value, i.e., u_i, t, and $c^{(i)}$. The fluid properties are denoted by ρ_o-the density, ν-the kinematic viscosity, k-the thermal conductivity, R-the universal gas constant, and α-the mass diffusivity. g represents the gravitational force, δ_{ij} the Kronecker delta and $F^{(i)}$ the frequency factor and $E^{(i)}$ the activation energy of the (i)-th chemical species, with τ denoting time. Equations [1] through [4] represent the conservation of momentum, energy, and mass for a turbulent medium. These relations are formally indeterminate since the Reynolds averaging procedure has introduced the unknowns $\overline{u_i u_j}$, $\overline{tu_j}$ and $\overline{c^{(i)} u_j}$, which describe the turbulent diffusion processes. Attempts are currently being made to solve these equations (3); however, they are of value even in this form since they show that the concentration at a point is due to convection, turbulent transport, viscous transport, and generation or destruction. There is a strong interaction between concentration, temperature, velocity and the chemical reactions themselves. Note that the terrain and external transport features enter the process through the boundary conditions. This balance is shown schematically in Figure 1.

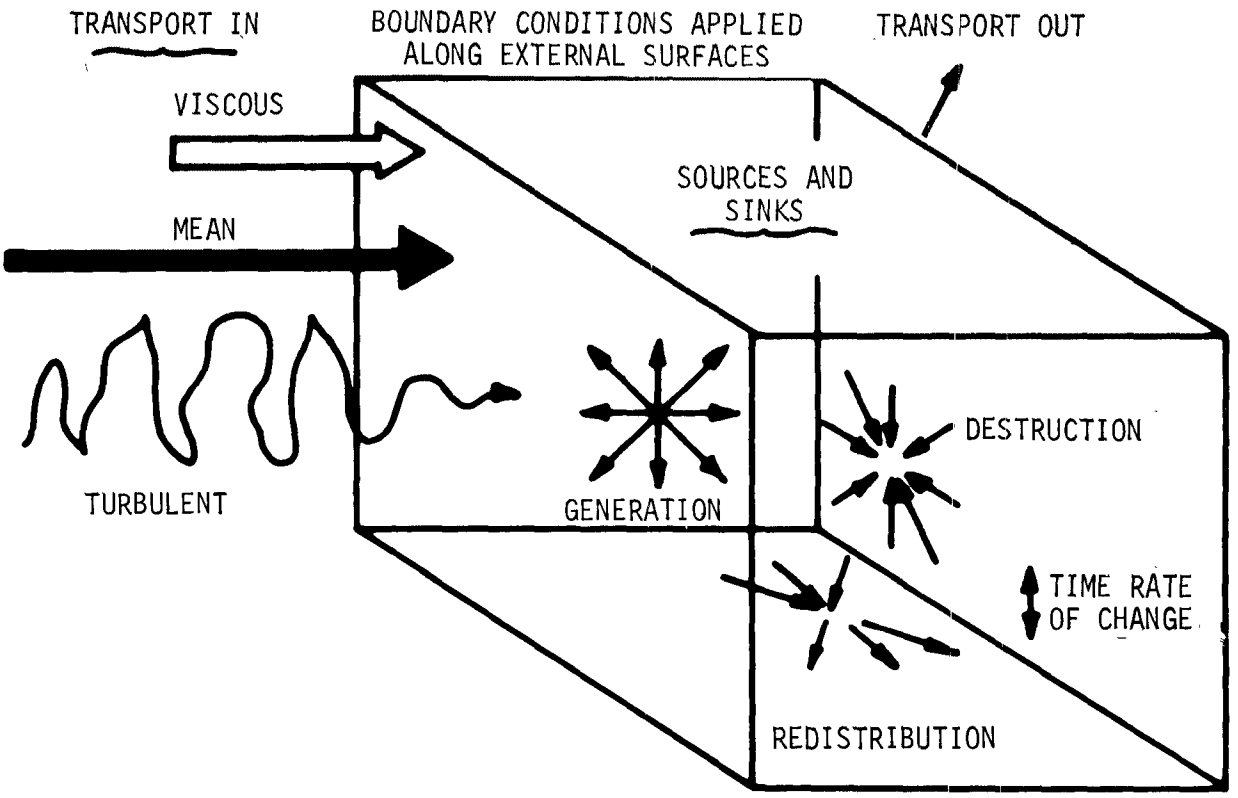

Figure 1. Processes Represented by the Transport Equations.

With this phenomenological description of the oxidant generation transport process in mind, the Indianapolis Center for Advanced Research (ICFAR) in conjunction with the City of Indianapolis, State of Indiana, Environmental Protection Agency-Region V (in 1974), and a consortium of local businesses instituted a continuing study of ozone levels in and around Indianapolis. This paper will summarize the major findings of three years of ground level and altitude measurements and attempt to interpret the results in terms of the previously described phenomena.

GROUND LEVEL MEASUREMENTS

The ground level measurements were initiated in June of 1974 using six monitoring stations. Their location relative to Indianapolis and Marion County is shown in Figure 2. These locations have been used throughout the three years of the study with some minor changes. All data was taken according to EPA guidelines (6) with the data quality assurance tasks performed in 1974 by EPA contractors (7) and by the Indiana Air Pollution Control Division in subsequent years.

While ground level measurements do not in general reveal substantial insight into the ozone generation/transport mechanisms, they do serve to define the magnitude of the problem and can be used to estimate the contribution of various processes to over-all oxidant levels. In this context, the following results were obtained from both the 1974 (8) and 1975 (9) studies.

A unique relative ordering existed between the sites in ozone concentration, which did not change significantly with wind direction. This implies that wave-like ozone excursions that have been noted in the Los Angeles Basin (10) do not occur in Indianapolis. The substantial terrain differences may account for this.

A high degree of correlation existed in the daily profile or time rate of change of ozone measured at each site with no decrease in this correlation with increasing distance. This is illustrated in Figure 3. This result in conjunction with the lack of correlation between site ordering and wind direction indicates that horizontal is much smaller than vertical mixing. Furthermore, the time rate of change of concentration is in balance with vertical diffusion processes and the generation (destruction) term. This is indicative of elevated, remote natural or anthropogenic sources. This may be due to photochemical generation at the surface, stratospheric ozone (11, 12), and/or a cyclic vertical ozone or ozone precursor transport process (10).

Ozone levels in the incoming air at upwind rural background sites often exceeded the federal standard. This is illustrative of long range transport of ozone and/or ozone precursors (13, 14, 15).

No statistically significant differences were found for daily average ozone concentrations between weekends and weekdays; however, the percentage of weekend violations of the hourly standard was higher than for weekdays. Moreover, traffic density in the area of each site showed a negative relationship with the relative ordering of sites on measured levels, i.e., inner city, high traffic density sites showed low ozone levels while upwind and downwind, low traffic density sites showed higher ozone levels. This suggests

increased turbulence and scavenging towards the center of the city (16, 17).

Measured ozone levels had a strong positive correlation with temperature and solar radiation. This is also a commonly noted effect and is due to enhanced reaction rates through $F^{(i)} \exp(-E^{(i)}/RT)$ and increased turbulent mixing as a result of $g\overline{T}'\delta_{i3}/T_o$.

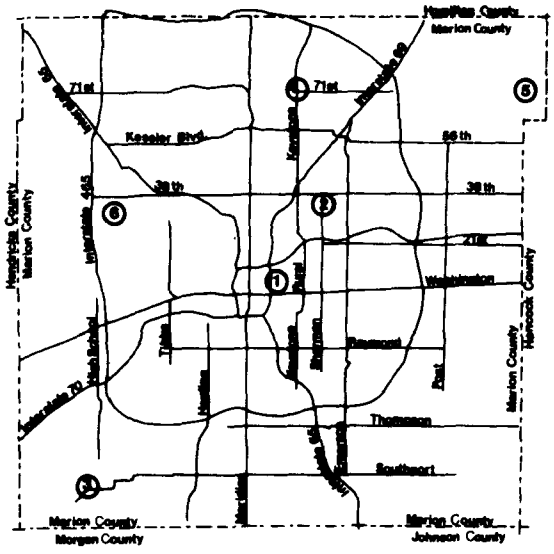

Figure 2. Monitoring Sites.

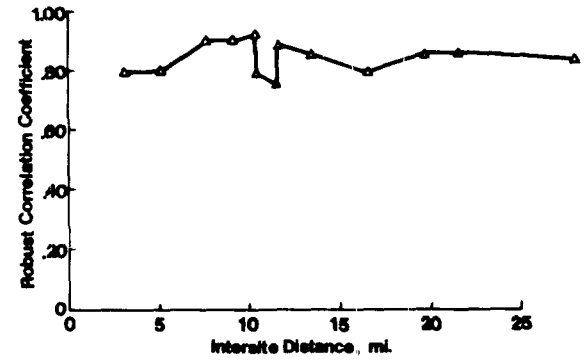

Figure 3. Intersite Distance Robust Correlation Coefficient.

In addition to the ozone measurements, some nitrogen dioxide (NO_2) and non-methane hydrocarbons (NMHC) measurements have been carried out. The relationship between the maximum daily ozone concentration and the 6:00-9:00 a.m. NO_2 and NMHC is shown in Figures 4 and 5. This indicates a low correlation, i.e., approximately 0.35, in both cases. While this cannot be interpreted as non-correlated in an absolute sense, it does indicate a weak direct relationship.

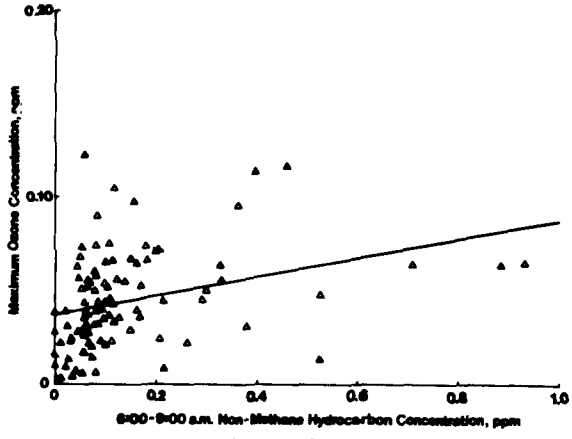

Figure 4. Maximum Ozone and Morning NO_2 Concentrations - 1975.

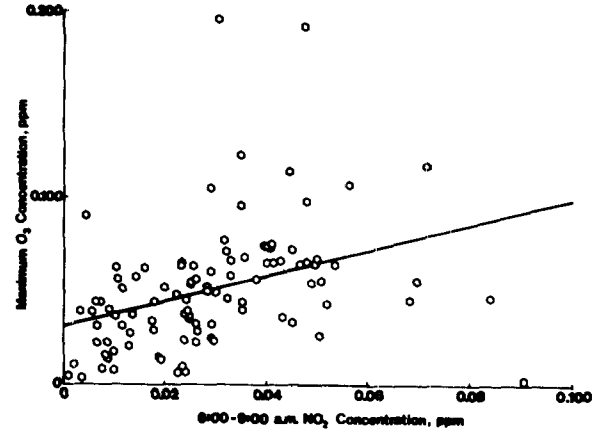

Figure 5. Maximum Ozone and Reactive Hydrocarbon Concentrations - 1975.

ALTITUDE MEASUREMENTS

Since the velocity, temperature, and concentration fields are inherently

three-dimensional and time-dependent in nature, a series of altitude measurements has been carried out in conjunction with the previously discussed ground level measurements (7, 8, 9, 12). All experiments have been conducted with a fixed wing aircraft, an AID and a Dasibi ozone monitors--corrected for altitude effects following reference 12--and a thermistor for temperature measurements. Three separate types of aircraft flights have been conducted: vertical spirals above a ground station from altitudes of a few hundred feet to approximately 30,000 ft.; horizontal traverses from county line to county line (see Figure 2) from 2000 to 15,000 ft.; and, long range horizontal traverses from state line to state line at a series of altitudes.

Some typical results for the vertical spiral flights are shown in Figures 6 through 12. Figures 6 through 8 show a discontinuous and/or intermittent behavior. These spikes do not indicate a smooth ozone profile but rather irregularly shaped "lumps." Mechanisms must be in existence to maintain this structure since diffusive processes would, over a period of time, normally yield a fairly uniform distribution.

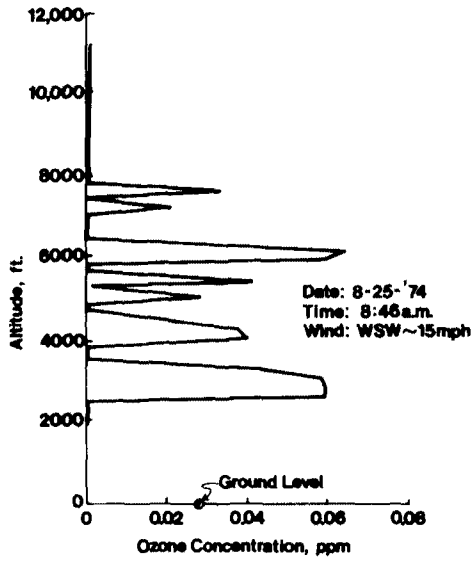

Figure 6. Ozone Concentration and Altitude - Indianapolis.

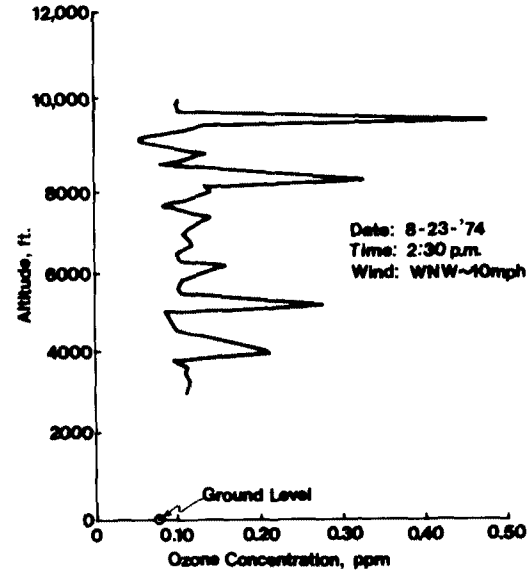

Figure 7. Ozone Concentration and Altitude - Indianapolis.

Figures 9 through 11 demonstrate a more uniform distribution typical of a well mixed layer. Note that Figures 9 and 12 approach a high ozone concentration at the higher altitudes. This is consistent with an elevated source. Figure 12 also shows two distinct strata of high ozone at lower altitudes along with a low ground level concentration. This may be due to ground level generation and transportation aloft and/or transportation downward from a high level source with ground level scavenging.

The processes that occur within the atmospheric surface layer are of particular importance and show somewhat different behavior than those aloft. A series of these measurements is shown in Figure 13 for both summer and afternoon conditions. Although the concentration gradients are quite different

near the ground, they approach the same value aloft. Similar results are reported in reference 18. This particular set of values is indicative of a "blanket" of ozone covering the entire area during the measurement period. Both afternoon curves indicate a well mixed layer with nearly uniform concentration. However, the night between the two afternoons indicates a low ground level concentration with values aloft approaching those of the afternoons. This phenomenon could be caused by an ozone reservoir blanketing the area with continual scavenging at the surface. At night, when no photochemical processes are present and vertical transport is limited by the inversion, the surface ozone is destroyed. However, in the afternoon, with enhanced vertical transport and photochemical processes, the surface concentration approaches that of the blanket.

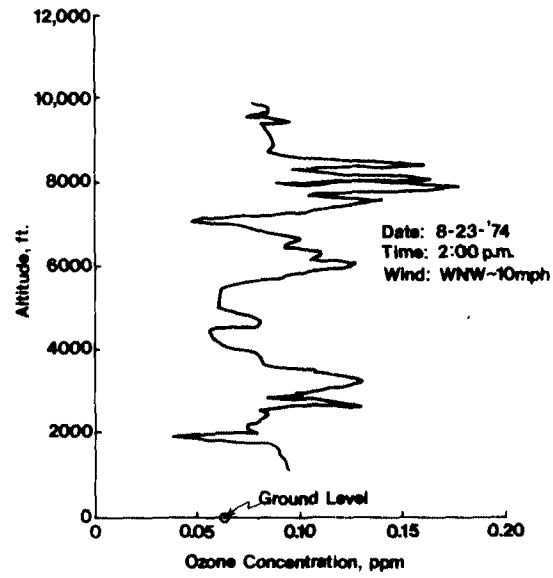

Figure 8. Ozone Concentration and Altitude - Indianapolis.

Horizontal flights at a series of altitudes were also carried out. Figure 14 shows that there are significant departures from uniform stratification of ozone concentration with the principal demarcation located at about 4000 ft. This sharp delineation often occurs on days with high ozone concentration (Figures 9 and 12).

Cross-country flights generally indicate constant or slowly varying ozone values with distance from Indianapolis at constant altitudes. Figure 15 shows a typical result and corresponds to conditions in Figure 13. The origin of the deep spikes is unknown--they were not generally present. The "steady" ozone values were observed to extend upwind and laterally to approximately 70 miles--the extent of the flight. Figure 16 shows results obtained from another cross-country flight. Again reasonably uniform ozone values occur for the length of the traverse--approximately 300 miles. This condition corresponds to the vertical traverse of Figure 11.

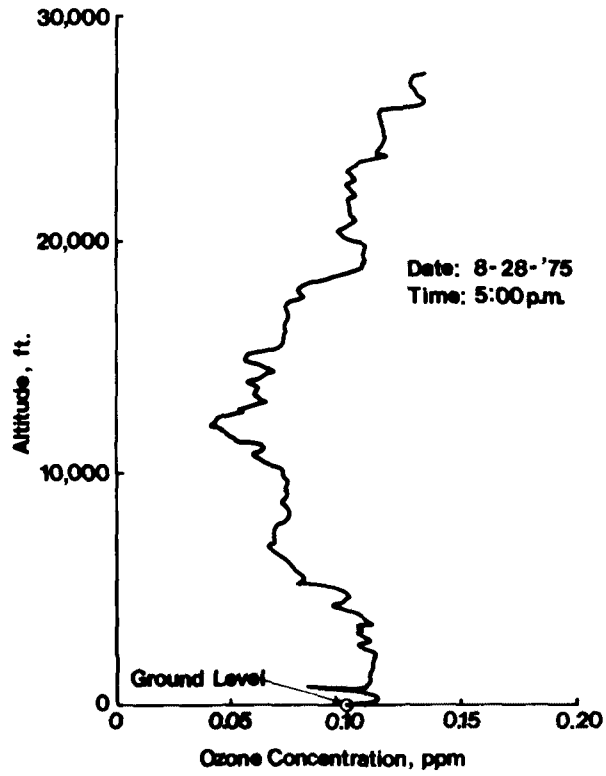

Figure 9. Ozone concentration and altitude - 1975.

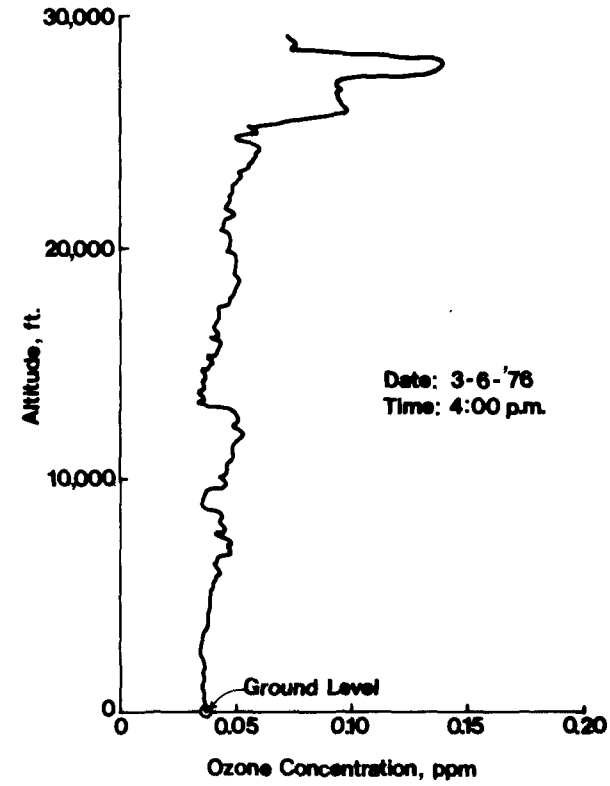

Figure 10. Ozone concentration and altitude - 1976.

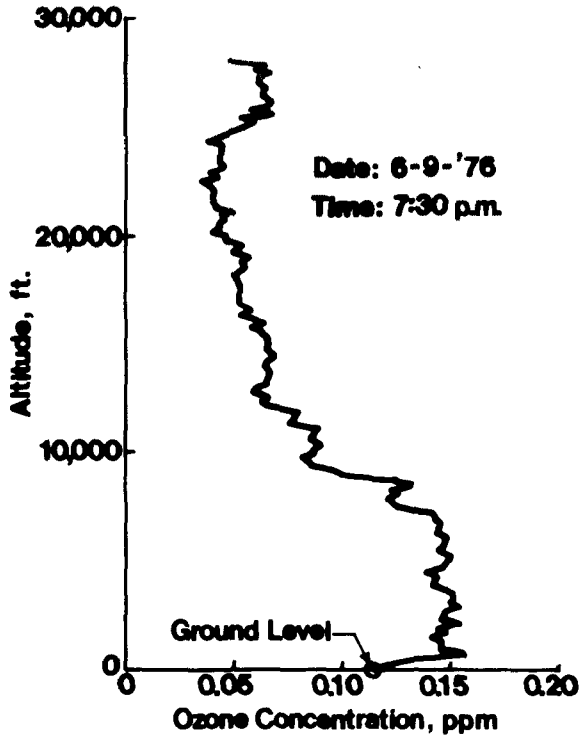

Figure 11. Ozone concentration and altitude - 1976.

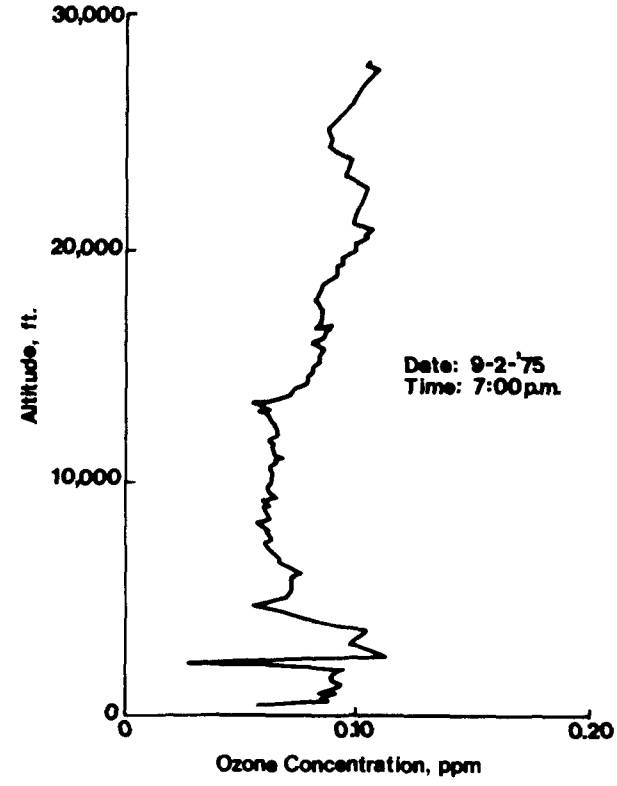

Figure 12. Ozone-altitude data over Northwest Indianapolis.

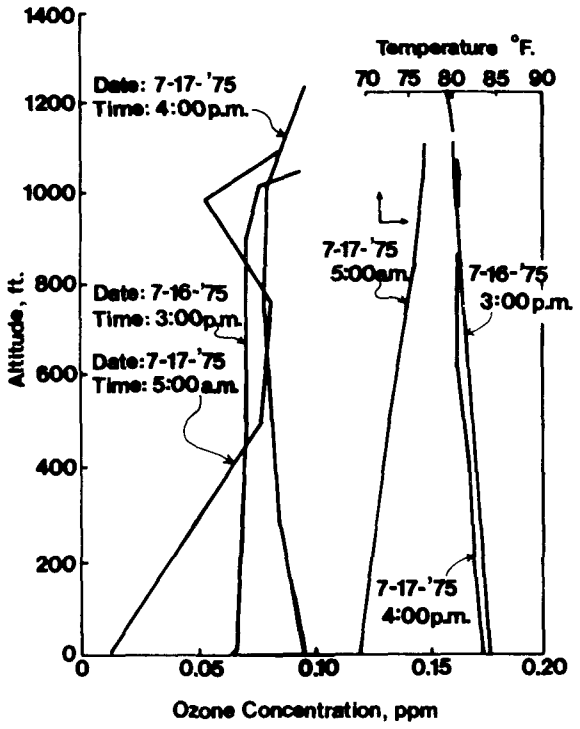

Figure 13. Ozone concentration and altitude, 25-hr. period, Indianapolis.

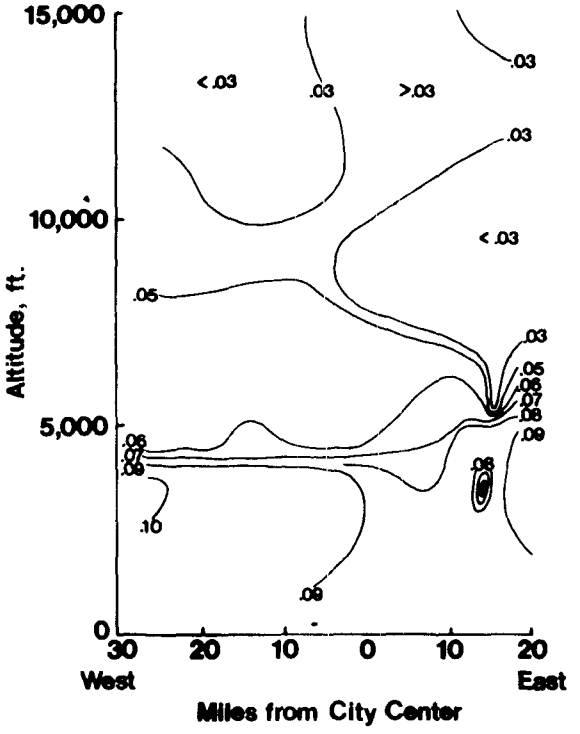

Figure 14. Ozone concentration over Indianapolis, 7-29-75, 5:00-8:00 p.m. Numbers on plot denote lines of constant ozone concentration.

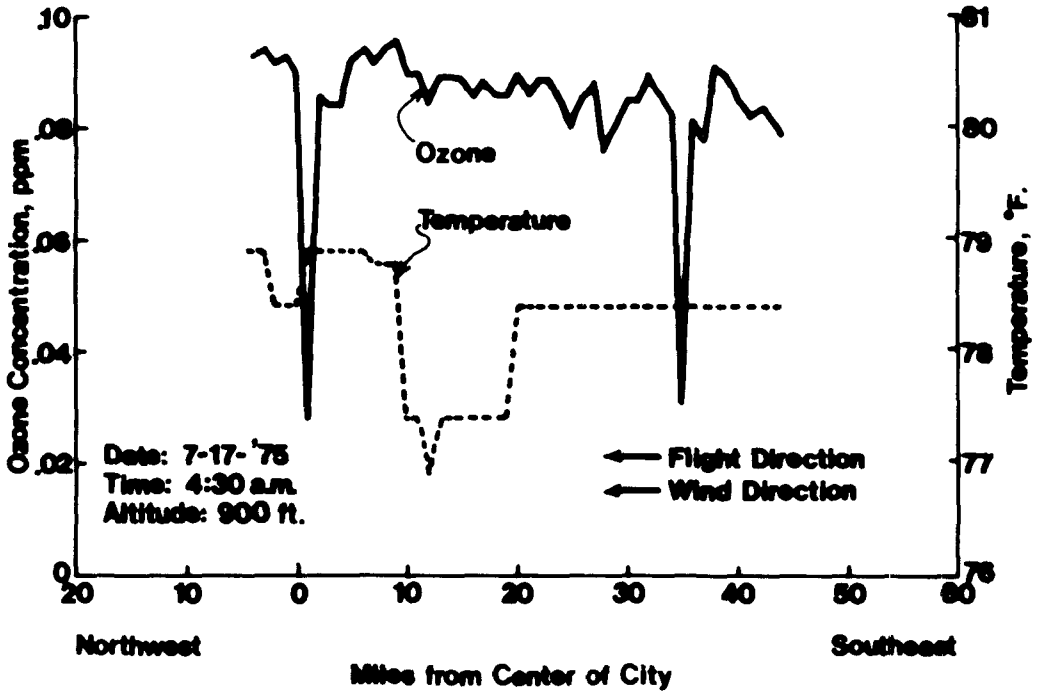

Figure 15. Ozone Concentration and Temperature Upwind of Indianapolis at 900 Feet Altitude.

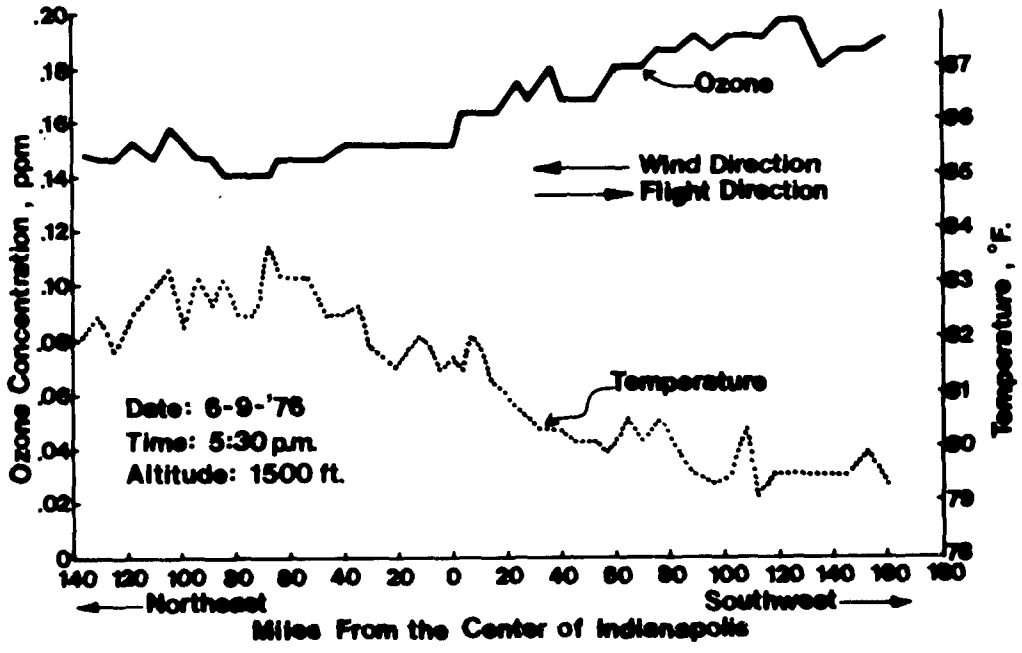

Figure 16. Ozone Concentration and Temperature Near Indianapolis.

Even though many different ozone profiles are encountered, a few general characteristics can be noted. First, ozone levels do not change appreciably over long distances at constant altitude both upwind and laterally as long as no frontal activity is encountered. Secondly, ground level concentrations change in a diurnal pattern--mornings usually having lower values with high values in the afternoon. Ozone levels at altitudes of a few thousand feet tend to remain reasonably constant diurnally--barring gross meteorological changes. Afternoon ozone concentrations have similar values both at the surface and aloft. This may be due to scavenging of ozone at the surface during the night and morning hours and then afternoon surface increases resulting from both photochemical processes and enhanced vertical mixing. Finally, ozone concentrations at altitudes of 25,000 ft. are often quite high indicating potential ozone transport from the stratosphere.

UPPER AIR METEOROLOGICAL STUDY

In an effort to isolate meteorological transport of ozone-rich air from the more conventional sources due to photochemical formation and surface advection, a meteorological study (19) was conducted of a high ozone incidence that occurred on February 24, 25, and 26, 1976. During this time period both Dayton and Indianapolis measured ozone levels exceeding the current standards. A study of area and national surface maps indicated that advection and/or long range transport from an adjacent urban center to Indianapolis or Dayton was unlikely.

To explore other possible causes, a series of vertical cross-sections were plotted extending from the surface to 50,000 ft. The cross-sections originated at International Falls, Minn. (INL) and followed an irregular path through Green Bay, Wis. (GRB), Dayton, Ohio (DAY), Huntington, W. Va. (HTS)

and Greensboro, N. C. (GSO). For both dates, the wind aloft and the location of the tropopause were plotted (see Figures 17 and 18). These figures show a low-level jet located immediately below the break in the tropopause. If the high-speed jet is an ozone rich wind stream originating near the tropopause break and gradually descending, winter occurrences of high ground level ozone concentrations could be more easily explained. While this phenomena is unlikely during the summer months it may well explain unusual occurrences during the late fall, winter and spring.

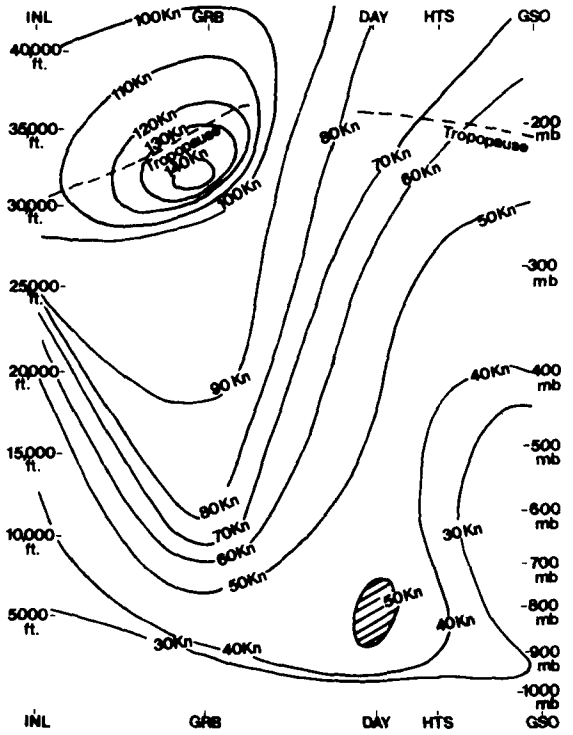

Figure 17. Vertical cross-section of Atmosphere over Midwest - February 29, 1976.

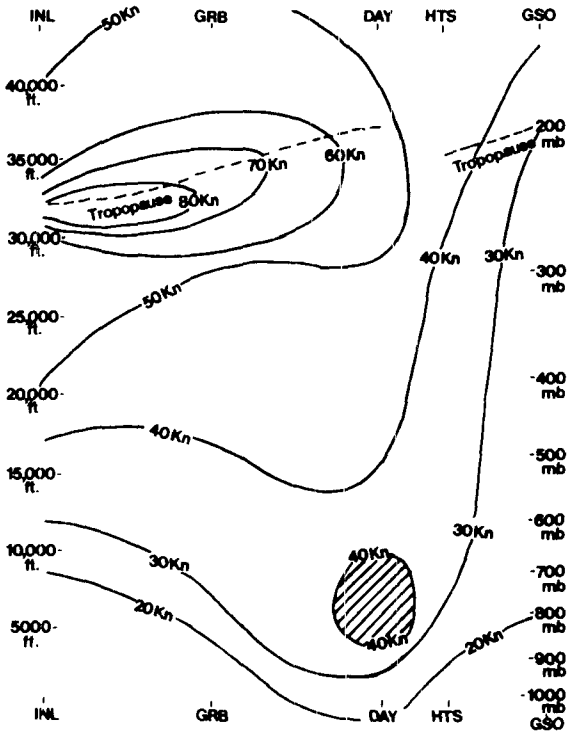

Figure 18. Vertical cross-section of Atmosphere over Midwest - February 25, 1976.

CONCLUSIONS

The diversity of the test data indicates that meteorological, transport, and photochemical processes all could be important contributors to ground and altitude ozone levels. Under a given set of conditions, one process may dominate or all three processes may make equal contributions. As a result, it is difficult to draw general conclusions. Categorization of ozone profiles according to atmospheric stability might prove useful--unfortunately a broad enough data base is not yet available for this purpose.

Even though the phenomena cannot be described in concise terms, results indicate that for the Indianapolis area wave-like migrations of ozone and/or ozone precursors are not a major contributor to ground level concentrations. Furthermore, vertical mixing seems to dominate other processes with either a surface or elevated source supplying the ozone. During a winter period,

stratospheric sources have been identified. This is not necessarily the predominant contributor in the summer with ozone and/or ozone precursors, vertical transport and re-entrainment coupled with photochemical generation equally likely. All in all, ozone generation and transport in an urban environment is extremely complex and additional data is required before an in-depth understanding of the phenomena involved can be reached. Such an understanding would then hopefully lead to an effective control strategy.

REFERENCES

1. "Requirements for Preparation, Adoption and Submittal of Implementation Plans," Federal Register, 36, August 1971, p. 15486.

2. "Air Quality Criteria for Photochemical Oxidants," National Air Pollution Control Association, Durham, N. C., March 1970, p. 4-3.

3. Bradshaw, P. An Introduction to Turbulence and its Measurements, Pergammon Press, Oxford, England, 1971.

4. Lumley, J. L. and H. A. Panofsky. The Structure of Atmospheric Turbulence Interscience Publishers, New York, N. Y. 1964.

5. Beer, J. M. and N. A. Chigier. Combustion Aerodynamics, John Wiley and Sons, Inc., New York, N. Y. 1972.

6. Guidelines for Development of a Quality Assurance Program, Reference Method for Measurement of Photochemical Oxidants, EPA Monitoring Series No. EPA-R4-73-028c, June 1973, Office of Research and Monitoring, U. S. Environmental Protection Agency, Washington, D. C.

7. Waltz, E. W. and D. Raichart. "Indianapolis 1974 Summer Ozone Study - Data Documentation Report," Indianapolis Center for Advanced Research, April 1975.

8. Lovelace, D. E., et al. "Indianapolis 1974 Summer Ozone Study," The Indianapolis Center for Advanced Research, February 1975.

9. Haering, G. W. "Interim Air Quality Report," Indianapolis Center for Advanced Research, March 1976.

10. Blumenthal, D. L. and W. H. White. "The Stability and Long Range Transport of Ozone or Ozone Precursors," Paper No. 75-07.4, Air Pollution Control Association, Boston, Mass., June 1975.

11. Sticksel, P. R. "The Stratosphere as a Source of Surface Ozone," Paper No. 75-07.6, Air Pollution Control Association, Boston, Mass., June 1975.

12. Cook, P. P. and R. C. Bourke. "Correction of Ozone-Altitude Data and Stratospheric-Source Implications," Air Pollution Control Association Journal, June 1976.

13. Wolff, G. T., et al. "Aerial Ozone Measurements over New Jersey, New

York and Connecticut," Paper No. 75-58.6, Air Pollution Control Association, Boston, Mass., June 1975.

14. Rabino, R. A. "Ozone Transport," Paper No. 75-07.1, Air Pollution Control Association, Boston, Mass., June 1975.

15. Price, J. H., et al. "Estimation of Minimum Achievable Oxidant Levels by Trajectory Analysis: Implications for Oxidant Control," Paper No. 75-07.2, Air Pollution Control Association, Boston, Mass., June 1975.

16. Cleveland, W. S., et al. "Sunday and Workday Variations in Photochemical Air Pollutants in New Jersey and New York," Science, Vol. 186, pg. 1037, 1974.

17. Levitt, S. B. and Chock, D. P. "Weekday-Weekend Pollutant and Meteorological Studies of the Los Angeles Basin," Paper No. 75-51.1, Air Pollution Control Association, Boston, Mass., June 1975.

18. "Control of Photochemical Oxidants - Technical Basis and Implications of Recent Findings," U. S. EPA. Research Triangle Park, North Carolina, July 15, 1975.

A "TEXAS SIZE" OZONE EPISODE TRACKED TO ITS SOURCE

J. W. Hathorn III and H. M. Walker*

ABSTRACT

Between September 25 and October 1, 1975, a widespread ozone (O_3) episode occurred in Texas. Tracks of monitoring data for the period August 20 to October 31 clearly show evidence of this episode completely across the state. In addition, evidence is offered that most instances of high O_3 at all sites are related to widespread episodes.

The frequent, regional ozone episodes experienced in the Eastern United States are probably caused, in part, by the transport of ozone-rich stratospheric air to the earth's surface. Numerous vertical ozone profiles have shown that there is increased ozone concentrations within the frontal layer and currently-accepted frontal models indicate that this ozone is probably of stratospheric origin.

An analysis of the space and time continuity of a front's low-level structure demonstrates that the stable layer over the region experiencing an ozone episode was actually the remnant of a cold front that had pushed through several days earlier. The stable layer disappeared and reappeared at several stations indicating that it was losing its identity as it dissipated. Any air within the stable layer would have been mixed in the lower troposphere. Since this stable layer is the remnant of a cold front, its increased ozone content could have caused an/or "seeded" an ozone episode.

Stratospheric ozone accompanying the frontal system of September 24 is believed to have initiated the photochemical oxidation sequence broadly across the state. This sequence built to episodic levels, which peaked during the period discussed.

INTRODUCTION

The frequent occurrence of regional ozone (O_3) episodes in the eastern United States suggests that their cause is related to repetitive meteorological patterns.

This paper seeks to analyze such patterns and develop a more detailed understanding of the regional episode. The subject of this study is the

*J. W. Hathorn III, Applied Meteorology, Inc., Houston, Texas.
H. M. Walker, Monsanto Co., Texas City, Texas.

week-long episode occurring in Texas between September 25 and October 1, 1975.

This was plainly a major episode that extended to practically all of the monitoring sites of the state network.

Figure 1 presents time plots of daily ozone peaks for the 2 1/2 month period beginning on August 20th. Part 1A depicts patterns for Houston, Aldine, Texas City, and El Paso, which are shown with the one-week period under discussion being outlined. As a result of this work, another widespread episode was noted during the period September 14-17, 1975. This episode is also outlined. Both of these episodes are sharply defined at all sites.

Figure 1-C extends the analysis to Corpus Christi, Orange, and Fort Worth and adds high quantity data sets from two non-urban Texas sites. The Port O'Connor data was obtained courtesy of DuPont and the Athens data (by Radian Corporation) was obtained courtesy of Texas Utilities. Again, all tracks show the effect of both episodes, although, in the case of the rural Athens sites, three of the four effects are manifest as maxima in the data actually peaking below the 0.08 ppm ambient air standard.

Figure 1-B shows tracks for Clute, San Antonio, Dallas, Austin, Nederland, and the other El Paso site. All sites but Austin reacted to the September 14-17 episode, and all but El Paso (Campbell) to the September 25 through October 1 episode. The latter observation was unexpected in view of the sharp episode effect displayed by the other El Paso monitor during that period.

Figure 1-D depicts Houston sites operated by the Houston City Air Pollution Control Department and adds a track for Lake Charles, Louisiana, obtained courtesy of the Louisiana Air Control Commission. The Houston sites strongly evidenced the episodes. The Lake Charles track shows slight evidence of the two episodes.

Considering all four sections of Figure 1 together, one sees the persistence of these two episodes that covered the state. Closer inspection of all tracks suggests that additional episodes could have been defined for the periods August 21-23, October 6-7, and October 29-30. These would also have had relatively wide coverage. In fact, for the entire 73-day period one might well conclude that <u>most</u> periods of high ozone at <u>all</u> sites occurred as manifestations of broad ozone episodes.

Figure 2 presents time patterns of ozone for a number of the sites hour-by-hour during the episode. The strong diurnal pattern is clearly evident in the cities with the highest emissions of various sorts. Thus, the Houston sites have the highest peaks and the greatest number of hours of essentially zero ozone each night. Conversely, rural Athens barely reached the National Ambient Air Standard (NAAS) during the episode but exhibited little diurnal variation and has relatively high ozone levels throughout the night many nights. Port O'Connor has a pattern similar to Athens with occasional reversion to a more urban-type pattern. El Paso's pattern is surprisingly similar to that of Houston. Texas City's is characterized

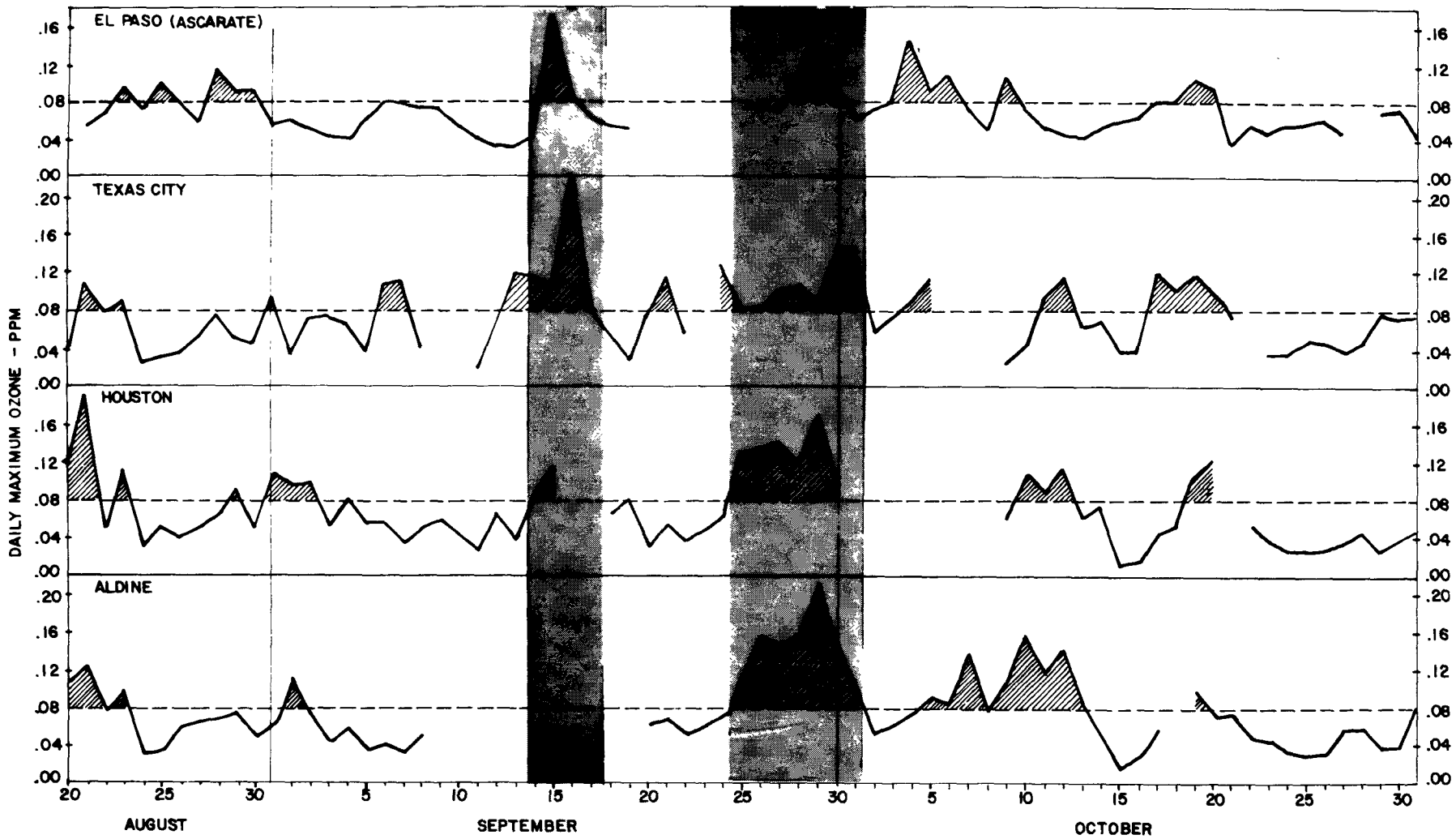

Figure 1-a. Daily peaks - various Texas sites, August 20 - October 31, 1975.

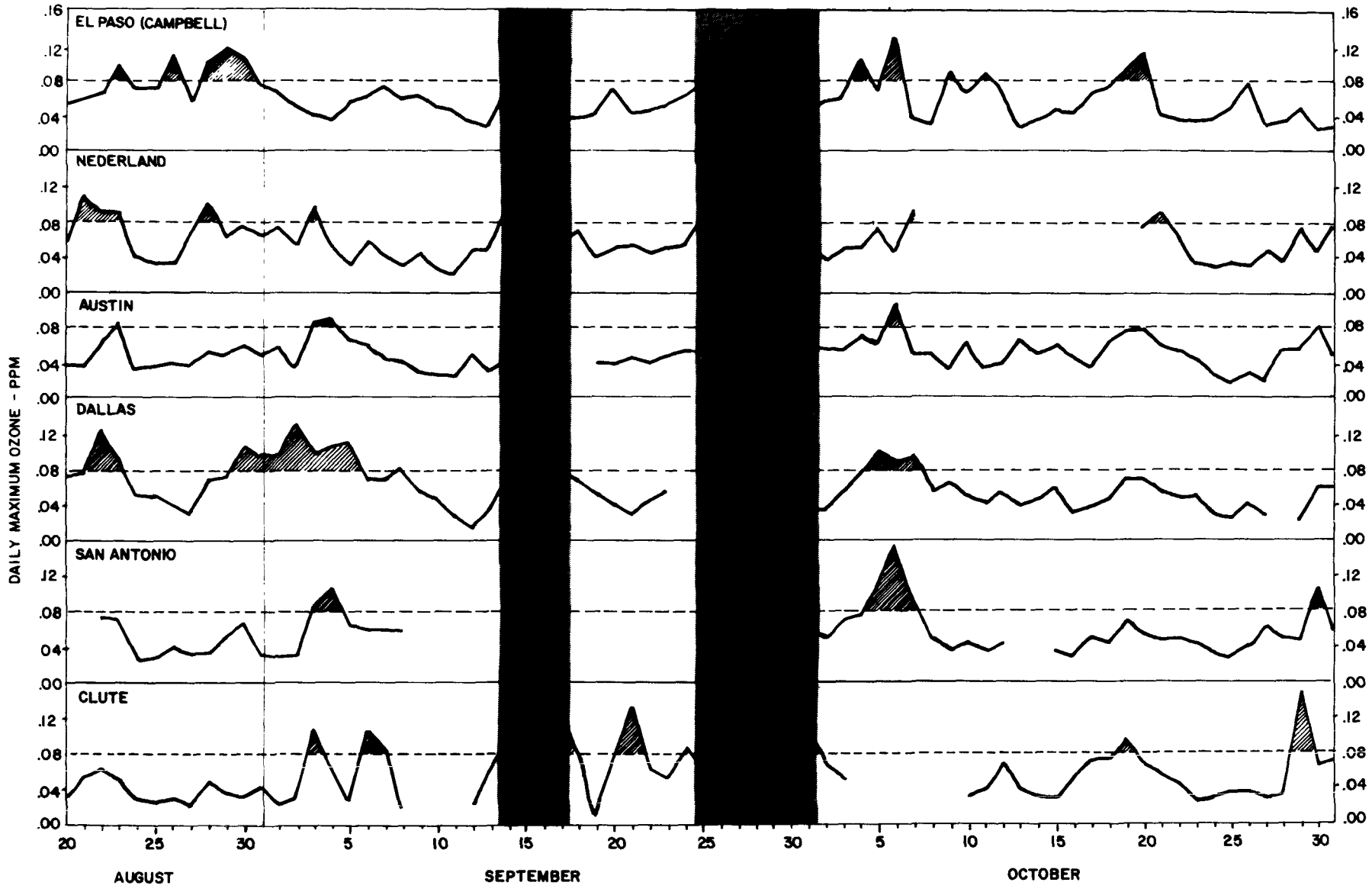

Figure 1-b. Daily peaks - various Texas sites, August 20 - October 31, 1975.

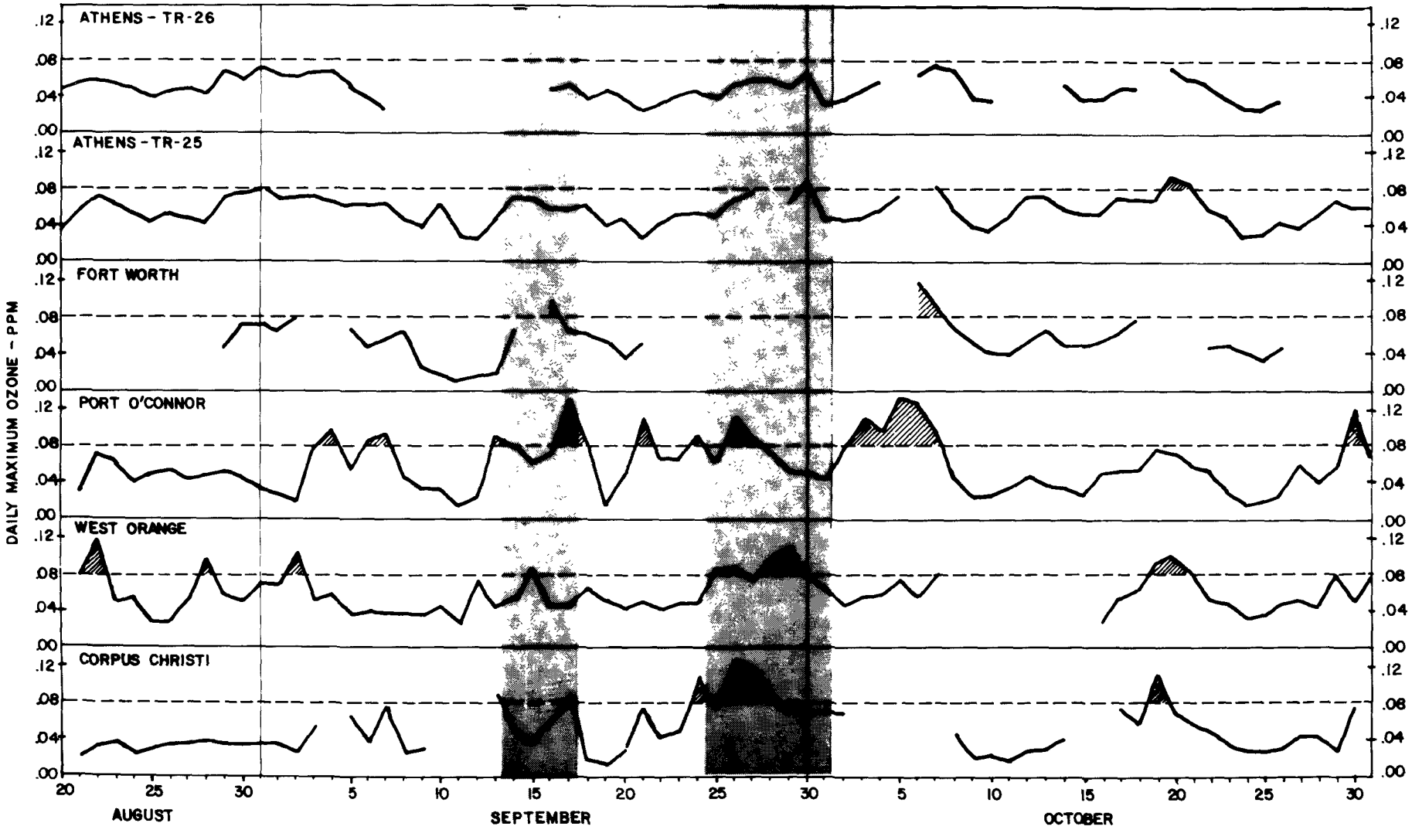

Figure 1-c. Daily peaks - various Texas sites, August 20 - October 31, 1975.

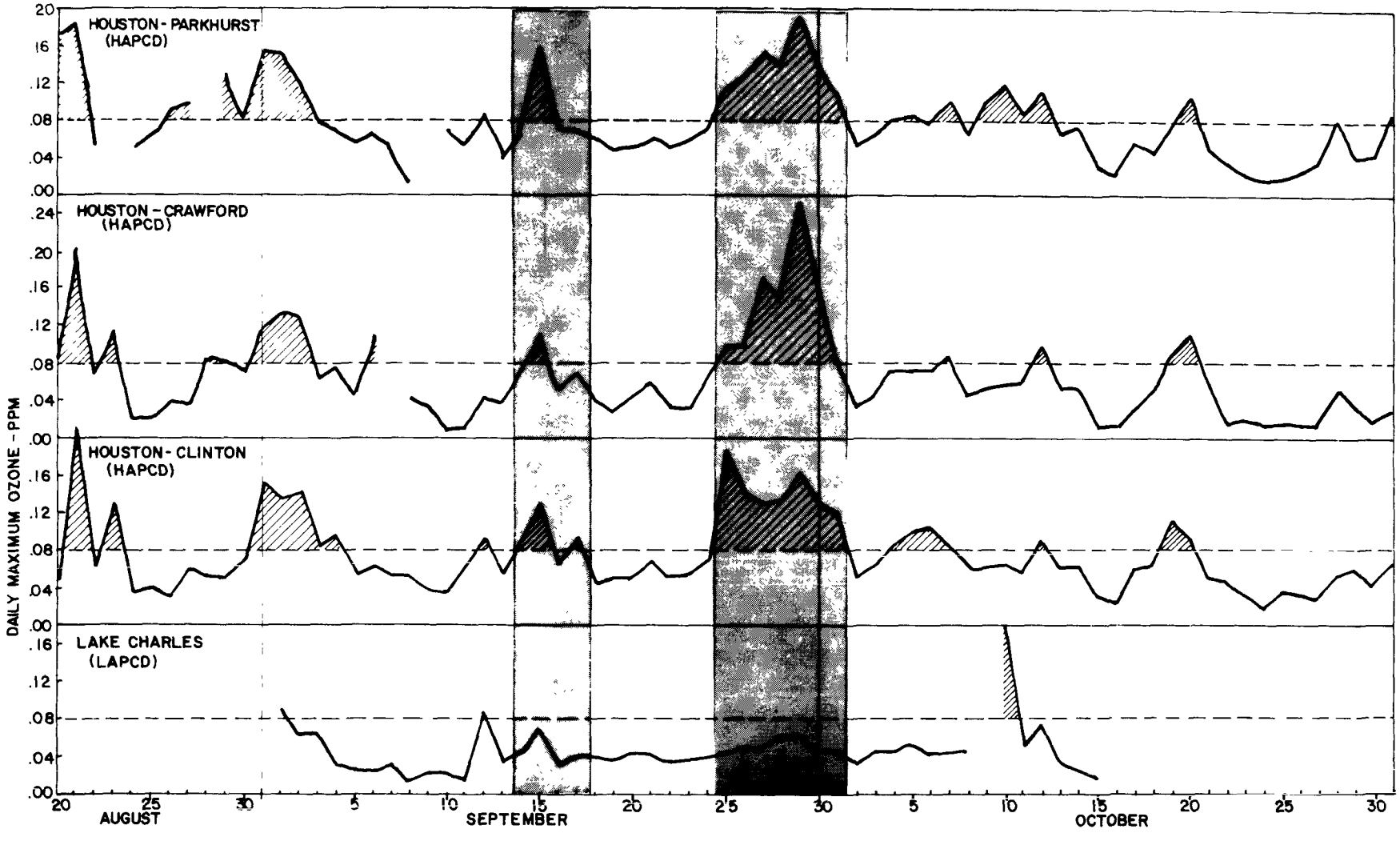

Figure 1-d. Daily peaks - various sites, August 20 - October 31, 1975.

by many high nighttime hours -- probably indicative of winds directly off the Gulf. This was somewhat unexpected since Texas City in general has relatively high levels of both hydrocarbons and ozone.

Since it is more than 750 airline miles from El Paso to Orange, the event of September 25 to October 1 was truly of synoptic proportion -- far beyond the scale of any local pollution situation.

Previous data suggests that ozone episodes that cover large regions recur with a typical set of characteristics as follows:

1. High ozone concentrations will persist for several days.

2. Both rural and urban monitoring stations throughout the region, whether upwind or downwind of urban or industrial areas, will experience the episode.

3. Concentrations of other contaminants will not necessarily be high.

4. Ozone concentrations rise sharply after sunrise and decrease sharply in the evening.

5. Usually, the wind is from the southern quadrant and there is a large subtropical anticyclone (i.e., high pressure area) located east to northeast of the region experiencing the episode; (i.e., the event is "on the backside of a HIGH.")

6. The frequency of occurrences is high (e.g., in Texas, more than three times in some months).

The data of Figures 1 and 2 confirm that the episode under study possessed most of these characteristics. Additional monitoring information revealed that characteristic #3 was apparently applicable; the concentrations of other contaminants were not uniformly nor especially high. Item #6, the weather characteristics will now be discussed in detail.

SYNOPTIC WEATHER SITUATION FOR THE SEVEN-DAY EPISODE

The synoptic weather situation leading up to the seven-day ozone episode began with a cold front passing through Texas between September 18 and 20. Figure 3 presents the surface weather map for September 20, 1975, for 7:00 a.m. EST, and also shows the locations of two vertical cross-sections (A-A' and B-B', heavy dashed lines) to be discussed later.

The cold front merges with Hurricane Eloise on the afternoon of September 22, in the central Gulf of Mexico (Figure 4) and became stationary along the Atlantic Coast of the United States until September 28, while the remnants of the hurricane moved up the coast toward Nova Scotia (Figures 5 through 7).

On September 26 (Figure 6), a high pressure area following the cold front moved into the central United States (Missouri) and then drifted

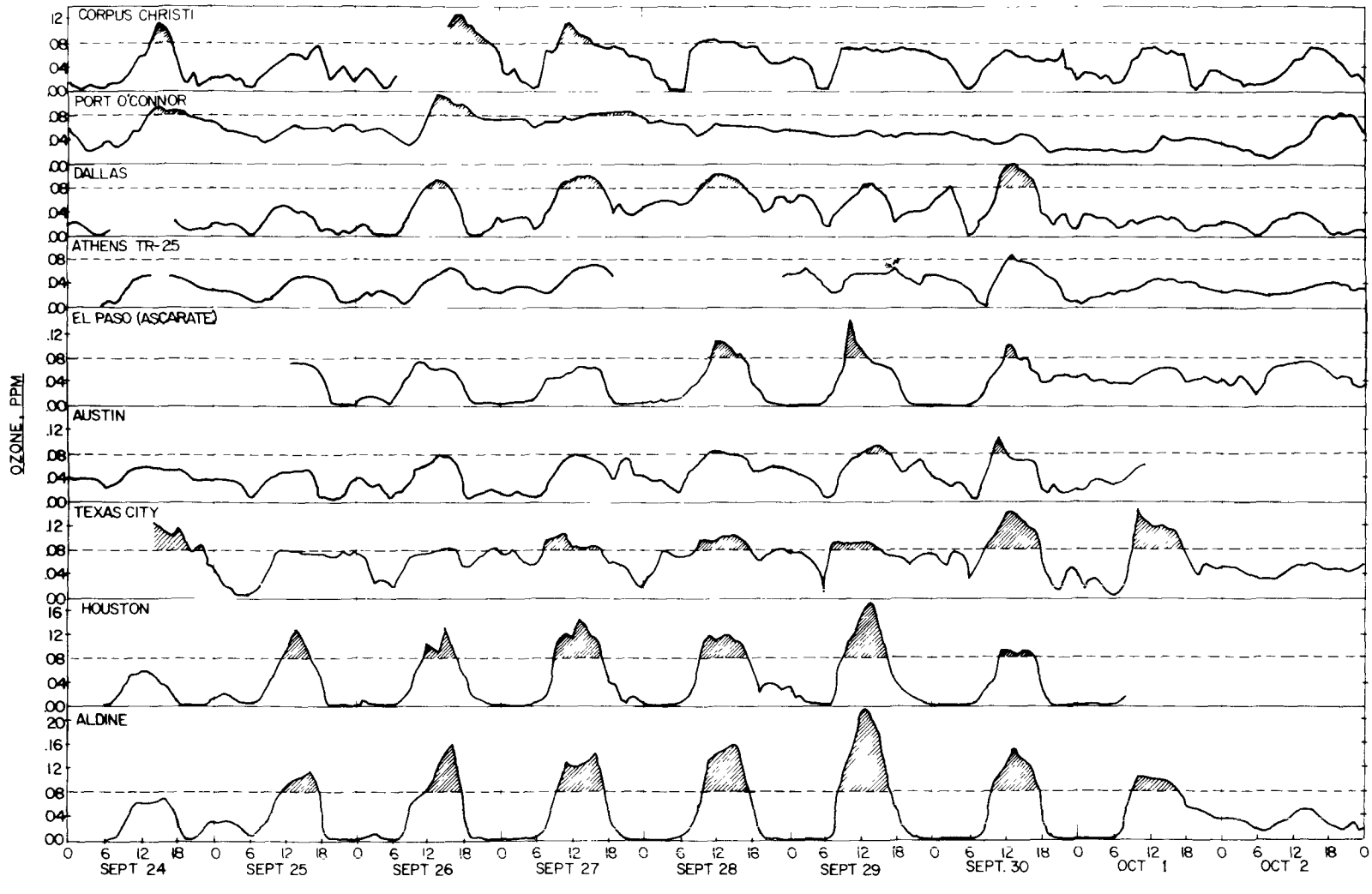

Figure 2. Hourly data, September 24 - October 2, 1975.

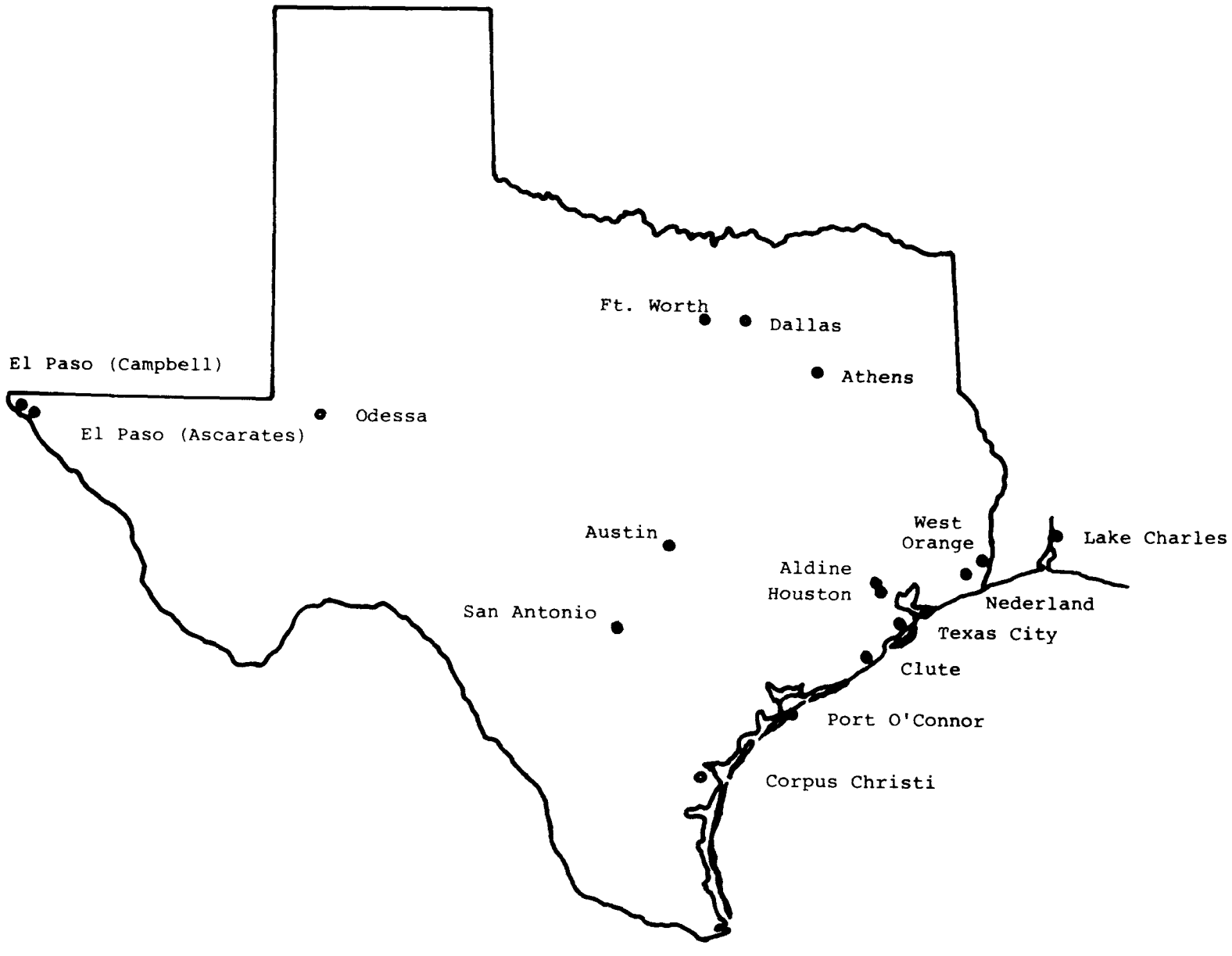

Figure 2-b. Reporting stations.

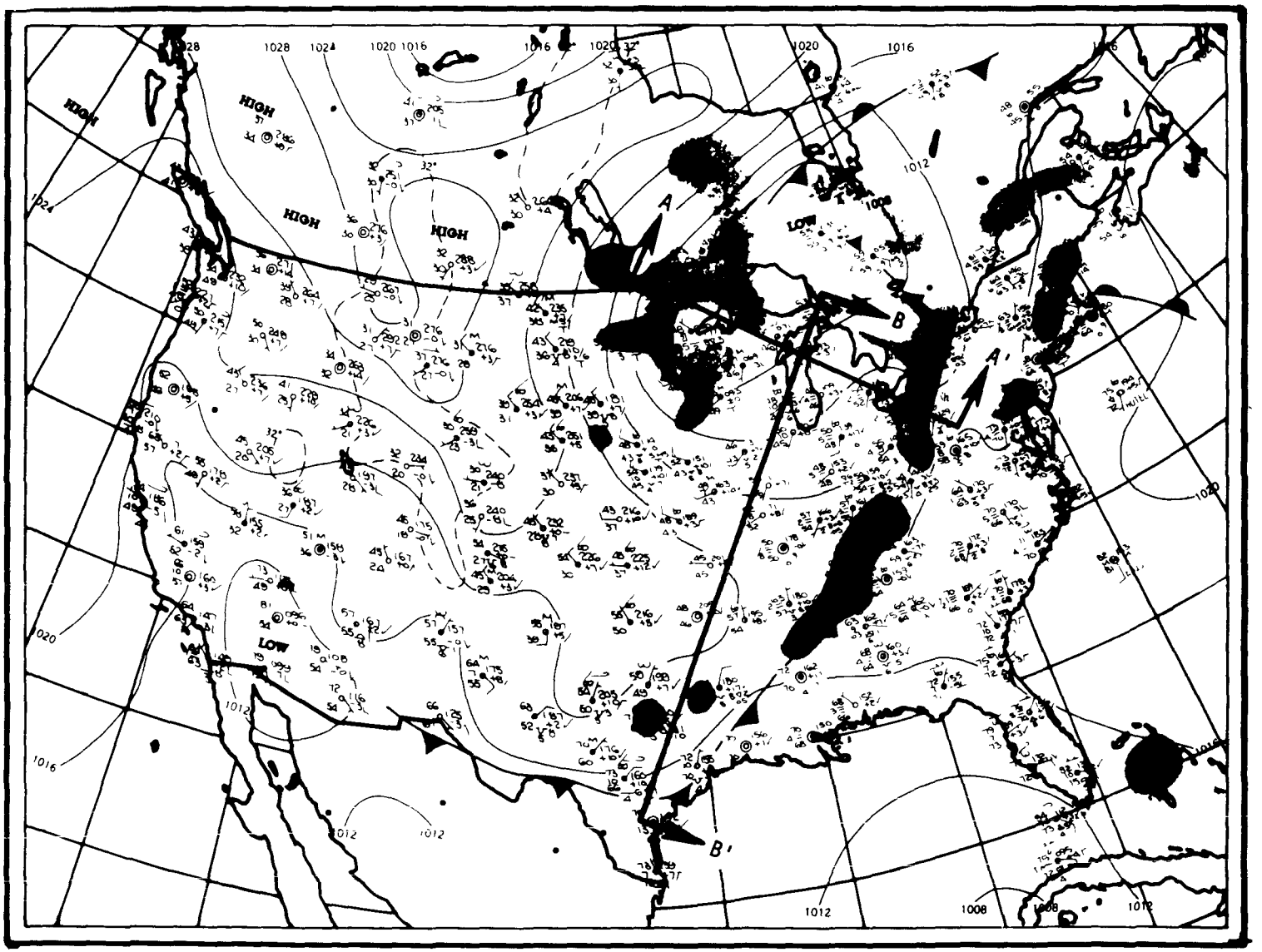

Figure 3. Surface Weather Map for September 20, 1975, 7:00 a.m. EST with locations for cross-sections A-A' and B-B'.

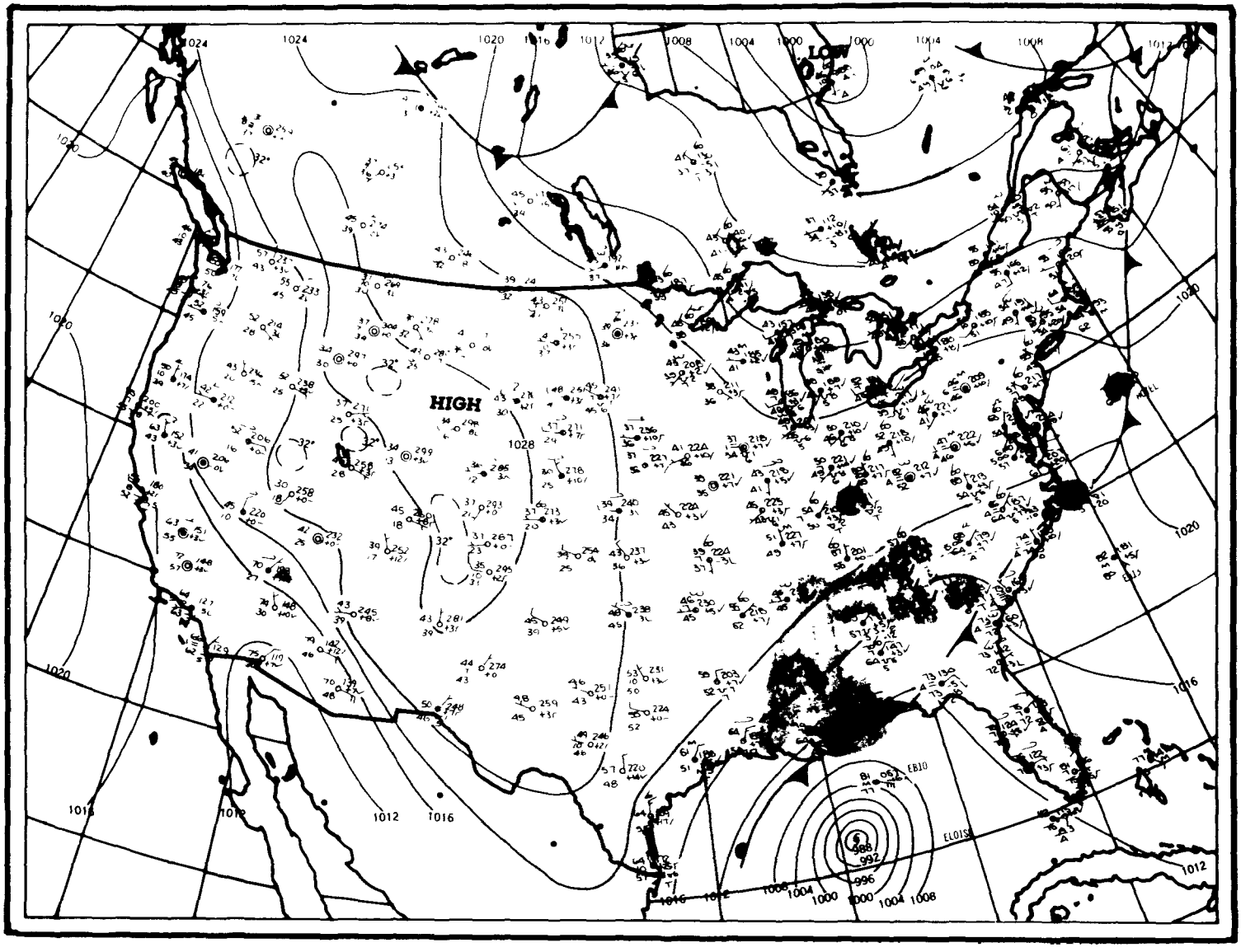

Figure 4. Surface Weather Map for September 22, 1975, 7:00 a.m. EST.

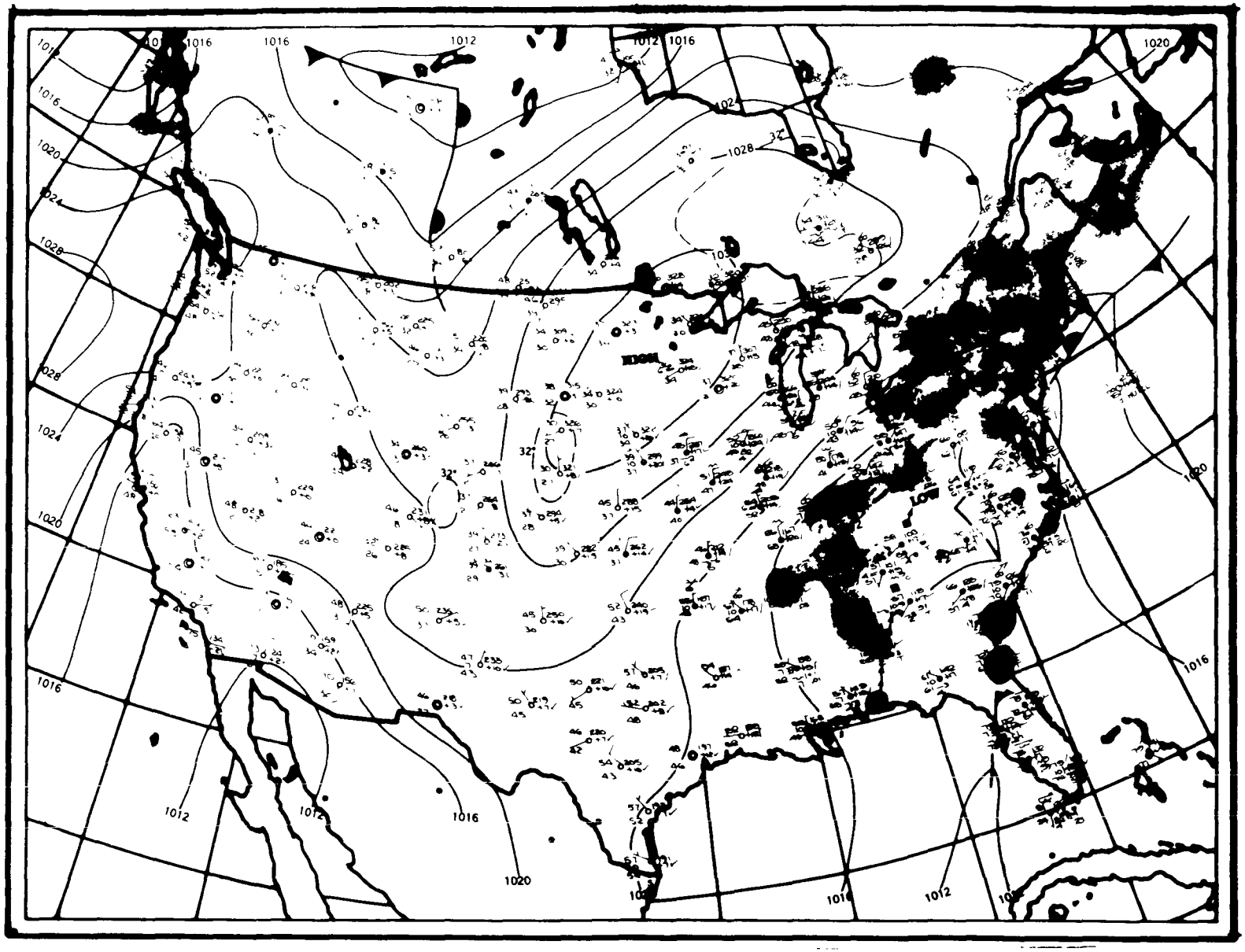
1016
1012
1016
1020
1028
1024
1020
1016
1012
1016
1020
1012
1016
1012
1016
1020
1016
1012
1016
1020
1016
1012
1016
1020
1028
1024
1020
1016
1012
1016
1020
1016
1012
1016
1020
1016
1012
1016

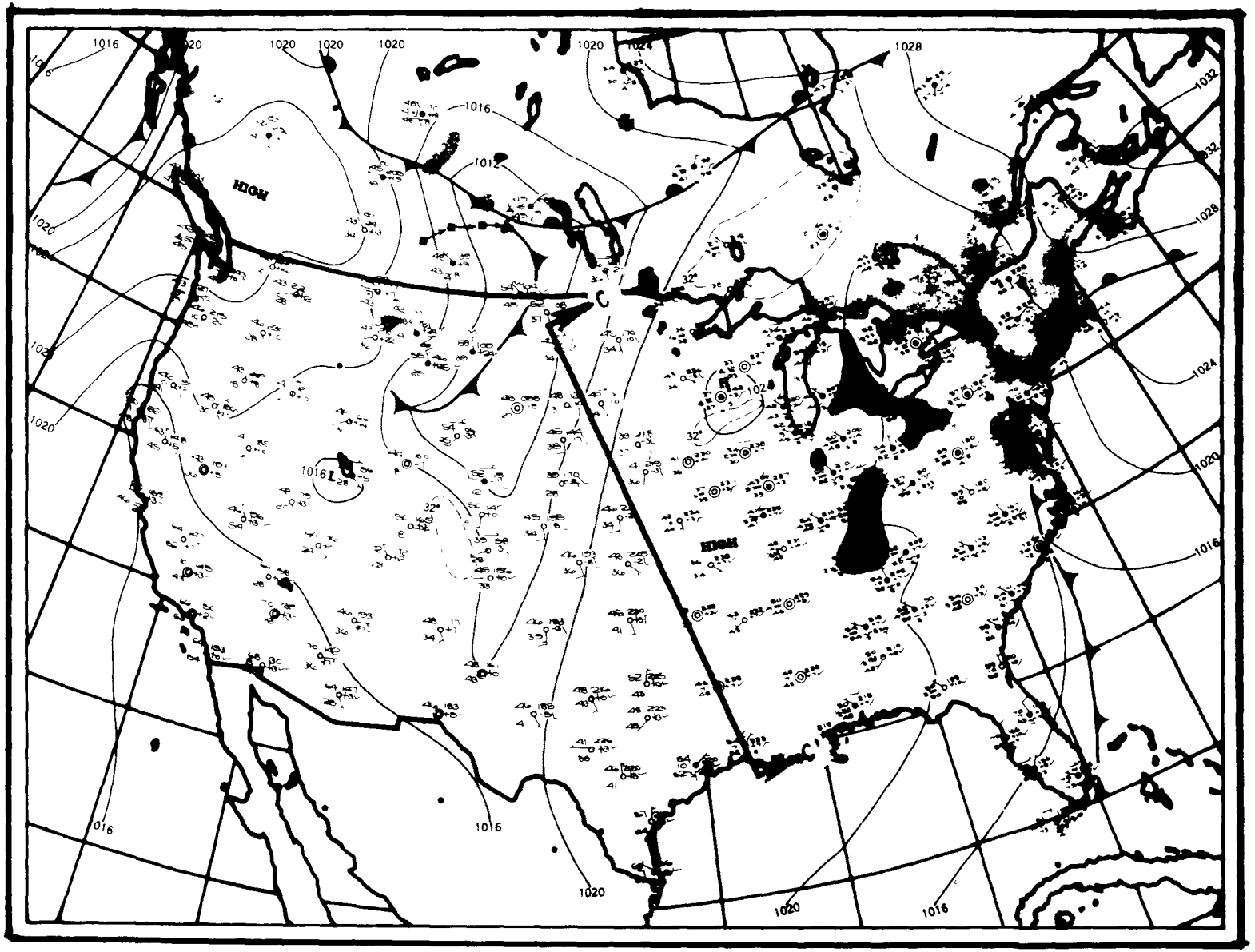

Figure 6. Surface Weather Map for September 26, 1975, 7:00 a.m. EST with location for cross-section C-C'.

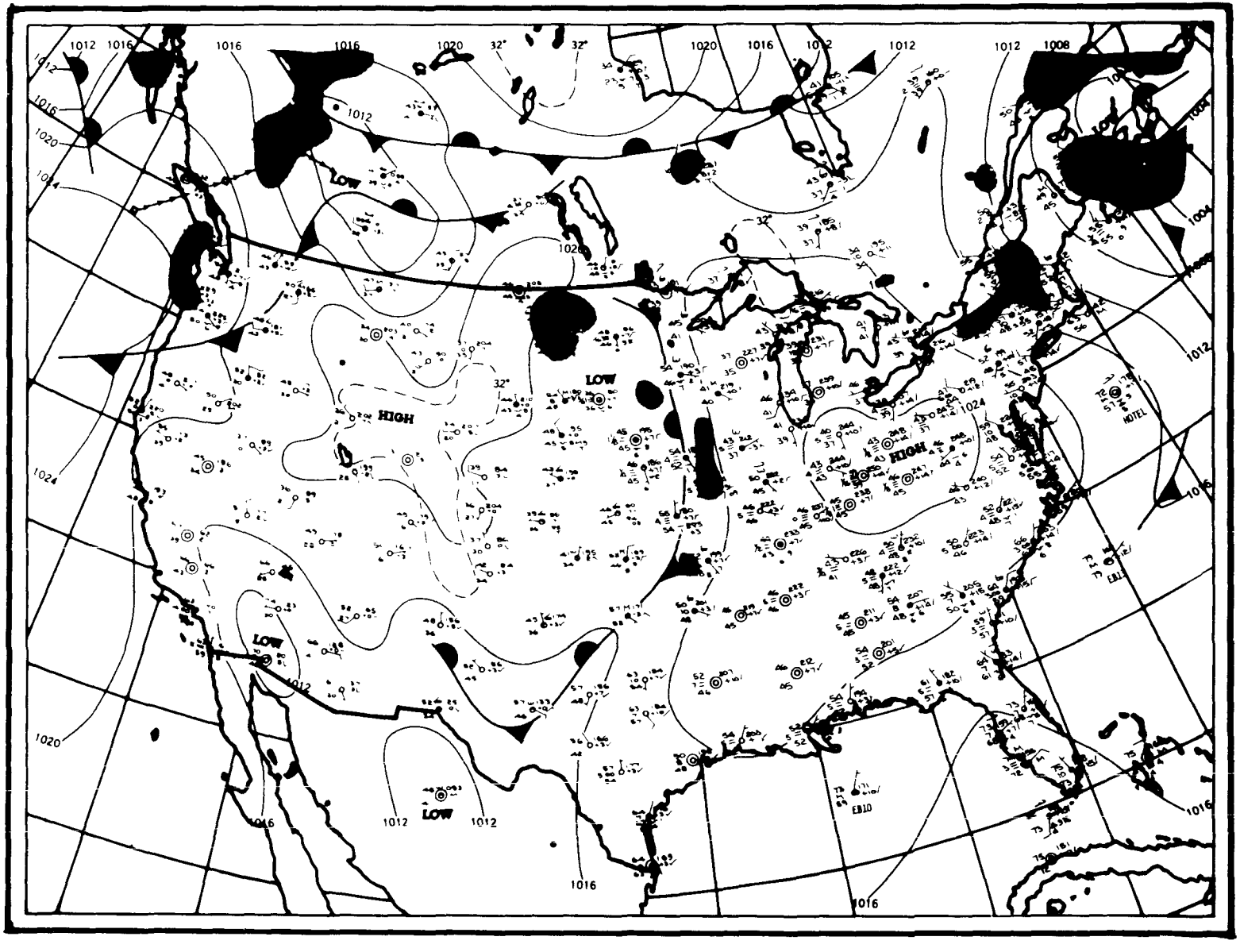

Figure 7. Surface Weather Map for September 28, 1975, 7:00 a.m. EST.

slowly east-northeastward until on October 1 (Figure 8) it was located in the Atlantic Ocean. During the seven-day period from September 25 through October 1, Texas was located on "the backside of this HIGH" and experienced generally southerly flow. These were the seven days during which the ozone episode occurred.

Those familiar with synoptic weather patterns recognize this sequence of events (except for Hurricane Eloise) as rather typical.

THREE-DIMENSIONAL STRUCTURE OF THE ATMOSPHERE FOR THE EPISODE

To understand how an ozone episode in Texas beginning on September 25 was caused by stratospheric ozone, the three-dimensional structure of the cold front in both space and time (beginning on September 20) must be examined. Vertical cross-sections perpendicular to the front at its steepest point (Section A-A' in Figure 3) and parallel to the front (Section B-B' in Figure 3) describe the front's three-dimensional structure during the early development stage. A time series of vertical temperature profiles show the transition continuity from the development stage to the dissipation stage. Then, another vertical cross-section shows the structure of the front in its dissipation stage.

A vertical cross-section from International Falls, Minnesota, to Pittsburgh, Pennsylvania (see Section A-A' in Figure 3) is presented in Figure 9. The cold front intersects the surface near Pittsburgh, passes over Flint, Michigan, and Green Bay, Wisconsin, before it intersects the tropopause in central Wisconsin. The cold front is undergoing rapid development indicated by potential temperatures within the lower frontal layer (dashed lines indicate constant potential temperature, i.e., isentropes) not yet equalling those at the tropopause over International Falls. (There is another stable layer over Pittsburgh, Flint, and Green Bay that can be identified as the remnants of another cold front that had pushed through the area several days earlier.) The cold front is moving rapidly (about 9 miles per hour) eastward.

Another cross section (B-B' on Figure 3) through Green Bay that essentially parallels the cold front until it intersects the ground just south of Longview, Texas is shown in Figure 10. The frontal remnant that was also noted in Figure 9 can be identified in Figure 10 as well.

These cross-sectional analyses (Figures 9 and 10) indicate that fronts are continuous layers that can cover large areas. In addition, the layer itself can persist in time. To illustrate persistence, a time-series of vertical temperature profiles measured at Longview, Texas, from September 19 through September 28 are presented in Figure 11. The cold front passed Longview on the afternoon of September 19 and is identified as a shaded area on all subsequent profiles. Between September 22 and 23, the front decreased in altitude from 8,700 feet to 5,800 feet (conserving its original potential temperature) and remained at about that altitude throughout the seven-day episode.

The temperature profiles for September 23 through 28 have the "typical"

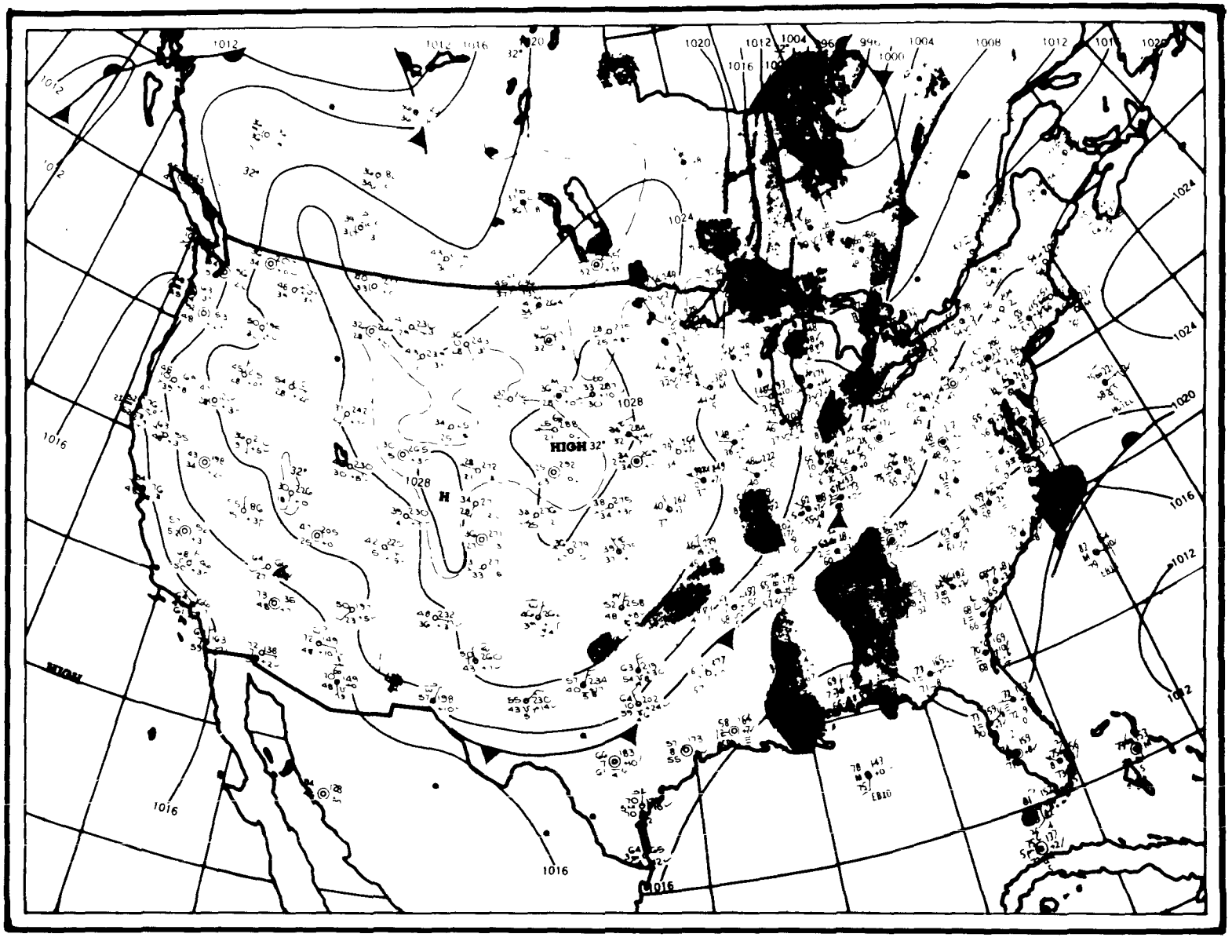

Figure 8. Surface Weather Map for October 1, 1975, 7:00 a.m. EST.

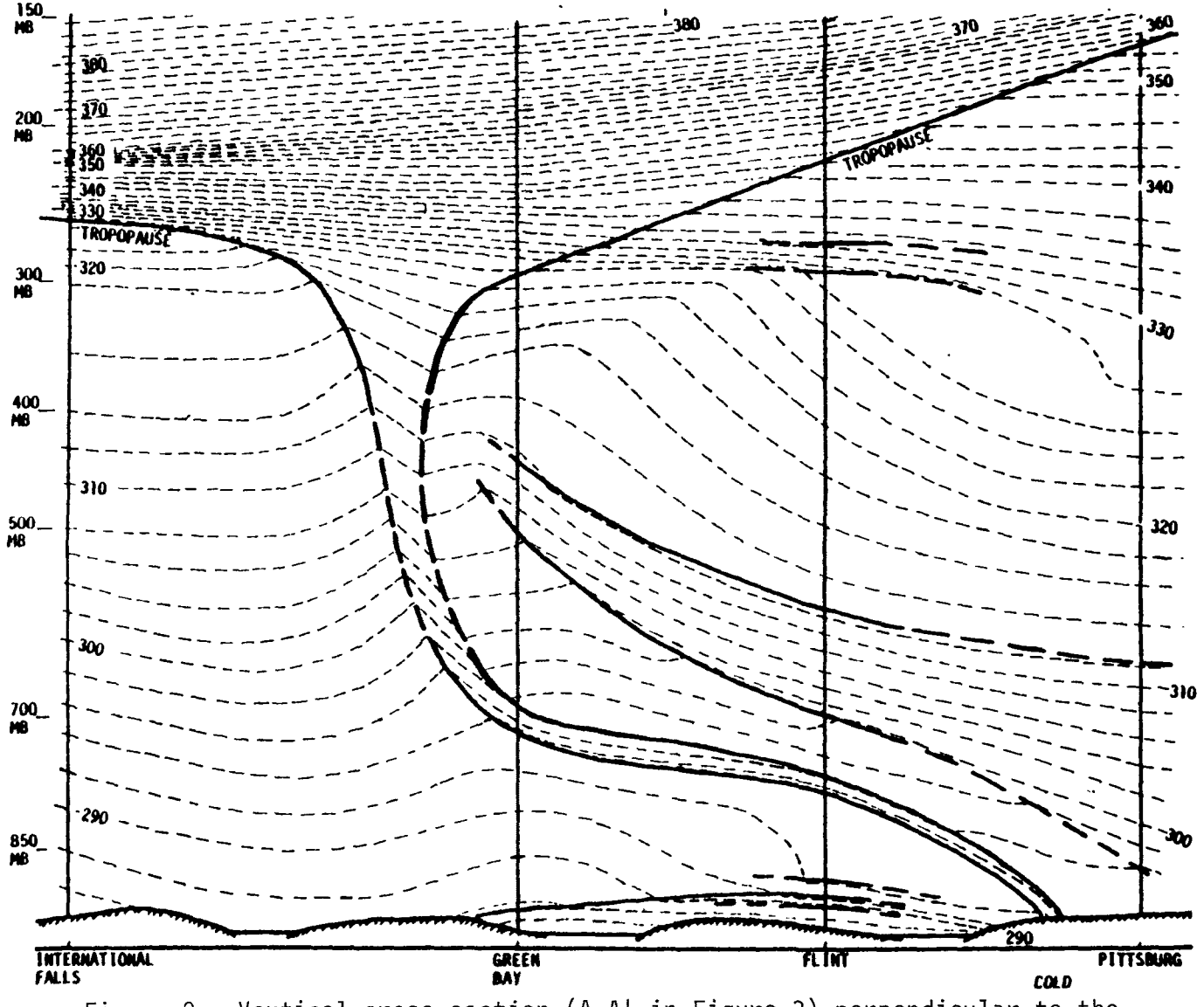

Figure 9. Vertical cross-section (A-A' in Figure 3) perpendicular to the cold front on September 29, 1975, 7:00 a.m. EST indicating frontal surfaces, stable layers, and the tropopause (heavy lines) and the potential temperatures ($^{\circ}$K, dashed lines).

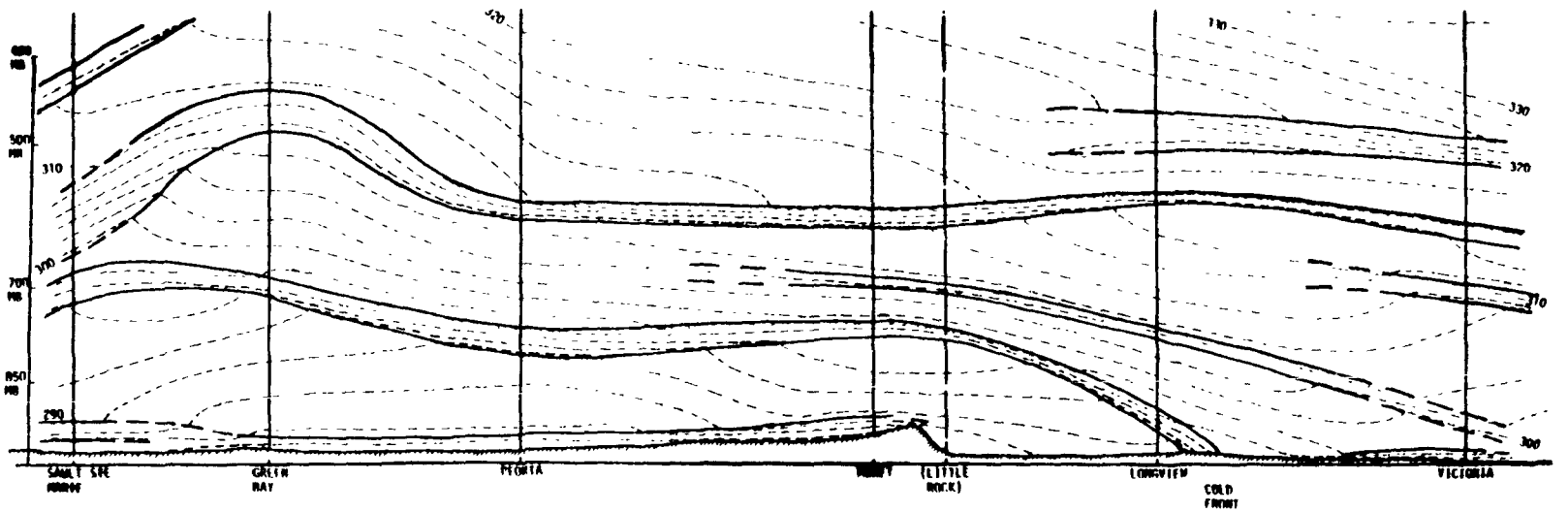

Figure 10. Vertical cross-section (B-B' on Figure 3) parallel to the cold front on September 20, 1975, 7:00 a.m. EST. The cold front intersecting the ground near Longview, Texas is the same as that shown merging with the tropopause in Figure 9.

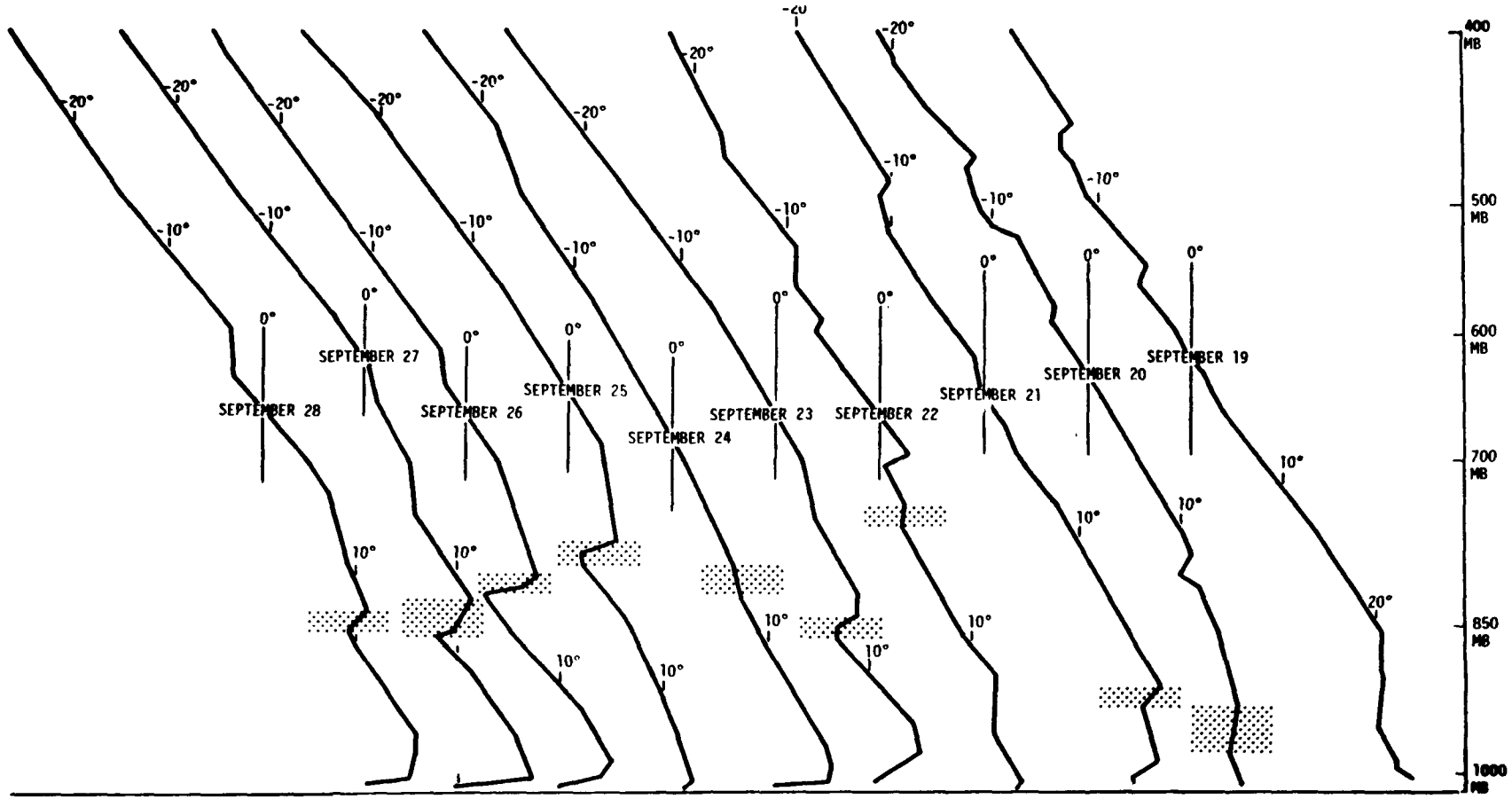

Figure 11. Vertical temperature profiles for September 19, 1975, 7:00 a.m. EST through September 28, 1975, 7:00 a.m. EST indicating the cold front-stable layer's persistence for the period. (Shaded layer is the front.)

appearance of those when air is subsiding over a stable layer. This is consistent with the circulation patterns aloft over Texas for this period.

Having now demonstrated that the cold front that passed through Texas between September 19 and 21 actually remained over the area as a stable layer through September 28, a cross-sectional analysis (Figure 12) indicates that the layer covered not just Texas but the entire central United States. (The cross-section is identified as C-C' on Figure 6.) The cold front-stable layer can be identified over Longview, Texas, but not over Lake Charles, Louisiana, on September 26. This indicates that the atmosphere over Lake Charles has become well mixed and has destroyed the stable layer. Any air that was previously in the stable layer is now mixed throughout the lower troposphere.

Two days later the stable layer reappeared at Lake Charles but disappeared over Del Rio, Texas (Figure not included). This sporatic disappearance (i.e., mixing) and reappearance of a "frontal remnant-stable layer" is a typical occurrence on the "backside of a HIGH." There, the trailing edge of the cold front is losing its identity as other meteorological phenomena begin to dominate. The speed with which the cold front-stable layer loses its identity depends on the speed of motion of the High pressure area. A slowly drifting HIGH may result in several disappearances and reappearances of the layer.

STRUCTURE OF A FRONT AND ASSOCIATED OZONE MEASUREMENTS

FRONTAL MODEL

The three-dimensional structure of a front has been modeled by Reed and Danielsen, 1959, by analyzing the discontinuities in the temperature and wind fields at the frontal and tropopause surfaces. Their model, after which the analysis in Figure 9 is patterned, describes the front as a layer of air whose upper and lower surfaces are tied to the tropopause ahead of and behind the front, respectively. Air within the frontal layer can actually have the same potential temperature (i.e., be on the same isentropic surface) as air in the stratosphere.

Vertical Motion Within the Frontal Layer

More recently, Shapiro, 1969, examined the detailed vertical motions in the upper frontal zone using a high-resolution numerical technique. He has shown that there can be downward motion of air of up to 0.15 meters per second within the upper frontal zone. This downward moving air would conserve its potential temperature (i.e., flow along an isentropic surface) as it moved down in the frontal layer. Since it is stratospheric in origin, it contains high concentrations of ozone.

Observations of Ozone Within the Frontal Layer

Vertical profiles of ozone have been measured by several research programs. Figure 13 presents one such profile measured by the Air Force Cambridge Research Laboratory's (AFCRL) ozone program on May 7, 1963,

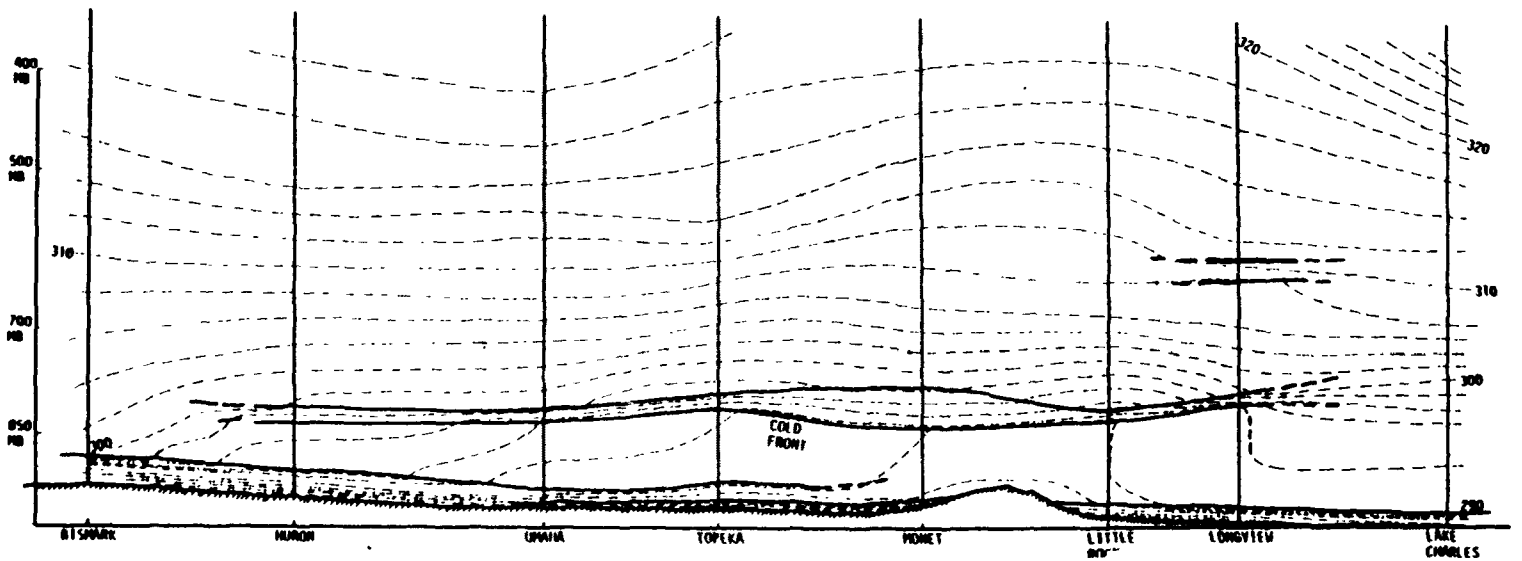

Figure 12. Vertical cross-section (C-C' on Figure 6) through the remnant of the cold front on September 26, 1975, 7:00 a.m. EST. Note that the cold front overlays the central United States from Huron, South Dakota, to Longview, Texas, yet had dissipated over Lake Charles, Louisiana.

7:12 a.m. EST, at Tallahassee Florida. This profile shows that as the ozonesonde (instrument package) ascended through a frontal layer at an altitude of about 8 km, there was an increase in ozone. Other profiles at Tallahassee and at other stations (Hering and Bordon, 1964, 1965, and 1967; and Carney, 1976) have indicated similarly that sometimes there are increased concentrations of ozone within frontal layers. This is probably stratospheric ozone being transported down an isentropic surface within the frontal layer.

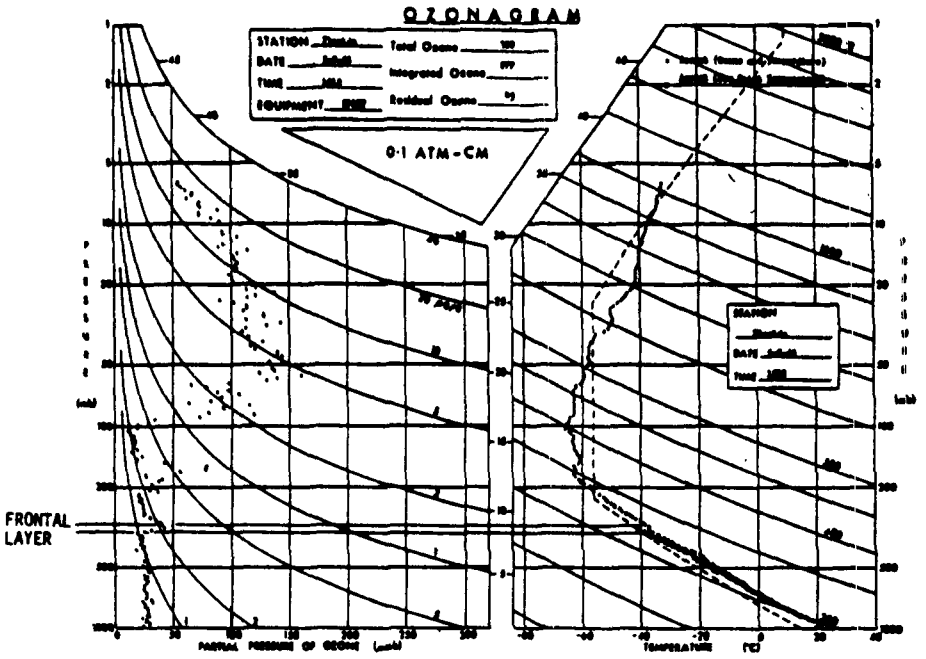

Figure 13. Vertical ozone profile (ozonagram) for Tallahassee, Florida, for May 7, 1963, 7:12 a.m. EST indicating that there was an increase of ozone concentrations measured by the ozonesonde as it ascended through a frontal layer.

While being transported down the inside of the front, the ozone will move with the general circulation at each level and will persist until, either destroyed by precipitation, washout, etc., or mixed into the lower tropospheric air. The general circulation over the backside of a HIGH has the required anticyclonic subsidence to mix the air within the "dissipating" frontal layer to the surface.

A Perspective Sketch of the Frontal Structure

To summarize the structure, a sketch of the three-dimensional perspective of the frontal surfaces (Figure 14) shows that they are essentially topological surfaces that connect the tropopause (a surface) to the earth's surface. Gridlines on the front's surface are sketched to show that the front at the trailing edge (left-hand side) has flattened and is almost horizontal. In addition, a section of these gridlines on

the leading and trailing edges of the front are omitted to show the thickness of the innerfrontal layer and to show the tendency for stratospheric air to flow downward within the layer. A jet stream maximum is indicated at about 200 millibars (mb) over the leading edge of the front and a low-level anticyclonic subsidence is indicated at the trailing edge.

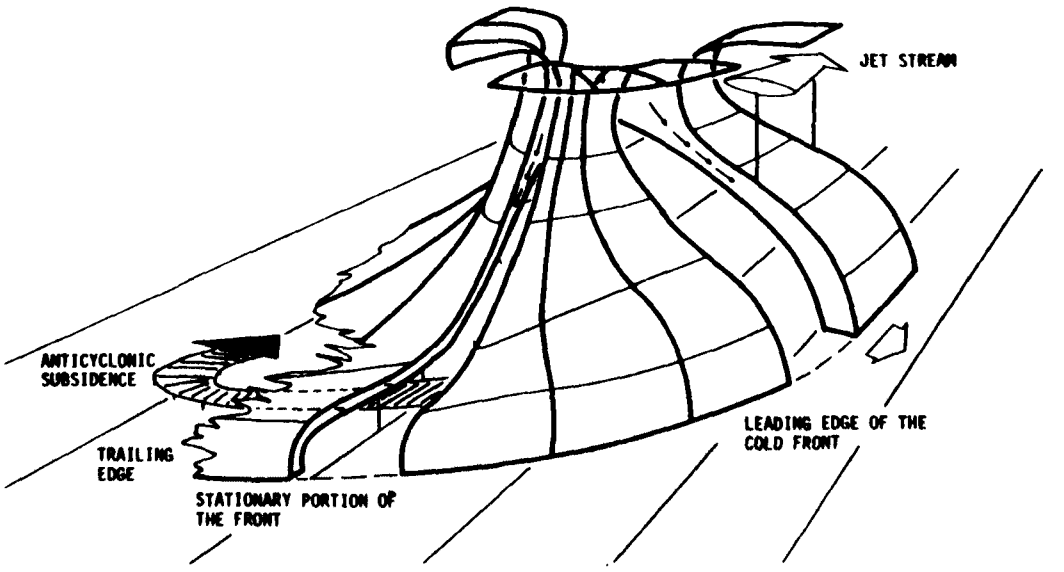

Figure 14. Artist's sketch of the structure of a cold front. Grid lines on the frontal surface are broken to show the thickness of the frontal layer near the leading and trailing edges. The tendency for stratospheric air to flow downward within the frontal layer is indicated. Also, the dissipation of the frontal layer near the trailing edge is indicated as well as the anticyclonic subsidence near that edge.

ROUTINE EVENTS LEADING TO AN EPISODE

The sequence of events leading up to the regional ozone episode is:

1. Ozone-rich stratospheric air begins to flow down inside the developing frontal layer at the upper levels.

2. Several days later, ozone from the upper rear portion of the front has moved (a) down within the frontal layer, and (b) around to a position near the trailing edge.

3. As the trailing edge dissipates and the air within the front mixes in the lower troposphere, ozone is transported to the earth's surface.

The meteorological analysis has provided a clearly feasible mechanism for bringing stratospheric ozone to the surface of the earth in Texas. The quantities involved are not definable by this analysis. However, reasonable

assumptions suggest that this injected ozone may amount to an appreciable part of, perhaps even a majority of, the ozone found at unpolluted rural sites. However, in urban areas it could hardly contribute more than a small portion of the total ozone burden.

Another phenomenon is believed to operate and exert a major influence. This is initiation or triggering. It is suggested that stratospheric ozone played the role of a free-radical oxidation initiator and triggered a gradual buildup of photochemical oxidation processes, which culminated in the episodic ozone levels of September 25 through October 1.

For the benefit of those unfamiliar with the details of chemical oxidation processes, let me comment that it is well known that hydrocarbon oxidation reactions employing oxygen proceed by free-radical sequences. However, an initial source of such radicals is required to initiate the process.

A dramatic example of the importance of initiation can be cited from one of Monsanto's commercial experiences. In the commercial production of cumene hydroperoxide, which is the first step in Monsanto's synthesis of phenol, cumene is oxidized with air. This reaction is initiated by providing an initial level of a percent or so of cumene hydroperoxide in the oxidation mixture. Thermal fragmentation of a portion of this initiator provides enough radicals to get the process going. It is exceedingly difficult to initiate the process if no peroxide is present. When Monsanto started up its plant in 1962, no oxidation occurred, even after 16 hours of bubbling air through hot cumene. When one pint of a dilute cumene hydroperoxide solution was added to a 21,000 gallon reactor, the reaction started briskly in less than three minutes. The applicable sequence of free-radical initiation and propagation steps is illustrated in Figure 15.

It is believed that initiation of this type provides the chemical path by which stratospheric ozone can initiate an ozone episode on a scale as broad as the entire state of Texas.

Significant levels of stratospheric ozone, though well below the NAAS, may become widely dispersed in the lower troposphere. This ozone can, by reaction with olefins, create ozonides that are unstable and cleave yielding diradicals. These diradicals can propagate hydrocarbon oxidation sequences of the type shown in Figure 15. Figure 16 illustrates part of this process.

Radicals from the hydrocarbon ozidation process can oxidize nitric oxide (NO) interferring with the nitrogen-dioxide photolytic cycle, causing a buildup of ozone (Figure 17). Note that the process of Figure 17 is conservative of free-radicals, allowing it to continue and to oxidize more and more NO. Every molecule of NO oxidized is, of course, equivalent potentially to creating one more molecule of ozone.

Critics of this suggestion will, no doubt, point out that the nitrogen dioxide photolytic cycle is capable of providing many oxygen atoms that might act as initiators for the oxidation of hydrocarbons. This may or may

INITIATION:

$$R\text{-}O\text{-}O\text{-}H \longrightarrow R\cdot + H\text{-}O\cdot$$

PROPAGATION:

$$R\text{-}H + H\text{-}O\cdot \longrightarrow H_2O + R\cdot$$

$$R\cdot + O_2 \longrightarrow R\text{-}O\text{-}O\cdot$$

$$R\text{-}O\text{-}O\cdot + R\text{-}H \longrightarrow R\text{-}O\text{-}O\text{-}H + R\cdot$$

ETC.

$$R = C_6H_5C\,(CH_3)_2$$

Figure 15. Free-radical initiation and propagation.

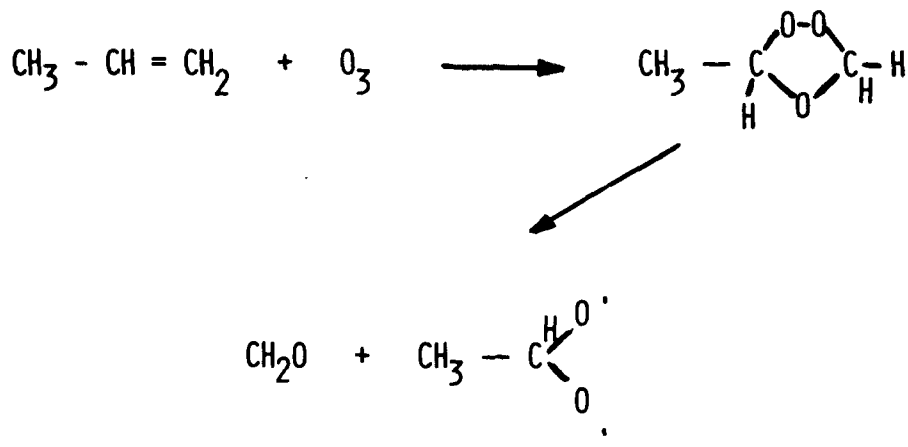

Figure 16. Hydrocarbon oxidation sequences.

$$R\text{-}CH_2\text{-}O\text{-}O\cdot + N\text{-}O \longrightarrow R\text{-}CH_2\text{-}O\cdot + NO_2$$

$$R\text{-}CH_2O\cdot \longrightarrow R\cdot + CH_2O$$

$$R\cdot + O_2 \longrightarrow R\text{-}O\text{-}O\cdot$$

$$R\text{-}O\text{-}O\cdot + N\text{-}O \longrightarrow R\text{-}O\cdot + NO_2$$

ETC.

Figure 17. Oxidation of Nitric Oxide, Nitrogen Dioxide photolytic cycle.

not be so. Oxygen atoms and various hydrocarbon free-radicals do not have the same energetic properties and ability to transfer with all moieties. Therefore, initiation of oxidation chain process in the manner suggested may be favored.

A factor favoring stratospheric ozone being the initiator is that it will be well mixed into many thousands of feet of the lower troposphere. Each day, as mixing begins, a fresh infusion downward can provide a source of make-up free-radical initiator to keep photochemical activity building.

Some confirmation of this view is obtained in the fact that it is now being observed in aerial plume studies (7, 8) that ozone concentration in downwind plumes seems to be closely related to upwind ozone concentrations feeding into the urban photochemical process.

It should also be noted that stratospheric ozone is not the only possible source of such initiation. Transported ozone and carryover ozone frequently observed in bands near the inversion level can act similarly. As suggested, ozonides, hydroperoxodes, and perhaps even peroxyacetylnitrate (PAN) can act as sources of free-radicals and carry the initiation process over from one day to the next.

There is certainly a great need to provide a chemical explanation for the broad scale ozone episode. Pollution, as a direct cause, is ruled out because of its invariability, the distances involved, and the involvement of unpolluted sites. Air stagnation is an unlikely cause because of the lack of an accompanying sharp or consistent buildup in other pollutants and because the rapid development in high ozone peaks frequently occurs before sufficient time has elapsed to permit such a buildup.

It is believed that the phenomenon discussed occurs primarily in continental polar air masses and involves their associated fronts. We believe that it occurs most often in the fall of the year in central United States but may be associated with intrusions in other seasons.

While we regret that we cannot offer unequivocal proof that the synoptic-scale ozone episode is triggered by an injection of stratospheric ozone, we believe that strong evidence exists that this may be the case. Future research efforts, particularly aerial studies, should make an effort to seriously test this thesis.

SUMMARY

The frequent, regional ozone episodes experienced in the eastern United States are probably caused, in part, by the transport of ozone-rich stratospheric air to the earth's surface. Numerous vertical ozone profiles have shown that there is increased ozone concentrations within the frontal layer, and currently-accepted frontal models indicate that this ozone is probably of stratospheric origin.

An analysis of the space and time continuity of a front's low-level structure demonstrates that the stable layer over the region experiencing an ozone episode was actually the remnant of a cold front that had pushed through several days earlier. The stable layer disappeared and reappeared at several stations indicating that it was losing its identity as it dissipated. Any air within the stable layer would have been mixed in the lower troposphere. Since this stable layer is the remnant of a cold front, its increased ozone content could have caused and/or "seeded" an ozone episode.

ACKNOWLEDGEMENTS

The kind cooperation of the staffs of the Texas Air Control Board, the Houston Air Pollution Control Department, the Louisiana Air Control Commission, the DuPont Company, Texas Utilities, and Radian Corporation in providing data is greatly appreciated.

REFERENCES

1. Carney, Thomas A., 1976. Vertical Distributions of Ozone as Evidence of the Role of Stratospheric Transport in the Spatial and Temporal Distribution of Tropospheric Ozone. In: Proceedings of the Ozone/Oxidants, Interactions with the Total Environment, Specialty Conference, Dallas, Texas, March 10-12, 1976. P. 234. (Thomas A. Carney, Tennessee Depart of Public Health, Division of Air Pollution Control, C2-220 Cordell Hull Building, Nashville, Tennessee 37219.)

2. Hering, W.S. and T R. Borden, Jr., 1964. Ozonesonde observations over North America, Vol. 2. Environmental Research Paper No. 38. Report AFCRL-64-30 (II), Air Force Cambridge Research Laboratories.

3. Hering, W. S. and T. R. Borden, Jr., 1965. Ozonesonde observations over North America, Vol. 3. Environmental Research Paper No. 133. Report AFCRL-64-30 (III), Air Force Cambridge Research Laboratories.

4. Hering, W.S. and T. R. Borden, Jr., 1967. Ozonesonde observations

over North America, Vol. 4. Environmental Research Paper No. 279. Report AFCRL-64-30 (IV), Air Force Cambridge Research Laboratories.

5. Reed, R. J. and E. F. Danielsen, 1959: Fronts in the vicinity of the tropopause. Arch. Meteoro. Geophy. Bioklim., AII, 1-17.

6. Shapiro, Melvyn A. On the Scale of Atmospheric Motions within Middle-Tropospheric Frontal Zones. NCAR Cooperative Thesis No. 18, Florida State University and Laboratory of Atmospheric Science, NCAR, 1969.

7. Dr. Max Shauck, Baylor University, private communication.

8. White, Blumenthal, et al., Meteorological Research, Inc., Paper to be presented at the International Conference on Photochemical Oxidant and Its Control, September 12-17, 1976, Raleigh, N. C.

APPLICATION OF 1960'S OZONE SOUNDING INFORMATION TO 1970'S SURFACE OZONE STUDIES

P. R. Sticksel*

ABSTRACT

It has been purported that high ozone levels in the lower troposphere are, at least partially, the result of ozone transport from the stratosphere downward along stable layers. A limited investigation of this hypothesis was conducted using ozone measurements made in the lower troposphere in 1963 and 1974 and the data from the North American upper air soundings of temperature and wind. Three-dimensional isentropic trajectories traced backward from the lower troposphere failed to confirm the hypothesis of continuous downward transport along stable layers. However, a sloping stable layer extending from coast to coast across the United States was identified for the May, 1963, case, and soundings into this layer at three widely-separated stations revealed higher-than-average ozone concentrations within the layer.

INTRODUCTION

This is a report on the testing of a hypothesis--that episodes of high surface ozone concentrations are at least partially the result of transport of stratospheric ozone downward along stable layers. These stable layers are hypothesized to (a) originate at breaks in the tropopause at higher latitudes, (b) follow surfaces of constant potential temperature downward, and (c) terminate within inversion layers near the surface. The basis for this hypothesis is observations of ozone maxima appearing at various levels in the troposphere during the upper atmosphere ozone sounding programs conducted in the 1960's. Kroening and Ney (1) identified "rivers" of high ozone concentrations exiting from the stratosphere at tropopause breaks and entering the upper troposphere.

In a recent paper, Sticksel (2) showed one example of a vertical cross section through the atmosphere from Florida to Greenland on which there was a sloping stable layer. The surface synoptic chart is Figure 1, and the cross section with the sloping layer is Figure 2. This stable layer (between the potential temperatures of 310°K and 315°K) appeared in many upper atmospheric soundings along the eastern coast of the Northern Hemisphere on May 15, 1963, at 1200 Greenwich Meridian Time (GMT). Ozone soundings at Tallahassee, Florida; Bedford, Massachusetts; and Churchill, Manitoba, all displayed ozone peaks along this surface of constant potential temperature (isentropic surface) (Figures 3a, 3d, 3e). At Thule, Greenland this isentropic surface was within

*Battelle Columbus Laboratories, Columbus, Ohio.

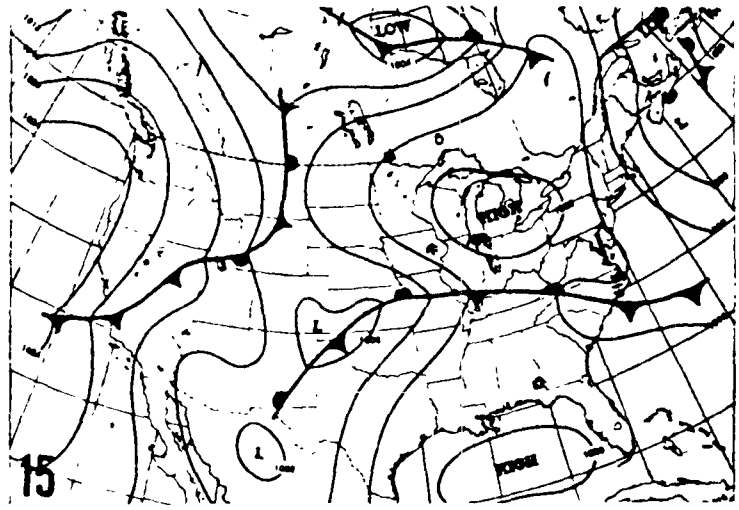

Figure 1. Surface synoptic map for 1200 GMT on May 15, 1963. (Weatherwise, August, 1963)

the stratosphere after passing through a break in the tropopause north of Churchill.

Sticksel (2) also noted that high concentrations of lower tropospheric ozone appearing on the Northern Hemisphere soundings of the 1960's followed a seasonal progression and recession from low latitudes to high latitudes and back again during the spring-summer-fall period. This movement corresponds to the seasonal progression and recession of the tropopause break poleward and equatorward.

This evidence for the transport of ozone between the stratosphere and surface is circumstantial. Proof of a continuous trajectory downward and a description of the mechanism of descent are required. If downward transport along a stable isentropic layer can be demonstrated, the horizontal extent of this movement should be determined.

ISENTROPIC TRAJECTORIES

The approach chosen for this investigation of possible stratosphere-to-surface transport was to study the pressure and wind patterns on isentropic surfaces. Pressure data for constructing the isentropic charts were obtained from the temperature-pressure soundings of the United States and Canadian rawinsonde networks. Wind speeds and directions were interpolated from the wind observations made during these same soundings.

Since one of the pieces of evidence for the stratosphere-to-surface hypothesis was the May 15, 1963, cross section, this date was chosen for the isentropic analysis. Work was done with both the θ=310°K and the θ=315°K surfaces. The 310°K surface intersected the Tallahassee sounding at 650 millibars (mb). This was the top of the ozone layer that extended from the ground to about four kilometers at this station (Figure 3a). Above this layer of high ozone there was a shallow layer in which ozone concentration dropped off

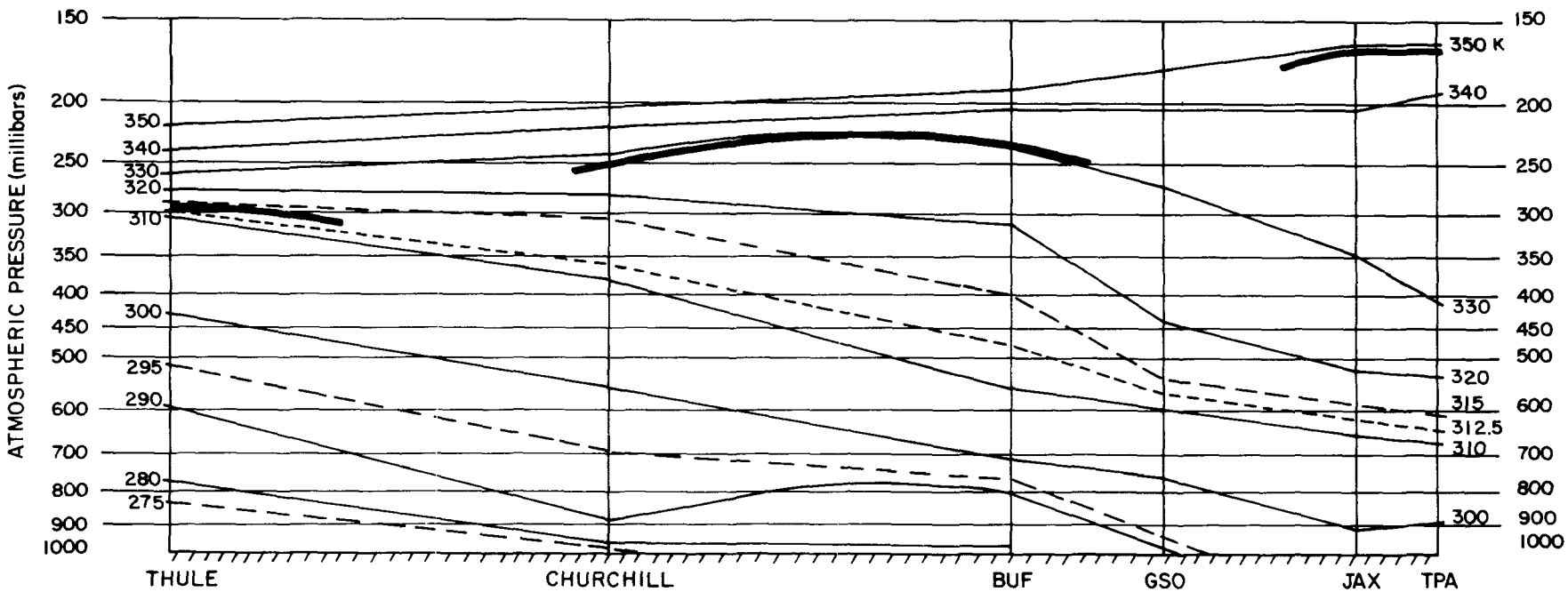

Figure 2. Vertical cross section of potential temperature through the atmosphere between Tampa, Florida, and Thule, Greenland, for 1200 GMT (8 a.m. EDT) on May 15, 1963. Potential temperatures are in degrees Kelvin. Heavy lines denote the tropopause position.

slightly and then a two-kilometer layer of concentrations equal to those in the surface layer. This upper layer is intersected by the 315°K isentropic surface. Both these surfaces were high enough so that they did not intersect the ground even in the mountainous portions of southwestern United States.

Since all processes in the free atmosphere tend to be largely adiabatic as long as there is no condensation, air particles should remain on the same isentropic surface unless saturation occurs (3). Other nonadiabatic atmospheric processes include radiational heating and cooling, evaporation, and convective activity (4).

Indications of the direction of vertical motion were obtained from the relationship between wind directions and isobars on the isentropic charts. Winds blowing toward higher pressure were evidence of descending motion. Generally air parcels moving from north to south on an isentropic surface in the Northern Hemisphere are descending toward lower altitudes. Some caution must be taken in these vertical motion determinations because the isentropic surface itself may also be moving. Thus, these rules are reliable only when movements are strong. If this is the case, the forward motion of the air relative to the surface is guaranteed (5).

Keeping these limitations of isentropic analysis in mind, an additional step was taken to determine the origins of the ozone-rich air. Trajectories were traced backward along the isentropic surfaces in 12-hour segments from one standard radiosonde launch time to the preceding launch time. These trajectories were graphically computed from the streamlines on the surfaces following the method given by Saucier (6). Trajectories, once constructed, should be viewed as surrounded by a region of uncertainty expanding with distance from the origin of the trajectory. In the case of the three-dimensional isentropic trajectories, the region of uncertainty can be visualized as cone-like. The base of the cone-like volume is an ellipse rather than a circle.

RESULTS

MAY 15, 1963

Figure 4 portrays the isentropic surface for 1200 Greenwich Meridian Time (GMT) on May 15, 1963. The surface has a depression (region of high pressure) over the Texas panhandle and a dome (region of low pressure) centered over northeastern Wyoming. The intersection of the θ=315°K surface with the tropopause occurs along a line running across Canada from the southwest to the northeast.

Streamline patterns on the surface generally follow the isobars. There is an anticyclonic divergence center on the Louisiana-Mississippi border. Some ascending motion is apparent in the western United States and some descending motion in the eastern United States. There is no strong descending motion from the Canadian area of the tropopause southward into the central or eastern United States.

The strongest winds on the surface would represent the greatest relative

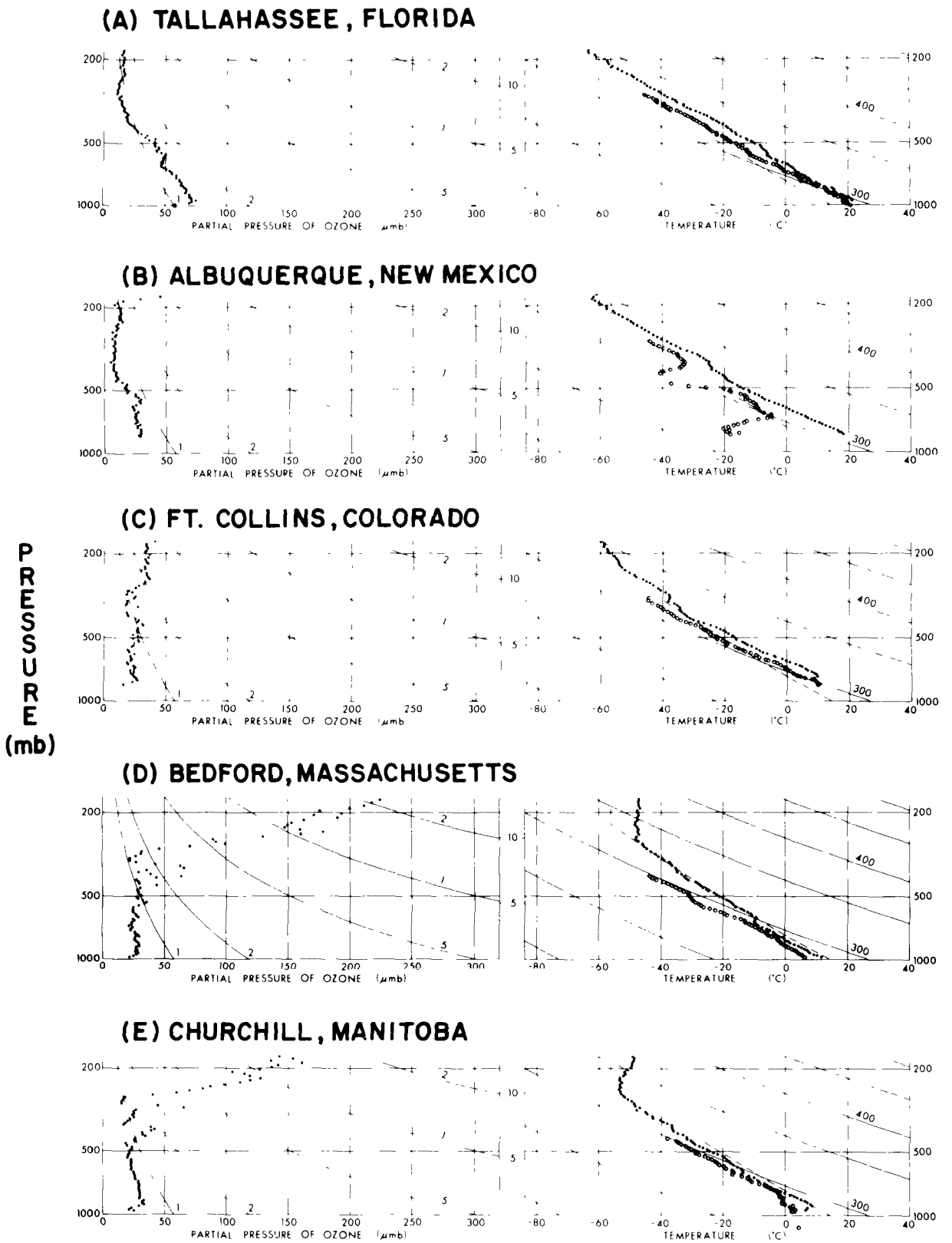

Figure 3. Ozonesonde soundings for 1200 GMT on May 15, 1963. (Hering and Borden, Vol. 2, 1965)

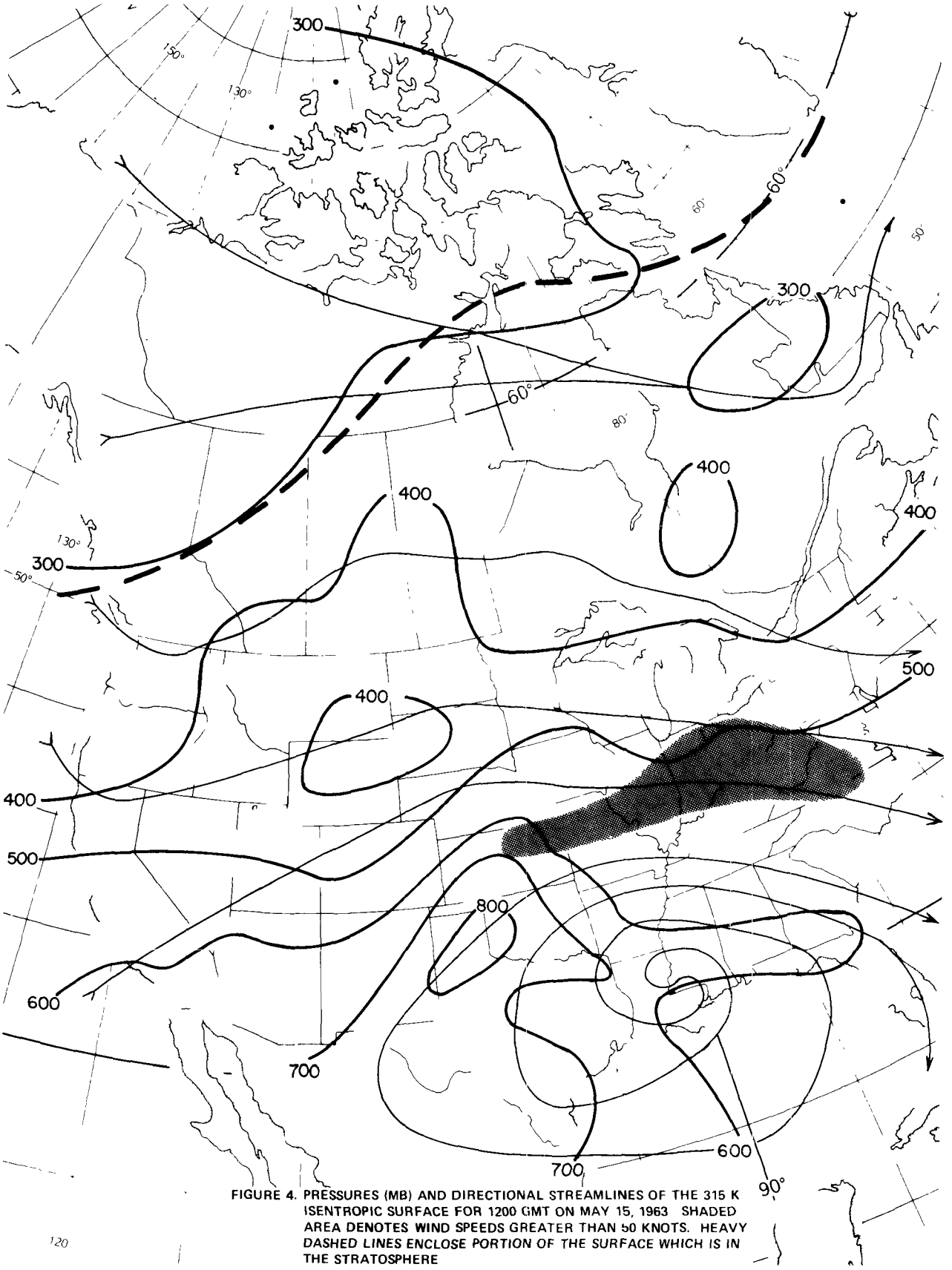

FIGURE 4. PRESSURES (MB) AND DIRECTIONAL STREAMLINES OF THE 315 K ISENTROPIC SURFACE FOR 1200 GMT ON MAY 15, 1963 SHADED AREA DENOTES WIND SPEEDS GREATER THAN 50 KNOTS. HEAVY DASHED LINES ENCLOSE PORTION OF THE SURFACE WHICH IS IN THE STRATOSPHERE

motion of the air to the surface and consequently the areas of most pronounced vertical motion. These wind maxima indicate strongest ascent over Kansas and Missouri with strongest descent occurring between Indiana and Virginia.

Isentropic trajectories were computed to determine whether the ozone-rich air that appeared along this surface at Tallahassee, Bedford, and Churchill could be traced backward in the direction of the tropopause. The results of these computations are displayed in Figure 5. The air that arrived above Tallahassee on May 15 (Trajectory No. 1) was above the Houston, Texas, region 48 hours earlier. This trajectory resembles the flow one would expect around the north side of the high pressure area located in the Gulf of Mexico. The motion along this trajectory was generally upward.

The Bedford trajectory (No. 2) followed a different path and indicated descent for the air parcel as it traveled southward from northern Canada to Massachusetts. However, it should be stated that none of the temperature soundings along this trajectory had a stable layer encompassing the isentropic surface.

Trajectory No. 3 from Churchill backward displayed not descending movement, but rather small ascending motion. The position of the air parcel 24 hours earlier was over northern British Columbia at a height that would have been within the stratosphere on May 15. However, on May 14, this location was still within the troposphere.

Although one must take into account the pitfalls accompanying the computation of isentropic trajectories, the ones described here should be representative of the true flow. One can conclude from these results that the high ozone concentrations observed at $\theta=315^{\circ}K$ on the May 15 soundings did not arrive there by direct transport from the stratosphere along a stable layer. In fact the ozone at the three stations probably came from three different source areas, even though their final potential temperatures were identical.

DAYTON, OHIO--1974

Calculation of an isentropic trajectory for the period of a recent oxidant study in Ohio provided some additional insight on the hypothesis of descending ozone parcels. On August 7, 1974, at 0000 GMT (8 p.m. EDT) a vertical ozone sounding made by an airplane over Dayton, Ohio, measured ozone concentrations of over 160 $\mu g/m^3$ in the layer between the surface and 1500 meters (7). The isentropic trajectory traced backward from this point and time is shown as trajectory No. 4 in Figure 5. This trajectory was calculated for the $\theta=300^{\circ}K$ surfaces. It terminated at 825 mb at Dayton, which was approximately 1800 meters above the ground and within the layer of high atmospheric ozone concentration. Forty-eight hours earlier this air was over central Wisconsin at 775 mb (an altitude of about 2300 meters), thus indicating descending motion. On the morning of August 6 (1200 GMT) the $300^{\circ}K$ surface was within a strong inversion layer. At the other 12-hour checkpoints along its journey the air parcel was within a layer that was slightly stable.

It is significant to compare the isentropic trajectory (solid line) with

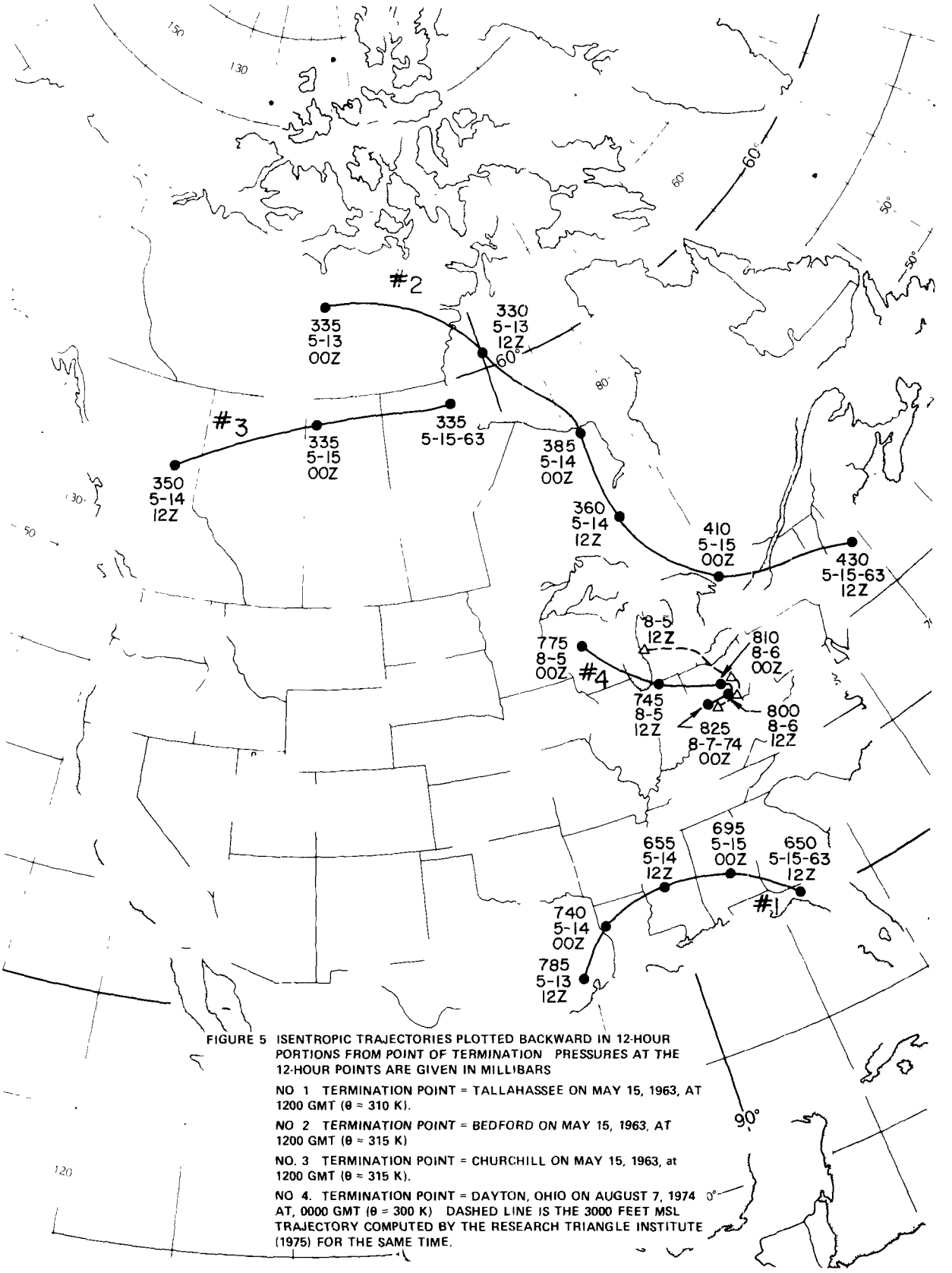

FIGURE 5 ISENTROPIC TRAJECTORIES PLOTTED BACKWARD IN 12-HOUR PORTIONS FROM POINT OF TERMINATION PRESSURES AT THE 12-HOUR POINTS ARE GIVEN IN MILLIBARS

NO 1 TERMINATION POINT = TALLAHASSEE ON MAY 15, 1963, AT 1200 GMT (θ = 310 K).

NO 2 TERMINATION POINT = BEDFORD ON MAY 15, 1963, AT 1200 GMT (θ = 315 K)

NO. 3 TERMINATION POINT = CHURCHILL ON MAY 15, 1963, at 1200 GMT (θ = 315 K).

NO 4. TERMINATION POINT = DAYTON, OHIO ON AUGUST 7, 1974 AT, 0000 GMT (θ = 300 K) DASHED LINE IS THE 3000 FEET MSL TRAJECTORY COMPUTED BY THE RESEARCH TRIANGLE INSTITUTE (1975) FOR THE SAME TIME.

a trajectory at 3000 feet (dashed line) originating at Wilmington, Ohio, (20 miles southeast of Dayton) computed by the Research Triangle Institute (8) for their concurrent oxidant study. The path and endpoints for the 36-hour extent of the RTI constant level trajectory are quite similar to those of the three-dimensional isentropic trajectory.

Additional Comment on the May, 1963, Case

A prediction of the paths of the May 15, 1963, isentropic trajectories could have been obtained from the 500 mb chart for that date (Figure 6). The path of the Tallahassee air parcel was dictated by the HIGH covering the southern United States. Control of the Bedford trajectory was exerted by the trough in the northeast, while the relatively straight isentropic trajectory from Churchill resembles the 500-mb contour pattern in that region.

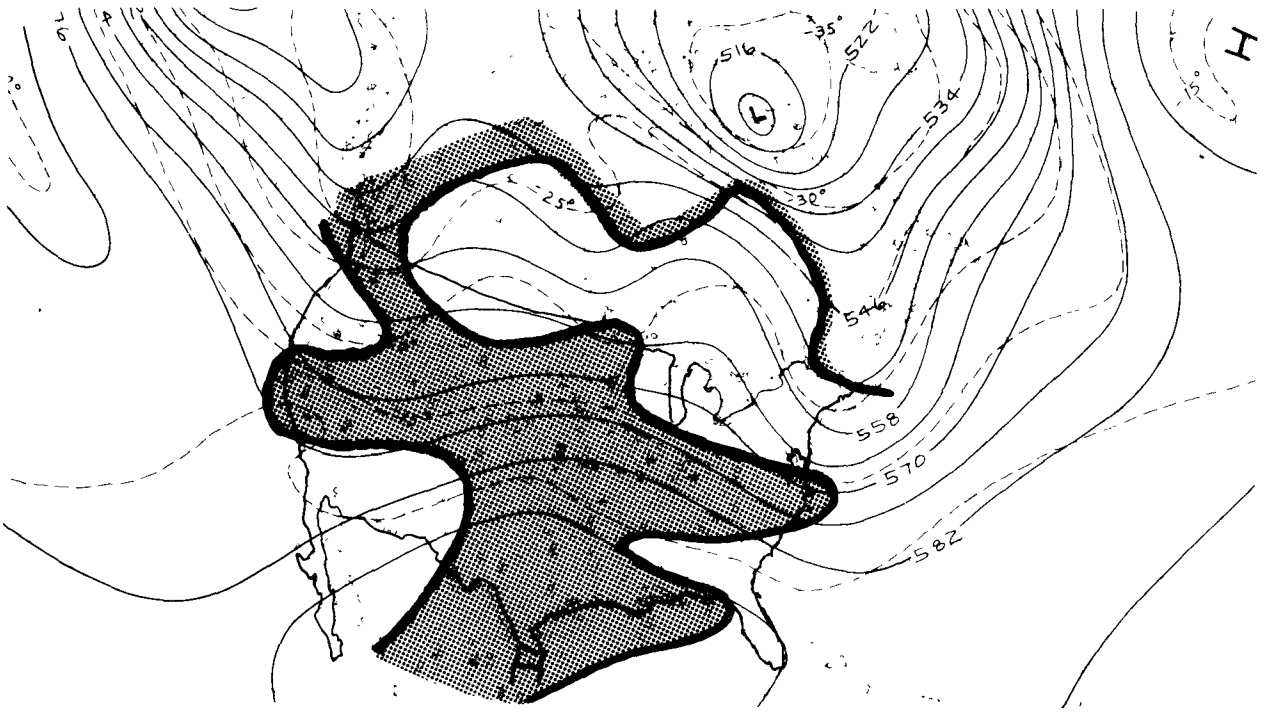

Figure 6. North American 500 mb chart for 1200 GMT on May 15, 1963. Shaded portions enclose areas for which the θ=315 K surface was within a stable layer.

Another interesting observation related to the 315°K isentropic surface is depicted in Figure 6. The shaded areas enclose all the stations for which the 1200 GMT soundings on May 15 had a stable or slightly stable layer encompassing some portion of the interval between 310°K and 320°K. This aerial representation shows a discontinuity in the stable surface occurring along a broad area near the U.S.-Canadian border. Any stratospheric ozone that reached the troposphere south of this discontinuity must not have proceeded along a direct trajectory. However, the pervasiveness of the stable layer over most of the United States suggests that there may have been an extensive layer of ozone related to the HIGH in Mexico. Closer inspection of the

soundings at Tallahassee, Albuquerque, New Mexico and Ft. Collins, Colorado (Figure 3) verifies that there was a deep layer of ozone above each station. The layer at Tallahassee contains two maxima--about 450 mb to 550 mb and 600 mb to the surface. At Albuquerque the ozone layer extends from 500 mb to the surface with a peak at 550 mb. At Ft. Collins there is an above-average ozone layer between 400 and 550 mb. Thus, the original hypothesis is supported in part. There may likely be a large layer of ozone sloping upward from low to high latitudes. The ozone in this layer is so extensive that its source is not anthropogenic. However, by turbulent mixing it can supply ozone to the surface layer, which supplements the man-created oxidants there. It is suggested that the stratosphere was the original source of this pervasive ozone layer and that it was associated with the subtropical HIGH. The mechanism of transfer downward is still to be determined.

CONCLUSIONS

From the results of this limited investigation the following conclusions were drawn:

(1) "Rivers" (inversion layers) of ozone extending from a tropopause break to the surface are not a reliable explanation for all high surface ozone concentrations. Further investigation may show that there is transport downward along slightly stable layers in some cases. In any event, the sharp ozone peaks observed in the upper troposphere do not isentropically descend unaltered to the surface where they produce ozone maxima.

(2) Layers of ozone extensive enough and deep enough to rule out anthropogenic sources were observed in the lower troposphere associated with a large subtropical HIGH at 500 mb. This suggests another descent mechanism associated with the development of synoptic scale systems.

(3) Predictions of isentropic trajectory paths can be made from the contours on isobaric surfaces where those surfaces are near the same pressure as the origin of the isentropic trajectory. Movement along contours from higher to lower latitudes will indicate descent. Movement from west to east will indicate little movement in the vertical direction.

REFERENCES

1. Kroening, J. L. and E. P. Ney, Atmospheric Ozone, J. Geoph. Res., 67: 1867-1875, 1962.

2. Sticksel, P. R., Occurrence and Movement of Tropospheric Ozone Maxima, In: Proceedings Ozone/Oxidant Interactions with the Total Environment Specialty Conference, Southwest Section Air Pollution Control Association, Dallas, Texas, 1976, pp. 252-267.

3. Byers, H. R., General Meteorology, 3rd Edition, McGraw-Hill Book Company, New York, New York, 1959, p. 146.

4. Oliver, V. J., and M. B. Oliver, "Construction and Use of Isentropic Charts," in Handbook of Meteorology, F. A. Berry, E. Bollay, and N. R. Beers, eds., McGraw-Hill Book Company, New York, New York, 1945, pp. 848-56.

5. Saucier, W. J., Principles of Meteorological Analysis, The University of Chicago Press, Chicago, Illinois, 1955, p. 255.

6. Ibid., p. 313.

7. Spicer, C. W., J. L. Gemma, D. W. Joseph, P. R. Sticksel, and G. F. Ward, "The Transport of Oxidant Beyond Urban Areas," Report by the Battelle Columbus Laboratories to the U.S. EPA, EPA-600/3-76-018, U.S. Environmental Protection Agency, Research Triangle Park, N.C., February, 1976, p. 189.

8. The Research Triangle Institute, Investigation of Rural Oxidant Levels as Related to Urban Hydrocarbon Control Strategies. EPA-450/3-75-036, U.S. Environmental Protection Agency, Research Triangle Park, N. C., March, 1975.

THE ROLE OF STRATOSPHERIC IMPORT ON TROPOSPHERIC OZONE CONCENTRATIONS

E. R. Reiter*

ABSTRACT

The effects of stratospheric ozone imports into the lower troposphere are studied through analogy to radioactive fallout, from ozonesonde measurements and from hourly ozone measurements at Zugspitze, Germany (3000 m above mean sea level (M.S.L.)). It is shown that the maximum allowable hourly concentration of 74.7 ppb of ozone (O_3) is exceeded by such imports on approximately 0.2 percent of the days in the cyclogenetically active regions of middle latitudes. The stratospheric circulation pattern that provides the ozone reservoir in the lower stratosphere appears to play a significant role in cases that provide O_3 concentrations in the lower troposphere two to three times in excess of the maximum allowable level set by EPA.

INTRODUCTION

The present federal standards of ozone (O_3) concentrations not to be exceeded for longer than one hour are 160 μg/m^3 (= 74.7 ppb, or 0.1238 μg/g). This value is transgressed relatively frequently even in rural areas away from known pollution sources (for references see Singh et al., 1975). The question arises to what extent stratospheric O_3 transported into the lower troposphere could lead to ambient ozone concentrations that either exceed the federal maximum level or produce such a high background level that even a modest industrial and/or photochemical contribution could push the concentration values over the "allowable" maximum.

To answer this question we have taken several approaches.

STRATOSPHERIC RESIDENCE TIMES OF AIR MASSES

Using data on the mean meridional circulation published by J. F. Luis in CIAP Monograph 1 (Reiter et al., 1975), together with case studies on eddy transport and tropopause height adjustments (Reiter, 1975a), the annual mass budget of the northern hemisphere stratosphere given in Table 1 was derived.

Observed residence times of nuclear debris in the stratosphere agree very well with these estimates.

From satellite data Lovill (1972) estimated the average global value of total ozone to be 303.3 Dobson units (or milli-atmospheric-centimeters at

*Colorado State University, Fort Collins, Colorado.

TABLE 1. MASS BUDGET OF THE STRATOSPHERE (IN PERCENT OF THE MASS EQUIVALENT TO ONE HEMISPHERIC STRATOSPHERE)

Seasonal adjustments of tropopause level	10%
Mean meridional circulation	43%
Stratospheric exchange between hemispheres	16%
Large-scale eddies (jet streams)	20%
Small-scale eddies (thunderstorms)	negligible
	89%

normal temperature and pressure). The total weight of the ozone column, therefore, is $6.495 \times 10^{-4} g/cm^2$, or 1.6565×10^9 tons in one hemisphere. If, according to Table 1, 73% of the air in the stratosphere is exchanged with the troposphere each year (the 16 percent of interhemispheric exchange within the stratosphere cannot be counted here), 1.2×10^9 tons of ozone should be affected by this transport in each hemisphere.

Regener and Aldaz (1969) determined the vertical flux of ozone to be 1.3×10^9 tons per year over the whole globe. A somewhat smaller flux of 0.804×10^9 tons per year over the globe was determined by Junge (1962, 1963; Fabian and Junge, 1970). Comparing these values with the above number for hemispheric transport, we arrive at the conclusion that only about half of the stratospheric ozone is available for transport into the troposphere. The ozone in the middle and upper stratosphere (above 15 to 20 km) is still photochemically active and subject to dissociation. (See Reiter et al., 1975, for data and references.) Therefore only ozone in the lower stratosphere can be considered as a potential source of tropospheric ozone.

OZONE AND RADIOACTIVE FALLOUT

Detailed data on radioactive fallout during the early 1960's are available from the U.S. Public Health Service Radiation Surveillance network. Excessive fallout concentrations in dry air at the ground usually could be ascribed to the import of tropospheric air into the stratosphere (for typical case studies see Reiter, 1972). Radioactive debris concentration measurements in the stratosphere are also available for this time period from Project Stardust. We have attempted to correlate stratospheric Strontium^{90} (Sr^{90}) concentrations (Seitz et al., 1968) with O_3 to arrive at Sr^{90}/O_3 ratios. For May-August 1963 we obtained an average ratio of 500 in the lower stratosphere of the northern hemisphere (Figure 1), with Sr given in dpm/1000 SCF (standard cubic feet) and O_3 given in $\mu g/g$. A correction has to be applied to this ratio, because the Sr^{90} data of May-August were actually compared with ozone concentrations of March-April. Using the relationship

$$N = N_o \exp(-t/T)$$

(where N is the extrapolated Sr^{90}/O_3 ratio for March-April; N_o is the value of this ratio at t = 0; T is the e-folding residence time of Sr^{90} in the

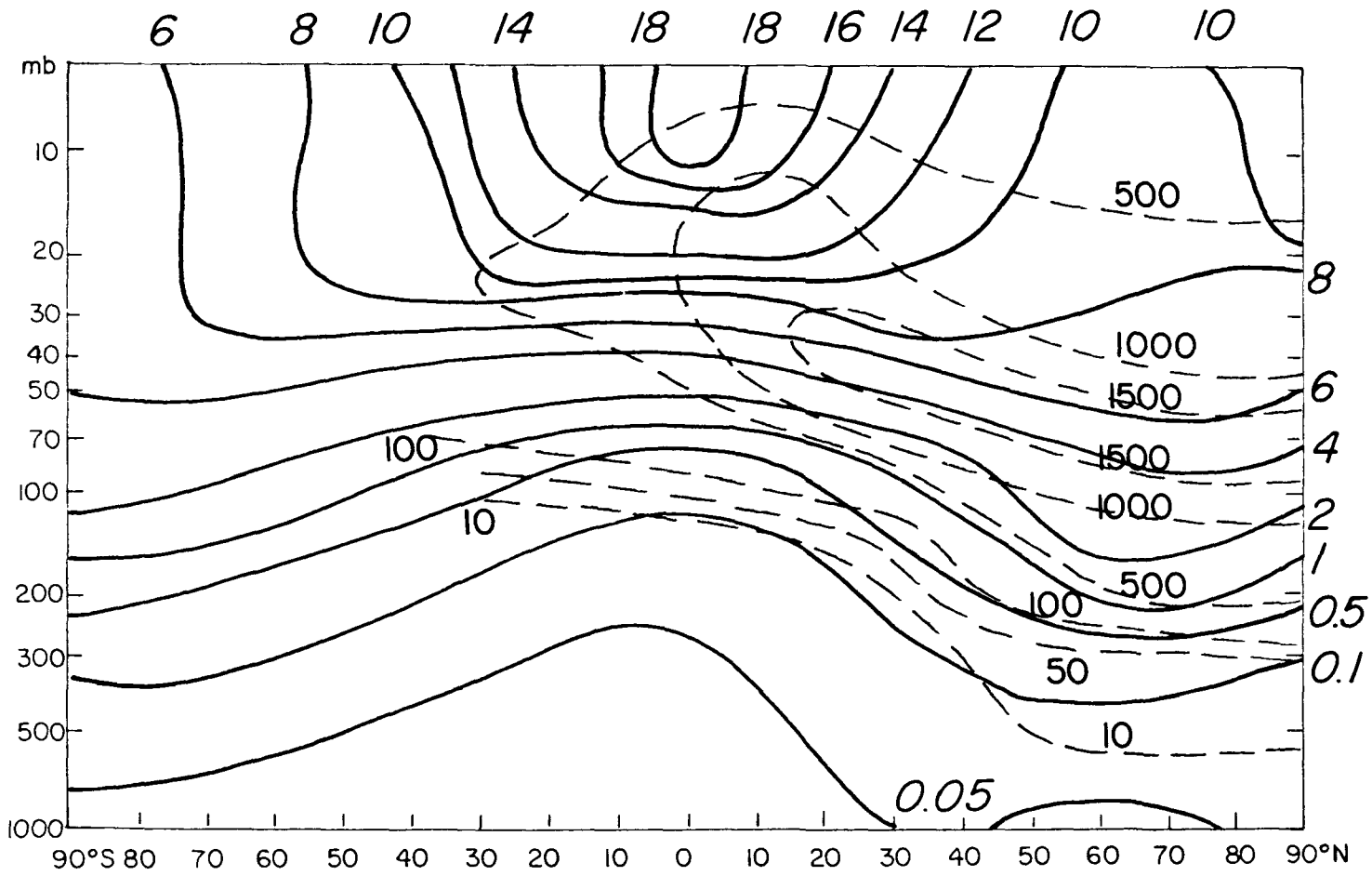

Figure 1. Mean ozone distribution for March-April (solid lines, slanting number, μg/g) and strontium^{90} distribution for May-August 1963 (dashed lines, vertical numbers, dpm/1000 SCF).

stratosphere, i.e., 14 months) we arrive at a correction factor of 1.24 for t = -3 months. Thus the representative Sr^{90}/O_3 ratio in the lower stratosphere for March-April 1963 was assumed to be 620. This value, together with others, is shown in Figure 2. The straight line in this diagram predicts the Sr^{90}/O_3 ratio under the assumptions that the stratospheric O_3 concentration remains invariant and the the Sr^{90} concentration is subject to an e-folding time of 14 months.

The Sr^{90}/O_3 ratios of 250 to 300 derived from measurements of September-November 1964 do not fit this straight line. We have to take into account, however, that ozone concentrations in the lower stratosphere are only half as high in fall than in spring (Dütsch, 1971). Therefore, to project the Sr^{90}/O_3 ratio measured in fall to O_3 concentrations as they would prevail during spring, the ratios of 250 to 300 would have to be reduced by a factor of 2 (dashed "box" in Figure 2) (Reiter, 1975b).

We can now proceed to estimate O_3 concentrations at ground level, that should have been encountered with surface radioactive fallout of stratospheric origin. Since in spring and summer of 1963 the bulk of radioactive fallout was due to the US and USSR test series of megaton devices conducted during 1962, we can estimate the contribution of Sr^{90} to the total radioactivity measured at ground level in 1963 to be of the order of 1% (Reiter, 1975b). By spring of 1964 the Sr^{90} contribution was of the order of 2%. A surface fallout value of 5 p C/m^3 observed in summer of 1963, therefore, should have contained approximately 0.05p C/m^3 of strontium, or 3.145 dpm/1000 SCF of Sr^{90}. With a Sr^{90}/O_3 ratio of 620 in the appropriate units the ozone concentration in this surface air should have been 0.0051 μg/g. With the same ratio of 620 the Federal maximum value of O_3 of 74.7 ppb would correspond to a Sr^{90} activity of 76.76 dpm/1000 SCF, or at least 7676 dpm/1000 SCF of total radioactivity. This amounts to 122 p C/m^3.

Figure 3 shows the average fallout over the U.S. Public Health Service Radiation Surveillance network during 1963. Discounting the high concentrations over Nevada, which most likely were due to local sources, we can conclude that the "natural" average background of stratospheric O_3 at the ground should be of the order of 3 to 5 percent of the federal hourly maximum value. Slightly higher values prevail in the lee of the Rocky Mountains, where chinook winds provide a rapid mechanism of transport of stratospheric air towards the ground.

The maximum fallout encountered during 1963 is shown in Figure 4. We should emphasize that these are 24-hour average values. Nevertheless they come within about 20 percent of the hourly allowable maximum value of equivalent ozone concentrations (Reiter, 1975b).

OZONESONDE MEASUREMENTS

We should expect that "instantaneous" measurements of O_3 concentrations will off and on reach considerably higher values than indicated by 24-hour average values, especially if rapid transport processes from the stratosphere are involved, with little mixing in the upper troposphere. To investigate this possibility we reviewed 1477 ozonesonde observations between December

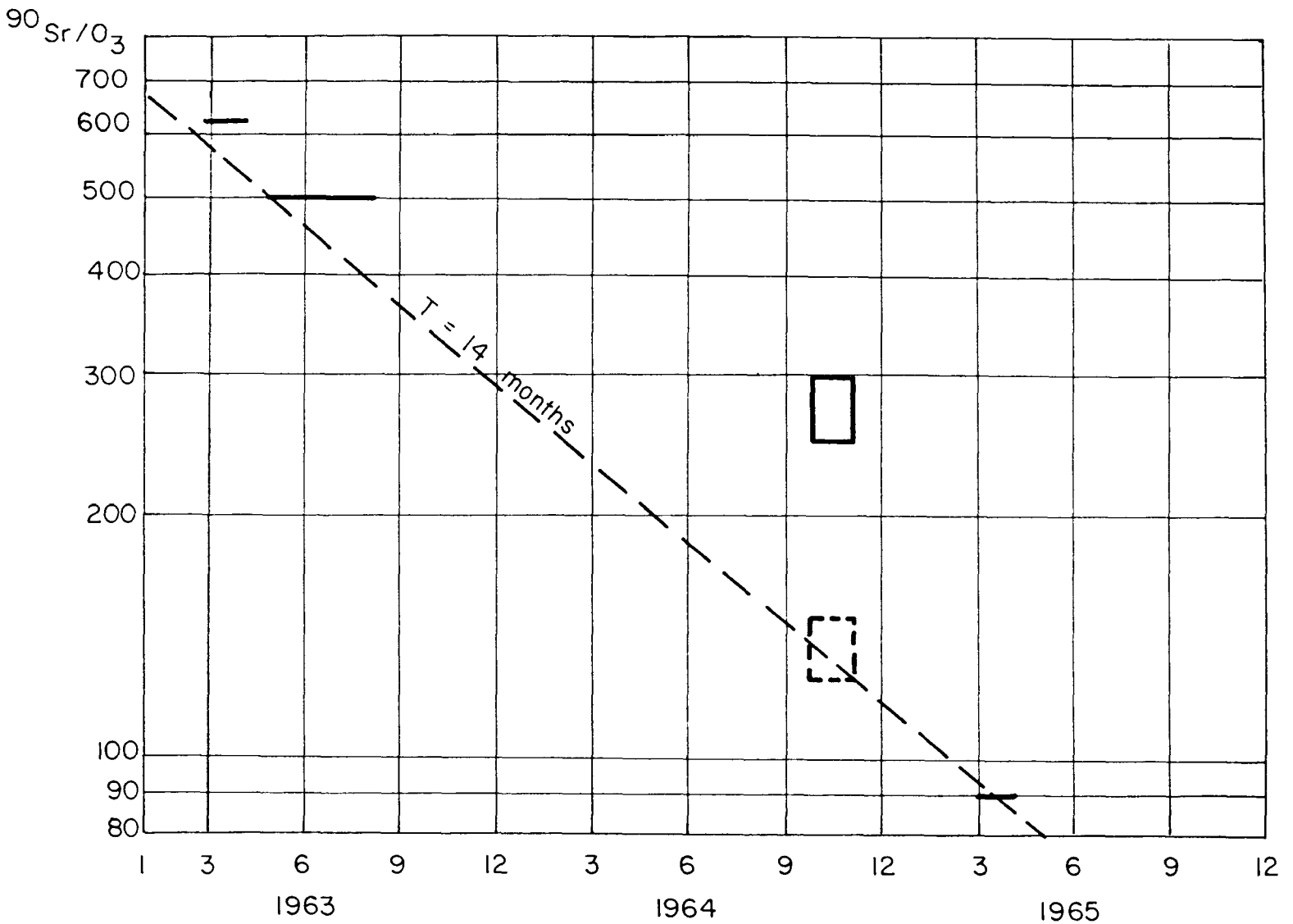

Figure 2. Sr^{90}/O_3 ratios as a function of time (see text for explanation).

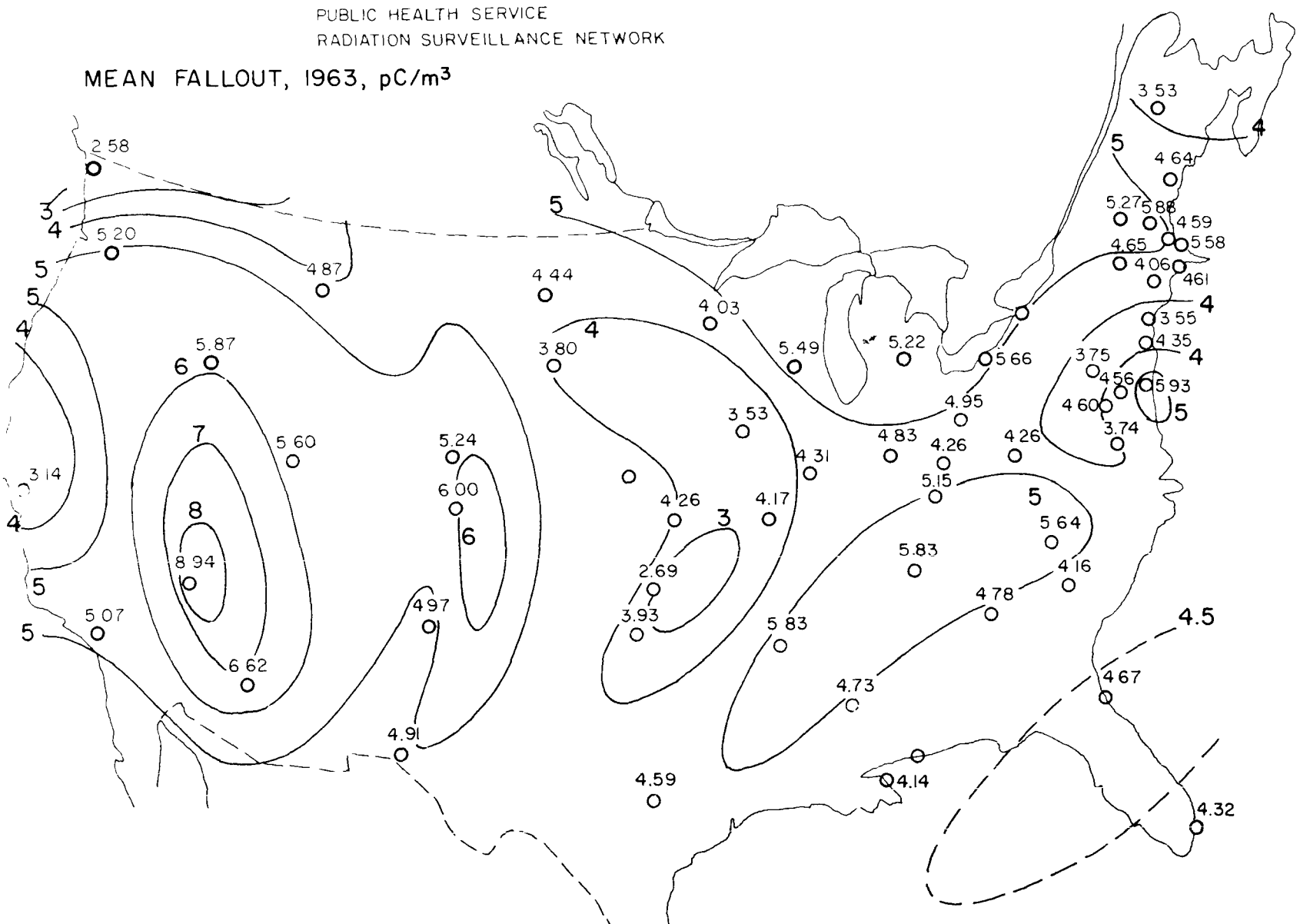

Figure 3. The average fallout over the U.S. Public Health Service Radiation Surveillance network during 1963.

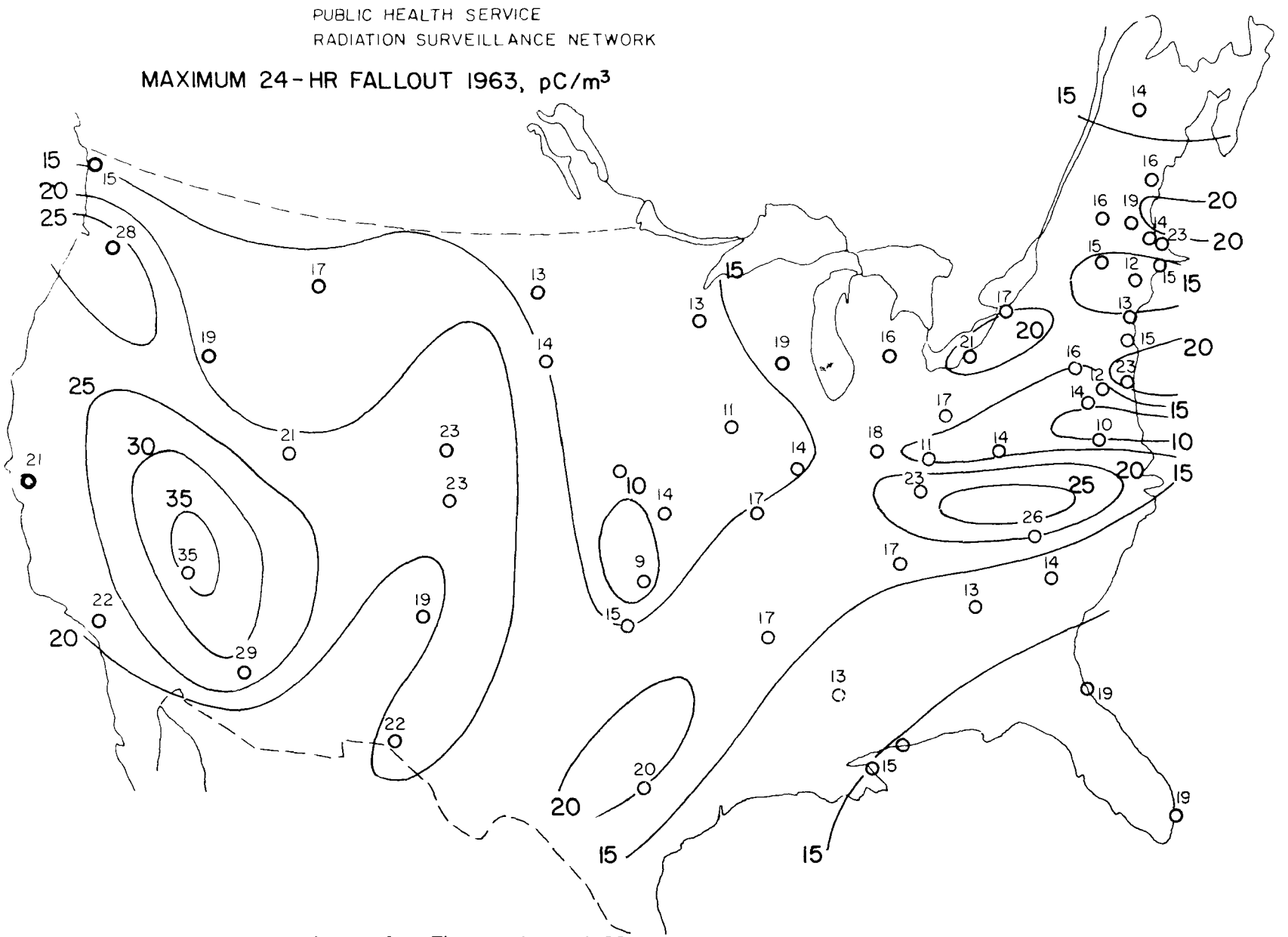

Figure 4. The maximum fallout encountered during 1963.

1962 and December 1965 (Hering, 1964; Hering and Borden, 1964, 1965a,b, 1967). Table 2 shows a frequency distribution of maximum O_3 mixing ratios (μg/g) below the 800-mb level (for the stations Albuquerque, New Mexico, and Ft. Collins, Colorado, below 750 millibars (mb)). The layer below this level was assumed to be characteristic of the planetary boundary layer (PBL). In approximately 2 percent of the soundings the hourly allowable maximum of 74.7 ppb or 0.1238 μg/g had been exceeded.

Of the 31 cases with excessive O_3 concentrations in the PBL, only three (i.e., 0.2% of the total sample) qualified as possible stratospheric air intrusions: Goose Bay, Canada, 5-2-1963, 0.15 μg/g; Tallahassee, Florida, 8-14-1963, 0.19 μg/g; and Seattle, Washington, 4-15-1964, 0.16 μg/g. All other cases (listed in Table 3) had to be suspect of tropospheric sources (Reiter, 1976a). Figures 5 and 6 show isentropic trajectories constructed backwards in time for the cases of Goose Bay and Tallahassee. The case of March 24, 1964, in which an ozonesonde intercepted high O_3 concentrations (ca. 3.5 μg/g) above the 500-mb level over Albuquerque, New Mexico, was not considered in the above statistics, because these excessive concentrations were encountered outside the PBL.

Since the ozonesondes intercepted layers with high O_3 concentrations away from the earth's surface we have to expect that these concentrations will be reduced by turbulent mixing processes within the PBL. Even though almost undiluted parcels of air can reach the ground on occasions when such layers are "tapped" by strong turbulence, the one-hour averaging process inherent in the maximum allowable value of 74.7 ppb will reduce these instantaneous "spikes" considerably. In analogy we could consider the peak gusts versus the one-hour average wind speed.

HOURLY OZONE OBSERVATIONS

Up to this point we considered daily average and instantaneous O_3 concentrations, neither of which is strictly comparable to hourly ozone concentrations. We were fortunate to receive hourly ozone data for 529 days, taken at Zugspitze, Germany (3000 m above M.S.L.) from August 1973 to February, 1976. These data were kindly supplied by Drs. Reinhold Reiter and H. J. Kantor of the Institut fuer atmosphaerische Umweltforschung at Garmisch-Partenkirchen, Germany.

In Figure 7 we have plotted a joint frequency distribution of hourly maximum O_3 concentrations in excess of the daily mean values (ppb) by classes of 2 ppb, and daily mean values by classes of 5 ppb. The maximum allowable value of 74.7 ppb would be exceeded to the right of the shaded line in this diagram. The "normal" scatter of observation points is produced partly by instrument noise, but mostly -- with above-average ozone concentrations -- by turbulent mixing processes acting upon stratospheric air intrusions.

Two observations depart significantly from the "normal" scatter of observation points. Table 4 gives the hourly O_3 concentrations which yielded the two points of excessive maximum concentrations in Figure 7. Since the allowable maximum value of 74.7 ppb was exceeded during 9 consecutive hours (by as much as a factor of 2.64) we should count this episode as only one day

TABLE 2. FREQUENCY DISTRIBUTION (NUMBER OF CASES, VERTICAL NUMERALS; PERCENT FREQUENCY, ITALICS) OF MAXIMUM OZONE MIXING RATIOS (μg/g) IN THE PLANETARY BOUNDARY LAYER AS MEASURED BY OZONESONDES

Station	μg/g 0-0.1	0.02	0.03	0.04	0.05	0.06	0.07	0.08	0.09	0.10	0.11	0.12	0.13	0.14	0.15	0.16	0.17	0.18	0.19	0.20	0.21	0.22	0.23	0.24	0.25	Σ
Thule,		6	23	15	18	10	4	3	3																	82
Greenland		*7*	*28*	*18*	*22*	*12*	*5*	*4*	*4*																	*100*
Fairbanks,		1	10	15	9	7	4	2	4	3	2															57
Alaska		*2*	*18*	*20*	*16*	*12*	*7*	*4*	*7*	*5*	*4*															*101*
Churchill,	1	10	13	13	12	16	15	8	4	2	4	2														100
Canada	*1*	*10*	*13*	*13*	*12*	*16*	*15*	*8*	*4*	*2*	*4*	*2*														*100*
Goose Bay,	3	17	34	25	20	13	8	4	1	2		1			2											130
Canada	*2*	*13*	*26*	*19*	*15*	*10*	*6*	*3*	*1*	*2*		*1*			*2*											*100*
Seattle,		25	28	22	23	11	15	9	4	3	1	2				2	1	1		1						148
Washington		*17*	*19*	*15*	*16*	*7*	*10*	*6*	*3*	*2*	*1*	*1*				*1*	*1*	*1*		*1*						*101*
Green Bay,		9	15	12	15	4	8	3	6	6	1	2														81
Wisconsin		*11*	*19*	*15*	*19*	*5*	*10*	*4*	*7*	*7*	*1*	*2*														*100*
Bedford,		21	45	32	33	28	15	17	13	8	3	3	1		1	1	3		2							226
Massachusetts		*9*	*20*	*14*	*15*	*12*	*7*	*8*	*6*	*4*	*1*	*1*	-		-	-	*1*		*1*							*99*
Ft. Collins,		26	35	27	25	18	9	9	12	1	2	1														165
Colorado		*16*	*21*	*18*	*15*	*11*	*5*	*5*	*7*	*1*	*1*	*1*														*99*
Pt. Mugu, California		1	3	3			1	2			1		1	2					1					2	1	18
Albuquerque,	2	35	36	29	28	21	18	18	7	3	3	3	1													204
New Mexico	*1*	*17*	*18*	*14*	*14*	*10*	*9*	*9*	*3*	*1*	*1*	*1*	-													*98*
Tallahassee,		8	21	13	11	19	20	13	10	7	4	1	3	1	2		1		1							135
Florida		*6*	*16*	*10*	*8*	*14*	*15*	*10*	*7*	*5*	*3*	*1*	*2*	*1*	*1*		*1*		*1*							*101*
Grand Turk Isl.	1	13	11	10	7	2	5	1																		50
Bahamas	*2*	*26*	*22*	*20*	*14*	*1*	*10*	*2*																		*100*
Balboa,	3	24	21	13	7	1	3	1	4	2	1	1														81
Canal Zone	*4*	*30*	*26*	*16*	*9*	*1*	*4*	*1*	*5*	*2*	*1*	*1*														*100*
Σ	10	196	295	229	208	150	125	90	68	37	22	16	6	3	5	3	5	1	4	1				2	1	1477
	1	*13*	*30*	*16*	*14*	*10*	*8*	*6*	*5*	*3*	*1*	*1*	(----------	----------	----------	----------	----------	----------	*2*	----------	----------	----------	----------	----------	----------	) *100*

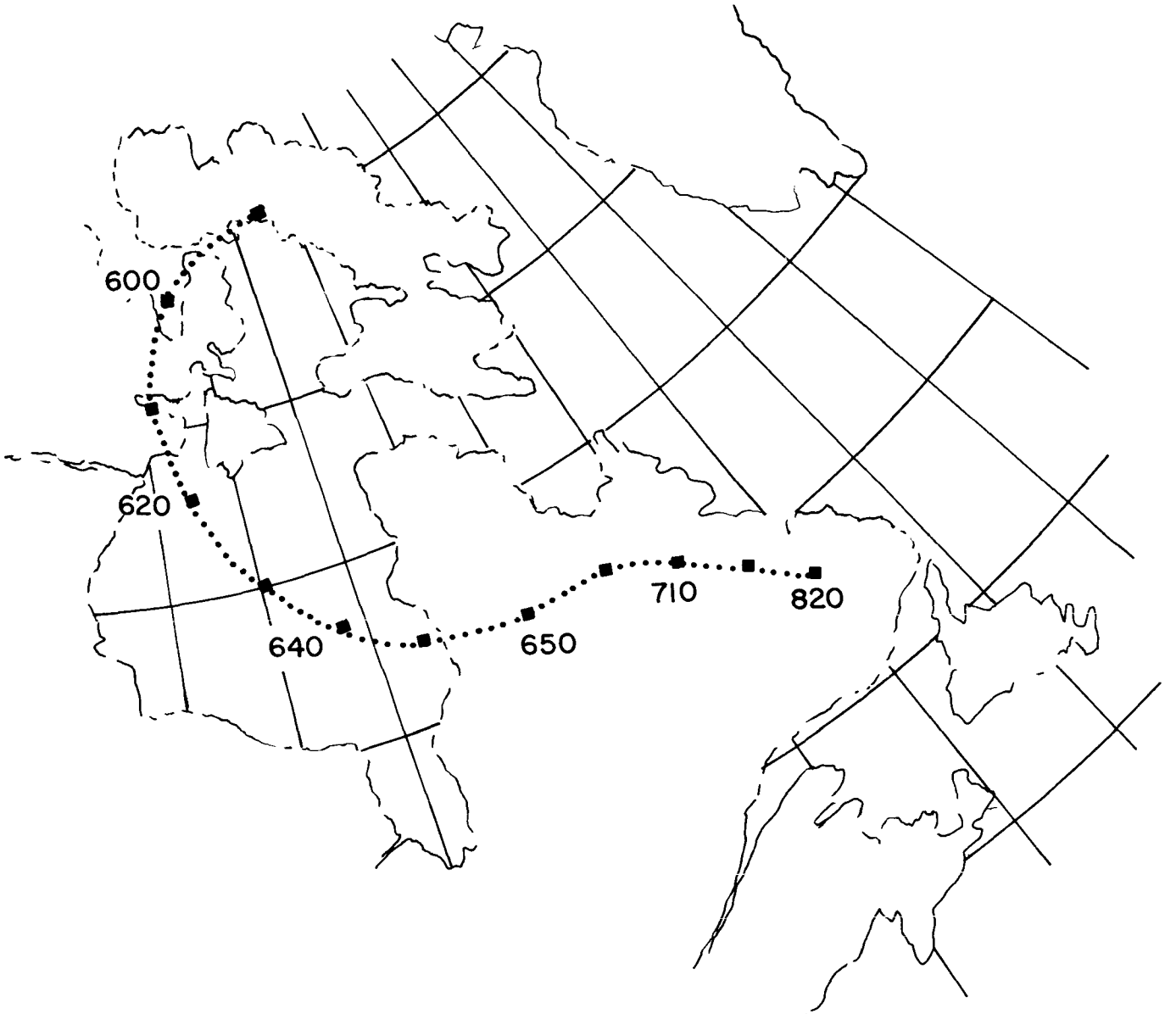

Figure 5. Composit 6-hour trajectory segments from April 29, 1963, 18 GMT to May 2, 1963, 12 GMT. Pressures in millibars are indicated next to dots corresponding to synoptic observation times.

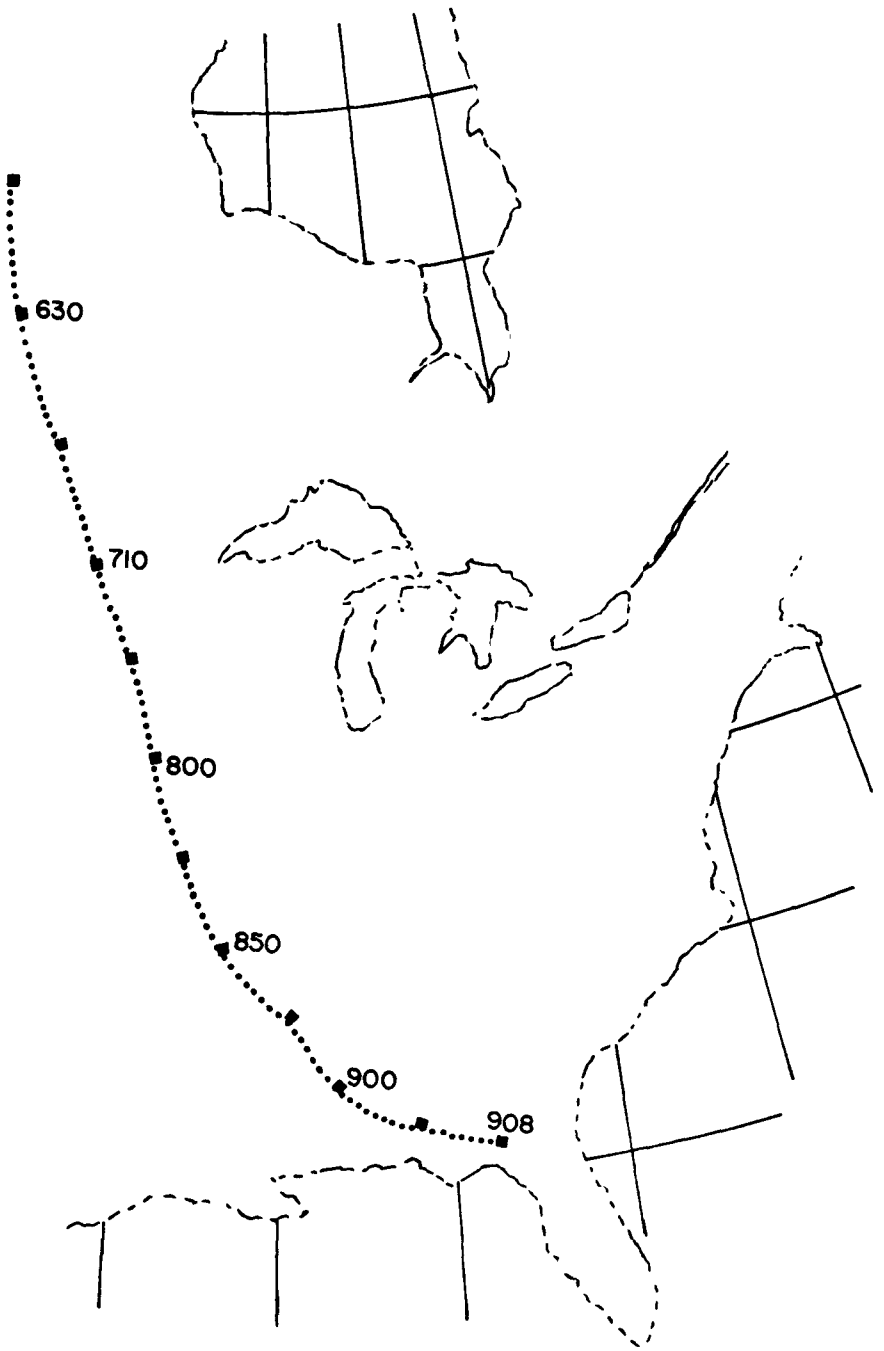

Figure 6. Composit 6-hour trajectory segments from August 11, 1963, 18 GMT to August 14, 12 GMT. Pressures in millibars are indicated next to dots corresponding to synoptic observation times.

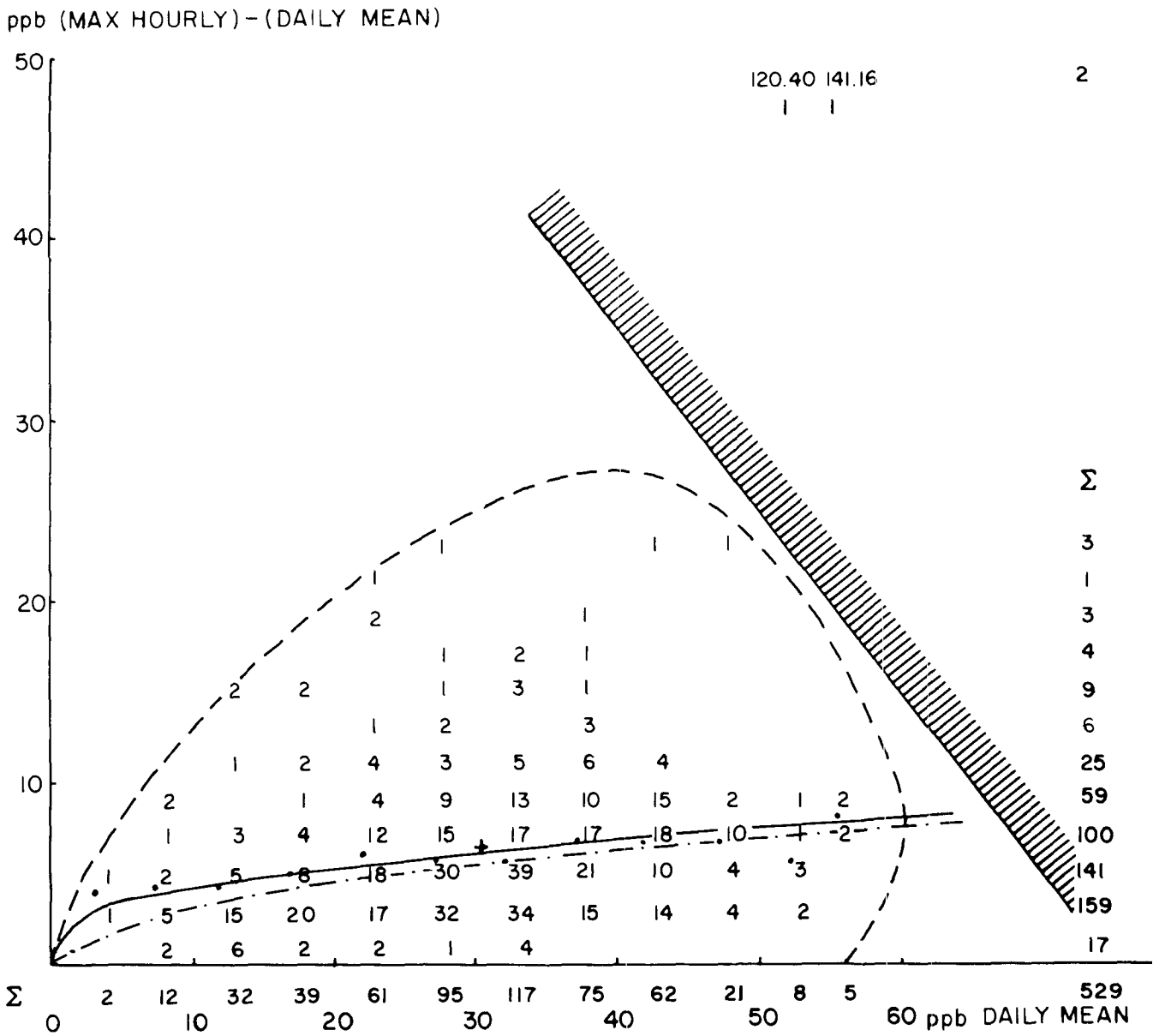

Figure 7. Difference between maximum hourly ozone concentrations (ppb) and daily mean concentrations as a function of daily mean concentrations, observed at Zugspitze (3000 m above M.S.L.) between August 1973 and February 1976. The frequency distribution by 5-ppb classes of the daily mean and 2-ppb classes of hourly maximum minus daily mean is given by the numbers in the diagram. The dashed line indicates the limits of the present data distribution. To the right of the shaded line the federal maximum value of 74.7 ppb would be exceeded. Dots indicate the mean values of (max. hourly - daily mean) in each class of daily mean values. The solid line gives an approximate best fit to these dots. The cross marks the mean value of both distributions, that of (max. hourly - daily mean) and that of the daily mean values. The dashed-dotted line approximates the position of the mode values in each class of daily mean concentrations. Note that two observations fall outside the plotted distribution.

TABLE 3. OZONE CONCENTRATIONS IN THE PLANETARY BOUNDARY LAYER EXCEEDING FEDERAL STANDARDS, ARRANGED BY DATE

Episode No.	Date	Maximum O_3 (μg/g)	Station
1	5-2-63	0.15	Goose Bay
2	5-15-63	0.13	Tallahassee
3	6-26-63	0.19	Bedford
4	7-3-63	0.17	Bedford
5	8-7-63	0.15	Bedford
6	8-14-63	0.19	Tallahassee
7	9-11-63	0.17	Tallahassee
8	9-11-63	0.17	Seattle
9	9-18-63	0.15	Tallahassee
10	1-20-64	0.17	Bedford
11	4-8-64	0.18	Seattle
12	4-15-64	0.16	Seattle
13	4-17-64	0.20	Seattle
14	4-20-64	0.13	Tallahassee
15	4-20-64	0.16	Seattle
16	7-1-64	0.13	Albuquerque
17	7-1-64	0.13	Bedford
18	7-15-64	0.17	Bedford
19	7-15-64	0.15	Goose Bay
20	8-26-64	0.19	Bedford
21	9-23-64	0.13	Tallahassee
22	1-22-65	0.15	Tallahassee
23	7-14-65	0.16	Bedford
24	10-6-65	0.19	Pt. Mugu
25	10-7-65	0.24	Pt. Mugu
26	10-8-65	0.24	Pt. Mugu
27	10-13-65	0.13	Pt. Mugu
28	11-3-65	0.14	Pt. Mugu
29	11-10-65	0.25	Pt. Mugu
30	12-1-65	0.14	Pt. Mugu
31	12-1-65	0.14	Tallahassee

rather than two (as plotted in Figure 7). This one day would then correspond to 0.2 percent of the total sample of days -- in correspondence to our observations over the U.S. (Reiter, 1976b).

Even though we have not yet carried out an isentropic trajectory analysis for this case, we are convinced that we are faced with a massive stratospheric air intrusion because: (a) Cosmogenic beryllium^7 (Be^7) concentrations rose significantly during that period (Table 5); (b) a cold front, associated

with a strong northwesterly jet stream, passed before the rise in O_3 concentrations.

TABLE 4. HOURLY OZONE CONCENTRATIONS (ppb), ZUGSPITZE (GERMANY) ON JANUARY 8 AND 9, 1975

January 8				January 9			
Time (hr.)	ppb	Time (hr.)	ppb	Time (hr.)	ppb	Time (hr.)	ppb
1	25.82	13	42.88	1	158.89	13	32.12
2	27.28	14	50.81	2	170.36	14	32.22
3	27.94	15	62.21	3	171.44	15	25.61
4	30.08	16	52.92	4	159.78	16	25.18
5	31.30	17	52.06	5	81.33	17	24.88
6	30.93	18	54.83	6	28.50	18	22.37
7	28.07	19	57.03	7	25.33	19	22.39
8	27.37	20	62.80	8	27.79	20	19.84
9	26.91	21	79.85	9	30.31	21	19.10
10	27.69	22	114.10	10	30.71	22	17.92
11	37.78	23	157.74	11	31.43	23	16.89
12	47.88	24	197.55	12	31.82	24	17.17

TABLE 5. THE DAILY AVERAGE Be^7 CONCENTRATIONS MEASURED AT ZUGSPITZE

7 January 1975	1.33 pc/m3	13 January 1975	14.60 pc/m3
8 January 1975	4.99 pc/m3	14 January 1975	11.84 pc/m3
9 January 1975	10.35 pc/m3	15 January 1975	15.29 pc/m3
10 January 1975	13.79 pc/m3	16 January 1975	7.10 pc/m3
11 January 1975	11.17 pc/m3	17 January 1975	5.71 pc/m3
12 January 1975	11.66 pc/m3	18 January 1975	2.98 pc/m3

Peculiar about this event are the excessive values of hourly O_3 concentrations. Rises in Be^7 concentrations and jet stream-associated stratospheric air intrusions were also involved in the statistical distribution shown in

Figure 7 without exceeding the maximum allowable hourly O_3 concentration value (Reiter, 1976b). The answer to this puzzle is given in Figure 8, showing the 100-mb surface of January 7, 1975, 00 GMT. The center of gravity of the stratospheric polar vortex, according to this map, lies over Europe in a rather anomalous position. It began to establish itself in this position on January 6. Sinking motions in the middle and lower stratosphere to the rear of the European trough helped to establish a low-stratospheric ozone reservoir with well above average concentration values. This reservoir was tapped by a typical stratospheric extrusion process.

We are convinced, therefore, that the departure of the two data points with excessive O_3 maxima in Figure 7 from the rest of the statistical distribution is not so much due to the peculiar absence of mixing in the troposphere, but to an anomalous behavior of the stratospheric circulation and to the establishment of an excessively strong ozone reservoir in the lower stratosphere.

We still will have to allow for the fact that the O_3 concentrations described above were measured at an elevation of 3000 m above M.S.L., i.e. above the normal height of the PBL. Mixing processes within the PBL should reduce these concentrations considerably, perhaps by as much as a factor of two.

CONCLUSIONS

The foregoing discussion shows that the maximum allowable hourly O_3 concentration of 74.7 ppb can be exceeded on occasion in the cyclogenetically active regions of middle latitudes, and especially under favorable trough positions in the stratospheric vortex. Such excessive concentrations in these regions have a probability of approximately 0.2 percent, measured in days of observations on an annual basis.

It is also apparent that natural background levels of stratospheric ozone in the lower troposphere can fluctuate considerably, and can reach 20%, perhaps 50% of the maximum allowable hourly level considerably more often (see Figure 7). Relatively small additions of anthropogenic O_3, under such conditions, will lead to ambient O_3 concentrations above 74.7 ppb.

ACKNOWLEDGEMENTS

The research reported in this paper was supported by an Environmental Protection Agency grant to Stanford Research Institute.

REFERENCES

Dütsch, H.U., 1971: Photochemistry of atmospheric ozone. Advances in Geophysics, 15, 219-322.

Fabian, P. and C.E. Junge, 1970: Global rate of ozone destruction at the earth's surface. Arch. Meteor. Geoph. Bioklim., Ser. A, 19(2), 161-172.

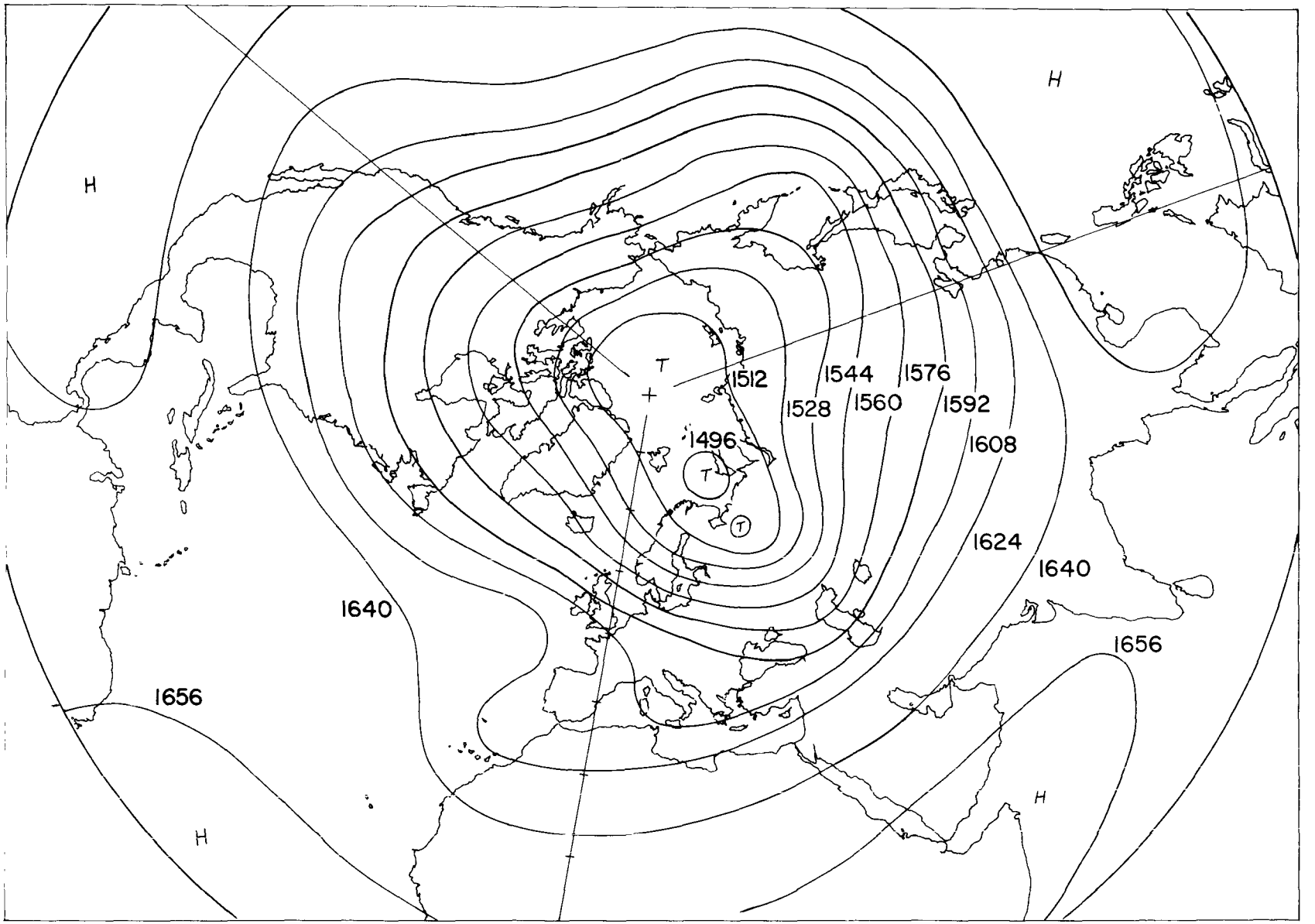

Figure 8. 100-mb map, 7 January, 1975, 00 GMT. (Taeglicher Wetterbericht, Deutscher Wetterdienst, Offenbach).

Hering, W.S., 1964: Ozonesonde observations over North America, Vol. 1. Report AFCRL-64-30(I), pp. 1-512, Air Force Cambridge Research Laboratories.

_____, and T.R. Borden, Jr., 1964: Ozonesonde observations over North America, Vol. 2. Report AFCRL-64-30(II), Air Force Cambridge Research Laboratories.

_____, and T.R. Borden, Jr., 1965a: Ozonesonde observations over North America, Vol. 3. Report AFCRL-64-30(III), Air Force Cambridge Research Laboratories.

_____, and T.R. Borden, Jr., 1965b: Mean distribution of ozone density over North America, 1963-1964. Report AFCRL-65-913, Air Force Cambridge Research Laboratories.

_____, and T.R. Borden, Jr., 1967: Ozonesonde observations over North America, Vol. 4. Report AFCRL-64-30(IV), Air Force Cambridge Research Laboratories.

Junge, C.E., 1962: Global ozone budget and exchange between stratosphere and troposphere. Tellus, 14(4), 363-377.

_____, 1963: Studies of global exchange processes in the atmosphere by natural and artificial tracers. J. Geophys. Res., 68(13), 3849-3856.

Lovill, J.E., 1972: The global distribution of total ozone as determined by the NIMBUS III Satellite Infrared Interferometer Spectrometer. Colorado State University, Ft. Collins, Colorado, Ph.D. Dissertation, 72 pp.

Regener, V.H. and L. Aldaz, 1969: Turbulent transport near the ground as determined from measurements of the ozone flux and the ozone gradient. J. Geophys. Res., 74(28), 6935-6942.

Reiter, E.R., 1972: Atmospheric transport processes, Part 3: Hydrodynamic tracers. U.S. Atomic Energy Commission, TID-25731, 212 pp.

_____, 1975a: Stratospheric-tropospheric exchange processes. Reviews of Geophysics and Space Physics, 13(4), 459-474.

_____, 1975b: The transport of radioactive debris and ozone from the stratosphere to the ground. Report to Stanford Research Institute, 22 November 1975, 36 pp.

_____, 1976a: Ozone concentrations in the lower troposphere as revealed by ozonesonde observations. Report to Stanford Research Institute, 24 March 1976, 106 pp.

_____, 1976b: Lower-tropospheric ozone in excess of Federal maximum value. Report to Stanford Research Institute, 28 June 1976, 39 pp.

_____, E. Bauer and S.C. Coroniti, 1975: The natural stratosphere 1974. CIAP Monograph No. 1, U.S. Department of Transportation.

Seitz, H., B. Davidson, J.P. Friend and H. W. Feely, 1968: Final report on Project Streak. Numerical models of transport, diffusion and fallout of stratospheric material. Isotopes, Inc., Westwood, New Jersey, Report No. NYO-3654-4, 97 pp.

Singh, H.B., W.B. Johnson and E.R. Reiter, 1975: The relation of oxidant levels to meteorochemical processes: A review of available research results and monitoring data. Stanford Research Institute: Interim Report, SRI Project 4432, 119 pp.

SESSION 9

THEORIES ON RURAL OZONE/OXIDATES

Chairman: B. Dimitriades
Environmental Protection Agency

RESEARCH TRIANGLE INSTITUTE STUDIES OF HIGH OZONE CONCENTRATIONS IN NONURBAN AREAS

L. A. Ripperton, J. J. B. Worth, F. M. Vukovich, and C. E. Decker*

ABSTRACT

The Research Triangle Institute has conducted field studies from 1970 through the summer of 1975 under sponsorship of the Environmental Protection Agency to help characterize the phenomonen of high rural ozone concentrations. The most significant results of these programs include the following: (a) As high pressure systems move across the U. S. from West to East, high ozone concentrations in a high pressure system are found in an area of approximately 60,000 sq. mi. and are associated with increasing population density; (b) the high ozone concentrations were found to occur on the trailing side of the high pressure system; (c) theoretical studies indicated that air in the leading edge of a high pressure system had been in the high pressure system a day or less, whereas the air on the trailing side of the high pressure system had been there two to six days; and, (d) the air that had been in the system longer had more time to accumulate ozone precursors and to allow reaction of less reactive alkanes.

BACKGROUND

Since the mid-1960's, hourly average ozone concentrations in excess of the National Ambient Air Quality Standard (NAAQS) for photochemical oxidants have been reported in areas previously thought to be remote and pollution free, and reached values of 0.1 ppm or greater (1, 2, 3, 4,5). An exhaustive survey of historical data has not been performed but the data presented by Junge provided substantial evidence that concentrations of 0.1 ppm had not occurred in rural areas as of the time of writing (1963) (6).

In the early days of the investigation of high rural ozone (O_3) a number of controversies arose. Considerable differences of opinion exist regarding the origin of these high concentrations of ozone in rural and semirural areas. One opinion was that ozone in the rural areas did not come from urban areas because ozone could not survive long distances of transport without destruction. Another was that synthesis of ozone did not occur in rural areas near the ground in classical smog reactions because oxides of nitrogen concentrations were too low to support such synthesis. Another opinion supported the thesis that this ozone descended from the stratosphere. One difficulty

*Research Triangle Institute, Research Triangle Park, North Carolina.

in the understanding of the chemistry of ozone generation in nonurban atmospheres is the paucity of oxides of nitrogen (NO_x) found there. Most of the NO_x measurements that have been made in the rural field studies have been in the noise level of the instrumentation available, around 0.005 ppm. Nevertheless, on second and third days of continuous smog chamber runs at RTI, NO_x concentrations of this level have produced ozone concentrations in excess of the NAAQS (7).

In the summers of 1970 (1), 1972 (2), 1973 (3), 1974 (4), 1975 (8), and 1976 (9), Research Triangle Institute (RTI) conducted field studies, under Environmental Protection Agency (EPA) sponsorship, that have helped characterize the phenomenon of high nonurban concentrations of ozone.

Some investigators have data indicating massive intrusion of stratospheric ozone into the troposphere, but the bulk of evidence obtained by RTI in these investigations favors the generation of ozone from anthropogenic precursors and the transport of this ozone and its precursors from a few miles to a few hundred miles in the lower levels of the troposphere. The following technical report describes the findings of the six previous summer studies conducted by RTI and subsequent conclusions drawn from these data.

FIELD STUDIES

In 1970, in response to an air pollution incident at and near Mt. Storm, West Virginia, RTI measured ozone concentrations of several hours duration that exceeded 0.1 ppm using a chemiluminescent (Rhodamine B) instrument (1). In the summer of 1972, RTI conducted a study of atmospheric ozone near Mt. Storm in Garrett County, Maryland, and Preston County, West Virginia. The 1972 study confirmed the earlier reports of high ozone concentrations; approximately 11 percent of 1,043 hourly measurements made at the Garrett County, Maryland Airport during the summer of 1972 exceeded the NAAQS. Similar findings were obtained at satellite locations around the base station at a radius of approximately 19 kilometers. Analysis of synoptic meteorological data, as well as an examination of ozone wind roses for the Garrett County Maryland Airport led to a hypothesis that the high ozone concentrations at this location developed within particular air masses that acquired and maintained their characteristics over broad geographic regions (2).

In the summer of 1973, in order to further assess the aerial extent of high rural ozone concentrations, RTI established a network of four monitoring sites for the measurement of ground-level ozone concentrations and conducted airborne measurements of ozone with an instrumented twin-engine aircraft. These four sites were located at or near McHenry, Maryland (Garrett County); Kane, Pennsylvania; Coshocton, Ohio; and Lewisburg, West Virginia. This study confirmed the hypothesis that the high rural ozone concentrations extended over a considerable area. For the summer and early fall of 1973, the NAAQS for photochemical oxidants was exceeded during 15 percent of 1,663 hours at Lewisburg; 37 percent of 1,652 hours at McHenry; 30 percent of 2,131 hours at Kane; and 20 percent of 1,785 hours at Coshocton (3).

In 1974, a study was conducted in Ohio to investigate the relationship between high rural oxidant levels and urban hydrocarbon control strategies.

All data obtained in the 1974 study showed strong evidence for the involvement of anthropogenic precursors and urban effluvia in the generation of the high ozone concentrations in rural areas. As a result of these investigations it was postulated that the high concentrations of ozone (produced by photochemical processes) found in nonurban portions of the area studied are primarily an air mass characteristic and will occur when a slow-moving high atmospheric pressure system passes over the region (4).

In 1975, RTI conducted a study for EPA to further investigate the relationship between high ozone concentration and high pressure systems and to determine the change in the concentration of ozone in the center of a high pressure system, as the system moves from an area of low population density to an area of high population density. Ozone, nitrogen oxides, and hydrocarbon data were collected at ground stations located in Bradford, Pennsylvania, Lewisburg, West Virginia, Creston, Iowa, and Wolf Point, Montana, and from an instrumented aircraft flying specified flight patterns. High ozone concentrations and the frequency of exceeding the NAAQS were found to be associated with high population density and high pressure (8).

In 1976, RTI under EPA sponsorship participated in the flight of DaVinci II, an Energy Research Development Administration (ERDA) sponsored manned balloon-borne experiment conducted in the St. Louis area during early June. Ozone and meteorological variables were monitored from a Lagrangian frame of reference over a twenty-four hour period. Data obtained from the balloon and on the ground indicate that high ozone concentrations (>0.13 ppm) were transported aloft undiminished for several hundreds of miles from an urban area (9).

For various reasons the characterization of high ozone systems in different parts of the country may be different. In this paper, RTI presents a summary of its findings and discusses suppositions with regard to high ozone concentrations in nonurban areas and the relationship between high ozone and high pressure systems, in particular high pressure systems that originate in Canada and the Northern Plans and sweep the area south of the Great Lakes and into the Atlantic Ocean.

RESULTS OF STUDIES

Observational data and theoretical considerations have indicated the following behavior of the diurnal maximum ozone concentrations in rural regions in the midwest and eastern portions of the United States as a high pressure system moves through the region (Figure 1). When the leading edge of a high pressure system passes through a rural region, the diurnal maximum ozone concentration generally begins to lower in value, and a relative minimum value usually occurs before the center of the high pressure system reaches the sampling station. A relative maximum value of the diurnal maximum ozone concentration is found on the back side of the high pressure system. It has been hypothesized that this distribution is related to the residence time of air in the high pressure system. Generally, the residence time is larger on the back side of that system (Figure 2). This allows time for air parcels to obtain large or critical concentration of ozone precursors, time for the generation of ozone from much less active precursors, and time for the accu-

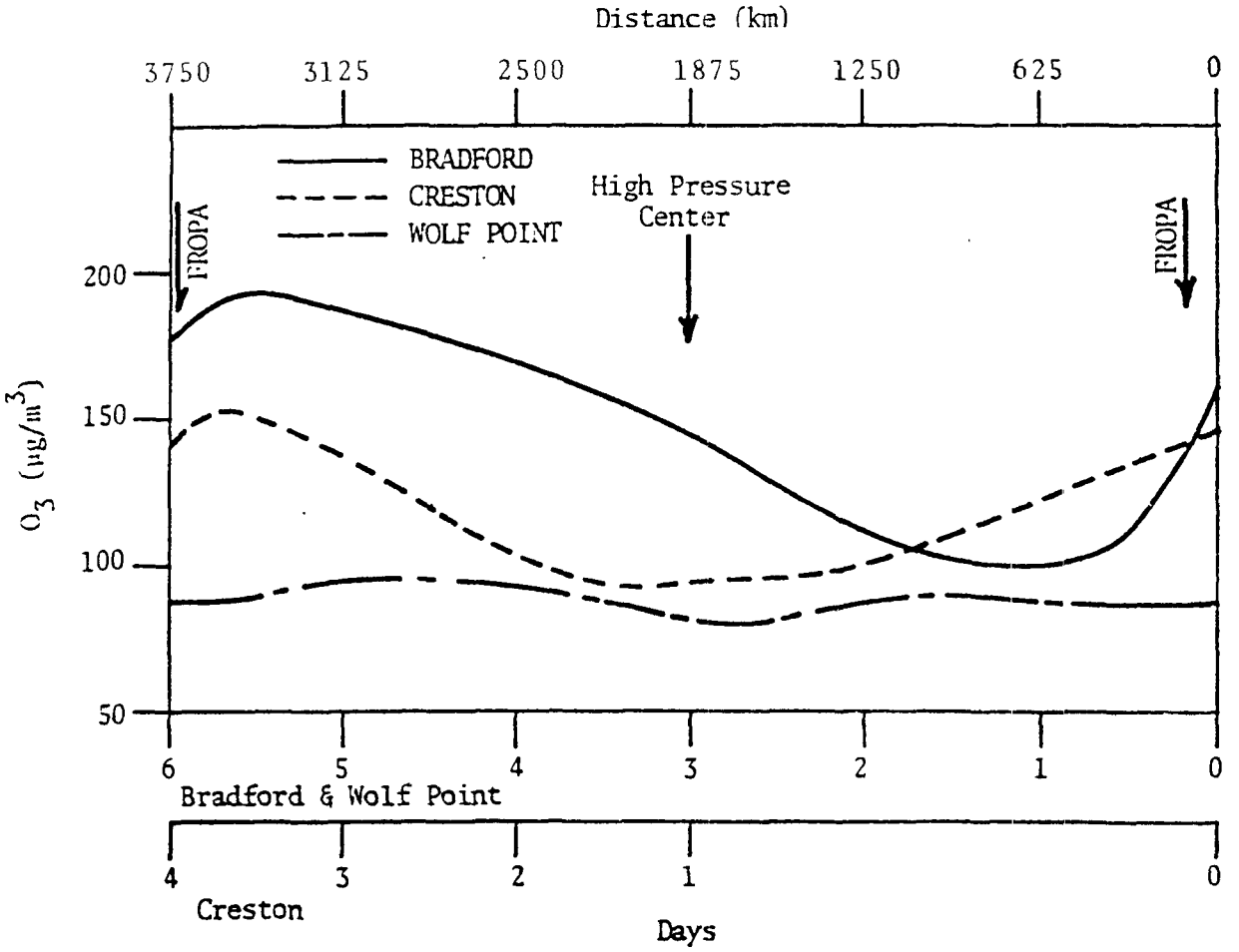

Figure 1. The temporal and spatial variations of the diurnal maximum ozone concentrations through a moving high pressure system based on the 1975 data at Wolf Point, Montana; Creston, Iowa; and Bradford, Pennsylvania.

mulation of ozone. Because of the difficulty of measuring low concentrations of NO_x and other precursors, this hypothesis has not been substantiated. It is suggested that the low concentration of NO_x that apparently exist in rural boundary layers is a result of rapid gas phase chemical reactions.

In the summer of 1975, the ozone concentration at Wolf Point, Montana, which was the western-most station in the 1975 array and in the Northern Plains never exceeded the NAAQS. Furthermore, Figure 1 shows that the diurnal maximum ozone concentration did not behave similarly to that found for stations further east; that is, the ozone concentration on the back side of the high was not a relative maximum. When the high pressure system reached Creston, Iowa, low concentrations of ozone were found on the eastern portion of the high pressure system and high concentrations on the back part of that system. This distributional characteristic of ozone in high pressure systems was most highly developed when the system reached Bradford, Pennsylvania (4).

There are two or three mechanisms that may be responsible for high ozone

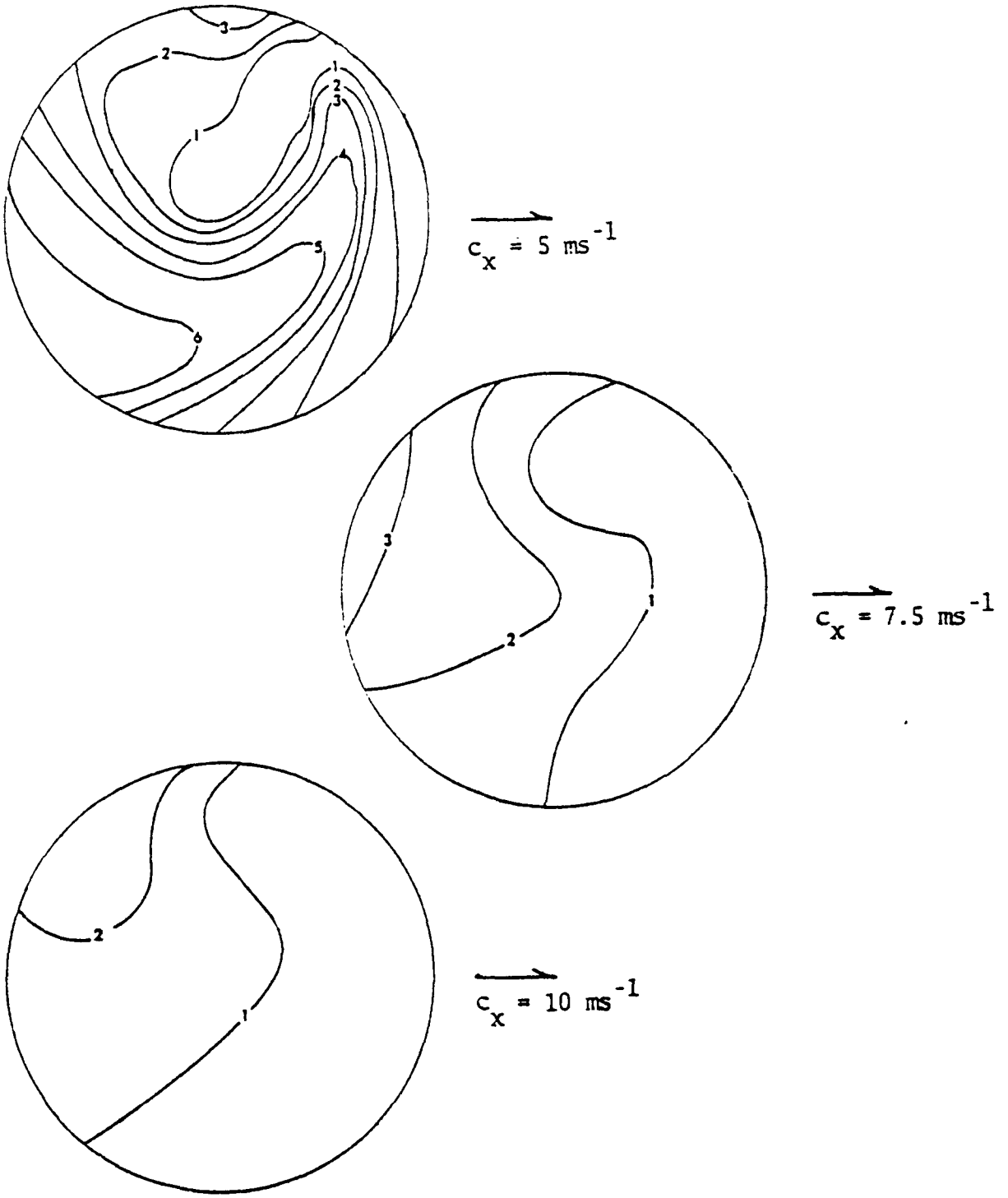

Figure 2. Hypothetical distribution of air parcel residence time (days) in a circular high pressure system versus system speed.

concentrations in rural regions associated with high pressure systems. One mechanism is synthesis. Another is vertical transport. And still another is horizontal transport. Theory and trajectory analyses suggest that within a high pressure system it is quite possible for air, although it moves slowly and without strong directional influence, to travel 400 miles within a 24-hour period. Data from the DaVinci II experiment have suggested that air reaching ozone concentrations of 0.13 to 0.14 ppm by late afternoon over the city of St. Louis was transported almost undiminished 150 miles across the State of Illinois into Indiana (Figure 3). The ozone concentrations in the air aloft remained at essentially the same concentrations; whereas, the air at the ground that was being monitored by a mobile van that kept the balloon in sight, behaved in the usual surface diurnal fashion and reached lower values at night. At the beginning of the next daylight period, the ozone concentration began to rise. This mechanism is believed to behave in the following manner.

In the rural region, air is mixed during the day through great depths. Throughout the mixing depth, the ozone concentration is generally homogenous. At night, when the nocturnal inversion is produced near the ground, the ozone concentration near the surface is reduced by gas phase destruction and by contact with the surface of the earth. The nocturnal inversion will prevent destructive agents from being injected into the layer above. Therefore, the ozone concentration in this layer will remain undepleted and will maintain itself overnight as is suggested by the data shown in Figure 3. Thus, a diurnal variation of ozone will be found in the surface layer whereas little or no diurnal variation will be found in the layer above the nocturnal inversion.

After sunrise two processes occur that cause that cause the increase in ozone near the surface. Solar and sensible heating erode the nocturnal inversion allowing air containing higher concentrations of ozone aloft to be mixed to the surface. Furthermore, the air in the surface layer has accumulated large concentrations of ozone precursors that will eventually be used to synthesize ozone. Data are not yet available from the DaVinci II experiment to test this hypothesis with calculations.

Many have attributed high ozone concentrations in rural regions to the near surface transport of so-called fossil ozone. In general, the half-life of ozone at night as indicated by RTI smog chamber studies and by observed data (Table 1) would be around 20 to 30 hours. This would not allow fossil ozone to be responsible for the high concentrations found in rural areas for more than two days without synthesis to maintain these concentrations.

It can be seen in Figure 4, which represents a series of flights made in 1974 at Wilmington, Ohio, that the ozone concentration increased with time through a layer from the surface, 1000 ft. mean sea level (MSL) to approximately the 6000 foot level (MSL). Computations made using these data and available meteorological data during the same period indicated that approximately 50 percent of the increase of ozone at the lower level and in the period 0704 Central Daylight Time (CDT) to 1320 CDT, could be explained by vertical mixing. However, vertical mixing accounts for only 10 percent of the increase between 1320 and 1656 CDT. At 1656 CDT, the vertical gradient is reversed

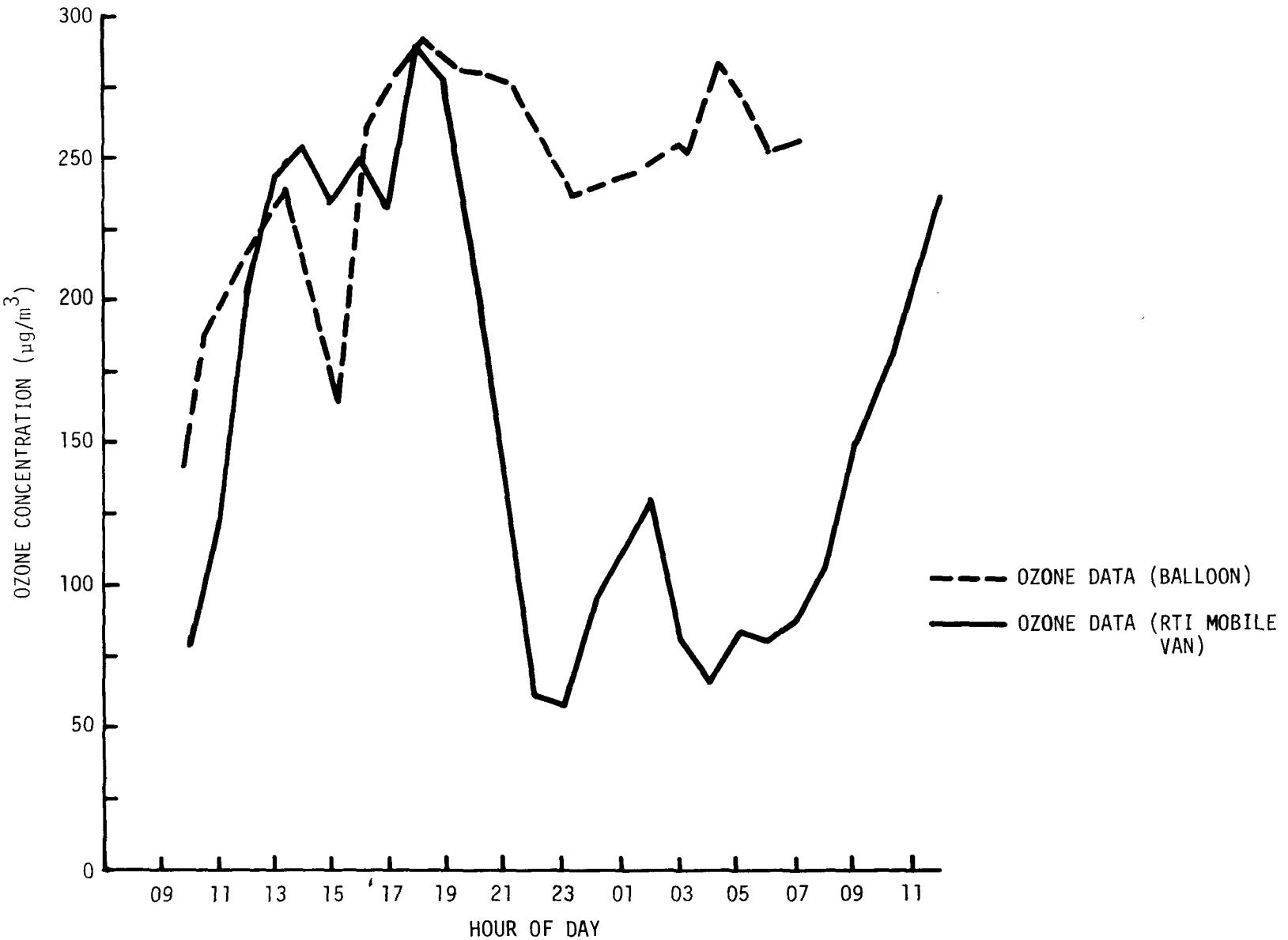

Figure 3. Airborne and ground-level ozone concentrations during the flight of DaVinci II (June 8-9, 1976).

TABLE 1. DARK PHASE OZONE HALF LIFE*

Station	Half-life Mean (hrs)	Std. Dev. (percent)	Range	Case Count
Bradford, Pennsylvania	13.1	15.2	2.8-75.9	65
Creston, Iowa	20.4	28.5	3.4-180.9	60
Wolf Point, Montana	15.4	15.9	3.6-70.7	61

*Half life was calculated using ozone data from the 1975 Summer Oxidant Study from 0200 to 0500, assuming a first order decay rate.

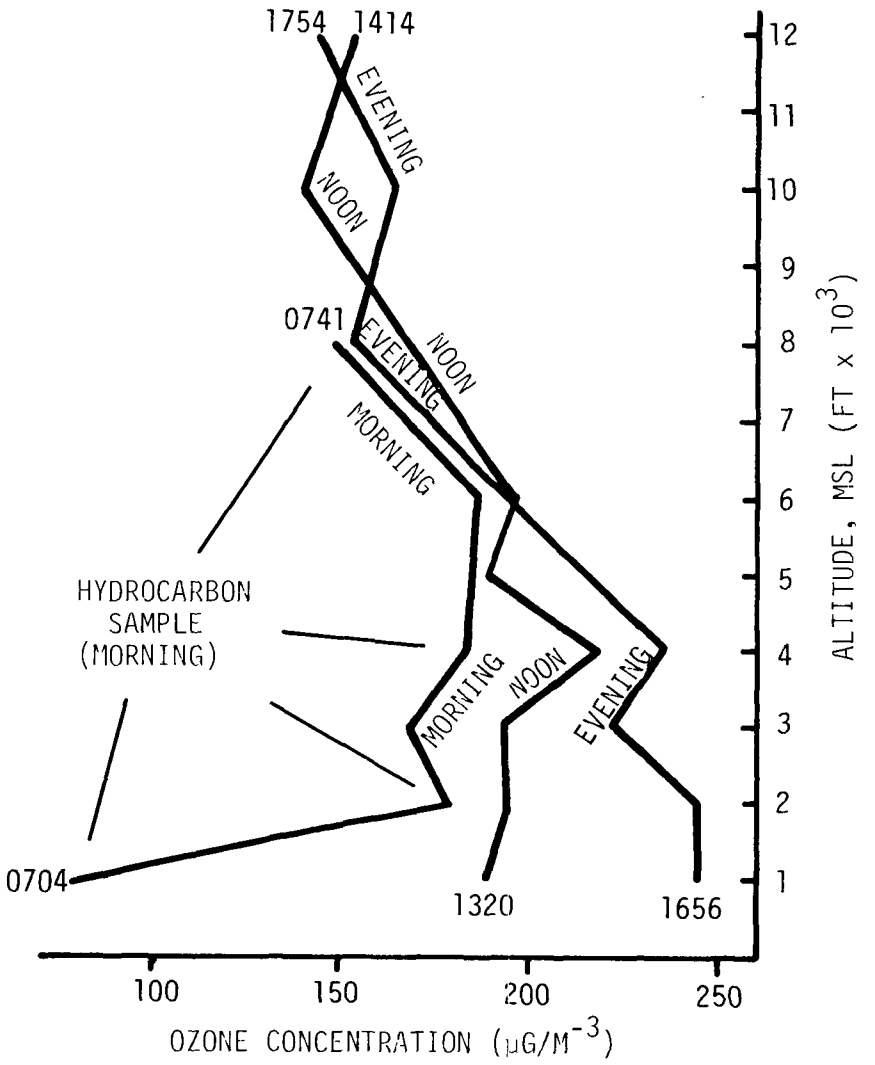

Figure 4. Ozone profile flight, Wilmington, Ohio, August 1, 1974.

such that the lower level is supplying ozone to the upper levels. This suggested that, in this latter case, since vertical mixing could not account for a major portion of the increase in ozone in the lower boundary layer, most of the increase from morning till late afternoon is due to synthesis.

That synthesis plays a part in producing high concentration of ozone in rural areas can be seen by the fact that in many cases rural sites exhibit a higher concentrations of ozone than do nearby urban sites (Table 2 and 3). The data in Figure 3 have suggested that synthesis accounted for most of the increase in ozone at lower levels. It has also been discussed that in the northern part of the United States, the high ozone that is associated with high pressure is found on the back side of an eastward moving high pressure system. This is thought to be due to the fact that as the system moves, air in the front part of the high pressure system has spent insufficient time in that system to accumulate ozone precursors and to be exposed to unimpeded solar radiation. On the back side of the high pressure system, we find air that has spent two to six days in that system. This air has had plenty of time to accumulate ozone precursors and has undergone many diurnal ozone cycles.

As the high pressure system moves east, population density increases and consequently the potential for greater emissions of hydrocarbons and NO_x. The polluted air from the cities injected into the system as it moves eastward will permit the generation of ozone. As has been shown in smog chamber work, an aged system with low concentrations of NO_x will generate high concentrations of ozone (greater than the NAAQS). The most active of the organic precursors, olefins, are also those that are most reactive in destroying ozone. These are reacted rapidly and the less reactive precursors are preserved to react later. The less reactive precursors can generate high ozone concentrations given enough time, and they do not destroy ozone very rapidly. The more aged the system the more favorable the conditions for retaining ozone that it generates.

As a result of the reported studies, the following hypothesis has been established for high ozone in the rural boundary layers in midwestern and eastern portions of the United States. Air parcels in high pressure systems moving from Canada across the Northern Great Plains pick up very little in the way of ozone precursors from the plains. What precursors are injected into the system are natural in origin because there are relatively few anthropogenic sources in this region. As the high pressure system moves further eastward across a line arbitrarily drawn from Fargo, North Dakota to Dallas, Texas, the population, according to the 1970 density map, increases quite rapidly from about ten people per square miles to 103 people per square mile. The accumulation of ozone precursors should increase considerably to the east of this line due to the increased potential for anthropogenic injection. It is doubtful that the rural population itself can contribute enough material to generate the ozone. However, the cities should produce enough precursor material to begin to generate large concentrations of ozone.

Results of these research programs imply that the control of hydrocarbons in any individual city will reduce, but not necessarily prevent, the occurrence of high rural ozone concentrations in excess of the NAAQS at any given rural site. The implication is that the release of hydrocarbons and oxides

TABLE 2. SUMMARY OF OZONE DATA FOR 1973 AND 1974 OXIDANT STUDIES

Station	Year	Type of Station	Average O_3 (ppm)	No. Hours $\geq$ 0.08 ppm	No. Hours	Hours $\geq$ 0.08 ppm (%)
McHenry, MD	1973	Rural	0.074	600	1622	37.0
Kane, PA	1973	Rural	0.065	639	2131	30.0
Coshocton, OH	1973	Rural	0.056	357	1785	20.0
Lewisburg, WV	1973	Rural	0.052	249	1663	15.0
Wilmington, OH	1974	Rural	0.052	259	1751	14.9
McConnelsville, OH	1974	Rural	0.057	262	2011	13.0
Wooster, OH	1974	Rural	0.047	262	1878	14.0
McHenry, MD	1974	Rural	0.057	262	2011	13.0
DuBois, PA	1974	Rural	0.056	341	1667	20.5
Canton, OH	1974	Urban	0.035	148	1829	8.0
Cincinnati, OH	1974	Urban	0.025	54	1548	3.5
Cleveland, OH	1974	Urban	0.031	51	1652	3.0
Columbus, OH	1974	Urban	0.033	113	1935	5.8
Dayton, OH	1974	Urban	0.035	114	1576	7.2
Pittsburgh, PA	1974	Urban	0.028	106	1622	6.5

of nitrogen from anthropogenic or biogenic sources, located in both urban or rural areas, all combine to generate appreciable quantities of ozone over widespread regions.

By the time the high pressure system reached Kansas City, cities have provided sufficient precursors for generation of a high concentration of ozone. Once the ozone system has been generated, anthropogenic effluents provide enough fuel for the process to continue. The denser the population becomes, the greater the amount of precursor material released and the higher the potential for producing large concentrations of ozone becomes. As the so-called city plume moves out, widens and is then added to the material injected from the rural regions and from smaller cities, ozone will be generated in concentration greater than the NAAQS. Eventually, the urban plumes, although they may be undetectable by other means, will have overlapped in such a way that they produced an areawide ozone phenomena.

TABLE 3. SUMMARY OF OZONE DATA FOR 1975 OXIDANT STUDY

Station	Year	Type of Station	Average O_3 (ppm)	No. hours $\geq$ 0.08 ppm	No. Hours	Hours $\geq$ 0.08 ppm (%)
Bradford, PA	1975	Rural	0.040	100	2332	4.3
Lewisburg, WV	1975	Rural	0.038	59	2386	2.5
Creston, IA	1975	Rural	0.035	17	2117	0.8
Wolf Point, MT	1975	Rural	0.028	0	2160	0.0
DeRidder, LA	1975	Rural	0.030	38	2994	1.3
Pittsburgh, PA	1975	Urban	0.030	227	2841	8.0
Columbus, OH	1975	Urban	0.022	43	2885	1.5
Poynette, WI	1975	Rural	0.038	126	2663	4.7
Cedar Rapids, IA	1975	Urban	0.025	6	2781	0.2
Des Moines, IA	1975	Urban	0.036	124	2528	4.9
Omaha, NB	1975	Urban	0.035	64	1787	3.6
Nederland, TX	1975	Urban	0.027	138	2714	5.1
Port O'Connor, TX	1975	Rural	0.027	99	2912	3.4
Austin, TX	1975	Urban	0.025	19	2504	0.8
Houston, TX	1975	Urban	0.026	141	2104	6.7

CONCLUSIONS

Some of the most significant conclusions of the RTI Summer Studies are the following. As high pressure systems moves across the United States, high ozone concentrations found in that system are associated with high population density. The data indicate that high concentrations of ozone observed at rural locations are generated in the lower troposphere. The air on the back side of an eastward-moving high pressure system experiences longer residence time than air in the leading edge of that system. Generally, high ozone is found on the back side of high pressure systems.

An areawide system (a radius of 225 miles or more) of high ozone concentrations can exist in which most features suggestive of a precursor origin have been smoothed out. However, a short range urban influence on both hydrocarbon and ozone concentration can be observed. The evidence indicates an observable urban influence extending as far as 150 miles downwind of the city.

Transport of fossil ozone can occur for several hundred miles. The delivery of high concentrations of ozone to rural sites depends on both the movement of so-called fossil ozone and the synthesis of fresh ozone from systems containing low concentrations of NO_x and hydrocarbons that are mainly alkanes and aromatics.

REFERENCES

1. Richter, H. G. Special Ozone and Oxidant Measurement in the Vicinity of Mt. Storm, West Virginia. Research Triangle Institute. Task Report, Task No. 3. NAPCA Contract No. 70-147, 1975.

2. Research Triangle Institute. Investigation of High Ozone Concentration in the Vicinity of Garrett County, Maryland, and Preston County, West Virginia. Issued as Environmental Protection Agency Report No. EPA-R4-73-019.

3. Research Triangle Institute. Investigation of Ozone and Ozone Precursor Concentrations at Non-Urban Locations in the Eastern United States, Phase I. Issued as Environmental Protection Agency Report No. EPA-450/3-74-034, May 1974.

4. Research Triangle Institute. Investigation of Rural Oxidant Levels as Related to Urban Hydrocarbon Control Strategies. Issued as Environmental Protection Agency Report No. EPA-450/3-75-035, March 1975.

5. Stasiuk, W. N. and P. E. Coffey. Rural and Urban Ozone Relationships in New York State, J.A.P.C.A., 24, 1974. pp. 564-568.

6. Junge, C. E. Air Chemistry and Radioactivity. Academic Press, New York, 1963. pp. 37-59.

7. Research Triangle Institute. Oxidant Precursor Relations Under Pollutant Transport Conditions. Final Report. Environmental Protection Agency Contract 68-02-1296, May 1976.

8. Research Triangle Institute. Study of the Formation and Transport of Ambient Oxidants in the Western Gulf Coast and Northcentral and Northeast Regions of the United States. Final Report. Environmental Protection Agency Contract No. 68-02-2048, August 1976.

9. Research Triangle Institute. Ambient Monitoring Aloft of Ozone and Precursors in the Vicinity of and Downwind of a City. Interim Report. Environmental Protection Agency Contract No. 68-02-2391, July 1976.

IMPORTANT FACTORS AFFECTING RURAL OZONE CONCENTRATION

F.L. Ludwig, W.B. Johnson, R.E. Ruff and H.B. Singh*

ABSTRACT

Statistical analyses of 120 air trajectories arriving at four different rural ozone monitoring sites in the eastern United States have been used to identify the emissions and meteorological conditions that are most closely studied by comparing the large-scale spatial distributions of maximum-hour ozone concentrations with corresponding weather patterns. The average air temperature during the last 12 hours of the trajectory was the best single descriptor of ozone concentrations; oxides of nitrogen emissions were significantly correlated with ozone but hydrocarbon emissions were not. The trajectory analyses also showed that ozone concentrations above 80 ppb were most frequently associated with light southwest winds and the absence of precipitation. The corresponding weather patterns are the warm air side of fronts and the western parts of anticyclones. In general, the studies showed violations of oxidant standards to extend over areas larger than the typical air quality control region, suggesting the necessity of revisions in the present control philosophies.

INTRODUCTION

The adoption of ambient air quality standards (AQS) brings with it some corollary concepts. The first of these is the air quality control plan. This is a concert of actions that will ensure that air quality will not violate the established standards. In practice, these control plans have been formulated for limited geographical regions under the assumption that the consequences of control measures--and conversely, of uncontrolled emissions--are quite limited in area.

Figure 1 shows the air quality control regions (AQCR) into which the eastern United States has been divided. Observations of high ozone concentrations in rural areas have raised the possibility that the consequences of pollutant emissions might be much more widespread than originally assumed when AQCRs were defined. Figure 2 shows the distribution of maximum-hour ozone concentrations in the eastern United States for May 22 1974. The shaded areas show where the federal standard of 80 ppb was exceeded. It is

*Stanford Research Institute, Menlo Park, California.

immediately apparent that the AQS are exceeded over areas that are much larger than the typical air quality control region. There are at least two possibilities for the widespread occurrence of high ozone levels:

- There are large-scale natural processes producing high ozone concentrations.
- The effects of man-made emissions are much more pervasive than originally thought.

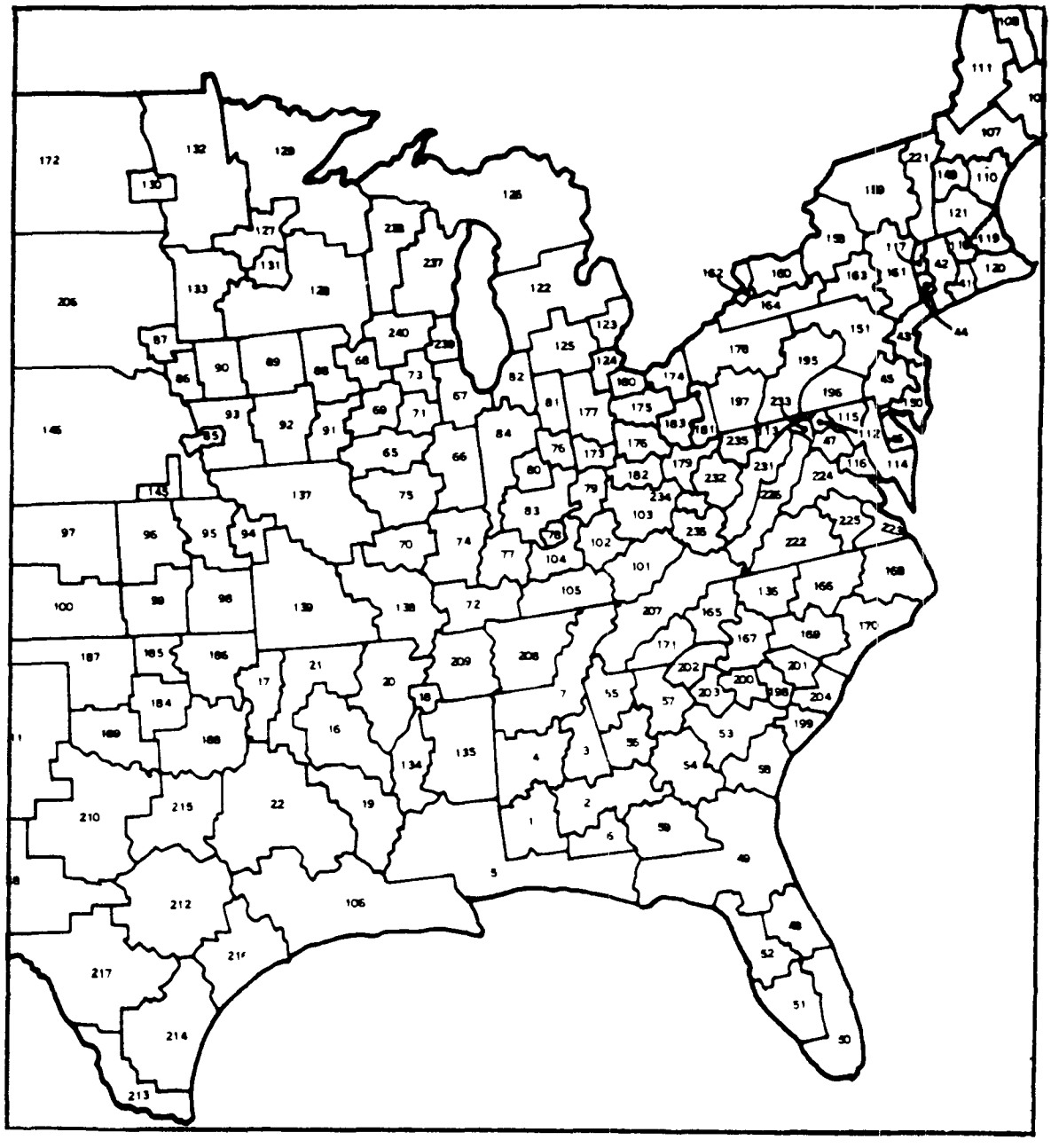

Figure 1. Federal Air Quality Control Regions

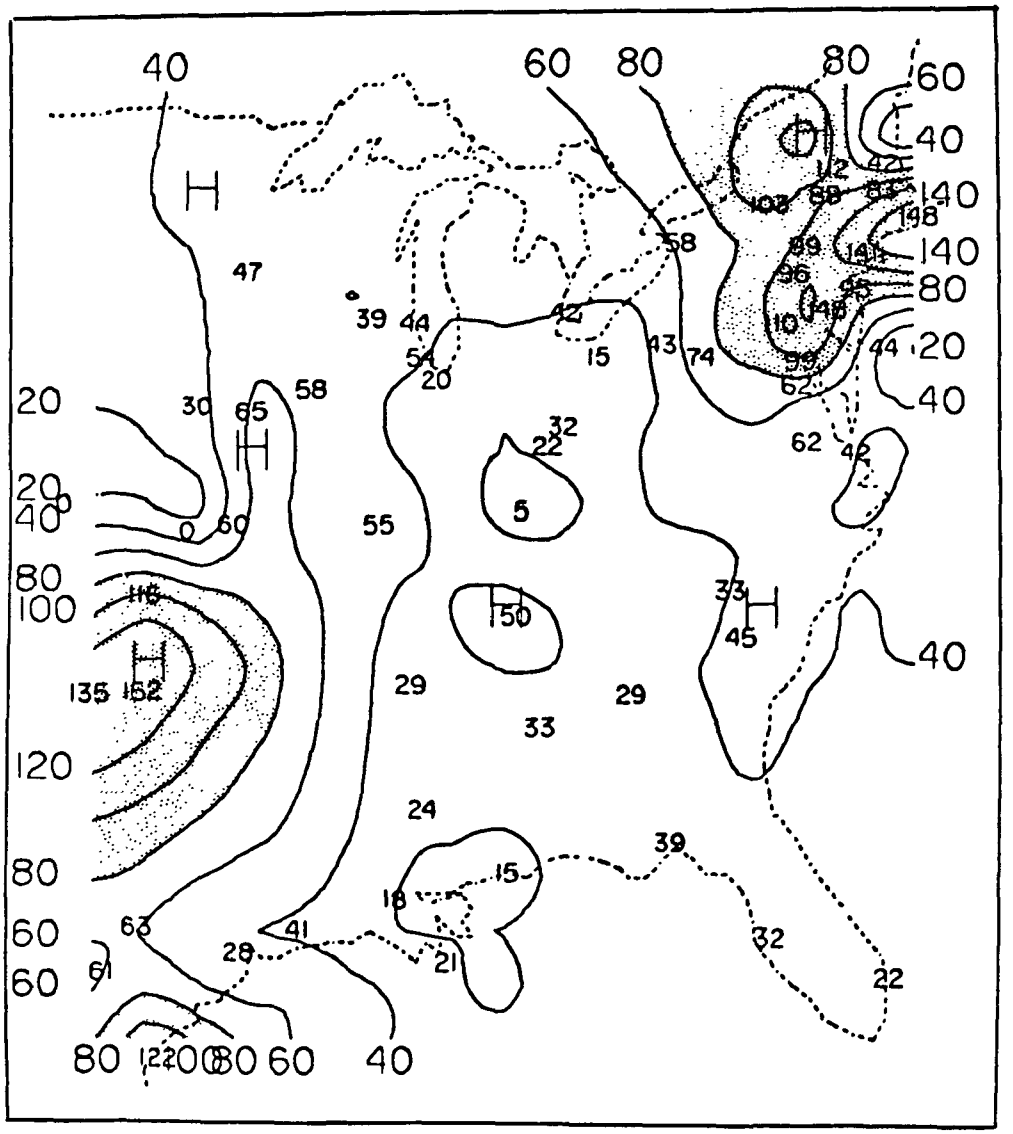

Figure 2. Distribution of maximum-hour O_3 concentrations for the eastern United States for 22 May 1974.

Both these possibilities have important consequences in the formulation and execution of emission control policies. This paper summarizes recent studies of the importance to the above explanations (Ludwig et al, 1976), with emphasis on the second explanation. This paper addresses two facets of the problem:

- The effects of meteorological conditions and emissions within the mixing layer on subsequent formation of ozone.
- The relationships between large-scale ozone patterns and synoptic weather features.

METHODS

A statistical approach was used to determine what tropospheric factors are important to ozone formation in rural areas. Four rural monitoring sites were chosen for study:

- McHenry, Maryland
- Queeny, Missouri
- Wooster, Ohio
- Yellowstone Lake, Wisconsin.

Thirty cases were chosen for analysis from the data collected at each of these stations during the summer of 1974. The emphasis was placed on cases with high ozone (O_3) readings. Fifteen cases were chosen for each site from among the days whose high-hour O_3 concentration was in the upper 20 percentile of the 1975 summer high-hour observations for that site. The remaining 15 cases for each site were split between days when the O_3 concentrations were among the bottom 20 percentile and days with near-median maximum hourly concentrations.

Once the 120 cases had been chosen, air trajectories were calculated by applying Heffter and Taylor's (1975) methods to the available rawinsonde and pilot balloon data. The resulting trajectories were then used to determine the air's history during the 60 hours preceding the observation. The air trajectories were plotted on maps provided by the Environmental Protection Agency (EPA) that show average annual emission densities of oxides of nitrogen (NO_x) and nonmethane hydrocarbons (NMHC) for each U.S. county. From these the emissions encountered were estimated for different segments of the trajectory; the average emission rates were corrected to account for the time of day and diurnal emission cycles.

The trajectories were also plotted on three-hour weather maps* to determine the weather prevailing at different times. The weather information was used to estimate the following factors suspected to be important to the production of ozone:

- Temperature
- Relative humidity
- Dewpoint
- Insolation
- Precipitation

---

*National Weather Service Synoptic Analyses are available from the National Climatic Center, Asheville, North Carolina.

- Atmospheric stability.

Temperature and dewpoint can be estimated directly from the weather maps and they can be used to derive relative humidity. Other factors have to be derived indirectly. The occurrence of precipitation, its type (e.g., rain, drizzle, and so forth) and a subjective classification of its character and intensity (e.g., continuous moderate, intermittant light, and so forth) are shown on the weather maps. The subjective classifications were assigned numbers approximately proportional to precipitation rates, based on the guidance provided to U.S. Air Force weather observers (U.S. Air Force, 1957). Insolation strength was estimated from cloud cover and solar elevation using a method described by Ludwig and Dabberdt (1972). Stability classification was based on Ludwig and Dabberdt's (1972) modification of Pasquill's (1961) methodology.

Using the Storage and Retrieval of Aerometric Data (SAROAD) data base, the large-scale distribution of maximun-hour ozone concentrations were determined for all 365 days of 1974. Smoothing techniques were used to suppress small-scale variability such as might be found within, and in the immediate vicinity, of cities. The smoothing also suppresses the effects of anomalous or erroneous readings. The maximum hourly average ozone concentrations were determined for each day and for each site. All the measurements taken in a single city were averaged and used as a single measurement representative of the entire city. The available observations were then used to interpolate for grid points, which served as the basis for subsequent isopleth analysis. The O_3 isopleths were then compared with the weather map for the same day (National Oceanic and Atmospheric Administration, 1974). The comparisons were subjective, but were guided by the results of the trajectory studies.

RESULTS

Once the average meteorological factors and emissions were determined for 12-hour segments of each of the 120 trajectories, linear correlations between the ozone concentrations and each of the meteorological and emissions indexes were calculated. In some cases there were important relationships that were not reflected in the linear correlation coefficients. For instance, linear correlation between O_3 concentration and precipitation is not particularly high, but there is an important relationship, as should be evident from the scatter diagram in Figure 3. In this diagram, the joint occurrences of ozone concentrations and precipitations index values are marked by the asterisks; if more than one case had approximately the same values, then the number of cases is shown instead of an asterisk. As noted earlier, the precipitation that occurred along the trajectory during the 12 hours before the observation generally prevents ozone concentrations from rising above 80 ppb. This probably arises from a combination of factors, such as washout of ozone or its precursors, and the concurrent limited sunshine and lower temperatures that are not conducive to ozone formation.

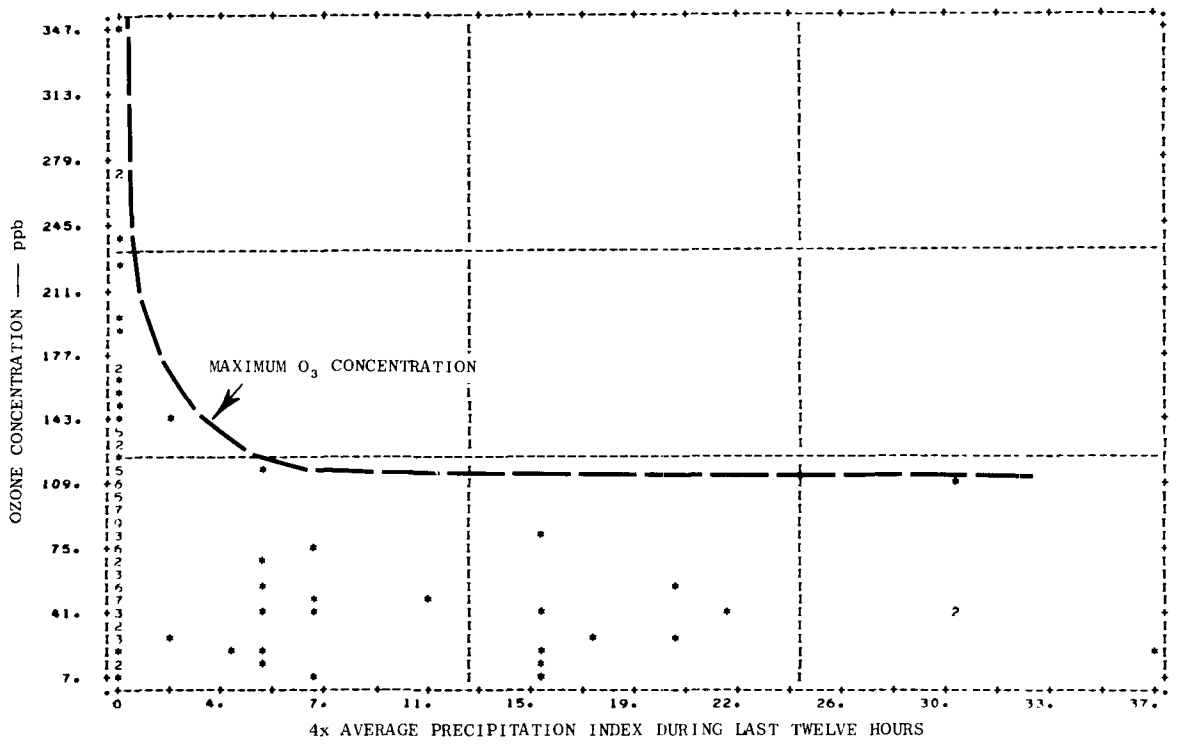

Figure 3. Scatter diagram of ozone concentration versus precipitation index during last 12 hours of trajectory.

Temperature was found to have the greatest linear correlation with observed ozone concentrations. Average temperature along the trajectory during the 12 hours preceeding the observation is especially important, with a linear correlation of 0.54. If temperature is used in a regression equation to describe ozone concentrations, the addition of other meteorological variables will not improve the specification very much, but inclusion of the NO_x emissions does help, raising the correlation to about 0.6. The hydrocarbon (HC) emissions are not significantly correlated with ozone concentration.

Several linear regression equations were formed using temperature and two emissions indexes (e.g., NO_x and HC during the last 12 hours of the trajectory, NO_x during the last 12 hours and during the preceding day) and NO_x and HC emissions throughout the preceding days weighted to emphasize the more recent emissions. There is little to choose among the different combinations; all achieved linear correlations with O_3 of about 0.6 and standard errors of estimate around 47 ppb.

However, it was apparent from scatterframs of observed ozone versus the values calculated from the regression that ozone concentrations greater than about 80 ppb had a different, and stronger, relationship with the predictors than do the lower concentrations. For this reason, separate regression equations were derived for those cases where the observed O_3 was less than 80 ppb and for those cases with higher values. Figure 4 illustrates the results of two such "piecewise" regressions. In

both cases, the temperature and emissions during the last 12 hours of the trajectory were used to predict the cases with $O_3 < 80$ ppb. The same variables were used in Figure 4a to predict the higher o ozone values; for Figure 4b the temperature was replaced with measures of insolation during the preceding 24 hours. The two-part regressions achieve correlations of about 0.8 between observed and estimated ozone concentrations and standard errors of about 35 ppb.

The fact that ozone concentrations can be so well predicted by emissions and meterological conditions to which the air was exposed during the preceding 12 hours does not ensure that events at earlier times are not influential. This is particularly true for air temperature and isolation. If we track the same air for several days, the temperatures and sunshine conditions will tend to be much the same from day to day and the values for one day would serve nearly as well in a linear regression equation as those from the next. The large spatial variability of emissions causes these indexes to be generally independent from one time period to the next. Thus, the fact that NO_x emissions along the air trajectory 24 to 36 hours earlier are significantly correlated with the observed ozone concentrations suggests that the influence of such emissions may presist for a considerable period of time.

For those cases where O_3 concentrations exceeded 80 ppb, the air had generally been within about 450 km of the observing site 12 hours earlier, and within 1150 km 36 hours before. Taken in conjunction with the data that indicate that some influence may presist for 36 hours or more, this suggests that the influence of emissions can be quite widespread.

When ozone concentrations were above 80 ppb, the air had come more often from a direction between south and west than from any of the other quadrants. Thus, when we have relatively high concentrations of ozone in rural areas, the causes for those concentrations are most likely to have occurred during the preceding day or so, and within about 1000 km to the southwest. Obviously, this is not an infalliable generation, but it does provide some guidance that might be useful in the formulation of control strategies. Furthermore, some justification for the generalization is found in the comparisons of large-scale distributions of maximum hourly ozone concentrations in the eastern United States with the concurrent synoptic weather patterns.

The findings of the trajectory studies have their counterparts in the interpretation of the larger scale ozone patterns. The preferred wind directions, the warm temperatures, and the sunny conditions associated with high ozone concentrations are characteristic of certain kinds of meteorological situation, and we might expect to find most areas of high ozone in connection with these meteorological conditions. Similarly, emissions in combination with wind speed and direction influences might be expected to produce some preferred geographical areas for high ozone concentration.

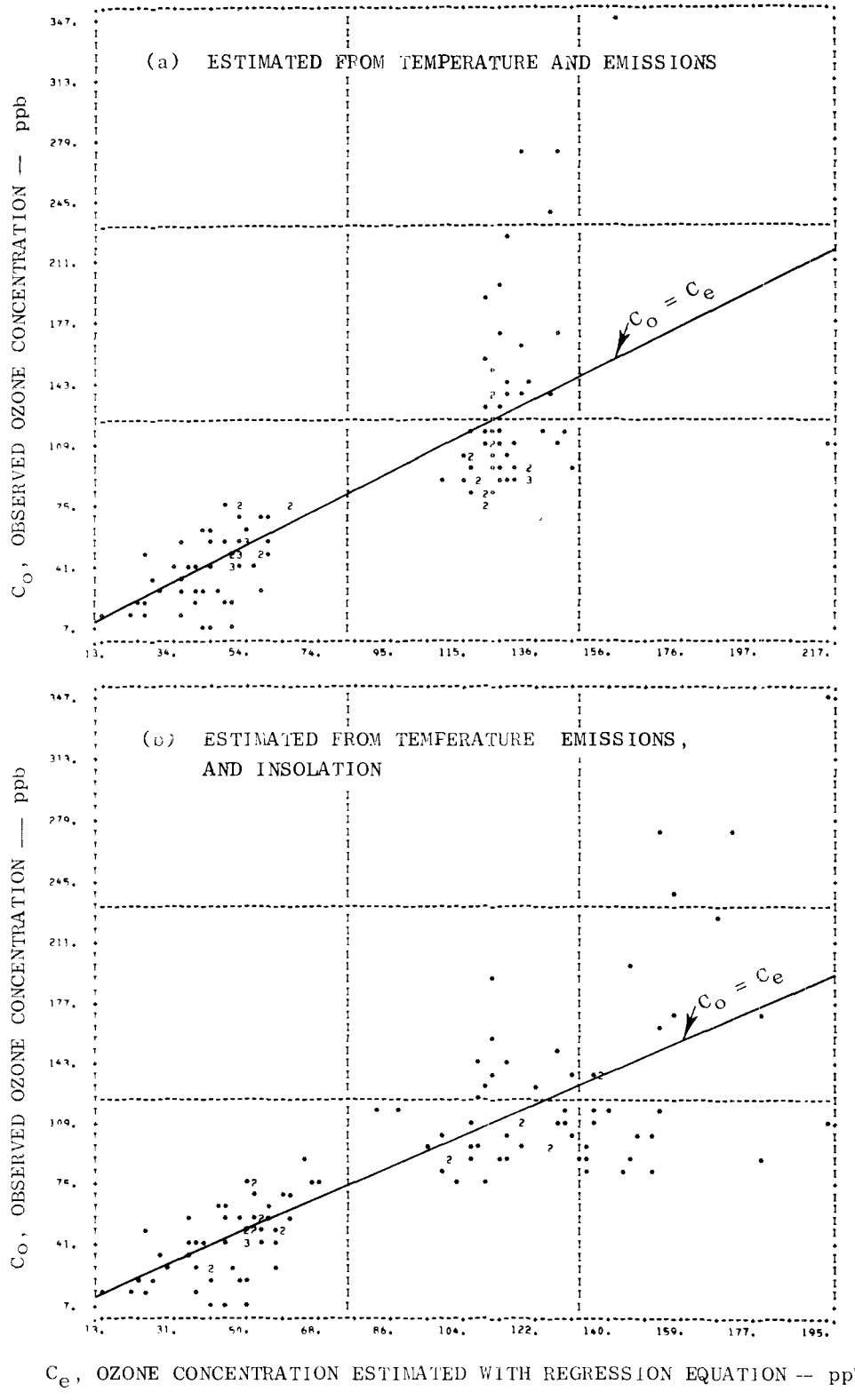

Figure 4. Estimated versus observed O_3 for two regression expressions.

The expected grographical and meteorological relationships have been found. The following geographical areas accounted for nearly all of the 1974 cases where O_3 exceeded 80 ppb:

- New England
- The area southwest of Lakes Erie and Ontario
- The areas south and southwest of Lake Michigan
- The Washington-Philadelphia Corridor
- The St. Louis-Ohio River Valley area
- The Texas-Louisiana Gulf Coast
- The Florida Peninsula
- The western parts of Oklahoma, Kansas, and Nebraska.

All but the last two regions are clearly identified with regions of major anthropogenic emissions. The Florida Peninsula appears to be an area where the frequent occurrence of meteorological conditions favorable to ozone production is more important than the emissions. As yet we have not found a satisfactory explanation for the frequent high ozone concentrations in the western parts of Oklahoma, Kansas, and Nebraska. If the data are all valid, then the following possibilities have to be considered: long-range transport of precursors from Texas, agricultural sources of NO_x, stratospheric ozone brought to the surface by the lee waves of the Rocky Mountains or by frequent cyclogenesis in the area. Figure 5 shows an example of ozone distribution in the eastern United States, with areas of high ozone concentration in several of the regions mentioned above.

The trajectory analyses showed that high ozone concentrations were more likely with warm temperatures, profuse sunshine, and light southwesterly winds. These conditions are associated with the warm air side of weather fronts and the western parts of anticyclones (high-pressure areas). Studies of stratospheric intrusion (e.g. Ludwig et al, 1976) indicate that this phenomenon is most likely behind strong cold fronts, in areas of cyclogenesis, and in the lee waves of large mountain ranges. It has also been found (Ludwig et al., 1976) that squall lines can be sites of stratospheric intrusion. Figure 6 is a schematic representation of the weather patterns that are most likely to be associated with high ozone concentrations in the eastern United States. Figure 7 is an example of the weather patterns and the corresponding distribution of maximum-hour ozone oxidant concentrations in the eastern United States. Figure 7 is an example of the weather patterns and the corresponding distribution of maximum-hour ozone oxidant concentrations in the eastern United States were associated with one of the expected synoptic patterns, especially those involving warm air and light southerly or westerly

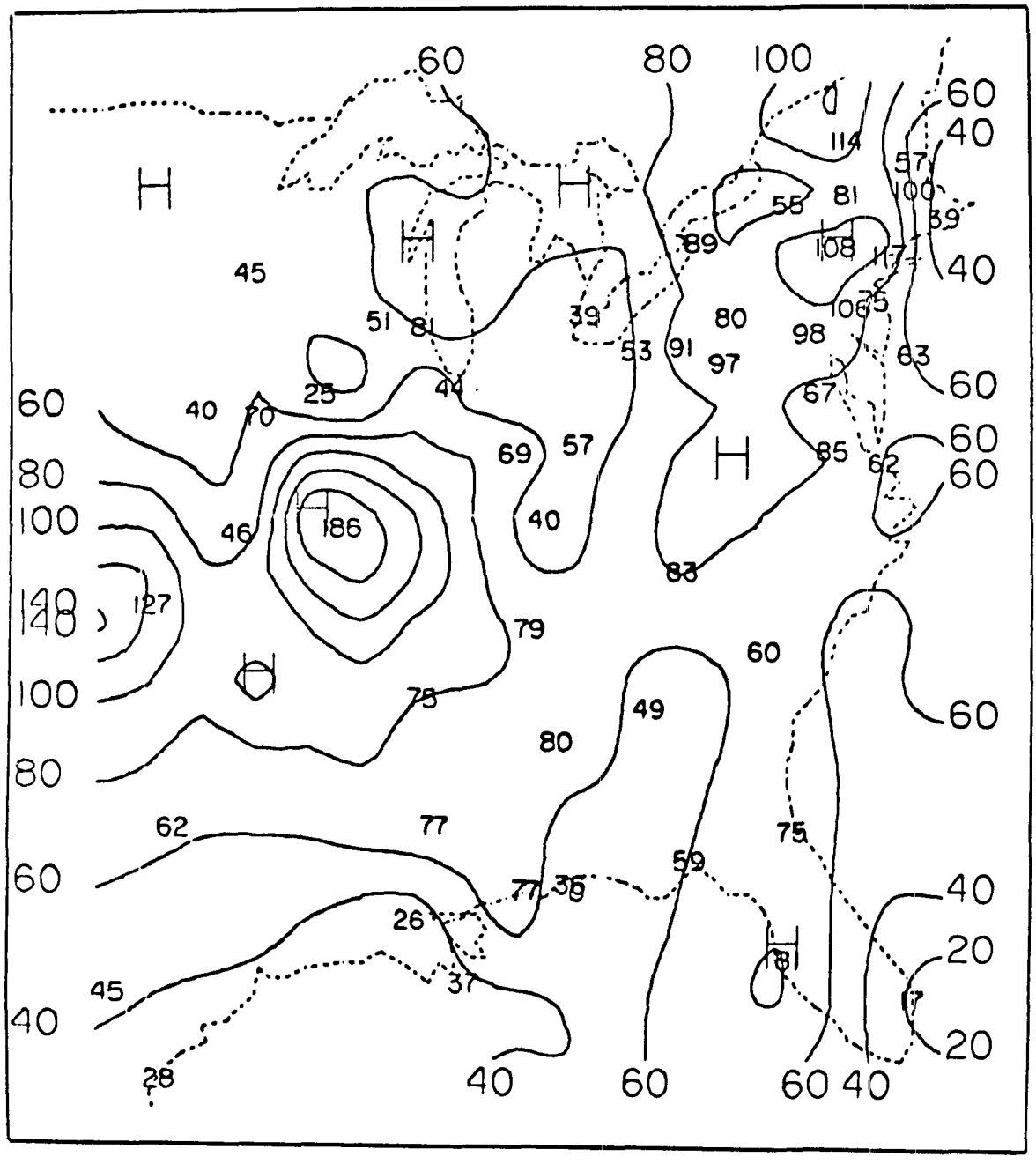

Figure 5. Example of O_3 distribution in the eastern United States on 14 June 1974.

winds.

APPLICATIONS

Some of the findings discussed above have been arrived at by different means elsewhere. The relationships with high pressure areas have been noted before (Envirohmental Protection Agency, 1975) and long-range transport has been demonstrated in several case

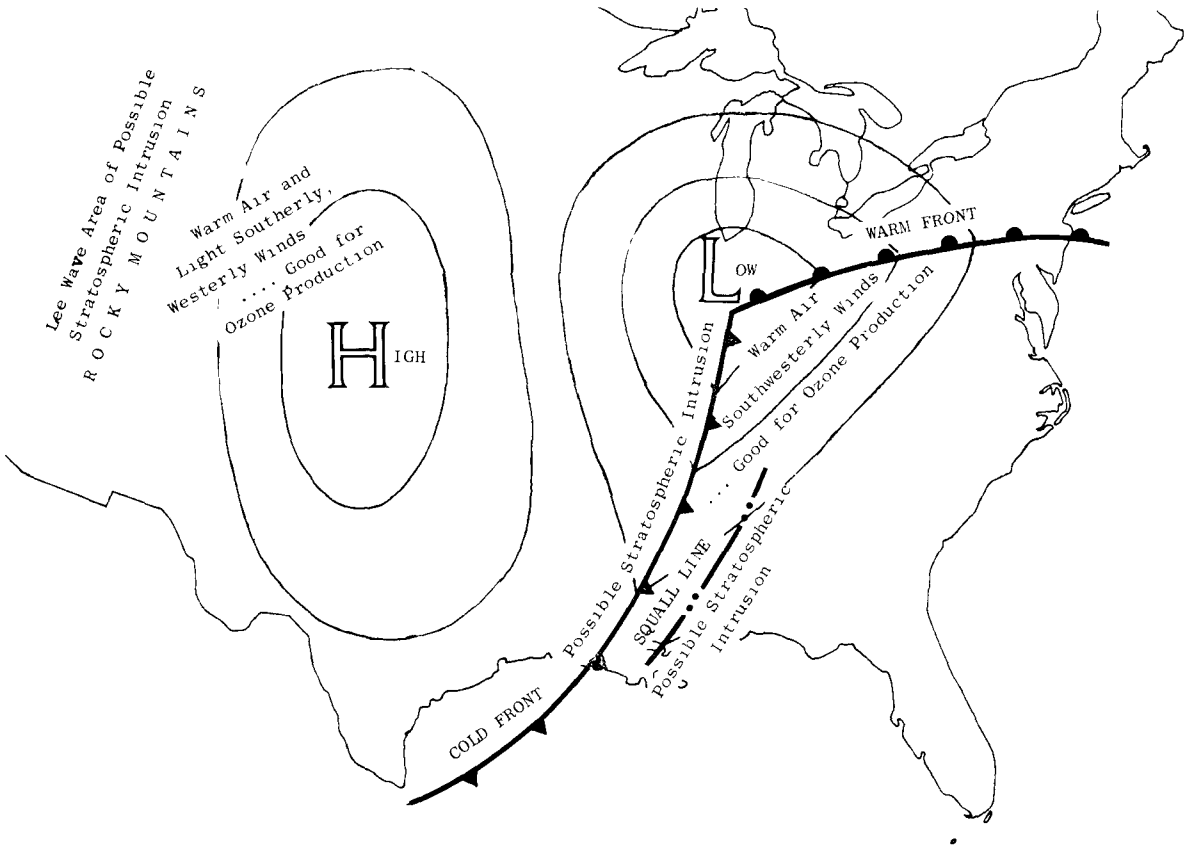

Figure 6. Schematic diagram showing parts of weather systems favorable for high ground level concentrations of ozone.

studies (Coffey and Stasiuk, 1975; Cleveland et al., 1975; Lyons and Cole, 1976; and Martinez and Meyer, 1976). The question arises, how can results of the kind reported here be applied to the problem of control strategy development?

The synoptic weather patterns that are associated with high ozone concentrations seem to be sufficiently well-defined that they can be used to defind spheres of influence for major anthropogenic source areas. In general, the regions influenced by a source will tend to be toward its northeast, but there are likely to be differences from one region of the country to another, because the orientation of the ozone-associated weather features will be different in different regions. The distance that a source's influence extends downwind could be estimated from trajectory analyses for specific weather situations of the kind known to be associated with high ozone concentrations. It appears that the influence of a source is not likely to last much longer than about 36 hours, and hence the distance traveled during such a period should define the outer limits of influence. The trajectory studies reported here, the dimensions of the high-ozone areas in the synoptic analyses and the results of other studies (Martinez and Meyers, 1976) all indicate that the areas of

21 JULY 1974

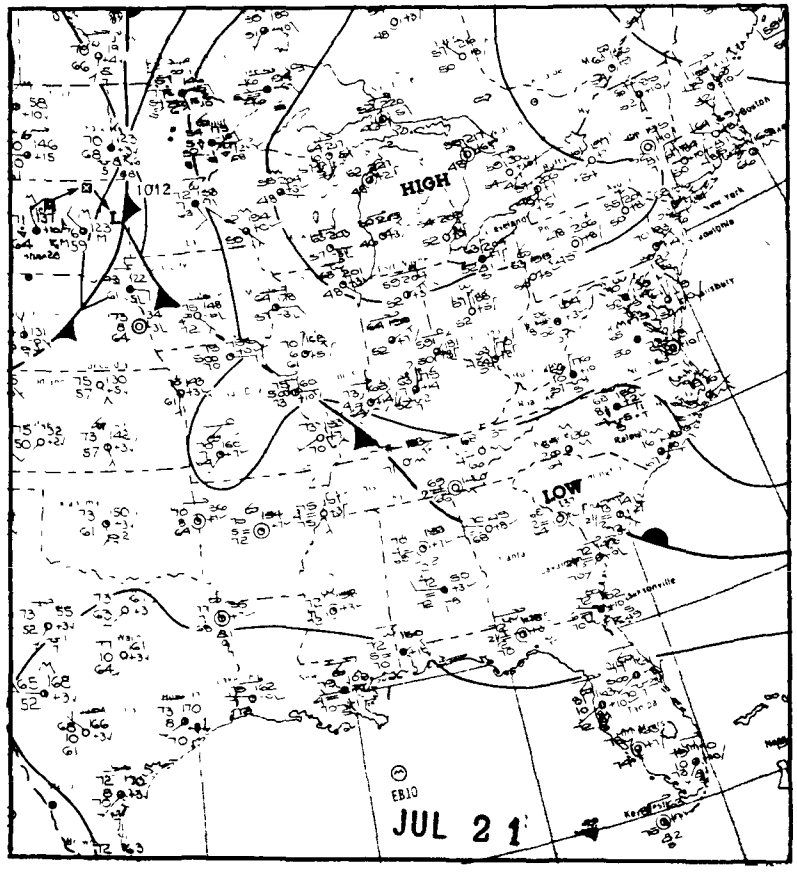

1200 GMT WEATHER MAP

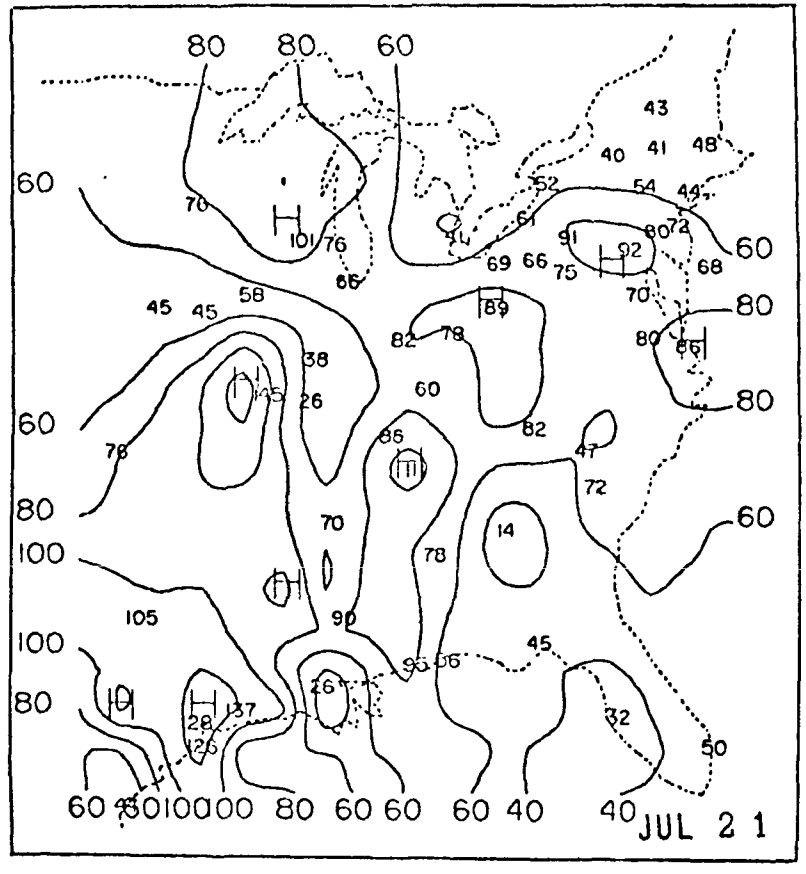

MAXIMUM-HOUR OZONE CONCENTRATIONS (ppb)

Figure 7. Maximum-hour ozone concentrations and weather patterns for the eastern United States, 21 July 1974.

influence of major sources have dimensions of more than a hundred kilometers. This is larger than most of the air quality control regions shown in Figure 1. Perhaps larger regions are more appropriate to the oxidant control problem and revisions should be considered.

ACKNOWLEDGMENTS

The support of the Environmental Protection Agency, Office of Air Quality Planning and Standards, under Contract No. 68-02-2084 is gratefully acknowledged. We have found the comments and other assistance of the Project Officer, Mr. Phillip Youngblood, to be most helpful.

Mr. Dale Coventry of EPA and Mr. R. Hows of Research Triangle Institute have provided much useful data, as has the staff of the National Climatic Center.

At SRI the following people have provided invaluable assistance: E. Shelar, R.L. Mancuso, J.H.S. Kealoha, A.H. Smith, R. Trudeau, P.B. Simmon, and L.J. Salas.

REFERENCES

Bruntz, S.M., W.S. Cleveland, B. Kleiner and J. L. Warner, 1974: The Dependence of Ambient Ozone on Solar Radiation, Wind, Temperature and Mixing Height. Proc. Symp. Atmos. Diff. and Air Poll., Santa Barbara, Calif. (Sept. 9-13), Amer. Met. Soc., pp.125-128.

Cleveland. W.S., B. Kleiner, J.E. McRae and J.L. Warner, 1975: The Analysis of Ground-level Ozone Data from New Jersey, New York, Connecticut and Massachusetts: Transport from the New York City Metropolitan Area. Undesignated Report, Bell Laboratories, Murray Hill, N.J., 63 pp.

Coffey, P. E. and W. N. Stasiuk, 1975: Evidence of Atmospheric Transport of Ozone into Urban Areas, Environ. Sci. and Tech., 9, 59-62.

Environmental Protection Agency, 1975: Control of Photochemical Oxidant--Technical Basis and Implications of Recent Findings. EPA Report 450/2-75-005, 37 pp.

Heffter, J.L. and A.D. Taylor, 1975: A Regional Continental Scale Transport, Diffusion and Deposition Model, Part I: Trajectory Model, Nat. Ocean. and Atmos. Admin. Tech. Memo. ERL ARC-50, pp. 1-16.

Ludwig, F.L., E. Reiter, E. Shelar, R.L. Mancuso, W.B. Johnson and P.B. Simmon, 1976: Meteorochemical Influence on Rural Ozone Concentrations, Final Report EPA Contract 68-02-2084, Stanford Research Institute, Menlo Park, California, Draft Submitted September 1976.

Lyons, W.A. and H.S. Cole, 1976: Photochemical Oxidant Transport: Mesoscale Lake Breeze and Synoptic-Scale Aspects. J. Appl. Meteorol. 15, 733-743.

Martinez, E. L. and E.L. Meyer, 1976: Urban-nonurban Ozone Gradients and their Significance, Presented at Air Poll. Cont. Assoc. Spec. Conf. on Ozone/Oxidants: Interactions with the total Environment, Dallas, Texas, March 12, 1976.

Pasquill, F., 1961: The Estimation of the Dispersion of Windborne Material, Meteorol. Mag. (London), 90, 33-49.

U.S. Air Force, 1957: On-the Job Training Program No. JP 25251, Weather Observer, Chapter 5.

A MECHANISM ACCOUNTING FOR THE PRODUCTION OF OZONE IN RURAL POLLUTED ATMOSPHERES

M. Antell*

ABSTRACT

In this report a kinetic model of rural smog is justified and presented. The model sets ozone (O_3), nonmethane hydrocarbon (NMHC), and nitrogen dioxide (NO_2) at measured levels. It assumes that the only organic species present in such smogs are "nonreactive" hydrocarbons and products of photo-oxidation of nonreactives. The concentration of the partially oxidized species is assumed to be at a level defined by their photochemical production and destruction. At measured levels of NO_2 and NMHC, ozone production is predicted to be large enough to account for ozone levels noted in rural smogs. The rate of net ozone production predicted is .0126 ppm/hr, aldehyde and ketone levels predicted are .010 ppm and .0093 ppm respectively for a system containing .007 ppm NO_2, .06 ppm O_3, and .02 ppm pentane.

INTRODUCTION

The purpose of this paper is to present a rough model of the mechanism of ozone production in polluted rural atmospheres. By indicating which reactions are of major import, it simplifies the task of developing sophisticated predictive models for smog production in very low concentration systems. The model presented is a simplified mathematical description of the production of ozone by an oxides of nitrogen-alkane system, at equilibrium with its products under average daytime insolation. Oxides of nitrogen (NO_x), alkane, and ozone (O_3) are varied in this model about levels measured in rural ozone-producing atmospheres. Solutions are reached for the concentration of intermediate smog products and of the net ozone production rate of such a system.

THESIS AND METHOD

The following line of reasoning was used to develop and justify this simplified steady-state model of the rural ozone-producing atmosphere.

BASIC ASSUMPTIONS

It appears that air masses generating ozone over the rural southeastern United States may reflect a pollution injection received more than a day earlier, perhaps over the industrial Midwest areas. The fact that these air masses are aged argued for modeling on the assumption that they are well mixed with

*U.S. Environmental Protection Agency, Washington, D. C.

respect to ozone precursors.

Reactive organic species injected into an air mass a day or more prior to its arrival over rural areas will be completely removed by ongoing active photochemistry. The bulk of alkanes so injected will remain unreacted.

The only reactive organic species remaining are those such as aldehydes and ketones that are replenished by the reaction of alkanes. In other words, pollutants injected into an air mass passing over densely populated areas undergo olefin photochemistry to leave alkanes and partially oxidized organics. If this reactive-depleted air mass then passes over areas of low emission density, it undergoes alkane photochemistry. During this phase, partially oxidized organic species promote the alkane photochemistry, which in turn maintains the concentration of partially oxidized species. This argument is the basis of an assumption that the rural ozone-producing atmosphere is characterized by a steady-state concentration of reactive species maintained and defined by a concentration of alkanes. The alkane species can be shown to be removed slowly enough to justify assuming its concentration to be invariant.

ASSUMED CONCENTRATIONS

We assume levels of anthropogenic pollutants in the range of those observed in rural ozone-producing air. These are:

- Ozone = .06 ppm (US EPA 1975)
- Nitrogen dioxide = .07 ppm (RTI 1974)
- Nitric oxide = .0019 based on assumption of photostationary concentration of O_3 and NO_x at an average daily insolation (Jeffries et al., 1976)
- Nonmethane organic FID (flame ionization detection) response (which includes hydrocarbons and several other organic species) has been measured in these smogs at .2 ppm C (RTI 1974). We conservatively set nonmethane hydrocarbon (NMHC) equal to .1 ppm C, or 1/2 of FID response.
- The concentration of other species - carbonyls, radicals - is poorly known. These concentrations are solved within the model.

For ease of analysis, in this model all hydrocarbon is assumed to be pentane, and all reactive intermediates are assumed to be those produced in pentane photo-oxidation.

KINETIC MODEL

Also, to simplify calculation, the qualitative lumped kinetic mechanism of Hecht et al. (1974) is used to set pertinent reactions and reaction rates. In this mechanism compounds within the classes alkane, ketone, aldehyde, etc. are each treated as having equivalent reaction rates and products. Further-

more, where several reactions follow an initiating reaction with high efficiency, these several are lumped together and treated as a single reaction of rate equal to initial reaction.

When the rate constants from Hecht et al. (1974) are used, the system is not highly ozone-productive. In particular, using the given concentrations of hydrocarbon, ozone, and NO_x, radical chains are terminated by peroxyacetyl nitrate (PAN) formation. The critical parameters creating this effect are the relative rates of reaction of peroxyacyl radical with NO vs. with NO_2. If instead of Hecht et al.'s (1974) evaluation of these contents, we utilize those of Niki et al. (1972), radical chains are lengthened considerably. Those rate constants applicable to peroxyacyl radical suggested by Niki et al. (1972) are utilized in this paper. To this author, this assumption is not unwarranted. The reaction rates suggested by Niki et al. (1972) preclude any significant PAN formation in irradiated hydrocarbon-NO_x systems prior to the point that $NO_2 >> NO$. In contrast, rates suggested by Hecht et al. (1974) imply significant PAN formation even when NO_2 = NO. Initial stages in NO-alkane smog chamber runs present a system in which NO, NO_2, and presumably peroxyacyl radical are present. However, these systems do not generate significant PAN until late in runs when NO is suppressed by net O_3 production (Altshuller, et al., 1969; Bufalini, et al., 1970).

The reactions, reaction rates, and overall reaction mechanism are listed in Tables 1, 2, and 3. The model attempts to maintain simplicity. It is noted that only a few reactions are of primary importance in the description of OH-HO_2 cycle mediated, alkane photo-oxidation. A number of reactions of secondary import are excluded in this analysis. Their exclusion is justified as they are relatively inefficient mechanisms for radical removal, or production, or recycling in the rural polluted atmosphere. We define "inefficient" competing reactions as those which react at rates less than, and generally much less than, 15% of the reactions modeled. Inefficient reactions include, for example, the reaction of hydroxyl radical (OH) with carbon monoxide (CO) and methane (CH_4), a variety of radical combination reactions, and production of OH by nitrous acid (HNO_2), nitric acid (HNO_3), or O_3 photolysis, or by reaction of O^3P (triplet atomic oxygen) with hydrocarbons.

MATHEMATICAL DESCRIPTION OF MODEL

The steady-state model is amenable to a mathematical description. Production rates of OH, HO_2, ketone, and aldehyde are set equal to their destruction according to the reactions, reaction constants, and reaction chains of Tables 1, 2, and 3. A tabulation of this mathematical description is seen in Table 4. It is noted that a "C" factor is included to allow for variation of relative reaction rates of peroxyacyl radical with NO and NO_2. "C" is the fractional percentage of peroxyacyl radicals converted to PAN. Aldehyde photolysis or reaction with OH is assumed to be only 1/3 effective for destruction of aldehyde. Two-thirds of the time aldehyde reactions will lead to production of the one carbon less aldehyde analogue which is "seen" in this model as no change at all.

In fact, we have assumed the aldehyde to be 1/3 propanal, 1/3 ethanal, and 1/3 methanal. This assumption is reasonably close to the proportion of

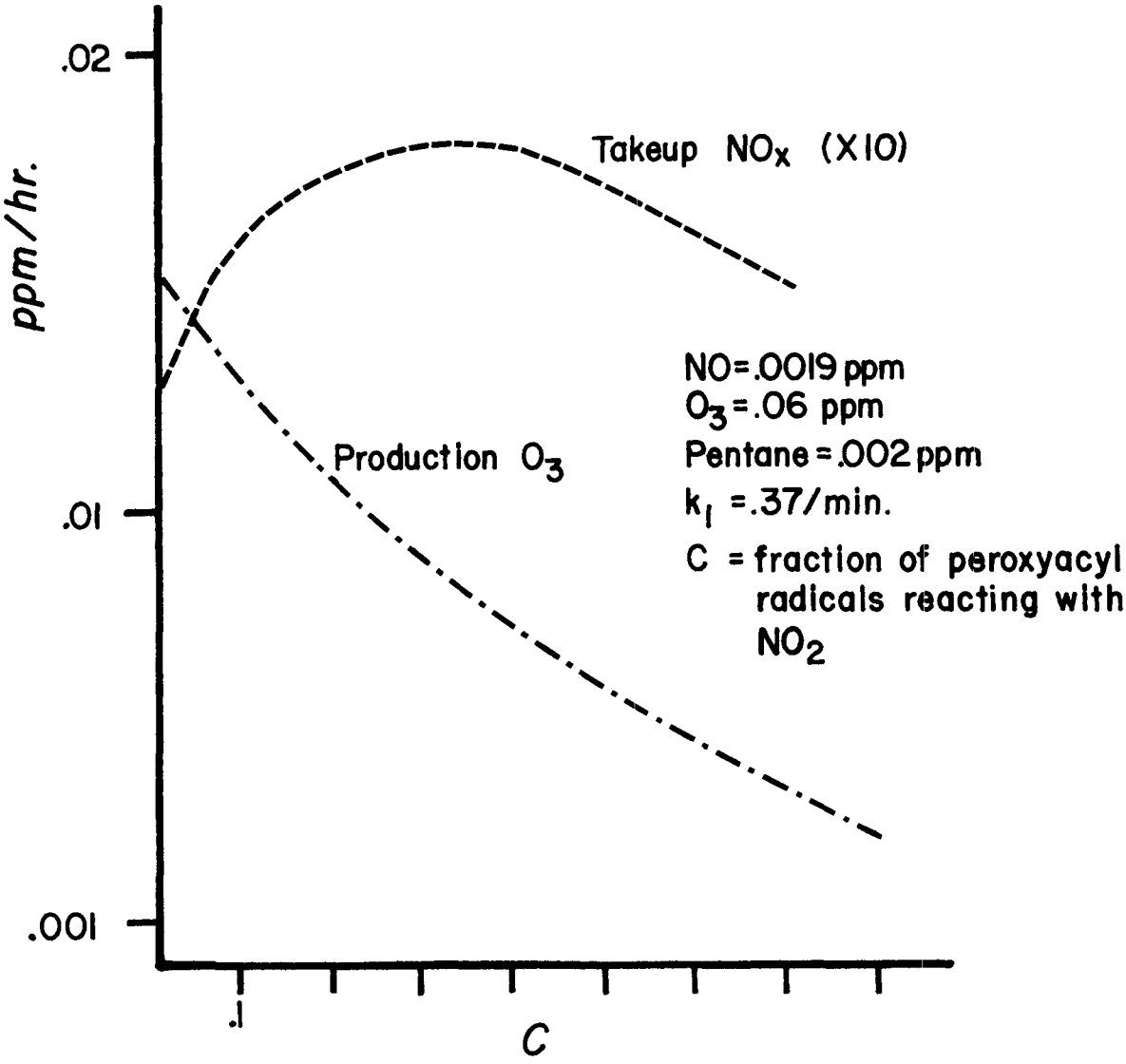

Figure 1. Effect of assumption of several rates of peroxyacyl reaction with NO_2 versus with NO.

aldehyde species that might be expected to be generated from pentane undergoing photo-oxidation. In any case, the system is not very sensitive to perturbation of this assumption.

BOUNDARY CONDITIONS

According to the above discussion, alkane hydrocarbon is consumed slowly enough to be considered a pseudo-conservative species. Any solution of the system of equations defined in this report, for which hydrocarbon take-up is greater than 1/2 of the assumed hydrocarbon concentration, violates the model's assumptions.

NO_x is a different case. It is consumed effectively during transport

TABLE 1. REACTIONS IN A RURAL ATMOSPHERE

(Groups of reactions are headed by the rate determining reactions. We later model on the reasonable assumption that the net reaction following a rate determining reaction occurs at the rate set by the initial reaction.)

1.	NO_2	$\xrightarrow{UV}$	$NO + O$
2.	$O + O_2$	$\longrightarrow$	O_3
3.	$O_3 + NO$	$\longrightarrow$	$NO_2 + O_2$
4i.	$RCHO$	$\xrightarrow{UV}$	$R\cdot + CHO$
4ii.	$R\cdot + O_2$	$\longrightarrow$	$ROO\cdot$
4iii.	$ROO\cdot + NO$	$\longrightarrow$	$RO\cdot + NO_2$
4iv.	$RO\cdot + O_2$	$\longrightarrow$	$HO_2 + R'CHO$
4v.	$\cdot CHO + O_2$	$\longrightarrow$	$CO + HO_2$
*NET 4	$RCHO + 3O_2 + NO$	$\longrightarrow$	$R'CHO + CO + NO_2 + 2HO_2$
**5i.	$RCHO + OH$	$\longrightarrow$	$RC = O$
5ii.	$RC^{=O} + O_2$	$\longrightarrow$	$RC^{=O}_{\diagdown OO}$
5iii.	$RC^{=O}_{\diagdown OO} + NO$	$\longrightarrow$	$RC^{=O}_{\diagdown O\cdot} + NO_2$
5iv.	$RC^{=O}_{\diagdown O\cdot} + O_2$	$\longrightarrow$	$ROO\cdot + CO_2$
5v.	$ROO\cdot + NO$	$\longrightarrow$	$RO\cdot + NO_2$
5vi.	$RO\cdot + O_2$	$\longrightarrow$	$R'CHO + HO_2$
NET 5	$RCHO + OH + 2O_2 + 2NO$	$\longrightarrow$	$R'CHO + 2NO_2 + CO_2 + HO_2$
6.	$HO_2 + NO$	$\longrightarrow$	$NO_2 + OH$
7.	$HO_2 + HO_2$	$\longrightarrow$	$H_2O_2 + O_2$
8.	$OH + NO_2$	$\longrightarrow$	HNO_3
9i.	$RCH_2R + OH + O_2$	$\longrightarrow$	$R\underset{H}{C}R^{OO\cdot}$
9ii.	$RC^{=OO\cdot}_{\diagdown R} + NO$	$\longrightarrow$	$RC^{-O\cdot}_{H\diagdown R} + NO_2$

(continued)

TABLE 1. (continued)

9iii.	$RC^{-O\cdot}_{H\ R}$ + O_2	$\longrightarrow$	$RC^{=O}_{R}$ + HO_2
NET 9	RCH_2R + OH + $2O_2$ + NO	$\longrightarrow$	$RC^{=O}_{R}$ + NO_2 + HO_2
10i.	$R_1C^{=O}R_2$	$\xrightarrow{UV}$	$R_1C^{=O}_{\cdot}$ + $R_2\cdot$
10ii.	$R_1C^{=O}_{\cdot}$ + O_2	$\longrightarrow$	$R_1C^{=O}_{OO\cdot}$
10iii.	$R_1C^{=O}_{OO\cdot}$ + NO	$\longrightarrow$	$R_1C^{=O}_{O\cdot}$ + NO_2
10iv.	$R_1C^{=O}_{O\cdot}$	$\longrightarrow$	$R_1\cdot$ + CO_2
10v.	$R_1\cdot$ and $R_2\cdot$ + O_2	$\longrightarrow$	ROO·
10vi.	ROO· + NO	$\longrightarrow$	RO· + NO_2
10vii.	RO· + O_2	$\longrightarrow$	R'CHO + HO_2
NET 10	$R_1C^{=O}_{R_2}$ + $5O_2$ + 3NO	$\longrightarrow$	R_1' CHO + R'_2 CHO + $2HO_2$ + $3NO_2$
11i.	$R_1'CH_2C^{=O}R_2$ + OH	$\longrightarrow$	$R_1CHC^{=O}R_2$
11ii.	$R_1CHC^{=O}R_2$ + O_2	$\longrightarrow$	$R_1C^{OO\cdot}HC^{=O}R_2$
11iii.	$R_1C^{OO\cdot}HC\ ^{O}R_2$ + NO + O_2	$\longrightarrow$	$R_1C^{=O}_{H}$ + $R_2C^{=O}_{OO\cdot}$ + NO_2
11iv.	$R_2C^{=O}_{OO\cdot}$ + NO + O_2	$\longrightarrow$	R_2'CHO + HO_2 + NO_2
***NET 11	$R_1CH_2C^{=O}R_2$ + $3O_2$ + 2NO + OH	$\longrightarrow$	R_1'CHO + R_2'CHO + HO_2 + CO_2 + $2NO_2$

*R' = alkyl radical of one less carbon than R.

**Note that the effect of reaction 5iib $RC^{O}_{OO\cdot}$ + NO_2 $\longrightarrow$ $RC\ ^{O}_{OO}NO_2$ would be:

NET 5b RCHO + OH + O_2 + NO_2 $\longrightarrow$ PAN

(reaction 10 and 11 are affected analogously).

***Reaction 11 is poorly characterized (NAQCAC 1976).

so the main source of NO_x in rural smog must be <u>in-situ</u> emissions, largely from mobile sources.

It need not be contradictory for the model to allow for a significant continual replenishment of NO_x and insignificant replenishment of organics from local automotive emissions. This is because the ratio of NO_x to organics

TABLE 2. RATE CONSTANTS OF REACTIONS IN TABLE 1 IN PPM^{-1} MIN^{-1} EXCEPT AS NOTED

1.	$NO_2 \longrightarrow NO + O$	k_1	= .37/min
2.	$O + O_2 \longrightarrow O_3$	k_2	= 2×10^{-4}
3.	$O_3 + NO \longrightarrow NO_2 + O_2$	k_3	= 20.8
4.	$RCHO \longrightarrow R^{\bullet} + {}^{\bullet}CHO$	k_4	= 2.5×10^{-3}/min
5.	$RCHO + OH \longrightarrow RC(=O)\bullet$	k_5	= 2.3×10^{4}
6.	$HO_2 + NO \longrightarrow NO_2 + OH$	k_6	= 7×10^{2}
7.	$HO_2 + HO_2 \longrightarrow H_2O_2$	k_7	= 5.3×10^{3}
8.	$OH + NO_2 \longrightarrow HNO_3$	k_8	= 1.5×10^{4}
9.	$RCH_2R + OH + O_2 \longrightarrow RC(-OO\bullet)R$	k_9	= 3.8×10^{3}
10.	$RC(=O)R \xrightarrow{UV} RC(=O)\bullet + \bullet R$	k_{10}	= 8.2×10^{-4}/min
11.	$RCH_2C(=O)R + OH \longrightarrow RC^{\bullet}HC(=O)R$	k_{11}	= 3.8×10^{3}

TABLE 3. REACTION PATHWAYS OCCURRING IN THE RURAL POLLUTED ATMOSPHERE. PATHWAYS LABELED BY REACTION GROUPS DISCUSSED IN TABLE 1

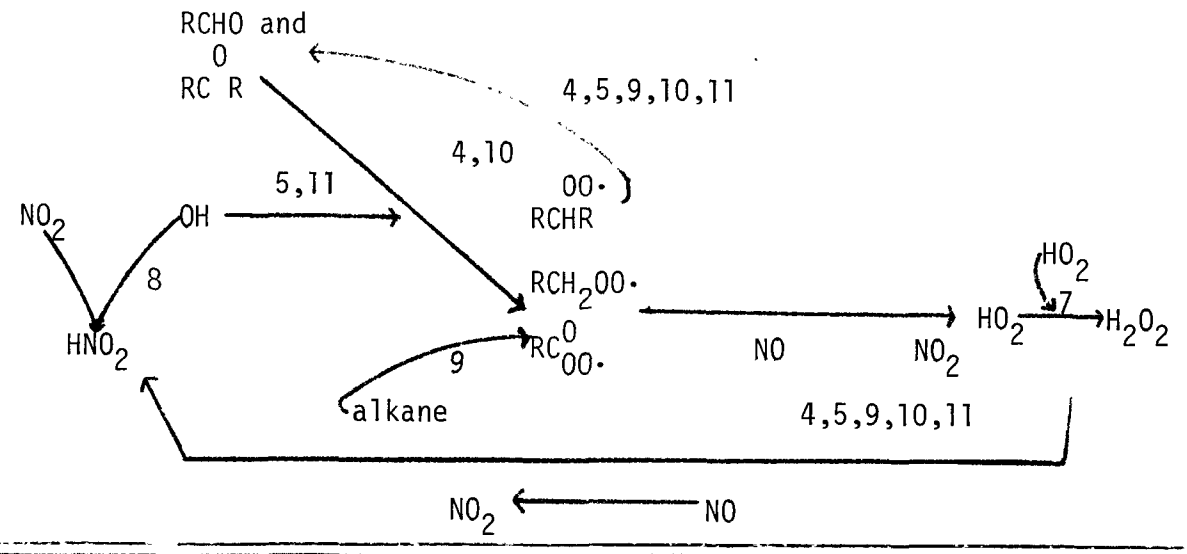

TABLE 4. SIMULTANEOUS STEADY STATE EQUATIONS DESCRIBING RURAL POLLUTED AIR

1. Production ketone = destruction ketone

$$(OH)\ (HC)\ 3.8 \times 10^{3} = [8.2 \times 10^{-4} + (OH)\ (3.8 \times 10^{3})]\ Ke$$

2. Production aldehyde = destruction aldehyde

$$Ke\ (2\text{-}C)\ 8.2 \times 10^{-4} + (2\text{-}C)\ (Ke)\ (OH)\ 3.8 \times 10^{3} =$$

$$[(.33 + C)\ (OH)\ 2.3 \times 10^{4} + (.33)\ 2.5 \times 10^{-3}]\ Al$$

3. Production OH = destruction OH

$$(HO_2)\ (NO)\ 700 =$$

$$(OH)\ (Hc)\ 5 \times 10^{3} + (OH)\ (Al)\ 2.3 \times 10^{4} + (OH)\ (Ke)\ 3.8 \times 10^{3} +$$

$$(OH)\ (NO_2)\ 1.5 \times 10^{4}$$

4. Production HO_2 = destruction HO_2

$$(2\text{-}c)\ (Ke)\ (16.4 \times 10^{-4}) + 2(Al)\ 2.5 \times 10^{-3} + (OH)\ (Hc)\ 3.8 \times 10^{3}$$

$$+ (OH)\ (Ke)\ (1\text{-}c)\ 3.8 \times 10^{3} + (OH)\ (Al)\ (1\text{-}c)\ 2.3 \times 10^{4} =$$

$$2\ (HO_2)^2\ 5.3 \times 10^{3} + (HO_2)\ (NO)\ (700)$$

where: Hc = hydrocarbon
Al = aldehyde
Ke = ketone
c = fraction of peroxyacyl radicals reacting with NO_2

mass emissions from (post 1969) automobiles is less than one (1), while optimum ozone production (particularly in alkane systems) is achieved at NO_x to hydrocarbon mass concentrations of 1:5 or greater. However, a boundary condition for NO_x replenishment is set by this argument.

Replenishment of NO_x and hydrocarbon is from the same automotive source. Given that the organic content of rural smog is a phenomenon of transport, then in-situ precursor replenishment should not be the major contribution (perhaps less than 20%) to organic concentrations. Therefore, the maximum uptake and replenishment of NO_x per day as mass concentration allowable under these boundary conditions is equal to 20% x mass of concentration of organics in rural smog x ratio of emissions of NO_x to organics. This term is equal to .02 ppm NO_x replenishment per day allowable maximum. Solutions of the equations proposed in this report for several concentrations of ozone, hydrocarbon, and NO_x are assayed against the above boundary conditions for hydrocarbon and NO_x takeup.

RESULTS

The effect of mathematically assuming a variety of rates of reaction of peroxyacyl radical with NO_2 and NO on ozone production is seen in Figure 1. O_3 = .06 ppm, NO_2 = .007 ppm, and hydrocarbon = .02 ppm pentane. C = .05 corresponds closely to the ratio of reactions used by Niki et al. (1971); C = .3 corresponds to that used by Hecht et al. (1974); C = .8 corresponds to that used by Dimerjian (1974).

The solution for the concentration of ketone, aldehyde, HO_2, OH, and net O_3 production per hour at these concentrations, at C = .1, are respectively $.936 \times 10^{-2}$, $.101 \times 10^{-1}$, $.684 \times 10^{-4}$, $.198 \times 10^{-6}$, and $.126 \times 10^{-1}$ ppm. The effect of variation of hydrocarbon and NO_2, and of ozone, on ozone production are shown in Figures 2 and 3.

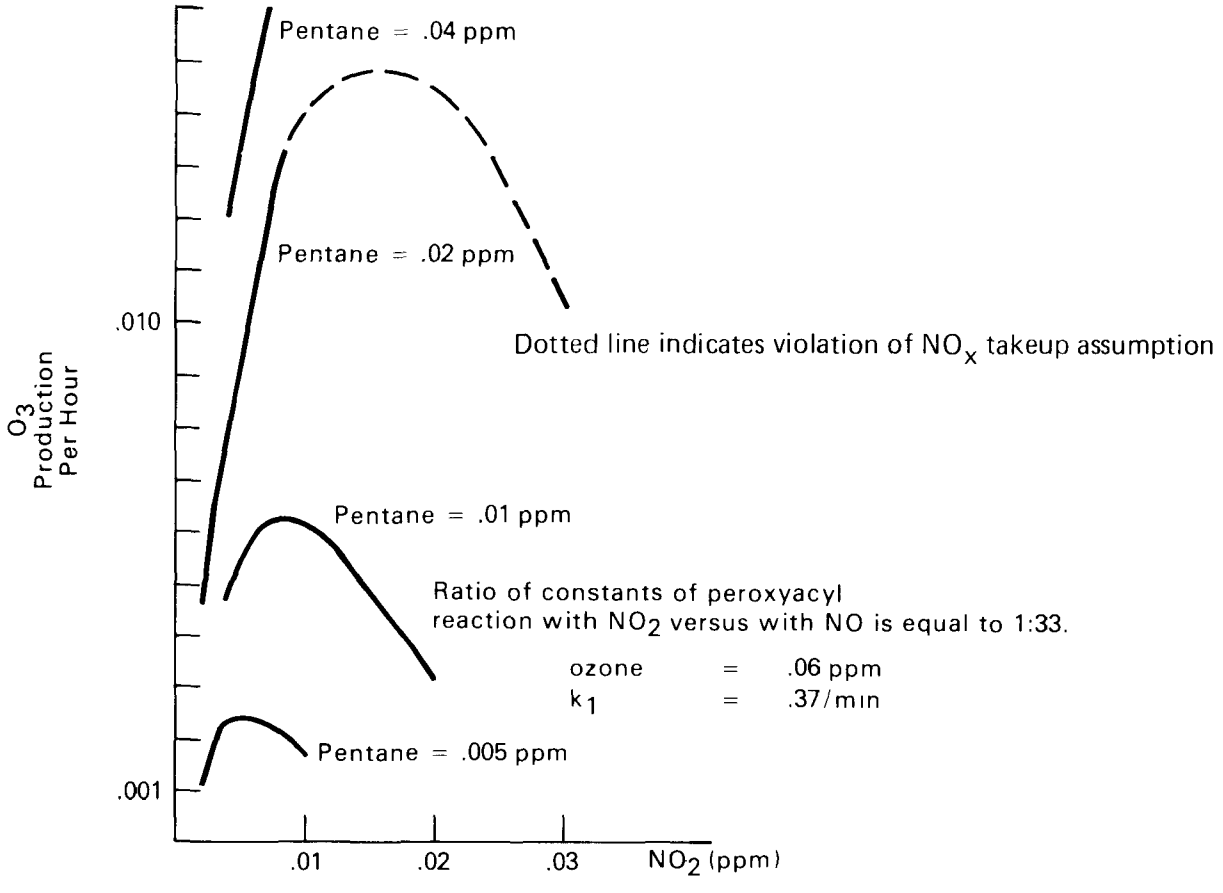

Figure 2. Effect of variation of initial concentrations of pentane and NO_x of ozone production and NO_x takeup.

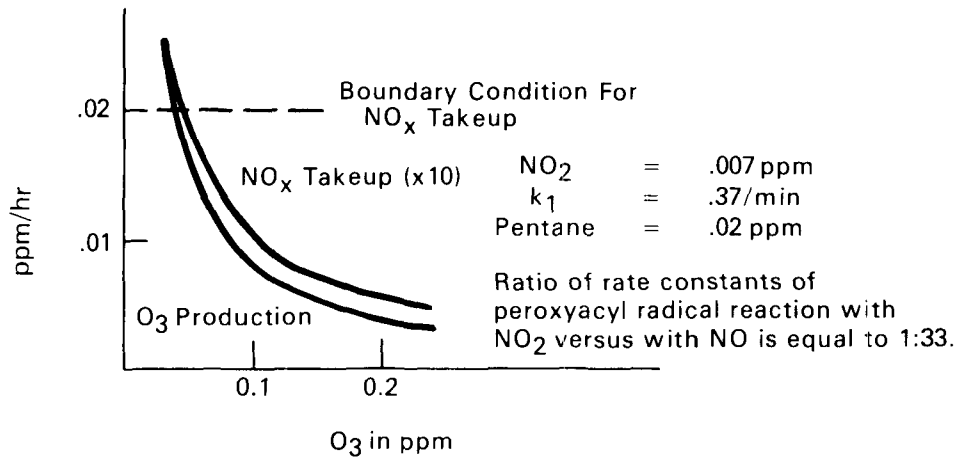

Figure 3. Effect of level of ozone on ozone production and NO_x takeup.

DISCUSSION OF RESULTS

Variation of the ratio of reaction of peroxyacyl radical with NO and NO_2 (Figure 1) is shown to strongly affect potential ozone formation in an alkane-NO_x system. The effect of variation of NO_x and hydrocarbon is expected. Their ratio, as well as absolute concentrations, strongly control net production of ozone. At measured levels of precursors, ozone production in rural smog systems is both NO_x and hydrocarbon concentration dependent. NO_x takeup as a percentage of NO_x concentration is significant so the system can only maintain ozone production over several hours by continued replenishment of NO_x. The model presented here is realistic only for systems containing ozone, hydrocarbon, and nitrogen oxides at close to measured levels. At conditions tending to create faster generation of ozone, the NO_x is taken up very quickly. Maintenance of levels of NO_x and organics in such systems would imply local sources of pollution contributing more of these ozone precursors than are contributed by long range transport. Such a condition violates several of the explicit assumptions of the model. In particular, local pollution sources of such magnitude would likely emit sufficient quantities of olefin to suppress alkane photo-oxidation.

CONCLUSIONS

The modeled production of O_3 from an alkane-NO_x system is shown to be highly dependent on the relative rates of reaction of peroxyacyl radical with NO_2 versus with NO. If those rates are near the extreme of rates reported in the literature, such systems can account for the amounts of ozone presently found in the rural east coast of the United States.

The mathematical model here presented also suggests the presence in rural polluted air of significant quantities (roughly .02 ppm) of carbonyl compounds. If such concentrations were observed, they would tend to support the theory that rural ozone in the U.S. is generally a phenomenon created by widespread, human generated, hydrocarbon and nitrogen oxide pollution.

TABLE 5. ALGORITHMS FOR SOLUTION OF NET PRODUCTION OF OZONE PER HOUR, AND THE NET TAKEUP OF HYDROCARBON AND NITROGEN OXIDE PER HOUR

Net O_3 production per hour* =

$$60\ [(HO_2)\ (NO)\ (700) + (Ke)\ (2\text{-}c)\ 8.2 \times 10^{-4} + 3.8 \times 10^{3}\ (Ke)\ (OH)\ (2\text{-}c) +$$

$$2\ AL\ 2.5 \times 10^{-3} + (Al)\ (OH)\ (1\text{-}c)\ 2.3 \times 10^{4}]$$

Takeup of hydrocarbon per hour =

$$60\ [\ 3.8 \times 10^{3}\ (OH)\ (Hc)\ ]$$

Takeup of nitrogen dioxide per hour** =

$$60\ [\ OH\ (1.5 \times 10^{4})\ (NO_2) + (C)\ Ke\ 8.2 \times 10^{-4} + (C)\ (Ke)\ (OH)\ 3.8 \times 10^{3}$$

$$+ (C)\ (Al)\ (OH)\ 2.3 \times 10^{4}\ ]$$

* O_3 production rate = rate of oxidation of NO by HO_2 + rate of oxidation of NO by ROO· and related species

** NO_2 takeup rate = rate of production of HNO_3 + rate of production of PAN

REFERENCES

Altshuller, A.P., S.L. Kopczynsk, D. Wilson, W. Lonneman, and F.D. Sutterfield. Photochemical Reactivities of N-Butane and other Paraffinic Hydrocarbon, 1969. Journal Air Pollution Control Association 19:787.

Bufalini, J. J., B. W. Gay, and S. L. Kopczynsk. 1970. Oxidation of N-Butane by Photolysis of NO. Environmental Science and Technology. 4:333-338.

Dimerjian, K. L., J. A. Kerr, and J. G. Calvert. 1974. The Mechanism of Photochemical Smog Formation. Advances in Environmental Science and Technology. 4:1-262.

Hecht, T. A., J. H. Seinfeld, and M. C. Dodge. 1974. Further Development of Generalized Kinetic Mechanism for Photochemical Smog. Environmental Science and Technology. 8:327-338.

Jeffries, H. E., J. E. Sickles II, L. A. Ripperton. 1976. Ozone Transport Phenomena Observed and Simulated. Paper 14.3 - Annual APCA Convention.

National Air Quality Criteria Advisory Committee. 1976. Final Report.

Niki, H., E. E. Daby, and B. Weinstock. 1972. Mechanisms of Smog Reactions. Advances in Chemistry Series - Ozone and Smog Reactions. New York.

Research Triangle Institute. 1974. Investigation of Ozone Precursor Concentrations at Non-Urban Locations in the Eastern United States.

U. S. Enviornmental Protection Agency. 1975. Control of Photochemical Oxidants - Technical Basis and Implications of Recent Findings. 35 p.

NET OZONE FORMATION IN RURAL ATMOSPHERES

T.Y. Chang and B. Weinstock*

ABSTRACT

A photochemical model was used to explain ozone (O_3) formation with alkane/oxides of nitrogen (NO_x) mixtures in smog chamber experiments designed to simulate rural conditions. In order to fit the smog chamber data, the model had to be modified to include an hydroxyl (HO) radical source and heterogeneous wall reactions. The unmodified model was applied to predict the effect on rural O_3 levels of less reactive hydrocarbons (HCs), which are left over from urban emissions and dispersed into rural areas. From this analysis, it is concluded that the leftover urban HCs make little contribution either to the generation of elevated rural ozone levels or to the increase of elevated levels already present. It is suggested instead that the major causes of elevated rural O_3 levels are the transport of high O_3 concentrations generated in urban areas and additional O_3 produced by reactions of fresh HC and NO_x emissions from local rural sources, both natural and man-made. Data from the 1974 Midwest study are found to be in agreement with the latter suggestion. Based on these findings, a method is proposed to correct hydrocarbon reactivity scales for the effect of dilution that occurs in the atmosphere. The analysis in this study is in disagreement with the justification presented for the new Environmental Protection Agency Policy Statement that severe control of all hydrocarbons, without regard to reactivity, will be necessary to reduce elevated rural O_3 levels.

INTRODUCTION

The observation of elevated ozone (O_3) concentrations in rural areas has become a matter of much interest in recent years. It has been suggested that less reactive hydrocarbon (HC) emissions from urban areas may contribute importantly to this phenomenon. These HCs, which are leftover after a single day of solar irradiation, are expected to be transported to rural areas, where they can react further on succeeding days and thereby contribute significantly, as some suggest, to the elevation of rural ozone concentrations. Their effect would be most pronounced under meteorological conditions, such as a high pressure system, when pollutants are not ventilated rapidly to the global atmosphere and are circulated over wide areas for many days. New smog chamber experiments have been made to simulate this behavior. In these ex-

*Ford Motor Company, Dearborn, Michigan.

periments, very long irradiation times and much higher initial hydrocarbon/oxides of nitrogen (HC/NO_X) ratios were used compared with those used in earlier experiments to simulate urban photochemistry. It was found that many HCs, previously found to be unreactive in urban simulations, produced significant concentration of ozone under the new conditions (1). These results appeared to support the above concept. Citing this as a basis, the Environmental Protection Agency (EPA) issued a Policy Statement (2) in which it was stated that HC reactivity no longer was essential to HC control strategy and that all HC emissions would be regulated in the future, without regard to their photochemical reactivity. It was advised that the previous strategy of the replacement of more reactive HCs by less reactive ones as a means of oxidant abatement, such as in Los Angeles Air Pollution Control District (LAAPCD) Rule 66(3), should be regarded now only as an interim measure and that future planning should consider complete HC control regardless of reactivity.

The objectives of this paper are to examine the validity of this new concept and of the use of smog chamber data as a simple representation of atmospheric behavior. In a recent paper (4), we have considered these questions with respect to methane and found that methane, on balance, will diminish elevated rural ozone levels contrary to the conclusions of a recent publication (5). Methane is so unreactive compared with other HCs, however, that generalizations cannot be drawn from its behavior. The methodology developed in that study (4) was modified for this paper to include higher alkanes and the behavior of the modified systems is taken as a prototype for the reactions of less reactive HCs. First, the modified photochemical model is used to explain the new smog chamber data. The model is applied next to evaluate the contribution of less reactive HCs to elevated rural ozone levels. The relevance of these findings to abatement strategy for elevated rural ozone levels is discussed next. Finally, some suggestions are made for a revised HC reactivity scale.

PHOTOCHEMICAL MODEL

The reference photochemical model used in this study is a modified version of a model used previously in a study of the methane-carbon monoxide-nitrogen oxides (CH_4-CO-NO_X) system (4). A list of reactions and rate coefficients is given in Appendix A. Reactions of alkanes with oxygen (O) and hydroxyl radicals (HO) and reactions involving radicals produced from alkane-O and alkane-HO reactions are added to the previous model. All types of alkyl groups are lumped together and represented by R. A parameter, β, is introduced

$$RO + O_2 = \beta RCHO + (1-\beta)HCHO + HO_2 \qquad R46)$$

to represent the fraction of total aldehydes produced that are not formaldehyde. The values of β are assumed to be 0, 1/2, 2/3, and 3/4 for methane, ethane, propane, and butane, respectively. The reaction,

$$HO_2 + NO_2 = HONO + O_2, \qquad R30)$$

also is added to the present model and a larger value for removal rate for nitric acid (HNO_3) [R57] is used. Rain-out removal for hydrogen peroxide (H_2O_2) and alkyl hydroperoxide (HOOR) is deleted. The photodissociation coefficients, R2 through R10, are assumed to be proportional to the photodissociation coefficient for nitrogen dioxide (NO_2), k_1.

The model used here incorporates the main features of the models of Niki et al. (6), Hecht et al. (7), Demerjian et al. (8), and Pitts et al. (9). Major uncertainties in photochemical models have been discussed by Hecht et al. (10), Durbin et al. (11), and Pitts et al. (9). The set of photochemical rate equations is strongly nonlinear. Therefore, absolute predictions of the photochemical model are somewhat uncertain. Relative trends of the photochemical behavior, however, are believed to be predicted by the model with good reliability.

ANALYSIS OF NEW SMOG CHAMBER DATA

As mentioned before, the new EPA smog chamber experiments (1) were designed to simulate rural atmospheric conditions. High initial HC/NO_x ratios, 8:1, were used compared with ratios of 2-3:1 used to simulate urban conditions in earlier experiments. Longer irradiation times also were used to simulate carry-over of urban emissions to rural areas. Data for the propane/NO_x system, run 194, (1) are given in Table 1. In a simulation with the unmodified photochemical model, less than 2 pphm O_3 was predicted after 430 min, much less than the observed maximum value of 11 pphm. This disagreement was not unexpected. Propane, like alkanes in general, should produce HO radicals very slowly in these experiments, with the consequence that there should be a very long induction period before the O_3 concentration builds up. The much more rapid production of O_3 seen in the actual experiment is a consequence of a substantial HO background common to all laboratory experiments (12).

An attempt to fit the experimental behavior was made in simulation 1 by the addition of a constant HO source of 3×10^{-4} ppm min^{-1} to the model. This approach also has been used by Pitts et al. (9). In addition, an O_3 removal term, $k_{55} = 1 \times 10^{-3}$ min^{-1}, was introduced to simulate the O_3 removal at the walls that is characteristic of smog chambers. A reasonable prediction of the experimentally observed NO_2 maximum and of the time to reach this maximum is obtained. An O_3 maximum still is not observed, however, and the 430 min. O_3 concentration predicted is much higher now than 11 pphm.

A different approach to produce an HO background was used in simulation 2. The rate constant, k_{20}, for the reaction,

$$NO + NO_2 + H_2O = 2\ HONO \qquad R20)$$

TABLE 1. EPA DATA AND SIMULATION RESULTS FOR PROPANE - NO_x[a]

	Maximum NO_2		Maximum O_3		At 430 min			
	Time (min)	Conc. (ppb)	Time (min)	Conc. (pphm)	HC (ppm)	NO_2 (ppb)	NO (ppb)	O_3 (pphm)
EPA Run No. 194	55	130	225	11.0	3.18	95[b]	<1.0	7.6
Sim. 1[c]	80	147	-	-	3.24	80	2.9	33
Sim. 2[d]	105	142	-	-	3.35	110	5.4	26
Sim. 3[e]	65	132	305	14.5	3.40	11	1.0	14
Sim. 4[f]	70	132	250	12.6	3.38	16	1.8	11

a $k_1 = 0.33\ min^{-1}$, $k_{dilution} = 2.2 \times 10^{-4}\ min^{-1}$, $k_{34} = 22\ ppm^{-1}\ min^{-1}$, $k_{35} = 3200\ ppm^{-1}\ min^{-1}$, $(H_2O) = 1 \times 10^4$ ppm; initial concentrations: (HC) = 4.0 ppm, (NO) = 180 ppb, (NO_2) = 20 ppb, (O_3) = 0 pphm.

b (NO_x) - (NO).

c $k_{55} = 1 \times 10^{-3}\ min^{-1}$, constant HO source = 3×10^{-4} ppm/min.

d $k_{20} = 1.9 \times 10^{-5}\ ppm^{-2}\ min^{-1}$, $k_{21} = 1.8\ ppm^{-1}\ min^{-1}$, $k_{55} = 1 \times 10^{-3}\ min^{-1}$.

e add $k_{19} = 1.5 \times 10^{-3}\ ppm^{-1}\ min^{-1}$., to d

f same as e except, $k_{55} = 3 \times 10^{-3}\ min^{-1}$.

was arbitrarily increased from 1.9×10^{-11} to $1.9 \times 10^{-5}\ ppm^{-2}\ min^{-1}$. The rate of the back reaction, k_{21}, was increased from 1.8×10^{-5} to $1.8\ ppm^{-1}\ min^{-1}$. By this adjustment, the concentration of HONO is built up quickly and this provides rapid HO source because nitrous acid (HONO) produces HO by photodissociation. This approach has been used independently by Sickles(13). Although the rate constant for the homogeneous formation of HONO by R20 is known to be slow (14,15), the heterogeneous rate on the walls is probably very much faster in smog chambers. The predicted O_3 is in better agreement than in simulation 1, but is still too high; an O_3 maximum still is not observed, and the time for the NO_2 maximum changes in the wrong direction. For simulation 3, the rate constant, k_{19}, for the homogeneous reaction,

$$N_2O_5 + H_2O = 2HNO_3, \qquad R19)$$

was increased from 1.5×10^{-5} used in simulation 2 to $1.5 \times 10^{-3}\ ppm^{-1}\ min^{-1}$ to represent the heterogeneous reaction that is likely to be of more

importance in smog chambers. With this modification, an O_3 maximum now is predicted and the agreement with the experimental observations is noticeably improved. In simulation 4, the effect of increasing the O_3 decay rate, k_{55}, from 1×10^{-3} to 3×10^{-3} min^{-1} was calculated and this improved the agreement with the experimental data further. Similar situations have been made for data obtained with the ethane/NO_X system. The same qualitative behavior for the model adjustments were observed and the quantitative agreement with the experimental data was again satisfactory.

Model calculations also were compared with the O_3 maxima observed in similar experiments that have been reported by Heuss (16). Using the same parameters as in simulation 4, the model predicted O_3 maxima of 7.8, 14, and 15 pphm compared with the experimental values of 8, 13, and 20 pphm for ethane, propane, and butane, respectively.

These simulations give insight into the importance of the HO background and of heterogeneous reactions to O_3 formation in smog chamber experiments. The agreement of the model predictions with the experimental data alternatively gives a measure of confidence of the reliability of the model for predictions of atmospheric behavior for alkane/NO_X mixtures.

SIMULATED RURAL ATMOSPHERIC PHOTOCHEMISTRY

Calculations with the unmodified photochemical model, i.e., without the changes made to take account of the idiosyncrasies of smog chambers, have been made to simulate rural atmospheric photochemistry. Steady state calculations were made at first to investigate the variation of the steady state O_3 with a variety of fixed HC and NO_X concentrations. For each fixed HC concentration the predicted O_3 concentration goes through a maximum as the fixed NO_X concentration is varied. As the fixed HC concentration is increased, the NO_X concentration corresponding to the O_3 maximum also increases, as does the O_3 maximum. From these steady-state calculations, it can be concluded that atmospheric O_3 concentrations are affected not only by the absolute concentration of both HC and NO_X, but also by the HC/NO_X ratio.

Time-dependent photochemical model calculations were made next. In the first set of calculations, the concentrations of HC and NO_X were kept constant, and the daily buildup of O_3 was predicted. These calculations were made to determine the sensitivity and time dependence of O_3 formation to the NO_X concentration and characteristic time of O_3 buildup. Some of the results are given in Table 2. The initial O_3 concentration was taken to be 4 pphm; that of propane to be 0.1 ppm (0.3 ppmC). The NO_X concentration was taken as a variable since reliable rural NO_X data are not available because of interferences in the measuring techniques that give rise to spuriously high NO_2 values. The photodissociation coefficient for NO_2 in min^{-1} used was:

$$k_1 = 0.66\ e^{-3.8/\cos X},\quad \cos X > 0$$
$$k_1 = 0,\quad \cos X < 0. \qquad (1)$$

TABLE 2. DAILY MAXIMUM O_3 IN PPHM: (HC) AND (NO_x) KEPT CONSTANT[a]

Day	(NO_x)=0.1 ppb	1 ppb	10 ppb
1	4.0	4.4	10
3	3.3	5.6	15
5	2.9	7.0	18
7	2.7	8.2	19
10	2.7	9.5	21
13	2.7	10.2	22

(propane) = 0.1 ppm, (CH_4) = 2 ppm, (CO) = 0.2 ppm, (H_2O) = 2 x 10^4 ppm and (NO_x) = 0.1, 1, 10 are kept constant.

Initial (O_3) = 4 pphm

a. The NO_x was initially pure NO_2.

The angle of inclination of the sun, X, is approximated by,

$$X = \pi(H/12 - 1), \qquad (2)$$

where H is the hour of day. The values of k_1 given by Equation (1) give a good approximation of measured values of k_1 by Sickles (13).

The amount of O_3 formed is seen to be sensitive to the NO_x concentration. When (NO_x) = 0.1 ppb, the daily maximum O_3 decays from 4 to 2.7 pphm. When (NO_x) = 1 ppb, the time for the O_3 concentration to double from 4 to 8 pphm is about a week, and the O_3 concentration approaches an asymptotic value of about 10 pphm. When (NO_x) = 10 ppb, the doubling time of the initial O_3 concentration is about one day and the asymptotic maximum O_3 is a little above 22 pphm. These calculations show that reliable measurements of NO_2 and a more quantitative understanding of NO_x chemistry are critical for a better understanding of rural O_3.

The next set of time-dependent calculations were made to simulate the effect of less reactive, "leftover" hydrocarbons in an urban plume on several ambient rural O_3 concentrations, ranging from 0-20 pphm. The reactants were given various initial concentrations that were allowed to decay continuously during the two days. Further details of the calculations and the results are given in Table 3. Propane, which can be considered as a prototype for less reactive, "leftover" hydrocarbons, was set at an initial concentration of 0.1

ppm (0.3 ppmC). This concentration is much higher than the concentrations observed for the less reactive hydrocarbons in the 1974 Midwest study (17). The NO_x was taken to be pure NO_2 initially at a concentration of 10 ppb. This concentration is at the upper limit of the NO_2 concentrations observed in the 1974 Midwest study (17), which generally ranged from 5-10 ppb. As mentioned before, the NO_2 measurements are probably too high, so that 10 ppb NO_2 should be significantly higher than rural NO_2 levels. The reason for the choice of these hydrocarbon and NO_2 concentrations was to represent extreme rural concentrations that would favor formation of elevated ozone levels.

TABLE 3. DAILY MAXIMUM O_3: (HC) AND (NO_x) ALLOWED TO DECAY

Initial Propane	Initial O_3 (pphm)	Maximum O_3 (pphm) 1st day	2nd day
0.1	0	4.1	4.3
0.1	4	7.4	Decreasing
0.1	10	11.4	11.2
0.1	15	15.3	Decreasing
0.1	20	Decreasing	Decreasing

Initial concentrations at 0600: (CH_4) = 2 ppm, (CO) = 0.2 ppm, (NO_2) = 10 ppb, (H_2O) = 2 x 10^4 ppm.

These calculations show a number of interesting characteristics of rural ozone behavior. The O_3 maxima on the second day are, except for one case, lower than those on the first day. This is a consequence of the rapid decay of NO_x during the first day. In general, it can be concluded that the relative residence time of NO_x is much shorter than that of propane under these simulated rural conditions. When the initial O_3 concentrations are 0 and 4 pphm, they build up to 4.1 and 7.4 pphm, respectively, in the first day. When the initial O_3 concentrations are 10 and 15 pphm, relatively little change in concentration occurs in the first day. When the initial O_3 concentration is 20 pphm, this concentration decreases continuously during the first day. From these calculations, it appears highly unlikely that less reactive, "leftover" hydrocarbons would generate elevated rural O_3 levels. At the concentrations that these HCs and NO_x are likely to be present in rural atmospheres, these HCs could contribute to the lowering of already existing elevated rural O_3 levels. In the following discussion, a more probable explanation of the elevated rural O_3 levels is offered.

DISCUSSION

It is reasonable to assume that the high ozone concentrations generated in urban areas are transported into rural areas, particularly under meteorological conditions that retard their dispersion into the global atmosphere. This will result in an elevation of the rural ozone levels above the natural background ozone concentration. The longer that the adverse meteorological conditions persist, the greater the effect will be, and the greater the size of the area affected. The degree to which the elevated rural ozone concentrations are further increased, sustained, or diminished by further photochemistry in the rural areas on succeeding days depends on the concentrations of both HCs and NO_x that are present there. The preceding analysis strongly suggests that the less reactive, "leftover" HCs of the urban plume will not contribute importantly to sustaining or increasing the elevated rural ozone levels. (Unreacted NO_x from urban areas, where it is present in excess, will also be transported to rural areas and contribute to ozone formation there, but this aspect of the problem will not be discussed here because of the lack of reliable rural NO_2 data.) A more likely explanation for the persistence and increase of elevated rural O_3 levels is the reactions of new HC (and NO_x) emissions in the rural areas from local sources, both natural and man-made. The relative amounts of natural and man-made sources of rural HCs and NO_x is an unresolved question, which will not be discussed further here.

The relative importance of "leftover" HCs compared to fresh HC emissions in rural photochemistry can be deduced from detailed measurements of rural HC compositions. If the "leftover" HCs from urban areas are present in significant concentrations, this should be evidenced by an accumulation of less reactive species compared to more reactive ones in the rural atmosphere. This is because the more reactive species are removed much faster than the less reactive ones. This effect is similar to a separation of more volatile species from less volatile ones by fractional distillation. Detailed HC compositions have been measured in the 1974 Midwest study (18). There is little evidence of such fractionation in all of these data, both in samples taken at the ground and aloft. Thus it would be plausible to conclude that, for the area studied and for the conditions that existed during the study, the atmospheric HCs observed were representative, in the main, of local emission sources.

Some very interesting data were taken on August 1, 1974, in this Midwest study. Ozone measurements were reported, as shown in Figure 1, at a variety of elevations for 0704-0741, 1320-1414, and 1656-1754 hours (Figure 58, page 122 in reference 17). Concurrent nonmethane HC (NMHC) measurements were made at the ground and aloft at 0704-0741 and at the ground at 1210-1315. The early morning profile supports the conclusion of the preceding paragraph. The NMHC concentrations of 105 and 113 ppbC at the ground and at 2000 ft., respectively, represent the sum of the "leftover" NMHC and the new NMHC emissions, which are trapped by the early morning ground inversion. The concentration of 58 ppbC at 4000 ft. is the "leftover" NMHC concentration in the mixing layer, which is being augmented by leakage from the ground inversion layer and diminished by leakage into the inversion layer. The 35 ppbC

at 8000 ft. is the "leftover" NMHC in the inversion layer, which is being augmented by leakage from the mixing layer and diminished by leakage into the global atmosphere. At 1210-1315 hours, the ground inversion probably has burned away, and the NMHC concentration at the ground is 89 ppbC, which is intermediate between the ground and mixing layer values observed in the early morning.

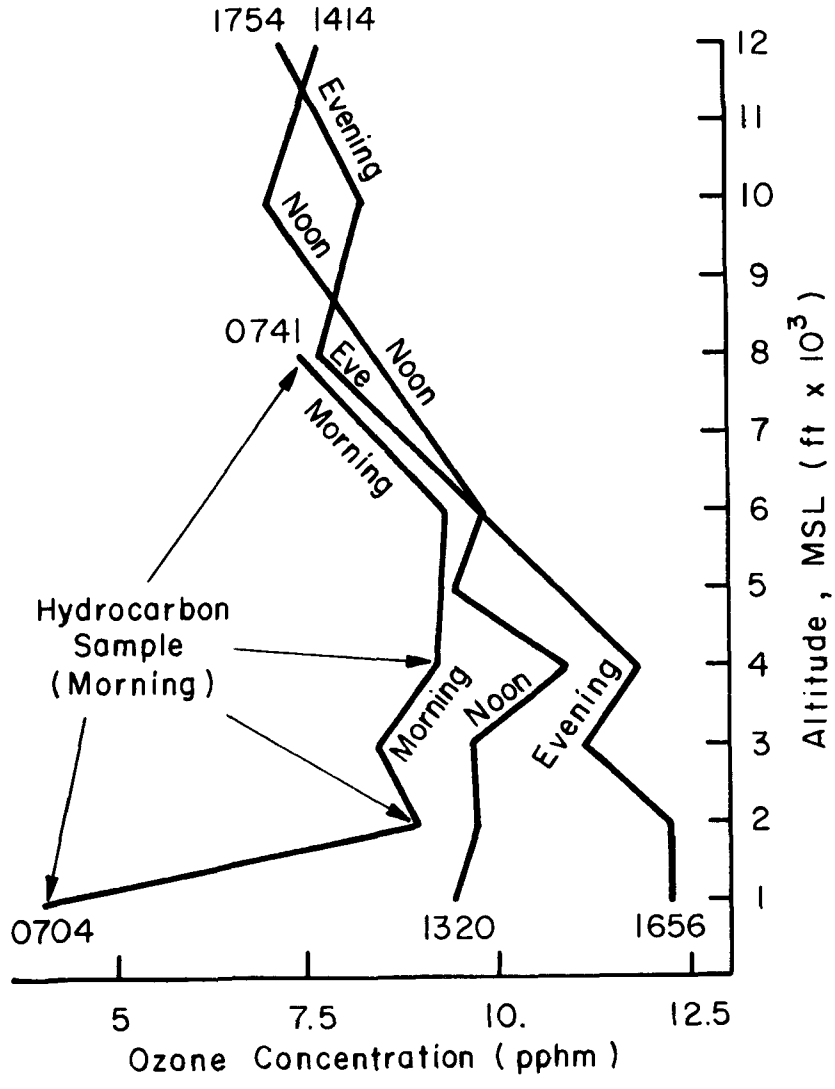

Figure 1. Ozone profile, Wilmington, Ohio, August 1, 1974 (17) TNMHC: 2000 ft., 113 ppbC; 4000 ft, 58 ppbC; 8000 ft., 35 ppbC at 0704-0741 hours; ground, 105 ppbC at 0745-9000 hrs; ground, 89 ppbC at 12-1315 hrs.

The ozone profiles are most revealing. The concentrations in the ground inversion layer in the early morning decrease markedly with decreasing altitude because of ground destruction of O_3. (The lines drawn in Figure 1 simply connect individual measurement points.) The concentrations in the mixing layer are relatively constant with altitude at about 9 pphm. This would be representative of an initially elevated O_3 level as analyzed in Table 3. The one point measured in the inversion layer is at about 7.5 pphm O_3. At noon, when the ground inversion has burned away, the O_3 concentrations in the mixing layer are constant with altitude at about 10 pphm, which is above the early morning 9 pphm value. The O_3 concentrations in the inversion layer are seen to be constant with altitude and unchanged from the early morning value. The evening measurements show the same trend. The concentration in the mixing layer has increased further to about 12 pphm, while that in the inversion layer is still at 7.5 pphm.

These data thus illustrate the explanation that is offered here for the elevated rural O_3 levels. The increase in the elevated O_3 concentration in the mixing layer is a consequence of reactions of fresh HCs (and NO_x) emitted into the mixing layer. It is likely that the "leftover" HCs there play only a minor role in augmenting this increase. There is no change in the elevated O_3 concentration in the inversion layer, because little fresh HCs are added there and it has mainly "leftover" HCs to react.

CONCLUSIONS

The preceding analysis and discussion disagrees with the conclusions in the new EPA Policy Statement (2). The extreme control of all HC emissions regardless of reactivity that is stated there to be necessary in order to resolve the rural O_3 problem is shown here to have a questionable basis. We conclude here instead that the present control strategy, based on reducing O_3 levels in urban areas, will also be effective in reducing rural O_3 levels. HC reactivity scales relevant to urban O_3 will be considered next.

In urban areas, the conversion of NO to NO_2 plays an important role in the time-dependent smog chemistry. (In rural areas, by contrast, the NO emissions are rapidly converted to NO_2 because of the excess O_3 present.) It has been pointed out that the NO-NO_2 conversion is driven largely by HO chain reactions, and a reactivity scale based on HO-hydrocarbon rate constants gives a representation of this (6). Pitts et al. recently have published a detailed study of this concept (19). Reactivity scales based on smog chamber data (20) are equivalent to this (6).

The NO-NO_2 conversion is only the first stage of O_3 production in urban areas as has been pointed out before (6). In the later stages of the reaction, the NO_2 is rapidly consumed and the O_3 concentration builds up. An HO reactivity scale does not give an adequate representation of these later stages of the reaction. In addition, HO reactivity scales do not take into account the dilution of the reactants by dispersion. As a consequence, we believe that HO reactivity scales overpredict the reactivity of less reactive hydrocarbons compared with more reactive hydrocarbons.

To take account of the later stages of the reaction in the reactivity scale, a factor should be introduced to express the effectiveness of different HCs in producing a net increase of radical species present. This would also improve the reactivity scale for the first stage of the reaction. Our understanding of the detailed chemical mechanism is not good enough at this time to make a reliable estimate of this factor. Qualitatively, we know that olefins are very effective in producing radical species because they often produce two new ones for each one they consume. Alkanes, on the other hand, more commonly break even in this respect, producing a single new radical for each one consumed. The failure to include this net radical production concept in the reactivity scale, then, qualitatively underpredicts the reactivity of more reactive species and overpredicts the reactivity of less reactive species.

Another factor should be introduced into the reactivity scale to take atmospheric dilution of smog precursors into account. It is proposed that this could be approximated by multiplying the HO rate constant for each HC by a fraction, which would represent the fraction of emissions of that HC which are consumed in the urban area in a single day. For very reactive HCs, this fraction would be unity. For very unreactive HCs, this fraction would be close to zero. This procedure is suggested by the findings in this paper that leftover HCs from urban areas contribute only marginally to subsequent O_3 formation. Such a procedure would, in part, remove the overprediction of the reactivity of less reactive HCs in the reactivity scales based on HO reactivity or equivalently based on smog chamber data.

An important corollary to these conclusions is worth mentioning. In the last few years, catalysts have been used to meet the HC emission standards for motor vehicles. One concomitant effect of the use of catalysts is to reduce the photochemical reactivity of the HC emissions (21). Therefore, the reduced HC emissions of catalyst-equipped vehicles should have a much more beneficial effect on urban O_3 reduction than was expected without taking this change of reactivity into account.

ACKNOWLEDGMENT

The authors would like to express appreciation to Hiromi Niki for many helpful discussions.

REFERENCES

1. Dimitriades, B. and S. B. Joshi. Application of Reactivity Criteria in Oxidant-Related Emission Control in U.S.A. In: Proceedings of this Conference.

2. "Policy Statement on Use of the Concept of Photochemical Reactivity of Organic Compounds in State Implementation Plans for Oxidant Control," U. S. EPA, January 29, 1976.

3. Los Angeles Air Pollution Control District, Rule 66.

4. Weinstock, B. and T. Y. Chang. Methane and Nonurban Ozone. Presented at the 69th Annual Meeting of the Air Pollution Control Association, Portland, Oregon, June, 1976.

5. Chameides, W. and D. H. Stedman. Ozone Formation from NO_x in Clean Air. Environ. Sci. Technol. 10: 150-153 (1976).

6. Niki, H., E. E. Daby and B. Weinstock. Mechanisms of Smog Reactions. Advanc. Chem. 113: 16-57, 1972.

7. Hecht, T. A., J. H. Seinfeld and M. C. Dodge. Further Development of Generalized Kinetic Mechanism for Photochemical Smog. Environ. Sci. Technol. 8: 327-339, 1974.

8. Demerjian, K. L., J. A. Kerr and J. G. Calvert. The Mechanism of Photochemical Smog Formation. Adv. Environ. Sci. Technol. 4: 1-262, 1964.

9. Pitts, Jr., J. N., G. J. Doyle, A. C. Lloyd and A. M. Winer. Chemical Transformations in Photochemical Smog and their Applications to Air Pollution Control Strategies. NSF-RANN Grant AEN 73-02904 A02, Second Annual Report, October 1, 1974 - September 30, 1975. University of California Statewide Air Pollution Research Center, Riverside, Calif.

10. Hecht T. A., M.-K. Liu and D. C. Whitney. Mathematical Simulation of Smog Chamber Photochemical Experiments. EPA-650/4-74-040. U. S. Environmental Protection Agency, Washington, D.C. 20460, 1974.

11. Durbin, P. A., T. A. Hecht and G. Z. Whitten. Mathematical Modeling of Simulated Photochemical Smog. EPA-650/4-75-026, U. S. Environmental Protection Agency, Washington, D. C., 1975.

12. Niki, H. and B. Weinstock. Recent Advances in Smog Chemistry, EPA Scientific Seminar on Automotive Pollutants, EPA-600/9-75-003, U. S. Environmental Protection Agency, Washington, D.C., February, 1975.

13. Sickles, II., J. E. Ozone-Precursor Relationships of Nitrogen Dioxide, Isopentane, and Sunlight Under Selected Conditions. Ph.D. Thesis, University of North Carolina, Chapel Hill, N.C., 1976.

14. Chan, W. H., R. J. Nordstrom, J. G. Calvert and J. H. Shaw. Kinetic Study of HONO Formation and Decay Reactions in Gaseous Mixtures of HONO, NO, NO_2, H_2O, and N_2. Environ. Sci. Technol. 10: 674-682, 1976.

15. Kaiser, E. W. and C. H. Wu. (To be published.)

16. Heuss, J. M. Photochemical Reactivity of Mixtures Simulating Present and Expected Future Concentrations in the Los Angeles Atmosphere. Presented at the 68th Annual Meeting of Air Pollution Control Association, #75-16.1, Boston, Mass., June, 1975.

17. Research Triangle Institute. Investigation of Rural Oxidant Levels as Related to Urban Hydrocarbon Control Strategies. EPA-450/3-75-036, U. S. Environmental Protection Agency, Research Triangle Park, N.C., 1975.

18. Detailed HC Analyses referred to in (17); available from W. A. Lonneman, U. S. EPA.

19. Darnall, Karen R., A. C. Lloyd, A. M. Weiner and J. N. Pitts, Jr. Reactivity Scale for Atmospheric Hydrocarbons Based on Reaction with Hydroxyl Radical. Environ. Sci. Technol. 10: 692-696, 1976.

20. Proceedings of the Solvent Reactivity Conference. U. S. Environmental Protection Agency, Research Triangle Park, N.C., EPA-650/3-74-010, November, 1974.

21. Powers, T. F. The Oxidant Formation Potential of Emissions from Catalyst Equipped Vehicles. In: Proceedings of Specialty Conference on Ozone-Oxidants-Interactions with the Total Environment. APCA Southwest Section, March 1976, pp. 189-200.

APPENDIX

List of Reactions and Rate Coefficients

	Reactions	Rate Coefficient (K_i)*
R1)	$NO_2 + HV = NO + O$	k_1
R2)	$HONO + HV = HO + NO$	$6.8E\text{-}2k_1$
R3)	$HOOH + HV = HO + HO$	$3.5E\text{-}3k_1$
R4)	$ROOH + HV = RO + HO$	$3.5E\text{-}3k_1$
R5)	$RCO_3H + HV = RO_2 + HO$	$3.5E\text{-}3k_1$
R6)	$O3 + HV = OD + O_2$	$3.5E\text{-}3k_1$
R7)	$HCHO + HV = HO_2 + HO_2 + CO$	$4.7E\text{-}3k_1$
R8)	$HCHO + HV = CO$	$1.1E\text{-}2k_1$
R9)	$RCHO + HV = RO_2 + HO_2 + CO$	$1.2E\text{-}3k_1$
R10)	$RNO_2 + HV = RO + NO$	$3.5E\text{-}3k_1$
R11)	$OD + M = O + M$	4.7E+4
R12)	$OD + H_2O = HO + HO$	3.1E+5
R13)	$O + O_2 + M = O_3 + M$	2.1E-5
R14)	$O_3 + NO = NO_2 + O_2$	2.5E+1
R15)	$O_3 + NO_2 = NO_3 + O_2$	4.8E-2
R16)	$NO + NO_3 = NO_2 + NO_2$	1.5E+4
R17)	$NO_2 + NO_3 = N_2O_5$	4.4E+3
R18)	$N_2O_5 = NO_2 + NO_3$	1.4E+1
R19)	$N_2O_5 + H_2O = NHO_3 + HNO_3$	1.5E-6
R20)	$NO + NO_2 + H_2O = HONO + HONO$	1.9E-11
R21)	$HONO + HONO = NO + NO_2 + H_2O$	1.8E-5
R22)	$NONO + HNO_3 = NO_2 + NO_2 + H_2O$	2.2E-2
R23)	$NO_2 + NO_2 + H_2O = HONO + HNO_3$	8.7E-9
R24)	$NO + HO = HONO$	1.2E+4
R25)	$NO_2 + HO = HNO_3$	1.5E+4
R26)	$CO + HO = HO_2$	2.1E+2
R27)	$HNO_2 + HO = NO_2 + H_2O$	3.1E+3
R28)	$HNO_3 + HO = NO_3 + H_2O$	1.9E+2

(continued)

APPENDIX (continued)

	Reactions	Rate Coefficient (K_j)*
R29)	$NO + HO_2 = NO_2 + HO$	7.0E+2
R30)	$NO_2 + HO_2 = HNO_2 + O_2$	3.5E+1
R31)	$HO_2 + HO = H_2O + O_2$	1.5E+5
R32)	$O_3 + HO_2 = HO + O_2 + O_2$	2.2E+1
R33)	$O_3 + HO = HO_2 + O_2$	8.3E+1
R34)	$HC_2 + O = RO_2 + HO$	k_{34}
R35)	$HC_2 + HO = RO_2 + H_2O$	k_{35}
R36)	$CH_4 + HO = RO_2 + H_2O$	1.1E+1
R37)	$HCHO + HO = HO_2 + CO + H_2O$	2.1E+4
R38)	$RCHO + HO = RCO_3 + H_2O$	2.1E+4
R39)	$HOOH + HO = HO_2 + H_2O$	1.2E+3
R40)	$ROOH + HO = RO_2 + H_2O$	1.2E3
R41)	$RCO_3H + HO = RCO_3 + H_2O$	1.2E+3
R42)	$NO + RO_2 = NO_2 + RO$	7.0E+2
R43)	$NO + RCO_3 = NO_2 + RO_2$	1.5E+3
R44)	$NO_2 + RCO_3 = PAN$	3.5E+1
R45)	$PAN = NO_3 + RO_2$	3.0E-3
R46)	$RO + O_2 = \beta RCHO + (1-\beta)\ HCHO + HO_2$	4.4E-3
R47)	$RO + NO = RNO_2$	1.2E+2
R48)	$RO + NO_2 = RNO_3$	1.1E+2
R49)	$HO_2 + HO_2 = HOOH + O_2$	4.9E+3
R50)	$HO_2 + RO_2 = ROOH + O_2$	4.9E+3
R51)	$RO_2 + RO_2 = RO + RO + O_2$	4.9E+2
R52)	$HO_2 + RCO_3 = RCO_3H + O_2$	4.9E+3
R53)	$RO_2 + RCO_3 = RO_2 + RO + O_2$	4.9E+2
R54)	$RCO_3 + RCO_3 = RO_2 + RO_2$	4.9E+2
R55)	$O_3 =$	0
R56)	$RNO_3 =$	1.0E-4
R57)	$HNO_3 =$	5.0E-4

* in ppm-min units

THE KINETIC OZONE PHOTOCHEMISTRY OF NATURAL AND PERTURBED NONURBAN TROPOSPHERES

T. E. Graedel and D. L. Allara*

ABSTRACT

The diurnal kinetic photochemistry of natural and perturbed nonurban tropospheres has been represented by a computation using emissions and reactions of terpenes, ammonia, hydrogen sulfide, and other organic and inorganic species. The computational results for the unperturbed case are simultaneously consistent with nonurban observations of monoterpenes, methane, ozone, oxides of nitrogen, hydrogen sulfide, ammonia, sulfur dioxide, acetone, and total nonmethane hydrocarbons, for nitric oxide, hydrogen sulfide, and ammonia emission rates adjusted to give observed concentrations. Substantial amounts of ozone (∿32 ppb peak) can be produced in remote area tropospheres by photochemical processes. The injection of additional nitric oxide (simulating that transported from urban areas) increases the formation of organic and inorganic nitrate compounds; the ozone peak concentration, however, decreases to ∿29 ppb.

INTRODUCTION

The chemistry of natural tropospheres is regarded as potentially significant to interactive ozone chemistry, the atmospheric carbon monoxide budget, and natural sulfate and acid rain production among other issues. Despite the importance of these issues, the chemical processes remain largely unexplored and the emission rates of the reactants poorly defined.

In this paper we present the results of calculations representing the natural and perturbed nonurban troposphere, particularly as they apply to the chemistry and resulting concentrations of ozone in nonurban areas. The calculations show that some ozone formation occurs naturally by photochemical processes on non-anthropogenic emissions, but that the addition of anthropogenic nitric oxide has only minimal effect on remote area ozone concentrations.

GASEOUS EMISSIONS INTO NATURAL TROPOSPHERES

A large number of gaseous species are emitted from natural sources; those whose emissions have been quantitatively assessed are listed in Table 1. Many of the emission rates are based on observed global concentrations and

* Bell Laboratories, Murray Hill, New Jersey.

estimated atmospheric residence times; in these cases the emission rate quoted is that needed to provide a balance between known or estimated source and removal rates. The emission estimates are therefore sensitive to errors in the estimated residence time and in the global concentration assessment and should, in general, be regarded as "order-of-magnitude"(11) numbers only further limitation is that natural emissions processes are not the same in all geographical locations. (Terpene emission rates based on data from forests obviously could not be expected to apply to desert areas, for example.) Although some of the emission mechanisms postulated or identified differ under different conditions of terrain and vegetation, it is premature to do more than to simulate an average natural area in this study. The results must thus be regarded as "bulk-averaged chemistry," rather than as being strictly applicable to any particular geographic location.

TABLE 1. NATURAL EMISSION RATES OF ATMOSPHERIC GASES

Molecule	Initial Emission* Rate Estimate	Reference	Final Emission* Rate Chosen
CH_4	1.30×10^{-11}	Ehhalt, 1974	1.52×10^{-13}@
H_2S	1.87×10^{-10}	Kellogg, et al., 1972	1.87×10^{-11}
NH_3	2.31×10^{-11}†	Robinson and Robbins, 1970	1.15×10^{-11}
NO	1.00×10^{-11}	Robinson and Robbins, 1970	1.00×10^{-11}
Isoprene	1.84×10^{-12}†§	Rasmussen, 1972	1.84×10^{-10}
α-Pinene	$1.84 \times 10^{-}$§	Rasmussen, 1972	1.84×10^{-10}

* Units are g cm^{-2} sec^{-1}.

† These rates are diurnally varied in accordance with the patterns illustrated in Paper I.

§ Total terpene emissions assumed to be equally divided between isoprene and α-pinene.

@ This is the amount needed to balance CH_4 loss by reaction with $H\dot{O}$ in the fully mixed planetary boundary layer of average depth 1 km. Diffusion loss of CH_4 to the stratosphere is not included in these computations.

Detailed discussions of the bases for and uncertainties in these emission rates are presented by Graedel and Allara (1976, referred to as "Paper I").

CHEMICAL REACTIONS IN NONURBAN TROPOSPHERES

The inorganic compounds present in urban and natural atmospheres are similar, as are the chemical reactions describing their interactions. For O-H-N chemistry, we utilize a set of 40 reactions identical to those of Groups 1 and 2 of Graedel, et al. (1976, referred to as "Paper II"). The sulfur chemistry of Paper II treated only oxidized sulfur compounds. We have therefore devised an appropriate reaction set for reduced sulfur, which is given in Paper I. The combined reaction set for compounds of sulfur totals 37 reactions. The chemistry of ammonia is also the subject of a newly devised reaction set, described in detail in Paper I.

A significant difference between the difference between the chemistry of urban and natural tropospheres is the composition of the complex organic compounds. Urban atmospheres contain a variety of species derived chiefly from automotive emissions, petroleum processing and handling, and evaporated paint solvents. Remote area organics are largely derived from botanically emitted terpenes. In each case eventual chemical breakdown of the long carbon chains produces simple products such as the aliphatic aldehydes. We have devised chemically reasonable reaction chains for α-pinene and isoprene in the presence of common atmospheric species. Examples of these chains are shown on Figures 1 and 2; full descriptions are given in Paper I.

The total chemical reaction set, including both organic and inorganic processes, contains 333 reactions involving 207 distinct chemical species.

METEOROLOGICAL INFLUENCES

The effects of meteorological variables upon the concentrations of chemical species in the atmosphere are substantial, and very complex techniques are sometimes utilized for the treatment of meteorological parameters. For studies that attempt to elucidate chemical mechanisms rather than detailed spatial structure, however, it appears sufficient to use somewhat simplified descriptions of the operational meteorology. Following the computational techniques of Paper II, therefore, we define the diurnally varying reaction volume by the mixing depth pattern specified therein and also use the diurnal variation in solar photon flux described. For the natural troposphere calculation we impose the further requirement of spatial homogeneity of emissions and terrain within the diurnal wind fetch; this allows advection to be neglected. Within the reaction volume thus defined, all chemical species are regarded as fully mixed, i.e., the concentrations of all species are spatially constant within the volume. The assumption of full mixing on a molecular scale appears to be relatively accurate during days of normal convective turbulence; near-uniform vertical concentrations of many chemical species have been measured at such times by airborne instruments (e.g., Blumenthal and White, 1975). Such an assumption is less valid during the stable nighttime hours, however, and we anticipate that our computation more accurately represents the physical mixing conditions that are present in the daytime troposphere.

RESULTS

The computed diurnal variations of a number of species in the unperturbed

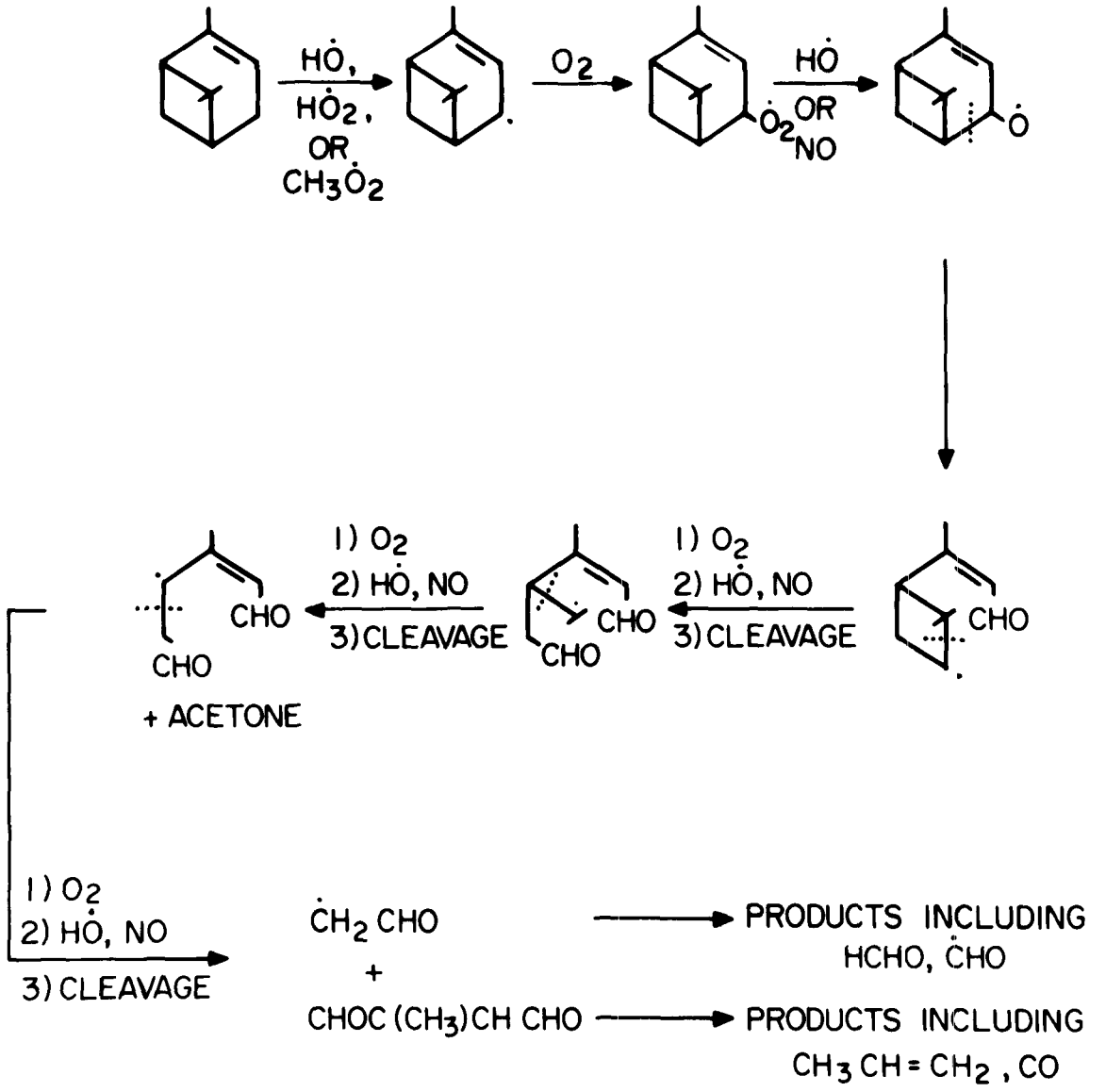

Figure 1. Schematic display of the chemical reaction sequence for hydrogen abstraction from α-pinene. The dots indicate the location of the unpaired electron bond; the dotted line shows the bond that cleaves on the subsequent rearrangement or disproportionation. The end products of the chain are relatively simple free radicals or stable molecules that participate in common atmospheric reactions. Some of the most significant of the products are indicated, but the chemical balance present in the actual equations is not necessarily reflected.

nonurban troposphere are illustrated in Figure 3. The comparison of these results with the sparse quantities of field data are discussed in detail in Paper I; the concentrations calculated agree to within a factor of ∿3 for nearly all species that have been measured in natural atmospheres and included in our study: nitrogen oxides (NO_x), ammonia (NH_3), hydrogen sulfide (H_2S), sulfur dioxide (SO_2), formaldehyde (HCHO), carbon monoxide (CO), methand (CH_4),

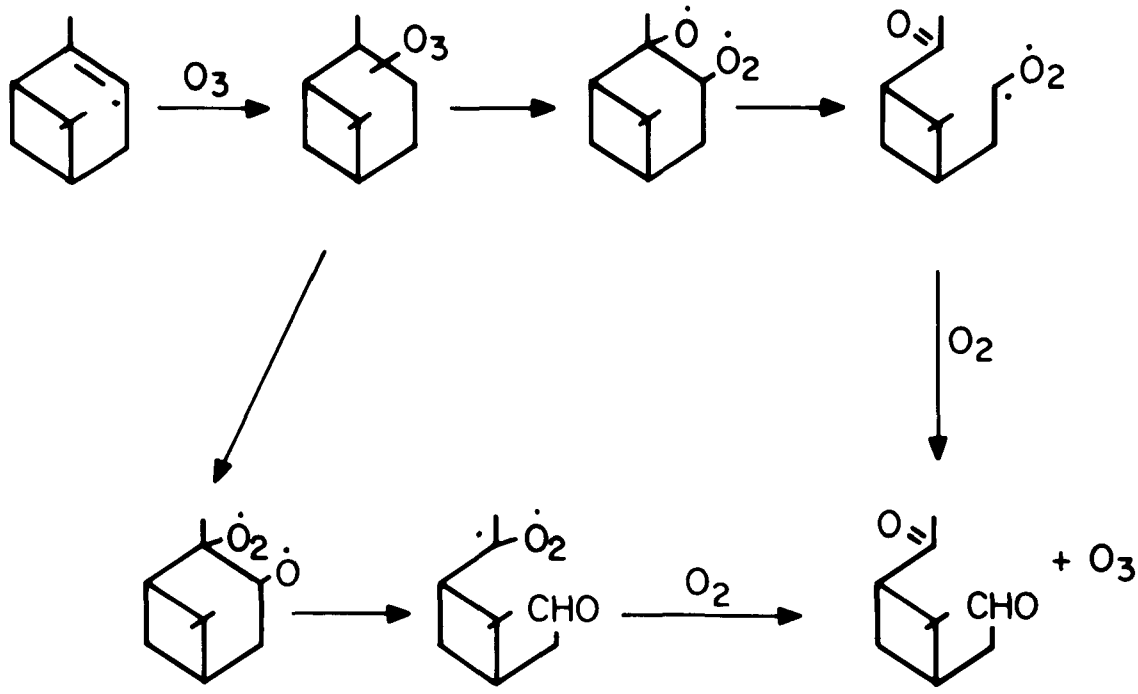

Figure 2. Schematic display of the chemical reaction sequences for ozone attack on α-pinene.

isoprene, α-pinene, acetone, and total nonmethane hydrocarbons. This is particularly satisfactory since formaldehyde and acetone are chemical products and thus validate the general chemical treatment as well as the emission and meteorological aspects of the computation.

The exception to the good agreement discussed above is ozone, whose concentration is generally measured at $\leq$ 60 ppb in nonurban areas, rather than the 32 ppb computed here. The ubiquitous presence of ozone in the mid-troposphere is well known, however, and the incorporation of this ozone into the expanding morning mixed layer is probable. This process (termed the incorporation of "fossil" ozone by Ripperton, 1974) is thus expected to increase the ozone concentrations in the lower troposphere. We are incorporating this effect into calculations now in progress and will report the results separately. The combined effects of local photochemistry and fossil ozone injection may be thought of as producing the natural ozone background in vegetated areas subject to normal stratospheric-tropospheric mixing processes.

A final consideration of interest is the effect of transported anthropogenic emissions on nonurban chemistry. Since remote areas have abundant sources of hydrocarbons and meagre sources of oxides of nitrogen, transport of the latter is more likely to influence the natural chemical cycles. To assess this effect, we add to the natural nitric oxide (NO) source strength an amount sufficient to maintain a daily NO_x concentration of $\sim$20 ppb (shown by Robinson (1976) to be indicative of the transport of urban air into nonurban regions). The response of the remote area ozone balance to this new source strength is rather small; the diurnal peak value decreasing from 32 ppb to 29 ppb. Similar results

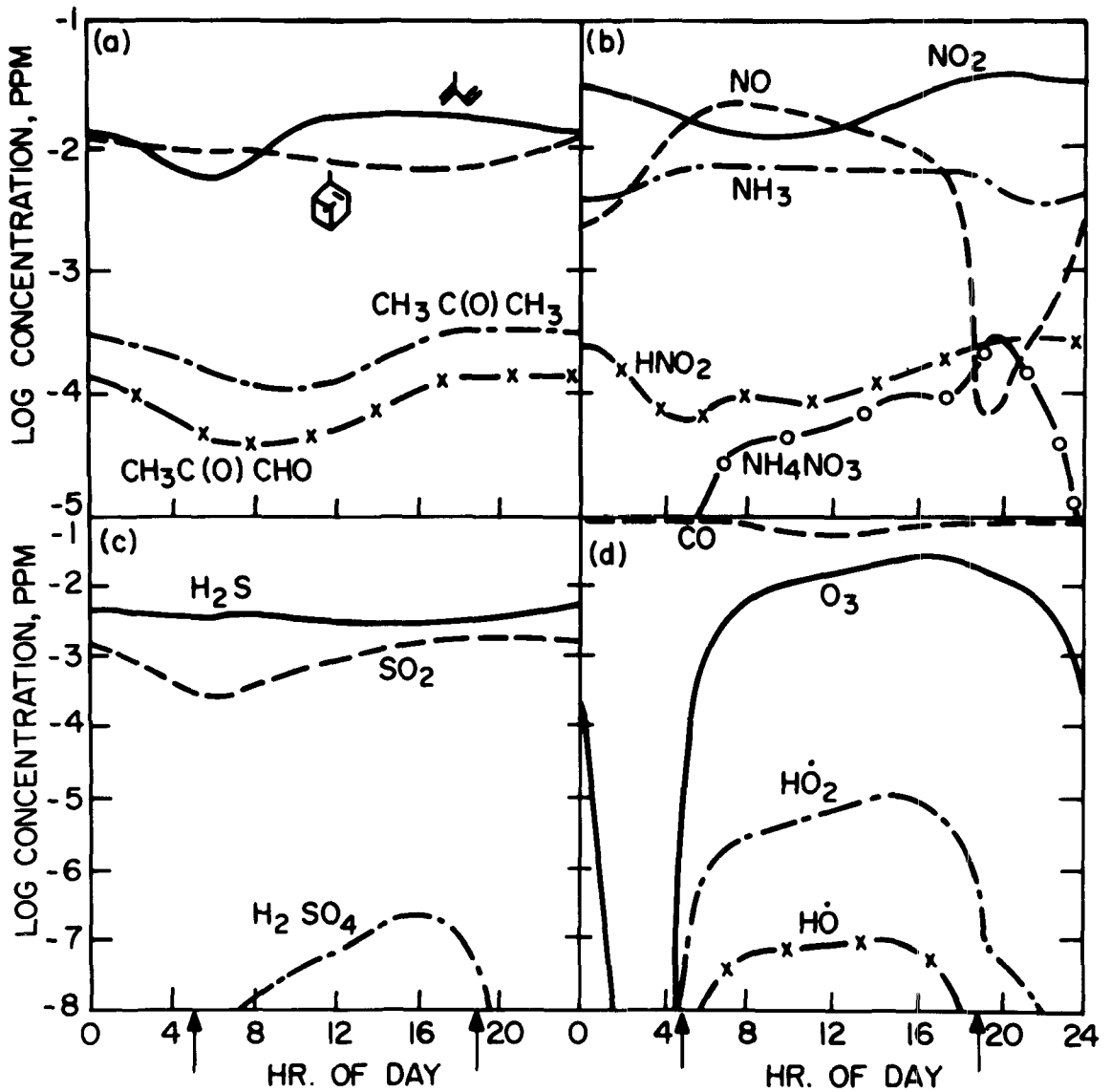

Figure 3. Computed diurnal concentrations of selected chemical species in the nonurban troposphere. Arrows on this figure indicate times of sunrise and sunset.

have been observed when rural Ohio air is "spiked" with NO (Rasmussen, 1975). The increased concentrations of NO and nitrogen dioxide (NO_2) from urban injection thus have little effect on ozone concentrations, since chemical buffering of the NO_2/NO ratio is strong, but increase the levels of inorganic and organic nitrate compounds. The computed ammonium nitrate peak concentration may be cited as an example of this effect; its computed values are 4 ppt (no NO injection) and 103 ppt (NO injection). Other nitrate compounds show similar effects.

SUMMARY

The chemistry of ozone in remote areas is complex and responds to a variety

of stimuli. The natural sources, together with photochemical and thermochemical processes, produce a rich spectrum of chemical reactions and generate moderate amounts of ozone. This photochemically produced ozone, together with any preexisting ozone in the nonurban troposphere, combine to form a naturally-produced ozone background. This natural background can be affected to some degree by the transport-generated injection of anthropogenic contaminants, but calculations representing the injection of NO show such perturbations to be minimal.

REFERENCES

Blumenthal, D. L., and W. H. White, The stability and long range transport of ozone or ozone precursors, paper presented at 68th Annual Meeting, Air Pollution Cont. Assoc., Boston, June 16, 1975.

Ehhalt, D. H., The atmospheric cycle of methane, Tellus, 26, 58-70, 1974.

Graedel, T. E., L. A. Farrow, and T. A. Weber, Kinetic studies of the photochemistry of the urban troposphere, Atmospheric Environment, (in press), 1976, Paper II).

Graedel, T. E., and D. L. Allara, The kinetic photochemistry of natural tropospheres, submitted for publication, 1976, (Paper I).

Kellogg, W. W., R. D. Cadle, E. R. Allen, A. L. Lazrus, and E. A. Martell, The sulfur cycle, Science, 175, 587-596, 1972.

Rasmussen, R. A., What do the hydrocarbons from trees contribute to air pollution?, J. Air Pollution Contr. Assoc., 22, 537-543, 1972.

Rasmussen, R. A., Recent field studies, in Scient. Sem. on Automotive Pollutants, EPA-600/9-75-003, Environmental Protection Agency, Washington, D. C., 1975.

Ripperton, L. A., Eastern United States high ozone concentrations: chemical aspects, Clean Air, 4 (16), 79-82, 1974.

Robinson, E., and R. C. Robbins, Gaseous nitrogen compound pollutants from urban and natural sources, J. Air Pollution Contr. Assoc., 20, 303-306, 1970.

Robinson, E., and R. A. Rasmussen, Identification of natural and anthropogenic rural ozone for control purposes, Proc. Specialty Conf. on Ozone/Oxidants-Interactions with the Total Environment, Pittsburgh: Air Pollution Contr. Assoc. 3-13, 1976.

SESSION 10

PHYSIOLOGICAL EFFECTS OF OXIDANTS - I

Chairman: J. Knelson
Environmental Protection Agency

ON THE RELATIONSHIP OF SUBJECTIVE SYMPTOMS TO PHOTOCHEMICAL OXIDANT

I. Mizoguchi, K. Makino, S. Kudou, and R. Mikami*

ABSTRACT

The daily incidences of acute subjective symptoms in 515 students of a junior high school were recorded for a 61-day period and were analysed in relation to environmental factors, especially prevalence of photochemical oxidants. Simple and multiple correlation analyses and multi-variate analysis were used to investigate the relationship between environmental factors and the symptoms. In addition, incidences of symptoms connected with predispositions, such as allergy, asthma, and orthostatic dysregulation, were compared under different oxidant levels. Eye irritation, throat irritation, shortness of breath, and headache correlated significantly ($p<0.001$) to ozone. Throat irritation, cough, and phlegm correlated significantly to sulfur dioxide, too. Humidity showed significant negative correlation to cough, lethargy, phlegm, throat irritation, and shortness of breath. Studies on the multiple correlation coefficients showed highly significant correlations between different pairs of environmental factors including oxidants and several symptoms. The result of a principal component analysis suggests that there are associations between oxidant, sulfur dioxide, suspended particulate matter and eye irritation, hoarseness, sore throat, headache, and so on. The incidences of the symptoms were compared with reference to the predispositions of the students. A significant increase in the incidence of cough was observed in asthma group; the orthostatic dysregulation group showed appreciable increases in the incidence of headache and lethargy in the days in which oxidant levels exceeded 0.15 ppm.

INTRODUCTION

During the summer many residents in metropolitan Tokyo and the Tokaido megalopolitan areas manifest symptoms caused by photochemical oxidants. This has become of considerable social concern in recent years. Hausknecht (1) reported that changes in chronic conditions related to oxidants and other weather factors were noted by eye complaints, asthma, and nose and throat complaints. In Japan similar reports (2, 3, 4) were recently published in journals and governmental reports. In our country, the deleterious effects of photochemical oxidants first attracted public attention when the shocking

*I. Mizoguchi, K. Makino, Tokyo Metropolitan Research Laboratory of Public Health, Tokyo, Japan.
S. Kudou, R. Mikami, School of Medicine, University of Tokyo, Tokyo, Japan.

episode at the Rissho Girls High School took place on July 18, 1970. Scores of girls playing handball on their campus suffered eye and throat irritation, and shortness of breath. More than 10 of them had trouble in breathing and temporary clouding of consciousness and were admitted to a neighboring hospital. Attacks like the Rissho High School episode have occurred a few times every year since then. The oxidant level in Tokyo is gradually rising. It is a most important problem for us to reveal the extent of actual effects of photochemical oxidants on health and to encourage control.

Since 1974 we have been conducting investigations on the relationship between multiple variables including subjective symptoms, photochemical oxidants, other air pollutants, meteorological factors, and clinical signs in students of a junior high school located in southeastern Tokyo (ca 12 km away from the center). In our investigation period, maximum oxidant concentration was 0.23 ppm, and clinical examinations were carried out under 0.17 ppm oxidant level. The values of respiratory function tests were not different from control values. The only signs we found were decreases in lysozyme activities and in the pH of tears (5). Analyzing the daily incidences of subjective symptoms related to environmental conditions presented several interesting clues, however.

MATERIALS AND METHOD

POPULATION AND SUBJECTIVE SYMPTOMS

The study population was composed of students of a public junior high school located in a southeastern area of Tokyo. Almost all students of this school live within 1.5 km from the school. Five hundred fifteen students recorded 17 symptoms every day from May 20th to July 19th, in 1974. These symptoms previously recorded in health diaries are shown in Table 1. The time and place in which each student became aware of symptoms were recorded. Subjective symptoms used were those which occurred from 8 am to 5 pm. Daily incidences of the symptoms are indicated by percentages of all 515 students. Frequencies of several symptoms and daily maximum oxidant and sulfur dioxide concentrations are shown in Figure 1. Stars at the top of Figure 1 indicate the days when maximum oxidant concentrations exceeded 0.15 ppm. It will be noticed that oxidant peaks correspond with peaks of frequencies of most symptoms. Such crude data were subjected to statistical procedures.

In order to examine incidences of the acute symptoms with reference to the predispositions of the students, three subgroups were picked out of all 515 students according to questionnaires (Table 2): allergy, asthma, and orthostatic dysregulation (O.D.). In Japan, O.D. is a present important problem in the field of school health administration. Although the concept has not been established completely, it seems that its entity is something different from postural hypotension. The criteria we used is shown in Table 3 (6). The number of students in each group were: Allergy group = 74, Asthma group = 20, O.D. group = 47; some overlapped each other.

TABLE 1. HEALTH DIARY

Check the proper space if you had symptoms below	Date	May 20 Mon.	May 21 Tues.	May 23 Wed.
1. Eye irritation				
2. Redness of conjunctiva				
3. Watering of eyes				
4. Blurred vision				
5. Cough				
6. Phlegm				
7. Sneeze				
8. Shortness of breath				
9. Hoarseness				
10. Sore throat				
11. Dizziness				
12. Headache				
13. Nausea				
14. Numbness of extremities				
15. Lethargy				
16. Abdominal pain				
17. Diarrhea				
Time when you had the symptoms		am pm	am pm	am pm
Place where you had symptoms: 1. Indoors 2. Playground 3. Outdoors 4. Outside school				
Duration		min hrs	min hrs	min hrs
Treatment (Ex: washing, gargling, etc.)				
Check if absent from school				
Reason for your absence				

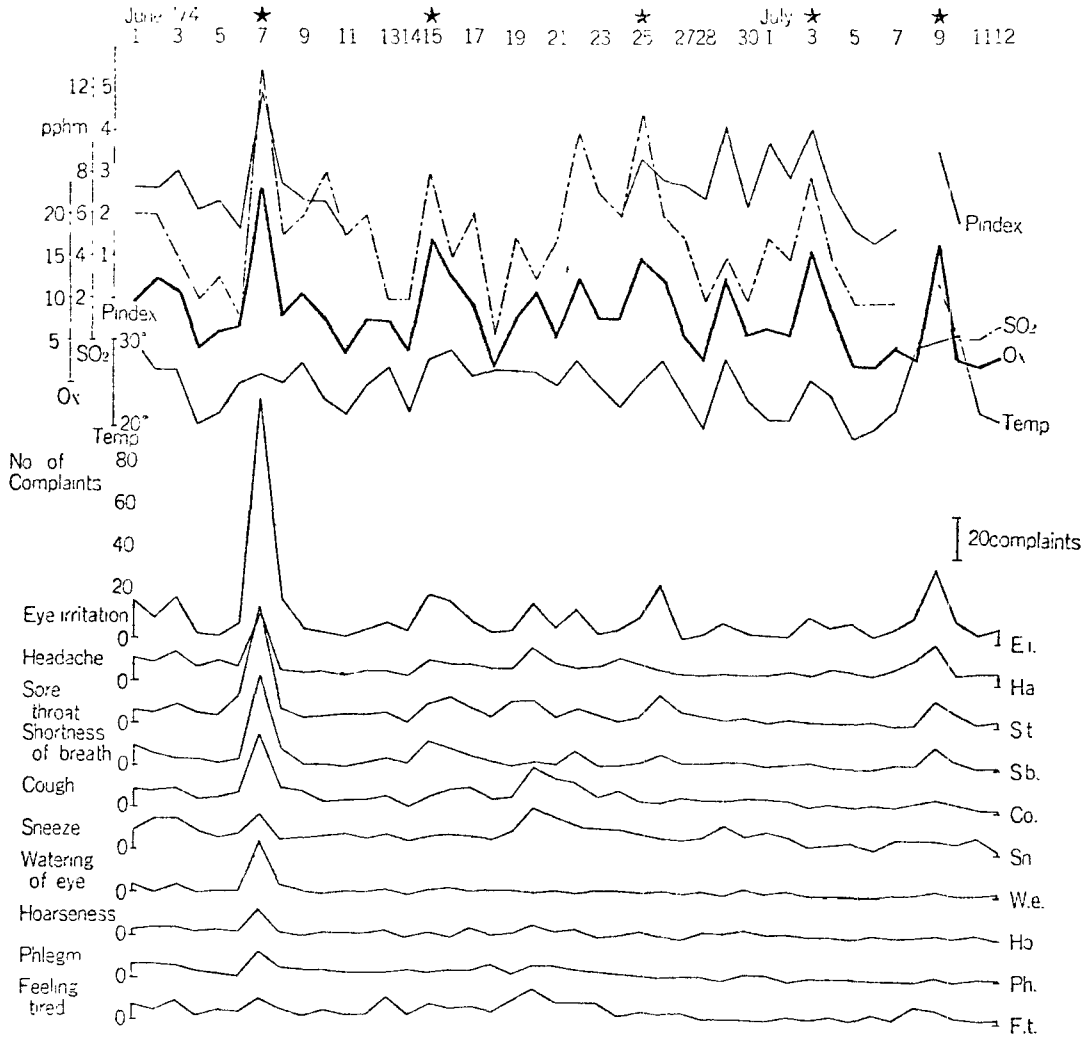

Figure 1. Correspondence of daily changes in subjective symptoms with oxidant concentrations.

AIR POLLUTION AND METEOROLOGICAL DATA

Oxidants, other air pollutants, and meteorological factors were measured every hour throughout this investigation period at a sampling room set up in the studied school. (Air pollutants and their measurement methods are shown in Table 4.) Meteorological factors obtained were temperature, relative humidity, wind speed, solar radiation, ultraviolet radiation, and visibility. Discomfort Index was calculated from temperature and humidity. Minimum values were used for humidity and visibility; maximum values of the other environmental variables were used.

TABLE 2. RATIOS OF YES TO ALL STUDENTS

QUESTIONNAIRES		%
1.	Having nausea	24
2.	Liable to be tired	22
3.	Liable to get carsick	19
4.	Frequently having headaches	18
5.	Frequently having sleep disturbances	14
6.	Liable to feel ill under difficult circumstances	13
7.	Liable to be irritated	12
8.	Liable not to feel refreshed in the morning	11
9.	Liable to feel dizzy	10
10.	Having urticaria	9
11.	Liable to be pale	6
12.	Frequently having eczema	5
13.	Having asthma attacks	4
14.	Liable to feel ill in a long erect posture	3
15.	Liable to palpitate or be short of breath after light exercise	3
16.	Having loss of appetite	3

TABLE 3. CRITERIA FOR GROUPING OF ORTHOSTATIC DYSREGULATION GROUP

	Major Symptoms		Minor Symptoms
	3	+	0
or	2	+	1
or	1	+	3

Major Symptoms: Nos. 6, 8, 9, 14, and 15 } From Questionnaire in
Minor Symptoms: Nos. 2, 3, 4, 11, and 16 } Table 2

TABLE 4. MEASURED ENVIRONMENTAL FACTORS

	Item	Method	
Air pollutants	O_x	Neutral Potassium Iodide	
	O_3	Chemiluminescence	
	SO_2	Conductimetric	
	NO	Saltzman	
	NO_2	Saltzman	
	HC(total)	Flame ionization	
	CO	Infrared absorption	
	Aerosol	Light scattering	
	SPM	High volume air sampler*	
	SO_4	Spectrometric*	
	NO_3	Spectrometric*	
	Aldehyde (total)	3-Methyl-2-Benzothiazolone hydrazone*	
One hour averaged for air pollutants *Four hours averaged			
Meteorological Factors		Temperature	^{o}C
		Relative humidity	%
		Discomfort Index	Calculated
Reading taken every hour			

STATISTICAL ANALYSIS

SIMPLE CORRELATION ANALYSIS

To study the relationship between the symptoms and environmental factors, simple correlation analysis was first adopted. Two variables were used: one was daily incidences of each symptom, the other was daily maximum value of each environmental factor for 61 successive days.

MULTIPLE CORRELATION ANALYSIS

Multiple correlation analysis was performed with three variables: one of the symptoms and a pair of environmental factors.

PRINCIPAL COMPONENT ANALYSIS

Principal component analysis is a mathematical and statistical method that has been used to derive principal components which represent a number of different variables. Variables of 17 symptoms and 14 environmental factors are analyzed. Principal components represent the degree of overlap or similarity among these variables as measured by correlation coefficients. Another interpretation is that principal components are synthetical characteristics that give weight to each variable and combine these variables primarily. Generally principal components are selected until the sum of ratios of the variances will exceed 60 per cent of the total variance. The ratio of 60 per cent is regarded to interpret most significant characteristics of the variables. The list of variables is contained in Table 7.

RESULTS

SIMPLE CORRELATION COEFFICIENTS

Figure 2 shows some typical variation of simple correlation coefficients between representative environmental pollutants and the symptoms. Exceedingly high correlation coefficients were noted between oxidant and eye irritation, sore throat, shortness of breath, headache, and blurred vision. The simple correlation pattern of ozone with variation of the symptoms, is noticed to be similar to that of oxidant. Sulfur dioxide and suspended particulate matter were revealed to have fairly high coefficient values to some symptoms such as sore throat, cough, phlegm, lethargy, and blurred vision. There are extremely high negative correlation coefficients between humidity and sore throat, cough, phlegm, lethargy, and sneezing. Besides there are significant ($p<0.01$) correlation between solar radiation and lethargy as well as between pollution index (Pindex) (8) and several symptoms. Table 5 is the list of all symptoms and environmental factors between which there are significant ($p<0.001$ and $p<0.01$) correlation coefficients (0.001 or 0.01 of significance level, used t-test, express extremely close associations). From mutual comparisons of values of the coefficients, the values of oxidant give us a large evaluation of contribution to occurrence of the symptoms. Wind speed and visibility have no significant correlation coefficients in spite of our expectation. The expectation came from observation of weather in the days when many students complained of mucous membrane irritations and respiratory symptoms.

MULTIPLE CORRELATION COEFFICIENTS

F-test was used to examine the significance of multiple correlation coefficients. Figure 3 shows that multiple correlation coefficients of subjective symptoms will change according to the pairs of air pollutants. Characteristic results of these analyses are significant from $p<0.005$ coefficients among several symptoms and pairs of environmental factors such as ox-SO_4, ox-Aldehyde, and ox-NO_3. Sulfate, nitrate, and aldehyde have no significant simple correlation coefficients to any symptoms, but their pairs, which include

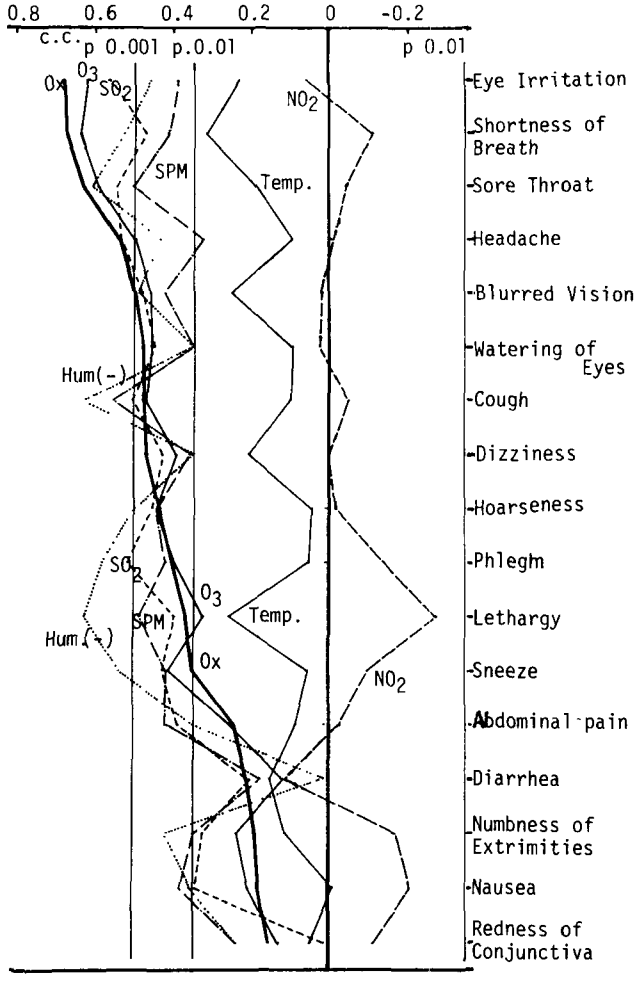

Figure 2. Changes in simple correlation coefficients between each environmental factor and symptoms.

oxidant, SO_2, or suspended particulate matter (SPM), have appreciably high values with several symptoms such as eye irritation, shortness of breath, sore throat, headache, blurred vision, watering of eyes, cough, dizziness, hoarseness, phlegm, and lethargy. If we adopt $p<0.01$ as the significant level, there are too many correlation coefficients to list in this limited space. For this reason, we adopted a severe significant level ($p<0.005$). In spite of this severe level, 29 combinations are listed in Table 6.

TABLE 5. EACH SYMPTOM AND ENVIRONMENTAL FACTOR BETWEEN WHICH THERE WAS A SIGNIFICANT SIMPLE CORRELATION COEFFICIENT

Symptoms	Environmental Factors p 0.001	p 0.01
Eye irritation	O_x, O_3, SO_2	Pindex, Hum(-), SPM, NO_3, Ald.
Shortness of breath	O_x, O_3, Hum(-)	SO_2, Pindex, SPM
Sore throat	O_x, Hum(-), O_3 SO_2, SPM	Pindex
Headache	SO_2, O_x	O_3, Hum(-), Pindex, NO_3
Blurred vision	O_x	Hum(-), SO_2, O_3, SPM, Pindex
Eye watering	---	Hum(-), Pindex
Cough	Hum(-), SO_2, SPM	O_x, O_3, Pindex
Vertigo	---	Pindex, O_x, SO_2, O_3, Ald., Hum(-), SPM, NO_3
Hoarseness	Hum(-)	Pindex, SO_2, O_3, O_x, SPM
Phlegm	Hum(-), SO_2	SPM, O_x, O_3, Pindex
Lethargy	Hum(-)	SPM, SO_2, O_x
Sneeze	Hum(-)	SO_2, SPM, O_3, O_x
Abdominal pain	---	SPM, SO_2, Hum(-)
Diarrhea	---	---
Numbness of extremities	---	Hum(-), SPM
Nausea	---	SPM, Hum(-)
Redness of conjunctiva	---	---

PRINCIPAL COMPONENTS

Three major principal components were produced, which altogether accounted for 63 per cent of the total variance of the data. These three principal components can be considered to have independent interpretation to each other and are shown in Table 7.

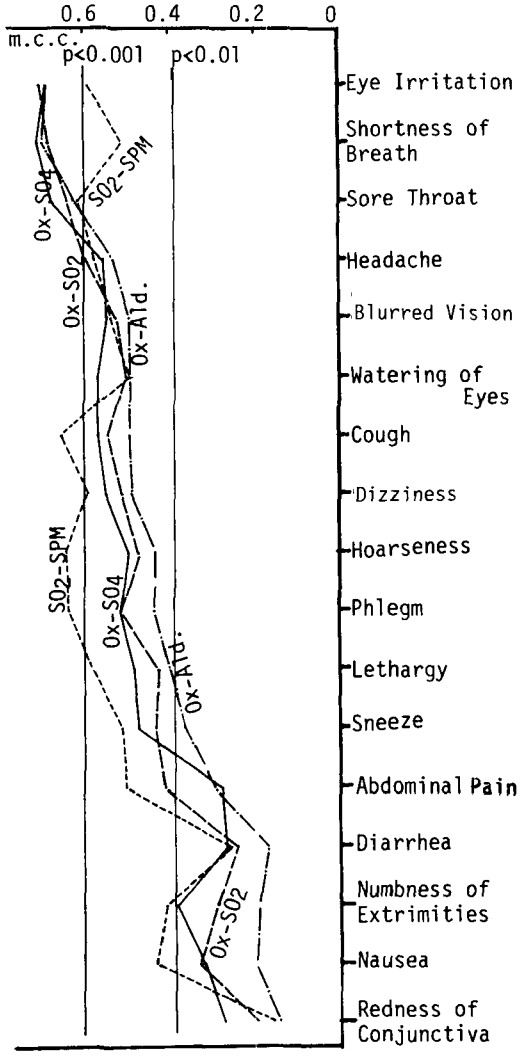

Figure 3. Changes in multiple correlation coefficients between each environmental factor and symptoms.

FIRST PRINCIPAL COMPONENT

The factor that has high loadings of variables is associated with respiratory symptoms such as sore throat and cough. Headache, eye irritation, hoarseness, blurred vision, shortness of breath, and phlegm follow. Thus, this principal component is associated with irritation of mucous membranes as well as respiratory symptoms. High loadings of headache, lethargy and dizziness suggest an association of this component with other systemic symptoms to some extent. In addition, oxidant, ozone, and sulfur dioxide have high

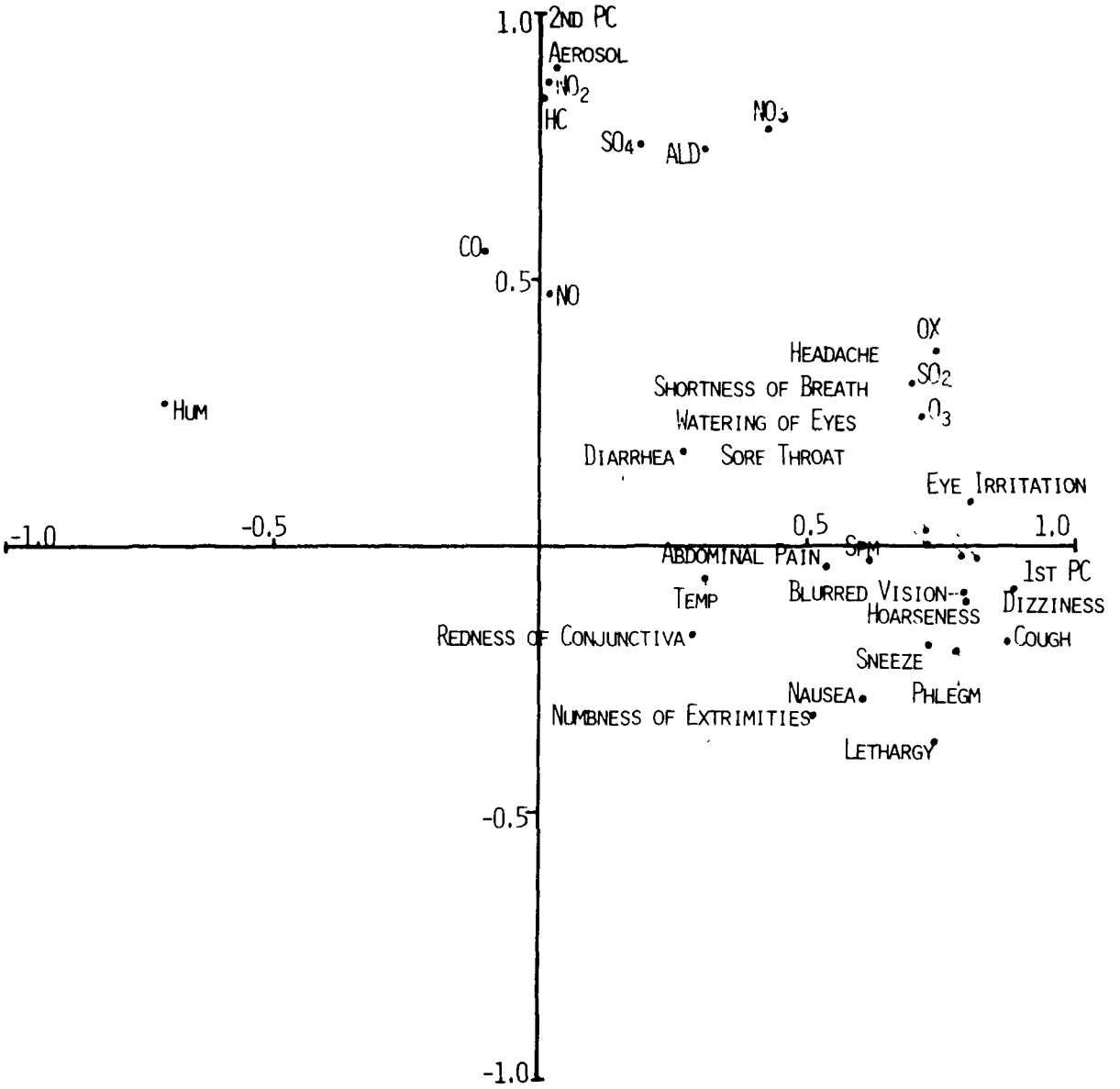

Figure 4. Distribution of the 1st principal components vs the 2nd principal components.

loadings, and it is recognized that oxidant affects symptoms mentioned above. The first principal component is considered to be a factor associated with "Photochemical Air Pollution."

TABLE 6. EACH SYMPTOM AND ENVIRONMENTAL FACTORS-COMPLEX BETWEEN WHICH THERE WAS A SIGNIFICANT MULTIPLE CORRELATION COEFFICIENT

Symptoms	Environmental Factors p 0.001
Eye Irritation	O_x-SO_2, O_x-SO_4, O_x-Ald., O_x-Temp., O_x-SPM, O_x-NO_3.
Shortness of Breath	O_x-SO_4, O_x-Ald., O_x-SO_2, O_x-Temp., O_x-NO_3, O_x-SPM.
Sore Throat	O_x-SO_4, O_x-SPM, O_x-SO_2, O_x-Temp., O_x-Ald., SO_2-SPM, O_x-NO_3.
Cough	SO_2-SPM, O_x-SPM, SPM-SO_4.
Hoarseness	SO_2-SPM, O_x-SPM, SPM-SO_4, SPM-NO_3, SPM-Ald.
Phlegm	SO_2-SPM, SO_2-SO_4.

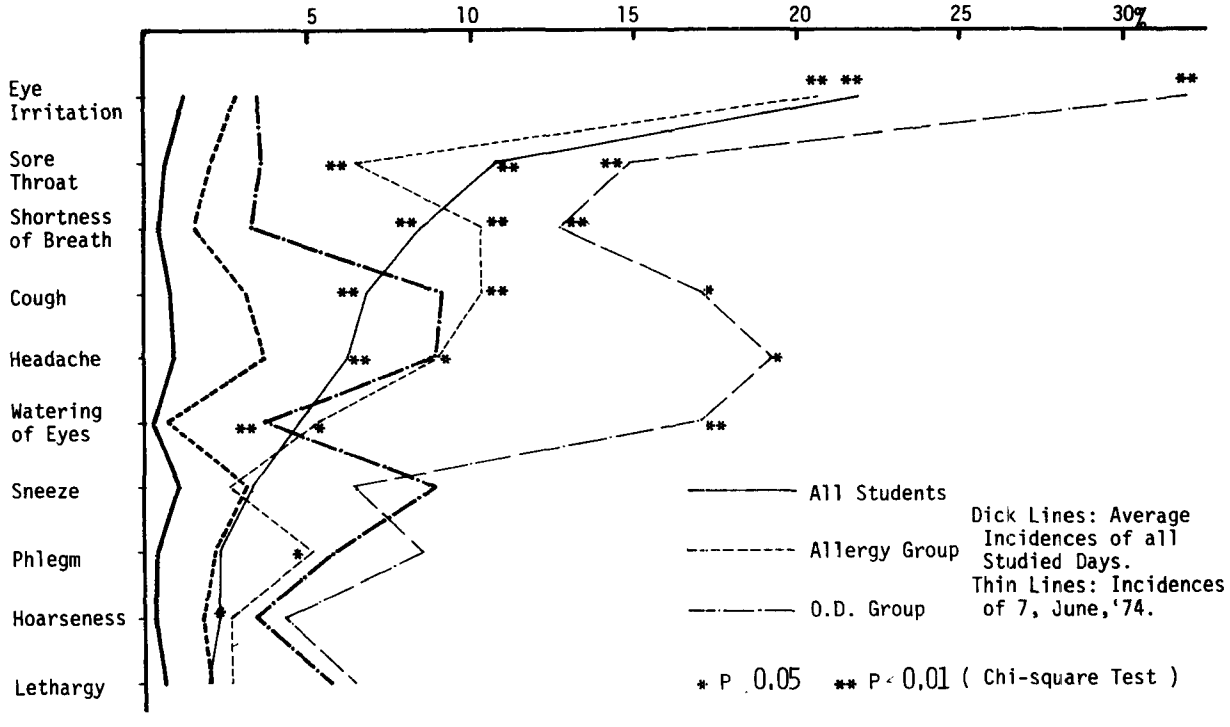

Figure 5. Changes in subjective symptoms related to oxidant concentration and subgroups. On June 7, 1974, oxidant concentration in Tokyo rose above 0.23 ppm.

TABLE 7. THE RELATIONSHIP AMONG SYMPTOMS, AIR POLLUTANTS, AND WEATHER FACTORS BY PRINCIPAL COMPONENTS ANALYSIS

Variables	1st PC	2nd PC	3rd PC
Air Pollutants & Weather Factors			
O_x	0.740	0.368	-0.386
O_3	0.717	0.249	-0.402
SO_2	0.691	0.309	-0.002
SO_4	0.187	0.752	-0.151
NO	0.016	0.476	-0.221
NO_2	0.013	0.872	0.176
NO_3	0.425	0.783	-0.029
CO	-0.104	0.555	0.604
Dust	0.024	0.900	0.143
SPM	0.618	-0.025	-0.075
Aldehyde	0.404	0.748	-0.047
HC	0.006	0.848	0.227
Temperature	0.310	-0.060	-0.632
Humidity	-0.706	-0.267	0.255
Symptoms			
Eye Irritation	0.813	0.086	-0.281
Redness of Conjuctiva	0.288	-0.164	-0.411
Watering of Eyes	0.722	0.031	-0.199
Blurred Vision	0.792	-0.087	0.021
Cough	0.879	-0.176	0.232
Phlegm	0.780	-0.197	0.302
Sneeze	0.726	-0.181	0.452
Shortness of Breath	0.789	-0.017	-0.371
Hoarseness	0.799	-0.095	0.280
Vertigo	0.881	-0.078	-0.125
Sore Throat	0.726	0.004	0.175
Headache	0.816	-0.020	0.136
Nausea	0.607	-0.284	0.444
Numbness of Extremities	0.510	-0.315	0.144
Lethargy	0.740	-0.361	0.234
Abdominal Pain	0.534	-0.036	0.376
Diarrhea	0.268	0.180	0.169

SECOND PRINCIPAL COMPONENT

Aerosol, nitrogen dioxide, hydrocarbon, nitrate, sulfur dioxide, aldehyde, and carbon monoxide have high loadings successively. These variables are the first air pollutants. The second principal component must be related to "High Air Pollution."

THIRD PRINCIPAL COMPONENT

Loadings of variables are less remarkable in this component, but this fact could be said to relate to "Temperature and Carbon Monoxide."

The variances of the first and second principal components account for 54 per cent of the total variance. The third accounts for only nine per cent and it does not have the features of factors that have high loadings. Other principal components have less per cent of variance than the third. In Figure 5, a scattering graph is drawn whose axes are first and second principal components. It shows that factors associated with photochemical oxidants are partial to right side and make a group, and that other factors distribute at random.

CONCERNING PREDISPOSITIONS

Figure 5 and Table 8 show changes in incidences of the symptoms both concerned with subgroups and also related to oxidant concentrations. The Chi-square test was carried out to examine differences between all days average incidences of all students and two subgroups: allergy and O.D. groups. In the allergy group, days averaged incidences of cough, phlegm, headache and dizziness were significantly ($p<0.05$) higher than those of all students. On the other hand, the O.D. group had significantly ($p<0.01$ or $p<0.05$) higher average incidences of most symptoms (indicated by single and double stars in column 4 of Table 8). The O.D. group seems to be a characteristic group; the O.D. students have a considerable number of complaints and have weak adaptability to changes in ambient conditions. In other words, they are most sensitive to the environment. The asthma group consists of too few examples to examine the differences; therefore we do not mention this group in this chapter.

Differences of the incidences which related to oxidant concentrations were tested separately in three different oxidant concentrations. The oxidant concentration was studied through all 75 days of the period. During the period, oxidant concentrations rose above 0.15 ppm during 5 days. It exceeded 0.23 ppm on June 7, 1974. A significant increase in the incidences in oxidant conditions is indicated by single ($p<0.05$) and double ($p<0.01$) stars in the 2nd, 3rd, 5th, 6th, 8th and 9th columns of Table 8 as well as in Figure 6. Figure 5 represents comparisons of incidences under varying oxidant levels.

In general, eye complaints, respiratory symptoms such as cough and shortness of breath and headache increase in the high oxidant conditions. While extremely significant increases of cough and phlegm are observed in the asthma group, the O.D. group shows characteristic increases of headache.

TABLE 8. INCIDENCES OF RESPECTIVE COMPLAINTS PER DAYS OF EACH SUBGROUP AND OXIDANT CONDITIONS (%)

	All Students			O.D. Group			Allergy Group		
	Av.	High O_x	Jun. 7	Av.	High O_x	Jun. 7	Av.	High O_x	Jun. 7
Eye Irritation	2.3	7.6**	21.9**	3.4	10.3**	31.9**	2.8	7.9**	20.5**
Sore Throat	1.2	3.5*	10.7**	3.7*	6.5	14.9**	2.0	2.7	6.4**
Shortness of Breath	0.8	2.8*	8.4**	3.2**	6.0	12.8**	1.5	3.4	10.3**
Cough	1.6	2.1	6.8**	9.1**	7.3	17.0*	3.1	3.4	10.3**
Headache	1.8	2.9	6.2**	9.0**	9.5	19.2	3.5*	4.5	9.0*
Watering of Eye	0.5	1.1*	4.7**	1.5*	3.5	17.0**	0.7	1.1	5.3*
Sneeze	2.0	1.7	3.3	8.9**	7.3	6.4	3.1	2.7	2.6
Phlegm	0.7	0.8	2.3	5.9**	6.0	8.5	2.1*	2.1	5.1*
Hoarseness	0.6	0.8	2.3*	3.4*	3.0	4.3	1.7	2.1	2.6
Lethargy	1.1	1.3	1.9	5.8**	4.7	6.4	2.0	1.6	2.6
Dizziness	0.4	0.7	1.2	2.4**	1.3	0.0	1.2*	2.4	2.7
Nausea	0.3	0.2	0.4	2.0**	1.7	2.1	0.8	0.5	2.6
Redness of Conjunctiva	0.3	0.4	0.6	1.3*	0.9	2.1	0.8	0.8	1.3
Abdominal Pain	0.5	0.6	0.4	2.3*	2.1	2.6	0.7	0.8	1.3
Diarrhea	0.1	0.2	0.2	0.8	0.9	0.0	0.5	1.1	1.3

* $p<0.05$
** $p<0.01$
Av.: Average incidences of all studied days (May 20-July 19, 1974).
High O_x: Average incidences of the 5 days when O_x concentrations rose above 0.15 ppm.
Jun. 7: O_x concentrations in Tokyo exceeded 0.23 ppm.

DISCUSSION

In this investigation period, weather in Tokyo was somewhat unusual. In June and early in July, wet and rainy days continue every year, in the so called Tsuyu season, but in 1974, Tsuyu season persisted until late in July and temperatures were lower than in more normal years. For this reason occurrences of photochemical smog in Tokyo were fewer and milder to some extent; therefore, signs except lysozymic activity and pH in tears may not have been found under this condition.

The searches for acute effects of air pollution through some respiratory function test (9, 10) and through the comparisons of frequencies and severities of attacks in asthma patients have been reported (11). These reports are excellent but do not focus on photochemical oxidant and leave something to analyse statistically.

There were some reports (12, 13) dealing with the effects of photochemical oxidant in which absenteeism and performance were used as parameters. Our study revealed that daily incidence of the symptoms correlated and associated closely with daily maximum oxidant concentration, as shown in this paper. It can be said that the subjective symptom is a more sensitive parameter.

Several problems remain, however, on the collection of daily frequencies of subjective symptoms related to photochemical oxidants. The first is evaluation for the bias occurring through the mental states of the students. If official smog warning information is given to a studied school, it is inevitable that mental situations and responses to the questionnaires in health diaries will change. We checked this bias by comparing frequencies of the symptoms with and without delivery of warning information at similar oxidant conditions. Results were not significantly different. However, more precise checking is required to evaluate this factor.

The second problem is a limit by which the students checked only symptoms recorded previously in health diaries. Acute effects of photochemical oxidant and other air pollutants may be more multifarious. The blank of free answer was not adopted in health diaries because of possible student reluctance to write. This might miss, however, other responses of the students to ambient conditions.

Means of delivery of health diaries is the third problem. From our experience, daily delivery and collection of diaries provoked more responses than at long intervals. In this investigation they were carried out monthly, and this interval may avoid excess responses. On the other hand, maintenance of constant concern of students was difficult.

It was reported (14) that most students who suffered from severe symptoms had allergic predisposition in the Rissho High School episode and other similar incidents. This research could not make a clear connection between allergic predisposition and severe symptoms. For the study concerning predisposition, more than 1500 samples are required because more than 50 at least are necessary as the population of a subgroup for statistical analysis in such a study period.

There are interactions and relations of photochemical oxidants to other air pollutants and weather conditions. Simple correlation analysis between these factors measured in this school to each other was carried out and reported (15). Its one point was that there were significant correlations between oxidants, ozone, sulfur dioxide, and suspended particulate matter. Our results from comparison of coefficient levels show, however, that oxidants contribute manifestly to occurrences of the specific symptoms.

Visibility and wind speed did not show significant correlation with any symptoms. However, short visibilities and slow wind speeds were pointed out on the days when many subjective symptoms were reported. This discrepancy comes from the fact that shortening of visibility is caused by smog and rain, and that slow wind speed not always bring about elevation of oxidant concentration. In a few cases of days when oxidant concentration exceeded 0.15 or 0.20 ppm, there were unusually scarce complaints of subjective symptoms. This problem requires more and different approaches. One of them is classification of air pollutants and weather conditions that vary in the day when many students complained of specific subjective symptoms.

REFERENCES

1. Hausknecht, R. Air Pollution: Effects reported by California Residents. Publ. California State Dept. Public Health, California, 1969.

2. Shimizu, T., and Y. Tsunetoshi, et al. Classified Subjective Symptoms of Junior High School Students Affected with Photochemical Air Pollution. J. of Japan Society of Air Pollution, 9(4); 734-741, 1975.

3. Makino, K., and I. Mizoguchi. Symptoms caused by Photochemical Smog. Japanese J. of Public Health, 22(8):421-430, 1975.

4. Sekizawa, N., et al. Effects of Tokyo Smog on Health. Annual Report of Tokyo Metropolitan Res. Institute for Environmental Protection, 5:206-227, 1974.

5. Shimizu, K., et al. Effect of Photochemical Smog on the Human Eye - Epidemiological, Biochemical, Opthalmological, and Experimental Studies. J. of Clinical Opthalmology, 30(4);407-418, 1976.

6. Ichihashi, Y., and M. Okuni, ed. Orthostatic Dysregulation. Chugai Med. Co. Ltd., Tokyo, 1974.

7. Okuno, T., H. Kume, T. Haga, and T. Yoshizawa. Multivariate Analysis. Nikkagiren Publ. Co. Ltd., Tokyo, 1975.

8. Babcock, L. R. A Combined Pollution Index for Measurement of Total Air Pollution. JAPCA, 20(10):653-659, 1970.

9. Toyama, T. Air Pollution and Its Health Effects in Japan. Arch Environ Health, 8:161-173, 1964.

10. Mcmillan, R. S., et al. Effects of Oxidant Air Pollution on Peak Expiratory Flow Rates in Los Angeles School Children. Arch Environ Health, 18:941-949, 1969.

11. Ishizaki, T., et al. Clinical Study of the Effect of Air Pollution upon Asthmatic Patients. J. of Japan Society of Air Pollution, 7(1):7-12, 1972.

12. Wayne, W. S. Oxidant Air Pollution and Athletic Performance. JAMA, 199:901-904, 1967.

13. Walborg, S. W., et al. Oxidant Air Pollution and School Absenteeism. Arch Environ Health, 19:315-322, 1969.

14. Mikami, R., and S. Kudo. Clinical Examination of Students Affected from Photochemical Smog. J. of Japanese Clinical Medicine, 31:2039-2044, 1973.

15. Mikami, R., et al. Survey Report on Health Effect of Photochemical Air Pollution, 1974, Tokyo B-Team. Bureau of Air Quality Control, Japan Environmental Protection Agency. Tokyo. 1975.

EFFECTS OF OZONE PLUS MODERATE EXERCISE ON PULMONARY FUNCTION IN HEALTHY YOUNG MEN

B. Ketcham, S. Lassiter, E. Haak, and J. H. Knelson*

ABSTRACT

Twenty healthy non-smoking male subjects were exposed to 0.6 ppm ozone for 2 hours in an environmental chamber. Each subject was seated at rest except for two 15-minute exercise periods on a bicycle ergometer. The exercise was sufficient to approximately double the resting heart rate. Subjects were asked to report any symptoms that occurred during the course of the chamber exposures and daily thereafter for the follow-up period. Pulmonary function studies included spirometry, maximum expiratory flow-volume curves, and body plethysmographic measurement of airway resistance and lung volumes. Changes in pulmonary function after 1 and 2 hours of ozone were compared to values obtained at the same times during a control 2-hour exposure to clean air. Most subjects exposed to ozone complained of cough, substernal chest pain, shortness of breath, and a decreased ability to maximally inspire. A few subjects continued with symptoms several hours post exposure. After 1 hour of ozone, maximal midexpiratory flow rate (MMFR), minute volumes (V_{25} and V_{50}), peak expiratory flow rate (PEFR), forced vital capacity (FVC), forced expired volume in 1 second (FEV_1), and inspiratory capacity (IC) were significantly decreased. After 2 hours of ozone exposure, decreases in these measurements were even greater, with the most marked change being a 35% reduction in mean MMFR over control. This test may be the most reliable and sensitive indicator of the adverse effects of ozone on lung function. Even though considerable individual variation in response was noted, it is concluded that a 2-hour 0.6 ppm ozone exposure, when coupled with moderate exercise, has a significantly detrimental effect on pulmonary function.

INTRODUCTION

Atmospheric photochemical reactions increase the oxidant content of the atmosphere, particularly over urban and industrialized areas (1). Ozone may account for as much as 90% of the total oxidant formed during periods of intense atmospheric photochemical activity (2). The genesis of very high hourly ozone concentrations during such phenomenon is now well understood (3). Some areas of Southern California have exceeded on many occasions, the maximum hourly ozone concentrations of 0.4 ppm (4,5). Moreover, recent reports indicate that the population at risk from oxidant pollution comprises a much larger segment of the population than previously estimated (6).

---

*U.S. Environmental Protection Agency, Research Triangle Park, North Carolina.

The present oxidant alert level is 0.6 ppm maximum 1-hour concentration. This level approximates peak smog episode levels found within the Los Angeles basin. This study was designed: (a) to better define the adverse health effects of short-term exposures to 0.6 ppm ozone utilizing a homogeneous group of human volunteers carefully selected to minimize intersubject variability and, (b) confirm earlier studies reporting impaired pulmonary function at these levels (7).

MATERIALS AND METHODS

Twenty healthy non-smoking male volunteers between the ages of 19 and 27 participated in this experiment. The mean anthropometric data for the group was: age, 22.7 years; weight, 73.4 kg; height, 180.1 cm. Normal healthy male subjects were selected by screening all candidates with a Minnesota Multiphasic Personality Inventory (MMPI), a complete medical history, a physical examination, and a complete blood cell count. Suitable subjects were candidates who were within normal limits on all screening tests. After obtaining informed consent to participate voluntarily in the study, final selection of the subjects was determined by an adequate performance in a chamber training session. Subjects were paid for the time of their participation at the rate of four dollars per hour. None of the subjects had a history of allergic, respiratory, or cardiac illness.

All exposures and the pulmonary function testing were conducted in a controlled environmental chamber (8'x8'x8') constructed of 1/2-inch plexiglass (8). Ozone was generated from pure oxygen using an OREC ozone generator and was injected into the chamber air-supply duct at a low pressure point. The air-ozone mixture was dispersed into the chamber through a perforated grill in the chamber ceiling. Ozone concentration was continuously monitored using a chemiluminescent analyzer (Bendix) and maintained to within $\pm$ 5% of the desired concentration.

Subjects were seated and resting in the chamber for the 2-hour protocol except for two 15-minute exercise periods on a bicycle ergometer (Quinton, Model 844) beginning at 30 and 90 minutes into exposure. The exercise was sufficient to approximately double resting heart rate as monitored by EKG. Subjects breathed filtered ambient laboratory air on control days (Friday a.m.) and 0.6 ppm ozone on exposure days (Monday a.m.) in an otherwise identical exposure protocol. A double blind protocol was not possible since the characteristic odor of ozone was readily detectable at the levels used. The ozone exposure always followed the air exposure because of the potential lingering effects of the ozone exposure.

Pulmonary function measurements for both the air and 0.6 ppm ozone exposures were made immediately prior to exposure (baseline) and after 1 and 2 hours of continuous exposure. These measures included spirometry (FVC, FEV_1, FEV_1/FVC, IC, FERV, and $FERV_1$), maximum expiratory flow-volume curves (MMFR, PEFR, V_{25}, V_{50}), and plethysmographic measurement (CPI, Model 1100) of airway resistance and lung volume. Spirometry was performed with the subject seated and breathing at tidal volume through a dry-seal rolling spirometer (Ohio, Model 840). At end-expiration (visually keyed) the subject inspired to total

lung capacity and performed forced vital capacity maneuvers. The subject then resumed tidal volume breathing for a few cycles and at the end of a normal expiration performed a forced expiratory reserve volume maneuver. All measurements were repeated at least three times. The output signals from the spirometer were used as input to (a) the x-y plotter (HP, Model 2FAM) for graphic displays of time-volume relationships, and (b) a PDP-12 computer programmed to perform time integration and differentiation of volume signals. Except for forced expiratory reserve volume and forced expiratory reserve volume in 1 second (FERV and $FERV_1$), all parameters were computer calculated. Plethysmographic measurements of airway resistance and lung volumes were calculated using the method of Dubois, et al. (9,10).

A multivariate, general, linear model was used for data analysis. Mean pre-exposure pulmonary function values for air and ozone were compared to changes at 1 and 2 hours, respectively.

RESULTS

Of the 20 subjects, 17 detected the ozone odor on entering the chamber on the exposure day. Those subjects who detected the smell of ozone were able to do so for a variable amount of time. Although some subjects reported that they became unaware of an odor after several minutes to an hour, seven subjects were aware of the ozone odor throughout the 2-hour exposure period, while three subjects did not detect the smell of ozone.

Immediately after the air and ozone exposures each subject completed a symptom questionnaire. An analysis of their responses has shown that exposure to 0.6 ppm ozone for 2 hours, when compared with exposure to air for 2 hours significantly increased the incidence and severity of certain symptoms. There was an increased incidence of severity of shortness of breath, cough, pain on deep inspiration, and chest pain with ozone exposure. These effects were most pronounced immediately post-exercise. Cough and pain on deep inspiration were the most commonly reported symptoms (see Figure 1). Four subjects complained of burning eyes during ozone exposure. This symptom was not noted during control sessions. A few subjects responded positively to sham symptoms of sneezing and/or paresthesias during the air and ozone exposures. However, these responses were not statistically significant. All symptoms were followed 24 and 48 hours after ozone exposure. Most symptoms resolved within 24 hours and no symptoms persisted beyond 48 hours.

Mean values for the pulmonary function tests performed are compared, and the significance of the difference determined using an analysis of variance (Table 1). The pulmonary parameters most affected by ozone exposure appear first. Significant decrements in air-flow parameters occurred after 1 hour of ozone exposure and were most evident in measurements of MMFR, PEFR, V_{25} and V_{50}. Significant reductions in FVC, FEV_1, FEV_1/FVC, and IC also occurred after 1 hour of ozone exposure. FERV, $FERV_1$, and airway resistance (R_{aw}) were decreased after 1 hour of ozone, but were of marginal statistical significance ($p \leq 0.05$, $p \leq 0.09$, $p \leq 0.08$, respectively). After 2 hours of ozone exposure, further significant reduction in MMFR, PEFR, V_{25}, V_{50}, FVC, FEV_1, FEV_1/FVC, and IC were observed. Moreover, the values for FVC, FEV_1, and IC were signi-

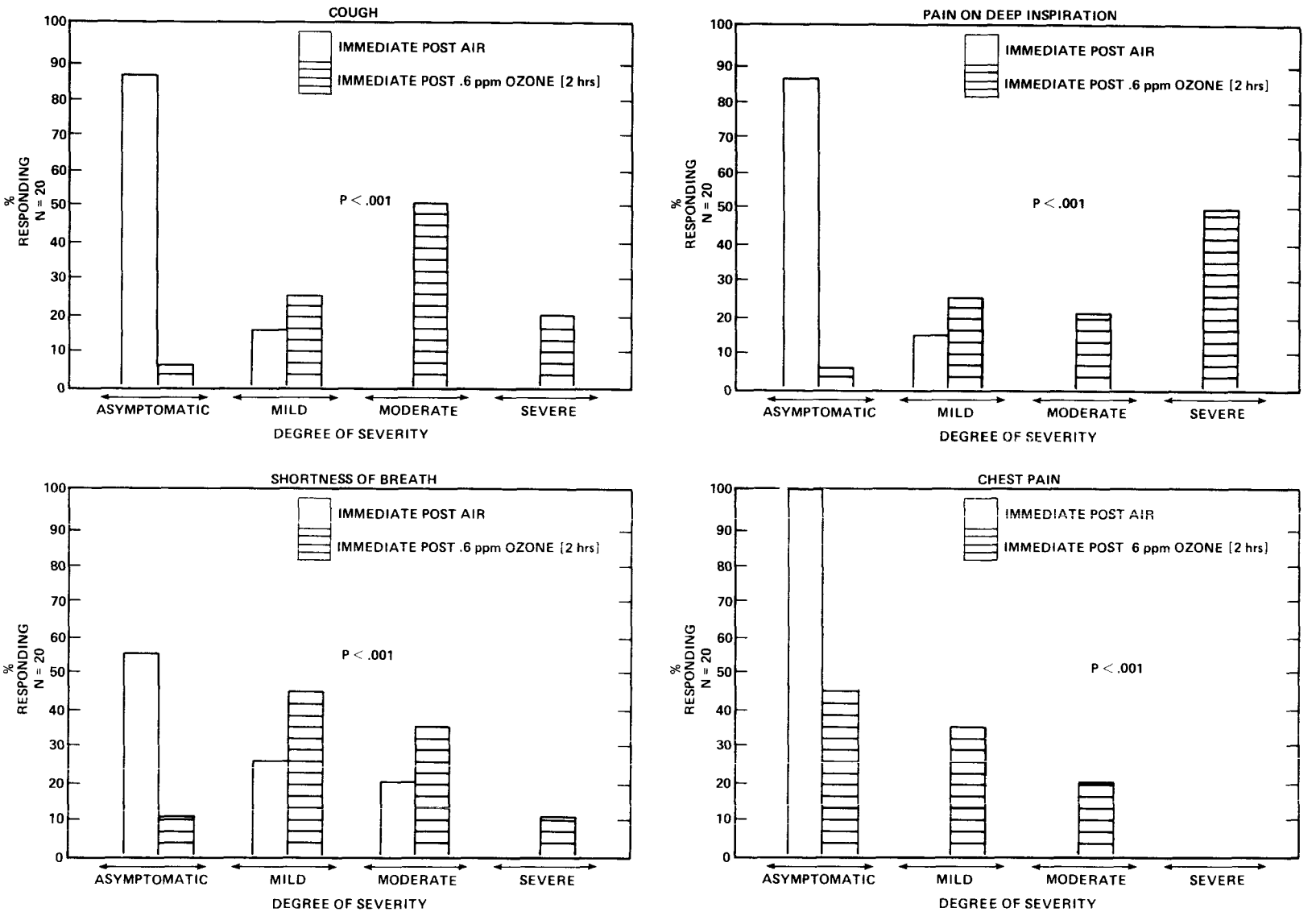

Figure 1. Significant symptoms; air vs. ozone.

TABLE 1. MEAN PULMONARY FUNCTION MEASUREMENTS AND RESULTS OF THE ANALYSIS OF VARIANCE FOR 20 SUBJECTS EXPOSED FOR 2 HOURS TO 1200 (0.6 ppm) OZONE AND CONTROL ATMOSPHERE OF AMBIENT AIR

	Control			O_3 (.6 ppm)			1 Hr Change on Air VS 1 Hr Change on Ozone	2 Hr Change on Air VS 2 Hr Change on Ozone
Variable	0 Hour	1 Hour	2 Hour	0 Hour	1 Hour	2 Hour	P	P
MMFR (L/sec)	5.03	5.01	5.00	4.82	3.54	3.13	.001	< .001
$\dot{V}_{25}$ (L/sec)	2.67	2.78	2.78	2.72	2.14	1.87	.04	.003
$\dot{V}_{50}$ (L/sec)	5.76	5.78	5.73	5.57	4.40	3.87	< .001	< .001
Peak Flow (L/sec)	9.83	9.83	9.57	10.15	7.63	7.15	< .001	< .001
FEV_1 (L)	4.43	4.51	4.54	4.51	3.57	3.23	< .001	< .001
FVC (L)	5.81	5.80	5.77	5.73	4.96	4.62	< .001	< .001
FVC Time (L)	3.69	3.53	3.23	3.91	4.39	4.85	NS(.27)	NS(.07)
IC (L)	3.72	3.71	3.65	3.65	3.19	2.87	< .001	.001
FEV/FVC (%)	76.4	78.00	78.00	77.80	72.50	70.30	.005	.002
FERV (L)	2.06	2.09	2.03	2.02	1.84	1.85	.05	NS(.24)
$FERV_1$ (L)	1.59	1.61	1.59	1.55	1.42	1.39	NS(.09)	NS(.06)
R_{aw} (cm H_2O/L/sec)	1.86	1.86	1.90	1.91	2.13	2.24	NS(.08)	NS(.27)
FRC (L)	3.905	3.902	3.894	3.895	4.017	4.141	NS(.58)	NS(.20)

P = the probability of the control vs exposure difference being due to chance.

ficantly lower after two hours of ozone exposure than with one hour of ozone exposure (see Figures 2 and 3). FVC time and $FERV_1$ were decreased after two hours of ozone, but were of marginal significance (p 0.07, p 0.06, respectively). Plethysmographic measurements of functional residual capacity (RFC) were not significantly affected by exposure to ozone, although small increases were observed.

No significant differences in heart rates were observed comparing air and ozone exposures either at rest or during exercise.

DISCUSSION

The results from this study clearly indicate that a 2-hour exposure to 0.6 ppm ozone, coupled with moderate exercise, produces significant pulmonary complaints as well as significant decrements in pulmonary function. Ozone inhalation resulting in adverse pulmonary effects had been well documented in many other human studies (7,11-16). Hackney et al. (11) after performing controlled human exposures to various ozone concentrations calculated an ozone threshold level for adverse effects in the 0.25 to 0.30 ppm range. Young, et al. (12) first noted that exercise increased the severity of the pulmonary effects of ozone, and other investigators have since corroborated these findings. Bates, et al. (13) exposed human subjects to 0.75 ppm ozone for 2 hours with and without intervening exercise. Their subjects demonstrated a dramatic increase in the degree of impairment of pulmonary function when ozone was coupled with moderate exercise.

In the present study, both volume and flow parameters were significantly adversely affected with ozone exposure. Preliminary findings also indicate an increase in respiratory volume (RV) and a decrease in total lung capacity (TLC). The most deleterious effects were observed in the flow parameters. This finding suggests that the most sensitive indicator of the adverse affects of ozone exposure on pulmonary function is reduced flow rate (see Table 2). This observation is consistent with those of Rummo, et al. (16) and Hazucha et al. (7). The reduction of MMFR is of particular significance in the present study, since this flow parameter was most adversely affected. The MMFR is derived from an effort-independent portion of the spirometric maneuver, and therefore, should not be influenced by subject cooperation or symptomology. Hazucha, et al. (7) studied six non-smoking subjects undergoing intermittent exercise exposed to 0.37 ppm or 0.75 ppm ozone for 2 hours and found decrements of MMFR to be a more sensitive indicator of ozone exposure than FEV_1. Those subjects exposed to 0.75 ppm ozone demonstrated decrements in MMFR similar to those reported in this study. These findings suggest that MMFR is the most sensitive and reliable flow-rate parameter for use as an indicator of the adverse pulmonary effects of ozone exposure.

In all exposures of this type, it is important to consider the relationship between the total dose of the exposure and the response. The total dose of ozone exposure is the product of the concentration and the exposure time. In these short-term exposures, ozone concentration has a greater influence on the magnitude of acute detrimental effects on pulmonary function than does exposure time. In a previous study from this laboratory, Rummo, et al. (16) exposed 22 subjects to 0.4 ppm ozone for 4 hours, total dose of 1.6 ppm·hours

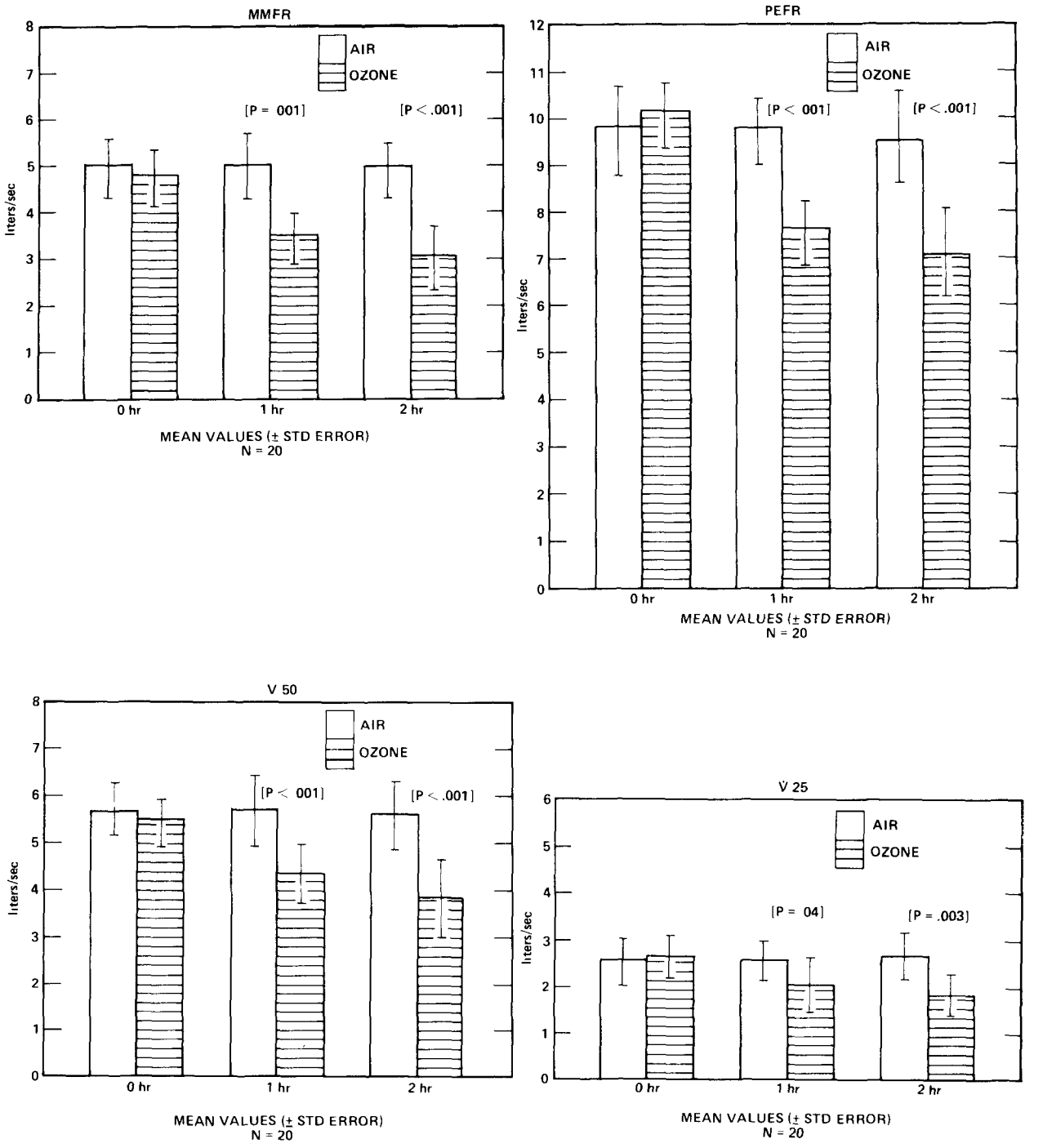

Figure 2. Changes in flow: air vs. ozone.

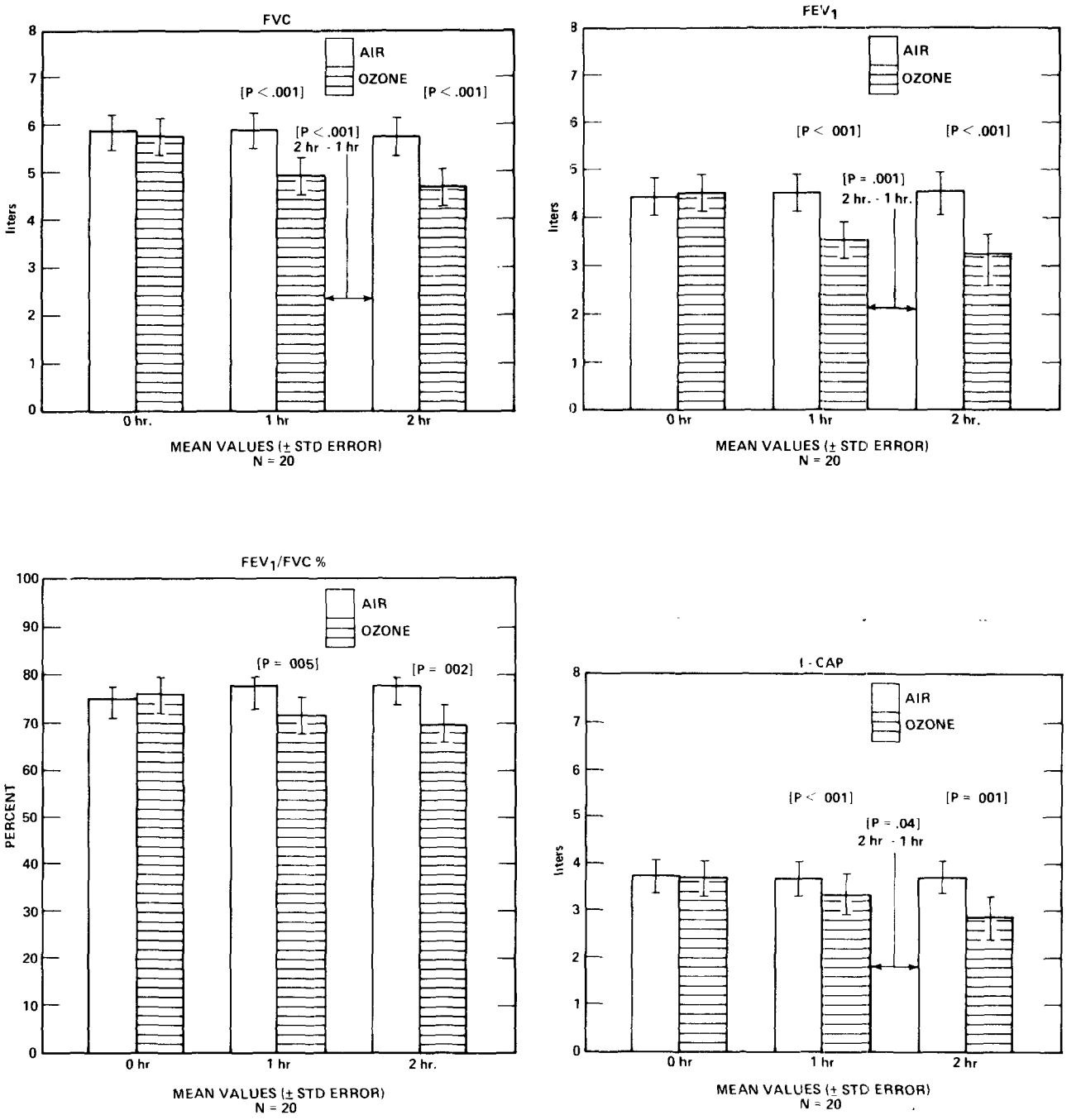

Figure 3. Changes in volume: air vs. ozone.

TABLE 2. % DEGRADATION, PULMONARY PARAMETERS, WITH 0.6 PPM OZONE
MEAN VALUES, N = 20

PARAMETER	TIME 1 Hr. (Ozone)	2 Hr. (Ozone)
MMFR	-26.4%	-35.1%
$\dot{V}_{25}$	-21.4%	-31.3%
$\dot{V}_{50}$	-21.1%	-30.6%
PEFR	-24.9%	-29.6%
FEV_1	-20.9%	-28.4%
FVC	-14.6%	-19.4%
IC	-12.7%	-21.4%

(2400 $\mu g \cdot hrs/m^3$). People with chronic lung disease may be sensitive to much lower concentrations of ozone than evaluated in this study. Although the present study was designed to evaluate adverse health effects produced by ozone at concentrations approaching peak smog levels, it must be emphasized that synergism may exist between ozone and sulphur dioxide (SO_2) as recently suggested by Hazucha, et al. (17). Thus, peak levels of ozone at lesser concentrations than those present here, in the presence of SO_2, may cause more marked symptoms as well as significant decrement in pulmonary function.

CONCLUSION

These results indicate that a 2-hour 0.6 ppm ozone exposure has important and immediate adverse effects on pulmonary function in healthy young men. We would expect these adverse effects of ozone on pulmonary function to be even more detrimental to the welfare of those who are not in good health. The large fraction of the population with chronic lung disease would probably be most sensitive to these adverse effects. Based on this study, which confirms earlier similar studies, 0.6 ppm ozone, even for 1 hour, is unacceptably high as an alert level if we are to assure protection of the general population. This conclusion is independent of any consideration of the potential synergism with simultaneous exposure to ozone and other pollutants, such as SO_2.

REFERENCES

1. National Air Pollution Control Administration, Nationwide Inventory of Air Pollution Emissions, 1968. Raleigh, N.C., August 1970.
2. Tabershaw, I. R., F. Ottoboni, and C. W. Cooper. Oxidants: Air Quality Criteria Based on Health Effects. Journal of Occupational Medicine, 10:9, p. 464-483, September 1968.
3. Williamson, S. J. Fundamentals of Air Pollution. Addison-Wesley Publishing Co., p. 301-305, Reading, Mass., 1973.
4. Blumenthal, D. L. Airborne Surveys in Urban Air Basins: Implications for Model Development. From Report on UC-ARB Conference "Technical Basis for Control Strategies of Photochemical Oxidant: Current Status and Priorities in Research" December 16-17, 1974, U.C. Riverside Statewide Air Pollution Research Center.
5. Maximum One-Hour Oxidant Concentrations. July 1973-June 1974. California Air Resources Board Publication 1975. 1, 1975.
6. Knelson, J. H., and R. L. Lee, Jr. Photochemical Oxidant Atmospheres: Origin, Fate and Public Health Implications. U. S. EPA/HERL/RTP, N.C. Unpublished.
7. Hazucha, M., F. Silverman, C. Parent, S. Field, and D.V. Bates. Pulmonary Function in Man after Short-term Exposure to Ozone. Arch. Environ. Health, 27:183-188, 1973.
8. Strong, A. A., R. Penley, and J. H. Knelson. Description of a Human Exposure System for Controlled Ozone Atmospheres. Unpublished.
9. DuBois, A. B., S. Y. Botelho, G. N. Bedell, R. Marshall, and J. H. Comroe, Jr. A Rapid Plethysmographic Method for Measuring Thoracic Gas Volume. J. Clin. Invest. 35:322-326, 1956.
10. DuBois, A. B., S. Y. Botelho and J. H. Comroe, Jr. A New Method for Measuring Airway Resistance in Man Using a Body Plethysmograph. J. Clin. Invest. 35:327-335, 1956.
11. Hackney, J. D., W. S. Linn, and D. C. Law, et al. Experimental Studies on Human Health Effects of Air Pollutants: III. Two-hour Exposure to Ozone Alone and in Combination with Other Pollutant Gases. Arch. Environ. Health, 30:385-390, 1975.
12. Young, W. A., D. B. Shaw, and D. V. Bates. Effects of Low Concentrations of Ozone on Pulmonary Function. J. Appl. Physiol. 19:765-768, 1964.
13. Bates, D. V., G. M. Bell, C.D. Burham, M. Hazucha, J. Mantha, L. D. Pengelly, and F. Silverman. Short-term Effects of Ozone on the Lung. J. Appl. Physiol. 32:176-181, 1972.
14. Kerr, H. D., T. J. Kulle, M. L. McIlhany, and P. Swidersky. Effects of Ozone on Pulmonary Function in Normal Subjects. Amer. Rev. Resp. Dis., 111:763-773, 1975.
15. Horvath, S. M., and L. J. Folinsbee. Effects of Low Levels of Ozone and Temperature Stress. EPA-600/1-76-001, March 1976.
16. Rummo, N. J., J. H. Knelson, S. Lassiter,and J. Cram. Effects of Ozone on Pulmonary Function in Healthy Young Men. Personal Communication, 1975.
17. Hazucha, M., and D. V. Bates. Combined Effects of Ozone and Sulfur Dioxide on Human Pulmonary Function. Nature 257:52, Sept. 1975.

EFFECTS OF OZONE AND NITROGEN DIOXIDE EXPOSURE OF RABBITS ON THE BINDING OF AUTOLOGOUS RED CELLS TO ALVEOLAR MACROPHAGES

J. G. Hadley, D. E. Gardner, D. L. Coffin, and D. B. Menzel*

ABSTRACT

The alveolar macrophage represents the primary line of defense in host protection against inhaled infectious organisms and is also exposed to high levels of air pollutants. Following exposure to oxidant gases, the ability of the host to resist airborne bacterial infection is severely impaired. To investigate possible damage by oxidant exposure on the alveolar macrophage's ability to recognize other cells, macrophages were isolated from rabbits and treated with a commercial preparation of wheat germ lipase. This preparation induced the binding of both heterologous (sheep) and autologous (rabbit) red blood cells (RBCs) to macrophages in the absence of antibody. The effective concentration for 50% rosette formation with the crude lipase preparation was 30 μg/ml for heterologous cells and 300 μg/ml for the autologous cells. When rabbits were exposed to 0.985 mg/m^3 (0.5 ppm) of ozone (O_3) for 3 hours or to 13.167 mg/m^3 (7 ppm) of nitrogen dioxide (NO_2) for 24 hours prior to the isolation of their macrophages, rosette formation induced by the wheat germ lipase was markedly enhanced. Control cells formed 7.2 ± 1.4% rosettes, compared to 66.0 ± 13.7% for O_3 treated cells and 51.7 ± 21.0% for NO_2 treated cells.

Treatment in vivo with oxidant gases at low concentrations results in the modification of the plasma membrane of macrophages. Such modification could well be involved in the recognition phenomena necessary for bacterial phagocytosis.

INTRODUCTION

The vital role played by the alveolar macrophage (AM) in host defense against airborn infectious organisms is well documented. Other studies have shown that exposure to environmental contaminants may severely impair the ability of the AM to attack, ingest, and destroy inhaled organisms. In the course of investigations on the characterization of the AM receptor for immunoglobulin G (IgG) and receptor alteration induced by atmospheric contaminants, it was observed that when monolayers of macrophages were treated with a commercial lipase preparation obtained from wheat germ, a massive and profound

*J. G. Hadley, D. E. Gardner, and D. L. Coffin, U.S. Environmental Protection Agency, Research Triangle, Park, North Carolina. D. B. Menzel, Duke University Medical Center, Durham, North Carolina.

increase in rosette formation was found on subsequent incubation of the treated macrophages with IgG-coated, sheep red blood cells. Since previous reports (1,2) had indicated no effect of lipase on antibody-mediated rosette formation, this apparent enhancement of receptor activity by the wheat germ lipase was investigated. The results from these experiments are the subject of the current report.

MATERIALS AND METHODS

ROSETTE FORMATION WITH PULMONARY MACROPHAGES

The basic experimental protocol for the experiments to be reported is outlined in Table 1. Briefly, following isolation by pulmonary lavage, the macrophages were washed by suspension and centrifugation. Cell concentration was adjusted to 1 x 10^6 cells per ml in phosphate-buffered saline solution, and 0.5 ml of the cell suspension was placed in wells of Lab Tek four-chambered tissue culture slides and incubated for 30 minutes at 37°C. AM's were attached to the bottom of the well as a monolayer of cells. Following incubation, the AM monolayers were rinsed, the desired concentration of wheat germ lipase added and allowed to stand at room temperature for 30 minutes. The monolayers were washed again with phosphate-buffered saline and 1.0 ml of a 1% suspension of either sheep (SRBC) or rabbit red blood cells (RRBC) added. Following a 30-minute incubation, the unattached red cells were removed by washing, and the remaining cells fixed with 1% gluteraldehyde and stained with Camco Quick

TABLE 1. GENERAL PROTOCOL

1.)	ISOLATION OF MACROPHAGES BY PULMONARY LAVAGE.
2.)	ATTACHMENT OF MACROPHAGES TO GLASS (37° X 30 MIN.).
3.)	INCUBATION WITH DESIRED CONC. OF LIPASE (24° X 30 MIN.).
4.)	3X RINSE OF MONOLAYERS.
5.)	INCUBATE WITH 1% SUSPENSION OF RBC'S (24° X 30 MIN.).
6.)	RINSE, FIXATION, AND STAINING OF CELLS.
7.)	% ROSETTE FORMATION DETERMINED UNDER OIL IMMERSION.

*ROSETTE = 4 OR MORE RBC's BOUND TO MACROPHAGE.

Stain. The slides were examined under oil emersion on a light microscope, and the percentage of rosette-forming cells determined. Positive rosette formation was taken as a macrophage with four or more RBC's bound to it. At least 200 cells were scored in each well.

RESULTS

The initial experiments with the lipase preparation were designed to characterize the rosette formation. Using unsensitized SRBC or RRBC, the log-dose response relationship with the concentration of lipase versus the percent rosette formation was determined (Figure 1). Using RBC's without any added IgG, wheat germ lipase promoted binding to the AM's in proportion to the amount of lipase added to the reaction mixture. Fifty percent rosette formation occurred with 30 μg/ml of lipase using SRBC, while 300 μg/ml of course and temperature dependence of the rosette formation are shown in Table 2. Rosette formation was determined following incubation with 1.0 mg/ml of lipase for the indicated times, followed by incubation with a 1% suspension of SRBC or RRBC for 30 minutes. The binding of the SRBC was rapid and essentially unaffected by temperature, while the binding of the RRBC was considerably slower and temperature dependent. Binding was complete after 15 minutes at room temperature.

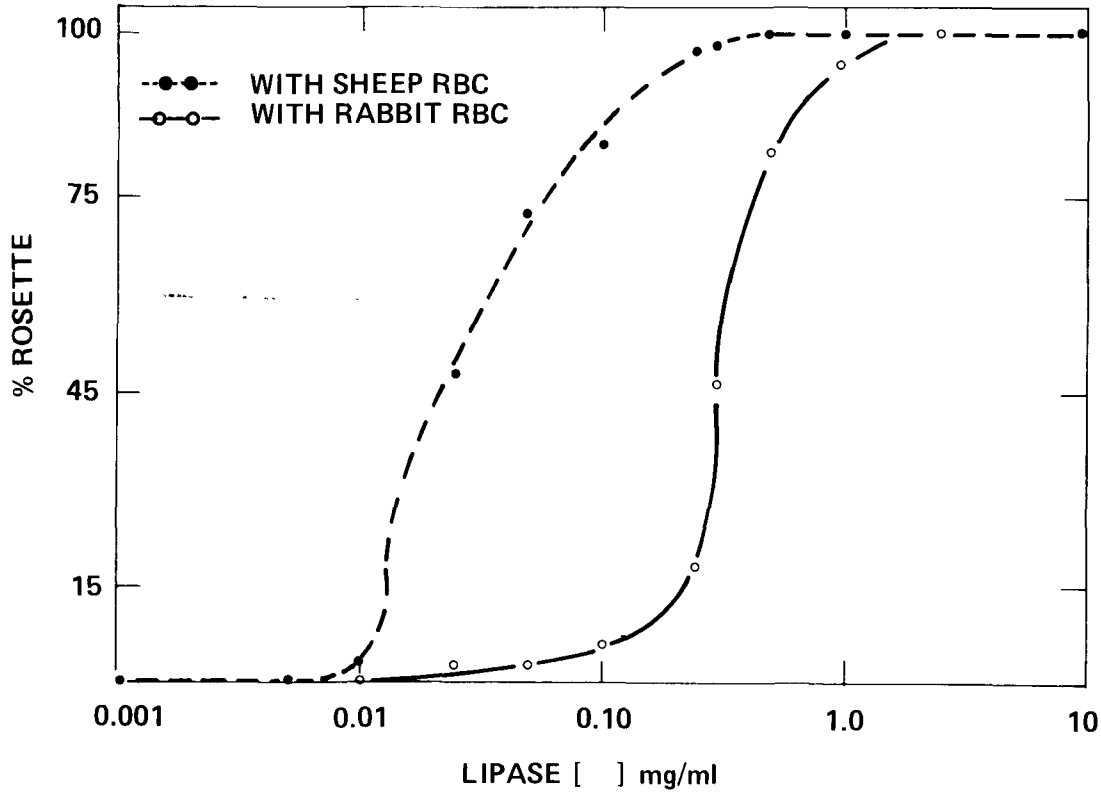

Figure 1. Effect of lipase concentration on rosette formation by rabbit alveolar macrophages.

TABLE 2. DEPENDENCE OF ROSETTE FORMATION ON TIME AND TEMPERATURE

% Rosette Formation

TIME IN MINUTES	WITH SHEEP RBC'S		WITH AUTOLOGOUS RABBIT RBC'S	
	24°	4°	24°	4°
0.5	67*	47	2	0
1.0	77	--	7.3	0
2.0	96	88	13.3	2
5.0	98	98	54	15
15.0	99	100	96	45

The binding of lipase to the AM's appears reversible, as indicated by the data in Figure 2. For these experiments, the macrophages were washed following treatment with the lipase preparation and incubated in media 199 at 37°C for the times indicated. At a specified time interval, the macrophages were rinsed; the red cell suspension added; and rosette formation determined as previously described.

Lipase-mediated rosette formation, with either RRBC or SRBC, could be completely inhibited by incubation with 1 mg/ml of ovomuchoid or 100 mM N-acetyl-D-glucosamine. These data suggest that the lipase-mediated rosette formation is akin to other membrane receptor phenomena suggested to function through glycosyl prosthetic groups of plasma membrane bound proteins (3).

The effect of ozone (O_3) and nitrogen dioxide (NO_2) exposure of rabbits on the rosette formation with autologous RBC's (RRBC) are shown in Table 3. In vivo exposure to 0.9815 mg/m^3 (0.5 ppm) of ozone for 3 hours had a marked effect on the rosette formation measured subsequently in vitro with lipase. Similarly, exposure to 13.17 mg/m^3 (7.0 ppm) of NO_2 for 24 hours augmented the lipase-mediated rosette formation of the isolated AM.

DISCUSSION

An intensive area of investigation in cell biology concerns the role of the plasma membrane of the cell in recognition of external stimuli. External stimuli, such as hormones, need not enter the cell to promote their action. Modern models of plasma membranes propose the existence of protein receptors intercalated within the liquid bilayer, but restricted in their movement to the plane of the membrane (3). These receptors conduct a large part of the

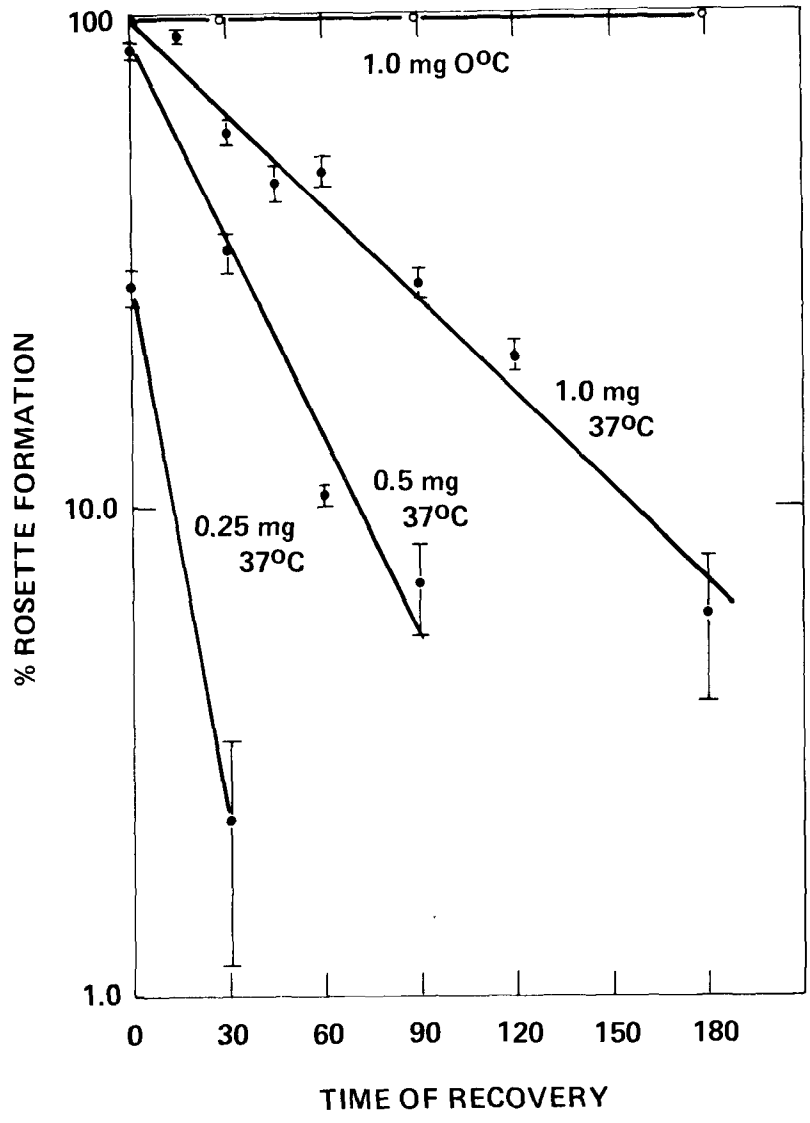

Figure 2. Recovery from lipase exposure.

commerce of the cell. The identification of specific plasma membrane receptors responsible for these phenomena is intimately related to such vital functions as recognition of aberrant cell types and external pathogens. Abberant cell types, such as those transformed into malignant cells or cancers, are characterized by increased numbers and/or affinity of these surface receptors (4,5). The receptors are generally complex proteins composed of both lipophilic and hydrophilic groups and are oriented within the membrane so as to present glycosyl prosthetic groups to the outside or external milieu of the cell. The receptors may act together in a "nearest neighbor effect" to promote their action through a complex network of ultramicrosocpic anatomy of the cell. Needless to say, environmental effects upon such vital functions of the cell, although seemingly subtle, have great potentials for the estimation of the effects of environmental pollutants upon the general health of the organism.

TABLE 3. EFFECT OF OXIDANT EXPOSURE ON LIPASE INDUCED ROSETTE FORMATION

CONCENTRATION OF LIPASE USED TO INDUCE ROSETTE FORMATION	% Rosette Formation		
	CONTROL	O_3[1]	NO_2[2]
0.1 mg/ml	7.2 ± 1.4 (5)	66.0 ± 13.7 (7)	51.7 ± 21 (3)
0.025 mg/ml	4.0 ± 2.4 (4)	37.2 ± 14.6 (6)	14.0 ± 2.9 (3)

[1]ANIMALS EXPOSED 3 hrs. TO 0.50 ppm O_3 PRIOR TO ISOLATION OF MACROPHAGES.

[2]ANIMALS EXPOSED 24 hrs. TO 7.0 ppm NO_2 PRIOR TO ISOLATION OF MACROPHAGES.

In the present study, a crude preparation of wheat germ lipase was used as a probe of the effects of the oxidant gases NO_2 and O_3 upon AM cell membrane receptors. The AM is of special interest because of its role in the protection of the organism against airborne infectious agents. To activate the defense mechanism of the AM, the AM must first recognize the infectious agent as foreign. Surface receptors, involving the fix complement (Fc) fragment of the IgG molecule, appear involved in this process (6).

Lipase promotes both SRBC and RRBC rosette formation in a concentration-dependent reversible fashion that can be inhibited with agents known to compete for binding with the glycosyl prostetic groups of membrane receptors. These data support the concept of the use of lipase as an index of injury to the AM. Exposure to relatively low concentrations of O_3 and NO_2 had profound effects upon the apparent number and/or affinity of receptors available to lipase and subsequently recognized by linkage to RBC. The actual concentrations of the oxidant gases causing these effects are difficult to estimate, since our knowledge of the alveolar concentration of these gases resulting from given ambient exposure is yet to be determined. A model of the concentration profile of O_3 in the rabbit lung is under development and suggests that the concentrations to which AM are exposed is significantly less than the ambient concentration (F. Miller, Personal Communication). Thus, while the O_3 and NO_2 concentrations used are greater than those generally experienced by the general public, they are still remarkable in the effect produced from a relatively brief exposure.

The chemical mechanism by which these effects are brought about can be speculated upon, but unfortunately is still not clearly known. Previously, we have suggested that both NO_2 and O_3 promote their toxic action through peroxidation of cell membrane unsaturated fatty acid (7,8). Since the membrane receptor proteins are intercalated into this lipid bilayer, peroxidation could well lead to perturbation of the conformation and topography of the receptors. Some receptors are known to be "cryptic" or "covert," which are revealed by transformation to malignant cells (10). Peroxidation of cell lipids could well convert the "cryptic" or "covert" receptors into "overt" or "unmasked" receptors and promote rosette formation. Alternately, peroxidation could restrict the dissociation of the receptors within the lipid bilayer and, therefore, change the topographic distribution of the receptors. A pooling of the receptors would increase binding by either closer association of the receptors (nearest neighbor enhancement or concomeric effects) or by concentration effects. Binding to large surfaces, such as RBC's, may require multiple molecular reactions to be stable, and, therefore, the aggrevation of receptors would be expected to promote binding (as evidenced by an increased rosette formation) mediated by the lipase. As is known from acute toxicity studies and from the rate of peroxidation promoted by O_3 and NO_2, O_3 is far more toxic and effective than NO_2. Both gases, in our hypothesis, should have the same qualitative effects, seen here as increased rosette formation, since the ultimate toxic lesion of the membrane is identical.

In terms of the immediate effect upon the organism after exposure to these oxidant gases, the alterations of the AM receptors possibly involved in pathogen recognition could help explain the known susceptiblility of oxidant-exposed animals to airborne pathogen (9). The short-term exposure needed to promote these effects and the potential relationship of the perturbation of these AM receptors to host defense mechanisms and potential long-term pathophysiology suggest great promise for this method as a sensitive probe of both the potential health effects of oxidant exposure and as an early indicator of damage.

REFERENCES

1. Howard, J. G. and B. Benacerraf, Brit. J. Exptl. Pathol. 47: 193, 1966.

2. Davey, M. J. and G. L. Asherson, Immunology 12: 13, 1967.

3. Nicolson, G. L. Biochem. Biophys. Acta. 457: 57, 1976.

4. Burger, M. M. Fed. Proc. 32: 1, 1973.

5. Burger, M. M. and A. R. Goldberg, Pro. Natl. Acad. Sci. 57: 359, 1967.

6. Cohn, Z. A., Fed. Proc. 34: 8, 1975.

7. Roehm, J. N., J. G. Hadley and D. B. Menzel, Arch. Environ. Health 23(2): 142, 1971.

8. Roehm, J. N., J. G. Hadley and D. B. Menzel, Arch. Interal. Med. 128: 88, 1972.

9. Coffin, D. L. Inhalation Carcinogenesis, AEC Symposium Series, 18:259, 1970.

RELATIONSHIPS BETWEEN NITROGEN DIOXIDE CONCENTRATION, TIME, AND LEVEL OF EFFECT USING AN ANIMAL INFECTIVITY MODEL

D. E. Gardner, F. J. Miller, E. J. Blommer, and D. L. Coffin*

ABSTRACT

The concentration of nitrogen dioxide (NO_2) in a polluted atmosphere is subject to wide variation, depending upon the peak traffic load, the industrial productivity, and various meteorological influences. This variation generally results in a low basal atmospheric concentration, which is superimposed with higher peaks that are usually of short duration and irregular occurrence. This variation in mode of exposure could play an important role in the determination of the toxicological effect of NO_2. Continuous and intermittent exposure studies were used to determine the relationship between biological response and length of exposure to various concentrations of NO_2. As the concentration decreased, the slope of the regression line decreased. After adjusting for total differences in concentration x time, the response for the two exposure modes was essentially the same. When a constant concentration x time level was employed, a short-term exposure to a high concentration produced a greater effect than exposure to a lower concentration administered over a longer period. Using these curves, the relationship between level of effect, concentration, and time can be determined. Results of these studies indicated that the frequency and amplitude of short-term peaks are of significance even though the exposure is interrupted with periods of zero concentration of NO_2.

INTRODUCTION

Nitrogen oxides formed in combustion processes are due to either (1) the thermal fixation of atmospheric nitrogen in the combustion air or (2) the conversion of chemically bound nitrogen in the fuel. In the United States, about one-half of the atmospheric nitrogen oxides is derived from products of automobile exhaust emissions and the remaining half is derived from stationary source emissions of various types. Concentration profiles for man-made oxides of nitrogen vary according to population density and combustion activity; therefore, significant elevations above the background level often occur.

Since atmospheric nitrogen dioxide (NO_2) is derived from nitric oxide, principally through the photochemical process, its concentration varies with the rate of combustion, the presence of other atmospheric pollutants, and various meteorological conditions--intensity of light, wind speed and direction, height of inversion layer, and temperature.

---

*U.S. Environmental Protection Agency, Research Triangle Park, North Carolina.

As a consequence of these variables, there are often low background levels of NO_2 on which higher diurnal peaks are superimposed. These peaks are usually of short duration and of irregular occurrence. Aerometric sampling devices provide air quality data expressed in terms of instantaneous hourly or daily integrated values. However, this data base is reduced to a simple annual arithmetic average and compared to the National Air Quality Standard for NO_2, which is set at an annual average of 100 $\mu g/m^3$ (.05 ppm). This average greatly minimizes the sporadic pollutant peaks that could be of toxicological importance. When such averages are used as indices of air pollution, the implication of the particular exposure profile on the health of the population at risk may not be immediately obvious.

Current literature contains little toxicological data that systematically compares the influence of mode of dose on the health effects of NO_2. Therefore, experiments were designed to examine and compare several different exposure regimens, using a single sensitive parameter--host resistance to respiratory infections. This model probably best reflects a summation of all the possible responses to the pollutant assault on the lung, such as edema, inflammation, and subtle immunological and cellular alterations (1).

Several species of animals have been employed in this model system to demonstrate the adverse effects of other environmental pollutants, such as irradiated automobile exhaust, (2) ozone (O_3), (3) nickel oxide (NiO), (4) ($CdCl_2$) (5) and manganese dioxide (MnO_2) (6). Influenza PR-8 virus, Klebsiella pneumoniae, Diplococcus pneumoniae, and Streptococcus pyogenes are examples of the types of microorganisms that have been used in these types of investigations. This model appears to be a sensitive biological indicator for toxicological studies.

EXPERIMENTAL METHODS

Pathogen-free, Swiss Albino female mice, strain CD-1, (Charles River Laboratory) weighing 20-25 gm, were exposed in a stainless steel chamber to various exposure regimes of NO_2. Each mouse was in an individual compartment, and was provided food and water ad libitum whenever exposures were for longer than three hours. Control animals were treated similarly. The NO_2 concentration within the chamber was monitored continuously by the standard chemiluminescence method (7). In addition, the chamber concentration was periodically (3 times/day) determined manually using the Saltzman method (8).

At various times during the exposure studies, groups of 20 mice were removed from the treatment chamber, combined with 20 control mice that had breathed only clean filtered air, and immediately exposed for 15 minutes to an aerosol of viable microorganisms (Streptococcus pyogenes, Group C). The organisms were grown in brain/heart infusion broth (Difco) for 24 hours before use. Prior to aerosolization, the organisms were washed three times and resuspended to a final concentration of approximately 10° organisms per cc. A 5.0 ml aliquot of this suspension was aerosolized and the microbes were delivered to the test animals immediately following the NO_2 exposure. The controls were again separated from the NO_2-exposed animals, and both groups were observed for 15 days in order to determine mortality rate. The data are reported as the dif-

ference in per cent mortality between the NO_2 test group and controls.

In addition to measuring the differences in mortality rates, a second parameter--the relative mean survival time--was also analyzed in order to determine the influence of exposure time and concentration on the mean survival period of the exposed animals. The relative mean survival time (RMST) reflects the average number of days the test animals lived during the experimental period.

It is calculated according to the equation:

$$RMST = \frac{(DxL) + \Sigma(AxB)}{n}$$

where "A" is the last day on which any individual mouse was alive; "B" is the number of mice surviving "A" days; "D" is the last day of the experiment (in this case 15); "L" is the number of mice alive on day "D"; "n" is the initial number of mice in the experimental group; and "Σ" represents the summation over the appropriate terms. The data are represented as the difference in relative mean survival time between the NO_2-exposed group and the controls.

RESULTS AND DISCUSSION

Using the increase in mortality as a biological endpoint for measuring the toxic effects of NO_2, studies were conducted in which the length of continuous exposure varied from a few minutes to several months. To date, six different concentrations have been studied, ranging from 0.94 mg/m^3 (0.5 ppm) NO_2 to 526.7 mg/m^3 (28 ppm) NO_2. Regression analysis was used for examining the interrelationship between per cent mortality and the length of exposure to NO_2. Figure 1 presents the regression equations for each of the concentrations studied. All of the regression lines were statistically significant at the .05 probability level. The experimental data base used to develop these curves is given in Table 1. When comparisons are made of the various lines, it is evident that with increasing concentrations, the slope of the regression line becomes steeper; that is to say, with increasing concentrations of NO_2, the rate of increase in mortality also increases. From these curves, various estimates can be derived for combinations of concentrations, lengths of exposure, and specific mortality responses. For example, the predicted length of exposure needed to produce a 20% increase in mortality varies from approximately 6150 hrs. for 0.94 mg/m^3 (0.5 ppm) NO_2 to one-half hour for 26.3 mg/m^3 (14 ppm) NO_2.

A common method for comparing the relationship of concentration and time to a specific toxic effect is on a concentration x time (CxT) basis. If no interaction occurred between concentration and time, then no statistical difference in response should be noted when either factor is varied, providing that the product remains a constant value.

Table 2 indicates that in the infectivity model the concentration has a greater influence on the observed effect than does the length of exposure. For each of the given CxT, there is a gradient response in mortality that would not be expected if the effect of NO_2 were directly related to concentration and time. To illustrate this point, at a CxT of 21, the overall expected average

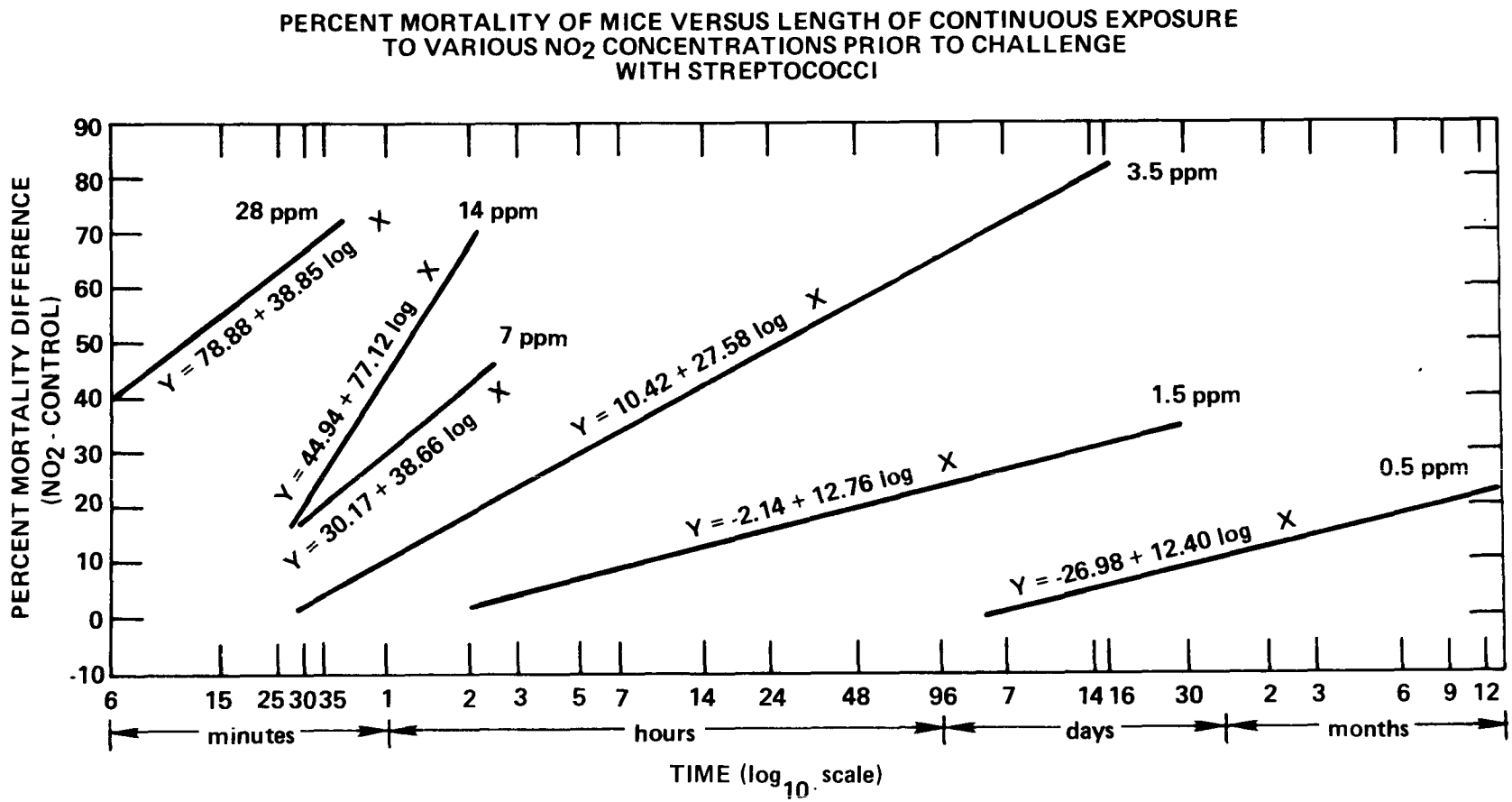

Figure 1. Per cent mortality of mice versus length of continuous exposure to various NO_2 concentrations prior to challenge with streptococci.

TABLE 1. EXPERIMENTAL DATA FROM STUDIES DESIGNED TO DETERMINE THE EFFECTS OF CONTINUOUS EXPOSURE TO VARIOUS NO_2 CONCENTRATIONS WITH TIME[a]

.5 ppm NO_2		1.5 ppm NO_2		3.5 ppm NO_2	
Exposure Length (Hours)	% Mortality (NO_2-Control)	Exposure Length (Hours)	% Mortality (NO_2-Control)	Exposure Length (Hours)	% Mortality (NO_2-Control)
168	.8	2	6.7	.5 (5)	10.0
336	5.1	5	0.0	1 (10)	8.0
720	5.0	8	24.4	2 (2)	12.5
1440	10.0	18	25.0	3 (10)	19.0
2160	19.9	24	15.6	5 (2)	37.5
4320	23.7	96 (6)	10.8	7 (14)	34.3
6480	12.3	126	35.0	14 (4)	45.0
8760	23.4	168 (4)	25.0	24 (7)	49.3
		222	25.0	48 (8)	56.3
		336 (4)	31.3	96	75.0
		504 (3)	45.0	168	85.0
				384	65.0

7.0 ppm NO_2		14.5 ppm NO_2		28 ppm NO_2	
.5 (6)	20.8	.5 (3)	23.3	.10 (5)	41.6
1.0 (6)	29.2	1.0 (3)	38.3	.25 (5)	53.6
1.5 (6)	28.3	1.5 (3)	66.7	.42 (5)	60.6
2.0 (6)	49.2	2.0 (3)	65.0	.58 (5)	73.6

[a]The number of replicate experiments in indicated in parentheses.

mortality increase would be 45.1%. However, the predicted mortality value from Figure 1 varied from a low of 12.5% obtained with 2.8 mg/m^3 (1.5 ppm) x 14 hrs. to a high of 74% obtained with 52.7 mg/m^3 (28 ppm) x 3/4 hr. This indicates that in this system concentration is a more important factor in eliciting the toxicological response than is time.

TABLE 2. THE INFLUENCE OF CONCENTRATION AND TIME ON ENHANCEMENT OF MORTALITY RESULTING FROM VARIOUS NO_2 CONCENTRATIONS[a]

Concentration (ppm)	Concentration X Time					
	7		14		21	
	Time (hrs)	% Mortality	Time (hrs)	% Mortality	Time (hrs)	% Mortality
1.5	4.7	6.4	9.3	10.2	14.0	12.5
3.5	2.0	18.7	4.0	27.0	6.0	31.9
7.0	1.0	30.2	2.0	41.8	3.0	48.6
14.0	.5	21.7	1.0	44.9	1.5	58.5
28.0	.25	55.5	.5	67.2	.75	74.0

[a]These are predicted values obtained from Figure 1.

Thus, in order to examine the adverse effects of this pollutant, it becomes necessary to clearly define the exact exposure pattern. The experiments described thus far provide information on what might be expected if the exposure regimen were of a continuous, nonvarying pattern. The CxT data indicated that substantially different effects can result from varying the exposure scheme. Also, since ambient concentrations of NO_2 are irregular, sporadic, and follow a diurnal mode, it was of interest to include in the study an intermittent exposure regimen and to compare those responses to those from the continuous exposure.

In order to test the effect of concentration and time, mice were intermittently exposed for 7 hrs./day, 7 days/wk to either 2.8 mg/m^3 (1.5 ppm) NO_2 or 6.6 mg/m^3 (3.5 ppm) NO_2. At various times animals were removed and given the bacterial challenge, and their response was compared to the animals exposed continuously.

Figure 2 illustrates the results from continuous and intermittent exposure to 6.6 mg/m^3 (3.5 ppm) NO_2 for periods up to 15 days. There was a noticeable increase in per cent mortality for each experimental group with increasing length of exposure. But for each given length of exposure, there was no statistical difference ($p = 0.05$) between the continuous and the intermittent exposure groups. After adjusting the data for actual exposure time, and thus for total difference in CxT, the per cent mortality rate in the two exposure modes was essentially the same (Table 3).

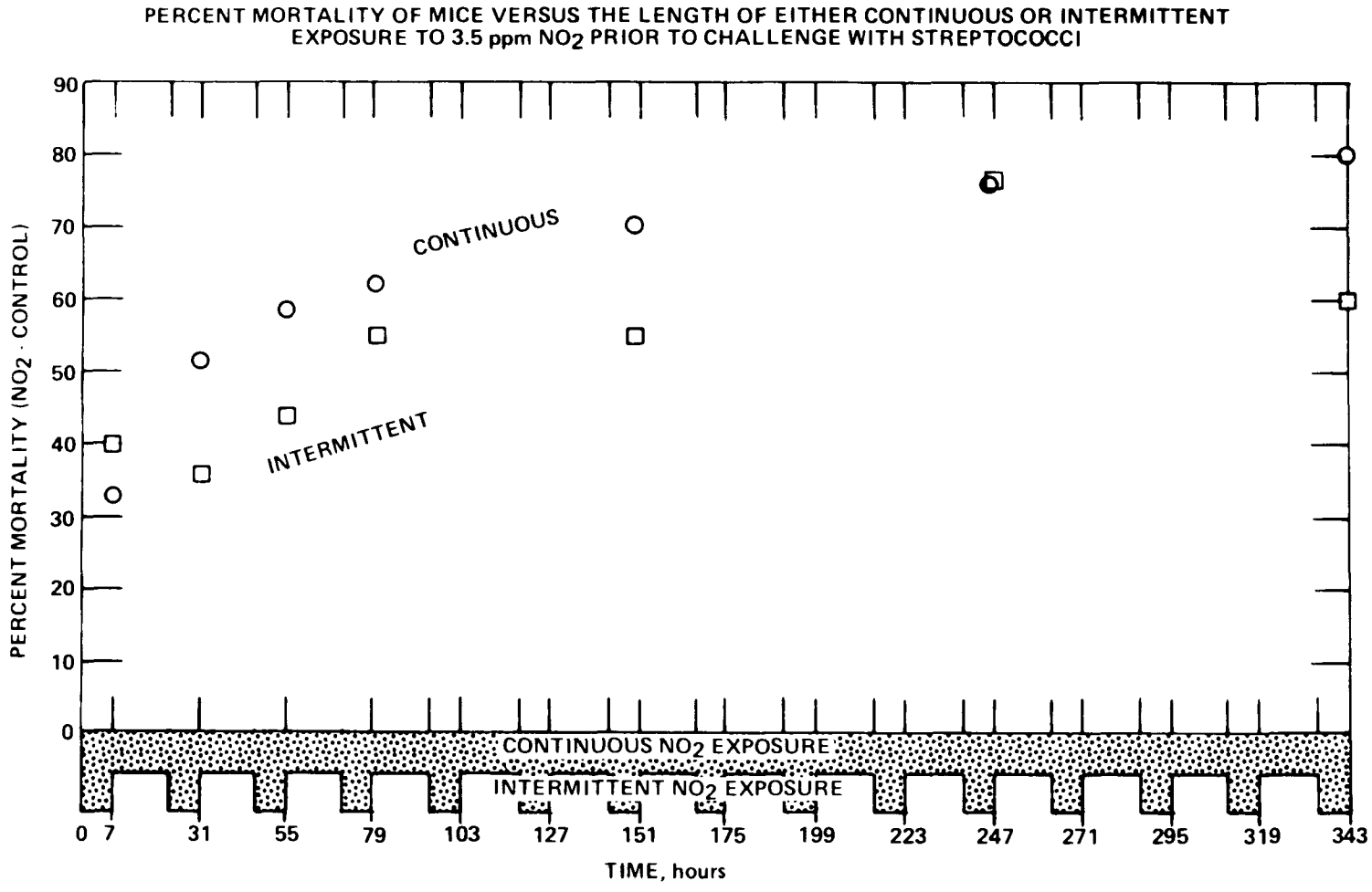

Figure 2. Per cent mortality of mice versus the length of either continuous or intermittent exposure to 3.5 ppm NO_2 prior to challenge with streptococci.

TABLE 3. A COMPARISON OF THE EFFECTS OF CxT AND MODE OF EXPOSURE TO 3.5 ppm NO_2 ON PERCENT MORTALITY

Concentration X Time	Exposure Mode: Intermittent % Mortality	Exposure Mode: Continuous % Mortality
49.0	37	42
73.5	43	47
98.0	55	50
171.5	55	57
269.5	75	62
367.5	60	66

Similar studies conducted at a lower concentration of NO_2 (2.8 mg/m^3) produced a different response (Figure 3). Again, there was a significant increasing linear relationship with duration of exposure. However, initially the mortality rate was significantly higher in mice exposed to the pollutant continuously as compared to the intermittent treatment. This difference became indistinguishable following 14 days of exposure.

The question arises as to the cause of the variation in the early response between the continuous and intermittent exposure at 2.8 mg/m^3 (1.5 ppm). From the continuous exposure curves (Figure 1), a statistically significant increase in mortality of approximately 15% would not be expected earlier than 24 hr. at this low level of NO_2. Thus, during the first 4 initial periods of intermittent exposure, the accumulated CxT is below this critical threshold, whereas the continuous exposure exceeds this 24 hr. criteria and hence causes a significant increase in mortality. After the seventh intermittent exposure to 2.8 mg/m^3 (1.5 ppm) NO_2, the pollutant produces a significant increase in mortality, and the effect begins to approach that of the continuous exposure group.

In conjunction with measuring the increase in mortality, a second endpoint was used to illustrate the relationship between concentration and length of exposure. The relative mean survival times for mice continually exposed to the three higher concentrations of NO_2 (13.2, 26.3 and 52.7 mg/m^3) are given in Table 4. The data demonstrate that at the concentrations and exposure periods studied, the survival time of the NO_2-exposed mice was significantly less than those in the control group. The relative mean survival time decreased with increasing concentration and correlated with the mortality enhancement presented in Table 2.

The relative mean survival times at lower concentrations of NO_2 (2.8 and 6.6 mg/m^3) are seen in Table 5 where a comparison is made between continuous and

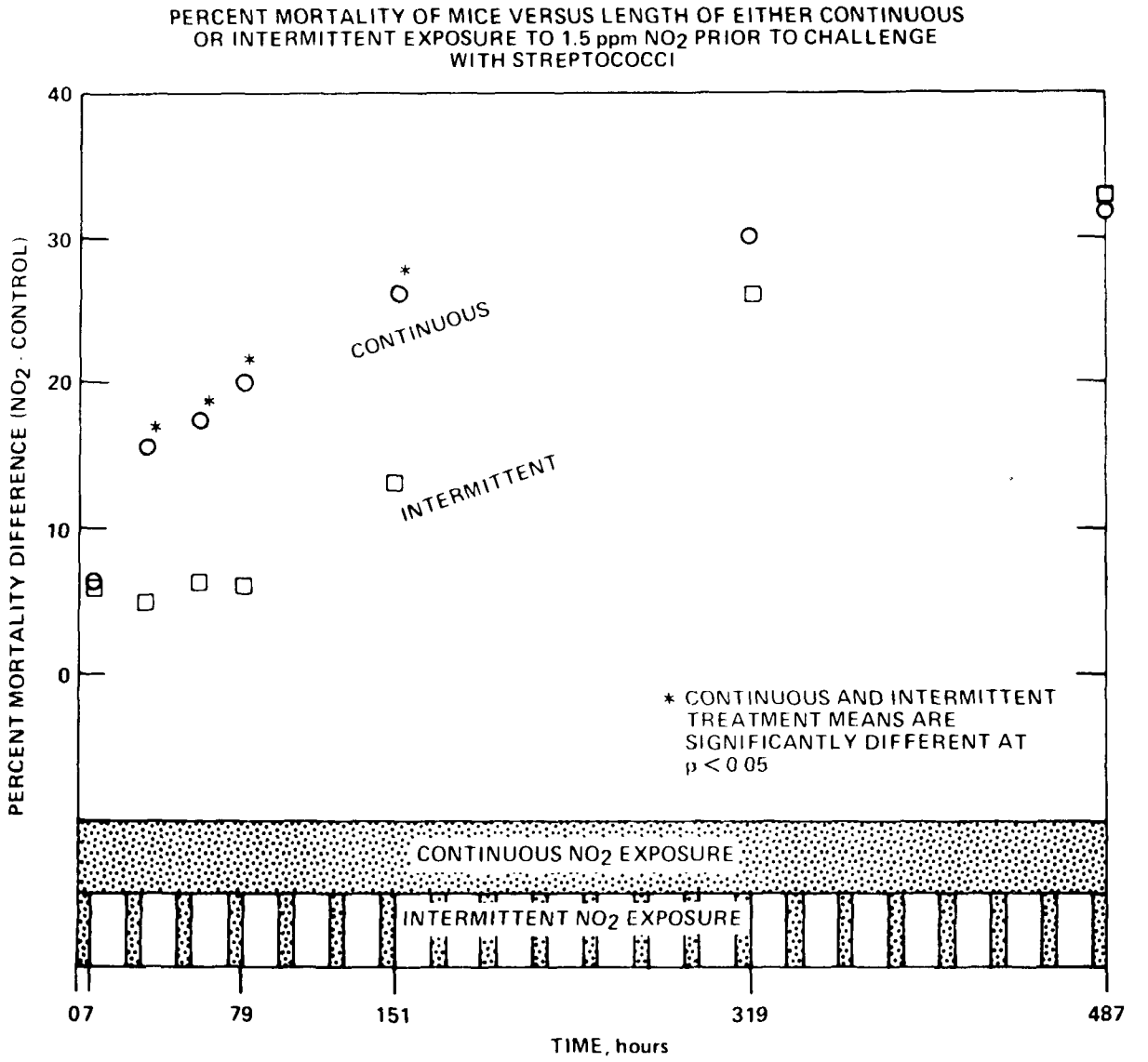

Figure 3. Per cent mortality of mice versus length of either continuous or intermittent exposure to 1.5 ppm NO_2 prior to challenge with streptococci.

intermittent exposure. Consistent statistical differences in the rate of survival were seen after 4 or more intermittent exposures to 6.6 mg/m^3 (3.5 ppm) NO_2. All continuous exposures at this level of NO_2 produced statistically different relative mean survival times, as compared to control. However, the pattern of statistical difference for the 2.8 mg/m^3 (1.5 ppm) exposure mode was somewhat ambiguous. This may reflect a decrease in sensitivity of this parameter as compared to the mortality model system, or it may reflect simply a lesser response to this lower level of NO_2.

TABLE 4. THE EFFECTS OF 7, 14, AND 28 ppm OF NO_2 ON RELATIVE MEAN SURVIVAL TIME (RMST) IN MICE EXPOSED FOR VARIOUS LENGTHS OF EXPOSURE[a]

C x T	NO_2 Concentration (ppm)	Time (hrs)	Difference in RMST (days)	Standard Error
2.8	28	.10	-2.99	.77
3.5	7	.50	-1.51	.72
7.0	7	1.00	-2.28	.43
7.0	14	.50	-1.43	.84
7.0	28	.25	-4.61	.47
10.5	7	1.50	-1.93	.50
11.7	28	.42	-4.76	.74
14.0	7	2.00	-4.03	.84
14.0	14	1.00	-2.65	.10
16.3	28	.58	-6.56	.64
21.0	14	1.50	-5.60	.33
28.0	14	2.00	-5.97	.10

[a]The number of replicate experiments for each C x T level was 6, 3, and 5 for 7, 14, and 28 ppm NO_2, respectively.

SUMMARY

This study has described variations in response with different concentrations, modes, and durations of NO_2 exposure. Continuous exposure to different levels of NO_2 resulted in a family of linear regression lines that related increase of mortality with duration of exposure. As the concentration of NO_2 increased, the slope of the resulting linear regression also increased.

The relationship between concentration and time produced significantly different mortality responses, although CxT was held constant. The ranking of the effects in the infectivity model suggests that concentration is the more important factor for a fixed CxT level. However, deleterious effects can also result from chronic exposure to low levels of NO_2, as evidenced by significantly increased mortality with long-term exposure to 0.94 mg/m^3 (.5 ppm) NO_2.

This seemingly contradictory role that time plays with respect to host responses to bacterial infections may indicate that there is more than one mechanism of NO_2 injury. At higher levels of NO_2 and for shorter time periods, the destructive action of this pollutant may be primarily on the pulmonary alveolar macrophage (9). These cells are postulated to be the chief pulmonary defense against inhaled infectious agents, and a variety of environmental pollutants have been shown to alter the functioning of these cells (9,10,11,12). However, after long-term, low-level exposures, certain anatomical and biochem-

ical changes do occur, such as desquamation of type 1 epithelial cells (13), loss of lung recoil (14), and pulmonary emphysema (15,16). Therefore, the observed increase in mortality at 0.94 mg/m^3 (0.5 ppm) NO_2 may indicate that the effects of this pollutant can be mediated through numerous subtle alterations in several host defense mechanisms.

Of particular importance were the results obtained when comparisons were made between intermittent and continuous exposure to 2.8 and 6.6 mg/m^3 (1.5 and 3.5 ppm) NO_2. Differences in mortality responses between the two exposure modes may be resolved on the basis of CxT. These data indicate the importance that short-term peaks may have upon responses to environmental pollutants. Consequently, air quality standards that do not account for the frequency and amplitude of such spikes may allow excess risk. At the present time, research is being conducted to investigate the effects resulting from the superimposition of spikes on lower basal concentrations of NO_2.

TABLE 5. THE EFFECTS OF INTERMITTENT AND CONTINUOUS EXPOSURE TO 1.5 AND 3.5 PPM NO_2 ON RELATIVE MEAN SURVIVAL TIME IN MICE EXPOSED FOR VARIOUS PERIODS[a]

Consecutive Exposures	Intermittent Regimen			Continuous Regimen		
	1.5 ppm NO_2, 7 hrs./day			1.5 ppm NO_2, 24 hrs./day		
	C x T	Difference in RMST		C x T	Difference in RMST	
2	21.0	.46	(4, .64)	72.0	1.08	(4, .83)
3	31.5	- .55	(4, .20)	108.0	- .58	(4, .75)
4	42.0	- .79	(5, .16)	144.0	- .78	(6, .46)
7	73.5	-1.34	(8, .50)	252.0	-1.95	(5, .97)
14	147.0	-2.16	(6, .52)	504.0	-2.42	(3, .58)
21	220.5	-2.88	(2, 1.03)	864.0	-4.05	(3, 1.13)
	3.5 ppm NO_2, 7 hrs./day			3.5 ppm NO_2, 24 hrs./day		
	C x T	Difference in RMST		C x T	Difference in RMST	
2	49.0	-2.83	(3, 1.12)	168.0	-4.67	(7, .56)
3	73.5	-.93	(4, 1.65)		No Data	
4	98.0	-3.59	(4, .97)	336.0	-6.95	(1, -)
7	171.5	-3.48	(3, .71)	588.0	-7.1	(1, -)
11	269.5	-4.90	(3, 1.85)		No Data	
15	367.5	-5.55	(2, .05)	1260.0	-5.85	(1, -)

[a]Numbers in parentheses represent sample size and standard error, respectively.

REFERENCES

1. Coffin, D. L. and D. E. Gardner. Interaction of Biological Agents and Chemical Air Pollutants. Ann. Occup. Hyg., 15:219-234, 1972.

2. Coffin, D. L. and E. J. Blommer. Acute Toxicity of Irradiated Auto Exhaust. Arch. Environ. Health, 15:36-37, 1967.

3. Coffin, D. L., E. J. Blommer, D. E. Gardner and R. S. Holzman. Effect of Air Pollution on Alteration of Susceptibility to Pulmonary Infection. In: Proceedings of 3rd Annual Conference on Atmospheric Contamination in Confined Space, Aerospace Medical Research Lab., Dayton, Ohio, 1968. pp. 71-80.

4. Port, C. D., J. D. Fenters, R. Ehrlich, D. L. Coffin and D. E. Gardner. Interaction of Nickel Oxide and Influenza Infection in the Hamster. In: Abs. Env. Proceedings Conference on Heavy Metals in the Environment, Environ. Health Perspectives, 10:268, 1975.

5. Gardner, D. E., F. J. Miller, J. W. Illing and J. M. Kirtz. Potentiation of Respiratory Infections by Inhalation of Cadmium. FASEB Meeting, Anaheim, Calif, 1976. (To be presented.)

6. Maigetter, R. A., J. Findlay, J. D. Fenters and R. Ehrlich. Effect of Manganese Dioxide on Resistance to Respiratory Infection. Abs. Am. Soc. of Microbiology, Chicago, Ill., 1974. Paper #E142, p. 85.

7. National Primary and Secondary Ambient Air Quality Standards: Reference Method for Determination of Nitrogen Dioxide. Federal Register, 38(110):15174, 1973.

8. Saltzman, B. E. Selected Methods for Measurement of Air Pollutants. PHS Publication No. 999-AP-11, U. S. Dept. of Health, Education and Welfare, 1965.

9. Gardner, D. E., R. S. Holzman and D. L. Coffin. Effects of Nitrogen Dioxide on Pulmonary Cell Populations. J. of Bact., 98:1041-1043, 1969.

10. Waters, M. D., D. E. Gardner, C. Aranyi and D. L. Coffin. Metal Toxicity for Rabbit Alveolar Macrophages _In Vitro_. Env. Res., 9:32-47, 1975.

11. Coffin, D. L., D. E. Gardner and R. S. Holzman. Influence of Ozone on Pulmonary Cells. Arch. Environ. Health, 16:633-636, 1968.

12. Goldstein, E., M. C. Eagle and P. D. Heoprich. Effect of Nitrogen Dioxide on Pulmonary Defense Mechanisms. Arch. Environ. Health, 26:202-204, 1973.

13. Freeman, G., L. T. Juhos, N. J. Furiosi, R. Mussender, R. J. Stephens and M. J. Evans. Pathology of Pulmonary Disease from Exposure to

Ambient Gases. Arch. Environ. Health, 29:203-210, 1974.

14. Buel, G. C., Y. Tokiwa and P. K. Mueller. Lung Collagen and Elastin Denaturation *In Vivo* Following Inhalation of NO_2. Air Pollution Control Assn. Meeting, San Francisco, Calif., June 1966. APCA Paper No. 66-7.

15. Freeman, G., R. J. Stephens, S. C. Crane and M. J. Furiosi. The Subacute Nitrogen-Induced Lesion of the Rat Lung. Arch. Environ. Health, 18:609-612, 1969.

16. Ehrlich, R. and M. C. Henry. Chronic Toxicity of Nitrogen Dioxide. I. Effects on Resistance to Bacterial Pneumonia. Arch. Environ. Health, 17:860-865, 1968.

DEVELOPMENT OF OZONE TOLERANCE IN MAN

M. Hazucha, C. Parent, and D.V. Bates*

ABSTRACT

The development of tolerance to ozone (O_3) has been investigated in young healthy subjects, using dynamic lung function measurements as assessment criteria.

Each of the sixteen subjects, divided into four groups, underwent three 2-hour exposures in the following sequence: Group A: 0.4 ppm O_3, 1-2 months delay, 0.2 ppm O_3, 1 day separation, 0.4 ppm O_3; Group B: 0.2 ppm 1 day, 0.4 ppm, 1-2 months, 0.4 ppm; Group C: 0.6 ppm, 1-2 months, 0.2 ppm 3 days, 0.6 ppm; Group D: 0.6 ppm, 1-2 months, 0.4 ppm, 3 days, 0.6 ppm.

No development of tolerance was observed in groups B and C. The measured decrements in lung function were comparable to decreases obtained after single exposures to the same ozone concentration. Group A showed slight adaptation to ozone on the third exposure compared to first exposure. However, these relative improvements in function were not statistically significant. Considerably smaller decreases on the third exposure were observed in group D, indicating development of tolerance. The most sensitive tests appeared to be maximal midexpiratory flow rate (MMFR) and maximum expiratory flow rate (MEFR) 50%, which "improved" by more than 10%.

Our results have demonstrated that pre-conditioning to ozone will induce tolerance in man, but only after threshold concentration and sufficient development period is reached. However, the afforded tolerance was not completely protective since it did not diminish the gravity and the extent of subjective symptoms. Furthermore, it did not completely prevent some decrease in lung function.

INTRODUCTION

A review of air quality data for ozone (O_3) over the last several years revealed that while peak concentrations have tended to decrease, the level of the highest average one-hour concentration is becoming greater. Furthermore, the frequency and the percentage of time during which ozone concentrations

---

*M. Hazucha and C. Parent, McGill University, Montreal, Quebec, Canada.
M. Hazucha, present address: Environmental Protection Agency, University of North Carolina, Chapel Hill, North Carolina.
D. V. Bates, University of British Columbia, Vancouver, B.C. Canada.

exceed certain levels set by regulating agencies is also increasing (1, 2). These trends, as well as growing numbers of cities and localities reporting appearance of ozone in the monitored atmosphere clearly increases the probability of multiple exposures of the same population to higher levels of ozone (1).

Data obtained from a number of animal studies strongly indicates that under certain conditions of exposure duration, O_3 concentration, and a delay time between exposures previously exposed animals are more resistant to subsequent exposure stress than animals that were not pre-conditioned. Pre-exposed animals were less susceptible to microbial infection (3), exhibited decreased mortality (4, 5) and had less extensive pathological changes (6).

To date, however, very few studies have been reported on the effects in man of multiple exposure to ozone (7). Moreover, all but the very recent study by Hackney et al. (8) are incomplete, and thus difficult to interpret. They exposed three groups of subjects to 0.5 ppm ozone at different periods of the year. The group tested at the end of summer, i.e., at the end of the Los Angeles peak oxidant season, showed the mildest response while the group tested in winter was the most affected. Their results suggest that preconditioning of subjects by ambient ozone exposures makes them more tolerant to subsequent oxidant loading, the tolerance being defined as "the protection afforded the respiratory system against otherwise toxic pollutant by pre-exposure to a dose of that same pollutant" (5).

The present study was designed to evaluate the functional response of the respiratory system of man to multiple exposures to ozone and to examine possible tolerance development under such conditions.

MATERIAL, METHODS, AND PROTOCOL

SUBJECTS AND EXPOSURE FACILITY

The subjects for this study were drawn from among students who volunteered to participate in the experiment. Their age ranged from 19 to 29 years and all but 4 were non-smokers.

All subjects were exposed individually in a Plexiglas environmental chamber. Concentration of ozone in the chamber was continuously monitored by two Mast O_3 meters and one chemiluminescent O_3 analyzer (McMillan 1100). Temperature and water vapor were also continuously monitored and recorded. Relative humidity typically ranged from 37 to 45%, and the temperature varied from 21 to 23°C. A complete technical description of the exposure facilities was reported by Bates et al. (9).

EXPOSURE PROTOCOL

The sixteen subjects for this study were randomly divided into 4 groups, each group consisting of 4 subjects. Each subject underwent individually three consecutive exposures: a "control", a "pre-exposure" and a "challenge" exposure. Table 1 shows ozone concentration sequence and a time delay schedule

TABLE 1. EXPOSURE PROTOCOL (2 HOURS, INTERMITTENT EXERCISE)

Group	No. of Subjects	1st Exposure	Delay	2nd Exposure	Delay	3rd Exposure
A	4	C-0.4ppm	1-2 months	P-0.2ppm	1 day	E-0.4ppm
B	4	P-0.2ppm	1 day	E-0.4ppm	1-2 months	C-0.4ppm
C	4	C-0.6ppm	1-2 months	P-0.2ppm	3 days	E-0.6ppm
D	4	C-0.6ppm	1-2 months	P-0.4ppm	3 days	E-0.6ppm

C: "control exposure"

P: "pre-exposure" or "pre-treatment"

E: "challenge exposure"

Concentrations are expressed in parts per million (ppm) in weight of air.

between these exposures. Since there is good evidence that the development of tolerance takes 1-3 days after pre-exposure (4) a delay period of 1 day for groups A & B and 3 days for groups C & D was chosen. The long delay period of 1-2 months represented an estimated time necessary for the disappearance of tolerance, should it have developed following the first exposure (4, 5).

All experiments followed the standard protocol of 15 minute periods of light exercise (≈70W) alternating with 15-minute rest periods, for 2 hours. During each exposure subjects were tested three times: before, at 1 hour, and after 2 hours of exposure. Details of the methodology have been fully described elsewhere (9, 10).

PULMONARY FUNCTION TESTS

Testing consisted of a respiratory symptom questionnaire and spirometry. The seated subject performed 3-5 forced vital capacity maneuvers (FVC) at each testing period. The FVC was determined by integration of the flow signal from a #3 Fleisch pneumotachograph and an H-P PM 270 transducer. The spirograms were recorded on a Visicorder 1706 (Honeywell). The signal was also recorded on an FM tape recorder (Thermoionic, T300) for later processing. The three largest FVC curves from each testing period were used for further calculations.

The values of all dynamic tests were expressed as the percentage of the zero-hour (before exposure) value for their respective exposures. Mean and standard error as well as the analysis of variance computations were done on an IBM 360/370 computer. The analysis of variance test was carried out using a modified Scientific Subroutine Package program.

RESULTS

CLINICAL FINDINGS

The four groups, described in terms of average age, height, and weight are presented in Table 2. Each group included one smoker whose smoking habits are also listed in Table 2. Since the composition of the groups was quite homogeneous, as is evident from the closeness of the means, the influence of the above physiological factors on in-between groups analysis was minimal.

The clinical findings and sampling rate corrected ozone concentrations during each experiment appear in Table 3. Measured O_3 concentrations were very close to the desired concentrations and except for one exposure (B.B.) they were all within 0.05 ppm of each other within each group.

The first and most common symptom to appear was throat irritation (Table 3). It usually appeared after 1 hour of exposure and was followed by cough and substernal pain. Three subjects (H. S., K. W., S.T.) experienced conjunctivitis after the "challenge" exposure. Objective examination immediately after the exposure disclosed respiratory rhonchi in subject R. A.

TABLE 2. MEANS OF PHYSICAL CHARACTERISTICS OF SUBJECTS BY GROUPS

Group	Age (years)	Height (cm)	Weight (kg)	Comments
A	22.4	168.8	57.8	L.Y. ex-smoker for 2 weeks before exp.
B	21.3	170.8	67.0	B.B. smoker, 25 cig/day
C	23.0	176.0	62.5	R.K. smoker, 3 cig/day
D	23.0	173.0	66.8	A.T. smoker, 1-2 pipes/day

All other subjects nonsmokers.

These were possibly due to increased mucous secretion as they disappeared after coughing. Frequent extrasystoles were noticed in subject N. I. after "pre-exposure." Further questioning elicited a history of extrasystoles occurring when under stress. A clinical examination later did not disclose any abnormal cardiovascular findings. The same subject, when exposed to higher concentrations, had subjective difficulty in taking a deep breath towards the end of exposure but showed no arrhythmia. When comparing the symptomatology og the three exposures for all groups, the symptoms reported during the "pre-exposure" (lower ozone levels) were of lesser intensity than in the other exposures, which was expected based on previous work that showed more subjective complaints at the higher ozone levels (10,11). No indication of reduced susceptibility or tolerance during the "challenge" exposure could be obtained on the basis of symptomatology. All symptoms disappeared a few hours after exposure and no residual effects could be noticed 24 hours after the experiment.

LUNG FUNCTION TESTS

The mean changes in lung function during each ozone exposure after one and two hours are shown in Figures 1 through 4. The average values $\pm$ S.E. (ordinate) representing percent deviation from the initial value before each exposure (0 hr) of the five function tests are plotted in sequence for all three exposures (abscissa).

TABLE 3. EXPOSURE CONCENTRATIONS AND CLINICAL FINDINGS

Group/ Subject	Control							Pre-exposure							Challenge						
	$\bar{x}$ O_3 conc. (ppm)	Throat irritation	Substernal pain	Cough	Conjunctivitis	Excessive sweating	Others	$\bar{x}$ O_3 conc. (ppm)	Throat irritation	Substernal pain	Cough	Conjunctivitis	Excessive sweating	Others	$\bar{x}$ O_3 conc. (ppm)	Throat irritation	Substernal pain	Cough	Conjunctivitis	Excessive sweating	Others
A. R.L.	0.40	▮▮	▮▮	-	-	-	-	0.22	▮▮	-	-	-	-	-	0.40	-	▮▮▮	▮▮▮	-	-	-
J.S.	0.39	▮▮	-	▮▮	-	-	-	0.22	-	-	-	-	-	-	0.40	▮▮	▮▮	-	-	-	-
H.S.	0.38	▮▮	▮▮	▮▮	-	-	-	0.23	▮▮	▮▮	▮▮	-	-	-	0.37	▮▮	▮▮	▮▮	▮	-	-
L.Y.	0.41	▮▮	▮▮	-	-	-	-	0.24	-	-	-	-	-	-	0.37	-	-	-	-	-	-
B. D.A.	0.41	▮▮	-	-	-	-	-	0.21	▮▮	-	▮▮	-	-	-	0.44	▮▮	-	▮▮	-	-	-
B.B.	0.39	-	-	-	-	-	-	0.30	-	-	-	-	-	-	0.39	-	-	-	-	-	-
H.D.	0.39	▮▮	▮▮	▮▮	-	-	-	0.24	▮▮	-	▮▮▮	-	-	-	0.38	▮▮▮	▮▮▮	▮▮▮▮	-		-
K.W.	0.41	-	-	-	-	-	-	0.22	-	-	-	-	-	-	0.38	▮▮	▮▮	▮▮	▮	-	-
C. R.K.	0.63	▮	▮	▮	-	-	-	0.21	-	-	-	-	-	-	0.66	▮	▮	▮	-	-	-
D.D.	0.65	▮▮	▮▮	▮▮	-	-	-	0.21	-	-	-	-	-	-	0.63	▮▮	▮▮	▮▮	-	-	-
M.M.	0.57	-	-	▮	-	-	-	0.23	-	-	-	-	-	-	0.65	▮	-	▮	-	-	-
P.K.	0.60	-	-	-	-	-	-	0.21	-	-	-	-	-	-	0.59	▮	-	-	-	-	-
D. R.A.	0.57	▮▮	▮▮	▮▮	-	▮	-	0.40	▮▮	▮▮	▮▮	-	-	*	0.60	▮	▮	-	-	-	-
N.I.	0.63	▮▮▮	▮▮▮	▮▮▮▮	-	-	**	0.42	▮▮	▮▮	▮▮▮	-	-	***	0.61	▮▮▮	▮▮▮	▮▮▮▮	-	-	**
S.T.	0.61		-	-	-	-	-	0.39	-	-	-	-	-	-	0.58	-	-	-	▮	-	-
A.T.	0.58	▮▮	▮▮	▮▮	-	-	-	0.42	▮	▮▮	▮▮	-	-	-	0.62	-	▮	▮	-	-	-

* Inspiratory rhonchus present at the end of experiment in right lower lobe.

** Difficulty in taking deep breaths.

*** Frequent extrasystoles at the end of the experiment.

▮ = 1+ ▮▮ = 2+ ▮▮▮ = 3+ ▮▮▮▮ = 4+

The one-hour values in group A (Figure 1) show a greater decrease in "pre-exposure" than the other two exposures. The largest average decrease of 7.5% in this exposure was measured for MEFR 50%, while maximal mean changes in "control" and "challenge" exposures were less than 5%. None of the one-hour function changes in this group for any exposure reached a significance level of 0.05. The average two-hour data show a different pattern for all three

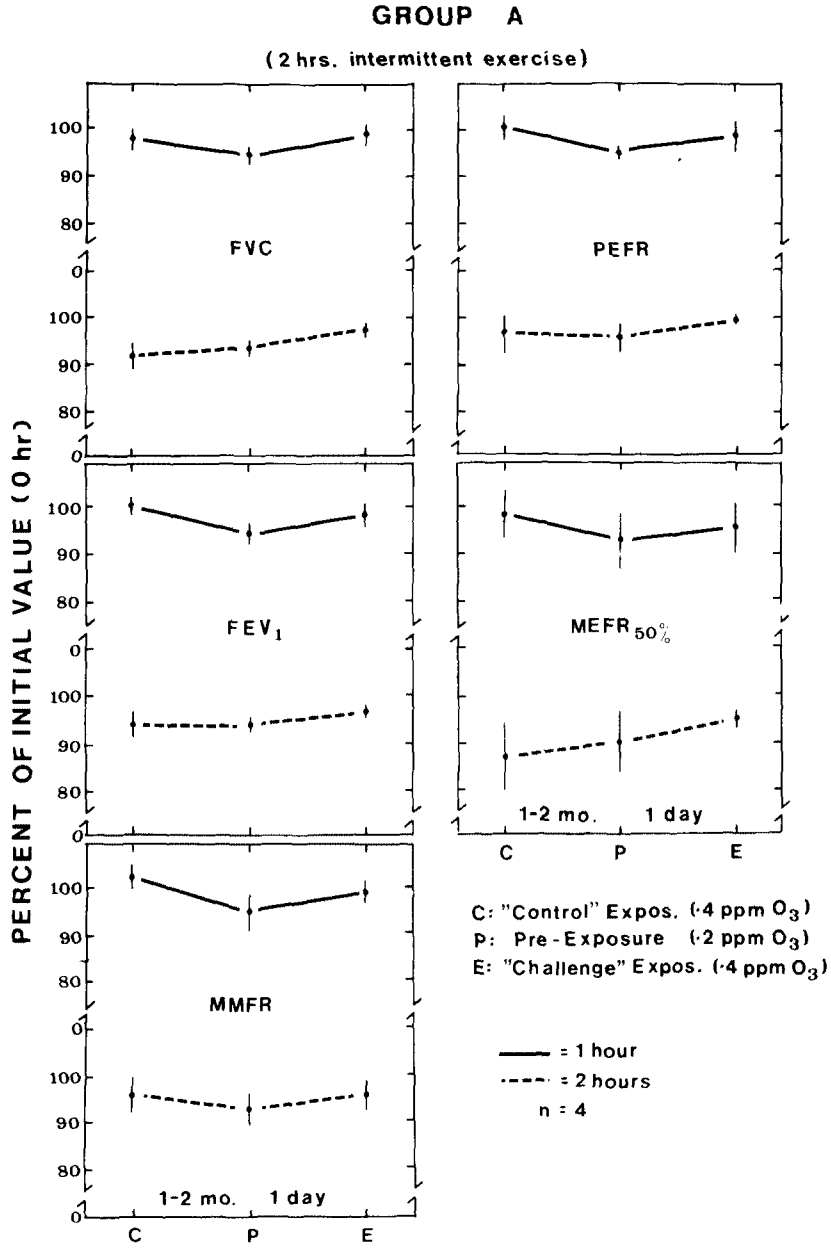

Figure 1. Changes in dynamic lung function tests (FVC, FEV_1, MMFR, PEFR, $MEFR_{50\%}$) in "control" exposure , "pre-exposure" and "challenge" exposure. All exposures were of two hours duration with intermittent exercise. Mean values for 4 subjects after one hour (solid line) and two hours (broken line) are expressed as percentage of the 0-hour mean value of each exposure. Bars represent standard errors. The exposure time sequence is given on the abscissa.

exposures. In general, the "control" exposure (0.4 ppm) produced greater decreases in lung function than the "challenge" exposure (0.4 ppm), with "pre-exposure" values being in between. However, no statistically significant differences were found using a three-way analysis of variance.

In group B (Figure 2) the pattern of lung function changes was similar to that in group A, except MEFR 50%, which dropped by 14% (86.0 ± 8.0) during one-hour "pre-exposure" and by 23.8% (76.2 ± 12.2) during two-hour "challenge" exposure testing. Corresponding decreases in group A were 7.5 ± 5.1% and 5.3 ± 1.6%, respectively. The difference between "challenge" and "control" exposure, which in this series was the last experiment instead of being the first one, were much smaller than in group A. Again, larger standard errors made it impossible to appreciate any difference between the results of these two exposures, and statistical significance was not attained in three-way analysis of variance.

Figure 3 shows the results obtained in group C. Since the subjects were exposed to a higher concentration of ozone the changes during "control" exposure (0.6 ppm) were greater, while values in the "pre-exposure" experiment (0.2 ppm) were very close to the ones obtained using corresponding levels of O_3 in group A and B. The third, "challenge" exposure (0.6 ppm) results were depressed to about the same degree as corresponding data in "control" exposure. The most sensitive tests were MMFR and MEFR 50%. After two hours the MMFR decreased 21.7% in the "control" exposure and by 25.5% in the "challenge" exposure. The slightly more sensitive MEFR 50% decreased by 23.5% and 26.6% respectively. The test data differences between these two groups were not statistically significant. However, if compared to "pre-exposure" data, the two-hour values for both 0.6 ppm O_3 series were significantly lower ($p < 0.05 - 0.01$).

The typical response pattern of group C changed completely after the concentration of O_3 in "pre-exposure" testing was increased to 0.4 ppm. These data, from group D, are presented in Figure 4. Although the changes in pulmonary function during the "control" exposure (0.6 ppm) are quite comparable to group C data, the "challenge" exposure (0.6 ppm) produced the smallest functional response of the three exposures. Despite the higher concentration of O_3 in the "challenge" exposure, the mean decreases from 0 hr. for both one- and two-hour test periods were smaller than in the "pre-exposure." Again, the most sensitive test to reflect these changes appeared to be MMFR, which compared to "control" exposure improved by 11.2% after two hours of breathing O_3 at "challenge" level. It was the only test to demonstrate significantly less deterioration ($p<0.05$) than was observed during "control" exposure. All other pulmonary function tests, although considerably improved, did not reach statistical significancy ($p<0.05$) mainly because of larger S. E.

DISCUSSION

Although the development of tolerance to ozone has been demonstrated in many animal studies (4, 5, 14) the possibility of adaptation to ozone in human subjects was first considered by Hackney et al. (12) when discussing the results of their multi-exposure experiments. The results of comparative studies on subjects exposed at two different laboratories under similar

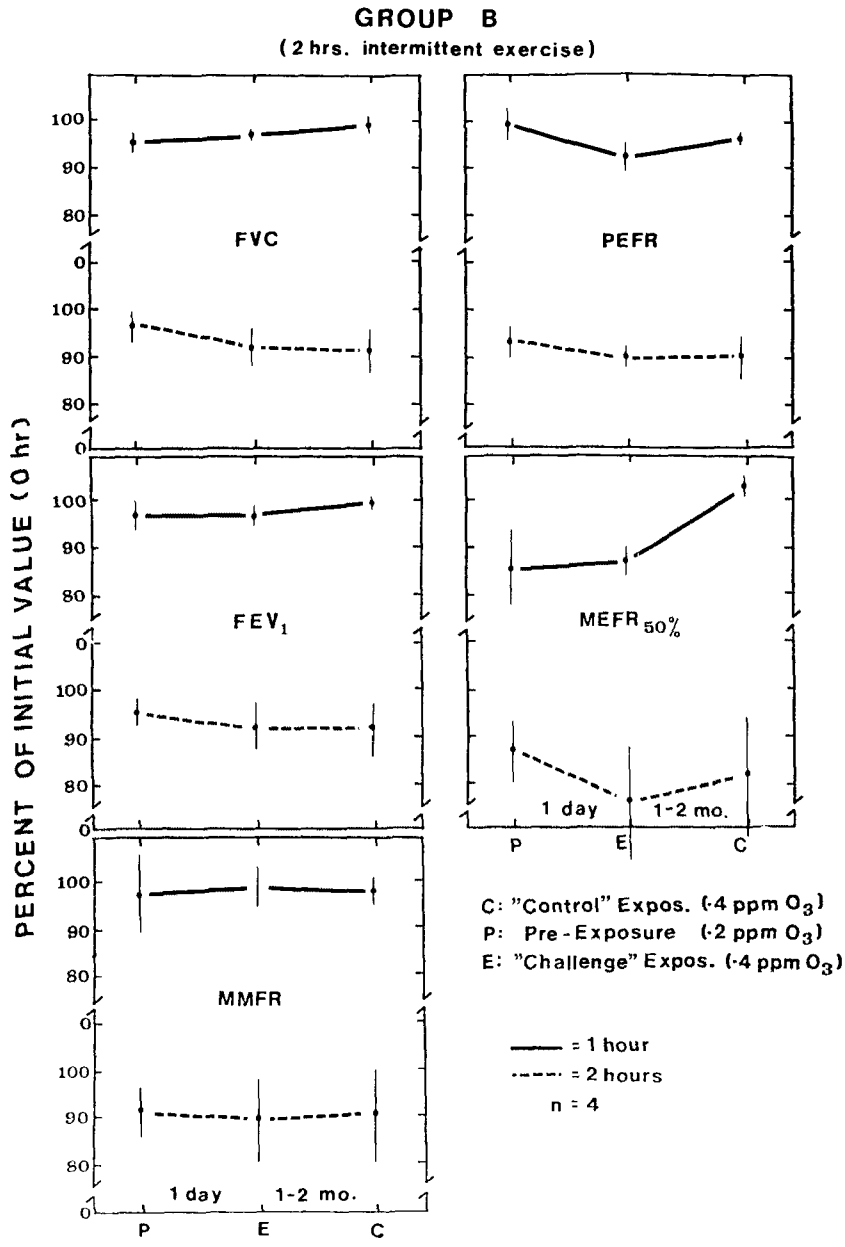

Figure 2. Changes in dynamic lung function tests (FVC, FEV_1 , MMFR, PEFR, $MEFR_{50\%}$) in "pre-exposure," "challenge" and "control" exposures. Abscissa and ordinate as in Figure !. However, subjects first underwent "pre-exposure" and "challenge" exposure, followed by 1-2 months later by "control" exposure. Values are means $\pm$ S. E. (n=4).

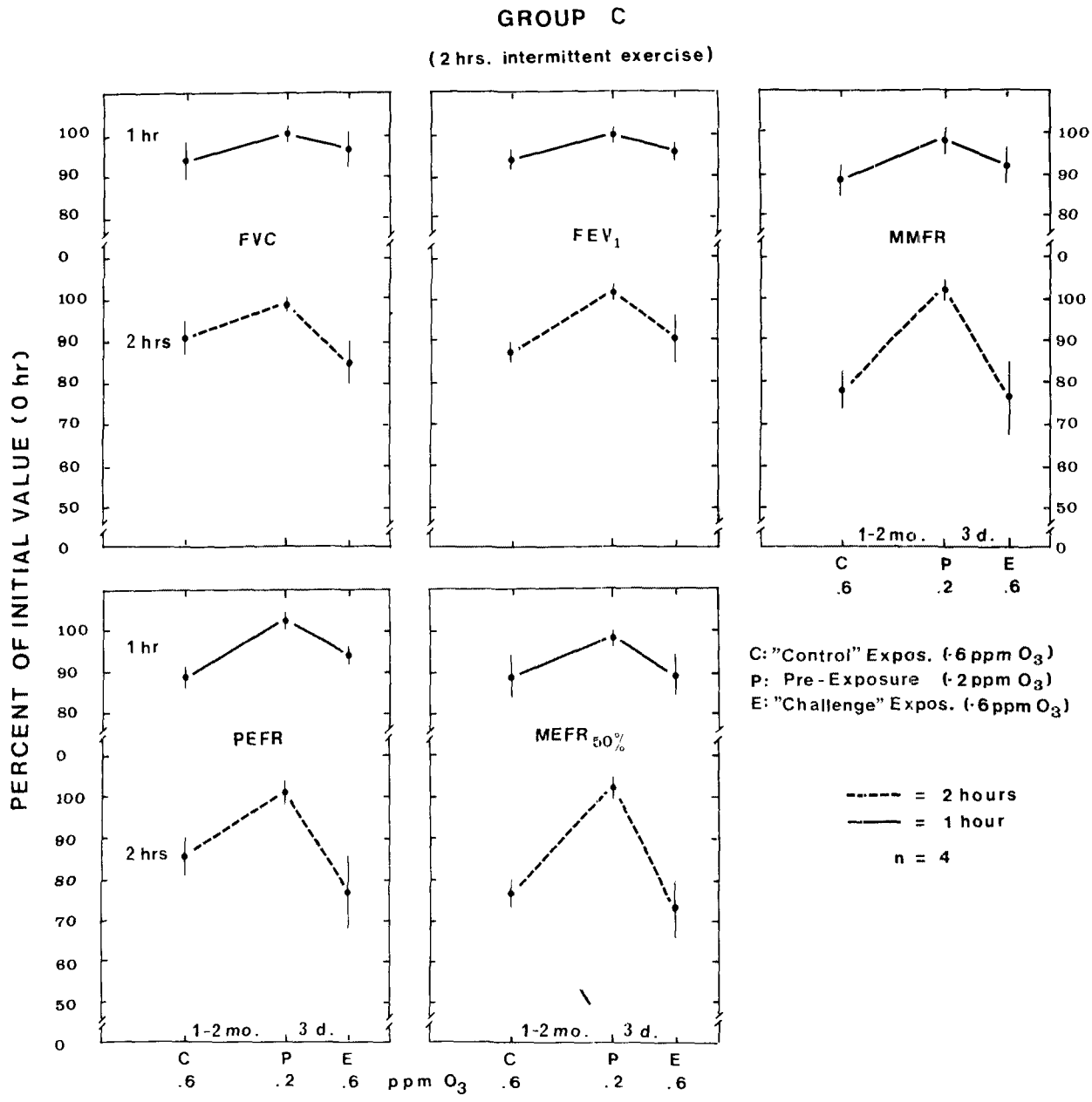

Figure 3. Changes in dynamic lung function tests (FVC, FEV_1, MMFR, PEFR, $MEFR_{50\%}$) for "control" exposure, "pre-exposure" and "challenge" exposure of four subjects. All exposures were of two hours with intermittent exercise. Lung function values are expressed as percentage of the 0-hour value in each exposure. The exposure sequence is displayed on the abscissa.

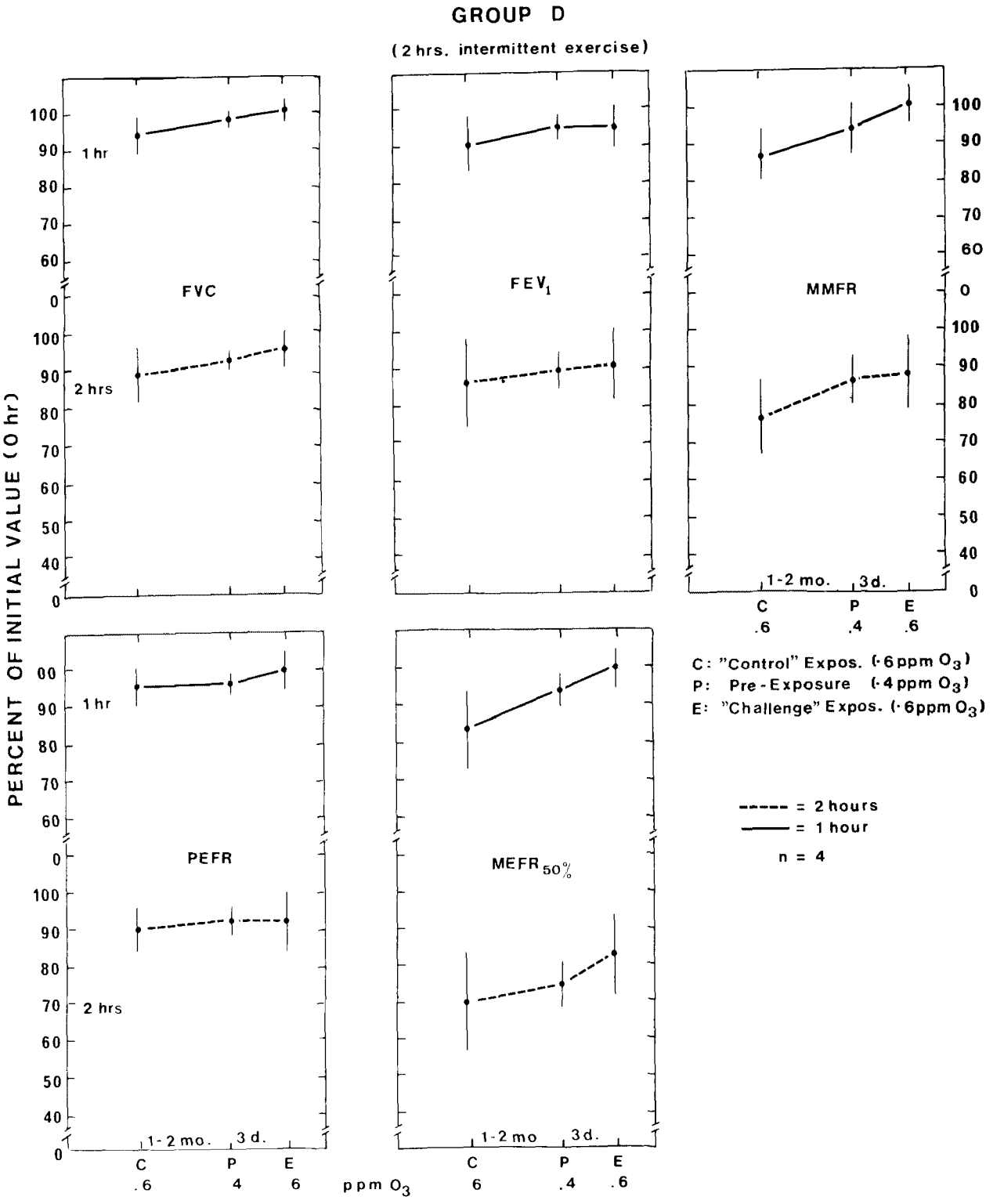

Figure 4. Changes in dynamic lung function tests (FVC, FEV_1, MMFR, PEFR, $MEFR_{50\%}$) for "control" exposure, "pre-exposure" and "challenge" exposure. Results are expressed as % of the 0-hour value in each exposure. Exposure time sequence is shown on the abscissa. Values are means ± S. E.

conditions (13) and data obtained from sequential exposures of the same subjects (8) provides further supporting evidence that tolerance can develop after repeated exposures to ozone.

In the present study groups, B and C did not show any adaptation in successive ozone exposures. Observed changes in dynamic lung function at different levels of ozone and days of exposure corresponded to decreases in lung function similar to those reported after single exposure (10, 15). It is of interest and importance to note that our data measured in group C, 0.6 ppm O_3, correlates closely with the data obtained on 20 subjects exposed under similar conditions and protocol by Ketcham et al. (16) and presented at this conference. Group A showed some signs of adaptation but the differences in mean values between "control" and "challenge" exposures were small and statistically insignificant. The only group that showed clear tolerance development, as indicated by smaller decreases in response on "challenge" exposure (0.6 ppm) after pre-conditioning to 0.4 ppm O_3, was group D.

At the present time the proposed action of various homeostatic and local mechanisms likely to explain tolerance development is not clearly understood (17). Numerous attempts have been made to study hormonal (18), immunologic (19), and pharmacological (4) mechanisms in the development of tolerance, but the results obtained have been incomplete, inconclusive, and often contradictory. Probably the most extensively studied effects in this category have been those induced via lung receptors. Changes in ventilatory parameters and reflex-mediated bronchoconstriction indicate that ozone-produced substances can reach and act on these receptors (20). Thus, it is conceivable that during pre-conditioning the threshold of these lung receptors could be modified, and consequently the response to a "challenge" exposure will be less marked. However, such alteration of bronchomotor tone, whether reflex or local, combined with other homeostatic mechanisms can only partially explain our findings.

Unilateral pulmonary exposures have shown that lung pre-treated with ozone is protected against the toxic effects of ozone challenge while at the same time unexposed lung was afforded no protection to these effects (21). These findings strongly indicate that tolerance can be induced by some local changes. The experimental evidence that ozone can penetrate to the alveoli and alter surface active material might explain at least some of these changes (22). Altered production of surfactant can constitute a convenient mechanism for explaining tolerance not only at the alveolar level but also in terms of changed lung mechanics. Our data have demonstrated considerable improvement not only of central airways impairment but also improved functioning of impaired peripheral airways. Furthermore local irritation of smooth bronchiolar muscle causing narrowing of the airways is possibly suppressed or prevented by altered chemistry of the surrounding tissue. It has been well documented that antioxidants protect against ozone insults (23). Changes in the concentration of vitamin E in the pulmonary tissue for example may affect the pulmonary response to ozone in some way and thus facilitate tolerance development. Furthermore, depressed activities of various hydrolytic enzymes may lessen ozone effects as well (24). Whether any or all these changes are pertinent to our observations is difficult to say, but certainly both homeostatic and local mechanisms are responsible for diminished response in "challenge" exposure.

Our studies demonstrated that the extent of the changes induced by the challenge exposure depends primarily on the ozone concentration during pre-conditioning and the time interval between pre-conditioning and challenge exposures. However, because of the small size of the groups, more extensive experiments are needed to better define the delay time required for tolerance development and the minimum concentrations of ozone required to produce subsequent tolerance. Moreover, we cannot be sure that this adaptation process yields a truly "protective effect" because the mechanisms involved are unclear, and the final consequence of such adaptation cannot be evaluated without understanding the mechanisms by which it is achieved.

ACKNOWLEDGMENTS

This investigation was supported by grants from the Quebec Medical Research Council and the Canadian Thoracic Society.

REFERENCES

1. Monitoring and Air Quality Trends Report, 1973, EPA-450/1-74-007, 1974.

2. Air Quality Monitoring Report, Ontario Ministry of Environment, 1971.

3. Coffin, D. L. The relationship of infectious agents and air pollutants. Presented at the Inter-Regional Symposium on Air Quality Criteria and Guides, World Health Organization, Geneva, Switzerland, October 5-9, 1970.

4. Matzen, R. N. Development of tolerance to ozone in reference to pulmonary edema. Am. J. Physiol. 190: 84-88, 1957.

5. Stokinger, H. E., W. D. Wagner, and P. G. Wright. Studies on ozone toxicity. I. Potentiating effects of exercise and tolerance development. Arch. Ind. Health 14: 158-162, 1956.

6. Scheel, L. D., O. J. Dobrogorski, J. T. Mountain, J. L. Svirbely, and H. E. Stokinger. Physiologic, biochemical, immunologic and pathologic changes following ozone exposure. J. Appl. Physiol. 14: 67-80, 1959.

7. Hallet, W. Y. Effects of ozone and cigarette smoke on lung function. Arch. Environ. Health 10: 295-302, 1965.

8. Hackney, J. D., W. S. Linn, D. C. Law, et al. Experimental studies on human health effects of air pollutants: III. Two-hour exposure to ozone alone and in combination with other pollutant gases. Arch. Environ. Health, 1975, 30, 385.

9. Bates, D. V., G. Bell, C. Burnham, M. Hazucha, J. Mantha, L. D. Pengelly, and F. Silverman. Problems in studies of human exposure to air pollutants. Can. Med. Assoc. J. 103: 833-837, 1970.

10. Bates, D. V., G. M. Bell, C. D. Burnham, M. Hazucha, J. Mantha, L. D. Pengelly, and F. Silverman. Short-term effects of ozone on the lung. J. Appl. Physiol. 32: 176-181, 1972.

11. Goldsmith, J. R., and J. A. Nadel. Experimental exposure of human subjects to ozone. J. Air. Pollut. Contr. Assoc. 19: 329-330, 1969.

12. Hackney, J. D., W. S. Linn, J. G. Mohler, et al. Experimental studies on human health effects of air pollutants: II. Four-hour exposure to ozone alone and in combination with other pollutant gases, Arch. Environ.Health, 1975, 30, 379.

13. Hackney, J. D., W. S. Linn, S. K. Karuza, R. D. Buckley, D. C. Law, D. V. Bates, M. Hazucha, L. D. Pengelly, and F. Silverman. Health effects of ozone exposure in Canadians vs. Southern Californians. Am. Review Respiratory Disease III (6): 902, June 1975.

14. Mittler, S., M. King, and B. Burkhardt. Toxicity of O_3. Arch. Ind. Health 15: 191, 1957.

15. Hazucha, M., F. Silverman, C. Parent, S. Field, and D. V. Bates. Pulmonary function in man after short-term exposure to ozone, Arch. Environ. Health, 1973, 27, 183.

16. Ketcham, B. et al. The effects of ozone plus moderate exercise on pulmonary function in healthy young men. In: Proceedings of the Int. Conf. on Photochemical Oxidant Pollution and its Control, 1976, U. S. Environmental Protection Agency, Research Triangle Park, N. C.

17. Fairchild, E. J. Tolerance mechanism. Arch. Environ. Health. 14: 111-124, 1967.

18. Fairchild, E. J. Neurohumoral factors in injury from inhaled irritants. Arch. Environ. Health 5: 79-86, 1963.

19. Gregory, A. R., and L. A. Ripperton. Effect of neonatal thymectomy on ozone tolerance in mice. Read before the Toxicology Session of the American Hygiene Conference, Houston, 1965.

20. Wilddicombe, J. G., and G. M. Sterling. The autonomic nervous system and breathing. Arch. Intern. Med. 126: 311-329, 1970.

21. Alpert, S. M., and T. R. Lewis: Ozone tolerance studies utilizing unilateral lung exposure. J. Appl. Physiol, 1971, 31, 243.

22. Mendenhall, R. M., and H. E. Stokinger. Films from lung washings as a mechanism model for lung injury by ozone. J. Appl. Physiol. 17: 28-32, 1962.

23. Tappel, A. L. Vitamin E as the biological lipid antioxidant. Vitamins Hormones 20: 493-510. 1962.

24. Gardner, D. E., T. R. Lewis, S. M. Alpert, D. J. Hurst, and D. L. Coffin. The role of tolerance in pulmonary defense mechanisms. Arch. Environ. Health 25: 432-438, 1972.

SESSION 11

PHYSIOLOGICAL EFFECTS OF OXIDANTS - II

Chairman: J. Knelson
Environmental Protection Agency

TOXIC INHALATION OF NITROGEN DIOXIDE IN CANINES

T. L. Guidotti and A. A. Liebow*

ABSTRACT

An experimental design of bronchial intubation and independent ventilation in beagles permitted precise delivery of 37.2 ppm of nitrogen dioxide (NO_2) to the left lung, but preserved the right lung as a subject-specific control. Serial measurements of oxygen uptake by the exposed lung showed an early reversible decline averaging 65%, best explained by the induction of a ventilation-perfusion inequality. Ultrastructural studies were augmented by morphometric analysis and revealed NO_2-induced changes in the interstitium compatible with early interstitial edema, very scant alveolar epithelial desquamation, and swelling with increased numbers of pinocytotic vesicles in the capillary endothelium, all appearing in the exposed lung. Early acute exposure to NO_2 appears to alter gas exchange and has its earliest visible toxic effect on the pulmonary capillary endothelium with the subsequent induction of interstitial edema. The magnitude of these changes in the lower concentration ranges, characteristic of photochemical air pollution, deserve study.

INTRODUCTION

The high clearance of nitrogen dioxide (NO_2) in the upper respiratory tract complicates pathophysiologic studies on the inhalation of this oxidant, which is a gas of major importance in photochemical air pollution. This clearance varies among species of animals and approaches 90% in dogs (1, 2). An experimental technique of unilateral, left mainstem bronchial cannulation bypasses the upper airway and preserves the right lung as a matched unexposed control. In this manner direct effects of inhaled NO_2 may be demonstrated unclouded by variations in technique, exposure, or individual animal sensitivity.

MATERIALS AND METHODS

Five purebred beagle dogs weighing approximately 13.5 kg, between 9 and 12 months of age, were examined, X-rayed for pulmonary disease, dewormed,

*T. L. Guidotti, the Johns Hopkins University School of Medicine, Baltimore, Maryland;
A. A. Liebow, University of California at San Diego, School of Medicine, La Jolla, California.

quarantined, and given intramuscular penicillin prophylaxis a week before the experiment. Under intravenous sodium thiamylal anesthesia with atropine, a specially designed stainless steel cannula was intubated and sealed the left mainstem bronchus. The left lung was ventilated by a Harvard pump delivering a premixed atmosphere of air and 37.2 ppm NO_2 by way of the cannula. The right lung received the same atmosphere, without NO_2, through a sealed airway surrounding the cannula. Connection to a Gaensler-Collins® bronchospirometer (Warren E. Collins, Inc.) allowed serial measurement of the oxygen uptake by each lung every 30 minutes. Selected physiological variables were also measured serially: heart rate, core temperature, hematocrit, methemoglobin, plasma hemoglobin, leukocyte count and differential, and breath sounds on auscultation of the thorax.

Following four hours of observation, the animals were sacrificed with a lethal intravenous injection of barbiturate. The lungs and heart were dissected promptly en bloc, and the trachea and main pulmonary artery were cannulated. A solution of 2.5% glutaraldehyde in 0.2 M sodium cacodylate buffered to between pH 7.25 and 7.40, warmed to 37.0°C., and checked for isotonicity at 300 mOsm by freezing point depression, was used as the fixative (3). The lungs were perfused by siphon with fixative under a pressure of 30 cm of water by way of the trachea and under 35 cm of water pressure by way of the pulmonary trunk; they were also totally immersed in fixative, all for over two hours.

Preparation for light microscopy consisted of paraffin embedding, sectioning, and staining of the slides with hematoxylin and eosin. Electron microscopy required further division into 1 mm^3 cubes, postfixation with 2% osmium tetroxide in sodium cacodylate buffer, dehydration with ethanol, and embedding in araldite resin. Thin sections (< 450 Å) were stained with uranyl acetate and lead citrate and were examined on copper grids under transmission electron microscopy. Photographs of 110 fields were matched between control and exposed lung tissue as being identical in anatomic and histologic location, magnification, contract, and experimental animal subject. The features of these were analyzed using the morphometric techniques of Weibel and colleagues (5, 6), i.e., stereological properties of the epithelium, interstitial space, capillary endothelium, and endothelial pinocytotic vesicles were compared statistically by the analysis of variance between control and exposed lungs, using the frequency of interception of points and lines on an overlying standard geometric grid. This system allowed calculation of volume proportions and surface-to-volume ratios for each structure.

RESULTS

The oxygen uptake by both lungs and by the exposed (left) lung alone is presented for each experimental animal in Figure 1. Oxygen uptake by the exposed lung fell abruptly and markedly within the first half-hour of exposure, to an average 65% of the initial value ($P < 0.01$). This fall was reversible and occurred despite a slightly increased ventilatory frequency (initial mean 48 increasing to 55) and an unchanged tidal volume (mean 55 ml). After subsequent recovery, the oxygen uptake invariably declined again, to a persistently lower oxygen uptake by the exposed lung ($P < 0.05$). In one animal in

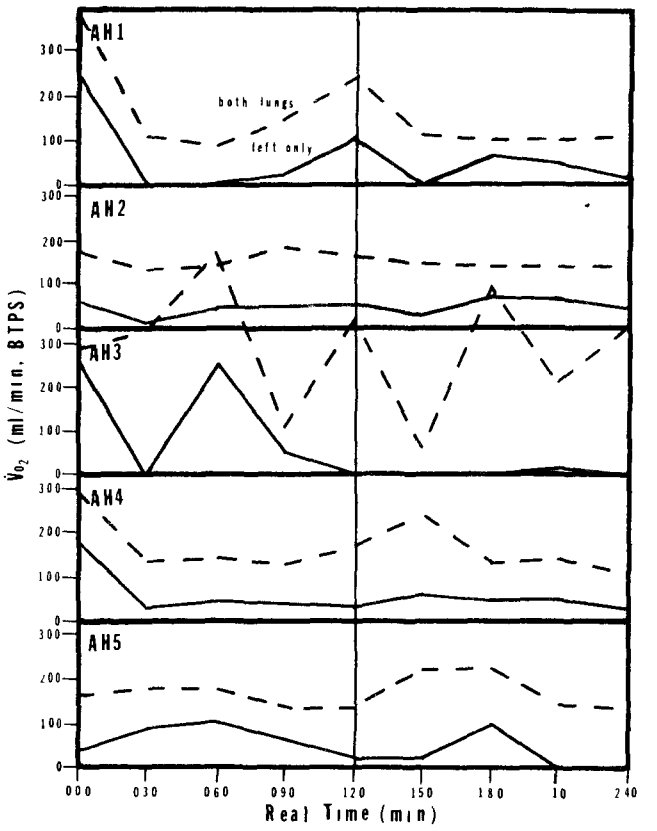

Figure 1. Oxygen uptake by both lungs and by the exposed (left) lung alone.

which blood gases were measured, the initial P_{O_2} of 96 fell to 65 torr in the first half hour, with changes of P_{CO_2} and pH from 40.5 and 7.39 to 33.5 and 7.30, respectively.

The heart rate, core temperature, hematocrit, plasma hemoglobin, leukocyte count and differential all were within normal limits for beagles and sustained no significant changes. On auscultation of the thorax, rales appeared earlier on the exposed side (mean 67 minutes vs. 108 minutes on the unexposed side).

Examination by light microscopy showed no visible evidence of pathologic change in either side, control or experimental. Ultrastructural examination revealed several subtle differences, however. The interstitium was compact and highly structured throughout the control tissue, but discrete areas of reduced density and loose structure were visible in many fields of exposed tissue, often adjacent to capillaries (Figure 2). This ultrastructural pattern is compatible with early interstitial edema. The capillary endothelium was highly variable in width and in the frequency of vesicles, on both sides; an impression of increased endothelial redundancy was noted in the exposed tissue (Figure 3). The capillary lumen was in all fields and there was no variation in the width nor breach of integrity of the endothelial basement membrane. An isolated event of epithelial desquamation in the exposed lung was the only noteworthy observation of the epithelium. Mitochrondria were seldom seen with sufficient resolution to assess swelling.

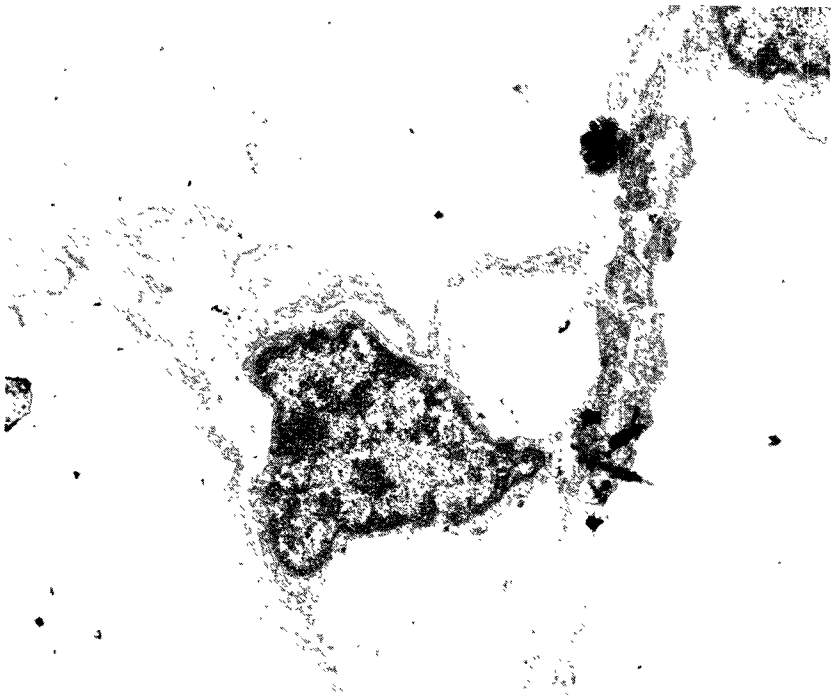

Figure 2. Disorganization of structure in the interstitium in the exposed lung.

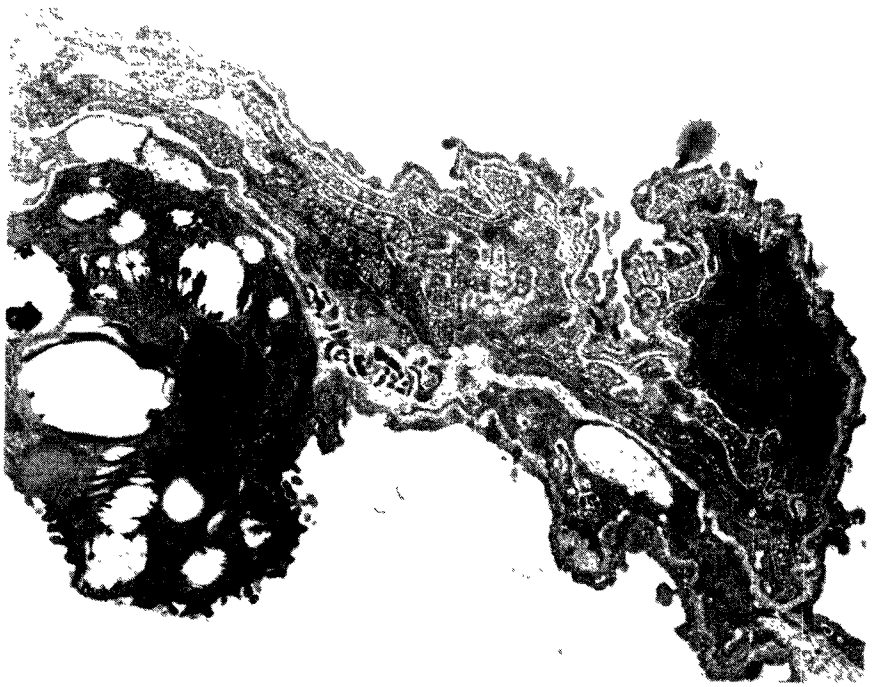

Figure 3. Endothelial redundancy and increased frequency of vesicles in the exposed lung.

Morphometric analysis of the paired prints added considerable information in Table 1.

TABLE 1. MORPHOMETRIC ANALYSIS

Ultrastructural Feature	Volume Ratio[a]		Surface-to-Volume Ratio[b]		Anal. Var.[c]
Exposed or Control:	E	C	E	C	P
Alveolar:Capillary Barrier[d]	0.222	0.215	4.340	4.166	<0.01
Alveolar Epithelium	0.104	0.090	0.028	0.033	>0.10
Interstitium	0.169	0.185	0.335	0.287	>0.10
Capillary Endothelium	0.108	0.087	0.872	0.521	<0.01
Endothelial Vesicles	0.167	0.081	---	---	<0.01

a,b. Where P_i = collective number of test grid points falling on structure i in multiple microscopic sections, P_T = total number of test points overlying all sections surveyed, and N_i = the collective number of intersections between the margins of structure i and a large arbitrary number of test grid lines of length Z overlying multiple sections, then the volume ratio $V_i/V_T = P_i/P_T$ and the surface-to-volume ration $S_i/V_i = 4N_i/ZP_i$ for structure i. (refs. 5, 6)

c. The observation subjected to analysis of variance was P_i.

d. The sum of epithelium, interstitium, and endothelium.

The entire alveolar:capillary barrier, as the sum of its three structures (see Note d, Table 1), was significantly larger in dimension in the exposed lung than in the control. The alveolar epithelium alone was not significantly different. The interstitium presented an increased surface-to-volume ratio with a comparable volume ratio, suggesting a deformity in shape toward the more globoid on the exposed side. The capillary endothelium is markedly, significantly altered with a greater volume ratio, greater surface-to-volume ratio, and increased frequency of vesicles on the exposed side. These findings imply increased thickness, more convoluted shape, and a more dense concentration of pinocytotic vesicles.

DISCUSSION

The study design of unilateral exposure by cannulation permits complicating factors of individual subject variation, experimental manipulation, and position under anesthesia to affect both lungs equally and simultaneously in one animal. Secondary effects of local tissue injury, local reflexes, and systemic toxicity are, if not prevented, minimized.

The bronchospirometric finding of a marked reversible reduction in oxygen uptake parallels the finding that humans inhaling lesser concentrations of NO_2 experience acutely reduced carbon monoxide diffusing capacity, reduced arterial blood oxygen tension, and alterations in pulmonary arterial perfusion, all within 30 minutes of exposure and all reversibly (7, 8). Oxygen uptake was used to assess gas exchange because it is a direct and sensitive measurement of mass displacement, whereas arterial oxygen saturation is a product of several variables. Of the four processes that affect alveolar-capillary gas exchange, hypoventilation was prevented mechanically and there was no anatomic basis for shunting. Morphometric studies by others suggest that the small increase in alveolar-capillary barrier dimension is not sufficient to inhibit gas exchange (9). Also, interstitial edema as a cause of such a block would not be so rapidly reversible. The most satisfactory explanation for the bronchospirometric findings is that inhalation of NO_2 in the 30 to 40 ppm range is capable of inducing redistribution of pulmonary perfusion, and may compound the resulting ventilation-perfusion inequality by inducing regional variations in airway resistance. Such alterations in perfusion (7) and ventilation (8) are suggested for humans in this range of dosage.

Morphometric analysis assisted greatly in the identification and interpretation of ultrastructural changes. Four key observations characterized the exposed tissue:

- Loosening of the interstitial structure and deformation of the interstitial space, implying incipient interstitial edema;
- Increased dimension of the capillary endothelium and increased redundancy of the surface, implying selective toxicity, and the endothelial cell first to be affected;
- Increased endothelial activity as evidenced by the number of vesicles, suggesting a membrane-based metabolic response to NO_2 toxicity;
- Scant early epithelial desquamation, confirming the role of endothelial rather than epithelial cell alteration in the earliest phase of cytotoxicity.

The first two effects plausibly explain the increased dimension of the entire alveolar-capillary barrier after exposure. Recognition of the endothelial cell, which is metabolically very active, as the earliest cell to be affected establishes a tentative sequence for the cellular lesions seen by others (10).

CONCLUSIONS

The concentration (37.2) ppm of NO_2 employed in this study, with its unique system of unilateral pulmonary exposure, produces a subtle toxic effect on the pulmonary capillary endothelium and induces interstitial edema. It also causes a functional deterioration of gas exchange, which is best explained as a pharmacologically or reflexly mediated maldistributution of pulmonary perfusion and ventilation.

An impressive body of information has accumulated to describe the pulmonary effects of NO_2 inhalation (11). Their potential interactions can be organized into a tentative integrated scheme as in Table 2. The role of local peripheral reflexes and of central nervous system reflexes is omitted only because of a lack of information, yet these surely must play a significant role in the integrated response.

Toxic inhalation of NO_2 is a complex process, and the study of its component interactions is assembling a picture of generalized diffuse alveolar damage. The task remaining is to determine the relative sequence and magnitude of the interactions in the ranges of exposure to photochemical air pollution.

REFERENCES

1. Dalhamn, T., and J. Sjöholm. Studies on SO_2, NO_2, and NH_3: Effect on Ciliary Activity in Rabbit Trachea of Single in Vitro Exposure and Resorption in Rabbit Nasal Cavity, Acta. Physiol. Scand., 58:287-291, 1963.

2. Vaughan, T. R., L. F. Jenelle, and R. T. Lewis, Long-Term Exposure to Low-Levels of Air Pollutants, Arch. Environ. Health., 19:45-50, 1969.

3. Gil, J., and E. R. Weibel, The Role of Buffers in Lung Fixation with Glutaraldehyde and Osmium Tetroxide., J. Ultrastruct. Res., 25:331-348, 1968.

4. Gil., J., Ultrastructure of Lung under Physiologically Defined Conditions, Arch. Int. Med., 217:896-902, 1970.

5. Weibel, E. R., G. S. Kistler, and W. F. Scherle, Practical Stereological Methods for Morphometric Cytology, J. Cell Biol., 30:23-38, 1966.

6. Wiebel, E. R., Stereological Principles for Morphometry in Electron Microscopic Cytology., Int. Rev. Cytol., 26:235-302, 1969.

7. Von Nieding, G., et al., Akute Wirkung von 5 ppm NO_2 auf die Lupgen- und Kreislauffunktion des gesunden Menschen., Int. Arch. Arbeitsmed, 27:234-243, 1970.

8. Von Nieding, G., et al., Studies of the Acute Effects of NO_2 on Lung Function: Influence on Diffusion, Perfusion, and Ventilation in the Lungs, Int. Arch. Arbeitsmed., 31:61-72, 1973.

TABLE 2. SCHEMA OF THE PATHOPHYSIOLOGY OF INHALED NITROGEN DIOXIDE

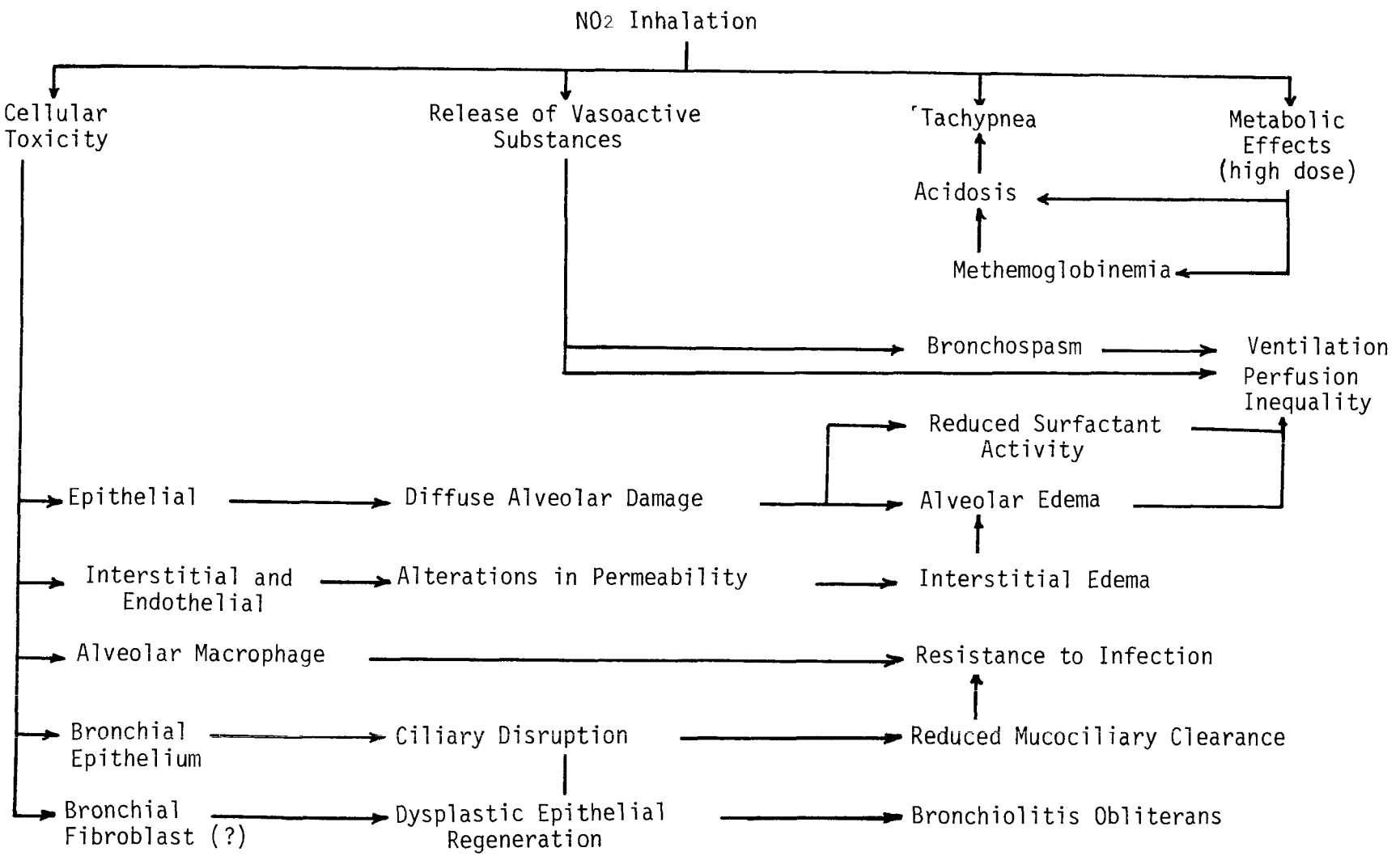

9. Dillman, G., D. Henschler, and W. Thoenes, Stickstoffdioxydwirkung an der Lungenalveole der Maus: Morphometrischelektronmikroskopische Untersuchungen, Arch. Toxikol, 23:55-65, 1967.

10. Dowell, A. R., K. H. Kilburn, and P. C. Pratt, Short-term Exposure to Nitrogen Dioxide: Effects on Pulmonary Ultrastructure, Compliance, and the Surfactant System, Arch. Int. Med., 128:74-80, 1971.

11. Guidotti, T. L., Toxic Inhalation of the Higher Oxides of Nitrogen, M.D. Thesis, University of California at San Diego School of Medicine, La Jolla, California, 1975, 119 pp.

THE EFFECT OF OZONE ON THE VISUAL EVOKED POTENTIAL OF THE RAT SUPERIOR COLLICULUS AND VISUAL CORTEX

B. W. Berney, R. S. Dyer, and Z. Annau*

ABSTRACT

The possibility that exposure to low levels of ozone may change central nervous system (CNS) responses to sensory stimulation was examined using the averaged evoked potential technique. Rats with recording electrodes chronically implanted in either superior colliculus or visual cortex were exposed to either 0.00 ppm, 0.50 ppm, 0.75 ppm, or 1.00 ppm ozone for 140 minutes. Amplitudes and latencies of evoked potentials recorded during the last 20 minutes of exposure were compared to pre-exposure recordings. No amplitude changes were found in the cortex or in the superior colliculus. Latencies tended to increase with increasing concentration of ozone. Several explanations for this effect are possible, although at present the most likely is that ozone produces CNS changes by peripheral irritation, which may lead to increased intraocular pressure.

INTRODUCTION

Among possible deleterious effects of ozone is alteration of central nervous system (CNS) function. Previous work concerning the effect of ozone on the CNS has been reported by Xintaras et al. (16), who acutely exposed rats that were chronically implanted with electrodes to 0.5 – 1.0 ppm ozone and recorded summated evoked potentials from the superior colliculus (SC) and visual cortex (VC). Unfortunately, their presentation of findings was not quantitative, and thus the findings are difficult to interpret. The present work was undertaken, therefore, to quantitatively assay the effect of low levels of ozone upon the rat CNS.

The method selected for measurement of CNS function was the visual evoked response in unanesthetized rats. The principal of the flash-evoked potential, a type of visual evoked response, is that a brief, bright visual stimulus evokes a neural response that can be recorded from various locations along the visual pathway. The average of many responses gives a characteristic wave form when monitored from certain neuroanatomical structures along the visual tract. The evoked potential is similar to the EEG, in that what is recorded

---

*The John Hopkins University, Baltimore, Maryland.
B. W. Berney is now at Environmental Control, Inc., Rockville, Maryland.

is generally accepted to be a reflection of post synaptic potentials summated across many neurons. The evoked potential differs from the EEG by representing the response of a group of neurons to a sudden stimulus. It therefore allows evaluation of the way in which the brain processes a standard signal under different experimental conditions.

The sensitivity of this test demonstrated by an earlier carbon monoxide (CO) study indicated that it may be a useful measure of CNS changes induced by other potentially toxic agents, in this case ozone (2). To take full advantage of the apparent sensitivity of this technique, the present protocol follows closely the one used by Dyer and Annau (1). All ozone levels used in this experiment were 1 ppm or less to permit evaluation of the CNS at levels below those generally accepted as necessary for producing such gross physiological changes as pulmonary edema.

MATERIALS AND METHODS

Twenty adult male, Long-Evans hooded rats (Blue Spruce Farms) weighing 350-550 grams were anesthetized with 1.5 cc Equithesin and implanted with .25 mm Nichrome wire as electrodes using a stereotaxic unit. Fourteen rats were implanted with a bipolar electrode with tip separation of approximately 1 mm. This electrode was lowered into the SC 5.5 mm posterior to bregma, 1.5 lateral and about 4 mm deep according to the Atlas of Skinner (13). Six rats to be used in VC recordings were fitted with 0-80 stainless steel screws, which served as electrodes. One screw was placed 5.5 mm posterior to bregma and 3.5 lateral over the visual cortex. A second screw was placed 1 mm posterior to bregma and 2 mm lateral over the frontal cortex. This electrode served as reference for the VC electrode. In addition, each rat had a screw placed in the skull over the frontal sinus to be used as a ground. The electrodes were all connected to an Amphenol receptacle, which was subsequently cemented to the skull. At least 1 week was allowed for recovery from surgery before any recordings were made.

After dilation of the pupils with atropine to assure uniformity of pupil diameter, the animals were connected to a recording apparatus by means of an Amphenol plug and Microdot mininoise shielded cable. They were then placed in a 8 x 20 x 38 cm plexiglas chamber with reflecting surfaces on all walls, ceiling, and floor. A portion of one wall included a window through which the lamp from a Grass PS-2 photostimulator provided the 1.5×10^6 cp 10 usec visual stimulus.

A PDP-8 computer triggered the photostimulator every 2.5 sec. Neural activity was passed through a Tektronix 122 preamplifier with high and low frequency filters set at 10 Khz and 0.2 hz respectively. The computer summated and averaged 240 msec epochs following each stimulus, and the resulting averaged evoked potential was displayed on an oscilloscope, where a cursor controlled by one analog channel and a teletype could be used to obtain a printout of the latency and amplitude of any point on the waveform. In this study, each averaged evoked potential was obtained from 500 flashes.

Ozone was produced by passing compressed air over 4 x 4 watt germicidal bulbs (General Electric, G4S11), which were mounted inside a sealed glass aquarium. During exposure runs the ozone-air mixture was passed into the recording chamber at 7 liters per minute (LPM), which was equivalent to 8.7 air changes per minute. The same flow was used when air was passed through the chamber for pre-exposure and 0.00 ppm control runs.

Ozone was monitored in the recording chamber by means of a Mast oxidant meter (Mast Development Co., Davenport, Iowa). The meter was monitored visually, with flow adjustments made when necessary. The meter was calibrated at the National Bureau of Standards (Gaithersburg, Md.) before the experiment and verified by calibration against a known concentration of ozone post-experimentally.

The protocol consisted of 10 min of habituation to the 0.4 hz flashes followed by averaging the responses to 500 flashes to obtain a pre-exposure evoked potential. During this time, the animal was exposed to 7 LPM of compressed air. Immediately after the pre-exposure evoked potential was obtained, a 140-minute exposure to one of several concentrations of ozone (0.00, 0.50, 0.75, or 1.00 ppm) was begun. After 110 minutes of exposure a second 10 minute flash habituation period occurred, and following this the averaged response to 500 flashes was again obtained. The percentage change from pre-exposure control was then evaluated for each peak-to-peak amplitude and for each peak latency. A dose-response curve was determined from these data for each evoked potential component by averaging the percentage changes across animals at each concentration of ozone. In order to eliminate aberrant readings due to sickness, conjunctival inflammation or other acute conditions, individual runs were eliminated if the pre-exposure value of P3-N4 amplitude was less than one-half of the average of all pre-exposure amplitudes of P3-N4 for the particular animal. Animals with P3-N4 values below 80 μvolts were also eliminated. At least 1 week was allowed to elapse between exposures to ozone.

Upon death, the animals were perfused with saline followed by formalin, and the electrodes were removed. The brains were frozen and sectioned at 90 μ to confirm proper placement of the electrodes. Cresyl violet stain was used. Only animals with proper placement of electrodes in the SC were used in the data analyses.

RESULTS

The output of the CNS from the monitored regions gave a characteristic waveform for both the SC and VC. These waveforms were similar to typical flash-evoked potentials obtained from the SC and VC as characterized by Dyer and Annau (1). Typical waveforms are displayed in Figures 1 and 2 for the SC and VC, respectively. The P1, P2, and N4 peaks in the SC waveforms are the most stable on both a trial-to-trial and day-to-day basis (1). In the results to be presented, evaluation of percentage change from pre-exposure control of peak-to-peak amplitudes (e.g., P3-N4) and latencies (e.g., P1, N4) were used to determine CNS response to the pollutant ozone.

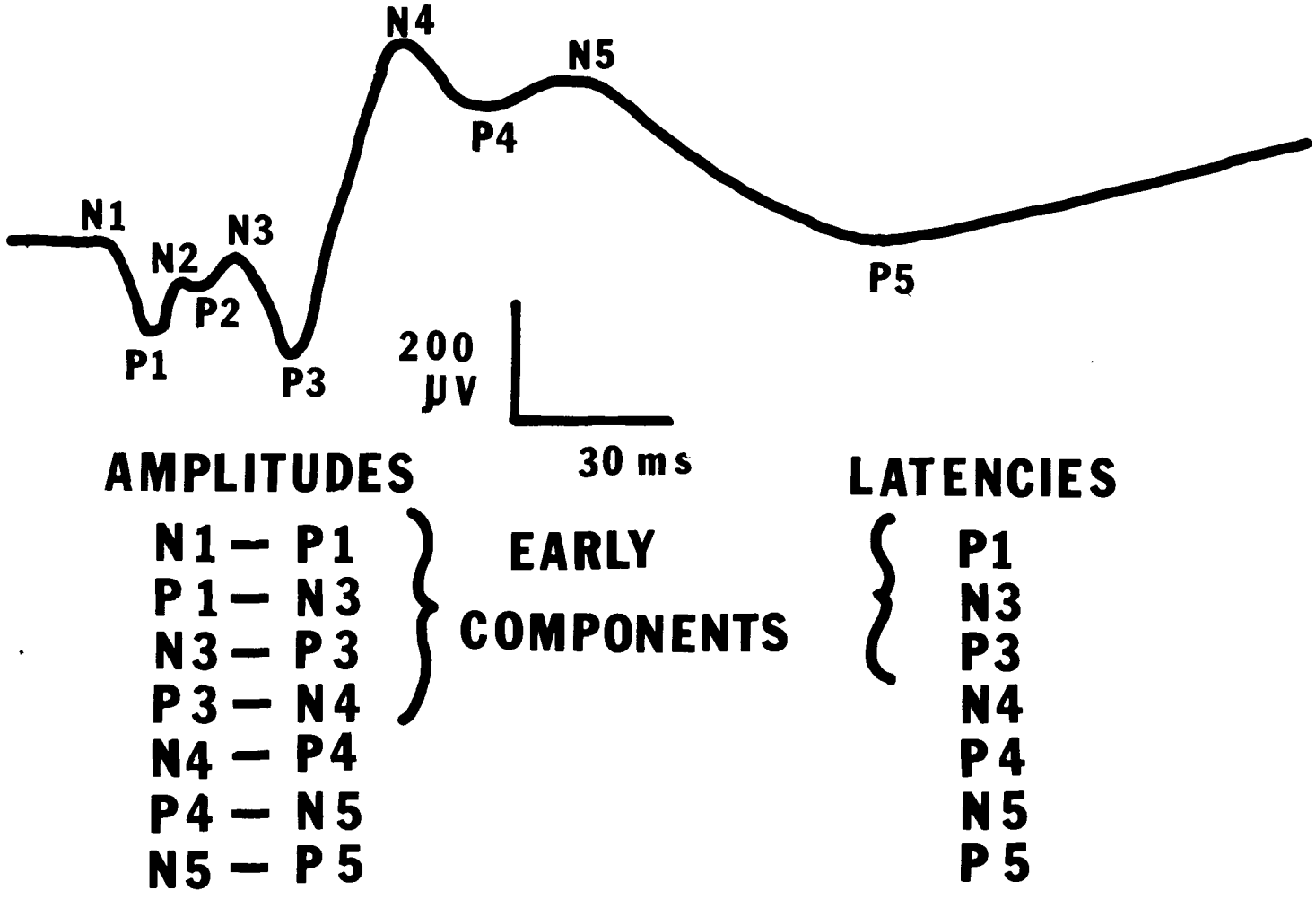

Figure 1. Normal superior colliculus evoked potential.

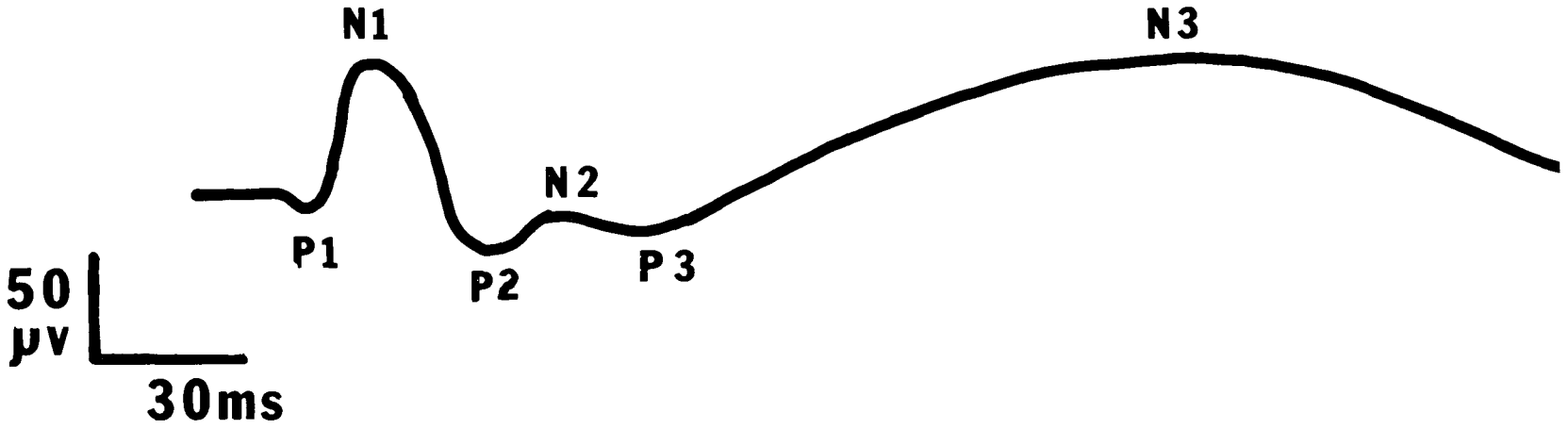

AMPLITUDES

P1 — N1
N1 — P2
P2 — N3

EARLY COMPONENTS

LATENCIES

N1
P2
N3

Figure 2. Normal visual cortex evoked potential.

SUPERIOR COLLICULUS

The peak-to-peak amplitudes that were selected for analysis were N1-P1 and P3-N4. Latencies evaluated were those at N1, P3, and N4.

A general increase in amplitude of the P3-N4 and N1-P1 components resulted from exposure to ozone. However, a repeated measures analysis of variance revealed no significant overall effect for either N1-P1 ($F_{3,21}$=.51, p>.10) or P3-N4 ($F_{3,21}$=1.13, p>.10) amplitude. The three peaks analyzed for changed latency showed a tendency toward increased latency with progressively higher concentrations of ozone. Again a repeated measures analysis of variance was performed, and it was found that although there was no significant overall effect, both P1 ($F_{3,21}$=2.99; .10>p>.05) and P3 ($F_{3,21}$=2.42; .100>p>.05) approached significance. A planned comparison between the 1.00 and 0.00 ppm latencies revealed a significant difference for P3 (t_7=2.46; p<.05) but not P1 (t_7=1.83; p>.05). A trend analysis indicated significant linear trends for both P1 ($F_{1,21}$=7.94; p<.05) and P3 ($F_{1,21}$=6.53; p<.05).

VISUAL CORTEX

Repeated measures analyses performed upon visual cortex amplitudes revealed no significant overall effect (F's < 1.20, p's > .10). Figure 3 illustrates the latency changes for the N1, P2, and P3 components. These changes parallel each other as they all peak at 0.75 ppm, then show a downward trend at 1 ppm. A repeated measures analysis failed to confirm an overall significant effect of ozone upon visual cortex evoked potential latencies ($F's_{3,15}$ < 2.20; p's >.10).

DISCUSSION

In considering these results, it should be emphasized that the concentration x time (C x T) value is only 25% of C x T levels found necessary to produce neurochemical (15) and evoked potential (6) changes in two other studies that made attempts to quantitatively evaluate the data. On the other hand, the C x T level of the present study was equal to (at 0.5 ppm) or greater than the C x T level reported to be effective by Xintaras et al. (16). A characteristic of the evoked potential, even under the carefully controlled conditions of the present experiment, is variability. Since attempts to control this variability and statistically evaluate the data are not discussed by Xintaras et al. (16), it appears reasonable to assume that the effect they described is more a reflection evoked potential variability than ozone.

At best the present results can be considered as supporting the contention that evoked potentials can be affected by exposure to ozone, if the C x T value is high enough. The trend in the present study was toward increased latencies in the superior colliculus recordings. Clearly, before definitive statements can be made, more subjects must be tested both at the exposure levels used here and at higher levels.

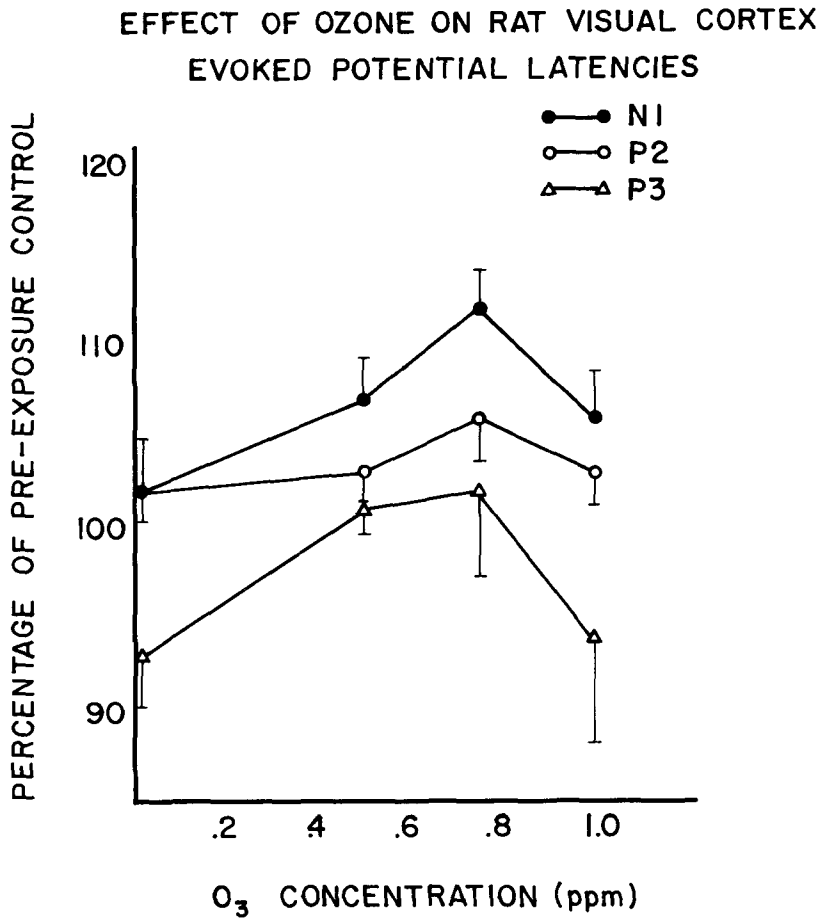

Figure 3. Effects of O_3 upon visual cortex latencies.

Ozone presents an interesting problem for the neurophysiologist, first because of the conflict raised by the present results regarding whether or not there is an effect upon CNS function, and secondly, if there is an effect, accounting for its mechanism. A number of mechanisms are possible. First, one might suppose that CNS effects might be secondary to a systemic response involving a pulmonary or vascular effect. Many studies (4, 8, 12) have demonstrated pulmonary function changes as well as edemagenesis in O_3-exposed rodents. Should this be the mechanism of effect, one would expect changes in blood chemistry of rats exposed to 1 ppm O_3 for two hours. Preliminary results from our laboratory indicate that blood chemistries of rats so exposed are essentially unaltered, and thus it appears unlikely that either hypoxia or hypocapnia could account for altered CNS function. A second, and perhaps more plausible, mechanism is one by which CNS changes are described as secondary to

peripheral irritation. Both the nasal mucosa and the ocular conjunctiva become irritated at low O_3 exposure levels. Irritation of nasal mucosa could be expected to stimulate both the olfactory nerve and the trigeminal nerve. The olfactory nerve might certainly be expected to produce a heightened arousal, mediated by reticular activation. Although one might postulate that this could increase amplitudes of evoked potentials in all sensory systems, it is unlikely that such arousal would increase latencies. Increased latencies are more generally associated with CNS depression, not activation.

There is some indirect evidence that changes in O_3 levels may be associated with changes in intraocular pressure (5) and visual function in humans (7). Since mechanical stimulation of the sensory branches of the trigeminal nerve can produce elevations in intraocular pressure (9), these effects are not difficult to understand. Furthermore, increases in intraocular pressure might well be expected to increase evoked potential latencies and amplitudes, although in cats the magnitude of increased pressure required is quite high (14).

In conclusion it appears that two-hour exposures to 0.5 or 0.75 ppm O_3 produce very little if any effect upon flash-evoked potentials from the visual cortex or superior colliculus. At 1.0 ppm O_3 a small increase in latency is observed, and this may be accounted for by peripherally induced changes in intraocular pressure.

ACKNOWLEDGMENTS

This work was supported by a grant-in-aid from Fight for Sight, Inc. (G553), and NIH grants ES00454, HL10342, ES0034.

REFERENCES

1. Dyer, R. S. and Annau, Z. Superior colliculus visual evoked potentials in unanesthetized rats. Presented to Society for Neuroscience, New York, November 1975a.

2. Dyer, R. S. and Annau, Z. Effects of carbon monoxide and hypoxia on visual evoked potentials in the rat. Presented to Federation of American Societies for Experimental Biology, Atlantic City, 1975b.

3. Dyer, R. S., Eacho, P., Jenko, P. G. and Olton, D. S. Septal stimulation, light aversion and visual evoked potentials in the rat. Neuroscience Abstracts, 1976, 2, in press.

4. Gardner, D. E., Illing, J. W., Miller, F. J. and Coffin, D. L. The effect of ozone on pentobarbital sleeping time in mice. Res. Com. Clin. Path. Pharm., 9:689-700, 1974.

5. Huerkamp, B. and Zieglitz, W. Arrangehalt der Luft und Glaukon. Von Graefes Arch. Opthal. Munich, 154:507, 1953.

6. Johnson, B. L., Orthoefer, J. C., Lewis, T. R. and Xintaras, C. The effect of ozone on brain function in Clinical Implications of Air Pollution Research, December 5-9, 1974.

7. Legerwerff, J. M. Prolonged ozone inhalation and its effects on visual parameters. Aerospace Med., 34:479-486, 1963.

8. Murphy, S. D., Ulrich, C. E., Frankowitz, S. H. and Xintaras, C. Altered function in animals inhaling low concentrations of ozone and nitrogen dioxide. J. Amer. Ind. Hyg. Assn., 25:246-253, 1964.

9. Perkins, E. S. Influence of the fifth cranial nerve on the intraocular pressure of the rabbit eye. Brit. J. Opthal., 41:257-300, 1957.

10. Powell, E. W. and Hoelle, D. F. Septotectal projections in the cat. Exp. Neurol., 18:177-183, 1967.

11. Pribram, K. H. and Kruger, L. Functions of the olfactory brain. Ann. N. Y. Acad. Sci., 58:109-138, 1954.

12. Schell, L. D., Dobroyorski, O. J., Mountain, J. T., Svirbely, J. L. and Stokinger, H. E. Physiologic, biochemical, immunologic and pathologic changes following ozone exposure. J. Appl. Physiol., 14:67-80, 1959.

13. Skinner, J. E. Neuroscience: A Laboratory Manual. W. B. Saunders Co., Philadelphia, 1971.

14. Takeda, Y., Nakai, Y. and Takaori, S. Analysis of evoked responses in the visual pathway of cats with elevation of the intraocular pressure. Brain Res., 43:373-381, 1972.

15. Trams, E. G., Lauter, C. J., Brandenburger-Brown, E. A. and Young, O. Cerebral cortical mechanism after chronic exposure to ozone. Arch. Env. Health, 24:253-259, 1972.

16. Xintaras, C., Johnson, G. L., Ulrich, C. E., Terrill, R. E. and Sobecki, M. F. Application of the evoked response technique in air pollution toxicology. Toxicol. Appl. Pharmacol., 8:77-87, 1966.

HEALTH EFFECTS OF SHORT-TERM EXPOSURES TO NO_2-O_3 MIXTURES

R. Ehrlich, J. C. Findlay, J. D. Fenters, and D. E. Gardner*

ABSTRACT

The effects of single and multiple daily 3-hour exposures to nitrogen dioxide (NO_2) and ozone (O_3) mixtures on the resistance to streptococcal pneumonia were investigated. The concentrations of NO_2 ranged from 2.8 to 9.4 mg/m^3 (1.5 to 5.0 ppm) and of O_3 from 0.1 to 0.98 mg/m^3 (0.05 to 0.5 ppm). The effect of a single exposure to the mixture was additive, whereby the excess mortality rates were equivalent to those induced by the inhalation of each individual pollutant. The ability to clear inhaled bacteria from the lungs was diminished in mice exposed to the NO_2-O_3 mixtures for 3 hours. This impairment was manifested by the increased frequency of isolation of <u>*streptococcus*</u> *from te lungs for up to 6 days after the respiratory challenge. Excess mortalities observed after 20 daily 3-hour exposures suggested that a synergistic effect might be present upon repeated inhalation of pollutant mixtures that made them more effective in reducing resistance to respiratory infection. The results emphasize the need for establishment of primary air quality standards for short-term NO_2 exposures.*

INTRODUCTION

Results of experimental studies clearly demonstrate that inhalation of either ozone (O_3) or nitrogen dioxide (NO_2) significantly enhances the susceptibility to bacterial pneumonias (Miller and Ehrlich, 1958; Coffin and Gardner, 1972; Ehrlich, 1966). Only sparse data are available on the effects of exposures to mixtures of these two pollutants on the resistance to respiratory infections, however. To elucidate such effects, studies were conducted in mice exposed to ozone, nitrogen dioxide, or a mixture of the two and then challenged with <u>Streptococcus</u> aerosol. This experimental model was employed because of its demonstrated sensitivity and responsiveness at ambient concentrations of air pollutants. Moreover, the model reflects the overall toxic response of the respiratory system, such as inflammation, edema, cellular necrosis, reduced macrophage function, and ciliostasis. Thus, it indicates the impairment of the basic defense mechanisms in the lung by the combined exposure to air pollutants and the superimposed infectious challenge.

*R. Ehrlich, J. C. Findlay, and J. D. Fenters IIT Research Institute, Chicago, Illinois.
D. E. Gardner, U. S. Environmental Protection Agency, Research Triangle Park, North Carolina.

METHODS

ANIMALS

Female CF-1 (ARS, Madison, Wisconsin), and CD_2F_1 mice (Murphy Laboratory, Plainfield, Indiana) were used in the experiments. The 5 to 8-week old mice were quarantined for 7 to 14 days before being used in the studies. During the quarantine and throughout the experiments, the mice were housed in groups of eight in stainless steel shoe-box cages. Food and water were provided *ad libitum*. For the 3-hour exposures to the pollutants and during the infectious challenge, the mice were housed individually in separate compartments of specially designed stainless steel wire cages.

EXPOSURE CHAMBERS

Four identical 120 x 60 x 60 cm (432 liters) Plexiglas chambers were used for exposure to air pollutants or filtered air. The air stream carrying the pollutants entered the chambers from the top of one side and was exhausted at the top of the opposite site. Homogeneous distribution of the pollutants was further assured by the continuous operation of a small blower during the animal exposures. To prevent ammonia build-up, deodorized cage boards were placed on the floor of each chamber. The compressed air supplied to the exposure chambers was dried and purified by passage through an Alemite filter (Model 7620, Steward Warner, Chicago, Illinois) and a disposable air purifier and flow equalizer (Koby Inc., Malboro, Massachusetts). Temperature in the exposure chambers was maintained at 24 $\pm$ 2°C at ambient humidity $\leq$ 40% RH).

NITROGEN DIOXIDE (NO_2)

A 1 percent NO_2 gas mixture in balanced air, 99.5% pure, (Matheson, Joliet, Illinois) was diluted with filtered air in a glass mixing chamber then passed into the animal exposure chamber at a rate of 60 $\pm$ 5 liters/minute. The NO_2 concentration was monitored continuously by a NO-NO_2-NO_X chemiluminescent analyzer (Model 8101B, Bendix Corporation, Ronceverte, West Virginia) and was expressed in ppm or gm/m^3 (ppm x 1.88 = mg/m^3).

OZONE (O_3)

A high-voltage generator (IITRI) was used to convert filtered air to O_3. To provide the desired concentration, O_3 was diluted with filtered air in a glass mixing chamber then passed into the animal exposure chamber at a rate of 60 $\pm$ 5 liters/minute. The O_3 concentration was monitored continuously with an O_3 chemiluminescent analyzer (Model OA 310, Meloy Laboratories, Springfield, Virginia) and was expressed in ppm or mg/m^3 (ppm x 1.96 = mg/m^3).

NO_2-O_3 MIXTURE

To obtain the NO_2 and O_3 mixture, each gas was introduced into a separate glass vessel then combined in a glass mixing chamber. The gas mixture was then passed into the animal exposure chamber at a rate of 60 $\pm$ 5 liters/minute. Concentration of the gases in the exposure chamber was monitored continuously with the NO_X and O_3 chemiluminescent analyzers.

INFECTIOUS CHALLENGE

Streptococcus (S. pyogenes, Group C isolated from a pharyngeal abcess of a guinea pig) was used for the infectious challenge. To maintain the stock culture, mice were injected intraperitoneally with a suspension of Streptococcus and killed 24 hours later. Heart blood was incubated on blood agar for 48 hours at 37°C., and the isolated Streptococcus colonies were inoculated in Todd Hewitt broth (BBL). After an 18-hour incubation at 37°C., the growth was harvested and approximate 1-ml aliquotes were frozen at -70°C. For the infectious challenge, the thawed bacteria were regrown in Todd Hewitt broth for 18 hours at 37°C. Before dissemination, the optical density of the suspension was adjusted in 0.1% peptone water to approximately 65% density as measured at 440 μm in a Spectronic 20 densitometer.

AEROSOL CHALLENGE

Infectious challenge was performed in a 400-liter Plexiglas aerosol chamber (71 x 61 x 92 cm) contained in a microbiological safety cabinet. Temperature in the aerosol chamber was maintained at 24 ± 2°C and humidity at 65 ± 5% RH. A continuous flow nebulizer (DeVilbiss Model 84) was used to produce the bacterial aerosol. Filtered air was supplied to the inlet of the nebulizer at a flow rate of approximately 8 liters/minute. Mice in individual compartments were exposed to the aerosol for 10 minutes, then removed from the chamber and held for 14 days in a clean-air isolated animal room.

The inhaled dose of bacteria in the lungs was determined by killing three mice immediately after the infectious challenge. The lungs were removed, weighed, and homogenized in sterile 0.1% peptone water. The suspension was diluted, plated on blood agar, and the colonies counted after 48-hours incubation at 37°C. The inhaled dose of viable bacteria ranged from 10 to 30 x 10^3 organisms per gram of lung tissue.

EXPERIMENTAL PROTOCOL

In the single exposure experiments, mice were exposed for 3 hours to the individual pollutants and corresponding pollutant mixtures. For repeated exposure studies, mice were exposed to the pollutants daily for 3 hours, 5 days/week, for 1, 2, or 4 weeks. Control mice were treated identically but were exposed to filtered air rather than air containing the pollutants. Within 1 hour after termination of 1 hour exposures to the pollutants, groups of 24 mice representing all experimental and control conditions were simultaneously infected by the respiratory route with airborne streptococcus. After the infectious challenge, the mice were held in a clean-air isolation room for 14 days, during which time mortality rates and survival times were determined daily.

RESULTS

SINGLE EXPOSURE

Previous reports from our laboratories (Ehrlich, 1966) have indicated that a single 2-hour exposure of mice to 6.58 mg/m^3 (3.5 ppm) NO_2 significantly

increased the mortality resulting from a superimposed bacterial pneumonia initiated by inhalation of airborne Klebsiella pneumoniae. Similar increases in mortality after a 3-hour exposure to 0.16 mg/m^3 (0.08 ppm) O_3 and challenge with Streptococcus aerosol were reported (Coffin and Gardner, 1972). To provide unified data and to more closely define the dose-response relationship, mice were exposed for 3 hours to various concentrations of either NO_2 or O_3 then challenged with Streptococcus aerosol.

The death rates obtained during numerous replicate exposures to the pollutants are summarized in Figure 1. The mortality of mice infected but not exposed to pollutants represent the total number of control mice used in all experiments. This mortality rate (26.6%) was used to estimate the significance of changes induced by exposures to the pollutants. The statistical significance of the differences was determined by a chi-square test with a 2x2 contingency table. A signficiant increase in death rates over the control mortality was observed upon the 3-hour exposure to 0.2 mg/m^3 (o.1 ppm) O_3 or 3.76 mg/m^3 (2.0 ppm) NO_2. Moreover, a linear relationship was present between the concentration of the pollutants and mortality rates with a correlation coefficient of 0.969 for NO_2 and 0.996 for O_3.

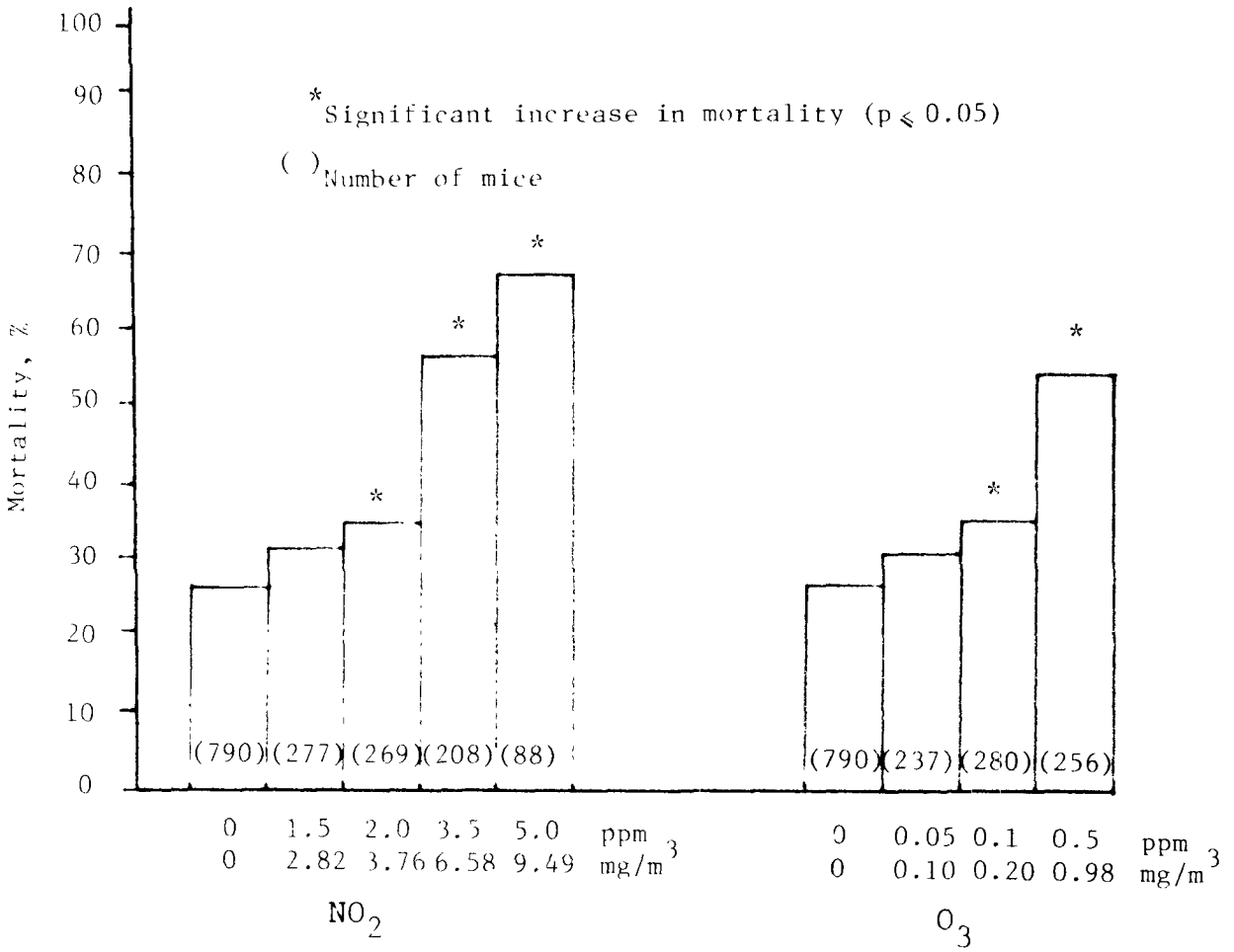

Figure 1. Mortality rates in mice exposed for 3 hours to O_3 or NO_2 and challenged with Streptococcus aerosol.

To determine the effects of inhalation of air pollutant mixtures, mice were exposed to selected concentrations of NO_2, O_3, NO_2-O_3 mixture, or to filtered air. The four groups, usually consisting of 24 mice each, were simultaneously challenged with Streptococcus aerosol. Thus, the mortality rates could be compared in each individual exposure experiment and results of replicate experiments could be pooled for statistical analysis. The differences between mortality rates observed in mice exposed to the pollutants and challenged with Streptococcus aerosol and the corresponding control mice challenged with infectious agent only during each exposure were calculated. Data representing a minimum of four replicate experiments for each concentration of each pollutant are summarized in Table 1. The data indicate that the effect of the 3-hour inhalation of NO_2-O_3 mixtures was additive. In most instances, the differences in mortality rates were equivalent to the sum of those resulting from inhalation of each individual pollutant.

TABLE 1. EXCESS MORTALITIES IN MICE EXPOSED FOR 3 HR TO POLLUTANTS AND CHALLENGED WITH STREPTOCOCCUS OVER THOSE IN CORRESPONDING INFECTED CONTROLS

NO_2, mg/m^3 (ppm) \ O_3, mg/m^3 (ppm)	Excess Mortality, %			
	0	0.1 (0.05)	0.2 (0.1)	0.98 (0.5)
0	0	5.4	7.2	28.6*
2.82 (1.5)	-1.7	4.6	4.2	23.9*
3.76 (2.0)	14.3*	22.0*	-	56.2*
6.58 (3.5)	28.2*	-	38.5*	68.7*
9.40 (5.0)	35.7*	-	-	65.3*

*Significant change in mortality from corresponding infected controls ($p \leq 0.05$).

MULTIPLE EXPOSURES

In studies of the effects of multiple short-term exposures, mice were exposed to the pollutants daily for 3-hours, 5 days/week, for 1, 2, and 4 weeks. Within 1 hour after termination of the final exposure the mice, along with control mice exposed to filtered air, were challenged with Streptococcus aerosol. Two mixtures of the pollutants were included in the experiments: 3.76 mg/m^3 (2.0 ppm) NO_2 and 0.10 mg/m^3 (0.05 ppm) O_3, and 2.82 mg/m^3 (1.5 ppm) NO_2 and 0.20 mg/m^3 (0.1 ppm) O_3. Thus, each mixture contained a concentration of one of the two pollutants, exposure to which previously resulted in excess mortality. The results of two replicate experiments for each exposure regimen are summarized in Figure 2. The excess mortalities are based on exposure of 48 mice at each experimental point to the 2.82 mg/m^3 (1.5 ppm) NO_2

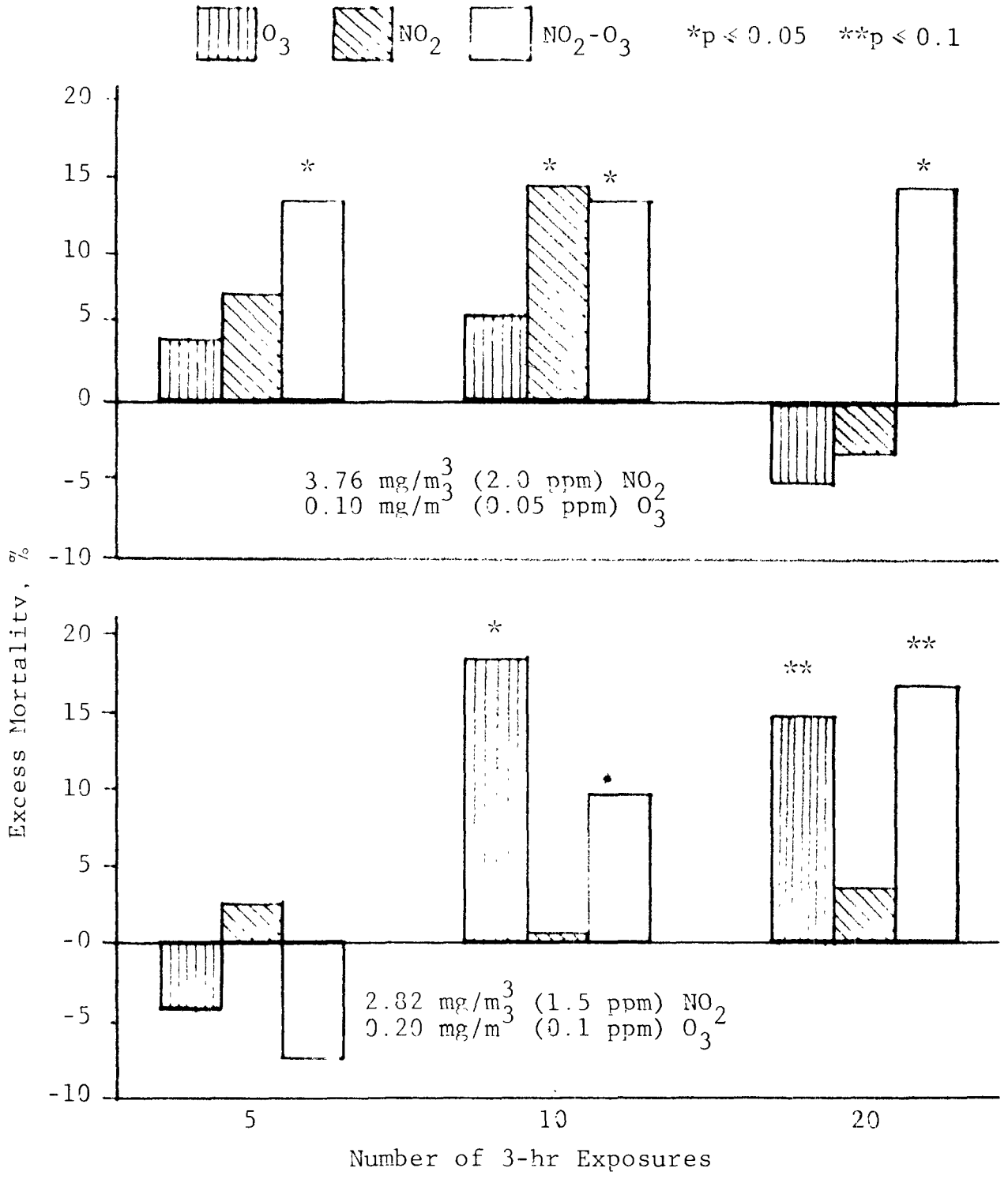

Figure 2. Excess mortality in mice after multiple daily 3 hour exposures to the NO_2-O_3 mixture and challenge with Streptococcus aerosol.

and 0.20 mg/m^3 (0.1 ppm) O_3 mixture, and 104 mice to the 3.76 mg/m^3 (2.0 ppm) NO_2 and 0.10 mg/m^3 (0.05 ppm) O_3 mixture.

Repeated daily exposure to the mixture consisting of 3.76 mg/m^3 (2.0 ppm) NO_2 and 0.10 mg/m^3 (0.05 ppm) O_3 followed by the infectious challenge resulted in a significant excess of deaths over those observed in control mice. The excess mortalities were present irrespective of the number of daily 3-hour exposures. Death rates increased somewhat after five daily exposures to 3.76 mg/m^3 (2.0 ppm) NO_2 alone, were significantly higher after 10 exposures, but did not differ from control mice after 20 exposures. Only small changes in mortality rates were seen after five to 20 daily exposures to 0.10 mg/m^3 (0.05 ppm) O_3 alone. The results indicate that daily 3-hour exposures to either NO_2 or O_3 had no major effect on the mortality rates. On the other hand, daily exposures to the NO_2-O_3 mixture containing the same concentration of each pollutant resulted in significant excess mortalities. This suggests a synergistic relation between the two pollutants that makes them more effective in reducing resistance to respiratory infection.

Results of daily 3-hour exposures to a mixture consisting of 2.82 mg/m^3 (1.5 ppm) NO_2 and 0.20 mg/m^3 (0.1 ppm) O_3 indicated that O_3 was the primary contributing factor, inducing the excess mortalities. There was no remarkable differences in mortalities at any of the exposure conditions after five daily exposures. However, after 10 or 20 exposures to O_3 per se or the NO_2-O_3 mixture there were marked excess deaths. Inasmuch as excess mortalities seen upon inhalation of the mixture were approximately the same as those observed in mice exposed to O_3 only, it can be assumed that they were due to the presence of O_3 in the mixture.

LUNG CLEARANCE OF INHALED BACTERIA

The effects of inhalation of pollutants on clearance of viable Streptococcus from the lungs were investigated in mice after a single 3-hour exposure to mixtures consisting of 6.58 mg/m^3 (3.5 ppm) NO_2 and 0.20 mg/m^3 (0.05 ppm) O_3. Within 1 hour after termination of exposure to the pollutants, the mice were challenged with airborne Streptococcus. Immediately after the infectious challenge, five mice were killed, the lungs removed, weighed, homogenized and cultured quantitatively. These initial counts (zero hour) expressed as the number of viable bacteria per gram of lung were considered as 100%. Thereafter, groups of five mice, either exposed to filtered air or the NO_2-O_3 mixture were killed at 1, 2, 3, 4, and 5 hours, and at 1, 2, 3, and 6 days after the respiratory challenge and their lungs were assayed in an identical manner.

The hourly counts were calculated as percent recovery of those present at the zero hour. The clearance rates of viable bacteria determined by the least square method showed a marked delay after exposure to the 6.58 mg/m^3 (3.5 ppm) NO_2 and 0.20 mg/m^3 (0.1 ppm) O_3 mixture. The time required to clear 50% of the inhaled bacteria in control mice was approximately 81 minutes, and in those exposed to the pollutants, 131 minutes. No differences were seen in bacterial clearance from the lungs upon exposure to 3.76 mg/m^3 (2.0 ppm) NO_2 and 0.10 mg/m^3 (0.05 ppm) O_3 mixture.

The daily clearance rates were calculated as the number of mice having viable Streptococcus in the lungs out of the total number of mice killed on a given day. The effects of exposure to both mixtures of the pollutants were much more pronounced over this extended assay period (Table 2). Among the mice exposed to 6.58 mg/m^3 (3.5 ppm) NO_2 and 0.20 mg/m^3 (0.10 ppm) O_3 mixture 15/19 (79%) and to 3.76 mg/m^3 (2.0 ppm) NO_2 and 0.10 mg/m^3 (0.05 ppm) O_3 mixture 16/19 (89%) showed viable Streptococcus in the lungs, whereas among the corresponding controls 7/20 (35%) and 8/20 (40%) were positive. Thus, it is apparent that the capacity to clear inhaled bacteria was impaired by the single 3-hour inhalation of NO_2-O_3 mixtures.

TABLE 2. RETENTION OF INHALED VIABLE STREPTOCOCCUS IN LUNGS OF MICE EXPOSED FOR 3 HR TO NO_2- O_3 MIXTURES

	NO_2 - O_3 Concn. mg/m^3 (ppm)			
	6.58 - 0.20 (3.5 - 0.1)		3.76 - 0.10 (2.0 - 0.05)	
	Positive/Total*		Positive/Total	
Day of Assay	Control	Expt	Control	Expt
1	2/5	5/5	0/5	4/4
2	3/5	3/5	2/5	4/5
3	0/5	3/4	4/5	3/4
6	2/5	4/5	2/5	5/5

*Number of mice showing viable Streptococcus out of total number of mice assayed.

DISCUSSION

It is well recognized that effects of air pollutants may be additive or synergistic with each other as well as with other environmental stresses. Such combined effects can be ascribed to a variety of factors: e.g., one pollutant affecting the site of deposition of another, one pollutant affecting the lung clearance mechanisms so that the second one cannot be removed, or one pollutant producing an effect in the lung that makes it more vulnerable to the effects of the second pollutant. Occasionally, the type of interaction can be predicted on the basis of the chemical composition of each component. More often it is not possible to forecast the effect of pollutant mixtures, however, and empirical experimental studies must be conducted.

Only sparse experimental data are available on the effects of exposure to mixtures of NO_2 and O_3 on the resistance to respiratory infections. Coffin and Bloomer (1967) reported increased mortality rates in mice exposed for 4 hours to light-irradiated automobile exhaust then infected with airborne Streptococcus. The NO_2 concentrations in the exhaust gas was 0.56 mg/m^3 (0.3 ppm) approximately tenfold below that reported to enhance the susceptibility to respiratory infection (Ehrlich, 1966). However, concentrations of oxidants were within the effective range of O_3, where threshold values of 0.20 mg/m^3 (0.1 ppm) have been reported (Coffin and Gardner, 1972). Thus, the authors ascribed the changes in resistance to infection primarily to the presence of oxidants. Goldstein et al. (1974) studied the pulmonary defense mechanisms in mice exposed to mixtures of NO_2 and O_3 and infected with airborne Staphylococcus aureus. Mice were exposed to the mixtures for either 17 hours before or 4 hours after infectious challenge. The authors concluded that the effects, expressed as bactericidal dysfunction in the lungs, were present when the level of either pollutant approximated its individual threshold value; 13.2 mg/m^3 (7.0 ppm) NO_2 and 0.78 mg/m^3 O_3 (0.4 ppm) O_3 for the 4-hour exposure.

Results of our studies clearly demonstrate the additive effects of NO_2 and O_3 during a single 3-hour exposure, when superimposed with an infectious challenge. Moreover, the results of 20 daily 3-hour exposures suggest a synergistic effect upon repeated inhalation of a mixture of the two pollutants.

To further assess the interaction between the two pollutants, regression analysis was applied to the excess mortality data obtained during exposures to the NO_2-O_3 mixtures. The least-square lines plotted in Figure 3 make it possible to estimate the increase in deaths that can be expected upon exposure to 2.82, 3.76, or 6.58 mg/m^3 (1.5, 2.0, or 3.5 ppm) NO_2 in presence of various concentrations of O_3 or, conversely, upon exposure to 0.10, 0.20, or 0.98 mg/m^3 (0.05, 0.1, or 0.5 ppm) O_3 in conjunction with various concentrations of NO_2. The accuracy of the extrapolations is related to the death rates of mice challenged with the infectious agent and exposed to either NO_2 or O_3 alone, inasmuch as these rates served as the zero point in the estimation of the least-square lines. The data show that a marked increase in mortality rates of infected mice can be expected upon a 3-hour exposure to a mixture of NO_2 and O_3 in concentrations frequently encountered in ambient urban pollution.

Results of our studies reemphasize the necessity of the establishment of primary air quality standards for short-term exposures to NO_2. The data provide estimates concerning the health effects of single and multiple short-term exposures to NO_2 alone or in the presence of O_3. It appears, therefore, that the primary air quality standards should consider the concommitant control of NO_2 and O_3 at any one time, e.g., NO_2 should not exceed X concentration when O_3 is present in Y concentration.

ACKNOWLEDGEMENTS

The authors are indebted to Ms. S. Daseler and Mr. J. Hingeveld for their technical assistance.

The studies were supported by funds provided by the U.S. Environmental Protection Agency under Contracts No. 68-02-1267 and 68-02-2274.

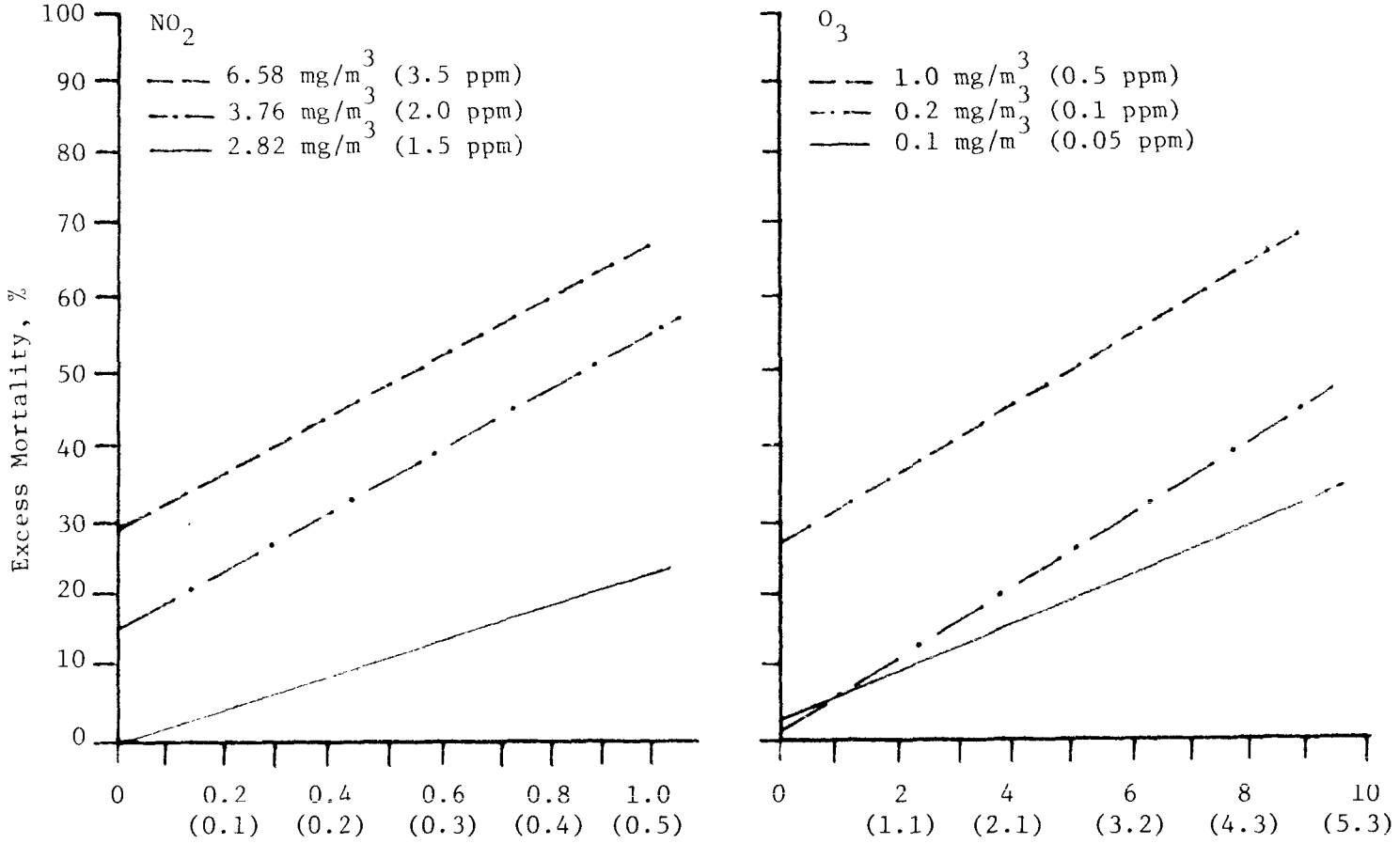

Figure 3. Estimated excess mortalities at various concentrations of NO_2-O_3 mixtures.

REFERENCES

1. Coffin, D. L., and E. J. Blommer, Acute Toxicity of Irradiated Auto Exhaust Indicated by Mortality from Streptococcal Pneumonia, Arch. Environ. Health, 15:36-38, 1967.

2. Coffin, D. L., and D. E. Gardner, Interaction of Biological Agents and Chemical Pollutants, Ann. Occup. Hyg., 15:219-234, 1972.

3. Ehrlich, R., Effect of Nitrogen Dioxide on Resistance to Respiratory Infection, Bacteriol. Rev., 30:604-614, 1966.

4. Goldstein, E., D. Warshauer, W. Lippert, and B. Tarkington, Ozone and Nitrogen Dioxide Exposure, Arch. Environ. Health, 28:85-90, 1974.

5. Miller, S., and R. Ehrlich, Susceptibility to Respiratory Infections of Animals Exposed to Ozone, J. Infect. Dis., 103:145-149, 1958.

TECHNICAL REPORT DATA
(Please read Instructions on the reverse before completing)

1 REPORT NO EPA-600/3-77-001a	2	3 RECIPIENT'S ACCESSION NO.
4 TITLE AND SUBTITLE INTERNATIONAL CONFERENCE ON PHOTOCHEMICAL OXIDANT POLLUTION AND ITS CONTROL Proceedings: Volume I		5 REPORT DATE January 1977 6. PERFORMING ORGANIZATION CODE
7 AUTHOR(S) Basil Dimitriades, Editor		8 PERFORMING ORGANIZATION REPORT NO.
9 PERFORMING ORGANIZATION NAME AND ADDRESS Environmental Sciences Research Laboratory Office of Research and Development U.S. Environmental Protection Agency Research Triangle Park, N.C. 27711		10. PROGRAM ELEMENT NO. 1AA603 11 CONTRACT/GRANT NO
12 SPONSORING AGENCY NAME AND ADDRESS Environmental Sciences Research Laboratory Office of Research and Development U.S. Environmental Protection Agency Research Triangle Park, N.C. 27711		13. TYPE OF REPORT AND PERIOD COVERED In-house 14. SPONSORING AGENCY CODE EPA-ORD

15 SUPPLEMENTARY NOTES

This Conference was sponsored by the US-Environmental Protection Agency with the patronage of the Organization for Economic Cooperation and Development.

16. ABSTRACT

The proceedings consist of 97 technical papers covering such areas as analytical methods for photochemical oxidants and precursors; causes of urban, suburban, and non-urban oxidant; biological effects; oxidant control strategies; and trends in emissions and emission control technology. The International Conference was held in Raleigh, N.C. in September 1976.

17. KEY WORDS AND DOCUMENT ANALYSIS

a. DESCRIPTORS	b. IDENTIFIERS/OPEN ENDED TERMS	c. COSATI Field/Group
*Air pollution		13B
*Ozone		07B
*Photochemical reactions		07E

18 DISTRIBUTION STATEMENT RELEASE TO PUBLIC	19 SECURITY CLASS (This Report) UNCLASSIFIED 20 SECURITY CLASS (This page) UNCLASSIFIED	21 NO. OF PAGES 592 22. PRICE

EPA Form 2220-1 (9-73)